AIP Conference Proceedings

scitation.org/journal/apc

Volume 2325

International Conference on Analysis and Applied Mathematics (ICAAM 2020)

Mersin, Turkey • 23–30 September 2020

Editors • Allaberen Ashyralyev, Charyyar Ashyralyyev, Abdullah S. Erdogan, Alexey Lukashov and Makhmud Sadybekov

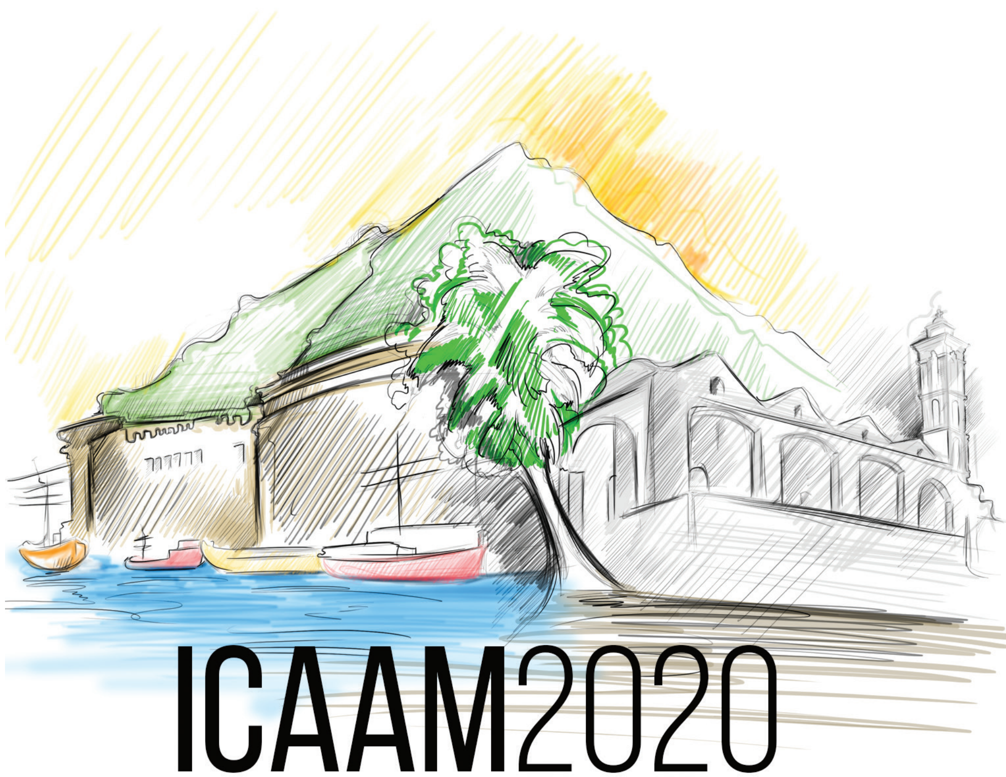

AIP Publishing

AIP Conference Proceedings

Volume 2325

ISBN: 978-0-7354-4069-2

ISSN: 0094-243X

scitation.org/journal/apc

AIP Publishing

AIP Conference Proceedings

International Conference on Analysis and Applied Mathematics (ICAAM 2020)

Volume 2325

Conference collection

International Conference on Analysis and Applied Mathematics (ICAAM 2020)

Mersin, Turkey
23–30 September 2020

Editors

Allaberen Ashyralyev
Near East University, Nicosia, Turkey

Charyyar Ashyralyyev
Gumushane University, Gumushane, Turkey

Abdullah S. Erdogan
Palm Beach State College, Palm Beach Gardens, United States of America

Alexey Lukashov
Saratov State University, Saratov, Russia

Makhmud Sadybekov
Institute of Mathematics and Mathematical Modeling, Almaty, Kazakhstan

Sponsoring Organizations
Near East University
Institute of Mathematics and Mathematical Modeling
Analysis & PDE Center Ghent University

All papers have been peer reviewed.

AIP Publishing

Melville, New York, 2021
AIP Conference Proceedings

Volume 2325

To learn more about AIP Conference Proceedings visit **http://proceedings.aip.org**

Editors

Allaberen Ashyralyev
Near East University
Department of Mathematics
Mersin 10
Nicosia, 99138
Turkey

Peoples' Friendship University of Russia
Department of Mathematics
Ulitsa Miklukho-Maklaya, 6
Moskva, 117198
Russia

Email: aallaberen@gmail.com

Charyyar Ashyralyyev
Gumushane University
Department of Mechanical Engineering
Baglarbashy Mahallesi
Gumushane, 29100
Turkey

Email: charyar@gmail.com

Abdullah S. Erdogan
Palm Beach State College
3160 PGA Boulevard
Palm Beach Gardens, FL
33410
United States of America

Email: aserdogan@gmail.com

Alexey Lukashov
Saratov State University
Department of Mathematics and Mechanics
Astrahanskaya
Saratov, 410012
Russia

Institutskiy per. Dolgoprudny
Moscow 141701
Russia

Email: alexey.lukashov@gmail.com

Makhmud Sadybekov
Institute of Mathematics and Mathematical Modeling
Differential Equations
Pushkina 125
Almaty, 050010
Kazakhstan

Email: sadybekov@math.kz

ISBN 978-0-7354-4069-2
ISSN 0094-243X
Printed in the United States of America

AIP Conference Proceedings, Volume 2325
International Conference on Analysis and Applied Mathematics (ICAAM 2020)

Table of Contents

Preface: Fifth International Conference on Analysis and Applied Mathematics (ICAAM 2020)

The main objective of ICAAM is to promote and inspire new developments in mathematics and mathematical applications. For reaching our goal, we provide a forum for researchers and scientists who are working in the fields of Analysis and Applied Mathematics to share and exchange their ideas and recent research works.

The COVID-19 pandemic has brought unprecedented challenges both for people and the math society. We are deeply saddened to hear the loss of previous ICAAM series participants. For being strong during the pandemic, as ICAAM community, we encourage one another to continue our research. This volume is one of the fruitful results of this encouragement.

This volume is a collection of 70 selected extended abstracts. These papers are presented at the Fifth International Conference on Analysis and Applied Mathematics (ICAAM 2020) which was held in North Cyprus, Turkey. The selection of the papers included in this volume is based on an international peer review procedure. The selected extended abstracts examine wide ranging and cutting edge developments in various areas of Analysis and Applied Mathematics. The papers give a taste of current research. We feel the variety of topics will be of interest to both graduate students and researchers.

We would like to thank:

- The Scientific Committee of ICAAM 2020 for their help and support.
- The distinguished invited speakers for their difficult task and for their acceptance to give keynote lectures on their respective fields of expertise.
- The Organizing Committee of ICAAM 2020 for their help and support.
- Special thanks to Prof. Evren Hincal, Prof. Deniz Agirseven, Prof. Yasar Sozen, Assoc. Prof. Maksat Ashyraliyev, Assoc. Prof. Ozgur Yildirim, Asst. Prof. Bilgen Kaymakamzade, Lecturer Nezihal Gökbulut for their valuable assistance and their help in typesetting of this volume.
- Special thanks to the American Institute of Physics for the inclusion of these Proceedings into the famous series of the AIP Conference Proceedings.
- Special thanks and acknowledgments to the main organizer of the conference Near East University, Lefkosa (Nicosia), Mersin 10, Turkey and co-organizers of the conference Institute of Mathematics and Mathematical Modeling, Almaty, Kazakhstan and Analysis & PDE Center, Ghent University, Belgium for their sponsorship.

International Conference on Analysis and Applied Mathematics (ICAAM 2020)
AIP Conf. Proc. 2325, 010001-1–010001-2; https://doi.org/10.1063/12.0003133
Published by AIP Publishing. 978-0-7354-4069-2/$30.00

Professor Allaberen Ashyralyev,
Near East University, Lefkosa (Nicosia), Mersin 10, Turkey and Peoples' Friendship University of Russia, Russian Federation

Professor Charyyar Ashyralyyev,
Gumushane University, Gumushane, Turkey

Professor Abdullah S. Erdogan,
Palm Beach State College, Palm Beach Gardens, FL, USA

Professor Alexey Lukashov,
Saratov State University and Moscow Institute of Physics and Technology, Moscow, Russian Federation

Professor Makhmud Sadybekov,
Institute of Mathematics and Mathematical Modeling, Almaty, Kazakhstan

October 2020

Optimal Investment Decision on Green Energy

Tynysbek Sh. Kalmenov,[a)] Vladislav S. Hachikyan,[b)] Gani A. Besbayev,[c)] and Aizat Sh. Aimakhanova[d)]

Institute of Mathematics and Mathematical Modeling, Almaty, Kazakhstan

[a)]*Corresponding author: kalmenov@math.kz*
[b)]*Electronic mail: vhachikyan@mail.ru*
[c)]*Electronic mail: besbayev@math.kz*
[d)]*Electronic mail: aimakhanova@math.kz*

Abstract. In this note we present that the optimal investment decision can be characterized by two boundaries that satisfy a system of coupled integral equations of Fredholm type and propose a numerical algorithm for resolution.

INTRODUCTION

The problem considered in this paper involves two underlying processes, for the spark spread and the electricity price, as well as embedded optimal stopping time problems for the operating decisions of the coal plant and the timing and selection decisions of the power plant operator. In order to keep the analysis as simple as possible, yet analytically tractable, we are led to model the spark spread directly, assuming an arithmetic Brownian motion. For the electricity price we use a geometric Brownian motion as is standard in the literature on renewable power generation (see [1, 2, 3, 4, 5]).

In this paper, we examine the optimal investment in power production projects when two competing technologies, a coal-fired plant or a wind farm, are considered. We present that the immediate investment policy is characterized by a pair of boundaries satisfying a system of coupled integral equations of the Fredholm type and provide a new algorithm to compute its solution. The value of the investment project has an early investment premium representation consisting of two components, each tallying the local gains achieved when investment in a given technology is optimal.

MAIN RESULTS

Theorem 1 *The optimal investment boundaries solve the pair of coupled integral equations,*

$$G_1(b_X(y)) = \pi(b_X(y), y; b_X, b_Y), \tag{1}$$

$$G_2(b_Y(x)) = \pi(x, b_Y(x); b_X, b_Y), \tag{2}$$

for $y > 0$ and $x \in \mathbb{R}$, where $\pi(x,y;b_X,b_Y)$ represents the early investment premium (EIP) defined as,

$$\pi(x,y;b_X,b_Y) = \pi_1(x,y;b_X) + \pi_2(x,y;b_Y), \tag{3}$$

$$\pi_1(x,y;b_X) = -\mathsf{E}_{x,y}\left[\int_0^\infty e^{-rt} H_1(X_t) I(X_t \geq b_X(Y_t))dt\right], \tag{4}$$

$$\pi_2(x,y;b_Y) = -\mathsf{E}_{x,y}\left[\int_0^\infty e^{-rt} H_2(Y_t) I(Y_t \geq b_Y(X_t))dt\right]. \tag{5}$$

Proof of Theorem 1. Let us assume that the operator faces the finite maturity T selection option problem,

$$V(x,y;T) = \sup_{t\leq\tau\leq T} \mathsf{E}_{x,y}\left[e^{-r\tau}\max(V_1(X_\tau) - K_g, W(Y_\tau) - K_w)\right], \tag{6}$$

International Conference on Analysis and Applied Mathematics (ICAAM 2020)
AIP Conf. Proc. 2325, 020001-1–020001-4; https://doi.org/10.1063/5.0040339
Published by AIP Publishing. 978-0-7354-4069-2/$30.00

for $x \in I\!R$, $y > 0$ and $T > 0$. Standard arguments of American options pricing theory provides the early exercise premium representation, i.e., the decomposition of American-style derivative into the European counterpart and early exercise premium (see [6, 7]),

$$V(x,y;T) = V^e(x,y;T) + \pi(t,x;b_X^T,b_Y^T,T), \tag{7}$$

where V^e is the expected discounted payoff at T,

$$V(x,y;T) = \mathsf{E}_{x,y}\left[e^{-rT}\max(V_1(X_T)-K_g, W(Y_T)-K_w)\right], \tag{8}$$

and the early exercise premium depends on the exercise surfaces (b_X^T, b_Y^T) and given as follows,

$$\pi(x,y;b_X^T,b_Y^T,T) = \pi_1(x,y;b_X^T,T) + \pi_2(x,y;b_Y^T,T), \tag{9}$$

$$\pi_1(x,y;b_X^T,T) = -\mathsf{E}_{x,y}\left[\int_0^T e^{-rt}H_1(X_t)I(X_t \geq b_X^T(t,Y_t))dt\right], \tag{10}$$

$$\pi_2(x,y;b_Y^T,T) = -\mathsf{E}_{x,y}\left[\int_0^T e^{-rt}H_2(Y_t)I(Y_t \geq b_Y^T(t,X_t))dt\right], \tag{11}$$

for $x \in I\!R$, $y > 0$ and $T > 0$. We now let $T \to +\infty$, it is clear then that $V(x,y;T) \to V(x,y)$, $b_X^T(t,y) \to b_X(y)$ and $b_Y^T(t,x) \to b_Y(x)$ for any given t, x and y. The European part then vanishes as e^{-rT} dominates and $\pi(x,y;b_X^T,b_Y^T,T) \to \pi(x,y;b_X,b_Y)$ so that

$$V(x,y) = \pi(x,y;b_X,b_Y) \tag{12}$$

for $x \in I\!R$ and $y > 0$. If now insert $x = b_X(y)$ and $y = b_Y(x)$, respectively, we arrive at the system of two integral equations (1)-(2). Theorem 1 shows that the boundaries solve a system of coupled integral equations. These equations derive from the Early Investment Premium (EIP) representation of the value of the project considered by the operator. As there are two subregions, the EIP premium $\pi(x,y;b_X,b_Y)$ has two components corresponding respectively to the value of investing when the coal-fired technology is optimal ($\pi_1(x,y;b_X)$) and when the wind technology is optimal ($\pi_2(x,y;b_Y)$). Because each premium component depends on its corresponding boundary, the equations are coupled. Hence, the boundary b_X depends on b_Y, and conversely.

This characterization of the optimal investment boundaries is reminiscent of the characterization typically obtained for the exercise boundaries of American max-call options (e.g., [4]). Although the structural form of the two systems appears similar, they differ in several respects. First, in (1)-(2) there is no term relating to a European option component. This follows from the assumption that the project endlessly lived. In this case, the residual value on The end date disappears. Secondly, equations do not have a recursive structure in time or space. Lack of recursiveness in time comes from the endless horizon of the nature of the problem. Lack of recursiveness in space is due to the fact that boundaries their respective premium domains. As a result, the integral equations not a typical Volterra type, as with the standard American option price Problems. Third, investment payments are related to non-linear, exponentially affine function of the base variable. Unlike The standard max call has a linear return in the exercise area. Finally, underlying variables evolve in accordance with geometric Brownian motion and arithmetic Brownian motion. This mix of processes invalidates scaling properties found in standard models based on geometric Brownian motion.

The system of coupled integral equations (1)-(2) can, in principle, be used to compute the optimal investment boundaries. One of the difficulties in implementing an algorithm based on these equations is the unboundedness of the domains over which boundaries are defined. The next result, which describes the asymptotic behavior of the boundaries, helps to address this issue. It shows that boundaries have linear growth and provides their exact slopes. We extract these slopes from the system of integral equations (1)-(2), and are not aware of any other method to achieve this. This shows another advantage and highlights the informational content of these equations.

Lemma 2 *The following identities hold,*

$$\lim_{y \uparrow +\infty} \frac{b_X(y)}{y} = b_X^\infty, \tag{13}$$

$$\lim_{x\uparrow+\infty}\frac{b_Y(x)}{x}=b_Y^\infty, \tag{14}$$

where the slopes b_X^∞ and b_Y^∞ can be computed, respectively, as

$$b_X^\infty=\frac{\gamma_w\int_0^\infty e^{-\delta_Y t}\int_{-\infty}^\infty \varphi(z_1)\Phi\left(-\frac{\frac{1}{\sigma_Y\sqrt{t}}\left(\log(b^\infty)-\left(\mu_Y+\frac{1}{2}\sigma_Y^2\right)t\right)-\rho z_2}{\sqrt{1-\rho^2}}\right)dz_1\,dt}{\gamma_g/r-\gamma_g\int_0^\infty e^{-rt}\int_{-\infty}^\infty \varphi(z_1)I\left(\left(\mu_Y-\frac{1}{2}\sigma_Y^2\right)t+\sigma_Y\sqrt{t}z_1<0\right)dz_1\,dt}, \tag{15}$$

$$b_Y^\infty=\frac{\gamma_g\int_0^\infty e^{-rt}\int_{-\infty}^\infty \varphi(z_1)I(b^\infty\exp\left\{\left(\mu_Y-\frac{1}{2}\sigma_Y^2\right)t+\sigma_Y\sqrt{t}z_1\right\}<1)\,dz_1\,dt}{\gamma_w/\delta_Y-\gamma_w\int_0^\infty e^{-\delta_Y t}\int_{-\infty}^\infty \varphi(z_2)\Phi\left(\frac{1}{\sqrt{1-\rho^2}}\left((\mu_Y/\sigma_Y+\sigma_Y/2)\sqrt{t}+\rho z_2\right)\right)dz_2\,dt}, \tag{16}$$

and where the product of the slopes $b^\infty=b_X^\infty b_Y^\infty$ is the unique solution to

$$b^\infty=\frac{\int_0^\infty e^{-\delta_Y t}\int_{-\infty}^\infty \varphi(z_1)\Phi\left(-\frac{\frac{1}{\sigma_Y\sqrt{t}}\left(\log(b^\infty)-\left(\mu_Y+\frac{1}{2}\sigma_Y^2\right)t\right)-\rho z_1}{\sqrt{1-\rho^2}}\right)dz_1\,dt}{1/r-\int_0^\infty e^{-rt}\int_{-\infty}^\infty \varphi(z_1)I\left(\left(\mu_Y-\frac{1}{2}\sigma_Y^2\right)t+\sigma_Y\sqrt{t}z_1<0\right)dz_1\,dt}$$

$$\times\frac{\int_0^\infty e^{-rt}\int_{-\infty}^\infty \varphi(z_1)I(b^\infty\exp\left\{\left(\mu_Y-\frac{1}{2}\sigma_Y^2\right)t+\sigma_Y\sqrt{t}z_1\right\}<1)\,dz_1\,dt}{1/\delta_Y-\int_0^\infty e^{-\delta_Y t}\int_{-\infty}^\infty \varphi(z_2)\Phi\left(\frac{1}{\sqrt{1-\rho^2}}\left((\mu_Y/\sigma_Y+\sigma_Y/2)\sqrt{t}+\rho z_2\right)\right)dz_2\,dt}. \tag{17}$$

In these formulas, φ and Φ are the standard normal cdf and pdf, respectively. We also have that $b_X^\infty\cdot y\le b_X(y)$ for any $y>0$ and $b_Y^\infty\cdot x\le b_Y(x)$ for any $x\in\mathbb{R}$.

Having obtained the system of integral equations, the expression for the early investment premium π and the asymptotic behavior of the boundaries, we now propose a numerical algorithm to compute the pair of boundaries (b_X,b_Y). We note that this approach can be extended to other perpetual multidimensional timing problems.

As noted above, the integral equations are not of Volterra type and this is in contrast to standard situations in American option problems where the time-dependent boundaries are solutions to recursive integral equations, which can be solved by backward induction. In our case, the equations are of Fredholm type, i.e., to extract $b_Y(x)$ we need to know the values of $b_Y(\widetilde{x})$ for both $\widetilde{x}<x$ and $\widetilde{x}>x$. Thus, we do not have recursive induction in x. However, we make use of the following iterative procedure. Let us choose some initial curves $(b_X^0(y),b_Y^0(x))$ for $x\in\mathbb{R}$ and $y>0$, and then, recursively, define $b_X^n(y)$ and $b_Y^n(x)$ as solutions to the algebraic equations,

$$G_1(b_X^n(y))=\pi(b_X^{n-1}(y),y;b_X^{n-1},b_Y^{n-1}), \tag{18}$$

$$G_2(b_Y^n(x))=\pi(x,b_Y^{n-1}(x);b_X^{n-1},b_Y^{n-1}), \tag{19}$$

for $y>0$, $x\in\mathbb{R}$ and $n\ge 1$. The intuition behind this recursive approach is that if the sequence of boundaries (b_X^n,b_Y^n) converges as $n\to\infty$, the equations in the limit correspond to the integral equations satisfied by the exercise boundaries (b_X,b_Y).

The advantage of this method is that, at step n, the right-hand sides are fixed and do not depend on b_X^n and b_Y^n, and the left-hand sides are increasing functions of $b_X^n(y)$ and $b_Y^n(x)$, respectively. Thus, there are unique solutions to both equations. In fact, as G_2 is affine in y, we have an explicit expression for $b_Y^n(x)$. The same is not true for G_1, because of its nonlinear structure, so that we have to solve that algebraic equation.

Let us now describe the natural candidate for the initial values of the sequence, namely (b_X^0,b_Y^0). As we identified lower bounds for (b_X,b_Y), we define initial values as follows,

$$b_X^0(y)=\begin{cases}b_X^g,\ y<b_X^g/b_X^\infty\\ b_X^\infty y,\ y\ge b_X^g/b_X^\infty\end{cases}, \tag{20}$$

and

$$b_Y^0(x) = \begin{cases} b_Y^w, \ x < b_Y^w / b_Y^\infty \\ b_Y^\infty x, \ x \geq b_Y^w / b_Y^\infty. \end{cases} \tag{21}$$

We then iterate for $n = 1, 2, \ldots$ until the variation $\left(b_X^n(y) - b_X^{n-1}(y), b_Y^n(x) - b_Y^{n-1}(x)\right)$ falls below a predetermined tolerance threshold. The complete details of the algorithm such as truncation, discretization, interpolation and extrapolation of the state space and boundaries are given in a separate work.

ACKNOWLEDGMENTS

This research is financially supported by a target program BR05236656 from the Ministry of Science and Education of the Republic of Kazakhstan.

REFERENCES

1. I. Bakke, S. E. Fleten, L. I. Hagfors, V. Hagspiel, and B. Norheim, Journal of Commodity Market **3(1)**, 54–69 (2016).
2. T. K. Boomsma, N. Meade, and S. E. Fleten, European Journal of Operational Research **220(1)**, 225–237 (2012).
3. M. Brennan and E. S. Schwartz, Journal of Business **58(2)**, 135–157 (1985).
4. P. Carr, R. Jarrow, and R. Myneni, Mathematical Finance **2(2)**, 87–106 (1992).
5. J. P. Decamps, T. Mariotti, and S. Villeneuve, Economic Theory **28(2)**, 425–448 (2006).
6. S. Deng, B. Johnson, and A. Sogomonian, "Spark Spread Options and the Valuation of Electricity Generation Assets," in *Proceedings of the 32nd Hawai International Conference on System Sciences*, 1–7, 1999.
7. G. Peskir, Journal of Theoretical Probability **18(3)**, 499–535 (2005).

Towards the Theory of Boundary Value Problems on Non-Smooth Manifolds

Vladimir Vasilyev[a)]

Chair of Applied Mathematics and Computer Modeling, Belgorod State National Research University, Pobedy street 85, Belgorod 308015, Russia

[a)]*Corresponding author: vladimir.b.vasilyev@gmail.com*

Abstract. We suggest some constructions to develop the theory of boundary value problems on manifolds with a non-smooth boundaries. We discuss basic principles for such a theory and describe main results that we have obtained to this time. Further, we show how these results are related to the theory of boundary value problems on non-smooth manifolds.

INTRODUCTION

In this paper we would like to present basic ideas and results which can be useful for constructing the theory of boundary value problems for elliptic pseudo-differential equations on manifolds with a non-smooth boundary.

There are a lot of books [1, 2, 3, 4, 5, 6] in which similar problems are discussed but they use distinct methods and consider certain "singular manifolds" of other types.

Some papers are very closed to this text [7, 8, 9] but these are related to algebraical aspects of such a theory.

The paper [10] is classified as asymptotical aspect of such a theory, some author's studies and results can be found in [11, 12].

Author's results were presented in the book [13]. Generally these results concerned to the two-dimensional situation. Here we present our main ideas and results which are under consideration last years [11, 12, 14, 15, 16, 17, 18] and these latter considerations are related to multi-dimensional case especially. Here we continue these studies and give certain concrete constructions for special boundary value problems.

BASIC PRINCIPLES

We use a few basic principles on which the theory holds. We will describe briefly all these postulates because these are very simple and give the key for understanding the theory. As a model we will take the following operator

$$u(x) \longmapsto \int_D A(x,x-y)u(y)dy, \quad x \in D, \tag{1}$$

where $A(x,y)$ is "kernel" of the operator, i.e. $A(x,y) = F^{-1}_{\xi\to y}\tilde{A}(x,\xi)$, F is the Fourier transform,

$$\tilde{u}(\xi) = (Fu)(\xi) = \int_{\mathbb{R}^m} e^{ix\cdot\xi}u(x)dx,$$

$D \subset \mathbb{R}^m$ is a bounded domain (for simplicity) with a boundary ∂D. Such operator (1) is called a pseudo-differential operator in D [19] with the symbol $\tilde{A}(x,\xi)$.

We will suppose here that the symbol $A(x,\xi)$ satisfies some smoothness properties (for example, $A(x,\xi)$ is continuously differentiable on $\overline{D}\times\mathbb{R}^m$) and the condition

$$c_1(1+|\xi|)^\alpha \le |A(x,\xi)| \le c_1(1+|\xi|)^\alpha, \quad \alpha \in \mathbb{R}.$$

Let us note the latter condition guarantees the boundedness of the operator (1) in Sobolev–Slobodetskii spaces $H^s(D) \to H^{s-\alpha}(D)$ [19].

The main problem of the theory is describing Fredholm properties of the operator (1).

Definition 1 *Operator (1) is called an elliptic operator if*

$$ess \inf_{x\in\overline{D},\xi\in\mathbb{R}^m} |A(x,\xi)| > 0.$$

International Conference on Analysis and Applied Mathematics (ICAAM 2020)
AIP Conf. Proc. 2325, 020002-1–020002-10; https://doi.org/10.1063/5.0040277
Published by AIP Publishing. 978-0-7354-4069-2/$30.00

Such symbol is called elliptic symbol.

It is convenient considering operators (1) in Sobolev–Slobodetskii spaces $H^s(D)$ [19]. We will remind the definition [19]. By definition, this space consists of functions (distributions) u from $H^s(\mathbb{R}^m)$ which supports belong to $\overline{D}$. A norm in the space $H^s(D)$ is induced by the $H^s(\mathbb{R}^m)$-norm

$$||u||_s = \left(\int\limits_{\mathbb{R}^m} |\tilde{u}(\xi)|^2 (1+|\xi|)^{2s} d\xi \right)^{1/2},$$

where the sign $\sim$ over u denotes its Fourier transform

$$\tilde{u}(\xi) = \int\limits_{\mathbb{R}^m} u(x(e^{ix\cdot\xi} dx.$$

Everywhere below we consider only elliptic symbols, and $\widetilde{H}(D)$ denotes the Fourier image of the space $H(D)$.

Local principle

This principle was introduced by I.B. Simonenko [20] more than a half-century ago. It asserts in a simplest form that an operator of a special type operator of a local type) has Fredholm property iff all certain other operators (its *local representatives*) have the same property. It seems there is no news but the essential point is that local representative of an operator can have more simple structure than the starting general operator. As we will see below it is real fact.

Complicated Operator at a Boundary Point

This concept is related to the first principle. We will explain it for the case when the boundary ∂D is a smooth surface. This case includes two types of local representatives. If the point $x_0 \in D$ is an inner point then a neighborhood of the point is diffeomorphic to $\mathbb{R}^m$ and the local representative of the the operator (1) looks as follows

$$u(x) \longmapsto \int\limits_{\mathbb{R}^m} A(x_0, x-y)u(y)dy, \quad x \in \mathbb{R}^m. \tag{2}$$

To obtain Fredholm property (= invertibility property) for such operator(2) in "local" Sobolev–Slobodetskii space $H^s(\mathbb{R}^m)$ it is necessary and sufficient to require the ellipticity condition [19, 20].

If the point $x_0 \in \partial D$ is a boundary point then a neighborhood of the the point is diffeomorphic to half-space $\mathbf{R}^m_+ = \{x \in \mathbf{R}^m : x = (x_1, ..., x_m), x_m > 0\}$ (rectification of a boundary), and the local representative of the the operator (ref1) looks as follows

$$u(x) \longmapsto \int\limits_{\mathbb{R}^m_+} A(x_0, x-y)u(y)dy, \quad x \in \mathbb{R}^m_+. \tag{3}$$

The latter operator (3) acts in "local" Sobolev–Slobodetskii spaces $H^s(\mathbb{R}^m_+)$. Such operators (3) are called usually Wiener–Hopf operators. The ellipticity condition for their invertibility is not enough. Principal role takes factorization technique based on classical Riemann boundary value problem [19]. The dimension of a kernel (co-kernel) of the operator (3) is defined by so called index of factorization. We denote it by $_{m-1}(x_0)$, generally it depends on the point $x_0 \in \partial D$.

Conjugation Problem and Factorizability Principle at a Boundary Point

This idea was applied by the author earlier [13] and it related to a new type of local representatives of the operator (1). They appear when the boundary ∂D includes some singular points in which smoothness property does not hold.

For example, if $x_0 \in \partial D$ such that its neighborhood is diffeomorphic to a cone $C \subset \mathbb{R}^m$ and a neighborhood of ∂D transforms to a neighborhood of ∂C then local representative of the operator (1) is the following

$$u(x) \longmapsto \int\limits_C A(x_0, x-y)u(y)dy, \quad x \in C, \tag{4}$$

and we need to study invertibility properties of the operator (4) in "local" Sobolev–Slobodetskii space $H^s(C)$. Therefore, if you want to do it or not you must invent how to find the inverse operator for (4).

Multidimensional Riemann boundary value problem and the wave factorization

For this purpose the author has studied a certain multidimensional variant of Riemann boundary value problem [13]. It appears if we try to apply the Fourier transform to study the operator (4). As a result we obtain some multidimensional singular integral equation with a special kernel; this equation is a generalization of one-dimensional singular integral equation with the Cauchy kernel.

Bochner kernel Let C be a convex cone non-including a whole straight line. This kernel is defined by the formula

$$B(z) = \int\limits_C e^{iy\cdot z}dy, \quad z = x + i\tau, \quad \tau \in \overset{*}{C},$$

where $\overset{*}{C} = \{x \in \mathbf{R}^m : x \cdot y > 0, y \in C\}$. The Bochner kernel is holomorphic function in radial tube domain $T(\overset{*}{C}) = \mathbf{R}^m + i\overset{*}{C} \subset \mathbf{C}^m$ [21, 22, 23]. Only one cone exists in the real line, and for this case the Bochner kernel transforms into Cauchy kernel.

Conjugation problem Up to now there is no any way to solve such singular integral equations excluding the Wiener–Hopf method (= method of Riemann boundary value problem). This method is based on a special representation for coefficient of conjugation problem (or in other words for the symbol of a "local operator"). The author has used this idea for the multidimensional Riemann boundary value problem and has introduced the concept of wave factorization for an elliptic symbol.

If we consider the cone $\mathbb{R}^k \times C^{m-k}$ where C^{m-k} is a convex cone in $\mathbb{R}^{m-k}$ non-including a whole straight line then the existence of k-wave factorization for the symbol $\tilde{A}(\cdot,\xi)$ with respect to the cone C^{m-k} means the following. The symbol $A(\cdot,\xi)$ admits the representation

$$A(\cdot,\xi'',\xi') = A_{\neq}(\cdot,\xi'',\xi') \cdot A_{=}(\cdot,\xi'',\xi'),$$

where $\xi'' = (\xi_1,\cdot,\xi_k), \xi' = (\xi_{k+1},\cdot,\xi_m)$, factors $A_{\neq}(\cdot,\xi'',\xi'), A_{=}(\cdot,\xi'',\xi')$ admit holomorphic continuation with respect to the ξ' (for fixed ξ'') into radial tube domains $T(\overset{*}{C}{}^{m-k}), T(-\overset{*}{C}{}^{m-k})$ respectively with some estimates in which the index ${}_k$ of k-wave factorization takes part (one can find the rigorous definition in [13]). The value of the ${}_k$ is essential for a solvability of corresponding conjugation problem.

Unfortunately, existence of k-wave factorization is one of main problems, that's why this is the third postulate.

GENERAL CONCEPT: OPERATOR APPROACH

As we have seen there are distinct types of "local operators" (2),(3),(4) for the operator (1). We will denote all such operators by unified formula

$$u(x) \longmapsto \int\limits_{D_{x_0}} A(x_0, x-y)u(y)dy, \quad x \in D_{x_0}, \tag{5}$$

meaning D_{x_0} as one of above domains.

It is convenient to consider the operator A on a manifold with such a family of local representatives in Sobolev–Slobodetskii spaces $H^s(D)$ for which its "local" variant will be the space $H^s(D_{x_0})$.

Definition 2 *Symbol of the operator (1) is called the operator function $A(x) : D \to \{A_x\}_{x\in D}$ which is a family of local representatives of the operator (1). The operator (1) is called an elliptic operator if its symbol consists of invertible operators.*

In other words, symbol of the operator (1) is operator family (5) when x_0 varies in $\overline{D}$.

Canonical Domains and Model Operators

Definition 3 *Canonical domains in Euclidean space $\mathbb{R}^m$ is such a domain which is diffeomorphic to one of the following cones: $\mathbb{R}^m, \mathbb{R}^m_+, \mathbb{R}^k \times C^{m-k}, k = 0,1,\cdots,m-2$, where C^{m-k} is a convex cone in $\mathbb{R}^{m-k}$ non-including a whole straight line.*

Remark 1 If we put by definition $\mathbb{R}^m \times C^0 \equiv \mathbb{R}^m, \mathbb{R}^{m-1} \times C^1 \equiv \mathbb{R}^m_+, \mathbb{R}^0 \times C^m \equiv C^m$ then an arbitrary canonical domain will be a cone of the type $\mathbb{R}^k \times C^{m-k}, k = 0,1,\cdots,m-2,m-1,m$.

Definition 4 *A model operator is called an operator of type (5) in some canonical domain with the symbol $\tilde{A}(\cdot,\xi)$ non-depending on a spatial variable.*

Manifolds with a Singular Boundary

To define a domain (manifold) D with a singular boundary we will introduce different types of neighborhoods. For a smooth compact manifold all neighborhoods $\{U_j\}$ have the same type, these are diffeomorhic to $\mathbb{R}^m$. But if a manifold has a smooth boundary even then there are two types of neighborhoods related to a place of a neighborhood, namely inner neighborhoods and boundary ones. For inner neighborhood U such that $U \subset \mathring{D}$ we have the diffeomorphism $\omega : U \to \mathbb{R}^m$. For a boundary neighborhood such that $U \cap \partial D \neq \emptyset$ we have another diffeomorphism $\omega_1 : U \to \mathbb{R}^m_+$. May be this boundary ∂D has some singularities like conical points and wedges. A conical point at the boundary is such a point for which its neighborhood is diffeomorphic to the cone C^m, a wedge point of codimension $k, 1 \leq k \leq m-2$, is such a point for which its neighborhood is diffeomorphic to the cone $\mathbb{R}^k \times C^{m-k}$. So if the manifold D has such singularities we suppose that we can extract certain k-dimensional sub-manifolds, namely $(m-1)$-dimensional boundary ∂D, and k-dimensional wedges $D_k, k = 0,\cdots,m-2$; D_0 is a collection of conical points.

Operators on Manifolds

If D is a compact domain (manifold) then there is *a partition of unity*. It means the following. For every finite open covering $\{U_j\}_{j=1}^k$ of the manifold D there exists a system of functions $\{\varphi_j(x)\}_{j=1}^k, \varphi_j(x) \in C^\infty(D)$, such that

- $0 \leq \varphi_j(x) \leq 1$,
- $supp\ \varphi_j \subset U_j$,
- $\sum\limits_{j=1}^{k} \varphi_j(x) = 1$.

So we have

$$f(x) = \sum_{j=1}^{k} \varphi_j(x) f(x)$$

for arbitrary function f defined on D.

Since an every set U_j is diffeomorphic to an open set $D_k^j = \mathbb{R}^k \times C^{m-k}$ for some k we have corresponding diffeomorphisms $\omega_j : U_j \to D_k^j$. Further for a function f defined on D we compose mappings $f_j = f \cdot \varphi_j$ and as far as $supp\ f_j \subset U_j$ we put $\hat{f}_j = f_j \circ \omega_j^{-1}$ so that $\hat{f}_j : D_k^j \to \mathbb{R}$ is a function defined in a domain of m-dimensional space $\mathbb{R}^m$.

On the manifold D we fix a finite open covering and a partitions of unity corresponding to this covering $\{U_j, f_j\}_{j=1}^n$ and choose smooth functions $\{g_j\}_{j=1}^n$ so that $supp\ g_j \subset V_j, \overline{U_j} \subset V_j$, and $g_j(x) \equiv 1$ for $x \in supp\ f_j, supp\ f_j \cap (1-g_j) = \emptyset$.

Definition 5 *The operator A on the manifold D can be represented in the form*

$$A = \sum_{j=1}^{n} f_j \cdot \hat{A}_j \cdot g_j + T,$$

where $T : H^s(D) \to H^{s-\alpha}(D)$ is a compact operator, $\hat{A}_j$ is one of model operators (5) in which the change of variables ω_j was done.

Fredholm Properties

Invertibility of local operators First conclusion from the local principle is the following.
Theorem 1 *The operator A has Fredholm property iff it is an elliptic operator.*

Let us denote ${}_k(x)$ the indices of k-wave factorization of the symbol $A(x,\xi)$ with respect to the cone $C^{\underline{m-k}}$ at points $x \in M_k, k = 0,1,\cdots,m-2$ and assume that the functions ${}_k(x), k = 0,1,\cdots,m-1$, can be continued into M_k because it is possible $M_k \cap M_{k-1} \neq \emptyset$.
Proposition 1 *Let the classical symbol $A(x,\xi)$ admits k-wave factorization with respect to the cone C^{m-k} with indices ${}_k(x), k = 0,1,\cdots,m-2$ satisfying the conditions*

$$|{}_k(x) - s| < 1/2, \quad \forall x \in M_k, \quad k = 0,1,\cdots,m-1. \tag{6}$$

Then the operator $A : H^s(M) \to H^{s-\alpha}(M)$ has Fredholm property.
Remark 2 *Let us note that $(m-1)$-wave factorization is usual factorization in Eskin's sense and it always exists [19].*

On boundary conditions Let us suppose that one of conditions (6) does not hold. It means that there is at list one point $x_o \in \partial D$. If x_0 is a smoothness point at the boundary ∂D then you can look [19]. We suppose here that x_0 is a conical point so that $D_{x_0} = C$ and for this this convex cone C its boundary is given by the equation $x_m = \varphi(x')$. Moreover we suppose that ${}_0(x_0) - s = n + \varepsilon, |\varepsilon| < 1/2$. Then the local representative A_{x_0} is not invertible, but it is possible to describe its kernel [16, 17].

Let C be a convex cone in the space $\mathbb{R}^m$, and this cone does not include any whole straight line, it is important because we use the theory of analytic functions of several complex variables [21, 22, 23]. Moreover we suppose that a surface of this cone is given by the equation $x_m = \varphi(x'), x' = (x_1,\cdots,x_{m-1})$, where $\varphi : \mathbb{R}^{m-1} \to \mathbb{R}$ is a smooth function in $\mathbb{R}^{m-1} \setminus \{0\}$, and $\varphi(0) = 0$.

Let us introduce the following change of variables

$$\left\{ \begin{array}{rcl} t_1 &=& x_1 \\ t_2 &=& x_2 \\ \cdots && \\ t_{m-1} &=& x_{m-1} \\ t_m &=& x_m - \varphi(x') \end{array} \right.$$

and we denote this operator by $T_\varphi : \mathbb{R}^m \to \mathbb{R}^m$ so that points from lower half-space will be fixed.
Theorem 2 *A kernel of the operator A_{x_0} in the space $H^s(C)$ consists of functions of the following type*

$$A_{\neq}^{-1}(\xi) V_{-\varphi} F \left(\sum_{k=0}^{n-1} c_k(x') \delta^{(k)}(x_m) \right),$$

where $A_{\neq}(\xi)$ is factor of 0-wave factorization for the symbol $A(x_0,\xi)$, δ is the Dirac mass-function, and $V_{-\varphi}$ is a special integral operator defined by changes of variables in m-dimensional space and the Fourier transform, $c_k(x')$ are arbitrary functions from the space where $H^{s_k}(\mathbf{R}^{m-1})$, $s_k = s - {}_0(x_0) + k + 1/2$, $k = 0,1,2,...,n-1$.

We have the a priori estimate

$$||u||_s \leq const \sum_{k=0}^{n-1} [c_k]_{s_k},$$

where $[\cdot]_{s_k}$ denotes the $H^{s_k}(\mathbb{R}^{m-1})$-norm.

Therefore, to obtain invertibility for such operator A_{x_0} and to annihilate the kernel we need to add some additional conditions. As a rule such conditions are chosen as boundary conditions.
Remark 3 *It is very unpleasant but it may be happened that we need distinct number of conditions for different placements of the point x_0. But I think such a problem is now very far from nearest ones.*

DESCRIPTION OF OPERATOR V_φ AND ITS PROPERTIES

To obtain explicit expression for V_φ we need to choice a concrete cone. We consider here $C \equiv C_+^a = \{x \in \mathbb{R}^m : x = (x', x_m), x_m > a|x'|, a > 0\}$, the notation $T_\varphi \equiv T_a, V_\varphi \equiv V_a$ and use the transmutation formula

$$FT_a^{-1} = V_{-a}F.$$

Let us fix $u \in S(\mathbb{R}^m)$ and evaluate

$$(FT_a^{-1}u)(\xi) = \int\limits_{\mathbb{R}^m} e^{iy\cdot\xi}(T_a^{-1}u)(y)dy = \int\limits_{\mathbb{R}^m} e^{iy\cdot\xi'}u(y', y_m + a|y'|)dy$$

$$= \int\limits_{\mathbb{R}^m} e^{ix\cdot\xi}e^{-i\xi_m a|x'|}u(x', x_m)dx'dx_m = \int\limits_{\mathbb{R}^m} e^{ix'\cdot\xi'}e^{-i\xi_m a|x'|}\hat{u}(x', \xi_m)dx',$$

where $\hat{u}(x', \xi_m)$ denotes the Fourier transform of the function $u(x', x_m)$ with respect to the variable x_m. According to properties of the Fourier transform we denote

$$F_{x'\to\xi'}(e^{-i\xi_m a|x'|}) \equiv K_a(\xi', \xi_m),$$

and obtain an integral representation for the operator V_{-a}:

$$(FT_a^{-1}u)(\xi) = \int\limits_{\mathbb{R}^m} K_a(\xi' - \eta', \xi_m)\tilde{u}(\eta', \xi_m)d\eta',$$

where $K_a(\xi', \xi_m)$ is the Fourier image of corresponding distribution.

Since the function $e^{-i\xi_m a|x'|}$ is not integrable in $\mathbb{R}^{m-1}$ we need some regularization method , and we mean the latter formula as follows

$$\lim_{\tau\to 0} F_{x'\to\xi'}(e^{-iz_m a|x'|}), \quad z_m = \xi_m - i\tau, \quad \tau > 0,$$

so that

$$(FT_a^{-1}u)(\xi) = \lim_{\tau\to 0+}\int\limits_{\mathbb{R}^m} K_a(\xi' - \eta', z_m)\tilde{u}(\eta', \xi_m)d\eta',$$

According to above

$$F_{x'\to\xi'}(e^{-iz_m a|x'|}) = \int\limits_{\mathbb{R}^{m-1}} e^{ix'\cdot\xi'}e^{-iz_m a|x'|}dx',$$

and we cam use certain technical methods developed in [24] to find the following representation.
Proposition 2 *The function K_a has the following form*

$$K_a(\xi', z_m) = \frac{iaz_m 2^{m-1}\pi^{\frac{m-2}{2}}\Gamma(m/2)}{\left(\xi_1^2 + \xi_2^2 + \cdots \xi_{m-1}^2 - a^2 z_m^2\right)^{m/2}},$$

where $z_m = \xi_m - i\tau, \tau > 0$.

So, we have

$$(V_{-a}\tilde{u})(\xi) = \lim_{\tau\to 0+} \frac{1}{\pi^{m/2}} \int\limits_{\mathbb{R}^{m-1}} \frac{iaz_m\Gamma(m/2)\tilde{u}(\eta', \xi_m)d\eta'}{(|\xi' - \eta'|^2 - a^2z_m^2)^{m/2}}. \tag{7}$$

Corollary 1 *If $a \to 0$ then*

$$(V_0\tilde{u})(\xi) = \lim_{a\to 0}\lim_{\tau\to 0+} \frac{1}{\pi^{m/2}} \int\limits_{\mathbb{R}^{m-1}} \frac{iaz_m\Gamma(m/2)\tilde{u}(\eta', \xi_m)d\eta'}{(|\xi' - \eta'|^2 - a^2z_m^2)^{m/2}} = \tilde{u}(\xi', \xi_m).$$

Corollary 2 *If $\xi_m \to 0$ then*

$$\lim_{\xi_m\to 0}(V_{-a}\tilde{u})(\xi) = \lim_{\xi_m\to 0}\lim_{\tau\to 0+} \frac{1}{\pi^{m/2}} \int\limits_{\mathbb{R}^{m-1}} \frac{iaz_m\Gamma(m/2)\tilde{u}(\eta', \xi_m)d\eta'}{(|\xi' - \eta'|^2 - a^2z_m^2)^{m/2}} = \tilde{u}(\xi', 0)$$

Theorem 3 *The kernel of the equation (5) consists of functions of the following type*

$$\tilde{u}(\xi) = A_{\neq}^{-1}(\xi)\left(\sum_{k=1}^{n}\tilde{C}_k(\xi, \xi_m)\xi_m^{k-1}\right),$$

where

$$\tilde{C}_k(\xi, \xi_m) = (V_{-a}\tilde{c}_k)(\xi', \xi_m).$$

Thus, for unique identification of the functions $\tilde{C}_k(\xi', \xi_m)$ we need some additional conditions. We consider some variants below.

Case $m = 2$

First, we need to note that 2-dimensional case was studied without operator V_φ, but to verify this way we have constructed the operator V_φ for this case also. Second, for 2-dimensional case we have only one type of a cone (excluding rotations) $C_+^a = \{x \in \mathbb{R}^2 : x = (x_1, x_2), x_2 > a|x_1|, a > 0\}$. Thus, we have the following boundary function $\varphi(x_1) = a|x_1|$. For this function we have evaluated the operator V_φ [16] using analytic properties of the Fourier transform, and it looks as follows

$$(V_a\tilde{u})(\xi) = \frac{\tilde{u}(\xi_1 + a\xi_2, \xi_2) + \tilde{u}(\xi_1 - a\xi_2, \xi_2)}{2}$$

$$+v.p.\frac{i}{2\pi}\int\limits_{-\infty}^{+\infty}\frac{\tilde{u}(\eta, \xi_2)d\eta}{\xi_1 + a\xi_2 - \eta} - v.p.\frac{i}{2\pi}\int\limits_{-\infty}^{+\infty}\frac{\tilde{u}(\eta, \xi_2)d\eta}{\xi_1 - a\xi_2 - \eta}.$$

Case $m = 3$

We have a lot of cones in this case, and we consider some of them.

4-sided angle. The boundary function for this case is the following $\varphi(x) = a_1|x_1| + a_2|x_2|$, i.e. the conical surface is described by the equation $x_2 = a_1|x_1| + a_2|x_2|$. The cone looks as follows $C_{a_1a_2} = \{x \in \mathbb{R}^3 : x_2 > a_1|x_1| + a_2|x_2|\}$. Let us introduce two operators defined on functions of three variables

$$(S_1u)(\xi_1,\xi_2,\xi_3) = v.p\frac{i}{2\pi}\int\limits_{-\infty}^{+\infty}\frac{u(\tau,\xi_2,\xi_3)d\tau}{\xi_1-\tau},$$

$$(S_2u)(\xi_1,\xi_2,\xi_3) = v.p\frac{i}{2\pi}\int\limits_{-\infty}^{+\infty}\frac{u(\xi_1,\eta,\xi_3)d\eta}{\xi_2-\eta}.$$

If we will denote corresponding operator by $T_{a_1a_2}$ (change of variables) and its transmutation operator by $V_{a_1a_2}$ then we obtain

$$(V_{a_1a_2}\tilde{u})(\xi_1,\xi_2,\xi_3) = \frac{\tilde{u}(\xi_1-a_1\xi_3,\xi_2-a_2\xi_3,\xi_3)+\tilde{u}(\xi_1+a_1\xi_3,\xi_2-a_2\xi_3,\xi_3)}{4}$$

$$+\frac{1}{2}(S_1\tilde{u})(\xi_1+a_1\xi_3,\xi_2-a_2\xi_3,\xi_3)-\frac{1}{2}(S_1\tilde{u})(\xi_1-a_1\xi_3,\xi_2-a_2\xi_3,\xi_3)$$

$$+\frac{\tilde{u}(\xi_1-a_1\xi_3,\xi_2+a_2\xi_3,\xi_3)+\tilde{u}(\xi_1+a_1\xi_3,\xi_2+a_2\xi_3,\xi_3)}{4}$$

$$+\frac{1}{2}(S_1\tilde{u})(\xi_1+a_1\xi_3,\xi_2+a_2\xi_3,\xi_3)-\frac{1}{2}(S_1\tilde{u})(\xi_1-a_1\xi_3,\xi_2+a_2\xi_3,\xi_3)$$

$$+\frac{(S_2\tilde{u})(\xi_1-a_1\xi_3,\xi_2+a_2\xi_3,\xi_3)+(S_2\tilde{u})(\xi_1+a_1\xi_3,\xi_2+a_2\xi_3,\xi_3)}{2}$$

$$+(S_1S_2\tilde{u})(\xi_1+a_1\xi_3,\xi_2+a_2\xi_3,\xi_3)-(S_1S_2\tilde{u})(\xi_1-a_1\xi_3,\xi_2+a_2\xi_3,\xi_3)$$

$$-\frac{(S_2\tilde{u})(\xi_1-a_1\xi_3,\xi_2-a_2\xi_3,\xi_3)-(S_2\tilde{u})(\xi_1+a_1\xi_3,\xi_2-a_2\xi_3,\xi_3)}{2}$$

$$-(S_1S_2\tilde{u})(\xi_1+a_1\xi_3,\xi_2-a_2\xi_3,\xi_3)+(S_1S_2\tilde{u})(\xi_1-a_1\xi_3,\xi_2-a_2\xi_3,\xi_3).$$

This case was studied in [17] (see also [25]) and here we give the final form only

Circle cone. According to the formula (7) we have for C_+^a

$$(V_{-a}\tilde{u})(\xi_1,\xi_2,\xi_3) = \lim_{\tau\to 0+}\frac{1}{\pi^{3/2}}\int\limits_{\mathbb{R}^2}\frac{iaz_3\Gamma(3/2)\tilde{u}(\eta_1,\eta_2,\xi_3)d\eta_1d\eta_2}{\left((\xi_1-\eta_1)^2+(\xi_2-\eta_2)^2-a^2z_3^2\right)^{3/2}}.$$

Multidimensional and Complicated Cases

There are a lot of cones in multidimensional Euclidean space which can be constructed from those that we have considered. We will enumerate some of them.

- $\mathbb{R}^k \times C_+^a \subset \mathbb{R}^{k+m}$;
- $C_{a_1a_2} \times C_+^a \subset \mathbb{R}^{m+3}$;
- $(0,+\infty) \times C_+^a \subset \mathbb{R}^{m+1}$;
- $(0,+\infty) \times C_+^a \times C_{a_1a_2} \subset \mathbb{R}^{m+4}$;
- $\mathbb{R}^k \times (0,+\infty) \times C_+^a \times C_{a_1a_2} \subset \mathbb{R}^{k+m+4}$.

For every of these cases we will obtain special type of the integral operator V_φ, and every particular case will generate its own formula for a general solution. We will consider such possibilities in forthcoming publications.

INTEGRAL CONDITION AND SOLVABILITY

Taking into account Theorem 2 we consider the equation with a model operator

$$(Au)(x) = 0, \quad x \in C_+^a, \tag{8}$$

in the cone C_+^a with symbol $A(\xi)$ for $n=1$. Then we have the following formula for a general solution in view of (7)

$$\tilde{u}(\xi) = A_{\neq}^{-1}(\xi) V_{-a} \tilde{c}_0(\xi')$$

with an arbitrary function $c_0 \in H^{s-+1/2}(\mathbb{R}^{m-1})$. Let us suppose that the following condition

$$\int\limits_{-\infty}^{+\infty} u(x', x_m) dx_m = g(x'), \tag{9}$$

where $g(x')$ is given function from $H^{s+1/2}(\mathbb{R}^{m-1})$. According to the Fourier transform properties we have

$$\tilde{u}(\xi', 0) = \tilde{g}(\xi'),$$

and taking into account Corollary 2 we can find $\tilde{c}_0(\xi')$ immediately from the equality

$$\tilde{u}(\xi', 0) = A_{\neq}^{-1}(\xi', 0) \tilde{c}_0(\xi'),$$

more exactly

$$\tilde{c}_0(\xi') = A_{\neq}(\xi', 0) \tilde{g}(\xi').$$

Therefore, we can formulate the following result.

Theorem 4 *The boundary value problem (8), (9) has unique solution in the space $H^s(C_+^a)$ for arbitrary given function $g(x') \in H^{s+1/2}(\mathbb{R}^{m-1})$ of the following type*

$$\tilde{u}(\xi', \xi_m) = \frac{A_{\neq}^{-1}(\xi', \xi_m)}{\pi^{m/2}} \lim_{\tau \to 0+} \int\limits_{\mathbb{R}^{m-1}} \frac{iaz_m \Gamma(m/2) A_{\neq}(\eta', 0) \tilde{g}(\eta') d\eta'}{(|\xi' - \eta'|^2 - a^2 z_m^2)^{m/2}}, \quad z_m = \xi_m - i\tau, \quad \tau > 0.$$

A priori estimate

$$||u||_s \leq const [g]_{s+1/2}$$

holds.

CONCLUSION

Here we have tried to show how much possibilities gives the developed approach, and how we can find some integral representations for certain boundary value problems. General concepts of this approach was described in author's papers [26, 27] but as you see there are a lot of difficulties to realize these ideas. But we hope that this point of view can be useful and can give a new impulse to develop the theory.

REFERENCES

1. V. Kozlov, V. Maz'ya, and J. Rossmann, *Spectral Problems Associated with Corner Singularities of Solutions to Elliptic Equations* (AMS, Providence, RI, 2001).
2. S. Nazarov and B. A. Plamenevsky, *Elliptic Problems in Domains with Piecewise Smooth Noundaries* (Walter de Gruyter, Berlin – New York, 1994).

3. V. E. Nazaikinskii, A. Y. Savin, B.-W. Schulze, and B. Y. Sternin, *Elliptic Theory on Singular Manifolds* (Chapman & Hall/CRC, Boca Raton, 2006).
4. J. Egorov and B.-W. Schulze, *Pseudo-Differential Operators, Singularities, Applications* (Birkhäuser-Verlag, Basel, 1997).
5. B.-W. Schulze, *Boundary Value Problems and Singular Pseudo-Differential Operators* (J. Wiley, Chichester, 1998).
6. B.-W. Schulze, B. Sternin, and V. Shatalov, *Differential Equations on Singular Manifolds; Semiclassical Theory and Operator Algebras* (Wiley–VCH, Berlin, 1998).
7. A. Dynin, Proc. Nat. Acad. Sci. USA **75**, 4668–4670 (1978).
8. A. Dynin, Integr Equat. Oper. Theory **9**, 537–556 (1986).
9. A. Dynin, Integr Equat. Oper. Theory **10**, 554–576 (1987).
10. B. Sternin, Trudy Moskov. Mat. Obsh. (in Russian) **15**, 346–382 (1966).
11. V. B. Vasilyev, "Asymptotical analysis of singularities for pseudo differential equations in canonical non-smooth domains," in *Integral Methods in Science and Engineering. Computational and Analytic Aspects*, edited by C. Constanda and P. J. Harris (Birkhauser, Boston, 2011) pp. 379–390.
12. V. Vasilyev, Bound. Value Probl. **116**, 1–14 (2017).
13. V. Vasil'ev, *Wave Factorization of Elliptic Symbols: Theory and Applications. Introduction to the Theory of Boundary Value Problems in Non-Smooth Domains* (Kluwer Academic Publishers, Dordrecht–Boston–London, 2000).
14. V. Vasilyev, Math. Bohem. **39**, 333–340 (2014).
15. V. Vasilyev, Adv. Dyn. Syst. Appl. **9**, 227–237 (2014).
16. V. Vasilyev, Opusc. Math. **39**, 109–124 (2019).
17. V. Vasilyev, Math. Meth. Appl. Sci. **41**, 9252–9263 (2018).
18. V. B. Vasilyev, "Pseudo-differential operators on manifolds with a singular boundary," in *Modern Problems in Applied Analysis*, edited by P. Drygas and S. Rogosin (Birkhauser, Cham, 2018) pp. 169–179.
19. G. Eskin, *Boundary Value Problems for Elliptic Pseudodifferential Equations* (AMS, Providence, RI, 1981).
20. I. Simonenko, *Local Method in the Theory of Translation Invariant Operators and Their Envelopes* (CVVR (in Russian), Rostov on Don, 2007).
21. V. Vladimirov, *Methods of the Theory of Functions of Many Complex Variables* (Dover Publications, Mineola, NY, 2007).
22. V. Vladimirov, *Generalized Functions in Mathematical Physics* (Mir Publishers, Moscow, 1979).
23. S. Bochner and W. Martin, *Several Complex Variables* (Princeton Univ. Press, Princeton, NY, 1948).
24. E. M. Stein and G. Weiss, *Introduction to Fourier Analysis on Euclidean Spaces* (Princeton Univ. Pres, Princeton, 1971).
25. V. Vasilyev, Lobachevskii J. Math, **41**, 917–925 (2020).
26. V. Vasilyev, Demonstr. Math. **52**, 361–369 (2019).
27. V. Vasilyev, Symmetry **64**, 1–12 (2020).

About Optimal Feedback Control Problem for Motion Model of Nonlinearly Viscous Fluid

Allaberen Ashyralyev,[1,2,3,a)] Victor Zvyagin,[4,b)] and Andrey Zvyagin[5,c)]

[1)] *Department of Mathematics, Near East University, Nicosia, Mersin 10, Turkey*
[2)] *Peoples' Friendship University of Russia (RUDN University), Ul Miklukho Maklaya 6, Moscow 117198, Russia*
[3)] *Institute of Mathematics and Mathematical Modeling, 050010, Almaty,Kazakhstan*
[4)] *Voronezh State University, Univesitetskay sq. 1, 394018, Voronezh, Russia*
[5)] *Voronezh State Pedagogical University, Lenina st. 86, 394043, Voronezh, Russia*

[a)] *Electronic mail: allaberen.ashyralyev@neu.edu.tr*
[b)] *Electronic mail: zvg_vsu@mail.ru*
[c)] *Corresponding author: zvyagin.a@mail.ru*

Abstract. The optimal feedback control problem for the initial–boundary value problem describing a motion of a nonlinearly viscous fluid is considered in the paper. The existence of an optimal solution that gives a minimum to a given quality functional is proved. To prove the existence of an optimal solution the topological approximation method for investigation of hydrodynamic problems is used.

INTRODUCTION

The motion of an incompressible nonlinearly viscous fluid in a bounded domain $\Omega \subset R^n$, $n = 2,3$, on the time interval $[0,T]$ $(T < \infty)$ is described by the following initial–boundary value problem

$$\frac{\partial v}{\partial t} + \sum_{i=1}^{n} v_i \frac{\partial v}{\partial x_i} - \text{Div } \left[2\mu\big(I_2(v)\big)\varepsilon(v)\right] + \text{grad } p = f, \tag{1}$$

$$\text{div } v = 0, \qquad v|_{t=0} = v_0(x), \qquad v|_{\partial\Omega\times[0,T]} = 0. \tag{2}$$

Here $v(x,t)$ is a vector–function of the velocity of a fluid particle at a point $x \in \Omega$ at a time $t \in [0,T]$; p is a pressure function in a fluid; f is the density of external forces; ε is the strain rate tensor $\varepsilon(v) = \big(\varepsilon_{ij}(v)\big)$, $\varepsilon_{ij}(v) = \frac{1}{2}\big(\frac{\partial v_i}{\partial x_j} + \frac{\partial v_j}{\partial x_i}\big)$, tensor $I_2(v)$ is determined by the equality

$$I_2^2(v) = \varepsilon(v) : \varepsilon(v) = \sum_{i,j=1}^{n} [\varepsilon_{ij}(v)]^2 .$$

Here for arbitrary square matrices $A = (a_{ij})$ and $B = (b_{ij})$ the symbol $A : B = \sum_{i,j=1}^{n} a_{ij} b_{ij}$ is used. The symbol Div M is denoting the divergence of the tensor $M = (m_{ij})$, i.e. the vector

$$\text{Div } M = \Big(\sum_{j=1}^{n} \frac{\partial m_{1j}}{\partial x_j}, \ldots, \sum_{j=1}^{n} \frac{\partial m_{nj}}{\partial x_j}\Big).$$

This mathematical model was in detail studied at works of Professor V.G. Litvinov (see [1]), where natural restrictions on the viscosity of a fluid under consideration are given through properties of the function $\mu : \mathbb{R}_+ \to \mathbb{R}$. $\mu(s)$ should be a continuously differentiable scalar function at $s \geq 0$ for which inequalities

a) $0 < C_1 \leq \mu(s) \leq C_2 < \infty$;

b) $-s\mu'(s) \leq \mu(s)$ as $\mu'(s) < 0$;

c) $|s\mu'(s)| \leq C_3 < \infty$

International Conference on Analysis and Applied Mathematics (ICAAM 2020)
AIP Conf. Proc. 2325, 020003-1–020003-4; https://doi.org/10.1063/5.0040387
Published by AIP Publishing. 978-0-7354-4069-2/$30.00

are hold. Hereinafter, C_i denotes various constants.

The question of solutions existence for this problem have been considered at works of V.G. Litviniv (see, for example, [1]), P.E. Sobolevskii [2], V.G. Zvyagin [3] and et al.

In this paper the optimal feedback control problem for the system of equations (1)–(2) is considered. A large number of works have been devoted to the study of control problems (see [4, 5, 6]). However, while control problem for linear systems is more or less studied, control problem for nonlinear systems remains a serious problem (even for finite–dimensional or local domains). Control (optimal control) problem of a fluid motion using external forces often arises in practice. Solving such problems a control is usually selected from some given (finite) set of controls. In this paper we consider the control of external forces, which depend on the velocity of a fluid. Such problems are called feedback problems (see, for example, [7, 8, 9, 10, 11, 12] and the bibliography therein). This allows us to more accurately choose a control. Since in this case the control is not selected from a finite set of available controls but belongs to the image of some multivalued map (it's natural that some conditions are imposed on this map).

In this paper solutions existence to the feedback control problem for a nonlinearly viscous fluid model (1)–(2) is studied. Also the existence of an optimal solution to the problem under consideration that gives a minimum to a given bounded quality functional is proved.

STATEMENT OF THE PROBLEM AND MAIN RESULTS

Let introduce main notations and auxiliary statements.

By $L_p(\Omega)$, $1 \leqslant p < \infty$, we denote the set of measurable p–integrable vector–functions $v : \Omega \to \mathbb{R}^n$. By $W_p^m(\Omega)$, $m \geqslant 1$, $p \geqslant 1$, we denote the Sobolev spaces. By $C_0^\infty(\Omega)^n$ we denote the space of infinitely differentiable vector–functions defined in Ω ranging in $\mathbb{R}^n$ and compactly supported in Ω. $\mathscr{V}$ is the set $\{v \in C_0^\infty(\Omega)^n, \operatorname{div} v = 0\}$. H is the closure of $\mathscr{V}$ with respect to the norm $L_2(\Omega)$ and V is the closure of $\mathscr{V}$ with respect to the norm $W_2^1(\Omega)$.

Let consider the main space in which weak solutions of the problem under consideration will be studied:

$$W_1 = \{v : v \in L_2(0,T,V) \cap L_\infty(0,T;H), v' \in L_1(0,T,V^*)\}.$$

The space W_1 is considered with the norm

$$\|v\|_{W_1} = \|v\|_{L_2(0,T,V)} + \|v\|_{L_\infty(0,T;H)} + \|v'\|_{L_1(0,T,V^*)}.$$

Let the multivalued map $\Psi : W_1 \multimap L_2(0,T,V^*)$ which we will use to define feedback. We will specify restrictions on the control. Assume that Ψ satisfies conditions:

(Ψ1) The map Ψ is defined on W_1 and has nonempty compact convex values;

(Ψ2) The map Ψ is compact and upper semicontinuous (i.e. for any given $v \in W_1$ and an open set $Y \subset L_2(0,T,V^*)$ with $\Psi(v) \subset Y$ there exists a neighborhood $U(v)$ with $\Psi(U(v)) \subset Y$);

(Ψ3) The map Ψ is globally bounded; that is, there exists a constant $C > 0$ such that

$$\|\Psi(v)\|_{L_2(0,T,V^*)} := \sup\{\|u\|_{L_2(0,T,V^*)} : u \in \Psi(v)\} \leq C \text{ for all } v \in W_1;$$

(Ψ4) The map Ψ is weakly closed, which means that if $\{v_l\}_{l=1}^\infty \subset W_1, v_l \rightharpoonup v_0, u_l \in \Psi(v_l)$ and $u_l \to u_0$ in $L_2(0,T,V^*)$ then $u_0 \in \Psi(v_0)$.

We will consider a weak statement of the optimal feedback control problem for the initial–boundary value problem (1)–(2). By feedback we understand the condition

$$f \in \Psi(v). \tag{3}$$

Definition 1 *A pair of functions $(v,f) \in W_1 \times L_2(0,T,V^*)$ is a weak solution to the feedback control problem* (1)–(2)*, if for every $\varphi \in V$ and almost all $t \in [0,T]$ it satisfies the identity*

$$\langle v', \varphi \rangle - \int_\Omega \sum_{i,j=1}^n v_i v_j \frac{\partial \varphi_j}{\partial x_i}\, dx + 2\int_\Omega \mu(I_2(v))\varepsilon(v) : \varepsilon(\varphi)\, dx = \langle f, \varphi \rangle, \tag{4}$$

the initial condition $v(0) = v_0$ and the feedback condition (3).

Hereinafter, $\langle v', \varphi \rangle = (\dfrac{\partial v}{\partial t}, \varphi)$.

The first result of this paper is

Theorem 1 *Let the multivalued map* Ψ *satisfies* $(\Psi 1)-(\Psi 4)$ *and viscosity of the fluid under consideration satisfies* $a)-c)$. *Then there is at least one weak solution* $(v_*, f_*) \in W_1 \times L_2(0,T,V^*)$ *to the feedback control problem* (1)–(3).

Denote by $\Sigma \subset W_1 \times L_2(0,T;V^*)$ the set of all weak solutions to the feedback control problem (1)–(3). Consider an arbitrary quality functional $\Phi : \Sigma \to \mathbb{R}$ satisfying conditions

$(\Phi 1)$ There exists a number γ such that $\Phi(v,f) \geqslant \gamma$ for all $(v,f) \in \Sigma$.

$(\Phi 2)$ If $v_l \rightharpoonup v_*$ in W_1 and $f_l \to f_*$ in $L_2(0,T;V^*)$, then $\Phi(v_*, f_*) \leqslant \varliminf\limits_{m\to\infty} \Phi(v_l, f_l)$.

As an example of this functional, we can take

$$\Phi(v,f) = \int_0^T \|v(t) - u_*(t)\|_V \, dt + \int_0^T \|f(t)\|^2_{V^*} \, dt.$$

Here u_* is some specified velocity field. This functional characterizes the deviation of velocity from the required, and its minimum yields the minimal deviation of velocity from the one specified by the minimal control.

The main result of this paper is

Theorem 2 *Let the multivalued map* Ψ *satisfies* $(\Psi 1)$–$(\Psi 4)$, *viscosity of the fluid under consideration satisfies* $a)-c)$ *and quality functional* Φ *satisfies* $(\Phi 1), (\Phi 2)$. *Then the optimal feedback control problem* (1)–(3) *has at least one weak solution* (v_*, f_*) *such that*

$$\Phi(v_*, f_*) = \inf_{(v,f)\in\Sigma} \Phi(v,f).$$

The proof of Theorems 1 and 2 is based on the topological approximation method for hydrodynamic problems investigation (see [13]). For this, at first, we obtain the operator interpretation of the problem under consideration (operator inclusion) in suitable function spaces. Further, due to the fact that operators in the obtained operator inclusion do not have necessary properties we consider a problem that approximates the original one (in this case, it is also an operator inclusion, but with better operators that have required properties and in better functional spaces). Then, on the based of a priori estimates of solutions and the topological degree theory for multivalued vector fields the solutions existence to the approximation problem is proved. And, finally, it is shown that from the sequence of solutions to the approximation problem we can consider a subsequence that converges (in a sense) to a solution of the original operator inclusion. After proving solvability of the control problem, it is shown that in the set of solutions there is at least one solution that gives a minimum to a given quality functional (this is why this type of problem is called the optimal feedback control problem for a fluid motion). The developed method has been successfully applied in a number of fluid dynamics models to prove the existence of solutions, in feedback optimal control problems, in problems of the existence of attractors and pullback attractors and others (see [8, 9, 10, 11, 14, 15, 16, 17]).

ACKNOWLEDGMENTS

The research of the first author was funded by Russian Foundation for Basic Research (project number 20-01-00051). The research of the second author was funded by Russian Foundation for Basic Research (project number 19-31-60014).

REFERENCES

1. V. G. Litvinov, *Motion of a Nonlinearly Viscous Fluid* (Nauka, 1982).
2. P. E. Sobolevskii, Dokl. Akad. Nauk SSSR. **285**, 44–48 (1985).
3. V. T. Dmitrienko and V. G. Zvyagin, Abstract and Applied Analysis **2**, 1–45 (1997).

4. J. L. Lions, *Optimal Control of Systems Governed by Partial Differential Equations* (Springer, 1971).
5. A. V. Fursikov, *Optimal Control of Distributed Systems. Theory and Applications* (Amer. Math. Soc., 2000).
6. F. Abergel and R. Temam, Theor. Comput. Fluid Dyn. **1**, 303–325 (1990).
7. V. Zvyagin, V. Obukhovskii, and A. Zvyagin, J. Fixed Point Theory and Appl. **16**, 27–82 (2014).
8. A. V. Zvyagin, Siberian Mathematical Journal **54**, 640–655 (2013).
9. A. V. Zvyagin, Differential Equations **49**, 246–250 (2013).
10. A. V. Zvyagin, Doklady Mathematics **93**, 270–272 (2016).
11. A. V. Zvyagin and V. G. Zvyagin, Siberian Advances in Mathematics **29**, 137–152 (2019).
12. A. V. Zvyagin, Doklady Mathematics **99**, 299–302 (2019).
13. V. G. Zvyagin, J. Math. Sci. **201**, 830–858 (2014).
14. A. V. Zvyagin, Russian Mathematics (Iz. VUZ) **55**, 90–92 (2011).
15. A. V. Zvyagin, Russian Mathematical Surveys **74**, 549–551 (2019).
16. A. V. Zvyagin, Doklady Mathematics **88**, 730–733 (2013).
17. A. V. Zvyagin, Discrete and Continuous Dynamical Systems **28**, 6305–6325 (2018).

Löwner Evolution as Itô Diffusion

Hülya Acar[1, a)] and Alexey L. Lukashov[2, 3, b)]

[1)] *Düzce University, Düzce, Turkey*
[2)] *Moscow Institute of Physics and Technology, Moscow, Russia*
[3)] *Department of Mechanics and Mathematics, Saratov State University, Saratov, Russia*

[a)] *Electronic mail: hulyaacar98@gmail.com*
[b)] *Corresponding author: alexey.lukashov@gmail.com*

Abstract F. Bracci, M.D. Contreras, S. Díaz Madrigal [3] proved that any evaluation family of order d is described by a generalized Löwner chain. G. Ivanov and A. Vasil'ev considered randomized version of the chain and found a substitution which transforms the chain to an Itô diffusion.We generalize their result to vector randomized Löwner chain and prove there are no other possibilities to transform such Löwner chains to Itô diffusions.

INTRODUCTION

In [7] the authors introduce new evolution families of conformal maps on the unit disk satisfying an invariance property typically associated with Schramm-Löwner evolution (SLE). In particular, they found a substitution which transforms their evolution family into an Itô diffusion.

We refer to [2] for a nice survey and to [6] for another type of evolution families of conformal maps on the unit disk.

In our work, we denote by $\check{C}$ the set of functions $f(z,\mathbf{x})$ from $C^n(\mathbb{D}\times\mathbb{R}^n)$ such that these functions have continuous derivatives up to order n, $\frac{\partial f}{\partial z}$ doesn't vanish and $H(\mathbb{D})$ is the set of analytic functions in unit disc $\mathbb{D}$. Let function $p:\mathbb{D}\times[0,\infty)\to\mathbb{C}$ measurable in t, holomorphic in z, $p(0,t)=1$ and $\Re(p(z,t))\geq 0$ for all $z\in\mathbb{D}$ and $t\geq 0$ (such functions p are called Herglötz functions). We take Herglötz function of $p(w,t)=\tilde{p}\left(\frac{w}{\tau(t)}\right)$ in this form and τ depends on some independent Brownian motions, denotes by $\tau(t)=\tau(\mathbf{B}_t)$ where $\mathbf{B}_t=(B_t^1,B_t^2,\ldots,B_t^n)$.

MAIN RESULTS

Theorem 1. *Let us consider Löwner random differential equation*

$$\begin{cases} \frac{d\phi_t(z,w)}{dt} = \frac{(\tau_1(t,w)-\phi_t(z,w))^2}{\tau_1(t,w)}\tilde{p}\left(\frac{\phi_t(z,w)}{\tau_1(t,w)}\right) \\ \phi_0(z,w)=z \end{cases} \tag{1}$$

where $|\tau_1(t,\omega)|=1$ for each fixed $w\in\Omega$ (Ω is a sample space) and $\tilde{p}$ is an arbitrary Herglötz function. Suppose $\psi_t=m(\phi_t,B_t^{(1)},B_t^{(2)},\ldots,B_t^{(n)})$ where $B_t^{(i)}$ are independent Brownian motions, $m\in\check{C}$ and $\tau_1(t,\omega)=\tau(\mathbf{B}_t)$ then, ψ_t is an $n\times 1$ dimensional Itô diffusion with coefficients from $H(\mathbb{D})$ for an arbitrary Herglötz function $\tilde{p}$ if and only if $\tau(\mathbf{B}_t)=e^{\mathbf{k}\cdot\mathbf{B}_t}$ where $\mathbf{k}=(k_1,\ldots,k_n)$ and $\mathbf{k}\in\mathbb{C}^n$.

Furthermore the infinitesimal generator of ψ_t (when it is an Itô diffusion) is given by this form

$$A=\left(-\frac{z}{2}|\mathbf{k}|^2+(1-z)^2\tilde{p}(z)\right)\frac{d}{dz}-\frac{1}{2}|\mathbf{k}|^2 z^2\frac{d^2}{dz^2}. \tag{2}$$

Proof. For $n=1$ sufficiency part was proved by G. Ivanov and A. Vasilev. We use similar argument to prove sufficiency for arbitrary n. By the complex Itô formula, the process

$$\frac{1}{\tau(\mathbf{B}_t)}=e^{-ik_1B_t^{(1)}-ik_2B_t^{(2)}-\ldots-ik_nB_t^{(n)}}$$

International Conference on Analysis and Applied Mathematics (ICAAM 2020)
AIP Conf. Proc. 2325, 020004-1–020004-5; https://doi.org/10.1063/5.0040353
Published by AIP Publishing. 978-0-7354-4069-2/$30.00

satisfies the stochastic differential equation (SDE)

$$
\begin{aligned}
d(e^{-ik_1B_t^{(1)}-\ldots-ik_nB_t^{(n)}}) = -\sum_{j=1}^{n} ik_j e^{-ik_1B_t^{(1)}-\ldots-ik_nB_t^{(n)}} dB_t^{(j)} \\
-\tfrac{1}{2}\sum_{j=1}^{n} k_j^2 e^{-ik_1B_t^{(1)}-\ldots-ik_nB_t^{(n)}} dt.
\end{aligned}
\tag{3}
$$

Let us denote $\psi_t(z,w) = \frac{\phi_t(z,w)}{\tau(\mathbf{B}_t)}$. Applying the integration by parts formula for ψ_t, we obtain

$$
\begin{aligned}
d(\psi_t) &= \phi_t d(e^{-ik_1B_t^{(1)}-\ldots-ik_nB_t^{(n)}}) + (e^{-ik_1B_t^{(1)}-\ldots-ik_nB_t^{(n)}})d\phi_t \\
&= -i\psi_t \mathbf{k}\cdot d\mathbf{B}_t + (-\tfrac{|\mathbf{k}|^2}{2}\psi_t + (\psi_t-1)^2\tilde{p}(\psi_t))dt
\end{aligned}
\tag{4}
$$

So ψ_t is an Itô diffusion in $\mathbb{R}^n$.

Now for the necessity part, from our supposition $\psi_t = m(\phi_t, B_t^{(1)},\ldots,B_t^{(n)})$. Apply Itô formula;

$$
d(\psi_t) = \frac{\partial m}{\partial x} d\phi_t + \sum_{i=1}^{n} \frac{\partial m}{\partial y_i} dB_t^{(i)} + \frac{1}{2}\sum_{i=1}^{n} \frac{\partial^2 m}{\partial y_i^2} dt. \tag{5}
$$

and if (5) is an $n\times 1$ dimensional Itô diffusion with analytic coefficients then there are functions $f_i \in H(\mathbb{D})$ such that

$$
\frac{\partial m}{\partial y_i} = f_i(m(x,\mathbf{y})). \tag{6}
$$

Taking derivative of (6) with respect to y_j we obtain

$$
\frac{f_i'(m(x,\mathbf{y}))}{f_i(m(x,\mathbf{y}))} = \frac{f_j'(m(x,\mathbf{y}))}{f_j(m(x,\mathbf{y}))}.
$$

Hence

$$
(\ln f_i(z))' = (\ln f_j(z))'
$$

and

$$
f_i(z) = c_{ij} f_j(z). \tag{7}
$$

Let us denote

$$
f_i(z) = c_i f(z) \tag{8}
$$

and let $F(z)$ be an antiderivative of $\frac{1}{f(z)}$, hence

$$
F(m(x,\mathbf{y})) = \mathbf{c}\cdot\mathbf{y} + q(x)
$$

where $\mathbf{c} = (c_1,\ldots,c_n)$.

Since by supposition F' doesn't vanish, there exists an inverse function F^{-1} and

$$
m(x,\mathbf{y}) = F^{-1}(\mathbf{c}\cdot\mathbf{y} + q(x)). \tag{9}
$$

Let us denote

$$
F^{-1}(z) = G(z). \tag{10}
$$

Now for coefficients in dt, we have

$$
\frac{\partial m}{\partial x} d\Phi_t + \frac{1}{2}\sum_{i=1}^{n} \frac{\partial^2 m}{\partial y_i^2} dt = g(G(\mathbf{c}\cdot\mathbf{y} + q(x))dt,
$$

where g is an analytic function in $\mathbb{D}$. If we substitute (6), (8), and (10) then we get,

$$\begin{aligned} &G'(\mathbf{c}\cdot\mathbf{y}+q(x))q'(x)\tfrac{d\phi_t}{dt}+f'(G(\mathbf{c}\cdot\mathbf{y}+q(x)))f(G(\mathbf{c}\cdot\mathbf{y}+q(x)))\tfrac{1}{2}\sum_{i=1}^{n}c_i^2 \\ &= g(G(\mathbf{c}\cdot\mathbf{y}+q(x))), \end{aligned} \tag{11}$$

$$G'(\mathbf{c}\cdot\mathbf{y}+q(x))q'(x)\frac{(\tau(\mathbf{y})-x)^2}{\tau(\mathbf{y})}\tilde{p}(\frac{x}{\tau(\mathbf{y})}) = g_1(\mathbf{c}\cdot\mathbf{y}+q(x)), \tag{12}$$

where we denote

$$g_1(z) = g(z) - f'(z)f(z)\frac{1}{2}\sum_{i=1}^{n}c_i^2.$$

Definition of (9) shows that $G'(\mathbf{c}\cdot\mathbf{y}+q(x))$ doesn't vanish. Hence $g_1(\mathbf{c}\cdot\mathbf{y}+q(x))$ is not identically zero. So equation (12) can be written as

$$q'(x)\frac{(\tau(\mathbf{y})-x)^2}{\tau(\mathbf{y})}\tilde{p}(\frac{x}{\tau(\mathbf{y})}) = H_1(\mathbf{c}\cdot\mathbf{y}+q(x)), \tag{13}$$

where $H_1(z) = \frac{g_1(z)}{G'(z)}$.

Let us differentiate (13) with respect to x and y_i. Then we obtain two equalities:

$$\begin{aligned} &q''(x)\tfrac{(\tau(\mathbf{y})-x)^2}{\tau(\mathbf{y})}\tilde{p}(\tfrac{x}{\tau(\mathbf{y})}) - 2q'(x)\tfrac{(\tau(\mathbf{y})-x)}{\tau(\mathbf{y})}\tilde{p}(\tfrac{x}{\tau(\mathbf{y})}) + q'(x)\tfrac{(\tau(\mathbf{y})-x)^2}{\tau^2(\mathbf{y})}\tilde{p}'(\tfrac{x}{\tau(\mathbf{y})}) \\ &= q'(x)H_1'(\mathbf{c}\cdot\mathbf{y}+q(x)) \end{aligned} \tag{14}$$

and

$$\begin{aligned} &q'(x)\frac{(\tau(\mathbf{y})-x)\frac{\partial\tau(\mathbf{y})}{\partial y_i}(\tau(\mathbf{y})+x)}{\tau^2(\mathbf{y})}\tilde{p}(\tfrac{x}{\tau(\mathbf{y})}) - q'(x)\frac{(\tau(\mathbf{y})-x)^2\frac{\partial\tau(\mathbf{y})}{\partial y_i}x}{\tau^2(\mathbf{y})}\tilde{p}'(\tfrac{x}{\tau(\mathbf{y})}) \\ &= c_iH_1'(\mathbf{c}\cdot\mathbf{y}+q(x)); i=1,2,\ldots,n. \end{aligned} \tag{15}$$

Now (14) and (15) imply,

$$\begin{aligned} &q''(x)\tfrac{(\tau(\mathbf{y})-x)^2}{\tau(\mathbf{y})}\tilde{p}\left(\tfrac{x}{\tau(\mathbf{y})}\right) - 2q'(x)\tfrac{(\tau(\mathbf{y})-x)}{\tau(\mathbf{y})}\tilde{p}\left(\tfrac{x}{\tau(\mathbf{y})}\right) + q'(x)\tfrac{(\tau(\mathbf{y})-x)^2}{\tau^2(\mathbf{y})}\tilde{p}'\left(\tfrac{x}{\tau(\mathbf{y})}\right) \\ &= \tfrac{q'(x)}{c_i}\left[q'(x)\frac{(\tau(\mathbf{y})-x)\frac{\partial\tau(\mathbf{y})}{\partial y_i}(\tau(\mathbf{y})+x)}{\tau^2(\mathbf{y})}\tilde{p}\left(\tfrac{x}{\tau(\mathbf{y})}\right) - q'(x)\frac{(\tau(\mathbf{y})-x)^2\frac{\partial\tau(\mathbf{y})}{\partial y_i}x}{\tau^2(\mathbf{y})}\tilde{p}'\left(\tfrac{x}{\tau(\mathbf{y})}\right)\right]; \\ &i=1,2,\ldots,n. \end{aligned} \tag{16}$$

Take derivative of (16) with respect to y_i again ;

$$\left[\tilde{p}'\left(\frac{x}{\tau(\mathbf{y})}\right)\frac{x\frac{\partial\tau(\mathbf{y})}{\partial y_i}}{\tau^2(\mathbf{y})}(-q''(x)(\tau(\mathbf{y})-x)+3q'(x))-\frac{q'(x)x\frac{\partial\tau(\mathbf{y})}{\partial y_i}(\tau(\mathbf{y})-x)}{\tau^3(\mathbf{y})}\tilde{p}''\left(\frac{x}{\tau(\mathbf{y})}\right)\right.$$

$$\left.+q''(x)\frac{\partial\tau(\mathbf{y})}{\partial y_i}\tilde{p}\left(\frac{x}{\tau(\mathbf{y})}\right)\right]\cdot\left[q'(x)\frac{\frac{\partial\tau(\mathbf{y})}{\partial y_i}(\tau(\mathbf{y})+x)}{\tau(\mathbf{y})}\tilde{p}\left(\frac{x}{\tau(\mathbf{y})}\right)-q'(x)\frac{(\tau(\mathbf{y})-x)\frac{\partial\tau(\mathbf{y})}{\partial y_i}x}{\tau^2(\mathbf{y})}\tilde{p}'\left(\frac{x}{\tau(\mathbf{y})}\right)\right]$$

$$=\left[q'(x)\frac{\frac{\partial^2\tau(\mathbf{y})}{\partial y_i{}^2}\tau(\mathbf{y})(\tau(\mathbf{y})+x)-(\frac{\partial\tau(\mathbf{y})}{\partial y_i})^2x}{\tau^2(\mathbf{y})}\tilde{p}\left(\frac{x}{\tau(\mathbf{y})}\right)-\frac{q'(x)}{\tau^3(\mathbf{y})}(x\frac{\partial^2\tau(\mathbf{y})}{\partial y_i{}^2}\tau(\mathbf{y})(\tau(\mathbf{y})-x)\right. \tag{17}$$

$$\left.+3x^2(\frac{\partial\tau(\mathbf{y})}{\partial y_i})^2)\tilde{p}'\left(\frac{x}{\tau(\mathbf{y})}\right)+q'(x)\frac{(\tau(\mathbf{y})-x))x^2(\frac{\partial\tau(\mathbf{y})}{\partial y_i})^2}{\tau^4(\mathbf{y})}\tilde{p}''\left(\frac{x}{\tau(\mathbf{y})}\right)\right]\cdot\left[q''(x)(\tau(\mathbf{y})-x)\tilde{p}\left(\frac{x}{\tau(\mathbf{y})}\right)\right.$$

$$\left.-2q'(x)\tilde{p}\left(\frac{x}{\tau(\mathbf{y})}\right)+q'(x)(\tau(\mathbf{y})-x)\tilde{p}'\left(\frac{x}{\tau(\mathbf{y})}\right)\right];i=1,2,\ldots,n.$$

Observe that the functions $(\tilde{p}'(z))^2$, $\tilde{p}'(z)\,\tilde{p}(z)$, $(\tilde{p}(z))^2$, $\tilde{p}''(z)\,\tilde{p}(z)$, $\tilde{p}''(z)\,\tilde{p}'(z)$ and $(\tilde{p}''(z))^2$,where $\tilde{p}$ are arbitrary Herglötz functions, are independent. In fact they are independent even for $\tilde{p}(w)=\frac{1}{1-w}+a, a>0$, what can be checked by straightforward calculations. Hence coefficients in $(\tilde{p}'(z))^2$, $\tilde{p}'(z)\,\tilde{p}(z)$, $(\tilde{p}(z))^2$, $\tilde{p}''(z)\,\tilde{p}(z)$, $\tilde{p}''(z)\,\tilde{p}'(z)$and $(\tilde{p}''(z))^2$ in the left and right hand part of (17) coincide.
In particular,

$$x\left(\frac{\partial\tau(\mathbf{y})}{\partial y_i}\right)^2q''(x)=-\tau(\mathbf{y})\frac{\partial^2\tau(\mathbf{y})}{\partial y_i^2}q'(x) \tag{18}$$

and

$$q'(x)=-xq''(x). \tag{19}$$

Then

$$q(x)=\alpha\ln x, \tag{20}$$

where α is a constant. If we substitute this in (18) then we obtain

$$\left(\frac{\partial\tau(\mathbf{y})}{\partial y_i}\right)^2=\tau(\mathbf{y})\frac{\partial^2\tau(\mathbf{y})}{\partial y_i^2},1\le i\le n. \tag{21}$$

It is easy to see that any solution of system (21) can be written as

$$\tau(\mathbf{y})=h_1(y_2,\ldots,y_n)e^{y_1g_1(y_2,\ldots,y_n)}=\cdots=h_n(y_1,\ldots,y_{n-1})e^{y_ng_n(y_1,\ldots,y_{n-1})}, \tag{22}$$

where $h_1,\ldots,h_n$ are sufficiently smooth functions.Then

$$\frac{\partial^n\ln\tau(\mathbf{y})}{\partial y_1\ldots\partial y_n}=\frac{\partial^{n-1}g_1(y_2,\ldots,y_n)}{\partial y_2\ldots\partial y_n}=\cdots=\frac{\partial^{n-1}\partial g_n(y_1,\ldots,y_{n-1})}{\partial y_1\ldots\partial y_{n-1}}=c. \tag{23}$$

It gives the general solution of (23)

$$\ln\tau(\mathbf{y})=cy_n\ldots y_1+\tilde{g}_1(y_2,\ldots,y_n)+\ldots+\tilde{g}_n(y_1,\ldots,y_{n-1}), \tag{24}$$

where $\tilde{g}_1,\ldots,\tilde{g}_n$ are arbitrary sufficiently smooth functions. If we put this $\tau(\mathbf{y})$ in (16) and take coefficient of $\tilde{p}'(z)$, then we obtain

$$\frac{c_i}{t_i}=\prod_{k=1}^{n}y_k+\sum_{k=1,k\neq i}^{n}\frac{\partial\tilde{g}_k(y_1,...,\tilde{y}_i,...,y_n)}{\partial y_i}. \tag{25}$$

Taking derivative $\frac{\partial^{n-1}}{\partial y_2 \ldots \partial y_n}$ of (25) with $i=1$, we obtain $c=0$.

Moreover we claim that (24) and (25) imply $\tau(\mathbf{y}) = \exp(\mathbf{K}\cdot\mathbf{y})$. Indeed for $n=1$ it follows immediately from (21). For $n>1$ we take derivative of (25) with respect to $y_2, \ldots, y_{n-1}$ we obtain

$$\frac{\partial^{n-1}\tilde{g}_n(y_1, \ldots, y_{n-1})}{\partial y_1 \ldots \partial y_{n-1}} = 0.$$

Hence $\tilde{g}_n$ can be written as sum of functions of $n-2$ variables. By induction it implies $\tau(\mathbf{y}) = \exp(\sum_{i=1}^{n} K_i(y_i))$, and application of (21) finishes the proof of the necessity part.

We mainly use techniques of the Theorem 7.3.3. in [12] to prove formula (2) for the infinitesimal generator of ψ_t (when it is an Itô diffusion). ■

ACKNOWLEDGMENTS

Corresponding author would like to thank the Scientific and Technological Research Council of Turkey (TUBITAK-2211 Domestic Graduate Scholarship Program) for the financial support.

REFERENCES

1. E. Berkson and H. Porta, Michigan Math. J. **25(1)**, 101-115 (1978).
2. F. Bracci, M. D. Contreras, S. Diaz-Madrigal, and A. Vasil'ev, Classical and Stochastic Löwner-Kufarev Equations, in: Harmonic and Complex Analysis and its Applications, Trends Math., Birkhäuser,Basel, 39-134,(2013).
3. F. Bracci, M. D. Contreras, and S. Díaz-Madrigal, J. Reine Angew. Math. **672**, 1-37 (2012).
4. L.P.Duren, *Univalent Functions* (Springer-Verlag, New York, 1983).
5. G. M. Goluzin, *Geometrial Theory of Functions of a Complex Variable*, second ed. (Nauka, Moscow, 1966).
6. V. V. Goryainov, Mat. Sb. **206(1)**, 33–60 (2015).
7. G.Ivanov and A. Vasil'ev, Anal. Math. Phys. **1**,387-412 (2011).
8. H. H. Kuo, Introduction to Stochastic Integration (Springer, USA, 2006).
9. G. F. Lawler, *Conformally Invariant Processes in the Plane* (American Mathematical Society, USA 2005).
10. G. F. Lawler, An Introduction to the Stochastic L"owner evolution, in: Random Walks and Geometry, V. Kaimonovich, ed., De Gruyter, 261-293 (2004).
11. P. Mörters and Y. Peres, *Brownian Motion* (Cambridge University Press, New York, 2010).
12. B. Oksendal, *Stochastic Differential Equations*, sixth ed. (Springer-Verlag, New York, 2007).
13. C. Pommerenke, *Univalent Functions* (Vandenhoeck & Ruprecht, Göttingen, 1975).
14. S. Rohde and O. Schramm, Ann. of Math. **161(2)**, 883-924 (2005).
15. O. Schramm, Isr. J. Math. **118**, 221-288 (2000).
16. J. M. Steele, *Stochastic Calculus and Financial Applications*, second ed. (Springer-Verlag, New York, 2001).

Numerical Solution of the Nonlocal Reverse Parabolic Problem with Second Kind Boundary and Integral Conditions

Charyyar Ashyralyyev[1, 2, a)] and Ahmet Gönenç[1, 3, b)]

[1)] *Department of Mathematical Engineering, Gumushane University, Gumushane, 29100, Turkey*
[2)] *Department of Computer Technology, TAU, Ashgabat, Turkmenistan*
[3)] *Gumushane Vocational and Technical Anatolian School, Gumushane, 29100, Turkey*

[a)] *Electronic mail: charyar@gmail.com*
[b)] *Corresponding author: gonencahmet61@gmail.com*

Abstract. In this work, we consider approximation of nonlocal reverse parabolic problem with second kind boundary and integral conditions. Stability and coercive stability estimates for solution of difference scheme are obtained. Some illustrations of numerical results in examples of one and two dimensional reverse parabolic equations are presented.

INTRODUCTION

Some nonlocal boundary value problems for reverse parabolic differential equation are studied in [1-5] (see also references therein). Let Ω be unit open cube in R^n with boundary $\partial\Omega$, $\overline{\Omega} = S\Omega \cup \partial\Omega$, and

$$a_i : \Omega \to R, \psi : \overline{\Omega} \to R, \mu : [0,1] \to R, f : (0,1) \times \Omega \to R$$

be given functions, σ is known number ($\sigma > 0$), $\forall x \in \Omega$, $\forall i = 1,...,n, a_i(x) \geq a_0 > 0$.

In [4], nonlocal boundary value problem for multidimensional reverse parabolic equation with second kind boundary and integral conditions

$$\begin{cases} u_t(x,t) + \sum\limits_{r=1}^{n} \left(a_r(x) u_{x_r}(x,t)\right)_{x_r} - \sigma u(x,t) = f(x,t), x = (x_1,..,x_n) \in \Omega, 0 < t < 1, \\ u(x,1) = \int\limits_0^1 \mu(s) u(x,s) ds + \psi(x),\ x \in \overline{\Omega}, \\ \frac{\partial u}{\partial \vec{n}}(x,t) = 0,\ x \in \partial\Omega, 0 \leq t \leq 1 \end{cases} \tag{1}$$

was investigated. In the paper [5], approximation for multidimensional reverse parabolic differential equation with integral and Dirichlet boundary conditions was studied. Our purpose in this study is to construct stable difference scheme for nonlocal boundary value problem (1).

Introduce the grid spaces $\widetilde{\Omega}_h$ by

$$\widetilde{\Omega}_h = \{x_m = (h_1 m_1, \cdots, h_n m_n), m = (m_1, \cdots, m_n), m_i = 0, \cdots, N_i,\ N_i h_i = 1, i = 1, \cdots, n\}.$$

Let us take $\Omega_h = \widetilde{\Omega}_h \cap \Omega, S_h = \widetilde{\Omega}_h \cap \partial\Omega$. Let L_{2h} and W_{2h}^2 be spaces of the grid functions $v^h(x)$ defined on $\widetilde{\Omega}_h$, equipped with the corresponding norms

$$\left\|v^h\right\|_{L_{2h}} = \left(\sum_{x \in \widetilde{\Omega}_h} |v^h(x)|^2 h_1 \cdots h_n\right)^{1/2},$$

$$\left\|v^h\right\|_{W_{2h}^2} = \left\|v^h\right\|_{L_{2h}} + \left(\sum_{x \in \widetilde{\Omega}_h} \sum_{i=1}^n \left|(v^h(x))_{x_i \overline{x}_i,\, m_i}\right|^2 h_i\right)^{1/2}.$$

It is well known that the following operator

$$A_h^x u^h(x) = -\sum_{i=1}^n \left(a_i(x) u_{\overline{x}_i}^h(x)\right)_{x_i, j_i} + \sigma u^h(x),$$

International Conference on Analysis and Applied Mathematics (ICAAM 2020)
AIP Conf. Proc. 2325, 020005-1–020005-5; https://doi.org/10.1063/5.0040289
Published by AIP Publishing. 978-0-7354-4069-2/$30.00

acting in the space of grid functions $u^h(x)$ which satisfies the condition $Du^h(x)=0$ on $x\in S_h$ is a self-adjoint positive definite operator in L_{2h} (see [5]).

Applying A_h^x, nonlocal boundary value problem (1) can be replaced by the following difference scheme

$$\begin{cases} \frac{u_k^h(x)-u_{k-1}^h(x)}{\tau}-A_h^x u_{k-1}^h(x)=f^h(t_k,x), \quad 1\le k\le N,\ x\in\widetilde{\Omega}_h, \\ u_N^h(x)=\sum\limits_{j=0}^{N-1}\mu(t_j)u_j^h(x)\tau+\psi^h(x), x\in\widetilde{\Omega}_h. \end{cases} \tag{2}$$

Let τ and $|h|=\sqrt{\sum\limits_{i=1}^{n}h_i^2}$ be small positive real numbers.

Theorem 1 *Solution of difference scheme (2) obeys stability estimate:*

$$\left\|\left\{u_k^h\right\}_1^N\right\|_{\mathscr{C}_\tau(L_{2h})}\le M(\mu,\delta)\left[\left\|\psi^h\right\|_{L_{2h}}+\left\|\left\{f_k^h\right\}_1^N\right\|_{\mathscr{C}_\tau(L_{2h})}\right],$$

where positive constant $M(\mu,\delta)$ does depend on μ,δ, but is independent of $\tau,\psi^h(x),f_1^h(x),\cdots,f_{N-1}^h(x)$.

Theorem 2 *Solution of (2) satisfies the next coercive stability estimate:*

$$\left\|\left\{\tau^{-1}(u_k^h-u_{k-1}^h)\right\}_2^N\right\|_{\mathscr{C}_1^\alpha(L_{2h})}\le M(\mu,\delta)\left[\left\|\psi^h\right\|_{W_{2h}^2}+\left\|\left\{f_k^h\right\}_1^N\right\|_{\mathscr{C}_1^\alpha(L_{2h})}\right],$$

where positive constant $M(\delta,\mu)$ does depend on μ,δ, but is independent of $\tau,\psi^h(x),f_1^h(x),\cdots,f_{N-1}^h(x)$.

The proofs of Theorems 1 and 2 are based on coercive stability estimate for the solution of the elliptic difference problem with second kind boundary condition in L_{2h} [7] and the estimates (13) and (17) of paper [5].

NUMERICAL RESULTS

Now, we present numerical results to boundary value problems for reverse parabolic differential equation with second kind boundary and nonlocal integral conditions in 1D and 2D cases.

First, we consider boundary value problem for 1D reverse parabolic differential equation

$$\begin{cases} u_t(x,t)+(1+2x)^2u_{xx}(x,t)+4(1+2x)\ u_x(x,t)-u(x,t)=f(x,t), \\ f(x,t)=-4e^{-2t}\cos x\left(1+x+x^2\right)-4(1+2x)\ e^{-2t}\sin x\ ,\ 0<x<\pi,0<t<1, \\ u(x,1)=\int\limits_0^1 e^{-2\gamma}u(\gamma,x)\ d\gamma+\psi(x)\quad,\ \psi(x)=\cos x\left(e^{-2}+\frac{e^{-4}}{4}-\frac{1}{4}\right),0\le x\le\pi, \\ u_x(0,t)=0,u_x(\pi,t)=0,\ \ 0\le t\le 1. \end{cases} \tag{3}$$

The exact solution of problem (3) is $u(x,t)=e^{-2t}\cos x$.

Applying (2), we get the following difference scheme

$$\begin{cases} \frac{u_n^k-u_n^{k-1}}{\tau}+(1+2x_n)^2\frac{u_{n+1}^{k-1}-2u_n^{k-1}+u_{n-1}^{k-1}}{h^2}+4(1+2x_n)\frac{u_{n+1}^{k-1}-u_{n-1}^{k-1}}{2h}-u_n^{k-1}=f(x_n,t_k), \\ k=1,\cdots,N,\ n=1,\cdots,M-1, \\ u_n^N=\sum\limits_{j=0}^{N-1}e^{-2t_j}u_n^j\tau\ +\cos x_n\left(e^{-2}+\frac{e^{-4}}{4}-\frac{1}{4}\right),\ \ n=0,\cdots,M, \\ u_1^k=u_0^k,\ u_M^k=u_{M-1}^k,\ k=0,\cdots,N \end{cases} \tag{4}$$

for approximate solution of problem (3).
System of equation (4) can be rewritten in the matrix form

$$\begin{aligned} &A_n u_{n+1} + B_n u_n + C_n u_{n-1} = I_n \psi_n,\ n = 1,\cdots,M-1, \\ &u_0 = u_1, u_M = u_{M-1}. \end{aligned} \tag{5}$$

Here, ψ_n is $(N+1)\times 1$ column matrix, $I_n = I$ is identity matrix with $(N+1)$ rows, A_n, B_n, C_n are square matrices with $(N+1)$ rows and columns.

$$A_n = \begin{bmatrix} 0 & 0 & \cdots & 0 & 0 \\ a_n & 0 & \cdots & 0 & 0 \\ \vdots & \ddots & \cdots & \vdots & \vdots \\ 0 & 0 & \ddots & 0 & 0 \\ 0 & 0 & \cdots & a_n & 0 \end{bmatrix}, C_n = \begin{bmatrix} 0 & 0 & \cdots & 0 & 0 \\ c_n & 0 & \cdots & 0 & 0 \\ \vdots & \ddots & \cdots & \vdots & \vdots \\ 0 & 0 & \ddots & 0 & 0 \\ 0 & 0 & \cdots & c_n & 0 \end{bmatrix},$$

$$B_n = \begin{bmatrix} -e^{-2t_0}\tau & -e^{-2t_1}\tau & -e^{-2t_2}\tau & \cdots & -e^{-2t_{N-2}}\tau & -e^{-2t_{N-1}}\tau & 1 \\ b_n & s & 0 & \cdots & 0 & 0 & 0 \\ 0 & b_n & s & \cdots & 0 & 0 & 0 \\ \vdots & \ddots & \ddots & \ddots & \vdots & \vdots & \vdots \\ 0 & 0 & 0 & \ddots & s & 0 & 0 \\ 0 & 0 & 0 & \ddots & b_n & s & 0 \\ 0 & 0 & 0 & \cdots & 0 & b_n & s \end{bmatrix},$$

$$\begin{aligned} &a_n = \tfrac{(1+2x_n)^2}{h^2} + \tfrac{2(1+2x_n)}{h},\ b_n = -\tfrac{1}{\tau} - \tfrac{2(1+2x_n)^2}{h^2} - 1, \\ &c_n = \tfrac{(1+2x_n)^2}{h^2} - \tfrac{2(1+2x_n)}{h}, s = \tfrac{1}{\tau}, \\ &\psi_n = \left[\ \psi_n^0\ \ \ldots\ \ \psi_n^N\ \right]^t, u_j = \left[\ u_j^0\ \ \ldots\ \ u_j^N\ \right]^t, j = n-1, n, n+1, \\ &\psi_n^0 = \cos x_n \left(e^{-2} + \tfrac{e^{-4}}{4} - \tfrac{1}{4}\right),\ n = 1,\cdots,M-1, \\ &\psi_n^k = f(x_n,t_k),\ k = 1,\cdots,N,\ n = 1,\cdots,M-1. \end{aligned}$$

One can use modified Gauss elimination method for solving difference equations (4) numerically (see [7]).
Approximate solution of (4) is evaluated by

$$u_n = \alpha_{n+1} u_{n+1} + \beta_{n+1}, n = M-1,\cdots,1,$$

where

$$u_M = u_{M-1} = (A_{M-1} + B_{M-1} + C_{M-1}\alpha_{M-1})^{-1} (I_{M-1}\psi_{M-1} - C_{M-1}\beta_{M-1}),$$

$\alpha_1 = I$, β_1 is the column vector with $(N+1)$ zeros, α_n $(n = 2,\cdots,M-1)$ are square matrices with $(N+1)$ rows and columns and β_n $(n = 2,\cdots,M-1)$ are column matrices with $(N+1)$ rows such that

$$\alpha_{n+1} = -(B_n + C_n\alpha_n)^{-1} A_n, \beta_{n+1} = (B_n + C_n\alpha_n)^{-1} (I_n\psi_n - C_n\beta_n).$$

Table 1 shows error computed by

$$Eu_M^N = \max_{1\le k\le N-1} \left(\sum_{n=1}^{M-1} (u(x_n,t_k) - u_n^k)^2 h \right)^{\frac{1}{2}}$$

for different values of (N,M).

TABLE 1. Error output for DS (4).

(N,M)	**(10,10)**	**(20,20)**	**(40,40)**	**(80,80)**	**(160,160)**
Error	0.6194	0.3819	0.2264	0.1218	0.0630

Second, we consider the next boundary value problem for 2D reverse parabolic differential equation

$$\begin{cases} u_t(x,y,t)+(1+2x)^2u_{xx}(x,y,t)+4(1+2x)u_x(x,y,t) \\ +u_{yy}(x,y,t)-\ u(x,y,t)=f(x,y,t), \\ f(x,y,t)=-\left(4+(1+2x)^2\right)e^{-2t}\cos x\cos y-4(1+2x)e^{-2t}\sin x\cos y, \\ 0<x,y<\pi,\ 0<t<1, \\ u(1,x,y)=\int\limits_0^1 e^{-2\gamma}u(\gamma,x,y)\,d\gamma+\psi(x,y), \\ \psi(x,y)=\cos x\cos y(e^{-2}+\frac{e^{-4}}{4}-\frac{1}{4}),0\le x,y\le\pi, \\ u_x(t,0,y)=0,u_x(t,\pi,y)=0,\ 0\le y\le\pi,0\le t\le 1, \\ u_y(t,x,0)=0,u_y(t,x,\pi)=0,0\le x\le\pi,0\le t\le 1. \end{cases} \tag{6}$$

The exact solution of problem (6) is $u(t,x,y)=e^{-2t}\cos x\cos y$.

Introduce notations:

$$\psi_{m,n}=\psi(x_m,y_n)\,,\ n,m=\overline{0,M},\ f^k_{m,n}=f(t_k,x_m,y_n),\ k=\overline{0,N},\ n,m=\overline{0,M}.$$

Applying (2), we get difference scheme for approximate solution of nonlocal boundary value problem (6) in the next form

$$\begin{cases} \frac{u^k_{m,n}-u^{k-1}_{m,n}}{\tau}+(1+2x_m)^2\frac{u^{k-1}_{m+1,n}-2u^{k-1}_{m,n}+u^{k-1}_{m-1,n}}{h^2}+2(1+2x_m)\frac{u^{k-1}_{m+1,n}-u^{k-1}_{m-1,n}}{h} \\ +\frac{u^{k-1}_{m,n+1}-2u^{k-1}_{m,n}+u^{k-1}_{m,n-1}}{h^2}-u^{k-1}_{m,n}=f^k_{m,n},1\le k\le N-1,1\le n,m\le M-1, \\ u^k_{0,n}=0,\ u^k_{M,n}=0,\ 1\le k\le N-1, \\ u^k_{m,0}=0,\ u^k_{m,M}=0,1\le k\le N-1,1\le n,m\le M-1, \\ u^N_{m,n}=\sum\limits_{j=0}^{N-1}e^{-2t_j}u^j_{m,n}\tau+\cos x_n\cos y_m(e^{-2}+\frac{e^{-4}}{4}-\frac{1}{4}),1\le n,m\le M-1. \end{cases} \tag{7}$$

Difference problem (7) can be rewritten in the matrix form (5). Here A_n, B_n, C_n ,I are $K\times K$ square matrices, and I is the identity matrix, $f^{(n)},u_{n-1},u_n,u_{n+1}$ are the $K\times 1$ column matrices such that $K=(N+1)(M+1)$,

$$f^{(n)}=\left[\ f^0_{0,n}\ \cdots\ f^N_{0,n}\ \ f^0_{1,n}\ \cdots\ f^N_{1,n}\ \cdots\ f^0_{M,n}\ \cdots\ f^N_{M,n}\ \right]^t,$$
$$u_s=\left[\ u^0_{0,s}\ \cdots\ u^N_{0,s}\ \ u^0_{1,s}\ \cdots\ u^N_{1,s}\ \cdots\ u^0_{M,s}\ \cdots\ u^N_{M,s}\ \right]^t,s=n\pm 1,n.$$

Modified Gauss elimination method are used to evaluate solution of (7) via Matlab program. Error output for difference problem (7) is recorded for different values of $(N,M)=(10,10),(20,20),(40,40)$ which are computed by

$$Eu^N_M=\max_{1\le k\le N-1}\left(\sum_{n=1}^{M-1}\sum_{m=1}^{M-1}(u(x_n,y_m,t_k)-u^k_{n,m})^2h^2\right)^{\frac{1}{2}}.$$

Calculated errors in Tables 1 and 2 point out sufficiently good agreement with theorems on stability solution of corresponding difference schemes of boundary value problems for reverse parabolic differential equation with Neumann boundary and nonlocal integral conditions.

TABLE 2. Error output for DS (7).

(N,M)	**(10,10)**	**(20,20)**	**(40,40)**
Error	0.6075	0.2957	0.1655

REFERENCES

1. A. Ashyralyev, A. Dural, and Y. Sozen, Vestnik of Odessa National University: Mathematics and Mechanics **13**, 1-12 (2008).
2. C. Ashyralyyev, A. Dural, and Y. Sozen, Abstr. Appl. Anal. **2012**, 1–17 (2012).
3. C. Ashyralyyev, A. Dural, and Y. Sozen, AIP Conference Proceedings **1470**, 102-105 (2012).
4. C. Ashyralyyev, e-Journal of Analysis and Applied Mathematics **2018(1)**, 11-20 (2018).
5. C. Ashyralyyev, Math. Meth. Appl. Sci. **43**, 5369-5379 (2020).
6. A. Ashyralyev and P. Sobolevskii, Difference Schemes for Partial Differential Equations,Operator Theory Advances and Applications (Birkhauser Verlag, Basel, Boston, Berlin, 2004).
7. A. Samarskii, The Theory of Difference Schemes (Dekker, New York, 2007).
8. P. Sobolevskii, Difference Methods for the Approximate Solution of Differential Equations (Voronezh State University Press, Voronezh, Russia, 1975).

Lebesgue Constants for Rational Interpolation Processes and Inverse Rational Functions Mappings

Sergei Kalmykov[1, 2, a)] and Alexey Lukashov[3, 4, b)]

[1)] *School of mathematical sciences, Shanghai Jiao Tong University, 800 Dongchuan RD, Shanghai, 200240, China*
[2)] *Institute of Applied Mathematics FEB RAS, Vladivostok. 7 Radio str. 690041, Russia*
[3)] *Moscow Institute of Physics and Technology (National Research University), Dolgoprudny Moscow Region. 9 Institutskiy per. 141701. Russia*
[4)] *Saratov State University, Saratov, Astrakhanskaya, 83. 410012, Russia*

[a)] *Electronic mail: kalmykovsergei@sjtu.edu.cn*
[b)] *Corresponding author: alexey.lukashov@gmail.com*

Abstract. We estimate the Lebesgue constants of interpolation by rational functions on one or several intervals with fixed poles having accumulation points on the interval(s). To prove it we use an analogue of the inverse polynomial image method for rational functions with fixed poles.

INTRODUCTION

Interpolation by polynomials on real sets has a long history. Main books on interpolation theory (by A.A. Privalov [1] and by J. Szabados, P. Vertesi [2]) contain many results about it.

Recently several results about Lebesgue constants of interpolation processes on finite unions of intervals were obtained (see [3, 4]).

In [3] the authors used an estimate for Lebesgue constants of interpolation processes by rational functions with fixed poles from [5].

Interpolation by rational functions with fixed poles is not so well developed as polynomial case. First results were collected in A. Kh. Turetskii's book [6]. Later some of them were rediscovered by G. Min (more references can be found in [5, 7, 8].

One of the best choices for interpolation by polynomials on an interval is to use zeros of Chebyshev polynomials as nodes of interpolation. Their analogues for rational functions with fixed poles are Chebyshev-Markov rational functions deviated least from zero on an interval. Corresponding interpolation processes were introduced by V. N. Rusak [9] and the most general estimate for related Lebesgue constants is due to A. P. Starovoitov. The last estimate was generalized for the case of two intervals by second author in [10]. It included possible accumulation of fixed poles to the ends of the convex hull of the intervals. The estimate for the case of three or more intervals from [5] didn't allow to fixed poles to accumulate on the convex hull of the intervals. Our first result gives a class of interpolation matrices which allow an estimate of Lebesgue constants of interpolation by rational functions on several intervals with fixed poles having accumulation points on the intervals.

To prove it we develop an analogue of the inverse polynomial image method for rational functions with fixed poles.

Our second result gives an improved answer to a hypothesis by G. Min about the existence of poles with accumulation points on an interval which have an estimate of Lebesgue constants with logarithmic growth.

RESULTS

For any $s \geq 1$ let

$$-1 = a_1 < b_1 < \cdots < a_s < b_s = 1 \tag{1}$$

be a finite partition of the interval $[-1,1]$, and let

$$J_s = \bigcup_{i=1}^{s} [a_i, b_i] \tag{2}$$

be the corresponding set of intervals.

International Conference on Analysis and Applied Mathematics (ICAAM 2020)
AIP Conf. Proc. 2325, 020006-1–020006-4; https://doi.org/10.1063/5.0040354
Published by AIP Publishing. 978-0-7354-4069-2/$30.00

The Lebesgue function of interpolation on J_s by rational functions with fixed poles from the matrix of their reciprocal values

$$\mathfrak{A} = \{a_{k,n}\} \subset \mathbb{D} = \{z \in \mathbb{C} : |z| < 1\} \tag{3}$$

for the matrix of interpolation nodes

$$\mathfrak{M} = \{x_{k,n}, x_{n,n} < x_{n-1,n} < \cdots x_{1,n}\} \tag{4}$$

is defined as

$$\lambda_n(\mathfrak{M}, \mathfrak{A}, x) = \sum_{k=1}^{n} |\ell_{k,n}(\mathfrak{M}, \mathfrak{A}, x)|, \tag{5}$$

where

$$\ell_{k,n}(\mathfrak{M}, \mathfrak{A}, x) = \frac{\varpi_n(x)}{\varpi_n'(x_{k,n})(x - x_{k,n})}, \quad \varpi_n(x) = \prod_{k=1}^{n} \frac{x - x_{k,n}}{1 - a_{k,n}x}.$$

Furthermore, the Lebesgue constant is given by

$$\lambda_n(\mathfrak{M}, \mathfrak{A}) = \|\lambda_n(\mathfrak{M}, \mathfrak{A}, x)\|_{J_s}, \tag{6}$$

where $\|\cdot\|_K$ is the supremum norm on any compact set K.

Definition 1 (see e.g. [11]) *Let B be a domain in $\overline{\mathbb{C}}$ such that its boundary consists of finitely many disjoint piecewise smooth curves or arcs and let α be a closed subset of ∂B also consisting of arcs or curcves. We denote by $\omega(z, \alpha, B)$ a bounded harmonic function in B such that $\omega(z, \alpha, B) \to 1$ as z approaches interior points of α, and $\omega(z, \alpha, B) \to 0$ as z approaches interior points of $\partial B \setminus \alpha$. The function $\omega(z, \alpha, B)$ is called the harmonic measure of α with respect to B at a point z.*

Definition 2 *Matrix $\mathfrak{A}$ from* (3) *is called regular with respect to J_s, if for every $j = 1, \ldots, s$ and $n \geq s$ the sum of the harmonic measures of the interval $[a_j, b_j]$ with respect to $1/a_{k,n}$ is a positive integer, i.e.*

$$\sum_{k=1}^{n} \omega_j(1/a_{k,n}) = q_j, \quad q_j \in \mathbb{N}, \quad j = 1, \ldots, s. \tag{7}$$

Regularity of matrices of (reciprocal to) fixed poles is a natural notion, since it guarantees that for every $n \geq s$ J_s can be considered as an inverse image of an interval under suitable rational function of degree n with (reciprocal to) fixed poles given by n-th row of $\mathfrak{A}$. This rational function is a direct generalization to the case of several intervals of the Chebyshev-Markov rational functions. It can be written (up to a constant multiplier) in the form

$$\varpi_n(x) = \cos\left(\pi \sum_{k=1}^{n} \omega(1/a_{k,n}, J_s \cap [a_1, x], \mathbb{C} \backslash J_s)\right). \tag{8}$$

Denote

$$H(x) = \prod_{j=1}^{s} (x - a_j)(x - b_j), \tag{9}$$

$$\gamma_n(J_s, \mathfrak{A}x) = \sqrt{-H(x)}\pi \sum_{k=1}^{n} \omega'(1/a_{k,n}, J_s \cap [a_1, x], \mathbb{C} \backslash J_s), \quad x \in \operatorname{int} J_s. \tag{10}$$

Now we can formulate A.P. Starovoitov's theorem and two theorems from earlier papers of second author in these notations. We enumerate the reciprocal of poles in a row as follows: $a_{1,n} = \ldots = a_{\kappa_n,n} = 0$ (here $1/0 = \infty$), $a_{k,n} \neq 0$, $k = \kappa_n + 1, \ldots, n$, Re $a_{k,n} > 0, k = \kappa_n + 1, \ldots, n_1$, Re $a_{k,n} < 0, k = n_1 + 1, \ldots, n$, and for Im $a_{k,n} > 0$ Im $a_{k+1,n} = -$ Im $a_{k,n}$. Here we don't indicate possible dependence of n_1 of n.

Theorem 1 ([12], see also [10]) *Let $s = 1$ and the matrix of reciprocal values of poles $\mathfrak{A}$ has no accumulation points on $\{|z| = 1\}$ with possible exception for points $\{\pm 1\}$, which can be attained by nontangent paths, and satisfies the conditions*

$$\sum_{k=1}^{n_1} \frac{\sqrt{1-|a_{k,n}|}t}{1-|a_{k,n}|+t^2} \geq C_1 \quad \text{for} \quad \sqrt{1-\max_{1\leq k\leq n_1}|a_{k,n}|} \leq t \leq 1; \tag{11}$$

$$\sum_{k=n_1+1}^{n} \frac{\sqrt{1-|a_{k,n}|}t}{1-|a_{k,n}|+t^2} \geq C_2 \quad \text{for} \quad \sqrt{1-\max_{n_1+1\leq k\leq n}|a_{k,n}|} \leq t \leq 1. \tag{12}$$

Then for the matrix $\mathfrak{M}$ such that its n-th row consists of zeroes of ϖ from (8) *the estimate*

$$\lambda_n(\mathfrak{M},\mathfrak{A}) \leq C_3 \log \|\gamma_n(J_1,\mathfrak{A},\cdot)\|_{J_1} \tag{13}$$

holds.

Remark 1 *It is funny that this result (which was proved in 1984) answers the question posed in 1998 by [13] (Remark 2, p. 129) as an open problem (indeed it is easy to see that $a_{1,n} = \ldots = a_{n,n} = 1-1/n$ gives negative answer to Min's question).*

Theorem 2 *[10] Let $s = 2$, the matrix of reciprocal values of poles $\mathfrak{A}$ is regular with respect to J_2, has no accumulation points on $\{|z| = 1\}$ with possible exception for points $\{\pm 1\}$, which can be attained by non-tangent paths, and satisfies the conditions* (11),(12),

$$\min_{x\in J_2} \frac{\gamma_n(J_2,\mathfrak{A},x)}{\sqrt{(x-b_1)(x-a_2)}\gamma_n(J_2,\mathfrak{A},(a_2+1)/2))} \geq C_4, n \geq 2. \tag{14}$$

Then for the matrix $\mathfrak{M}$ such that its n-th row consists of zeroes of ϖ from (8) *the estimate*

$$\lambda_n(\mathfrak{M},\mathfrak{A}) \leq C_5 \log \|\gamma_n(J_2,\mathfrak{A},\cdot)\|_{J_2} \tag{15}$$

holds.

Theorem 3 *[5] Let $s \geq 1$, the matrix of reciprocal values of poles $\mathfrak{A} \subset \{|z| \leq r\}, 0 < r < 1$, is regular with respect to J_s. Then for the matrix $\mathfrak{M}$ such that its n-th row consists of zeroes of ϖ from* (8) *the estimate*

$$\lambda_n(\mathfrak{M},\mathfrak{A}) \leq C_7 \log n \tag{16}$$

holds.

Our results are as follows.

Theorem 4 *For any $s \geq 2$ and for any system* (2) *there exists a class of matrices of reciprocal values of poles $\mathfrak{A}$ which are regular with respect to J_s, the poles have accumulation points on J_s, including all points of the partition* (1) *and for the matrix $\mathfrak{M}$ such that its n-th row consists of zeroes of ϖ from* (8) *the estimate*

$$\lambda_n(\mathfrak{M},\mathfrak{A}) \leq C_8 \log \|\gamma_n(J_s,\mathfrak{A},\cdot)\|_{J_s} \tag{17}$$

holds.

In particular, there is a subclass of that class of matrices with the estimate (16).

Theorem 5 *Let F be a finite subset of $[-1,1]$. There exists a matrix of reciprocal values of poles such that every point of F is an accumulation point of the poles and the Lebesgue constants of the Chebyshev-Markov rational functions interpolation process on $[-1,1]$ with those poles are estimated by (16).*

The proof of Theorem 4 is quite analogous to the proof of [4] (Theorem 1), where instead of the inverse polynomial image of an interval it is necessary to consider inverse images of an interval by rational functions with fixed poles.

Concerning the proof of Theorem 5 one has to use the representation of the Chebyshev-Markov rational functions on $[-1,1]$:

$$M_m(x) = \cos\left(\sum_{j=1}^{m} \arccos \frac{x-a_j}{1-a_j x}\right).$$

Now for $F = \{x_1, \ldots, x_N\}$ and $m > N$ it is possible to get

$$\frac{1}{2\pi} \sum_{j=1}^{m} \arccos \frac{x_k - a_j}{1 - a_j x_k} \in \mathbb{N},\ k = 1 \ldots, N,$$

by the inverse function theorem since the related determinant is equal to a multiple of the Cauchy determinant.

Finally, the rational function $\mu_b(M_m(x))$, where $\mu_b(y) = \frac{y-b}{1-yb}$, $b \to 1+0$, satisfies the conditions of Theorem 5 for a suitable choice of a_j (they need to have accumulation points at 1).

ACKNOWLEDGMENTS

The first author supported by SJTU start-up grant program.

REFERENCES

1. A. A. Privalov, *Teoriya interpolirovaniya funktsiĭ. Kniga 1, 2* (Saratov. Gos. Univ., Saratov, 1990) pp. Book 1: 230 pp.; Book 2: pp. 231–424.
2. J. Szabados and P. Vértesi, *Interpolation of Functions* (World Scientific Publishing Co., Inc., Teaneck, NJ, 1990) pp. xii+305.
3. A. L. Lukashov and J. Szabados, Period. Math. Hungar. **72(2)**, 103–111 (2016).
4. A. Kroó and J. Szabados, J. Math. Anal. Appl. **436(2)**, 1165–1179 (2016).
5. A. Lukashov, Izv. Saratov Univ. (N.S.), Ser. Math. Mech. Inform. **5(1-2)**, 34–48 (2005).
6. A. Turetskii, *Teoriya interpolirovaniya v zadachakh.. Ch. 2* (Minsk: Vyshcheisha Shkola, 1977) pp. Book 1: 230 pp.; Book 2: pp. 231–424.
7. Y. A. Rovba and Y. V. Divruk, Izvestiya NAN Belarusi. Ser. fiz.-matem. nauk , 32–38 (2015).
8. Y. A. Rouba, K. A. Smatrytski, and Y. V. Divruk, J. Belorussian State Univ. Mathem. Inform. , 12–20 (2018).
9. V. N. Rusak, Dokl. Akad. Nauk BSSR **6**, 209–211 (1962).
10. A. L. Lukashov, Izv. Vyssh. Uchebn. Zaved. Mat. , 35–42 (1998).
11. G. M. Goluzin, *Geometric Theory of Functions of a Complex Variable*, Translations of Mathematical Monographs, Vol. 26 (American Mathematical Society, Providence, R.I., 1969) pp. vi+676.
12. A. Starovoitov, Izvestiya AN BSSR. Ser. fiz.-matem. nauk (1983).
13. G. Min, J. Approx. Theory **95(1)**, 123–145 (1998).
14. A. L. Lukashov, Izv. Ross. Akad. Nauk Ser. Mat. **68(3)**, 115–138 (2004).
15. S. Stoilow, *Teoria funcţiilor de o variabilă complexă. Vol. 2. Funcţii armonice. Suprafeţe Riemanniene*, In collaboration with C. A. Cazacu (Editura Academiei Republicii Populare Romîne, Bucharest, 1958) p. 378.

Mathematical Model of a Short Arc at the Blow-Off Repulsion of Electrical Contacts During the Transition from Metallic Phase to Gaseous Phase

Stanislav N. Kharin[1, 2, a)] and Targyn A. Nauryz[1, 2, b)]

[1)] *Institute of Mathematics and Mathematical Modeling, Almaty, Kazakhstan*
[2)] *Kazakh-British Technical University, Almaty, Kazakhstan*

[a)] *Corresponding author: staskharin@yahoo.com*
[b)] *Electronic mail: targyn.nauryz@gmail.com*

Abstract. The mathematical model describing the dynamics of temperature field in electrical contacts at the initial stage of a blow-off repulsion is presented. It is based on the Stefan problem for the disk of a short arc and two spherical domains for the liquid and solid zones. All coefficients in the equations such as the thermal and electrical conductivities, density, thermal capacity are dependent on the temperature. The analytical solution of this problem is obtained using the similarity principle. The results of calculation are compared with the data obtained in published papers and with the experimental data.

INTRODUCTION

Mathematical modeling of the electrical arc is very important to understand its dynamics and to estimate arc parameters because experimental methods give as a rule only the resulting information about arcing and arc erosion because of a fleeting process. General models describing phenomena in the arc plasma are based on the systems of partial differential equations of the magneto-hydrodynamics (MHD) [1, 2, 3, 4]. These models are too complicated for the practical investigation of the arc dynamics in electrical contacts. The non-stationary model presented in the paper [5] describes temperature and electromagnetic fields in a short electrical arc taking into account near-electrode phenomena. However, its application is also not so simple.

MATHEMATICAL MODEL

At the initial stage of the blow-off repulsion, when the arc is burning in the metal-dominated phase with following transition to the gas-dominated phase, it can be considered as a short arc, i.e. the occupied by the arc domain D_A has the form of a thin disk which radius $r = r_A(t)$ is much greater than the thickness $h = h(t)$ (Figure 1). The equation for

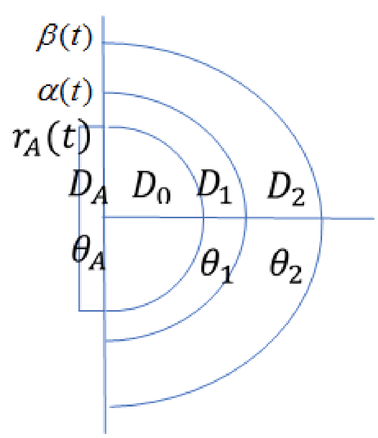

FIGURE 1. The axial contact cross-section of the spherical domains. D_A - is the disk occupied by the arc, D_0 - is the Holm sphere of the ideal conductivity, D_1 - is the sphere of metallic vapours, D_2 - is the sphere of liquid metal, $r > \beta(t)$ - is the solid zone

International Conference on Analysis and Applied Mathematics (ICAAM 2020)
AIP Conf. Proc. 2325, 020007-1–020007-6; https://doi.org/10.1063/5.0040412
Published by AIP Publishing. 978-0-7354-4069-2/$30.00

the temperature field of the arc $\theta_A(r,t)$ can be written in the form

$$c_A(\theta_A)\gamma_A(\theta_A)\frac{\partial\theta_A}{\partial t}=\frac{1}{r}\frac{\partial}{\partial r}\left(\lambda_A(\theta_A)r\frac{\partial\theta_A}{\partial r}\right)+\frac{j^2}{\sigma_A(\theta_A)}-W_r(\theta_A)-P(r,t). \tag{1}$$

Here $c_A(\theta_A),\gamma_A(\theta_A),\lambda_A(\theta_A),\sigma_A(\theta_A)$ are the coefficients of the heat capacity, density, thermal and electrical conductivity, respectively, $j=\dfrac{I(t)}{\pi r_A^2(t)}$ is the arc current density, $W_r(\theta_A)$ and $P(r,t)$ are the volumetric arc power radiation and power losses due to the arc heat conduction into contacts.

The temperature dependence of the coefficients [7] is presented in Figure 2 and Figure 3. The metallic arc phase

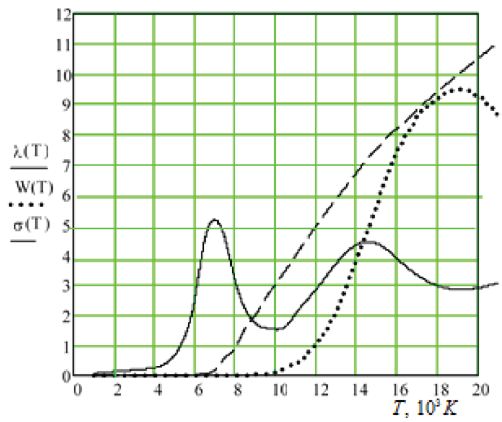

FIGURE 2. Temperature dependence of the thermal and electrical conductivity and radiation losses for the arc burning in air $\lambda(W/mK)$, $\sigma(10^3\Omega^{-1}m^{-1})$ and $W_r(10^9W/m^3)$

continues up to the time $t=t_{gi}$, when the temperature maximum at the center of the arc disk reaches the value of the gas ionization (approximately about 7000^0K)

$$\theta_A(0,t_{gi})=\theta_{g_i}. \tag{2}$$

Thus, for equation (1) we consider the domain

$$D_A: 0<t<t_{gi},\ \ 0<r<r_A(t), \tag{3}$$

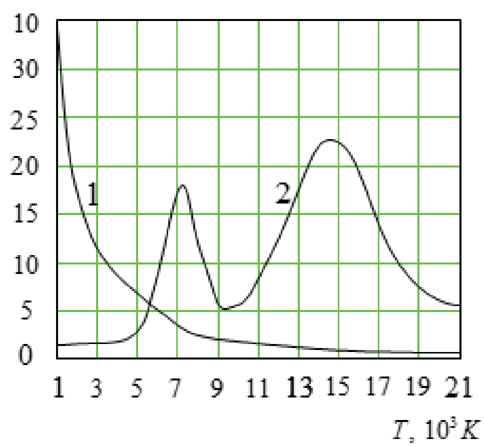

FIGURE 3. Temperature dependence of γ and c for the arc burning in air $1-\gamma, 10^2kg/m^3$, $2-c, 10^3J/kg\cdot K$

for the temperature range

$$\theta_{mi} < \theta_A(r,t) < \theta_{gi}, \tag{4}$$

where θ_{mi} is the temperature of the metallic vapor ionization (approximately about $5000^0 K$).

As can be seen from Figure 2, the arc radiation $W_r(\theta_A)$ can be neglected in the temperature range (4) and we should take into account only the power losses $P(r,t)$ due to the arc heat conduction into the zone of metallic vapour D_1 via the zone of the ideal thermal and electrical conductivity D_0 introduced by R. Holm [8]. This loss can be calculated using the formula

$$P(r,t) = -\frac{2\lambda_1}{h(t)} \frac{\partial \theta_1}{\partial r}\bigg|_{r=r_A(t)}. \tag{5}$$

It was shown in the paper [6] that the contact gap, i.e. the arc disk thickness $h(t)$, increases in the initial stage of the metallic arc phase at the blow-off repulsion due to the summary action of electromagnetic and vapor forces according to the expression

$$h(t) = h_0\sqrt{t}, \tag{6}$$

where the constant h_0 depends on the current amplitude I_0.

For the considered time interval $0 \leq t \leq t_{gi}$ it is possible to approximate the alternative current $I(t) = I_0 \sin(\omega t)$ by the expression

$$I(t) = k\sqrt{t}, \tag{7}$$

where

$$k = \frac{I_0 \sin(\omega t_{ig})}{\sqrt{t_{ig}}}. \tag{8}$$

Substituting the expressions (5) – (8) into the equation (1), we get

$$\begin{aligned} c_A(\theta_A)\gamma_A(\theta_A)\frac{\partial \theta_A}{\partial t} &= \frac{1}{r}\frac{\partial}{\partial r}\left(\lambda_A(\theta_A) r \frac{\partial \theta_A}{\partial r}\right) \\ &+ \frac{k^2 t}{\pi^2 r_A^4(t)\sigma_A(\theta_A)} - \frac{2\lambda_{1b}}{h_0\sqrt{t}}\frac{\partial \theta_1(r_A(t),t)}{\partial r}, \quad D_A: 0 < r < r_A(t),\ \ 0 < t < t_{jg}, \end{aligned} \tag{9}$$

where $\lambda_{1b} = \lambda_1(\theta_1(r_A(t))) = \lambda_1(\theta_{mi})$.

At the initial time the domain D_A collapses into a point $r = r_A(0) = 0$, where the temperature should be equal to the threshold of metal ionization temperature θ_{mi}:

$$\theta_A(0,0) = \theta_{mi}. \tag{10}$$

This temperature remains the same value on the boundary of the disk for $t > 0$:

$$\theta_A(r_A(t),t) = \theta_{mi}. \tag{11}$$

The arc heat flux passes through the sphere of ideal conductivity D_0 without any power losses and enters into vapor zone D_1 through the spherical surface $r = r_A(t)$ which temperature is the same like (11):

$$\theta_1(r_A(t),0) = \theta_{mi}. \tag{12}$$

The phenomena occurring in the vapor zone are too complicated for mathematical modeling in the frame of our approach, thus let us consider this zone as the thermal resistivity between the arc zone D_A and the liquid zone D_2 with a linearly decreasing temperature

$$\theta_1(r,t) = \theta_{mi} - \frac{r - r_A(t)}{\alpha(t) - r_A(t)}(\theta_{mi} - \theta_b), \ \ r_A(t) \leq r \leq \alpha(t). \tag{13}$$

The temperature fields of the liquid zone D_2 and the solid zone D_3 satisfy the heat equations

$$\begin{aligned} &c_i(\theta_i)\gamma_i(\theta_i)\frac{\partial\theta_i}{\partial t} = \frac{1}{r^2}\frac{\partial}{\partial r}\left(\lambda_i(\theta_i)r^2\frac{\partial\theta_i}{\partial r}\right), \\ &i=2 \ \rightarrow \ \alpha(t)<r<\beta(t), \\ &i=3 \ \rightarrow \ \beta(t)<r<\infty. \end{aligned} \tag{14}$$

The Stefan conditions hold on the interfaces of the phase transformations:

$$\begin{aligned} &\theta_2(\alpha(t),t)=\theta_b, \quad \theta_2(\beta(t),t)=\theta_3(\beta(t),t)=\theta_m, \\ &-\lambda_b\frac{\partial\theta_2(\alpha(t),t)}{\partial r} = L_b\gamma_b\frac{d\alpha}{dt}, \\ &-\lambda_2\frac{\partial\theta_2(\beta(t),t)}{\partial r} = -\lambda_3\frac{\partial\theta_3(\beta(t),t)}{\partial r}+L_m\gamma_m\frac{d\beta}{dt}. \end{aligned} \tag{15}$$

Here L_b, L_m are specific heats of evaporation and melting

$$\begin{aligned} &\lambda_b=\lambda(\theta_b), \\ &\lambda_2=\lambda(\theta_m), \ \text{ for liquid}, \\ &\lambda_3=\lambda(\theta_m), \ \text{ for solid}, \\ &\gamma_b=\gamma(\theta_b), \ \gamma_m=\gamma(\theta_m). \end{aligned}$$

The last boundary condition for the solid zone is

$$\theta_3(\infty,t)=0. \tag{16}$$

At the initial time all zones collapse into a point:

$$r_A(0)=\alpha(0)=\beta(0)=0. \tag{17}$$

The solution of the above-formulated problem can be found using the similarity principle.

SOLUTION OF THE PROBLEM

According to the similarity principle we represent the solution in the form

$$\theta_A(r,t)=u_A(\eta), \ \theta_i(r,t)=u_i(\eta), \ i=1,2, \tag{18}$$

where $\eta=\dfrac{r}{2a\sqrt{t}}$, $r_A(t)=a\sqrt{t}$, $\alpha(t)=\alpha_0\sqrt{t}$, $\beta(t)=\beta_0\sqrt{t}$. Then we get

$$\begin{aligned} &\frac{\partial\theta_A}{\partial t} = -\frac{1}{2t}\eta\frac{du_A}{d\eta}, \\ &\frac{1}{r}\frac{\partial}{\partial r}\left[r\lambda(u_A)\frac{\partial\theta_A}{\partial r}\right] = \frac{1}{4a^2t}\left[\lambda(u_A)u_A'(\eta)+\lambda'(u_A)u'(\eta)^2+\frac{\lambda(u_A)}{\eta}u_A'(\eta)\right], \end{aligned} \tag{19}$$

$$\frac{1}{r^2}\frac{\partial}{\partial r}\left[r^2\lambda(\theta_i)\frac{\partial\theta_i}{\partial r}\right] = \frac{1}{4a^2t}\left[\lambda(u_i)u_i'(\eta)+\lambda'(u_i)u_i'(\eta)^2+\frac{2\lambda(u_i)}{\eta}u_i'(\eta)\right] \tag{20}$$

and equation (9) takes the form

$$\begin{aligned} &\lambda_A(u_A)u_A'(\eta)+\lambda_A'(u_A)u_A'(\eta)^2 \\ &+\left[\frac{\lambda_A(u_A)}{\eta}+2a^2c_A(u_A)\gamma_A(u_A)\eta\right]u_A'(\eta) \\ &+\frac{4k^2}{\pi^2a^2\sigma_A(u_A)}, \quad 0<\eta<\frac{1}{2}. \end{aligned} \tag{21}$$

Similarly, the equations (14) can be written in the form

$$
\begin{aligned}
&\lambda_i(u_i)u_i''(\eta)+\lambda_i'(u_i)u_i'(\eta)^2+2\left[\frac{\lambda_i(u_i)}{\eta}+ac_i(u_i)\gamma_i(u_i)\eta\right]u_i'(\eta)=0,\\
&i=2,\ \rightarrow\ \frac{\alpha_0}{2a}<\eta<\frac{\beta_0}{2a},\\
&i=3,\ \rightarrow\ \frac{\beta_0}{2a}<\eta<\infty.
\end{aligned}
\tag{22}
$$

Thus, the problem is reduced to the solution of the ordinary differential equations (21), (22). The boundary conditions (12), (15) for these substitutions transform into expressions

$$u_A'(0)=0, \tag{23}$$

$$u_A(1/2)=\theta_{mi}, \tag{24}$$

$$u_2(\alpha_0/2a)=\theta_b, \tag{25}$$

$$u_2(\beta_0/2a)=u_3(\beta_0/2a)=\theta_m, \tag{26}$$

$$u_3(\infty)=0, \tag{27}$$

$$u_2'(\alpha_0/2a)=-\frac{L_b\gamma_b}{\lambda_b a}, \tag{28}$$

$$-\lambda_2u_2'(\beta_0/2a)=-\lambda_3u_3'(\beta_0/2a)+\frac{L_m\gamma_m}{a}. \tag{29}$$

The problem (21) – (29) can be solved using the Runge-Kutta method.

Sometimes, for an analytical analysis of the temperature dynamics, it is more convenient to reduce this problem to the system of the integral equations. In particular, equation (21) after the substitution

$$\lambda_A u_A(\eta)=V_A(\eta), \tag{30}$$

can be written in the form

$$V_A'(\eta)+L_A(\eta)V_A(\eta)=N(\eta), \tag{31}$$

where

$$
\begin{aligned}
L_A(\eta)&=\frac{1}{\eta}+2a^2M_A(u_A)\eta,\\
M_A(u_A)&=\frac{c_A(u_A)\gamma_A(u_A)}{\lambda_A(u_A)},
\end{aligned}
\tag{32}
$$

$$N_A(\eta)=-\frac{4k^2}{\pi a^2\sigma_A(u_A)}. \tag{33}$$

Equation (31) is equivalent to the non-linear integral equation

$$V_A(\eta)=\exp\left[-\int_0^\eta L_A(s)ds\right]\int_0^\eta N_A(s)\exp\left[-\int_0^\eta L_A(s_1)ds_1\right]ds. \tag{34}$$

Similarly, the equations (22) can be written in the form

$$V_i'(\eta) + L_i(\eta)V_i(\eta) = 0, \ \ i = 2,3, \tag{35}$$

where

$$V_i(\eta) = \lambda_i u_i(\eta), \tag{36}$$

$$\begin{aligned} L_i(\eta) &= \frac{1}{\eta} + 2a^2 M_i(u_i)\eta, \\ M_i(u_i) &= \frac{c_i(u_i)\gamma_i(u_i)}{\lambda_i(u_i)} \end{aligned} \tag{37}$$

or in equivalent form of integral equations

$$V_2(\eta) = \lambda_b\theta_b - \exp\left[-\int_{\eta}^{\beta_0/2a} L_2(\eta)d\eta\right], \tag{38}$$

$$V_3(\eta) = \lambda_b\theta_b - \exp\left[-\int_{\beta_0/2a}^{\eta} L_2(\eta)d\eta\right]. \tag{39}$$

The integral equations (34), (38), (39) are the equations of the Volterra type, and if the kernels of integral operators are differentiable, then these operators are contraction and the solution can be obtained by the iteration method.

CONCLUSION

1. The non-linear mathematical model of a short arc temperature at its transition from metallic to gaseous stages describes the dynamics of the flow-off repulsion of electrical contacts in a good agreement with experimental data.
2. The dynamics of increase of the radii of interfaces between zones of the phase transformations can be described by the self-similar law.
3. Generalizing of this model for the gaseous arc stage is possible by the replacement of the one-dimensional model of the arc disc for the two-dimensional model of the arc cylinder.

REFERENCES

1. E. Tomas and I. Browne, *Circuit Interruption* (Marcel Dekker, New York, 1984).
2. P. Slade, *Electrical Contacts. Principles and Applications* (CRC Press, Second Edition, 2014).
3. F. Karetta and M. Lindmayer, IEEE Transactions on Components Packaging and Manufacturing Technology, Part A **21(1)**, 95–103 (1998).
4. Xi. Liao, Xu. Zhou, K. Bo, and G. Zhai, 3-D Hydrodynamic Model of Metal Droplet Sputtering and Molten Pool Formation Under Electric Arc, in: Proc. Of 29th ICEC and 64th IEEE Holm Conference on Electrical Contacts, 2018, pp. 56–60.
5. S. N. Kharin, S. A. Kassabek, D. Salybek, and T. Ashymov, News of the National Academy of Sciences of the Republic of Kazakhstan, Physico-Mathematical Series **321(5)**, 19–24 (2018).
6. S. N. Kharin, Mathematical Model of the Short Arc Phenomena at the Initial Stage, in: Proc. 43-th IEEE Holm Conf. on Electrical Contacts, Philadelphia, USA, 1991, pp 289–305.
7. S. N. Kharin, H. Nouri, and M. Bizjak, IEEE Transactions on Components and Packaging Technologies **32(1)**, 180–190 (2009).
8. V. S. Engelsht, *Mathematical Modelling of the Electrical Arc* (ILIM Edition, Frunze, 1983, in Russian).

Weak Solvability of One Problem of Fractional Viscoelasticity Model with Memory

Vladimir P. Orlov[a)]

Voronezh State University, Universitetskaya pl. 1, 394 018 Voronezh, Russia

[a)]*Corresponding author: orlov_vp@mail.ru*

Abstract. We consider the motion of a multidimensional viscoelastic continuum which subjects some fractional constitutive law. The weak solvability of a corresponding initial-boundary value problem is established.

INTRODUCTION

A wide range of deformable media in the one-dimensional case is determined by means of a constitutive equation of the form (see [1])

$$\sum_{k=0}^{n}\sum_{i=0}^{s} a_{ki} D_{0t}^{\beta_{ki}} D^k \sigma = \sum_{k=0}^{m}\sum_{i=0}^{r} b_{ki} D_{0t}^{\beta_{ki}} D^k \varepsilon,\ 0 \le \beta_{ki} < 1. \tag{1}$$

Here ε is the deformation, σ means the stress, D_{0t}^{α} is a fractional Riemann-Liouville derivative of order $\alpha > 0$, $D^k = d^k/dt^k$, $n,s,r,k \in N_+$. In the case of some $\beta_{ki} \in (0,1)$ the equation (1) defines fractional models.

In contrast to the well-studied integer models (see, for example, [2, 3] and references therein), a nonlocal solvability for models with fractional derivatives are known to us only for the simplest fractional models (see [4, 5, 6]).

For some of such models stress tensor σ can be explicitly expressed via the strain rate tensor. Substitution of σ in the momentum equation leads to the appearance of integral terms. These integral terms exhibit the presence of memory in every point in space.

For various reasons, it is more realistic to take into account stresses-strains relation alongside the velocity field trajectories. In the case of a weak solvability this requires to the study of the corresponding Cauchy problem for the system of ODE in Sobolev spaces. The application of *RLF*-theory as well as nonlinear functional analysis and topological methods turns out to be productive to the study of some integer and fractional models (see [5, 7, 8]).

Our goal is to study the weak solvability of the second-grade fractional anti-Zener model (see [1]) with memory along the velocity field trajectories.

STATEMENT OF PROBLEM

We consider the motion of a viscoelastic continuum of a constant density (it is equal to one, for simplicity) occupying a bounded domain $\Omega \subset R^N$, $N = 2,3$, $\partial\Omega \in C^2$ on $Q_T = [0,T] \times \Omega$.

Let $v(t,x)$ be the velocity field of the continuum and $\mathscr{E}(v)$ be the strain rate tensor, i.e. the matrix with elements $\mathscr{E}_{ij}(v) = \frac{1}{2}(\partial v_i/\partial x_j + \partial v_j/\partial x_i)$. Let σ be the deviator of the stress tensor and I be the unit matrix. The multidimensional analogous of one-dimensional anti-Zener model AZ (see [1]) has the form

$$(I + a_1 D_{0t}^{\alpha})\sigma = (b_1 I_{0t}^{1-\alpha} + b_2 D_{0t}^{\alpha})\mathscr{E}(v), \quad 0 < \alpha < 1.$$

Here D_{0t}^{α} and I_{0t}^{α} denote fractional derivatives and integral, respectively.

Let $E(\lambda,t) = t^{\alpha-1}E_{\alpha,\alpha}(-\lambda t^{\alpha})$ where the Mittag–Lefler function $E_{\alpha,\beta}(t)$ is defined by the expression $E_{\alpha,\beta}(t) = \sum_{k=0}^{+\infty} t^k(\Gamma(\alpha k+\beta))^{-1}$, $t \in R^1$. Let

$$R_1(t,\tau) = \frac{1}{\Gamma(1-\alpha)}\int_{\tau}^{t} E(a_1^{-1}, t-s)(s-\tau)^{-\alpha}\, ds, \tag{2}$$

$$R_2(t,\tau) = E(-a_1^{-1}, t-\tau) = (t-\tau)^{\alpha-1}E_{\alpha,\alpha}(-a_1^{-1}(t-\tau)^{\alpha}). \tag{3}$$

International Conference on Analysis and Applied Mathematics (ICAAM 2020)
AIP Conf. Proc. 2325, 020008-1–020008-4; https://doi.org/10.1063/5.0040351
Published by AIP Publishing. 978-0-7354-4069-2/$30.00

The corresponding initial-boundary value problem has the form:

$$\partial v/\partial t+\sum_{i=1}^{N} v_i\partial v/\partial x_i-\mu_0\mathrm{Div}\,\mathscr{E}(v)-\mu_1\mathrm{Div}\int_0^t R_1(t,\tau)\,\mathscr{E}(v)(\tau,z(\tau;t,x))\,d\tau$$
$$-\mu_2\mathrm{Div}\int_0^t R_2(t,\tau)\,\mathscr{E}(v)(\tau,z(\tau;t,x))\,d\tau+\nabla p=f,\ \mathrm{div}\,v=0,\ (t,x)\in Q_T; \tag{4}$$

$$z(\tau;t,x)=x+\int_t^\tau v(s,z(s;t,x))\,ds,\quad 0\le t,\tau\le T,\quad x\in\overline{\Omega}; \tag{5}$$

$$v(0,x)=v^0(x),\ x\in\Omega;\ v|_{[0,T]\times\partial\Omega}=0. \tag{6}$$

The presence of Cauchy problem (5) in (4)–(6) means that the memory along trajectories $z(\tau;t,x)$ of velocity field v is taken into account.

AUXILIARY RESULTS AND NOTATIONS

Let $C_0^\infty(\Omega)^N$ be the set of infinitely differentiable compactly supported mappings of Ω in R^N. Let $\mathscr{V}=\{v: v\in C_0^\infty(\Omega)^N,\ \mathrm{div}\,v=0\}$. Functional spaces H and V (see [9], section III.1.4) are defined as the closure of $\mathscr{V}$ in the spaces $L_2(\Omega)^N$ and $W_2^1(\Omega)^N$, respectively. We denote by V^{-1} the space conjugate to V.

Symbol $\langle f,v\rangle$ means the action of a functional $f\in V^{-1}$ on an element $v\in V$.

Norms in the spaces H and $L_2(\Omega)^N$ will be denoted as $|\cdot|_0$, in V and $W_2^1(\Omega)^N$ as $|\cdot|_1$. Norms in the spaces V^{-1}, $W_2^{-1}(\Omega)^N$ and $W_2^{-1}(\Omega)^{N\times N}$ will be denoted by $|\cdot|_{-1}$. Symbol $(\cdot,\cdot)$ stands for the inner product in the Hilbert spaces $L_2(\Omega)$, H, $L_2(\Omega)^N$, $L_2(\Omega)^{N\times N}$. It is clear from the context in which of them the inner product is taken.

We consider the Cauchy problem (in integral form)

$$z(\tau;t,x)=x+\int_t^\tau v(s,z(s;t,x))\,ds,\quad 0\le t,\tau\le T,\quad x\in\overline{\Omega}. \tag{7}$$

If a vector-valued function $v\in L_1(0,T;C_0^1(\Omega)^N)$ then the problem (7) has nonlocal unique solution in the classical sense (see [10]). However, in the case of a summable vector function v the situation becomes more complicated and one needs to use a more general concept of solution.

Definition 1 *A regular Lagrangian flow (RLF) associated to divergence free v is a function $z(\tau;t,x)$, $(\tau;t,x)\in[0,T]\times[0,T]\times\overline{\Omega}$ which satisfies the following conditions: 1) for a.e. $x\in\Omega$ and every $t\in[0,T]$) function $\gamma(\tau)=z(\tau;t,x)$ is absolutely continuous and satisfies the equation (7); 2) for every $t,\tau\in[0,T]$ and an arbitrary Lebesgue-measurable set B with the Lebesgue measure $m(B)$ the relation $m(z(\tau;t,B))=m(B)$ holds; 3) for every $t_i,\in[0,T], i=1,2,3,$ and a.e. $x\in\overline{\Omega}$ the relation $z(t_3;t_1,x)=z(t_3;t_2,z(t_2;t_1,x))$ is valid.*

The basics of the *RLF* Theory one can find e.g. in [11]. Here we give this definition in the special case of a bounded domain Ω and divergence free field v.

The existence of unique *RLF* is known for $v\in L_1(0,T;W_p^1(\Omega)^N)$ (see [11]).

MAIN RESULTS

Let $W_1(a,b)=\{v:\ v\in L_2(a,b;V)\cap L_\infty(a,b;H),\ v'\in L_1(a,b;V^{-1})\}$. Here v' denotes the derivative with respect to t of a V^{-1}-valued function $v(t)$.

Definition 2 *Let $f \in L_2(0,T;V^{-1})$ and $v^0 \in H$. A weak solution to the problem (4)-(6) is a function $v \in W_1(0,T)$ satisfying the initial condition from (6) and the identity*

$$
\begin{aligned}
d(v,\varphi)/dt - \sum_{i=1}^{N}(v_i v, \partial\varphi/\partial x_i) + \mu_0(\mathscr{E}(v),\mathscr{E}(\varphi)) + \\
\mu_1\Big(\int_0^t R_1(t,\tau)\,\mathscr{E}(v)(\tau, z(\tau;t,\cdot))\,d\tau, \mathscr{E}(\varphi)(\cdot)\Big) + \\
\mu_2\Big(\int_0^t R_2(t,\tau)\,\mathscr{E}(v)(\tau, z(\tau;t,\cdot))\,d\tau, \mathscr{E}(\varphi)(\cdot)\Big) = \langle f,\varphi\rangle
\end{aligned}
\tag{8}
$$

for every $\varphi \in V$ and a.e. $t \in [0,T]$. Here z is the RLF associated to v.

Let us note that since the weak solution $v \in W_1(0,T)$ then there exists the unique *RLF* z associated to v.

Theorem 1 *Let $f \in L_2(0,T;V^{-1})$, $v^0 \in H$. Then the problem (4)–(6) has at least one weak solution.*

SCHEME OF PROOF OF THE MAIN RESULT

Let $S : D(S) \to H$ the Stokes operator, i.e. $S(u) = -\mathscr{P}\triangle u$, $u \in D(S) = W_2^2(\Omega)^N \cap \overset{\circ}{W}{}_2^1(\Omega)^N \cap H$. It is well known that operator S is self-adjoint positively defined in H. Consider the sequence of regularized problems depending on the numerical parameter $n = 1, 2, \ldots$

$$
\begin{aligned}
\partial v^n/\partial t + \sum_{i=1}^{N} v_i^n \partial((1+n^{-1}|v^n|^2)^{-1}v^n)/\partial x_i - \mu_0 \mathrm{Div}\,\mathscr{E}(v^n) \\
-\mu_1 \mathrm{Div}\int_0^t R_1(t,\tau,n)\,\mathscr{E}(v^n)(\tau, z^n(\tau;t,x))\,d\tau \\
-\mu_2 \mathrm{Div}\int_0^t R_2(t,\tau,n)\,\mathscr{E}(v^n)(\tau, z^n(\tau;t,x))\,d\tau + \nabla p^n = f, \quad (t,x) \in Q_T; \\
\mathrm{div}\, v^n = 0; \quad (t,x) \in Q_T; v^n(0,x) = v^0(x), \quad x \in \Omega, \; v^n|_{[0,T]\times\partial\Omega} = 0; \\
z^n(\tau;t,x) = x + \int_t^\tau \tilde{v}^n(s, z^n(s;t,x))\,ds, \quad 0 \le t,\tau \le T, \quad x \in \overline{\Omega}.
\end{aligned}
\tag{9}
$$

Here

$$
R_1(t,\tau,n) = \frac{1}{\Gamma(1-\alpha)}\int_\tau^t E(a_1^{-1}, t-s+n^{-1})(s-\tau+n^{-1})^{-\alpha}\,ds,
\tag{10}
$$

$$
R_2(t,\tau,n) = (t-\tau+n^{-1})^{\alpha-1}E_{\alpha,\alpha}(-a_1^{-1}(t-\tau+n^{-1})^{\alpha}),
\tag{11}
$$

$$
\tilde{v}^n = S_n v^n =: (I+n^{-1}S)^{-1}v^n\tau
\tag{12}
$$

and z^n is the *RLF* associated to the vector field $\tilde{v}^n$.

A weak solution $v^n \in W(0,T)$ to the problem (9) is defined as a function $v \in W(0,T)$ satisfying the initial condition from (9) and the identity

$$
\begin{aligned}
d(v^n,\varphi)/dt - \sum_{i=1}^{N}(v_i^n((1+n^{-1}|v^n|^2)^{-1}v^n, \partial\varphi/\partial x_i) + \mu_0(\mathscr{E}(v^n),\mathscr{E}(\varphi)) \\
+\mu_1\Big(\int_0^t R_1(t,\tau,n))\,\mathscr{E}(v^n)(\tau, z^n(\tau;t,\cdot))\,d\tau, \mathscr{E}(\varphi)(\cdot)\Big) \\
+\mu_2\Big(\int_0^t R_2(t,\tau,n))\,\mathscr{E}(v^n)(\tau, z^n(\tau;t,\cdot))\,d\tau, \mathscr{E}(\varphi)(\cdot)\Big) = \langle f,\varphi\rangle
\end{aligned}
\tag{13}
$$

for every $\varphi \in V$ and a.e. $t \in [0,T]$.

It follows from (12) that $\tilde{v}^n \in W(0,T)$ and therefore there exists *RLF* z^n associated to $\tilde{v}^n$. The weak solvability of problem (9) follows from [10].

Hence, we have constructed the sequence of weak solutions $v^n \in W(0,T)$ to the problems (9).

Next, we establish the validity of estimates

$$\sup_{0\le t\le T} |v^n(t,\cdot)|_0 + \|v^n\|_{L_2(0,T;V)} \le M(\|f\|_{L_2(0,T;V^{-1})} + |v^0|_0), \tag{14}$$

$$\|(v^n)'\|_{L_1(0,T;V^{-1})} \le M(1 + \|f\|_{L_2(0,T;V^{-1})} + |v^0|_0)^2 \tag{15}$$

where constant M that does not depend on n.

It follows from this that we can arrange the sequence v^n, $n = 1,2,\dots$ which converges to some $v \in W_1(0,T)$ weakly in $L_2(0,T;V)$, $*$-weakly in $L_\infty(0,T;H)$, strongly in $L_2(0,T;H)$ and $(v^n)'$ converges to v' in the sense of distributions.

The above mentioned properties of v^n and corresponding convergence properties of z^n (see [11]) allow to pass to the limit in (13) as $n \to +\infty$ and get the weak solution v to problem (4)–(6) .

ACKNOWLEDGMENT

This is a joint work with V.G. Zvyagin. The work was financially supported by the Russian Science Foundation, project No. 19-11-00146 and by the Russian Foundation for Basic Research, grant No. 20-01-00051.

REFERENCES

1. F. Mainardi and G. Spada, The European Physical Journal, Special Topics **193**, 133–160 (2011).
2. V. G. Zvyagin, J. Math. Sciences **124(5)**, 5321–5334 (2004).
3. V. G. Zvyagin and M. V. Turbin, *Mathematical Problems of Hydrodynamics of Viscoelastic Media* (Krassand, 2012, in Russian).
4. V. P. Orlov, D. A. Rode, and M. A. Pliev, Sib. Mat. J. **58(5)**, 1110–1127 (2017).
5. V. G. Zvyagin and V. P. Orlov, Discrete and Continuous Dynamical Systems, Series A **38(12)**, 6327–6350 (2018).
6. V. G. Zvyagin and V. P Orlov, Sib. Mat. J. **59(6)**, 1073–1089 (2018).
7. V. G. Zvyagin and V. P. Orlov, Nonlinear Analysis: TMA **172**, 73–98 (2018).
8. V. Zvyagin and V. Orlov, Discrete and Continuous Dynamical Systems, Series B **23(9)**, 3855–3877 (2018).
9. R. Temam, *Navier-Stokes Equations, Theory and Numerical Analysis* (AMS, Providence, RI, 2000).
10. V. G. Zvyagin and V. T. Dmitrienko, Differ. Equ. **38(1)**, 1731–1744 (2002).
11. G. Crippa and C. de Lellis, J. Reine Angew. Math. **616**, 15–46 (2008).

A Numerical Algorithm for the Hyperbolic Involutory Problem with the Neumann Condition

Allaberen Ashyralyev[1, 2, 3, a)] and Barez Abdalmohammed[1, b)]

[1)] *Department of Mathematics, Near East University, Nicosia, Mersin 10, Turkey*
[2)] *Peoples' Friendship University of Russia (RUDN University), Ul Miklukho Maklaya 6, Moscow 117198, Russian Federation*
[3)] *Institute of Mathematics and Mathematical Modeling, 050010, Almaty, Kazakhstan*

[a)] *Electronic mail: allaberen.ashyralyev@neu.edu.tr*
[b)] *Corresponding author: barez.osman@gmail.com*

Abstract. In the present paper, hyperbolic type involutory partial differential equations with the Neumann condition are studied. The first and second order of accuracy difference schemes for the numerical solution of the initial boundary value problem for one dimensional hyperbolic type involutory partial differential equations are presented. Some numerical results are provided.

INTRODUCTION

In the first time, in an experiment measuring the population growth of a species of water fleas, Nisbet([1]) tried to use delay differential equations with reversal time. He reversed time to get the solution of functional differential equations with given value of unknown function on one point. Such type functional differential equations are called the involutory differential equations. The time reversal problem is the special case of involutory problems.

Involutory partial differential equations have been studied in papers [2, 3]. The numerical algorithm for the solution of the initial boundary value problem for one dimensional partial differential equations was presented. Some numerical results were provided. Moreover, delay hyperbolic differential equations have been investigated by several authors in (see, [4, 5, 6, 7]).

Involutory hyperbolic partial differential equations are not investigated before. The present paper is devoted to study involutory hyperbolic partial differential equations. The first and second order of accuracy absolute stable difference schemes for the numerical solution of the initial boundary value problem for one dimensional involutory hyperbolic differential equations with the Neumann condition are constructed. Some numerical results are explained.

NUMERICAL ALGORITHM

We present the algorithm for the numerical solution of the initial boundary value problem

$$\begin{cases} \frac{\partial^2 u(t,x)}{\partial t^2} - u_{xx}(t,x) - bu_{xx}(-t,x) = -b\sin t\cos(x), \\ x \in (0,\pi), -\pi < t < \pi, \\ u(0,x) = 0, u_t(0,x) = \cos(x),\ x \in [0,\pi], \\ u_x(t,0) = u_x(t,\pi) = 0, t \in [-\pi,\pi] \end{cases} \tag{1}$$

for the one dimensional hyperbolic type involutory partial differential equation with the Neumann condition. The exact solution problem (1) is $u(t,x) = \sin t\cos(x), 0 \le x \le \pi, -\pi \le t \le \pi$. For the construction of the approximate solutions of problem (1), we define sets of grid points

$$[-T,T]_\tau = \{t_k : t_k = k\tau, -N \le k \le N, N\tau = T\},$$

$$[0,l]_h = \{x_n : x_n = nh,\ 0 \le n \le M, Mh = l\},$$

$$[-\pi,\pi]_\tau \times [0,\pi]_h$$

$$= \{(t_k,x_n) : t_k = k\tau, -N \le k \le N, N\tau = \pi, x_n = nh,\ 0 \le n \le M, Mh = \pi\}.$$

The construction difference schemes is based on Taylors decomposition on three points.

International Conference on Analysis and Applied Mathematics (ICAAM 2020)
AIP Conf. Proc. 2325, 020009-1–020009-5; https://doi.org/10.1063/5.0040291
Published by AIP Publishing. 978-0-7354-4069-2/$30.00

Theorem 1 ([8]) *Let the function $v(t)$ have a fourth order continuous derivative and $t_k, t_{k\pm1} \in [-T,T]_\tau$. Then the following relation holds*

$$v(t_{k+1})-2v(t_k)+v(t_{k-1})=\tau^2 v''(t_{k+1})+o(\tau^3), \tag{2}$$

$$v(t_{k+1})-2v(t_k)+v(t_{k-1})=\frac{\tau^2}{2}v''(t_k)+\frac{\tau^2}{4}\left[v''(t_{k+1})+v''(t_{k-1})\right]+o(\tau^4). \tag{3}$$

Now, we will give well-known approximation formulas for first and second order derivative for smooth functions

$$u''(x_n)=\frac{u(x_{n+1})-2u(x_n)+u(x_{n-1})}{h^2}+o(h^2), \tag{4}$$

$$\begin{cases} u'(0)=\frac{-u(2h)+4u(h)-3u(0)}{2h}+o(h^2), \\ u'(\pi)=\frac{u(\pi-2h)-4u(\pi-h)+3u(\pi)}{2h}+o(h^2), \end{cases} \tag{5}$$

$$v'(0)=\begin{cases} \frac{v(\tau)-v(0)}{\tau}+o(\tau), \\ \frac{-v(2\tau)+4v(\tau)-3v(0)}{2\tau}+o(\tau^2). \end{cases} \tag{6}$$

Applying formulas (2), (3), (4), (5) and (6), we present the following first order of accuracy difference scheme

$$\begin{cases} \frac{u_n^{k+1}-2u_n^k+u_n^{k-1}}{\tau^2}-\frac{u_{n+1}^{k+1}-2u_n^{k+1}+u_{n-1}^{k+1}}{h^2}-b\frac{u_{n+1}^{-k-1}-2u_n^{-k-1}+u_{n-1}^{-k-1}}{h^2} \\ =-b\sin t_{k+1}\cos(x_n), \\ -N+1\le k\le N-1,\ \ 1\le n\le M-1, \\ u_n^0=0, \frac{u_n^1-u_n^0}{\tau}=\cos x_n,\ 0\le n\le M, \\ u_1^k-u_0^k=0,\ u_M^k-u_{M-1}^k=0,\ -N\le k\le N \end{cases} \tag{7}$$

and second of accuracy difference scheme

$$\begin{cases} \frac{u_n^{k+1}-2u_n^k+u_n^{k-1}}{\tau^2}-\frac{u_{n+1}^{k}-2u_n^{k}+u_{n-1}^{k}}{2h^2}-\frac{u_{n+1}^{k+1}-2u_n^{k+1}+u_{n-1}^{k+1}}{4h^2} \\ -\frac{u_{n+1}^{k-1}-2u_n^{k-1}+u_{n-1}^{k-1}}{4h^2}-b\frac{u_{n+1}^{-k}-2u_n^{-k}+u_{n-1}^{-k}}{2h^2}-b\frac{u_{n+1}^{-k+1}-2u_n^{-k+1}+u_{n-1}^{-k+1}}{4h^2} \\ -b\frac{u_{n+1}^{-k-1}-2u_n^{-k-1}+u_{n-1}^{-k-1}}{4h^2}=-b\sin t_k\cos x_n, \\ -N+1\le k\le N-1,\ \ 1\le n\le M-1, \\ u_n^0=0, \frac{-u_n^2+4u_n^1-3u_n^0}{2\tau}=\cos x_n,\ 0\le n\le M, \\ -u_2^k+4u_1^k-3u_0^k=0,\ -3u_M^k+4u_{M-1}^k-u_{M-2}^k=0,\ -N\le k\le N \end{cases} \tag{8}$$

for the approximate solution of problem (1)
They are systems of algebraic equations and they can be written in the matrix form

$$\begin{cases} Au_{n-1}+Bu_n+Cu_{n+1}=D\varphi_n,\ 1\le n\le M-1, \\ u_0=u_1,\ \ u_M=u_{M-1} \end{cases} \tag{9}$$

for difference scheme (7) and

$$\begin{cases} Au_{n-1}+Bu_n+Cu_{n+1}=D\varphi_n,\ 1\le n\le M-1, \\ 3u_0=4u_1-u_2,\ \ 3u_M=4u_{M-1}-u_{M-2} \end{cases} \tag{10}$$

for difference scheme (8). Here A,B,C are $(2N+1)\times(2N+1)$ matrices and $D=I_{2N+1}$ is the identity matrix, φ_n and u_s are $(2N+1)\times 1$ column vectors

$$D\varphi_n = \begin{bmatrix} 0 \\ \tau\cos x_n \\ -b\sin t_{-N+1}\cos(x_n) \\ \cdot \\ -b\sin t_{N-1}\cos(x_n) \end{bmatrix}_{(2N+1)\times 1}, \quad u_s = \begin{bmatrix} u_s^{-N} \\ u_s^{-N+1} \\ \cdot \\ u_s^{N-1} \\ u_s^{N} \end{bmatrix}_{(2N+1)\times 1}$$

and

$$A=C=\begin{bmatrix}
0&0&0&0&\cdot&0&0&0&\cdot&0&0&0&0\\
0&0&0&0&\cdot&0&0&0&\cdot&0&0&0&0\\
0&0&a&0&\cdot&0&0&0&\cdot&0&d&0&0\\
0&0&0&a&\cdot&0&0&0&\cdot&d&0&0&0\\
\cdot&\cdot&\cdot&\cdot&\cdot&\cdot&\cdot&\cdot&\cdot&\cdot&\cdot&\cdot&\cdot\\
0&0&0&0&\cdot&a&0&d&\cdot&0&0&0&0\\
0&0&0&0&\cdot&0&a+d&0&\cdot&0&0&0&0\\
0&0&0&0&\cdot&d&0&a&\cdot&0&0&0&0\\
\cdot&\cdot&\cdot&\cdot&\cdot&\cdot&\cdot&\cdot&\cdot&\cdot&\cdot&\cdot&\cdot\\
0&0&d&0&\cdot&0&0&0&\cdot&0&a&0&0\\
0&d&0&0&\cdot&0&0&0&\cdot&0&0&a&0\\
d&0&0&0&\cdot&0&0&0&\cdot&0&0&0&a
\end{bmatrix}_{(2N+1)\times(2N+1)},$$

$$B=\begin{bmatrix}
0&0&0&0&\cdot&0&1&0&\cdot&0&0&0&0\\
0&0&0&0&\cdot&0&-1&1&\cdot&0&0&0&0\\
b&c&e&0&\cdot&0&0&0&\cdot&0&f&0&0\\
0&b&c&e&\cdot&0&0&0&\cdot&f&0&0&0\\
\cdot&\cdot&\cdot&\cdot&\cdot&\cdot&\cdot&\cdot&\cdot&\cdot&\cdot&\cdot&\cdot\\
0&0&0&0&\cdot&e&0&f&\cdot&0&0&0&0\\
0&0&0&0&\cdot&c&e+f&0&\cdot&0&0&0&0\\
0&0&0&0&\cdot&b+f&c&e&\cdot&0&0&0&0\\
\cdot&\cdot&\cdot&\cdot&\cdot&\cdot&\cdot&\cdot&\cdot&\cdot&\cdot&\cdot&\cdot\\
0&0&f&0&\cdot&0&0&0&\cdot&c&e&0&0\\
0&f&0&0&\cdot&0&0&0&\cdot&b&c&e&0\\
f&0&0&0&\cdot&0&0&0&\cdot&0&b&c&e
\end{bmatrix}_{(2N+1)\times(2N+1)},$$

$a=-\frac{1}{h^2}, b=\frac{1}{\tau^2}, c=-\frac{2}{\tau^2}, d=-\frac{b}{h^2}, e=\frac{1}{\tau^2}+\frac{2}{h^2}$ and $f=\frac{2b}{h^2}$ for the difference scheme (7) and

$$A=\begin{bmatrix}
0&0&0&0&\cdot&0&0&0&\cdot&0&0&0&0\\
0&0&0&0&\cdot&0&0&0&\cdot&0&0&0&0\\
b&a&b&0&\cdot&0&0&0&\cdot&0&d&c&d\\
0&b&a&b&\cdot&0&0&0&\cdot&d&c&d&0\\
\cdot&\cdot&\cdot&\cdot&\cdot&\cdot&\cdot&\cdot&\cdot&\cdot&\cdot&\cdot&\cdot\\
0&0&0&0&\cdot&a&b+d&c&\cdot&0&0&0&0\\
0&0&0&0&\cdot&b+d&a+c&b+d&\cdot&0&0&0&0\\
0&0&0&0&\cdot&c&b+d&a&\cdot&0&0&0&0\\
\cdot&\cdot&\cdot&\cdot&\cdot&\cdot&\cdot&\cdot&\cdot&\cdot&\cdot&\cdot&\cdot\\
0&0&d&c&\cdot&0&0&0&\cdot&b&a&0&0\\
0&d&c&d&\cdot&0&0&0&\cdot&b&a&b&0\\
d&c&d&0&\cdot&0&0&0&\cdot&0&b&a&b
\end{bmatrix}_{(2N+1)\times(2N+1)}$$

$$B=\begin{bmatrix} 0&0&0&0&\cdot&1&0&0&\cdot&0&0&0&0\\ 0&0&0&0&\cdot&-3&4&-1&\cdot&0&0&0&0\\ f&e&f&0&\cdot&0&0&0&\cdot&0&t&g&t\\ 0&f&e&f&\cdot&0&0&0&\cdot&t&g&t&0\\ \cdot&\cdot&\cdot&\cdot&\cdot&\cdot&\cdot&\cdot&\cdot&\cdot&\cdot&\cdot&\cdot\\ 0&0&0&0&\cdot&e&f+t&g&\cdot&0&0&0&0\\ 0&0&0&0&\cdot&f+t&e+g&f+t&\cdot&0&0&0&0\\ 0&0&0&0&\cdot&g&f+t&e&\cdot&0&0&0&0\\ \cdot&\cdot&\cdot&\cdot&\cdot&\cdot&\cdot&\cdot&\cdot&\cdot&\cdot&\cdot&\cdot\\ 0&0&d&c&\cdot&0&0&0&\cdot&e&f&0&0\\ 0&d&c&d&\cdot&0&0&0&\cdot&f&e&f&0\\ d&c&d&0&\cdot&0&0&0&\cdot&0&f&e&f \end{bmatrix}_{(2N+1)\times(2N+1)}$$

$a=\frac{-1}{2h^2}, b=-\frac{1}{4h^2}, c=\frac{-b}{2h^2}, d=\frac{-b}{4h^2}, e=-\frac{2}{\tau^2}+\frac{1}{h^2}, f=\frac{1}{\tau^2}+\frac{1}{2h^2}, g=\frac{b}{h^2}$ and $t=\frac{b}{2h^2}$ for the difference scheme (8). For the solutions of (9), we will apply modified Gauss elimination method by the following form

$$u_n=\alpha_{n+1}u_{n+1}+\beta_{n+1},\quad n=M-1,...,1,$$

where $u_M=(I-\alpha_M)^{-1}\beta_M$, $\alpha_j\ \ (j=1,...,M-1)$ are $(2N+1)\times(2N+1)$ square matrices, $\beta_j\ \ (j=1,...,M-1)$ are $(2N+1)\times 1$ column matrices,$\alpha_1=I$, $\beta_1$is zero matrices and

$$\begin{cases}\alpha_{n+1}=-(B+C\alpha_n)^{-1}A,\\ \beta_{n+1}=(B+C\alpha_n)^{-1}(D\varphi_n+C\beta_n),\ n=1,...,M-1.\end{cases}$$

For the solutions of (10), we will apply same modified Gauss elimination method by formula

$$u_n=\alpha_{n+1}u_{n+1}+\beta_{n+1},\quad n=M-1,...,1,$$

$$u_M=((B+4A)\alpha_M+C-3A)^{-1}\{-(B+4A)\beta_M+D\varphi_{M-1}\},$$

where $\alpha_j\ \ (j=1,...,M-1)$ are $(2N+1)\times(2N+1)$ square matrices, $\beta_j\ \ (j=1,...,M-1)$ are $(2N+1)\times 1$ column matrices defined by formula
,$\alpha_1=-(A-3C)^{-1}(B+4C)$, $\beta_1=(A-3C)^{-1}D\varphi_1$ and

$$\begin{cases}\alpha_{n+1}=-(B+C\alpha_n)^{-1}A, \alpha_1=-(A-3C)^{-1}(B+4C),\\ \beta_{n+1}=(B+C\alpha_n)^{-1}(D\varphi_n+C\beta_n), \beta_1=(A-3C)^{-1}D\varphi_1\\ n=1,...,M-1.\end{cases}$$

NUMERICAL ANALYSIS

The different values of N and M are recorded to the numerical solutions, and u_n^k represents the numerical solution of these difference schemes at $u(t_k,x_n)$. Table I is established for $N=M=40,80,160$ respectively and the errors are found by

$$E_M^N=\max_{-N\le k\le N,\ 0\le n\le M}|u(t_k,x_n)-u_n^k|. \tag{12}$$

If N and M are doubled, the values of the errors between the exact and approximate solution are decreases by a factor of approximately $1/2$ for the first order difference scheme (7) and $1/4$ for the second order of accuracy scheme (8). We presented the errors in this table and it shows the accuracy of difference schemes. The accuracy increases with the second order approximation.

TABLE 1. Error Analysis E_M^N

Difference schemes/$N=M$	40	80	160
(7)	0.0874	0.0365	0.0163
(8)	0.0080	0.0020	$5.0452e-04$

REFERENCES

1. R. M. Nisbet, "Delay-differential equations for structured populations," in *Structured-Population Models in Marine, Terrestrial, and Freshwater Systems*, edited by S. Tuljapurkar and H. Caswell (Springer US, Boston, MA, 1997) pp. 89–118.
2. A. Ashyralyev and A. M. Saeed Ahmed, AIP Conference Proceedings **2183**, 070010 (2019).
3. A. Ashyralyev and T. Abbas, AIP Conference Proceedings **2183**, 070015 (2019).
4. A. Ashyralyev and D. Agirseven, MDPI **7(12)**, 1-38 (2019).
5. N.Son and H. Thao, Journal of Intelligent and Fuzzy Systems **36(6)**, 6295-6306 (2019).
6. A. Ashyralyev and A. M. Sarsenbi, Stability of a hyperbolic equation with the involution, in: Springer Proceedings in Mathematics & Statistics **216(2019)**, pp 204-212. Springer.
7. Q. Zhang and C. Zhang, International Journal of Computer Mathematics **91(5)**, 964-982 (2014).
8. A. Ashyralyev and P. E. Sobolevskii, *New Difference Schemes for Partial Differential Equations* (Birkhauser Verlag, Basel, Boston, Berlin, 2004).

New Numerical Approach for Solving the Oseen Problem in a Convection Form in Non-convex Domain

Viktor A. Rukavishnikov[1, a)] and Alexey V. Rukavishnikov[2, b)]

[1)] *Computing Center of Far-Eastern Branch, Russian Academy of Sciences, Khabarovsk, Russia*

[2)] *Institute of Applied Mathematics of Far-Eastern Branch, Russian Academy of Sciences, Khabarovsk, Russia*

[a)] *Corresponding author: vark0102@mail.ru*
[b)] *Electronic mail: 78321a@mail.ru*

Abstract. In the paper, we consider stationary, linearized by Picard's iterations, Navier-Stokes equations governing the flow of a incompressible viscous fluid in the convection form in non-convex polygonal domain. An R_ν-generalized solution of the problem is defined. A weighted finite element method for finding an approximate R_ν-generalized solution is constructed. Numerically shown that the convergence rate does not depend on a value of the reentrant corner in the norm of the weighted Sobolev space.

INTRODUCTION

In the paper, we consider stationary, linearized by Picard's iterations, Navier-Stokes equations governing the flow of a incompressible viscous fluid in the convection form in non-convex polygon domain. An R_ν-generalized solution [1, 2, 3, 4, 5, 6] of the problem is defined. It is well known that for the well-posedness of the incompressible flow problem, the Ladyzhenskaya-Babuška-Brezzi (LBB) condition plays important role. We formulate and prove the weighted analogue of this condition in [7]. A weighted finite element method (see [7, 8, 9, 10, 11, 12]) for finding an approximate R_ν-generalized solution is constructed. A specially selected combination of them leads to an increase the order of convergence rate of an approximate solution to the exact one in relation to the classical finite element methods (FEM) or finite different schemes. The convergence rate is equal to one by the grid step in the norm of Sobolev weight space $\boldsymbol{W}^1_{2,\nu}(\Omega)$. Another advantage of this method is the simplicity of the solution determination which is an additional benefit for the numerical experiments.

PROBLEM STATEMENT. THE DEFINITION OF AN R_ν-GENERALIZED SOLUTION

Let $\boldsymbol{x} = (x_1, x_2)$ be an element of $\mathbb{R}^2$, where $d\boldsymbol{x} = dx_1\,dx_2$ and $\|\boldsymbol{x}\| = \sqrt{x_1^2 + x_2^2}$ are the measure and norm of $\boldsymbol{x}$, respectively. Let $\Omega \subset \mathbb{R}^2$ be a bounded domain with a boundary Γ, $\bar{\Omega} = \Omega \cup \Gamma$.

We write incompressible Navier-Stokes equations: find the velocity field $\boldsymbol{u} \equiv \boldsymbol{u}(\boldsymbol{x},t) = (u_1(\boldsymbol{x},t), u_2(\boldsymbol{x},t))$ and kinematic pressure $p \equiv p(\boldsymbol{x},t)$ which satisfy the system of differential equations, boundary and initial conditions

$$\frac{\partial \boldsymbol{u}}{\partial t} - \bar{\nu}\triangle\boldsymbol{u} + (\boldsymbol{u}\cdot\nabla)\boldsymbol{u} + \nabla p = \hat{\boldsymbol{f}}, \qquad \operatorname{div}\boldsymbol{u} = 0 \qquad \text{in} \qquad \Omega\times(0,T], \tag{1}$$

$$\boldsymbol{u} = \boldsymbol{g} \qquad \text{on} \qquad \Gamma\times(0,T], \qquad \boldsymbol{u}(\boldsymbol{x},0) = \boldsymbol{u}_0 \qquad \text{in} \qquad \Omega \tag{2}$$

with given force field $\hat{\boldsymbol{f}} = \hat{\boldsymbol{f}}(\boldsymbol{x},t)$ in $\Omega\times(0,T]$, $\boldsymbol{u}_0 = \boldsymbol{u}_0(\boldsymbol{x})$ in Ω, $\boldsymbol{g} = \boldsymbol{g}(\boldsymbol{x},t)$ on $\Gamma\times(0,T]$ and viscosity $\bar{\nu} > 0$. Let $\triangle, \nabla$ and div be the Laplace, gradient and divergence operators, respectively.

Using implicit time integration and linearization by Picard's iterative procedure of Eq. (1) (see [13]) we have

$$-\bar{\nu}\triangle\boldsymbol{u} + \alpha\,\boldsymbol{u} + \beta(\operatorname{curl}\boldsymbol{U}\times\boldsymbol{u}) + \eta\,(\boldsymbol{U}\cdot\nabla)\boldsymbol{u} + \nabla P = \boldsymbol{f}, \qquad \operatorname{div}\boldsymbol{u} = 0 \qquad \text{in} \qquad \Omega, \tag{3}$$

where $\boldsymbol{U} = (U_1, U_2)$ is approximation to $\boldsymbol{u} = (u_1, u_2)$, $\boldsymbol{f}$ is reformed force field. If a) $\alpha > 0, \beta = 1, \eta = 0, P = p + \frac{1}{2}\boldsymbol{u}^2$, $\operatorname{curl}\boldsymbol{U} = -\frac{\partial U_1}{\partial x_2} + \frac{\partial U_2}{\partial x_1}$, $a\times\boldsymbol{u} = (-au_2, au_1)^T$ we have the Oseen problem in a rotation form; b) $\alpha = \beta = \eta = 0, P = p$ — the Stokes problem; c) $\alpha > 0, \beta = 0, \eta = 1, P = p$ — the Oseen problem in a convection form.

The effective numerical approaches to solve a) and b) problems in non-convex polygonal domains were constructed and studied in [12] and [7, 11], respectively. In our research, we solve the system of Eq. (3) with the conditions c), i.

International Conference on Analysis and Applied Mathematics (ICAAM 2020)
AIP Conf. Proc. 2325, 020010-1–020010-6; https://doi.org/10.1063/5.0040324
Published by AIP Publishing. 978-0-7354-4069-2/$30.00

e.

$$-\bar{\nu}\triangle \boldsymbol{u}+\alpha \boldsymbol{u}+(\boldsymbol{U}\cdot\nabla)\boldsymbol{u}+\nabla P=\boldsymbol{f}, \qquad \text{div}\, \boldsymbol{u}=0 \quad \text{in} \quad \Omega, \qquad \boldsymbol{u}=\boldsymbol{g} \quad \text{on} \quad \Gamma, \tag{4}$$

where domain Ω has one internal corner greater than π on Γ with its vertex placed at the origin.

Denote by $\Omega_\delta^{'}=\{\boldsymbol{x}\in\bar{\Omega}:\|\boldsymbol{x}\|\le\delta<1,\delta>0\}$ the part of a δ-neighborhood of the origin that lies in $\bar{\Omega}$. Let $\rho(\boldsymbol{x})$ be a weight function: $\rho(\boldsymbol{x})=\{\|\boldsymbol{x}\|,\boldsymbol{x}\in\Omega_\delta^{'},\delta,\boldsymbol{x}\in\bar{\Omega}\setminus\Omega_\delta^{'}\}$. Let $L_{2,\gamma}(\Omega)$ and $W_{2,\gamma}^1(\Omega)$ be weighted spaces of functions $w(\boldsymbol{x})$ with bounded norms

$$\|w\|^2_{L_{2,\gamma}(\Omega)}=\int_\Omega \rho^{2\gamma}w^2 d\boldsymbol{x} \quad \text{and} \quad \|w\|^2_{W^1_{2,\gamma}(\Omega)}=\sum\nolimits_{|m|\le 1}\|\rho^\gamma|D^m w|\|^2_{L_2(\Omega)}, \tag{5}$$

respectively, where $D^m w=\frac{\partial^{|m|}w}{\partial x_1^{m_1}\partial x_2^{m_2}}$ $|m|=m_1+m_2, m_j\ge 0, j=1,2$ – integer and $\gamma\ge 0$. For $\boldsymbol{w}=(w_1,w_2)$ we define spaces $\boldsymbol{L}_{2,\gamma}(\Omega)$ and $\boldsymbol{W}^1_{2,\gamma}(\Omega)$ with norms $\|\boldsymbol{w}\|^2_{\boldsymbol{L}_{2,\gamma}(\Omega)}=\sum\limits_{j=1}^{2}\|w_j\|^2_{L_{2,\gamma}(\Omega)}$ and $\|\boldsymbol{w}\|^2_{\boldsymbol{W}^1_{2,\gamma}(\Omega)}=\sum\limits_{j=1}^{2}\|w_j\|^2_{W^1_{2,\gamma}(\Omega)}$, respectively. Let $W^1_{2,\gamma}(\Omega,\delta),\gamma>0$, be a set of function $w(\boldsymbol{x})$ from the space $W^1_{2,\gamma}(\Omega)$ with a bounded appropriate norm (5) satisfying the inequalities

$$\int_{\Omega\setminus\Omega_\delta^{'}}\rho^{2\gamma}w^2 d\boldsymbol{x}\ge C_1>0, \qquad |D^s w(\boldsymbol{x})|\le C_2\Big(\frac{\delta}{\rho(\boldsymbol{x})}\Big)^{\gamma+s} \quad \boldsymbol{x}\in\Omega_\delta^{'}, \qquad s=0,1, \tag{6}$$

where $C_2>0$ be a constant independent of s. Denote by $L_{2,\gamma}(\Omega,\delta)$ a set of functions from a space $L_{2,\gamma}(\Omega)$ satisfying inequalities (6) (for $s=0$) with a bounded appropriate norm (5). Let $L^0_{2,\gamma}(\Omega,\delta)=\{w\in L_{2,\gamma}(\Omega,\delta):\int_\Omega\rho^\gamma w d\boldsymbol{x}=0\}$. Denote by $W^{1,0}_{2,\gamma}(\Omega,\delta)(W^{1,0}_{2,\gamma}(\Omega,\delta)\subset W^1_{2,\gamma}(\Omega,\delta))$ a closure, with respect to the appropriate norm in (5), of infinitely-differentiable compactly supported functions in Ω, that satisfy (6). Let $W^{1/2}_{2,\gamma}(\Gamma,\delta)$ be a set of functions $\varphi(\boldsymbol{x})$ on Γ: $\varphi(\boldsymbol{x})\in W^{1/2}_{2,\gamma}(\Gamma,\delta)$ if there exists an extension $\Phi(\boldsymbol{x})$ in Ω from a set $W^1_{2,\gamma}(\Omega,\delta)$ so that $\Phi(\boldsymbol{x})|_\Gamma=\varphi(\boldsymbol{x})$, $\|\varphi\|_{W^{1/2}_{2,\gamma}(\Gamma,\delta)}=\inf_{\Phi|_\Gamma=\varphi}\|\Phi\|_{W^1_{2,\gamma}(\Omega)}$. If $\boldsymbol{w}=(w_1,w_2)$, then we define sets $\boldsymbol{W}^1_{2,\gamma}(\Omega,\delta)=\{\boldsymbol{w}:w_j\in W^1_{2,\gamma}(\Omega,\delta)\}$ and $\boldsymbol{L}_{2,\gamma}(\Omega,\delta)=\{\boldsymbol{w}:w_j\in L_{2,\gamma}(\Omega,\delta)\}$ with the norms of spaces $\boldsymbol{W}^1_{2,\gamma}(\Omega)$ and $\boldsymbol{L}_{2,\gamma}(\Omega)$, respectively. Similarly, we define sets $\boldsymbol{W}^{1,0}_{2,\gamma}(\Omega,\delta)$ and $\boldsymbol{W}^{1/2}_{2,\gamma}(\Gamma,\delta)$ in Ω and Γ, respectively. Known functions $\boldsymbol{U},\boldsymbol{f}$ and $\boldsymbol{g}$ in (2), (4) satisfy the conditions

$$\boldsymbol{U}\in\boldsymbol{W}^1_{2,\gamma}(\Omega,\delta), \qquad \boldsymbol{f}\in\boldsymbol{L}_{2,\gamma}(\Omega,\delta), \qquad \boldsymbol{g}\in\boldsymbol{W}^{1/2}_{2,\gamma}(\Gamma,\delta), \qquad \gamma\ge 0. \tag{7}$$

Define the bilinear and linear forms

$$a_\nu(\boldsymbol{u},\boldsymbol{v})=\int_\Omega\Big[\alpha\rho^{2\nu}\,\boldsymbol{u}\cdot\boldsymbol{v}+\bar{\nu}\nabla\boldsymbol{u}\cdot\nabla(\rho^{2\nu}\,\boldsymbol{v})+\rho^{2\nu}(\boldsymbol{U}\cdot\nabla)\boldsymbol{u}\cdot\boldsymbol{v}\Big]d\boldsymbol{x},$$

$$b_\nu(\boldsymbol{v},P)=-\int_\Omega P\ \text{div}\,(\rho^{2\nu}\boldsymbol{v})d\boldsymbol{x}, \qquad c_\nu(\boldsymbol{u},q)=-\int_\Omega \text{div}\,\boldsymbol{u}\,(\rho^{2\nu}\,q)\,d\boldsymbol{x}, \qquad l_\nu(\boldsymbol{v})=\int_\Omega\rho^{2\nu}\,\boldsymbol{f}\cdot\boldsymbol{v}d\boldsymbol{x}.$$

Definition 1 *The pair* $(\boldsymbol{u}_\nu,P_\nu)\in\boldsymbol{W}^1_{2,\nu}(\Omega,\delta)\times L^0_{2,\nu}(\Omega,\delta)$ *is called an* R_ν*-generalized solution of the Oseen problem in a convection form (4),* $\boldsymbol{u}_\nu$ *satisfies a condition (2) on* Γ*, if integral equalities*

$$a_\nu(\boldsymbol{u}_\nu,\boldsymbol{v})+b_\nu(\boldsymbol{v},P_\nu)=l_\nu(\boldsymbol{v}), \qquad c_\nu(\boldsymbol{u}_\nu,q)=0$$

hold for all pairs $(\boldsymbol{v},q)\in\boldsymbol{W}^{1,0}_{2,\nu}(\Omega,\delta)\times L^0_{2,\nu}(\Omega,\delta)$ *and given functions* $\boldsymbol{U}$, $\boldsymbol{f}$ *and* $\boldsymbol{g}$*, which satisfying (7) and* $\nu\ge\gamma$.

THE WEIGHTED FINITE ELEMENT METHOD

Now we construct a finite element scheme for the Oseen system (4), (2). We use the triangulation T_h which is barycenter refinement of a quasi-uniform triangulation Υ_h of $\bar{\Omega}$. First, we divide $\bar{\Omega}$ into a finite quantity of triangles L_i with sides of order h, L_i we call macro-elements. Second, we divide each $L_i\in\Upsilon_h$ into triangles K_{i_1},K_{i_2} and K_{i_3} using the barycenter of $L_i,K_{i_j}\in T_h$. So that, $\Omega_h=\bigcup_{L_i\in\Upsilon_h}L_i=\bigcup_{L_i\in\Upsilon_h}\big(\bigcup_{j=1}^3 K_{i_j}\big)=\bigcup_{K_s\in T_h}K_s$.

TABLE 1. The behavior of the error $\|\boldsymbol{u}-\boldsymbol{u}^h\|_{\boldsymbol{W}_2^1(\Omega_i)}$ of the generalized solution for different reentrant corners ω.

N ω	74	148	296
1.125π	8.157e-2	4.672e-2	2.703e-2
1.25π	2.013e-1	1.251e-1	7.849e-2
1.5π	3.649e-1	2.488e-1	1.707e-1

Let A_l and B_k be vertices and midpoints of the K_{i_j} sides, respectively. Then, 1) $Y_h = Y_h^\Omega \cup Y_h^\Gamma = \{A_l \cup B_k\}$, where Y_h^Ω and Y_h^Γ are sets of nodes for the velocity components in Ω and Γ, respectively; 2) $Z_h = \{N_i\}$ is a set of nodes for the pressure, where a node N_i coincides with a node A_l on the corresponding K_{i_j}. Now, we use Scott-Vogelius element pair [14], i. e. polynomials of second and first degrees to approximate the velocity components and pressure respectively: $S^h = \{w^h \in C(\Omega) : w^h|_K \in P_2(K), \forall K \in T_h\}$ and $G^h = \{q^h \in L_2(\Omega) : q^h|_K \in P_1(K), \forall K \in T_h\}$. Then, we define special sets of basis functions and describe a weighted finite element scheme. Nodes $M_s \in Y_h^\Omega$ and $N_m \in Z_h$ are associated with functions $\theta_s(\boldsymbol{x}) = \rho^{\nu^*}(\boldsymbol{x}) \cdot \varphi_s(\boldsymbol{x})$ and $\chi_m(\boldsymbol{x}) = \rho^{\mu^*}(\boldsymbol{x}) \cdot \psi_m(\boldsymbol{x}), s,m = 0,1,\ldots,$ $\varphi_s(\boldsymbol{x}) \in S^h, \varphi_s(M_j) = \delta_{sj}$ and $\psi_m(\boldsymbol{x}) \in G^h, \psi_m(N_j) = \delta_{mj}$, $s,m,j = 0,1,\ldots,$ where δ_{sj} is Kronecker delta, ν^* and μ^* are real constants.

Let V^h be a set of functions for the velocity components. If $\boldsymbol{w}_\nu(\boldsymbol{x}) = (w_{\nu,1}^h(\boldsymbol{x}), w_{\nu,2}^h(\boldsymbol{x})), w_{\nu,i}^h(\boldsymbol{x}) \in V^h$, then

$$w_{\nu,1}^h(\boldsymbol{x}) = \sum_k r_k^1 \cdot \theta_k(\boldsymbol{x}), \qquad w_{\nu,2}^h(\boldsymbol{x}) = \sum_k r_k^2 \cdot \theta_k(\boldsymbol{x}), \qquad r_k^i = \rho^{-\nu^*}(M_k) \cdot \hat{r}_k^i,\ i = 1,2. \tag{8}$$

Let V_0^h be a subset of V^h, such that $V_0^h = \{w^h \in V^h : w^h(M_k)|_{M_k \in Y_h^\Gamma} = 0\}$. Denote by Q^h a set of functions for a pressure. If $q_\nu^h(\boldsymbol{x}) \in Q_h$, then

$$q_\nu^h(\boldsymbol{x}) = \sum_l t_l \cdot \chi_l(\boldsymbol{x}), \qquad t_l = \rho^{-\mu^*}(N_l) \cdot \hat{t}_l. \tag{9}$$

Let $\boldsymbol{V}^h = V^h \times V^h, \boldsymbol{V}_0^h = V_0^h \times V_0^h$ and $\boldsymbol{V}^h \subset \boldsymbol{W}_{2,\nu}^1(\Omega_h,\delta), \boldsymbol{V}_0^h \subset \boldsymbol{W}_{2,\nu}^{1,0}(\Omega_h,\delta), Q^h \subset L_{2,\nu}^0(\Omega_h,\delta)$. The coefficients r_k^i and t_l in (8) and (9) are defined as a solution of a system (10) (see Definition 2 below) and coefficients $\hat{r}_k^i$ and $\hat{t}_l$ in (8) and (9) are the values at the nodes $M_k \in Y_h^\Omega$ and $N_l \in Z_h$, respectively.

Definition 2 *The pair $(\boldsymbol{u}_\nu^h, P_\nu^h) \in \boldsymbol{V}^h \times Q^h$ produced by the weighted FEM is called an approximate R_ν-generalized solution of the Oseen problem in a convection form (4), $\boldsymbol{u}_\nu^h$ satisfies a condition (2) at the nodes on Γ, if integral equalities*

$$a_\nu(\boldsymbol{u}_\nu^h, \boldsymbol{v}^h) + b_\nu(\boldsymbol{v}^h, P_\nu^h) = l_\nu(\boldsymbol{v}^h), \qquad c_\nu(\boldsymbol{u}_\nu^h, q^h) = 0 \tag{10}$$

hold for all pairs $(\boldsymbol{v}^h, q^h) \in \boldsymbol{V}_0^h \times Q^h$ and given functions $\boldsymbol{U}, \boldsymbol{f}$ and $\boldsymbol{g}$, which satisfying (7) and $\nu \geq \gamma$.

RESULTS OF NUMERICAL EXPERIMENTS

We present the results of numerical experiments to shaw advantage of our method to the Oseen problem (4), (2). Let $\Omega_i = (-1,1) \times (-1,1) \setminus \bar{\Xi}_i$ (see Figs. 1-2) be non-convex polygon domains with one internal corner ω_i greater than π: $\omega_1 = 1.125\pi, \omega_2 = 1.25\pi, \omega_3 = 1.5\pi$ on its boundary with the vertex located at the origin. We divide $\bar{\Omega}_i$ into a set of triangles $L_m \in T_h$, where L_m be a half of a square of the side h for $\omega_i, i = 2,3$, and a half of a closed square of the side h in $\bar{D}_1$, $D_1 = (-1,1) \times (0,1)$ and a half of a rectangle with sides h and $0.5h$ in $\bar{\Omega}_1 \setminus D_1$ for a corner ω_1. Denote by N the positive even number, so that $h \cdot N = 2$.

We take as an exact solution $(\boldsymbol{u}, P)$ of (4), (2) such one, which exhibits corner singularity phenomena in a neighborhood of a vertex located at the origin. In polar coordinates (r,φ) an exact solution has the following type

$$u_1(r,\varphi) = r^{\lambda_i} \cdot ((1+\lambda_i)\Theta(\varphi) \cdot \sin(\varphi) + \Theta'(\varphi) \cdot \cos(\varphi)), u_2(r,\varphi) = r^{\lambda_i} \cdot (\Theta'(\varphi) \cdot \sin(\varphi) - (1+\lambda_i)\Theta(\varphi) \cdot \cos(\varphi)),$$
$$P(r,\varphi) = -r^{\lambda_i - 1} \cdot \frac{(1+\lambda_i)^2\,\Theta'(\varphi) + \Theta'''(\varphi)}{1-\lambda_i},$$

TABLE 2. The influence of ν, δ and ν^* on the behavior of $\|\boldsymbol{u}-\boldsymbol{u}_\nu^h\|_{\boldsymbol{W}^1_{2,\nu}(\Omega_1)}$ of the R_ν-generalized solution, $\omega = 1.125\pi$.

ν	1.5						1.8					
δ	0.015			0.0175			0.015			0.0175		
N	74	148	296	74	148	296	74	148	296	74	148	296
ν^*												
$\lambda_1 - 1$	1.077e-4	5.360e-5	2.676e-5	1.513e-4	7.527e-5	3.758e-5	3.318e-5	1.650e-5	8.215e-6	4.196e-5	2.083e-5	1.037e-5
-0.175	1.005e-4	5.015e-5	2.493e-5	1.343e-4	6.700e-5	3.323e-5	3.084e-5	1.531e-5	7.611e-6	3.745e-5	1.853e-5	9.253e-6
-0.15	9.453e-5	4.695e-5	2.354e-5	1.173e-4	5.885e-5	2.914e-5	2.865e-5	1.418e-5	7.097e-6	3.364e-5	1.681e-5	8.374e-6
-0.125	9.351e-5	4.627e-5	2.313e-5	1.075e-4	5.320e-5	2.639e-5	2.747e-5	1.357e-5	6.789e-6	3.141e-5	1.574e-5	7.849e-6
-0.1	**8.955e-5**	**4.488e-5**	**2.247e-5**	**1.014e-4**	**5.048e-5**	**2.509e-5**	**2.709e-5**	**1.334e-5**	**6.645e-6**	**3.103e-5**	**1.550e-5**	**7.690e-6**
-0.075	9.312e-5	4.645e-5	2.311e-5	1.076e-4	5.315e-5	2.647e-5	2.721e-5	1.346e-5	6.683e-6	3.179e-5	1.575e-5	7.813e-6
-0.05	9.971e-5	4.958e-5	2.465e-5	1.106e-4	5.477e-5	2.725e-5	2.891e-5	1.435e-5	7.119e-6	3.243e-5	1.610e-5	8.008e-6
-0.025	1.076e-4	5.328e-5	2.656e-5	1.174e-4	5.808e-5	2.887e-5	3.094e-5	1.531e-5	7.613e-6	3.451e-5	1.704e-5	8.463e-6

TABLE 3. The influence of ν, δ and ν^* on the behavior of $\|\boldsymbol{u}-\boldsymbol{u}_\nu^h\|_{\boldsymbol{W}^1_{2,\nu}(\Omega_2)}$ of the R_ν-generalized solution, $\omega = 1.25\pi$.

ν	1.5						1.8					
δ	0.015			0.0175			0.015			0.0175		
N	74	148	296	74	148	296	74	148	296	74	148	296
ν^*												
$\lambda_2 - 1$	2.232e-4	1.110e-4	5.481e-5	2.706e-4	1.344e-4	6.684e-5	6.476e-5	3.217e-5	1.601e-5	8.350e-5	4.146e-5	2.066e-5
-0.3	2.022e-4	1.009e-4	5.045e-5	2.529e-4	1.259e-4	6.254e-5	5.927e-5	2.954e-5	1.473e-5	7.693e-5	3.822e-5	1.917e-5
-0.275	1.892e-4	9.392e-5	4.699e-5	2.271e-4	1.136e-4	5.683e-5	5.547e-5	2.745e-5	1.370e-5	7.085e-5	3.531e-5	1.749e-5
-0.25	1.816e-4	9.042e-5	4.523e-5	2.152e-4	1.065e-4	5.269e-5	5.331e-5	2.651e-5	1.318e-5	6.751e-5	3.340e-5	1.664e-5
-0.225	1.784e-4	8.832e-5	4.394e-5	**2.075e-4**	**1.027e-4**	**5.124e-5**	5.175e-5	2.595e-5	1.285e-5	6.473e-5	3.209e-5	1.593e-5
-0.2	**1.638e-4**	**8.210e-5**	**4.069e-5**	2.081e-4	1.032e-4	5.137e-5	5.129e-5	2.563e-5	1.278e-5	6.048e-5	3.031e-5	1.514e-5
-0.175	1.801e-4	8.964e-5	4.448e-5	2.153e-4	1.079e-4	5.345e-5	**5.123e-5**	**2.547e-5**	**1.266e-5**	**5.848e-5**	**2.899e-5**	**1.440e-5**
-0.15	1.878e-4	9.328e-5	4.649e-5	2.249e-4	1.122e-4	5.558e-5	5.261e-5	2.603e-5	1.297e-5	6.232e-5	3.133e-5	1.556e-5
-0.125	2.017e-4	1.011e-4	5.006e-5	2.347e-4	1.167e-4	5.786e-5	5.641e-5	2.803e-5	1.397e-5	6.841e-5	3.413e-5	1.697e-5
-0.1	2.169e-4	1.078e-4	5.331e-5	2.458e-4	1.222e-4	6.075e-5	6.021e-5	3.004e-5	1.491e-5	7.293e-5	3.609e-5	1.784e-5

where $\Theta(\varphi) = \frac{\sin((1+\lambda_i)\varphi)\cdot\cos(\lambda_i\omega_i)}{1+\lambda_i} - \cos((1+\lambda_i)\varphi) - \frac{\sin((1-\lambda_i)\varphi)\cdot\cos(\lambda_i\omega_i)}{1-\lambda_i} + \cos((1-\lambda_i)\varphi)$ and λ_i is the smallest positive root of the equation $\lambda\sin(\omega_i) + \sin(\lambda\,\omega_i) = 0$, which represent about 0.8008 for $\omega_1 = 1.125\pi$, about 0.6736 for $\omega_2 = 1.25\pi$, about 0.5445 for $\omega_3 = 1.5\pi$. Also, parameters α and $\bar{\nu}$ are equal to 1, $\boldsymbol{U} = 0.95\,\boldsymbol{u}$.

Numerical experiments were carried out on meshes with different step sizes h. The errors (for the velocity field) of the numerical approximations to the R_ν-generalized and generalized ($\nu = 0$, $\delta = 1$, $\nu^* = \mu^* = 0$) solutions were computed in the $\boldsymbol{W}^1_{2,\nu}(\Omega_i)$ and $\boldsymbol{W}^1_2(\Omega_i)$ norms, respectively, and as the module between exact and approximate solutions at the nodes M_k. We denote by δ^j a set of such nodes for the j-th component of the velocity field. The results of numerical experiments are showed in Tables 1-4 and Figs. 1-2. The values of parameters ν, ν^* and δ were derived numerically, the optimal values $\nu^*(\mu^* = \nu^*)$ for ν and δ are presented in bold type in columns of Tables 2-4.

CONCLUSION

The approximate R_ν-generalized solution (velocity field) by weighted FEM converges to the exact solution of the Oseen system in a convection form (4), (2) with the rate $\mathcal{O}(h)$ in the $\mathbf{W}^1_{2,\nu}(\Omega_i)$ norm for all corners ω_i and different δ and ν, Tables 2-4, while the approximate generalized solution by classical FEM has an $\mathcal{O}(h^{0.8})$ rate of convergence for a corner $\omega_1 = 1.125\pi$, $\mathcal{O}(h^{0.67})$ — for a $\omega_2 = 1.25\pi$, $\mathcal{O}(h^{0.55})$ — for a $\omega_3 = 1.5\pi$ in the $\mathbf{W}^1_2(\Omega_i)$ norm, Table 1.

TABLE 4. The influence of ν, δ and ν^* on the behavior of $\|\boldsymbol{u}-\boldsymbol{u}_\nu^h\|_{\boldsymbol{W}_{2,\nu}^1(\Omega_3)}$ of the R_ν-generalized solution, $\omega = 1.5\pi$.

ν	1.5						1.8					
δ	0.015			0.0175			0.015			0.0175		
N	74	148	296	74	148	296	74	148	296	74	148	296
ν^*												
λ_3-1	3.854e-4	1.915e-4	9.375e-5	5.195e-4	2.567e-4	1.276e-4	1.225e-4	6.064e-5	3.023e-5	1.845e-4	9.170e-5	4.557e-5
-0.425	3.481e-4	1.733e-4	8.609e-5	4.613e-4	2.278e-4	1.121e-4	1.114e-4	5.536e-5	2.756e-5	1.639e-4	8.124e-5	4.052e-5
-0.4	3.112e-4	1.540e-4	7.687e-5	4.141e-4	2.056e-4	1.030e-4	9.860e-5	4.876e-5	2.426e-5	1.498e-4	7.420e-5	3.688e-5
-0.375	3.034e-4	1.509e-4	7.534e-5	3.956e-4	1.963e-4	9.761e-5	9.435e-5	4.685e-5	2.334e-5	1.411e-4	7.021e-5	3.499e-5
-0.35	3.010e-4	1.499e-4	7.493e-5	3.883e-4	1.926e-4	9.556e-5	9.059e-5	4.490e-5	2.232e-5	1.266e-4	6.312e-5	3.147e-5
-0.325	2.964e-4	1.474e-4	7.298e-5	**3.705e-4**	**1.846e-4**	**9.180e-5**	8.429e-5	4.182e-5	2.087e-5	1.217e-4	6.049e-5	3.016e-5
-0.3	**2.761e-4**	**1.372e-4**	**6.829e-5**	3.896e-4	1.935e-4	9.618e-5	8.280e-5	4.097e-5	2.042e-5	**1.128e-4**	**5.619e-5**	**2.810e-5**
-0.275	2.951e-4	1.470e-4	7.299e-5	3.921e-4	1.949e-4	9.740e-5	**7.862e-5**	**3.890e-5**	**1.936e-5**	1.148e-4	5.743e-5	2.876e-5
-0.25	3.281e-4	1.631e-4	8.098e-5	4.249e-4	2.105e-4	1.042e-4	8.799e-5	4.354e-5	2.168e-5	1.213e-4	6.072e-5	3.027e-5
-0.225	3.548e-4	1.754e-4	8.732e-5	4.361e-4	2.165e-4	1.078e-4	9.716e-5	4.821e-5	2.399e-5	1.261e-4	6.276e-5	3.129e-5
-0.2	3.712e-4	1.846e-4	9.133e-5	4.702e-4	2.346e-4	1.170e-4	1.026e-4	5.103e-5	2.536e-5	1.303e-4	6.471e-5	3.227e-5

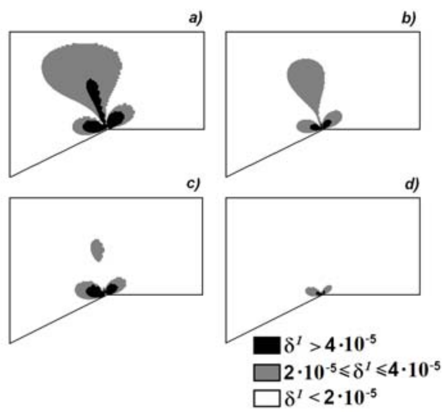

FIGURE 1. Distribution of the points M_k with errors δ^1 of the generalized $(\nu = 0, \delta = 1, \nu^* = \mu^* = 0)$ solution: a) N=148, b) N=296 and R_ν-generalized solution $(\nu = 1.8, \delta = 0.015, \nu^* = \mu^* = -0.175)$: c) N=148, d) N=296, $\omega_1 = 1.125\pi$.

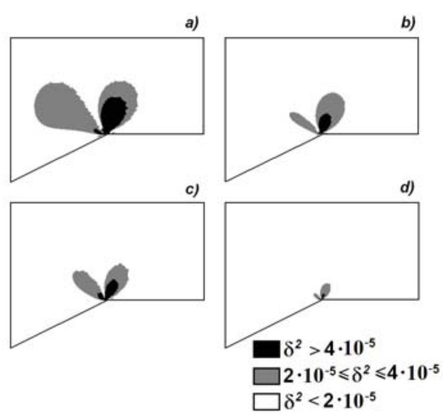

FIGURE 2. Distribution of the points M_k with errors δ^2 of the generalized $(\nu = 0, \delta = 1, \nu^* = \mu^* = 0)$ solution: a) N=148, b) N=296 and R_ν-generalized $(\nu = 1.8, \delta = 0.015, \nu^* = \mu^* = -0.175)$ solution: c) N=148, d) N=296, $\omega_2 = 1.125\pi$.

ACKNOWLEDGMENTS

Computational resources for the numerical experiments were provided by the Shared Services Center "Data Center of FEB RAS".

REFERENCES

1. V. A. Rukavishnikov, Doklady Akademii Nauk **337**, 447–449 (1994).
2. V. A. Rukavishnikov and A. G. Ereklintsev, Differential Equations **41**, 1757–1767 (2005).
3. V. A. Rukavishnikov and E. V. Kuznetsova, Differential Equations **43**, 550–560 (2007).
4. V. A. Rukavishnikov and E. V. Kuznetsova, Differential Equations **45**, 913–917 (2009).
5. V. A. Rukavishnikov, Doklady Mathematics **90**, 562–564 (2014).
6. V. A. Rukavishnikov and E. I. Rukavishnikova, Differential Equations **55**, 832–840 (2019).
7. V. A. Rukavishnikov and A. V. Rukavishnikov, Journal of Computational and Applied Mathematics **341**, 144–156 (2018).
8. V. A. Rukavishnikov, Russian Journal of Numerical Analysis and Mathematical Modelling **24**, 565–590 (2009).
9. V. A. Rukavishnikov and H. I. Rukavishnikova, Journal of Computational and Applied Mathematics **234**, 2870–2882 (2010).
10. V. A. Rukavishnikov and S. G. Nikolaev, Doklady Mathematics **88**, 705–709 (2013).
11. V. A. Rukavishnikov and A. V. Rukavishnikov, Bulletin South Ural State University., Ser. Mathematical Modelling, Programming and Computer Software **11**, 95–108 (2018).
12. V. A. Rukavishnikov and A. V. Rukavishnikov, Symmetry **11**, 1–17 (2019).
13. H. C. Elman, D. J. Silvester, and A. J. Wathen, *Finite Elements and Fast Iterative Solvers: with Applications in Incompressible Fluid Dynamics* (Oxford University Press, 2005).
14. L. R. Scott and M. Vogelius, Mathematical Modelling and Numerical Analysis **19**, 111–143 (1985).

A General Boundary Value Problem for Heat and Mass Transfer Equations with High Order Normal Derivatives in Boundary Conditions

Ermek Khairullin[a] and Aliya Azhibekova[b]

Satbayev University, 22a Satpaev str., Almaty, Kazakhstan

[a] *Electronic mail: khairullin_42_42@mail.ru*
[b] *Corresponding author: aliya.azhibek@gmail.com*

Abstract. A boundary value problem for the equations of heat and mass transfer in a half-space is considered, which contains in the boundary conditions derivatives of a higher order than the order of the derivative of a system of equations. The solution of the boundary problem is found in the form of a double layer potential. The lemma on finding the limit of the normal derivative of the finite order of the function in the neighborhood of the hyperplane $x_n = 0$ is given. Using the boundary conditions, a system of integro-differential equations (SIDE) is obtained. The characteristic part of the SIDE is solved by the method of Fourier-Laplace integral transforms. The conditions for the correctness and incorrectness of the problem, expressed in terms of the given constants and boundary conditions, are found. Using the regularization method, the SIDE is reduced to a system of Volterra-Fredholm integral equations. A theorem on the solvability of the boundary value problem for a parabolic system of heat and mass transfer equations is presented.

STATEMENT OF THE PROBLEM

In the articles [1, 2], boundary value problems for the heat equation are considered, when the boundary conditions contain derivatives of an order exceeding the order of the equation. Using the method of potentials, boundary value problems are reduced to integro-differential equations. Under the condition of solvability, the existence of solutions of boundary value problems is proved. In [3], a boundary value problem for an integro-differential equation in a half-space is considered, which contains in the boundary condition derivatives of a higher order than the order of the derivative of an equation. Using the regularization method, the boundary value problem is reduced to the Volterra-Fredholm integral equation.

Find a regular solution to the system:

$$\frac{\partial U_k(x,t)}{\partial t} = \lambda_k \Delta U_k(x,t), \; k = 1, \; 2 \tag{1}$$

in the domain $Q_T \equiv \left\{(x', x_n, t) : \; x' \in R^{n-1}, \; x_n \in R_+, t \in \left]0, T\right[\right\}$, with the initial and boundary conditions:

$$U_k(x,0) = 0, \tag{2}$$

$$\sum_{k=1}^{2} \left[\sum_{k_n=1}^{m_l} a_{l,k_n}^{(k)} \frac{\partial^{k_n} U_k(x,t)}{\partial {x_n}^{k_n}} + a_k^{(l)} U_k(x,t) \right] |_{x_n=0} = \varphi_l(x', t), \tag{3}$$

$$\left(x', t\right) \in Q_T^{(1)} = Q_T \backslash x_n, \; m_l \geq 1, \; l = 1, 2 \;,$$

where Δ is Laplace operator with respect to $x = (x_1, x_2, \ldots, x_n)$; λ_k are given positive constants, and $0 < \lambda_1 < \lambda_2$; $a_k^{(l)}$ and $a_{l,k_n}^{(k)}$ $(k = 1, 2)$ are given constants and $\varphi_l(x', t) \in C_{x', \, t}^{2, \, 1}\left(Q_T^{(1)}\right)$.

INTEGRAL REPRESENTATION OF THE SOLUTION

The solution of the boundary value problem (1)-(3) is found in the following form [4, 5]:

$$U_k(x,t) = -\Psi_k * G_{x_n}^{(k)}[x,t], \; k = 1, 2 \;, \tag{4}$$

International Conference on Analysis and Applied Mathematics (ICAAM 2020)
AIP Conf. Proc. 2325, 020011-1–020011-6; https://doi.org/10.1063/5.0041111
Published by AIP Publishing. 978-0-7354-4069-2/$30.00

where

$$G^{(k)}(x,t)=\frac{2\lambda_k \exp\left[-\frac{|x|^2}{4\lambda_k t}\right]}{\left[2\sqrt{\pi\lambda_k t}\right]^n},\ \ G^{(k)}_{x_n}(x,\ t)=\frac{\partial}{\partial x_n}G^{(k)}(x,\ t),$$

$$\Psi_k * G^{(k)}_{x_n}[x,t]=\int_0^t d\tau\int_{R^{n-1}}\Psi_k(\xi',\tau)G^{(k)}_{x_n}\left(x'-\xi',x_n,t-\tau\right)d\xi',$$

R^{n-1} is $(n-1)$-dimensional Euclidean space of points $x'=(x_1,x_2,\dots,x_{n-1})$ with the norm $|x'|=\sqrt{x_1^2+x_2^2+...+x_{n-1}^2}$; $\Psi_k(x',t)$ are unknown bounded continuous functions with partial derivatives of a sufficiently high order with respect to the variable x' and t.

REDUCING OF THE PROBLEM TO A SYSTEM OF INTEGRO-DIFFERENTIAL EQUATIONS (SIDE)

The functions $U_k(x,t)$ defined by (4) satisfy the system and the initial conditions. The unknown functions $\Psi_k(x',t)$ must be defined so that the functions $U_k(x,t)$ satisfy the boundary conditions (3).

We introduce the definitions of certain classes of functions denoted by $C^{m_i,\left[\frac{m_i}{2}\right]}_{x',\ t}\left(Q_T^{(1)}\right)$ and $\dot{C}^{m_i,\left[\frac{m_i}{2}\right]}_{x',\ t}\left(Q_T^{(1)}\right)$.

Definition 1 *The functions* $\Psi_i(x',t)\in C^{m_i,\left[\frac{m_i}{2}\right]}_{x',\ t}\left(Q_T^{(1)}\right)$, *if* $\Psi_i(x',t)$ *and all its derivatives* $F_i^{k_n}\left[D^{k'}_{x'}\Psi_i(x',t)\right]$ $\left(|k'|=\overline{0,\ m_i-2k_n},\ \ k_n=\overline{0,\left[\frac{m_i}{2}\right]}\right)$ *are continuous, where* $k'=(k_1,k_2,\dots,k_{n-1})$; $|k'|=k_1+k_2+\dots+k_{n-1}$; $D^{k'}_{x'}=D^{k_1}_{x_1},D^{k_2}_{x_2},\dots,D^{k_{n-1}}_{x_{n-1}}$, $D_{x_i}=\frac{\partial}{\partial x_i}\ \left(i=\overline{1,n-1}\right)$; $F_1\equiv\frac{\partial}{\partial t}-\lambda_1\Delta_{x'},\dots,F_i^{k_n}\equiv\left(\frac{\partial}{\partial t}-\lambda_i\Delta_{x'}\right)^{k_n}$, F_i^0 *is a unitary operator;* $\Delta_{x'}=\sum_{k=1}^{n-1}\frac{\partial^2}{\partial x_k^2}$; $\left[\frac{m_i}{2}\right]=\frac{m_i}{2}$ *or* $\frac{m_i-1}{2}$ *depending on whether* m_i *is an even or odd number.*

Definition 2 *The functions* $\Psi_i(x',t)\in\dot{C}^{m_i,\left[\frac{m_i}{2}\right]}_{x',\ t}\left(Q_T^{(1)}\right)$, *if* $\Psi_i(x',t)\in C^{m_i,\left[\frac{m_i}{2}\right]}_{x',\ t}\left(Q_T^{(1)}\right)$ *and satisfy the conditions*

$$F_i^{k_n}\left[D^{k'}_{x'}\Psi_i\left(x',t\right)\right]|_{t=0}=0,\ \ \left(\left|k'\right|=\overline{0,\ m_i-2k_n},\ k_n=\overline{0,\left[\frac{m_i}{2}\right]}\right).$$

Using Definitions 1 and 2, we state the Lemma.

Lemma 1 *If the functions* $\Psi_k(x',t)\in\dot{C}^{m_i,\left[\frac{m_i}{2}\right]}_{x',\ t}\left(Q_T^{(1)}\right)$, *then*

$$\lim_{x_n\to 0}\frac{\partial^{2k_n-1}U_k(x,t)}{\partial {x_n}^{2k_n-1}}=-\frac{1}{\left(\sqrt{\lambda_k}\right)^{2k_n}}{F_k}^{k_n}[\Psi_k]*G^{(k)}\left[x',0,t\right],\tag{5}$$

$$\lim_{x_n\to 0}\frac{\partial^{2k_n}U_k(x,t)}{\partial {x_n}^{2k_n}}=\frac{1}{(\sqrt{\lambda_k})^{2k_n}}{F_k}^{k_n}[\Psi_k].\tag{6}$$

To define $\Psi_k(x',t)$, the functions $U_k(x,t)$ are substituted in the boundary conditions (3), using (5)-(6) and the properties of the double layer potentials, we obtain the SIDE:

$$\sum_{k=1}^{2}\left[\sum_{k_n=0}^{\left[\frac{m_l}{2}\right]}\frac{a^{(k)}_{l,\ 2k_n}}{(\sqrt{\lambda_k})^{2k_n}}F_k^{k_n}\left[\Psi_k\left(x',t\right)\right]-\sum_{k_n=1}^{\left[\frac{m_l}{2}\right]}\frac{a^{(k)}_{l,\ 2k_n-1}}{(\sqrt{\lambda_k})^{2k_n-1}}F_k^{k_n}[\Psi_k]*G^{(k)}\left[x',0,t\right]+a^{(l)}_k\Psi_k\left(x',t\right)\right]=\varphi_l\left(x',t\right),$$

$$(l=1,2).\tag{7}$$

Let us consider the characteristic part of the system:

$$\sum_{k=1}^{2}\left[\frac{a_{l,\, m_l}(-1)^{m_l}}{(\sqrt{\lambda_k})^{m_l}}F_k^{\frac{m_l}{2}}\left[\Psi_k\left(x',t\right)\right]\right]=\Phi_l\left(x',t\right),\ (l=1,2), \tag{8}$$

where

$$\Phi_l\left(x',t\right)=\varphi_l\left(x',t\right)-\sum_{k=1}^{2}a_k^{(l)}\Psi_k\left(x',t\right)-\sum_{k=1}^{2}\left[\sum_{\nu=0}^{m_l-1}\frac{a_{l,\nu}^{(k)}(-1)^{\nu}}{(\sqrt{\lambda_k})^{\nu}}F_k^{\frac{\nu}{2}}\left[\Psi_k\left(x',t\right)\right]\right]. \tag{9}$$

Considering the right-hand side of the system (8) as a known function and assuming that Fourier integral transforms with respect to x' and Laplace transform with respect to t can be applied to the functions $\Psi_k\left(x',t\right)$ and $\Phi_k\left(x',t\right)$, we obtain:

$$\sum_{k=1}^{2}\left[\frac{a_{l,\, m_l}^{(k)}}{(\sqrt{\lambda_k})^{m_l}\left(\sqrt{2\pi}\right)^{n-1}}\int_0^{\infty}\left(\int_{R^{n-1}}F_k^{\frac{m_l}{2}}\left[\Psi_k\left(x',t\right)\right]exp\left[i\left(x',s'\right)\right]dx'\right)exp\left[-pt\right]dt\right]=\overline{\overline{\Phi}}_l\left(s',p\right), \tag{10}$$

where

$$\overline{\overline{\Phi}}_l\left(s',p\right)=\frac{1}{\left(\sqrt{2\pi}\right)^{n-1}}\int_0^{\infty}\left(\int_{R^{n-1}}\Phi_1\left(x',t\right)exp\left[i\left(x',s'\right)\right]dx'\right)exp\left[-pt\right]dt.$$

Integrating in (10) over the variable x' - m times, over the variable t - $\left[\frac{m}{2}\right]$ times and using the following equality

$$\frac{1}{\left(\sqrt{2\pi}\right)^{n-1}}\int_0^{\infty}\left(\int_{R^{n-1}}F_k^{\frac{m_l}{2}}\left[\Psi_k\left(x',t\right)\right]exp\left[i\left(x',s'\right)\right]dx'\right)exp\left[-pt\right]dt=\left(p+\lambda_k|s'|^2\right)^{\frac{m_l}{2}}\overline{\overline{\Psi}}_k\left(s',p\right),$$

we can find

$$\sum_{k=1}^{2}\frac{a_{l,\, m_l}^{(k)}}{(\sqrt{\lambda_k})^{m_l}}\left(\sqrt{p+\lambda_k|s'|^2}\right)^{m_l}\overline{\overline{\Psi}}_k\left(s',p\right)=\overline{\overline{\Phi}}_l\left(s',p\right). \tag{11}$$

The main determinant $\Delta\left(s',p\right)$ of the system:

$$\overline{\overline{\Delta}}\left(s',p\right)=\begin{vmatrix}\frac{a_{1,\, m_1}^{(1)}}{(\sqrt{\lambda_1})^{m_1}}\left(\sqrt{p+\lambda_1|s'|^2}\right)^{m_1} & \frac{a_{1,\, m_1}^{(2)}}{(\sqrt{\lambda_2})^{m_1}}\left(\sqrt{p+\lambda_2|s'|^2}\right)^{m_1}\\ \frac{a_{2,\, m_2}^{(1)}}{(\sqrt{\lambda_1})^{m_2}}\left(\sqrt{p+\lambda_1|s'|^2}\right)^{m_2} & \frac{a_{2,\, m_2}^{(2)}}{(\sqrt{\lambda_2})^{m_2}}\left(\sqrt{p+\lambda_2|s'|^2}\right)^{m_2}\end{vmatrix}.$$

If $\Delta\left(s',p\right)\neq 0$, then the problem is well posed and using the composition of operators

$$U_k\left(x,t\right)=\Phi_{1,\ \lambda_k}\left[F_{\lambda}^{-\frac{m_l}{2}}\left[\varphi_k\left(x',t\right),x_n\right]\right]$$

the problem reduces to a system of the Volterra-Fredholm type integral equations of the second kind with respect to unknown densities with an integrable singularity. The method of successive approximations is applied.

If $\Delta\left(s',p\right)=0$, then the well-known Lopatinsky condition is not fulfilled, therefore, it is necessary to study the roots of the equation:

$$\Delta_1\left(s',p\right)=a_{1,\, m_1}^{(2)}a_{2,\, m_2}^{(1)}\left(\sqrt{\frac{p+\lambda_1|s'|^2}{\lambda_1}}\right)^{m_1}\left(\sqrt{\frac{p+\lambda_2|s'|^2}{\lambda_2}}\right)^{m_2}\Delta_0\left(s',p\right)=0, \tag{12}$$

where

$$\Delta_0\left(s',p\right)=\frac{a_{1,\, m_1}^{(1)}a_{2,\, m_2}^{(2)}}{a_{1,\, m_1}^{(2)}a_{2,\, m_2}^{(1)}}-\left(\sqrt{\frac{\lambda_1}{\lambda_2}}\right)^{m_1-m_2}\left(\frac{\sqrt{p+\lambda_1|s'|^2}}{\sqrt{p+\lambda_2|s'|^2}}\right)^{m_1-m_2}.$$

It follows from (12) that the Lopatinsky condition is not satisfied if

$$\frac{a^{(1)}_{1,\,m_1}a^{(2)}_{2,\,m_2}}{(\sqrt{\lambda_1})^{m_1-m_2}}-\frac{a^{(2)}_{1,\,m_1}a^{(1)}_{2,\,m_2}}{(\sqrt{\lambda_2})^{m_1-m_2}}=0. \tag{13}$$

If $\left|a^{(1)}_{1,\,m_1}a^{(2)}_{2,\,m_2}\right|+\left|a^{(2)}_{1,\,m_1}a^{(1)}_{2,\,m_2}\right|\neq 0$, then we can assume that $a^{(2)}_{1,\,m_1}a^{(1)}_{2,\,m_2}\neq 0$. Then

$$\frac{a^{(1)}_{1,\,m_1}a^{(2)}_{2,\,m_2}}{a^{(2)}_{1,\,m_1}a^{(1)}_{2,\,m_2}}-\left(\frac{\lambda_1}{\lambda_2}\right)^{\frac{m_1-m_2}{2}}\left[\frac{\sqrt{\frac{p}{|s'|^2}+\lambda_2}}{\sqrt{\frac{p}{|s'|^2}+\lambda_1}}\right]^{m_1-m_2}=0. \tag{14}$$

If $m_1-m_2=2\nu+1$, then

$$\left[\sqrt{\frac{\frac{p}{|s'|^2}+\lambda_2}{\frac{p}{|s'|^2}+\lambda_1}}\right]^{2\nu+1}\left(\frac{\lambda_1}{\lambda_2}\right)^{\frac{2\nu+1}{2}}=\gamma, \tag{15}$$

where $\gamma=\frac{a^{(1)}_{1,\,m_1}a^{(2)}_{2,\,m_2}}{a^{(2)}_{1,\,m_1}a^{(1)}_{2,\,m_2}}$.

Applying a replacement $\frac{\sqrt{\frac{p}{|s'|^2}+\lambda_2}}{\sqrt{\frac{p}{|s'|^2}+\lambda_1}}=z$ to the last expression, where $z=h_1+ih_2$, $h_1>0$ and taking into account that $\frac{p}{|s'|^2}=\frac{\lambda_1 z^2-\lambda_2}{1-z^2}$, it is necessary that

$$Re\frac{p}{|s'|^2}=\frac{\left[\lambda_1\left(h_1^2-h_2^2\right)-\lambda_2\right]\left(1-h_1^2+h_2^2\right)-4\lambda_1 h_1^2h_2^2}{\left(1-h_1+h_2\right)^2+4h_1^2h_2^2}>0,$$

that is

$$\begin{cases}\lambda_1\left(h_1^2+h_2^2\right)-\left(\lambda_1+\lambda_2\right)\left(h_1^2-h_2^2\right)+\lambda_2<0,\\ h_1>0.\end{cases} \tag{16}$$

Thus, the Lopatinsky condition is not fulfilled if the equation

$$\left(\frac{\lambda_1}{\lambda_2}\right)^{\frac{2\nu+1}{2}}z^{2\nu+1}=\gamma \tag{17}$$

has roots in the domain (16). The roots of the equation (17) are

$$z_k=\sqrt{\frac{\lambda_2}{\lambda_1}}|\gamma|^{\frac{1}{2\nu+1}}\ exp\left[i\frac{2\theta+2k\pi}{2\nu+1}\right],$$

where $k=\overline{0,\,2\nu}$, $\theta=\begin{cases}0, & \gamma\geq 0,\\ \frac{\pi}{2}, & \gamma<0.\end{cases}$

Substituting z_k into the inequalities (15), we obtain

$$\begin{cases}\frac{\lambda_2}{\lambda_1}|\gamma|^{\frac{4}{2\nu+1}}-\frac{\lambda_1+\lambda_2}{\lambda_1}|\gamma|^{\frac{2}{2\nu+1}}\cos\frac{4(\theta+k\pi)}{2\nu+1}\ +1<0,\\ \cos\frac{2(\theta+k\pi)}{2\nu+1}\ >0,\end{cases}$$

which must be true for at least one of $k=\overline{0,\,2\nu}$.

Since

$$\bar{\tilde{L}}_{2\nu+1}\left(s',p\right)=\frac{1}{\left(\sqrt{\frac{p}{\lambda_1}+|s'|^2}\right)^2\left[\gamma-\left(\frac{\sqrt{\frac{p}{\lambda_2}+|s'|^2}}{\sqrt{\frac{p}{\lambda_1}+|s'|^2}}\right)^{2\nu+1}\right]}\ , \tag{18}$$

using the residue theory, we can find

$$\tilde{L}_{2v+1}\left(s',t\right)=\sum_{k^*=0}^{2v} res\left\{\frac{e^{pt}}{\left(\sqrt{\frac{p}{\lambda_1}+|s'|^2}\right)^2\left[\gamma-\left(\frac{\sqrt{\frac{p}{\lambda_2}+|s'|^2}}{\sqrt{\frac{p}{\lambda_1}+|s'|^2}}\right)^{2v+1}\right]},\ p=-q_k|s'|^2,\ q_k=\frac{\lambda_1 z_k^2-\lambda_2}{z_k^2-1}\right\},$$

where k^* are those numbers of k, for which $Re\ z_k>0$ in (17). So,

$$\tilde{L}_{2v+1}\left(s',t\right)=\sum_{k^*=0}^{2v}\frac{\lambda_2^{\frac{2v+1}{2}}e^{-a_k|s'|^2 t}}{\lambda_1^{\frac{2v-1}{2}}}\lim_{z\to z_k}\frac{(z-z_k)(z+z_k)}{\left(1-z_k^2\right)\left(z_k^{2v+1}-z^{2v+1}\right)},$$

or

$$\tilde{L}_{2v+1}\left(s',t\right)=\sum_{k^*=0}^{2v}\frac{2\left(\sqrt{\lambda_2}\right)^{2v+1}e^{-q_k|s'|^2 t}}{(2v+1)\left(\sqrt{\lambda_1}\right)^{2v-1}\left(1-z_k^2\right)z_k^{2v-1}}. \tag{19}$$

Applying the inverse Fourier transform with respect to the variable s', assuming that $q_k>0$, we obtain

$$L_{2v+1}\left(x',t\right)=\sum_{k^*=0}^{2v}\frac{2\left(\sqrt{\lambda_2}\right)^{2v+1}\left(1-z_k^2\right)^{n-3}exp\left[-\frac{|x'|^2}{4q_k t}\right]}{(2v+1)\left(\sqrt{\lambda_1}\right)^{2v-1}z_k^{2v-1}\left(2\sqrt{\pi q_k t}\right)^{n-1}}. \tag{20}$$

Using (20) and the known relation

$$\frac{1}{\left(\sqrt{p+\lambda_k|s'|^2}\right)^{\alpha}}:\to\frac{t^{\frac{\alpha}{2}-1}}{\Gamma\left(\frac{\alpha}{2}\right)}exp\left[-\lambda_k|s'|^2 t\right]$$

and also the Riemann-Mellin formula, from the system of equations (11) we can find

$$\Psi_k\left(x',t\right)=\sum_{\alpha=1}^{2}\int_0^t d\tau\int_{R^{n-1}}H_{k,\ \alpha}\left(x'-\xi',t-\tau\right)\Phi_\alpha\left(\xi',\tau\right)d\xi', \tag{21}$$

where the kernels $H_{k,\ \alpha}\left(x',t\right)$ satisfy the estimate:

$$\left|H_{k,\ \alpha}\left(x',t\right)\right|\leq M\frac{exp\left[-\delta\frac{|x'|^2}{t}\right]}{\left(\sqrt{t}\right)^n}, \tag{22}$$

here M and δ are positive constants.

REGULARIZATION OF THE SYSTEM (8)

Substituting the values of $\Phi_\alpha\left(x',t\right)$ from (9) into the system (8), we obtain:

$$\Psi_k\left(x',t\right)=\Phi_k\left(x',t\right)+\sum_{\alpha=1}^{2}\int_0^t d\tau\int_{R^{n-1}}H^{(1)}_{k,\ \alpha}\left(x'-\xi',t-\tau\right)\Psi_\alpha\left(\xi',\tau\right)d\xi', \tag{23}$$

where

$$\Phi_k\left(x',t\right)=\sum_{\alpha=1}^{2}\int_0^t d\tau\int_{R^{n-1}}H_{k,\ \alpha}\left(x'-\xi',t-\tau\right)\varphi_\alpha\left(\xi',\tau\right)d\xi', \tag{24}$$

the kernels $H_{k,\ \alpha}^{(1)}(x',t)$ satisfy the following estimate:

$$\left|H_{k,\ \alpha}^{(1)}(x',t)\right| \leq M_1 \frac{exp\left[-\delta_1 \frac{|x'|^2}{t}\right]}{\left(\sqrt{t}\right)^n}, \tag{25}$$

here M_1 and δ_1 are positive constants.

The system of integral equations (23) can be solved by the method of successive approximations based on the estimate (25).

The following theorem holds.

Theorem 2 *If $\varphi_k(x',t) \in C_{x',\ t}^{2,\ 1}\left(Q_T^{(1)}\right)$ and $q_k = \frac{\lambda_1 z_k^2 - \lambda_2}{z_k^2 - 1} > 0$ (z_k are roots of the characteristic equation), then the solution of the problem (1)-(3) exists and $U_k(x,t) \in C_{x,\ t}^{m_k,\ \left[\frac{m_k}{2}\right]}(Q_T)$, where the unknown functions $\Psi_k(x',t)$ are determined from the system of integral equations (23).*

REFERENCES

1. A. N. Tikhonov, Matem. Sbornik. **26**, 35–56 (1950), (in Russian).
2. E. I. Kim, Dokl. AN SSSR **140**, 553–556 (1961), (in Russian).
3. E. Khairullin, AIP Conf. Proc. **1759**, 020093 (2016).
4. Ye. Khairullin, G. Tulesheva, and A. Shakulikova, Vestnik KazNRTU **134(4)**, 561-567 (2019).
5. Ye. M. Khairullin, G. A. Tulesheva, and A. S. Azhibekova, A Multidimensional boundary value problem of heat and mass transfer, when the boundary conditions contain higher-order derivatives, in: Abstract Book of "International Conference of Actual Problems of Analysis, Differential Equations and Algebra", 161–162, 2019.

A Note on Hyperbolic Differential Equations on Manifold

Allaberen Ashyralyev,[1, 2, 3, a)] Yasar Sozen,[4, b)] and Fatih Hezenci[5, c)]

[1)] *Department of Mathematics, Near East University, Nicosia, Mersin 10, Turkey*
[2)] *Peoples' Friendship University of Russia (RUDN University), Ul Miklukho Maklaya 6, Moscow 117198, Russia*
[3)] *Institute of Mathematics and Mathematical Modeling, 050010, Almaty, Kazakhstan*
[4)] *Department of Mathematics, Hacettepe University, 06800 Beytepe, Ankara, Turkey*
[5)] *Department of Mathematics, Duzce University, 81620 Konuralp, Duzce, Turkey*

[a)] *Electronic mail: allaberen.ashyralyev@neu.edu.tr*
[b)] *Electronic mail: ysozen@hacettepe.edu.tr*
[c)] *Corresponding author: fatihhezenci@duzce.edu.tr*

Abstract. In this extended abstract, considering the differential equations on hyperbolic plane, we investigate and establish the well-posedness of boundary value problem for hyperbolic equations in Hölder spaces. Furthermore, we establish new coercivity estimates in various Hölder norms for the solutions of such boundary value problems for hyperbolic equations.

INTRODUCTION

In the study of boundary value problems for partial differential equations, the role played by the well-posedness (coercivity inequalities) in the study of boundary value problems for partial differential equations is well known (see, e.g. [1, 2, 3]).

The well-posedness of nonlocal boundary value problems for partial differential equations of hyperbolic type in in the Euclidean space has been studied extensively (see, e.g. [4, 5, 6, 7, 8, 9, 10, 11, 12] and the references therein). By considering the differential equations on hyperbolic plane, the present extended abstract investigates and establishes the well-posedness of nonlocal boundary value problems in Hölder spaces. Moreover, it establishes new coercivity estimates in various Hölder norms for the solutions of such boundary value problems for hyperbolic equations.

LAPLACE-BELTRAMI OPERATOR OF RIEMANNIAN MANIFOLD

The reader is referred to [13, 14] and the references therein for more information and unexplained subjects.

For an $n-$dimensional Riemannian manifold $(\mathscr{M}, g)$, the Laplace-Beltrami operator $\Delta_{\mathscr{M}}$ on real valued functions of $\mathscr{M}$ is locally $\frac{-1}{\sqrt{g}} \sum_{i,j=1}^{n} \frac{\partial}{\partial x_i} \left(g^{ij} \sqrt{g} \frac{\partial}{\partial x_j} \right)$, where $\sqrt{g} = \sqrt{\det(g_{ij})}$, (g^{ij}) is the inverse of (g_{ij}), and $g_{ij} = g\left(\frac{\partial}{\partial x_i}, \frac{\partial}{\partial x_j}\right)$.

Consider the $2-$dimensional hyperbolic plane $\mathbb{H}^2 = \left\{(x_1, x_2, x_3) \in \mathbb{R}^3, x_3 > 0 \mid x_1^2 + x_2^2 - x_3^2 = -1\right\}$ in the geodesic polar coordinates, namely, $\xi : (0,\infty) \times (0, 2\pi) \to \mathbb{H}^2$, $x_1 = \sinh(r)\cos\theta$, $x_2 = \sinh(r)\sin\theta$, $x_3 = \cosh(r)$, where $0 < r < \infty$, $0 < \theta < 2\pi$. We have

$$g_{\mathbb{H}^2} = \begin{bmatrix} 1 & 0 \\ 0 & \sinh^2(r) \end{bmatrix}, \quad \sqrt{\det g_{\mathbb{H}^2}} = \sinh(r), \; g_{\mathbb{H}^2}^{-1} = \begin{bmatrix} 1 & 0 \\ 0 & \frac{1}{\sinh^2(r)} \end{bmatrix}.$$

Furthermore, the Laplace-Beltrami operator of $\mathbb{H}^2$ in geodesic polar coordinates is

$$\Delta_{\mathbb{H}^2} = \frac{-1}{\sinh(r)} \left\{ \frac{\partial}{\partial r} \left(a_0(r,\theta) \frac{\partial}{\partial r} \right) + \frac{\partial}{\partial \theta} \left(a_1(r,\theta) \frac{\partial}{\partial \theta} \right) \right\},$$

where $a_0 = \sinh(r)$ and $a_1 = \frac{1}{\sinh(r)}$.

Stokes' Theorem and Divergence Theorem for manifolds state as follows.

Theorem 1 (Stokes' Theorem) *If $\mathscr{M}$ is an oriented complete Riemannian $n-$manifold with boundary, $\alpha \in \Omega^{n-1}(\mathscr{M})$ with compact support, and if $i : \partial\mathscr{M} \to \mathscr{M}$ is the inclusion map, then $\int_{\partial\mathscr{M}} i^*\alpha = \int_{\mathscr{M}} d\alpha$.*

International Conference on Analysis and Applied Mathematics (ICAAM 2020)
AIP Conf. Proc. 2325, 020012-1–020012-4; https://doi.org/10.1063/5.0040554
Published by AIP Publishing. 978-0-7354-4069-2/$30.00

Theorem 2 (Divergence Theorem) *Let $\mathscr{M}$ be a Riemannian manifold with boundary $\partial\mathscr{M}$ and X be a C^1-vector field on $\mathscr{M}$. Then, $\int_{\mathscr{M}} \mathrm{div}_g(X)\, dV_g = \int_{\partial\mathscr{M}} \langle X, \nu\rangle_g\, d\sigma_g$, where div_g denotes the divergence operator on $(\mathscr{M}, g)$, dV_g denotes the natural volume element on $(\mathscr{M}, g)$, and ν denotes the unit vector normal to $\partial\mathscr{M}$.*

From these theorems it follows

Theorem 3 (Green's Theorem) *If $(\mathscr{M}, g)$ is an oriented complete Riemannian manifold with boundary $\partial\mathscr{M}$, if $\psi \in C^1\left(\overline{\mathscr{M}}\right)$ and $\varphi \in C^2\left(\overline{\mathscr{M}}\right)$, then $\int_{\mathscr{M}} \psi \cdot \Delta_{\mathscr{M}}\phi\, dV_g = \int_{\mathscr{M}} \left\langle \nabla_g\psi, \nabla_g\phi \right\rangle dV_g - \int_{\partial\mathscr{M}} \psi \cdot \frac{\partial\phi}{\partial\nu} d\sigma_g$. Here, ∇_g denotes the gradient operator on the Riemannian manifold $(\mathscr{M}, g)$.*

Green's Theorem yields

Theorem 4 *[13, 14] Assume $(\mathscr{M}, g)$ is a complete Riemannian manifold without boundary. Then,*

1. *(Formal self-adjointness): $\left\langle \psi, \Delta_{\mathscr{M}}\phi \right\rangle_{L_2(\mathscr{M}, dV_g)} = \left\langle \phi, \Delta_{\mathscr{M}}\psi \right\rangle_{L_2(\mathscr{M}, dV_g)}$,*
2. *(Positivity): $\left\langle \Delta_{\mathscr{M}}\phi, \phi \right\rangle_{L_2(\mathscr{M}, dV_g)} \geq 0$.*

Here, $L_2(\mathscr{M}, dV_g)$ denotes the Hilbert space $\{f : \mathscr{M} \to \mathbb{R}; \langle \phi, \phi\rangle_{L_2(\mathscr{M}, dV_g)} := \int_{\mathscr{M}} \phi^2(x)\, dV_g(x) < \infty\}$.

Recall that for the simply connected constant (-1) Gaussian curvature space $\mathbb{H}^2$ we have $\lambda(\Omega) \geq \frac{1}{4}$, where $\Omega \subset \mathbb{H}^2$ is a normal domain [13].

NONLOCAL HYPERBOLIC DIFFERENTIAL EQUATION ON HYPERBOLIC PLANE

We consider the following relatively compact domain in the hyperbolic plane $\mathbb{H}^2$

$$\Omega = \xi((a,b)\times(c,d)) = \{(\sinh(r)\cos\theta, \sinh(r)\sin\theta, \cosh(r)) \in \mathbb{H}^2 : 0 < a < r < b < \infty, 0 < c < \theta < d < 2\pi\}.$$

Let us consider the mixed boundary value problem for hyperbolic equations in $\mathbb{H}^2$

$$\begin{cases} u_{tt}(t,x) + \Delta_{\mathbb{H}^2} u(t,x) = f(t,x), \quad (t,x) \in [0,1]\times\Omega, \\ u(0,x) = \sum\limits_{j=1}^{p} \alpha_j u(\lambda_j, x) + \varphi(x), \quad x \in \Omega, \\ u_t(0,x) = \sum\limits_{j=1}^{p} \beta_k u_t(\lambda_k, x) + \psi(x), \quad x \in \Omega, \\ 0 < \lambda_1 \leq \lambda_2 \leq \cdots \leq \lambda_p \leq 1, \\ u(t,x) = 0, \quad x \in \partial\Omega, \quad 0 \leq t \leq 1 \end{cases} \tag{1}$$

under the assumption

$$\sum_{j=1}^{p} |\alpha_j + \beta_j| + \sum_{j=1}^{p} |\alpha_j| \sum_{m=1,\, m\neq j}^{p} |\beta_m| < \left| 1 + \sum_{j=1}^{p} \alpha_j\beta_j \right|. \tag{2}$$

Here, $\Delta_{\mathbb{H}^2}$ denotes the Laplace-Beltrami operator on $(\mathbb{H}^2, g_{\mathbb{H}^2})$.

We prove

Theorem 5 *The solutions of problem (1) satisfy the following stability inequalities*

$$\max_{0\leq t\leq 1}\left(\| u_\phi(t,\cdot) \|_{L_2\left(\Omega, dV_{g_{\mathbb{H}^2}}\right)} + \| u_\theta(t,\cdot) \|_{L_2\left(\Omega, dV_{g_{\mathbb{H}^2}}\right)} \right) \leq M \left[\max_{0\leq t\leq 1} \| f(t,\cdot \|_{L_2\left(\Omega, dV_{g_{\mathbb{H}^2}}\right)} \right.$$
$$\left. + \left(\| \varphi_\phi \|_{L_2\left(\Omega, dV_{g_{\mathbb{H}^2}}\right)} + \| \varphi_\theta \|_{L_2\left(\Omega, dV_{g_{\mathbb{H}^2}}\right)} \right) + \| \psi \|_{L_2\left(\Omega, dV_{g_{\mathbb{H}^2}}\right)} \right],$$

$$\max_{0\le t\le 1}\left(\| u_{\phi\phi}(t,\cdot)\|_{L_2\left(\Omega,dV_{g_{\mathbb{H}^2}}\right)}+\| u_{\theta\theta}(t,\cdot)\|_{L_2\left(\Omega,dV_{g_{\mathbb{H}^2}}\right)}\right)$$

$$+\max_{0\le t\le 1}\| u_{tt}(t,\cdot)\|_{L_2\left(\Omega,dV_{g_{\mathbb{H}^2}}\right)}\le M\left[\max_{0\le t\le 1}\| f_t(t,\cdot)\|_{L_2\left(\Omega,dV_{g_{\mathbb{H}^2}}\right)}\right.$$

$$\left.+\| f(0,\cdot)\|_{L_2\left(\Omega,dV_{g_{\mathbb{H}^2}}\right)}+\left(\|\varphi_{\phi\phi}\|_{L_2\left(\Omega,dV_{g_{\mathbb{H}^2}}\right)}+\|\varphi_{\theta\theta}\|_{L_2\left(\Omega,dV_{g_{\mathbb{H}^2}}\right)}\right)+\left(\|\psi_{\phi}\|_{L_2\left(\Omega,dV_{g_{\mathbb{H}^2}}\right)}+\|\psi_{\theta}\|_{L_2\left(\Omega,dV_{g_{\mathbb{H}^2}}\right)}\right)\right].$$

Here, M is independent of $f(t,x)$, $\varphi(x)$, and $\psi(x)$.

We consider problem (1) as the following problem

$$\begin{cases} U_{tt}(t)+\mathbf{L}U(t)=F(t), \quad 0\le t\le 1, \\ U(0)=\sum_{j=1}^{p}\alpha_j U(\lambda_j)+\varphi, \\ U_t(0)=\sum_{j=1}^{p}\beta_k U_t(\lambda_k)+\psi, \\ 0<\lambda_1\le\lambda_2\le\cdots\le\lambda_p\le 1 \end{cases} \tag{3}$$

in the Hilbert space $H=L_2\left(\Omega,dV_{g_{\mathbb{H}^2}}\right)$ with the self-adjoint positive definite operator $\mathbf{L}=\Delta_{\mathbb{H}^2}$. Here, $\|U\|_{L_2\left(\Omega,dV_{g_{\mathbb{H}^2}}\right)}=\left(\int_\Omega U^2(x)dV_{g_{\mathbb{H}^2}}(x)\right)^{1/2}$, $dV_{g_{\mathbb{H}^2}}$ is the natural volume element of $\mathbb{H}^2$ obtained from metric tensor $g_{\mathbb{H}^2}$.

The proof of Theorem 5 is based on Theorem 6 with $H=L_2\left(\Omega,dV_{g_{\mathbb{H}^2}}\right)$, and Theorem 7 on the coercivity inequality for the solution of the elliptic differential problem in $L_2\left(\Omega,dV_{g_{\mathbb{H}^2}}\right)$.

Theorem 6 *([11, 12]) Let A be a self adjoint positive definite operator on a Hilbert space H, $\varphi\in D(A)$, $\psi\in D(A^{1/2})$, and $g(t)$ be continuously differentiable on $[0,1]$, and let the assumption (2) hold. Then, there exists a unique solution of*

$$\begin{cases} v_{tt}(t)+Av(t)=g(t), \quad 0\le t\le 1, \\ v(0)=\sum_{j=1}^{p}\alpha_j v(\lambda_j)+\varphi, \\ v_t(0)=\sum_{j=1}^{p}\beta_k v_t(\lambda_k)+\psi, \\ 0<\lambda_1\le\lambda_2\le\cdots\le\lambda_p\le 1 \end{cases}$$

and the following stability inequalities

$$\| v\|_{C(H)}\le M\left[\|\varphi\|_H+\| A^{-1/2}\psi\|_H+\| A^{-1/2}g\|_{C(H)}\right],$$

$$\| A^{1/2}v\|_{C(H)}\le M\left[\| A^{1/2}\varphi\|_H+\|\psi\|_H+\| g\|_{C(H)}\right],$$

$$\| v''\|_{C(H)}+\| Av\|_{C(H)}\le M\left[\| A\varphi\|_H+\| A^{1/2}\psi\|_H+\| g(0)\|_H\int_0^t\| g'(t)\|_H\,dt\right]$$

are valid. Here, M is independent of $g(t), t\in[0,1]$, φ,ψ, and $C(H)$ is the Banach space of the continuous functions $v(t)$ defined on $[0,1]$ with values in H, equipped with the norm

$$\|v\|_{C(H)}=\max_{0\le t\le 1}\|v(t)\|_H.$$

Theorem 7 *For the solutions of the elliptic differential problem*

$$\begin{cases} \Delta^{(r,\theta)}_{\mathbb{H}^2} u(x(r,\theta)) = \omega(\xi(r,\theta)), \quad (r,\theta) \in (a,b)\times(c,d), \\ u(\xi(r,\theta)) = 0, \quad (r,\theta) \text{ in boundary of } [a,b]\times[c,d] \end{cases}$$

the following coercivity inequality holds:

$$\|u_{rr}\|_{L_2\left(\Omega, dV_{g_{\mathbb{H}^2}}\right)} + \|u_{\theta\theta}\|_{L_2\left(\Omega, dV_{g_{\mathbb{H}^2}}\right)} \leq M||\omega||_{L_2\left(\Omega, dV_{g_{\mathbb{H}^2}}\right)}.$$

The proof of Theorem 7 is based on the following theorem.

Theorem 8 *[5] For the solutions of the elliptic differential problem*

$$\begin{cases} A^{\xi} u(\xi) = \omega(\xi), \quad \xi \in (\alpha_1,\beta_1)\times(\alpha_2,\beta_2), \\ u(\xi) = 0, \quad \xi \text{ in boundary } [\alpha_1,\beta_1]\times[\alpha_2,\beta_2] \end{cases}$$

the following coercivity inequality

$$\sum_{r=1}^{2} \|u_{\xi_r\xi_r}\|_{L_2((\alpha_1,\beta_1)\times(\alpha_2,\beta_2))} \leq M||\omega||_{L_2((\alpha_1,\beta_1)\times(\alpha_2,\beta_2))}$$

is valid, where $A^{\xi} = \sum\limits_{r=1}^{2} \frac{\partial}{\partial \xi_r}\left(a_r(\xi)\frac{\partial}{\partial \xi_r}\right)$ *and* $a_r \geq a > 0$.

REFERENCES

1. O. A. Ladyzhenskaya, V. A. Solonnikov, and N. N. Ural'tseva, *Linear and Quasilinear Equations of Parabolic Type* (American Mathematical Society, 1968).
2. O. A. Ladyzhenskaya and N. N. Ural'tseva, *Linear and Quasilinear Elliptic Equations* (Academic Press, 1968).
3. M. L. Vishik, A. D. Myshkis, and O. A. Oleinik, "Partial Differential Equations in: Mathematics in USSR in the Last 40 Years, 1917-1957", Fizmatgiz, Moscow, 1959, p. 563 (Russian).
4. A. V. Gulin, N. I. Ionkin, and V. A. Morozova, Differ. Equ. **37**, 970-978 (2001).
5. P. E. Sobolevskii, Trudy Nauchn. -Issled. Inst. Mat. Voronezh. Gos. Univ. **14**, 68 (1975).
6. P. E. Sobolevskii and L. M. Chebotaryeva, Izv. Vyssh. Uchebn. Zaved. Mat. **5**, 103-116 (1977).
7. H. O. Fattorini, *Second Order Linear Differential Equations in Banach Space* (Elsevier Science, 1985).
8. P. E. Sobolevskii and V. A. Pogorelenko, Sibirsk. Mat. Zh. **8**, 123-145 (1967).
9. A. Ashyralyev and P. E. Sobolevskii, *New Difference Schemes for Partial Differential Equations* (Birkhäuser, 2004).
10. A. Ashyralyev and P. E. Sobolevskii, Discrete Dyn. Nat. Soc. **2**, 183-213 (2005).
11. A. Ashyralyev and N. Aggez, Numer. Funct. Anal. Optim. **25**, 439-462 (2004).
12. A. Ashyralyev and O. Yildirim, Taiwanese J. Math. **14**, 165-194 (2010).
13. I. Chavel, *Eigenvalues in Riemannian Geometry* (Academic Press, 1984).
14. H. Urakawa, Adv. Stud. Pure Math. **22**, 347-406 (1993).

On the Ternary Semigroups of Homeomorphic Transformations of Bounded Closed Sets with Nonempty Interior of Finite-Dimensional Euclidean Spaces

Firudin Kh. Muradov[a)]

Department of Mathematics, Near East University, Nicosia, Mersin 10, Turkey

[a)]*Corresponding author: firudin.muradov@neu.edu.tr*

Abstract. Ternary semigroup is a universal algebra with an associative ternary operation. We give a characterization of bounded closed sets with nonempty interior of finite-dimensional Euclidean spaces by ternary semigroups of pairs of homeomorphic transformations.

INTRODUCTION

The theory of ternary algebraic systems was introduced by Lehmer in [1]. He investigated algebraic systems called triplexes. Sioson [6] studied ternary semigroups with special reference to ideals and radicals . Santiago and Sri Bala [11], [12] developed regular and completely regular ternary semigroups. In [10], Dutta, Kar and Maity studied intra-regular ternary semigroups. In [7], Wagner studied semiheaps. Regularity, Greens equivalences, complete simplicity (Gluskin [3]) have been studied for semiheaps. In [8] and [9] Mustafaev studied semiheaps of continuous and homeomorphic maps. In [2] Gluskin showed that semigroups of topological transformations of bounded closed sets with nonempty interior of finite-dimensional Euclidean spaces define those sets exactly up to homeomorphism. This paper is devoted to characterization of pairs of bounded closed sets with nonempty interior of finite-dimensional Euclidean spaces by ternary semigroups of pairs of homeomorphic maps between those sets.

A ternary semigroup is a nonempty set T together with a ternary operation $[abc]$ satisfying the associative law $[[abc]\,de] = [a\,[bcd]\,e] = [ab\,[cde]]$ for every $a,b,c,d,e \in T$. For convenience we shall denote by $[ABC]$ the set of all elements $[abc]$ where $a \in A, b \in B, c \in C$. The set $[AAA]$ is often denoted by $A^{[3]}$. As an example, any semigroup can be made into a ternary semigroup by defining the ternary product to be $[abc] = abc$. The set of all odd permutations under composition is a ternary semigroup. A nonempty subset A of a ternary semigroup T is called a *ternary subsemigroup* of T if $A^{[3]} \subseteq A$. A nonempty subset L of a ternary semigroup T is called a *left (right, lateral) ideal* of T if $[TTL] \subseteq L$ ($[LTT] \subseteq L, [TLT] \subseteq L$). A nonempty subset A of a ternary semigroup T is called a *two sided ideal* of T if it is a left and right ideal of T. A nonempty subset A of a ternary semigroup T is called an *ideal* of T if it is a left, right and lateral ideal of T. If the intersection K of all the ideals of a ternary semigroup T is not empty, we shall call K the *kernel* of T.

Let X and Y be two nonempty sets and let $F(X,Y)$ be the set of all pairs of functions (η,ϕ), where $\eta : X \to Y$ and $\phi : Y \to X$. The set $F(X,Y)$ is a ternary semigroup with respect to the ternary operation

$$[(\eta_1,\phi_1)(\eta_2,\phi_2)(\eta_3,\phi_3)] = (\eta_1\phi_2\eta_3, \phi_1\eta_2\phi_3),$$

where $(\eta_1\phi_2\eta_3)x = \eta_1(\phi_2(\eta_3(x)))$ and $(\phi_1\eta_2\phi_3)y = \phi_1(\eta_2(\phi_3(y)))$.

CHARACTERIZATION OF BOUNDED CLOSED SETS WITH NONEMPTY INTERIOR OF EUCLIDEAN $n-$SPACES BY TERNARY SEMIGROUPS OF HOMEOMORPHIC TRANSFORMATIONS

Let R be a finite-dimensional Euclidean space with the standard topology. Let Ω_1 and Ω_2 be two bounded closed sets of R such that $Int\Omega_i \neq \varnothing$ for $(i = 1,2)$. Denote by $HT_i(\Omega_i)$ the set of all homeomorphic maps from Ω_i to Ω_j, where $i,j = 1,2,(i \neq j)$. Let $B_i(\Omega_i)$ denote the set of all $a \in HT_i(\Omega_i)$ for which there is an $n-$sized element $E_a \subset \Omega_j$ (a set homeomorphic to some closed $n-$ball) such that $a\Omega_i \subset IntE_a$, $E_a \subset Int\Omega_j$. Let $HT(\Omega_1,\Omega_2) = HT_1(\Omega_1) \times HT_2(\Omega_2)$ be the set of all pairs of homeomorphic maps (a,b), where $a \in HT_1(\Omega_1)$, $b \in HT_2(\Omega_2)$. The set $HT(\Omega_1,\Omega_2)$ is a

International Conference on Analysis and Applied Mathematics (ICAAM 2020)
AIP Conf. Proc. 2325, 020013-1–020013-6; https://doi.org/10.1063/5.0040311
Published by AIP Publishing. 978-0-7354-4069-2/$30.00

ternary semigroup with respect to the ternary operation

$$[(a_1,b_1)(a_2,b_2)(a_3,b_3)] = (a_1b_2a_3, b_1a_2b_3).$$

Clearly, the set $B(\Omega_1,\Omega_2) = B_1(\Omega_1)\times B_2(\Omega_2)$ is a ternary subsemigroup and even an ideal of the ternary semigroup $HT(\Omega_1,\Omega_2)$.

If $a_1(\Omega_1)\subseteq a_2(\Omega_1)$ and $b_1(\Omega_2)\subseteq b_2(\Omega_2)$ for some $(a_1,b_1),(a_2,b_2)\in HT(\Omega_1,\Omega_2)$ we will write $(a_1,b_1)(\Omega_1,\Omega_2)\subseteq (a_2,b_2)(\Omega_1,\Omega_2)$.

Theorem 1 *Let R and R' be finite-dimensional Euclidean spaces. Let Ω_1 and Ω_2 be bounded closed sets of a finite-dimensional Euclidean space R and let Ω_1' and Ω_2' be bounded closed sets of a finite-dimensional Euclidean space R' such that $Int\Omega_i \neq \varnothing$, $Int\Omega_i' \neq \varnothing$ for $(i=1,2)$. The ternary semigroups $B(\Omega_1,\Omega_2)$ and $B(\Omega_1',\Omega_2')$ are isomorphic if and only if the spaces Ω_i and Ω_i' are homeomorphic $(i=1,2)$.*

Proof. Let Ω_1 and Ω_2 be bounded closed subsets of a finite-dimensional Euclidean space R and Ω_1' and Ω_2' be bounded closed subsets of a finite-dimensional Euclidean space R' . Suppose that $\xi_1:\Omega_1\to\Omega_1'$ is a homeomorphism of Ω_1 onto Ω_1' and $\xi_2:\Omega_2\to\Omega_2'$ is a homeomorphism of Ω_2 onto Ω_2'. Then the mapping $\varphi_{\xi_1,\xi_2}: B(\Omega_1,\Omega_2)\to B(\Omega_1',\Omega_2')$ defined by

$$\varphi_{\xi_1,\xi_2}(a,b) = \left(\xi_2 a\xi_1^{-1}, \xi_1 b\xi_2^{-1}\right)$$

is an isomorphism from $B(\Omega_1,\Omega_2)$ onto $B(\Omega_1',\Omega_2')$. The proof of the necessary condition follows from Lemmas 2-11.

Throughout this paper, the symbol φ denotes the isomorphism $\varphi: B(\Omega_1,\Omega_2)\to B(\Omega_1',\Omega_2')$.

Lemma 2 *Let (a,b) be any element of $B(\Omega_1,\Omega_2)$, and let (α,β) be an arbitrary point in $(Int\Omega_1\setminus b\Omega_2)\times(Int\Omega_2\setminus a\Omega_1)$. Then there are $(x,y),(u,v)\in B(\Omega_1,\Omega_2)$ such that*

$$[(a,b)(x,y)(a,b)] = [(a,b)(u,v)(a,b)], and\ \ (x,y)(\alpha,\beta)\neq(u,v)(\alpha,\beta).$$

Proof. Let (a,b) and (x,y) be any elements in $B(\Omega_1,\Omega_2)$ and (α,β) an arbitrary point in $(Int\Omega_1\setminus b\Omega_2)\times(Int\Omega_2\setminus a\Omega_1)$. The sets $(Int\Omega_1\setminus b\Omega_2)$ and $(Int\Omega_2\setminus a\Omega_1)$ contain closed $m-$balls E_1 and E_2 centered at the points α and β respectively, such that $E_1\subset(Int\Omega_1\setminus b\Omega_2)$ and $E_2\subset(Int\Omega_2\setminus a\Omega_1)$. Let f_i be an arbitrary homoemorphism of E_i, $(i=1,2)$ onto itself which maps each boundary point to itself and $f_1(\alpha)\neq\alpha, f_2(\beta)\neq\beta$. Denote by z_i the maps of Ω_i onto itself defined as $z_i(\eta_i)=\eta_i$ if $\eta_i\in\Omega_i\setminus E_i$ and $z_i(\eta_i)=f_i(\eta_i)$ if $\eta_i\in E_i$, $(i=1,2)$. Clearly, the maps z_i are the homeomorphisms of Ω_i onto itself, $(i=1,2)$. If $u=xz_1$, $v=yz_2$ then $(u,v)\in B(\Omega_1,\Omega_2)$ and $(u,v)(\alpha,\beta)\neq(x,y)(\alpha,\beta)$, but $(x,y)(\eta_1,\eta_2)=(u,v)(\eta_1,\eta_2)$ for every $(\eta_1,\eta_2)\in(\Omega_1\setminus E_1)\times(\Omega_2\setminus E_2)$, in particular, for every $(\eta_1,\eta_2)\in b\Omega_2\times a\Omega_1$. Consequently, $[(a,b)(x,y)(a,b)]=[(a,b)(u,v)(a,b)]$.

Lemma 3 *Let $(a_1,a_2),(b_1,b_2)\in B(\Omega_1,\Omega_2)$. The condition*

$$\forall(x_1,x_2),(y_1,y_2)\in B(\Omega_1,\Omega_2),\ [(a_1,a_2)(x_1,x_2)(a_1,a_2)] = [(a_1,a_2)(y_1,y_2)(a_1,a_2)] \tag{1}$$

$$\to [(b_1,b_2)(x_1,x_2)(b_1,b_2)] = [(b_1,b_2)(y_1,y_2)(b_1,b_2)]$$

is a necessary and sufficient for

$$(b_1,b_2)(\Omega_1,\Omega_2)\subseteq(a_1,a_2)(\Omega_1,\Omega_2)$$

Proof. Let $(b_1,b_2)(\Omega_1,\Omega_2)\subseteq(a_1,a_2)(\Omega_1,\Omega_2)$ and $[(a_1,a_2)(x_1,x_2)(a_1,a_2)]=[(a_1,a_2)(y_1,y_2)(a_1,a_2)]$. Then for every point $(\alpha_1,\alpha_2)\in Int\Omega_1\times Int\Omega_2$ there exists a point $(\beta_1,\beta_2)\in Int\Omega_1\times Int\Omega_2$ such that $(b_1,b_2)(\alpha_1,\alpha_2) = (a_1,a_2)(\beta_1,\beta_2)$. Furthermore, we have $a_1x_2a_1=a_1y_2a_1$ and $a_2x_1a_2=a_2y_1a_2$. Then it follows that $x_2a_1=y_2a_1$and $x_1a_2=y_1a_2$. Thus

$$b_1y_2b_1(\alpha_1) = b_1y_2a_1(\beta_1) = b_1x_2a_1(\beta_1) = b_1x_2b_1(\alpha_1),$$

$$b_2y_1b_2(\alpha_2) = b_2y_1a_2(\beta_2) = b_2x_1a_2(\beta_2) = b_2x_1b_2(\alpha_2).$$

The latter means that $[(b_1,b_2)(x_1,x_2)(b_1,b_2)] = [(b_1,b_2)(y_1,y_2)(b_1,b_2)]$.

Conversely, let $(a_1,a_2),(b_1,b_2)$ be any pairs of $B(\Omega_1,\Omega_2)$ and suppose that condition (1) is valid for every $(x_1,x_2),(y_1,y_2) \in B(\Omega_1,\Omega_2)$, but $(b_1,b_2)(\Omega_1,\Omega_2) \setminus \overline{(a_1,a_2)(\Omega_1,\Omega_2)} \neq \emptyset$. Pick the point $(\alpha_1,\alpha_2) = (b_1,b_2)(\beta_1,\beta_2)$ in $(b_1,b_2)(\Omega_1,\Omega_2) \setminus \overline{(a_1,a_2)(\Omega_1,\Omega_2)}$. It would then follow from Lemma 2 that

$$[(a_1,a_2)(x_1,x_2)(a_1,a_2)] = [(a_1,a_2)(y_1,y_2)(a_1,a_2)],$$

$$(x_1,x_2)(\alpha_1,\alpha_2) \neq (y_1,y_2)(\alpha_1,\alpha_2),$$

for some $(x_1,x_2),(y_1,y_2) \in B(\Omega_1,\Omega_2)$. Then

$$(b_1x_2b_1,b_2x_1b_2)(\beta_1,\beta_2) \neq (b_1y_2b_1,b_2y_1b_2)(\beta_1,\beta_2),$$

or

$$[(b_1,b_2)(x_1,x_2)(b_1,b_2)] \neq [(b_1,b_2)(y_1,y_2)(b_1,b_2)].$$

The latter inequality contradicts to condition (1). Therefore, $(b_1,b_2)(\Omega_1,\Omega_2) \subset (a_1,a_2)(\Omega_1,\Omega_2)$, or $b_1\Omega_1 \setminus a_1\Omega_1 \neq \emptyset$ and $b_2\Omega_2 \setminus a_2\Omega_2 = \emptyset$, or $b_1\Omega_1 \setminus a_1\Omega_1 = \emptyset$ and $b_2\Omega_2 \setminus a_2\Omega_2 \neq \emptyset$. Let, for example, $b_1\Omega_1 \setminus a_1\Omega_1 \neq \emptyset$, $b_2\Omega_2 \setminus a_2\Omega_2 = \emptyset$ hold. Clearly, $b_2\Omega_2 \subset a_2\Omega_2$. Pick the point $\beta \in b_1\Omega_1 \setminus a_1\Omega_1 \subset \Omega_2 \setminus a_1\Omega_1$ and the point $\alpha \in \Omega_1 \setminus a_2\Omega_2$. It would then follow from Lemma 2 that there exist $(x,y),(u,v)$ in B such that

$$[(a_1,a_2)(x,y)(a_1,a_2)] = [(a_1,a_2)(u,v)(a_1,a_2)],$$

$$(x,y)(\alpha,\beta) \neq (u,v)(\alpha,\beta).$$

Clearly, there exists $\gamma \in \Omega_1$ such that $\beta = b_1\gamma$. Then $b_1yb_1(\gamma) = b_1y(\beta) \neq b_1v(\beta) = b_1v(\gamma)$, that is

$$[(b_1,b_2)(x,y)(b_1,b_2)] \neq [(b_1,b_2)(u,v)(b_1,b_2)],$$

which contradicts to condition (1). We can prove analogous statement for the case $b_1\Omega_1 \setminus a_1\Omega_1 = \emptyset$ and $b_2\Omega_2 \setminus a_2\Omega_2 \neq \emptyset$.

Lemma 4 *If E_i is any closed ball in $Int\Omega_i$ and α_i is an arbitrary point in $IntE_i$, then there exists $(c_1,c_2) \in B(\Omega_1,\Omega_2)$ such that $\alpha_i \in Intc_j\Omega_j, c_i\Omega_i \subset IntE_j$, where $i,j = 1,2,(i \neq j)$.*

Lemma 5 *Let $(a_1,b_1),(a_2,b_2) \in B(\Omega_1,\Omega_2)$ such that*

$$(a_2,b_2)(\Omega_1,\Omega_2) \subseteq (a_1,b_1)(\Omega_1,\Omega_2).$$

Then

$$\varphi(a_2,b_2)\left(\Omega_1',\Omega_2'\right) \subset \varphi(a_1,b_1)\left(\Omega_1',\Omega_2'\right).$$

Proof. Let $(a_1,a_2),(b_1,b_2)$ be any two elements in $B(\Omega_1,\Omega_2)$ such that

$$(a_2,b_2)(\Omega_1,\Omega_2) \subseteq (a_1,b_1)(\Omega_1,\Omega_2).$$

If

$$\left[\varphi(a_1,b_1)\left(x_1',y_1'\right)\varphi(a_1,b_1)\right] = \left[\varphi(a_1,b_1)\left(x_2',y_2'\right)\varphi(a_1,b_1)\right] \tag{2}$$

is valid for some $(x_1',y_1'),(x_2',y_2') \in B(\Omega_1',\Omega_2')$ then there would have to be elements $(x_1,y_1),(x_2,y_2) \in B(\Omega_1,\Omega_2)$ such that $\varphi(x_1,y_1) = (x_1',y_1')$ and $\varphi(x_2,y_2) = (x_2',y_2')$ and therefore

$$[\varphi(a_1,b_1)\varphi(x_1,y_1)\varphi(a_1,b_1)] = [\varphi(a_1,b_1)\varphi(x_2,y_2)\varphi(a_1,b_1)].$$

From this we have

$$\varphi[(a_1,b_1)(x_1,y_1)(a_1,b_1)] = \varphi[(a_1,b_1)(x_2,y_2)(a_1,b_1)]$$

and since φ is an isomorphism of $B(\Omega_1,\Omega_2)$ onto $B(\Omega_1',\Omega_2')$ we have

$$[(a_1,b_1)(x_1,y_1)(a_1,b_1)] = [(a_1,b_1)(x_2,y_2)(a_1,b_1)].$$

Then it follows from Lemma 3 that

$$[(a_2,b_2)(x_1,y_1)(a_2,b_2)] = [(a_2,b_2)(x_2,y_2)(a_2,b_2)]$$

or

$$[\varphi(a_2,b_2)\varphi(x_1,y_1)\varphi(a_2,b_2)] = [\varphi(a_2,b_2)\varphi(x_2,y_2)\varphi(a_2,b_2)]$$

or

$$\left[\varphi(a_2,b_2)\left(x_1',y_1'\right)\varphi(a_2,b_2)\right] = \left[\varphi(a_2,b_2)\left(x_2',y_2'\right)\varphi(a_2,b_2)\right].$$

Since the last equality is valid for every $(x_1',y_1'),(x_2',y_2') \in B(\Omega_1',\Omega_2')$ satisfying (2), we have by Lemma 3 that $\varphi(a_2,b_2)(\Omega_1',\Omega_2') \subset \varphi(a_1,b_1)(\Omega_1',\Omega_2')$.

Lemma 6 *Let $(a_1,b_1),(a_2,b_2) \in B(\Omega_1,\Omega_2)$. If*

$$(a_1,b_1)(\Omega_1,\Omega_2) \cap (a_2,b_2)(\Omega_1,\Omega_2) \neq \varnothing$$

then $\varphi(a_1,b_1)(\Omega_1',\Omega_2') \cap \varphi(a_2,b_2)(\Omega_1',\Omega_2') \neq \varnothing$.

Lemma 7 *Let $(a_1,b_1),(a_2,b_2)$ be arbitrary elements of $B(\Omega_1,\Omega_2)$ and (u,v) be some fixed element of $B(\Omega_1,\Omega_2)$. The equation*

$$[(a_1,b_1)(u,v)(x,y)] = (a_2,b_2)$$

has a solution $(x,y) \in B(\Omega_1,\Omega_2)$ if and only if there exist $n-$sized elements $E_1 \subset Int b_1 u\Omega_1$ and $E_2 \subset Int a_1 v\Omega_2$ such that

$$(a_2,b_2)(\Omega_1,\Omega_2) \subset (Int E_1, Int E_2).$$

Let $(\alpha,\beta) \in Int\Omega_1 \times Int\Omega_2$. We say that an infinite sequence $\{(a_i,b_i)\}_{i=1}^{\infty}$ of elements $(a_i,b_i) \in B(\Omega_1,\Omega_2)$ has a limit (α,β) if the following conditions are satisfied:

a) $(\cap_{i=1}^{\infty} b_i\Omega_2, \cap_{i=2}^{\infty} a_i\Omega_1) = (\alpha,\beta)$,

b) for every i there exists an element (x_{i+1},y_{i+1}) such that

$$[(a_{i+1},b_{i+1})(a_i,b_i)(x_{i+1},y_{i+1})] = (a_{i+2},b_{i+2}).$$

A sequence $\{(a_i,b_i)\}_{i=1}^{\infty}$ of elements $(a_i,b_i) \in B(Int\Omega_1, Int\Omega_2)$converging to the point $(\alpha,\beta) \in Int\Omega_1 \times Int\Omega_2$ can be constructed, for example, as follows. Suppose that $E_1 \subset Int\Omega_1$ is a closed $n-$ball centered at α and $T_1 \subset Int\Omega_2$ is a closed $n-$ball centered at β. By Lemma 4 there exists $(a_1,b_1) \in B(\Omega_1,\Omega_2)$ such that $\alpha \in b_1\Omega_2 \subset Int E_1, \beta \in a_1\Omega_1 \subset Int T_1$. Suppose now that E_2 is a closed $n-$ball in $b_1\Omega_2$ and centered at α and T_2 is a closed $n-$ball in $a_1\Omega_1$ and centered at β. According to Lemma 4 there exists an element $(a_2,b_2) \in B(\Omega_1,\Omega_2)$ such that $\alpha \in b_2\Omega_2 \subset Int E_2, \beta \in a_2\Omega_1 \subset Int T_2$. Let $\alpha_1 = (b_2a_1)^{-1}(\alpha)$ and $\beta_1 = (a_2b_1)^{-1}(\beta)$. Let $A_1 \subset Int\Omega_1$ be a closed $n-$ball centered at α_1 and $B_1 \subset Int\Omega_2$ be a closed $n-$ball centered at β_1. Clearly, $\alpha \in b_2a_1A_1 \cap E_2, \beta \in a_2b_1B_1 \cap T_2$. Let $E_3 \subset Int(b_2a_1A_1 \cap E_2)$ be a closed $n-$ball centered at α, and let $T_3 \subset Int(a_2b_1B_1 \cap T_2)$ be a closed $n-$ball centered at β. According to Lemma 4 there exists an element $(a_3,b_3) \in B(\Omega_1,\Omega_2)$ such that $\alpha \in b_3\Omega_2$ and $b_3\Omega_2 \subset Int E_3, \beta \in a_3\Omega_1$ and $a_3\Omega_1 \subset Int T_3$. By Lemma 7 $x_2 = (a_2b_1)^{-1}a_3, y_2 = (b_2a_1)^{-1}b_3$ is the solution of the equation $[(a_2,b_2)(a_1,b_1)(x_2,y_2)] = (a_3,b_3)$. Assume now that the first n terms of the sequence are already found. Denote $\alpha_{n-1} = (b_na_{n-1})^{-1}(\alpha)$ and $\beta_{n-1} = (a_nb_{n-1})^{-1}(\beta)$. Suppose that $A_{n-1} \subset Int\Omega_1$ is a closed $n-$ball centered at α_{n-1} and $B_{n-1} \subset Int\Omega_2$ is a closed $n-$ball centered at β_{n-1}. Clearly, $\alpha \in b_na_{n-1}A_{n-1} \cap E_n, \beta \in a_nb_{n-1}B_{n-1} \cap T_n$. Let $E_{n+1} \subset Int(b_na_{n-1}A_{n-1} \cap E_n)$ be a closed $n-$ball centered at α, and let $T_{n+1} \subset Int(a_nb_{n-1}B_{n-1} \cap T_n)$ be a closed $n-$ball centered at β. According to Lemma 4 there exists an element $(a_{n+1},b_{n+1}) \in B(\Omega_1,\Omega_2)$ such that $\alpha \in b_{n+1}\Omega_2$ and $b_{n+1}\Omega_2 \subset Int E_{n+1}, \beta \in a_{n+1}\Omega_1$ and $a_{n+1}\Omega_1 \subset Int T_{n+1}$. By Lemma 7 $x_n = (a_nb_{n-1})^{-1}a_{n+1}, y_n = (b_na_{n-1})^{-1}b_{n+1}$ is the solution of the equation $[(a_n,b_n)(a_{n-1},b_{n-1})(x_n,y_n)] = (a_{n+1},b_{n+1})$. This sequence satisfies condition (b) and satisfies condition (a) if the sequences of radii of E_n and T_n converge to zero.

Lemma 8 *If the ternary semigroups $B(\Omega_1,\Omega_2)$ and $B(\Omega_1',\Omega_2')$ are isomorphic, then there exist a bijective map f from $Int\Omega_1 \times Int\Omega_2$ onto $Int\Omega_1' \times Int\Omega_2'$ and bijective maps ξ_i from $Int\Omega_i$ onto $Int\Omega_i'$ $(i=1,2)$ such that $f(\alpha,\beta) = (\xi_1\alpha,\xi_2\beta)$ for every $(\alpha,\beta) \in Int\Omega_1 \times Int\Omega_2$, .*

Proof. Let (α,β) be any point in $Int\Omega_1 \times Int\Omega_2$ and let $\{(a_i,b_i)\}_{i=1}^{\infty}$ be a sequence of elements $(a_i,b_i) \in B(\Omega_1,\Omega_2)$ converging to the point (α,β).Denote $\varphi(a_i,b_i)$ by (a_i',b_i').The sequence $\{(a_i',b_i')\}_{i=1}^{\infty}$ converges to the point (α',β'). Define a map $f:(\Omega_1,\Omega_2) \to (\Omega_1',\Omega_2')$ by $f(\alpha,\beta) = (\alpha',\beta')$. The point (α',β') does not depend on the choice of the sequence $\{(a_i,b_i)\}_{i=1}^{\infty}$ of elements $(a_i,b_i) \in B(\Omega_1,\Omega_2)$ converging to the point (α,β). The map f is one-to-one and there are one-to-one maps ξ_i from Ω_i onto Ω_i' for $(i=1,2)$ such that $\forall(\alpha,\beta) \in Int\Omega_1 \times Int\Omega_2, f(\alpha,\beta) = (\xi_1\alpha,\xi_2\beta)$.

Lemma 9 *For every $(\alpha,\beta) \in Int\Omega_1 \times Int\Omega_2$ and for every $(a,b) \in B(\Omega_1,\Omega_2)$ if $(\alpha,\beta) \in Int(a,b)(\Omega_1,\Omega_2)$ then $f(\alpha,\beta) = (\xi_1\alpha,\xi_2\beta) \in Int\varphi(a,b)(\Omega_1',\Omega_2')$. The map f is a homeomorphism from $Int\Omega_1 \times Int\Omega_2$ onto $Int\Omega_1' \times Int\Omega_2'$ and the maps ξ_i are homeomorphisms from $Int\Omega_i$ onto $Int\Omega_i'$ for $i=1,2$.*

Lemma 10 *Let (x,y) be an arbitrary element of $B(\Omega_1,\Omega_2)$ and (u,v) some fixed element of $B(\Omega_1,\Omega_2)$. The following equality holds for an arbitrary point $(\alpha,\beta) \in Int\Omega_1 \times Int\Omega_2$*

$$\varphi(x,y)\{\varphi(u,v)[(\xi_1,\xi_2)(\alpha,\beta)]\} = (\xi_1,\xi_2)\{(x,y)[(u,v)(\alpha,\beta)]\}.$$

Lemma 11 *The following equality holds for every $(a,b) \in B(\Omega_1,\Omega_2)$*

$$\varphi(a,b)\left(\Omega_1',\Omega_2'\right) = (\xi_1,\xi_2)(a,b)(\Omega_1,\Omega_2),$$

and so the spaces Ω_i and Ω_i' are homeomorphic $(i=1,2)$.

Theorem 12 *The ternary semigroup $B(\Omega_1,\Omega_2)$ is the kernel of the ternary semigroup $HT(\Omega_1,\Omega_2)$.*

Proof. The theorem is proved if we can show that $B(\Omega_1,\Omega_2)$ has no proper ideals. Let $(a_1,a_2),(b_1,b_2)$ be any two elements of $B(\Omega_1,\Omega_2)$. Show that there are $(x_1,x_2),(y_1,y_2) \in B(\Omega_1,\Omega_2)$ such that $[(x_1,x_2)(a_1,a_2)(y_1,y_2)] = (b_1,b_2)$. Let E be a closed $n-$ball containing the set Ω_1 and let E_1 be a closed $n-$ball contained in $Inta_2\Omega_2$. Let $b_1\Omega_1 \subset IntE_2$, where E_2 is an $n-$sized element in $Int\Omega_2$. Further, let E_3 and E_4 be closed $n-$balls in $Int\Omega_1$ such that $E_3 \subset IntE_4$. Denote by f a homeomorphism of an $n-$sized element E_2 onto E_3. Clearly, the set $fb_1(\Omega_1)$ is a closed set contained in $IntE_3$. Then there is a closed $n-$ball $E_5 \subset IntE_3$ such that $fb_1(\Omega_1) \subset IntE_5$. We denote the $n-$sized element $f^{-1}(E_5)$ by E_6. Denote by g a homeomorphism of an $n-$ball E onto E_3 such that $g(E_1) = E_5$. Take $x_1 = a_2^{-1}g^{-1}fb_1$ and $y_1 = f^{-1}g$. It is clear that $y_1a_2x_1 = b_1$. We can analogously select x_2 and y_2 such that $x_2a_1y_2 = b_2$. Thus, $B(\Omega_1,\Omega_2)$ is the kernel of the ternary semigroup $HT(\Omega_1,\Omega_2)$.

Theorem 13 *Let Ω_1 and Ω_2 be bounded closed subsets of a finite-dimensional Euclidean space R and Ω_1' and Ω_2' be bounded closed subsets of a finite-dimensional Euclidean space R'such that $Int\Omega_i \neq \emptyset$, $Int\Omega_i' \neq \emptyset$ for $i=1,2$. The ternary semigroups $HT(\Omega_1,\Omega_2)$ and $HT(\Omega_1',\Omega_2')$ are isomorphic if and only if the spaces Ω_i and Ω_i' are homeomorphic $(i=1,2)$.*

Proof. Let Ω_1 and Ω_2 be bounded closed subsets of a finite-dimensional Euclidean space R and Ω_1' and Ω_2' be bounded closed subsets of a finite-dimensional Euclidean space R' . Suppose that $\xi_1:\Omega_1 \to \Omega_1'$ is a homeomorphism of Ω_1 onto Ω_1' and $\xi_2:\Omega_2 \to \Omega_2'$ is a homeomorphism of Ω_2 onto Ω_2'. Then the mapping $\varphi_{\xi_1,\xi_2}: HT(\Omega_1,\Omega_2) \to HT(\Omega_1',\Omega_2')$ defined by

$$\varphi_{\xi_1,\xi_2}(a,b) = \left(\xi_2 a\xi_1^{-1}, \xi_1 b\xi_2^{-1}\right)$$

is an isomorphism from $HT(\Omega_1,\Omega_2)$ onto $HT(\Omega_1',\Omega_2')$. On the other hand, if the ternary semigroups $HT(\Omega_1,\Omega_2)$ and $HT(\Omega_1',\Omega_2')$ are isomorphic then it follows from Theorem 12 that the spaces Ω_i and Ω_i' are homeomorphic $(i=1,2)$.

REFERENCES

1. D. H. Lehmer, Am. J. Math. **54**, 329-338 (1932).
2. L. M.Gluskin, Izv. Vyssh. Uchebn. Zaved. Mat. **1**, 54 - 65 (1963) (in Russian).

3. L. M.Gluskin, *Completely Simple Semiheaps*, in: Theory of Semigroups and its Applications, vol.1, 179-197 (Saratov Gos. Univ., 1965, in Russian).
4. B. M. Schein, Amer. Math. Soc. Translat. **2(113)**, 123-181 (1979).
5. L. B. Shneperman, Sib. Math. J. **1**, 221-229 (1965).
6. F. M. Sioson, Math. Jpn. **10**, 63-84 (1965).
7. V. V. Wagner, Mat. Sb. NS **32(74)**, 545-632 (1953) (in Russian).
8. L.G.Mustafaev, Dokl. Akad. Nauk SSSR **215(3)**, 543-546 (1974) (in Russian).
9. L. G. Mustafaev, Dokl. Akad. Nauk SSSR **230(6)**, 1279-1281 (1976) (in Russian).
10. T. K. Dutta, S. Kar, and B. Maity, Discussiones Mathematicae, General Algebra and Applications **28**, 147-159 (2008).
11. M. L. Santiago and S. Sri Bala, Semigroup Forum **81**, 380-388 (2010).
12. M. L. Santiago and S. Sri Bala, J. Calcutta Math. Soc. **7**, 105 - 120 (2011).
13. G. Sheeja and S. Sri Bala, Quasigroups and Related Systems **21**, 103 - 116 (2013).

Sensitivity Analysis on the SEIR-SEI Model for the Dynamics of Blinding Trachoma

Salisu M. Muhammad,[1, a)] Evren Hincal,[1, 2, b)] Bilgen Kaymakamzade,[1, 2, c)] and Nezihal Gokbulut[1, 2, d)]

[1)] *Department of Mathematics, Near East University, Nicosia, Mersin 10, Turkey*
[2)] *Mathematics Research Center, Near East University, Nicosia, Mersin 10, Turkey*

[a)] *Electronic mail: salisumuhammadmuhammad@gmail.com*
[b)] *Electronic mail: evren.hincal@neu.edu.tr*
[c)] *Electronic mail: bilgen.kaymakamzade@neu.edu.tr*
[d)] *Corresponding author: nezihal.gokbulut@neu.edu.tr*

Abstract. In many engineering and science fields sensitivity analysis has become highly interesting. For the mathematical modeling of biological phenomena, researchers use sensitivity and uncertainty analysis because of its usefulness for defining important parameters for performance of the model. It can also help in the process of experimental analysis, reducing model order, estimating parameters, taking decisions or developing recommendations for decision-makers. Here, we illustrated the use of the local sensitivity analysis to explain the effect of various parameters on a threshold parameter, R_0, resulting from the study of a dynamics model inside the human-host. And it is confirmed from computed elasticity indices that the most sensitive parameter to basic reproduction number is (vector contact rate) followed by rates of transmission. Moreover, a detailed parameter estimation of the model parameters and model fitting presented with the use of field data cases from Northern Nigeria using least-square fitting method. Finally, the sensitivity analysis results shows that improving the rate of environmental hygiene and facial cleanliness will attract a consequential decrease in the size of basic reproduction number, which results in the declination of the disease transmission.

INTRODUCTION

Trachoma was one of 17 preventable diseases (NTDs) that the World Health Organization (WHO) prioritized for surveillance and elimination through protective therapies or improved prevention and treatment approaches [1]. NTDs appear to have been primarily responsible for chronic infectious diseases causing immense comorbidities. Nevertheless, long-term impairment in contrast with acute communicable diseases [1, 2] found to be relatively low deaths. Poverty-related lifestyles like substandard housing, insufficient sanitary conditions, inadequate access to clean water encourage the transmission of contagious disease [3].

C. Trachomatis can indeed spread through 2 primary ways. The first one is direct interaction with an infectious individual or garments interaction that had already encountered [4] infected eye discharges. Other paths involve spread through an eye-seeking fly [musca sobens] by contacting the leakage from such an afflicted person's face or nose [5]. The study provides alternative tools that can be used by planning officers to design a trachoma control program to achieve global eradication of trachoma as a public heath challenge as targeted by the world health organization.

Background

Mathematical models are used to understand the dynamics of the preventable diseases (particularly, Trachoma). Such approaches not just described the mathematical tool of contagious diseases but they often offer better information about the possible control and spread of the disease [6].
For the novel SEIR-SEI Trachoma model, the current study proposed a comprehensive local sensitivity analysis that considers both transmission to display the effect of different parameters in controlling epidemic so that the goal of the World Health Organization can be made feasible to eradicate trachoma as a public health problem by 2030. Some simulation results were obtained as a function of two different biological parameters with the aid of mesh plots for the reproductive number. Our new research article complimented some of the previously mentioned literary studies.

International Conference on Analysis and Applied Mathematics (ICAAM 2020)
AIP Conf. Proc. 2325, 020014-1–020014-5; https://doi.org/10.1063/5.0040299
Published by AIP Publishing. 978-0-7354-4069-2/$30.00

METHODOLOGY

TABLE 1. The state variables values $(Month^{-1})$ used in the model (1).

Variables	Interpretation
$S_h(t)$	Population of susceptible humans
$E_h(t)$	Population of exposed humans
$I_{hs}(t)$	Class of infected individuals with early stages of trachoma
$I_{hc}(t)$	Class of infected individuals with TT and CO stages of trachoma
$R_h(t)$	Population of recovered humans
$S_f(t)$	Class of exposed flies
$E_f(t)$	Population of exposed flies
$I_f(t)$	Class of infected flies

TABLE 2. The state parameters values $(Month^{-1})$ used in the model (1).

Parameters	Interpretation	Value	Source
Π_h	Human recruitment rate	25	[7, 8]
μ_h	Natural death rate of human	0.0014	[7, 8]
μ_f	Natural death rate of eye-seeking fly(musca sorvens)	1.354	[9, 10]
Π_f	Flies recruitment rate	1.5×10^6	Assumed
β_h	Rate of transmission from vector to host	0.08353	[7]
β_f	Rate of transmission from host to vector	0.07258	Assumed
δ_1	Progression rate from E_h to I_{hs}	4.72	[9, 10]
δ_2	Progression rate from I_{hs} to I_{hc}	0.0299	[7, 10]
τ	Progression rate from E_f to I_f	2.21	[9, 10]
φ	Rate at which human looses immunity	0.5	[11, 12]
σ_f	Vector Rate of biting	0.29	Assumed
ψ_1	Human recovery rate from exposed class	0.3	[11, 13, 14]
ψ_2	Human recovery rate from I_{hs}	0.1	[11, 13, 14]
ψ_3	Human recovery rate from I_{hc}	0.1428	[11, 13, 14]

LOCAL SENSITIVITY ANALYSIS

In this section, the local sensitivity analysis approach is employed to demonstrate the sensitivity of the R_0 in relation to individual parameters of the model. The basic reproduction number has been derived and characterized as the model's parameter-dependent output and the indicator of severity for the disease.

In this way, it was crucially involved and inspired to examine the monotonicity between the model parameters and the basic reproduction number. Earlier, the model's basic properties were demonstrated, detailing the positivity, and well-posedness of solutions. Our primary concern now is only to comprehend the sensitivity of the basic number of the reproduction in relation to the model's parameters. Here the basic reproduction number is

$$R_0 = \frac{\sqrt{P_2 P_1 P_3 P_4 \Pi_h \tau \Pi_f \beta_f \beta_h \delta_1 \mu_h \left(P_3 + \delta_2\right)} \sigma_f}{P_2 P_1 P_3 P_4 \Pi_h \mu_f}.$$

Meanwhile, we have the calculation of standardized local sensitivity index values of R_0^T proportional to the parameters in the trachoma model, where the parameters input relative to R_0^T

$$\rho = \left\{\Pi_h, \mu_h, \psi_3, \delta_2, \psi_2, \delta_1, \psi_1, \tau, \Pi_f \beta_f, \beta_h, \sigma_f, \mu_f\right\}.$$

Then, we display a normalized forward sensitivity index of R_0^T due to variance of the parameters.

By $\Gamma\omega^{R_0^T}$, we denote the normalized local sensitivity index of the R_0^T performance with respect to a (ω) parameter, where $\omega \in \rho$ is defined as

$$\Gamma_{\omega}^{R_0^T} = \frac{\partial ln(R_0^T)}{\partial ln(\omega)}.$$

[15, 16, 17, 18]. Using the above definition we computed the following indices for the output R_0^T with respect to every parameter presented in Table 2.

$$\begin{aligned}
\Gamma_{\sigma_f}^{R_0^T} &= \frac{\partial ln(R_0^T)}{\partial ln(\sigma_f)} = 1,\\
\Gamma_{\beta_h}^{R_0^T} &= \frac{\partial ln(R_0^T)}{\partial ln(\beta_h)} = \frac{1}{2},\\
\Gamma_{\beta_f}^{R_0^T} &= \frac{\partial ln(R_0^T)}{\partial ln(\beta_f)} = \frac{1}{2},\\
\Gamma_{\Pi_h}^{R_0^T} &= \frac{\partial ln(R_0^T)}{\partial ln(\Pi_h)} = -\frac{1}{2},\\
\Gamma_{\Pi_f}^{R_0^T} &= \frac{\partial ln(R_0^T)}{\partial ln(\Pi_f)} = \frac{1}{2},\\
\Gamma_{\tau}^{R_0^T} &= \frac{\partial ln(R_0^T)}{\partial ln(\tau)} = \frac{1}{2}\frac{\mu_h}{\mu_h+\tau},\\
\Gamma_{\delta_1}^{R_0^T} &= \frac{\partial ln(R_0^T)}{\partial ln(\delta_1)} = \frac{1}{2}\frac{\mu_h+\psi_1}{\delta_1+\mu_h+\psi_1},\\
\Gamma_{\delta_2}^{R_0^T} &= \frac{\partial ln(R_0^T)}{\partial ln(\delta_2)} = \frac{1}{2}\frac{(\psi_2-\psi_3)\delta_2}{(\delta_2+\mu_h+\psi_2)(\mu_h+\psi_3+\delta_2+)},\\
\Gamma_{\psi_1}^{R_0^T} &= \frac{\partial ln(R_0^T)}{\partial ln(\psi_1)} = -\frac{1}{2}\frac{\psi_1}{(\delta_1+\mu_h+\psi_1)},\\
\Gamma_{\psi_2}^{R_0^T} &= \frac{\partial ln(R_0^T)}{\partial ln(\psi_2)} = -\frac{1}{2}\frac{\psi_2}{(\delta_2+\mu_h+\psi_2)},\\
\Gamma_{\psi_3}^{R_0^T} &= \frac{\partial ln(R_0^T)}{\partial ln(\psi_3)} = -\frac{1}{2}\frac{(\delta_2\psi_3)}{(\mu_h+\psi_3)(\mu_h+\psi_3+\delta_2)},\\
\Gamma_{\mu_f}^{R_0^T} &= \frac{\partial ln(R_0^T)}{\partial ln(\mu_f)} = -1.
\end{aligned}$$

Based on the elasticity analysis above, one can quickly perceive whenever there is an increase in σ_f by 5%and all other parameters remained fixed, it will attract an increase of 5%to R_0^T demonstrated a good relation between R_0^T) and the model's parameters. In a similar manner, it clearly shows that adjusting the transmission rates, β_f, β_h, and recruitment rates of fly Π_f by 10% each, and maintaining other parameters unchanged, will generate an increase of 5% in R_0, that will also boost the incidence rate of trachoma in the populace. Likewise, increasing the parameter values τ and δ_1 by 1.0% (one point) in the simple reproduction amount R_0^T would correspondingly gain less than 1 *point* increment. Meanwhile, raising the parameter values μ_f and Π_h by 10% each will attract corresponding decreases of 10%and 5% respectively in R_0^T. Similarly, whenever we introduce increments of δ_1, ψ_1, ψ_2, $\psi_3$and μ_h by 1.0 percent, this will give us a consequential decrease of less than 1.0 percent in the basic reproduction number. Therefore, later are the most sensitive parameters to be targeted to achieve the goal of Global Trachoma Elimination as a Public Health Problem.
Using the produced coefficients of the normalized local sensitivity indices to illustrate the relative influences of each of the parameters on R_0^T is now quite enough used.

From 1, the elasticity indices recorded in the chart can be interpreted on the basis of the values given earlier in Table 1 and Table 2. It reveals that in changing the size of the basic reproduction number R_0^T the most sensitive and influential parameter is σ_f (the contact rate of the eye-seeking flies or the musca sovens) whose index value is $+1.0000$.

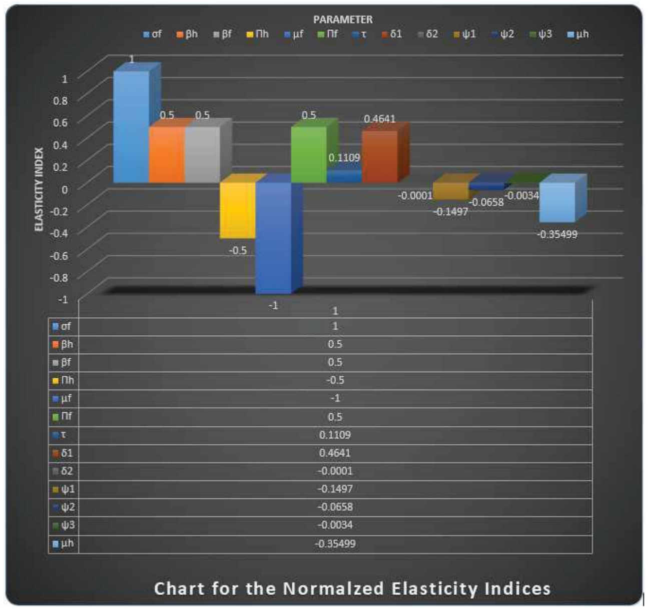

FIGURE 1. The local elasticity indices of R_o with respect to parameters of the model as presented in Table 1 and Table 2.

RESULTS AND DISCUSSION

R_0 is the most important quantity for understanding the extent to which an epidemic spreads. It is revealed that the effective use of the control scheme (SAFE) adopted by the WHO plays an important role in attaining desired elimination of trachoma as a major public health problem. Various kinds of biological parameters of the proposed Trachoma model have also been investigated. We obtained some numerical results using mesh plot and the parameter values in Table 2. The result as shown shows the significant increase in some model parameters with the variation.

CONCLUSION

We have considered a compartmental model of (Kermack-Mckenderick) type for the dynamics of chlamydia trachomatis earlier developed by (Salisu M.M. and Evren Hincal, 2020), where they confirmed that the local asymptotic stability of the disease-free equilibrium and the global asymptotic stability of the unique endemic equilibrium whenever the computed basic reproduction number R_0 is below unity and R_0 greater than one respectively. We have estimated the model parameters and fit the model with the use of field data cases from Northern Nigeria using least-square fitting method.

Moreover, we displayed the significance of the model parameters in changing the size of the basic reproduction number R_0^T. It is confirmed from computed elasticity indices that the most sensitive parameter to basic reproduction number is σ_f (vector contact rate), followed by rates of transmission (β_h and β_f), then the rest.

It shows that the effective use of the control scheme (SAFE) adopted by the WHO plays an important role in achieving targeted trachoma eradication by the WHO as a public health challenge over the next 10 years. We also obtained some simulation results as a function of two different biological parameters using mesh plots for the reproductive number R_0.

ACKNOWLEDGEMENTS

We wish to thank to the Department of Mathematics, Near East University, Cyprus for providing all the needful support.

REFERENCES

1. Neglected Tropical Diseases, http://www.who.int/neglected_diseases/diseases/en/ (accessed 4 October, 2020).
2. P. J. Hotez, M. Alvarado, M. G. Basanez, et. al., PLoS Negl. Trop. Dis. **8**, e2865 (2014).
3. P. J. Hotez, A. Fenwick, et. al., Lancet **373**, 1570-1575 (2009).
4. M. J. Burton and D. C. W. Mabey, PLoS Negl. Trop. Dis. **3**, e460 (2009).
5. P. M . Emerson, S. W. Lindsay, N. Alexander, et. al., Lancet **363**, 1093-1098 (2004).
6. F. Brauer and C. Castillo-Chavez, Mathematical Models in Population Biology and Epidemiology (New York, NY: Dordrecht Heidlberg London, 2012), pp. 134-146.
7. E. O. Omondi, F. Nyabadza, E. Bonyah, and K. Badu, Journal of Biological Systems **25**, 247-277 (2017).
8. Central Intelligence Agency: The World Fact Book, The World of a Nation: The Center of Intelligence, https://www.cia.gov/library/publications/the-worldfactbook (accessed February 2016).
9. Animal Diversity Web, Onchocerca volvulus, http://animaldiversity.org/accounts/Onchocerca_volvulus (accessed February 2016).
10. Onchocerciasis (On-kough-sir-ky-a-sis), Parasitic diseases, http://www.wellness proposals.com/health-care/handouts/parasitic-zoonotic-diseases/onchocerciasis-fact sheet.pdf ((accessed February 2016).
11. A. Pinsent and T. D. Hollingsworth, PLoS Negl. Trop. Dis. **12(10)**, (2018).
12. A. J. Shattock, M. Gambhir, H. R. Taylor, et. al., PLoS Negl. Trop. Dis. **9(4)**, 1-12 (2015).
13. M. Gambhir, M. G. Basanez, M. J. Burton, et. al., PLoS Negl. Trop. Dis. **3(6)**, e462 (2009).
14. N. C. Grassly, M. E. Ward, et. al., PLoS Negl. Trop. Dis. **2(12)**, e341 (2008).
15. A. V. Griensven, T. Meixner, S. Grunwald, et. al., Journal of Hydrology **324**, 10-23 (2006).
16. X. Zhou and H. Lin, Local Sensitivity Analysis (Springer US, Boston, MA, 2008).
17. X. Zhou and H. Lin, Global Sensitivity Analysis (Springer US,Boston, MA, 2008).
18. Z. Zi, IET Systems Bio. **456**, 336-346 (2011).

On the Asymptotic Formula for the Solution of Nonlocal Boundary Value Perturbation Problems for Hyperbolic Equations

Allaberen Ashyralyev[1, 2, 3, a)] and Ozgur Yildirim[4, b)]

[1)] Department of Mathematics, Near East University, Nicosia, Mersin 10, Turkey
[2)] Peoples' Friendship University of Russia (RUDN University), Ul Miklukho Maklaya 6, Moscow 117198, Russia
[3)] Institute of Mathematics and Mathematical Modeling, 050010, Almaty, Kazakhstan
[4)] Department of Mathematics, Yildiz Technical University, 34210, Istanbul, Turkey

[a)] Electronic mail: allaberen.ashyralyev@neu.edu.tr
[b)] Corresponding author: ozgury@yildiz.edu.tr

Abstract. In the present paper we consider the nonlocal boundary value perturbation problem

$$\begin{cases} \varepsilon^2 \frac{\partial^2 u(t,x)}{\partial t^2} - \left(a(x)\,u_x(t,x)\right)_x + \delta u(t,x) = f(t,x), \\ 0 < t < T, x \in (0,l), \\ u(0,x) = \alpha u(T,x) + \varphi(x), x \in [0,l], \\ u'(0,x) = \beta u'(T,x) + \psi(x), x \in [0,l], \\ u(t,0) = u(t,l), u_x(t,0) = u_x(t,l), 0 \le t \le T \end{cases}$$

for hyperbolic equation with an arbitrary $\varepsilon \in (0,\infty)$ parameter multiplying the derivative term. An asymptotic formula for the solution of this problem with a small ε parameter is presented.

INTRODUCTION

Singular perturbation problems are important in many fields such as quantum mechanics, fluid dynamics, solid mechanics, reaction–diffusion processes, aerodynamics etc. Asymptotic solutions are useful in various problems (see, e.g., [1, 2, 3, 4, 5]). In modeling some physical phenomena and problems in engineering, classical boundary conditions cannot describe the phenomenon precisely. Therefore, mathematical models of various physical, chemical, biological, or environmental processes often involve non-classical conditions, which are usually identified as nonlocal boundary conditions. This type of conditions project the cases when data on the domain boundary cannot be measured directly or when data on the boundary depend on the data inside the domain.

In this work, the nonlocal boundary value perturbation problem

$$\begin{cases} \varepsilon^2 \frac{\partial^2 u(t,x)}{\partial t^2} - \left(a(x)\,u_x(t,x)\right)_x + \delta u(t,x) = f(t,x), \\ 0 < t < T, x \in (0,l), \\ u(0,x) = \alpha u(T,x) + \varphi(x), x \in [0,l], \\ u'(0,x) = \beta u'(T,x) + \psi(x), x \in [0,l], \\ u(t,0) = u(t,l), u_x(t,0) = u_x(t,l), 0 \le t \le T \end{cases} \tag{1}$$

for hyperbolic equation is considered. Here $a(x), \varphi(x), \psi(x)$, and $f(t,x)$ are given sufficiently smooth functions, $\delta > 0$ is the sufficiently large number, $\varepsilon > 0$ is the arbitrary positive number. We will assume $a(x) \ge a > 0$ and $a(l) = a(0)$.

Stable difference schemes for nonlocal parabolic, hyperbolic, and elliptic problems, without parameter $(\varepsilon = 1)$, have been investigated by many authors (see, e.g., [6, 7, 8, 9, 10, 11, 12]).

ASYMPTOTIC FORMULA

In this section, we study the asymptotic formula for the solution of problem (1) under the assumption

$$|\alpha + \beta| < |1 + \alpha\beta\,|. \tag{2}$$

International Conference on Analysis and Applied Mathematics (ICAAM 2020)
AIP Conf. Proc. 2325, 020015-1–020015-3; https://doi.org/10.1063/5.0040357
Published by AIP Publishing. 978-0-7354-4069-2/$30.00

Theorem 1 *Suppose that assumption (2) is satisfied and the function $f(t,x)$ has $2m+3$ derivatives with*

$$\left\|f^{(2m+3)}(t,\cdot)\right\|_{L_2[0,l]} \leq M, 0 \leq t \leq T.$$

Then for small ε and even number m the following $(m+2)$-nd order asymptotic formula

$$u(t,x) = \sum_{i=0}^{m} \varepsilon^i \left[u_i(t,x) + v_i\left(\frac{t}{\varepsilon},x\right) + \omega_i\left(\frac{T-t}{\varepsilon},x\right)\right] + o\left(\varepsilon^{m+2}\right) \tag{3}$$

for the solution of problem (1) holds and for small ε and odd number m the following $(m+1)$-st order asymptotic formula

$$u(t,x) = \sum_{i=0}^{m} \varepsilon^i \left[u_i(t,x) + v_i\left(\frac{t}{\varepsilon},x\right) + \omega_i\left(\frac{T-t}{\varepsilon},x\right)\right] + o\left(\varepsilon^{m+1}\right) \tag{4}$$

for the solution of problem (1) holds, where the functions $u_i(t,x)$, $v_i\left(\frac{t}{\varepsilon},x\right)$, and $\omega_i\left(\frac{T-t}{\varepsilon},x\right)$ for $i \in \{1,2,...,m\}$, $x \in [0,l]$ are defined by the following formulas

$$u_0(t,x) = A^{-1}f(t,x), u_1(t,x) = 0, \tag{5}$$

$$u_i(t,x) = -A^{-1}u''_{i-2}(t,x), i = 2,...,m, \tag{6}$$

$$(v_i)_{\xi\xi}(\xi,x) + Av_i(\xi,x) = 0, i = 0,1,...,m, \tag{7}$$

$$(\omega_i)_{\mu\mu}(\mu,x) + A\omega_i(\mu,x) = 0, i = 0,1,...,m, \tag{8}$$

$$v_i(0,x) + \omega_i\left(\frac{T}{\varepsilon},x\right) - \alpha\left(v_i\left(\frac{T}{\varepsilon},x\right) + \omega_i(0,x)\right) = -u_i(0,x) + \alpha u_i(T,x), 1 \leq i \leq m, \tag{9}$$

$$v_0(0,x) + \omega_0\left(\frac{T}{\varepsilon},x\right) - \alpha\left(v_0\left(\frac{T}{\varepsilon},x\right) + \omega_0(0,x)\right) = \varphi(x) - u_0(0,x) + \alpha u_0(T,x), \tag{10}$$

$$(v_i)_\xi(0,x) - (\omega_i)_\mu\left(\frac{T}{\varepsilon},x\right) - \beta\left((v_i)_\xi(0,x) - (\omega_i)_\mu\left(\frac{T}{\varepsilon},x\right)\right) = u'_{i-1}(0,x) - \beta u'_{i-1}(T,x), 2 \leq i \leq m, \tag{11}$$

$$(v_0)_\xi(0,x) - (\omega_0)_\mu\left(\frac{T}{\varepsilon},x\right) - \beta\left((v_0)_\xi(0,x) - (\omega_0)_\mu\left(\frac{T}{\varepsilon},x\right)\right) = 0, \tag{12}$$

$$(v_1)_\xi(0,x) - (\omega_1)_\mu\left(\frac{T}{\varepsilon},x\right) - \beta\left((v_1)_\xi(0,x) - (\omega_1)_\mu\left(\frac{T}{\varepsilon},x\right)\right) = \psi(x) - u'_0(0,x) + \beta u'_0(T,x). \tag{13}$$

Here, M is a positive constant.

The proof of Theorem 1 is based on the self-adjointness and positivity in $L_2[0,l]$ of a differential operator A defined by the formula

$$Au(x) = -\frac{d}{dx}\left(a(x)\frac{du}{dx}\right) + \delta u(x)$$

with domain $D(A)=\left\{u\in W_2^2\left[0,l\right]:u\left(0\right)=u\left(l\right),u'\left(0\right)=u'\left(l\right)\right\}$, and on estimates

$$\|c\left(t\right)\|_{L_2[0,l]\to L_2[0,l]}\leq 1,\ \|A^{\frac{1}{2}}s\left(t\right)\|_{L_2[0,l]\to L_2[0,l]}\leq 1, t\geq 0.$$

Here $\{c\left(t\right), t\geq 0\}$ is a strongly continuous cosine operator-function (see, [13], [14]) defined by the formula

$$c\left(t\right)=\frac{e^{itA^{1/2}}+e^{-itA^{1/2}}}{2},$$

and $\{s\left(t\right), t\geq 0\}$ is a strongly continuous sine operator-function defined by the formula

$$s(t)u=\int_0^t c(s)u\,ds.$$

Then, it follows the formula

$$s\left(t\right)=A^{-1/2}\frac{e^{itA^{1/2}}-e^{-itA^{1/2}}}{2i}.$$

CONCLUSION

In this work, an asymptotic formula for the solution of nonlocal boundary value perturbation problem for hyperbolic equation is presented.

REFERENCES

1. M. Ashyraliyev, Filomat **31**, 1041–1049 (2017).
2. A. Ashyralyev and P. Sobolevskii, *New Difference Schemes for Partial Differential Equations in: Operator Theory and Appl.* (Birkhäuser Verlag, 2004).
3. A. Ilin, Math. USSR Izv. **34**, 261–279 (1990).
4. T. Kato, *Perturbation Theory for Linear Operators* (Springer-Verlag, 1995).
5. S. A. Lomov, *Introduction to the General Theory of Singular Perturbations* (American Mathematical Society, 1992).
6. A. Ashyralyev, Numerical Functional Analysis and Optimization **24**, 1–15 (2003).
7. A. Ashyralyev and A. Sarsenbi, Electronic Journal of Differential Equations **284**, 1–8 (2015).
8. A. Ashyralyev and O. Yildirim, Taiwanese Journal of Mathematics **14**, 165–194 (2010).
9. C. Ashyralyyev, Boundary Value Problems **74**, 1–22 (2017).
10. H. M. D. Gordezani and G. Avalishvili, Zhurnal Obchyslyuval'no Ta Prykladno I Matematyky **8**, 66–78 (2003).
11. V. A. Il'in and E. I. Moiseev, Differential Equations **23**, 803–810 (1987).
12. M. Sapagovas, Journal of Computer Applied Mathematics **1**, 89–98 (2003).
13. H. Fattorini, *Second Order Linear Differential Equations in Banach Space* (Notas de Matematica, North-Holland, 1985).
14. S. Piskarev and Y. Shaw, Taiwanese Journal of Mathematics **4**, 3585–3592 (1997).
15. S. G. Krein, *Linear Differential Equations in a Banach Space* (Moscow: Nauka, 1966).
16. G. I. Shishkin and V. L. Kolmogorov, *Numerical Methods for Singularly Perturbed Boundary Value Problems Modeling Diffusion Processes in: Singular Perturbation Problems in Chemical Physics, J. J. H. Miller ed, Advances in Chemical Physics Series* (J. Wiley and Sons, 1797).
17. C. Ashyralyyev, Numerical Functional Analysis and Optimization **38**, 1226–1243 (2017).

On the Source Identification Problem for Hyperbolic-Parabolic Equation with Nonlocal Conditions

Maksat Ashyraliyev,[1, a)] Allaberen Ashyralyev,[2, 3, 4, b)] and Viktor Zvyagin[5, c)]

[1)]*Department of Software Engineering, Bahcesehir University, 34353, Istanbul, Turkey*
[2)]*Department of Mathematics, Near East University, Nicosia, TRNC, Mersin 10, Turkey*
[3)]*Peoples Friendship University of Russia, Miklukho Maklaya 6, 117198, Moscow, Russia*
[4)]*Institute of Mathematics and Mathematical Modeling, 050010, Almaty, Kazakhstan*
[5)]*Voronezh State University, Universitetskaya 1, 394018, Voronezh, Russia*

[a)]*Corresponding author: maksat.ashyralyyev@eng.bau.edu.tr*
[b)]*Electronic mail: allaberen.ashyralyev@neu.edu.tr*
[c)]*Electronic mail: zvg_vsu@mail.ru*

Abstract. In the present paper, we establish the well-posedness of an identification problem for determining the unknown space-dependent source term in the hyperbolic-parabolic equation with nonlocal conditions. The difference scheme is constructed for the approximate solution of this source identification problem. The stability estimates for the solution of the difference scheme are presented.

INTRODUCTION

The problems for determining the unknown parameters in the partial differential equations have been studied extensively by many authors (see, e.g., [1, 2, 3, 4, 5, 6, 7] and the references given therein). Various source identification problems for hyperbolic-parabolic equations and the corresponding difference schemes for their approximate solutions have been recently investigated by the authors (see [8, 9, 10, 11]). However, source identification problems for hyperbolic-parabolic equations with nonlocal conditions have not been investigated well so far.

The present paper is devoted to the identification problem for finding the unknown space-dependent source term in the hyperbolic-parabolic differential and difference equations with nonlocal conditions. The stability of these source identification hyperbolic-parabolic problems is established.

STABILITY OF DIFFERENTIAL EQUATION

We consider the following source identification problem

$$\begin{cases} u_{tt}(t,x) - \big(a(x)u_x(t,x)\big)_x + \delta u(t,x) = p(x) + f(t,x),\ 0<x<\ell,\ 0<t<1, \\ u_t(t,x) - \big(a(x)u_x(t,x)\big)_x + \delta u(t,x) = p(x) + g(t,x),\ 0<x<\ell,\ -1<t<0, \\ u(t,0) = u(t,\ell),\ u_x(t,0) = u_x(t,\ell),\ -1 \le t \le 1, \\ u(0^+,x) = u(0^-,x),\ u_t(0^+,x) = u_t(0^-,x),\ 0 \le x \le \ell, \\ u(-1,x) = \varphi(x),\ \int\limits_0^1 u(s,x)ds = \psi(x),\ 0 \le x \le \ell \end{cases} \tag{1}$$

for one-dimensional hyperbolic-parabolic differential equation with nonlocal boundary conditions. Under compatibility conditions problem (1) has a unique smooth solution $\big(u(t,x), p(x)\big)$ for the given smooth functions $a(x) \ge a > 0$, $x \in (0,\ell)$, $a(\ell) = a(0)$, $\varphi(x)$, $\psi(x)$, $x \in [0,\ell]$, $f(t,x)$, $t \in [0,1]$, $x \in [0,\ell]$, $g(t,x)$, $t \in [-1,0]$, $x \in [0,\ell]$ and constant $\delta \ge 2$.

Theorem 1 *Suppose that $\varphi, \psi \in W_2^2[0,\ell]$. Let function $f(t,x)$ be continuously differentiable in t on $[0,1] \times [0,\ell]$ and function $g(t,x)$ be continuously differentiable in t on $[-1,0] \times [0,\ell]$. Then the solution of the identification problem (1) satisfies the stability estimates*

$$\|u\|_{C([-1,1],L_2[0,\ell])} + \left\|(A^x)^{-1}p\right\|_{L_2[0,\ell]} \le M_1(\delta)\left[\|\varphi\|_{L_2[0,\ell]} + \|\psi\|_{L_2[0,\ell]} + \|f\|_{C([0,1],L_2[0,\ell])} + \|g\|_{C([-1,0],L_2[0,\ell])}\right], \tag{2}$$

International Conference on Analysis and Applied Mathematics (ICAAM 2020)
AIP Conf. Proc. 2325, 020016-1–020016-4; https://doi.org/10.1063/5.0040269
Published by AIP Publishing. 978-0-7354-4069-2/$30.00

$$
\begin{aligned}
&\|u\|_{C^{(2)}([0,1],L_2[0,\ell])} + \|u\|_{C^{(1)}([-1,0],L_2[0,\ell])} + \|u\|_{C([-1,1],W_2^2[0,\ell])} + \|p\|_{L_2[0,\ell]} \\
&\qquad \le M_2(\delta)\left[\|\varphi\|_{W_2^2[0,\ell]} + \|\psi\|_{W_2^2[0,\ell]} + \|f\|_{C^{(1)}([0,1],L_2[0,\ell])} + \|g\|_{C^{(1)}([-1,0],L_2[0,\ell])}\right],
\end{aligned}
\tag{3}
$$

where $M_1(\delta)$ and $M_2(\delta)$ do not depend on $\varphi(x)$, $\psi(x)$, $f(t,x)$ and $g(t,x)$.

Here, the Sobolev space $W_2^2[0,\ell]$ is defined as the set of all functions $u(x)$ defined on $[0,\ell]$ such that $u(x)$ and the second order derivative function $u''(x)$ are both locally integrable in $L_2[0,\ell]$, equipped with the norm

$$
\|u(x)\|_{W_2^2[0,\ell]} = \left(\int_0^\ell |u(x)|^2\,dx\right)^{\frac{1}{2}} + \left(\int_0^\ell |u''(x)|^2\,dx\right)^{\frac{1}{2}}.
$$

Problem (1) can be written in the following abstract form

$$
\begin{cases}
u''(t) + Au(t) = p + f(t),\ 0 < t < 1, \\
u'(t) + Au(t) = p + g(t),\ -1 < t < 0, \\
u(0^+) = u(0^-),\ u'(0^+) = u'(0^-), \\
u(-1) = \varphi,\ \int_0^1 u(s)ds = \psi
\end{cases}
$$

in a Hilbert space $L_2[0,\ell]$ with self-adjoint positive definite operator $A = A^x$ defined by the formula

$$
A^x u(x) = -(a(x)u_x)_x + \delta u \tag{4}
$$

with domain

$$
D(A^x) = \{u(x) \mid u(x), u_x(x), (a(x)u_x)_x \in L_2[0,\ell], u(\ell) = u(0), u_x(\ell) = u_x(0)\}. \tag{5}
$$

Here, $f(t) = f(t,x)$ and $g(t) = g(t,x)$ are given abstract functions, $u(t) = u(t,x)$ is unknown function and $p = p(x)$ is the unknown element of $L_2[0,\ell]$. Therefore, the proof of Theorem 1 is based on the self-adjointness and positive definiteness of the space operator A^x with the domain $D(A^x) \subset W_2^2[0,\ell]$ (see [12]).

STABILITY OF DIFFERENCE SCHEME

We construct the first order of accuracy difference difference scheme in t for the approximate solution of source identification problem (1). The discretization of source identification problem (1) is carried out in two steps.

In the fist step, the spatial discretization is carried out. We define the grid space

$$
[0,\ell]_h = \{x = x_n \mid x_n = nh,\ 0 \le n \le M,\ Mh = \ell\}.
$$

Let us introduce the Hilbert space $L_{2h} = L_2([0,\ell]_h)$ of the grid functions $\phi^h(x) = \{\phi^n\}_0^M$ defined on $[0,\ell]_h$, equipped with the norm

$$
\|\phi^h\|_{L_{2h}} = \left(\sum_{x\in[0,\ell]_h} |\phi^h(x)|^2 h\right)^{1/2}.
$$

To the differential operator A^x defined by the formula (4) with domain (5), we assign the difference operator A_h^x by the formula

$$
A_h^x \phi^h(x) = \{-(a(x)\phi_{\bar{x}}^n)_x + \delta\phi^n\}_1^{M-1}, \tag{6}
$$

acting in the space of grid functions $\phi^h(x) = \{\phi^n\}_0^M$ and satisfying the following conditions

$$
\phi^0 = \phi^M, \quad \phi^1 - \phi^0 = \phi^M - \phi^{M-1}.
$$

Here

$$\phi_{\bar{x}}^{n} = \frac{\phi^{n} - \phi^{n-1}}{h},\ 1 \le n \le M, \quad \phi_{x}^{n} = \frac{\phi^{n+1} - \phi^{n}}{h},\ 0 \le n \le M-1.$$

It is well-known that A_h^x, defined by (6), is a self-adjoint positive definite operator in L_{2h}. With the help of A_h^x, the first step of the discretization process results in the following identification problem

$$\begin{cases} u_{tt}^h(t,x) + A_h^x u^h(t,x) = p^h(x) + f^h(t,x),\ x \in [0,\ell]_h,\ 0 < t < 1, \\ u_t^h(t,x) + A_h^x u^h(t,x) = p^h(x) + g^h(t,x),\ x \in [0,\ell]_h,\ -1 < t < 0, \\ u^h(0^+,x) = u^h(0^-,x),\ u_t^h(0^+,x) = u_t^h(0^-,x),\ x \in [0,\ell]_h, \\ u^h(-1,x) = \varphi^h(x),\ \int\limits_0^1 u^h(s,x)ds = \psi^h(x),\ x \in [0,\ell]_h. \end{cases} \tag{7}$$

In the second step, we replace the identification problem (7) with the following first order of accuracy difference scheme

$$\begin{cases} \dfrac{u_{k+1}^h(x) - 2u_k^h(x) + u_{k-1}^h(x)}{\tau^2} + A_h^x u_{k+1}^h(x) = p^h(x) + f_k^h(x),\ f_k^h(x) = f^h(t_k,x),\ x \in [0,\ell]_h,\ 1 \le k \le N-1, \\ \dfrac{u_k^h(x) - u_{k-1}^h(x)}{\tau} + A_h^x u_k^h(x) = p^h(x) + g_k^h,\ g_k^h(x) = g(t_k,x),\ x \in [0,\ell]_h,\ -N+1 \le k \le 0, \\ N\tau = 1,\ t_k = k\tau,\ -N \le k \le N,\ u_1^h(x) - u_0^h(x) = u_0^h(x) - u_{-1}^h(x),\ x \in [0,\ell]_h, \\ u_{-N}^h(x) = \varphi^h(x),\ \sum\limits_{k=1}^{N} u_k^h(x)\tau = \psi^h(x),\ x \in [0,\ell]_h. \end{cases} \tag{8}$$

Theorem 2 *Let τ and h be sufficiently small numbers. Then, for the solution $\left\{\left\{u_k^h(x)\right\}_{-N}^{N}, p^h(x)\right\}$ of difference scheme (8) the following stability estimates*

$$\max_{-N \le k \le N} \|u_k\|_{L_{2h}} + \left\|(A_h^x)^{-1} p^h\right\|_{L_{2h}} \le M_1(\delta)\left[\left\|\varphi^h\right\|_{L_{2h}} + \left\|\psi^h\right\|_{L_{2h}} + \max_{-N+1 \le k \le 0}\left\|g_k^h\right\|_{L_{2h}} + \max_{1 \le k \le N-1}\left\|f_k^h\right\|_{L_{2h}}\right],$$

$$\max_{1 \le k \le N-1}\left\|\frac{u_{k+1}^h - 2u_k^h + u_{k-1}^h}{\tau^2}\right\|_{L_{2h}} + \max_{-N+1 \le k \le 0}\left\|\frac{u_k^h - u_{k-1}^h}{\tau}\right\|_{L_{2h}} + \max_{-N \le k \le N}\left\|u_k^h\right\|_{W_{2h}^2} + \left\|p^h\right\|_{L_{2h}}$$
$$\le M_2(\delta)\left[\left\|\varphi^h\right\|_{W_{2h}^2} + \left\|\psi^h\right\|_{W_{2h}^2} + \left\|g_0^h\right\|_{L_{2h}} + \max_{-N+1 \le k \le -1}\left\|\frac{g_k^h - g_{k-1}^h}{\tau}\right\|_{L_{2h}} + \left\|f_1^h\right\|_{L_{2h}} + \max_{2 \le k \le N-1}\left\|\frac{f_k^h - f_{k-1}^h}{\tau}\right\|_{L_{2h}}\right]$$

hold, where $M_1(\delta)$ and $M_2(\delta)$ do not depend on τ, h, f_k^h, $1 \le k \le N-1$, g_k^h, $-N+1 \le k \le 0$, $\varphi^h(x)$ and $\psi^h(x)$.

Difference scheme (8) can be written in the following abstract form

$$\begin{cases} \dfrac{u_{k+1}^h - 2u_k^h + u_{k-1}^h}{\tau^2} + A_h u_{k+1}^h = p^h + f_k^h,\ 1 \le k \le N-1, \\ \dfrac{u_k^h - u_{k-1}^h}{\tau} + A_h u_k^h = p^h + g_k^h,\ -N+1 \le k \le 0, \\ u_1^h - u_0^h = u_0^h - u_{-1}^h,\ u_{-N}^h = \varphi^h,\ \sum\limits_{k=1}^{N} u_k^h \tau = \psi^h \end{cases}$$

in a Hilbert space L_{2h} with operator $A_h = A_h^x$ defined by formula (6). Here, $f_k^h = f_k^h(x)$ and $g_k^h = g_k^h(x)$ are given abstract functions, $u_k^h = u_k^h(x)$ is unknown mesh function and $p^h = p^h(x)$ is the unknown mesh element of L_{2h}. Therefore, the proof of Theorem 2 is based on the self-adjointness and positive definiteness of the space operator A_h in L_{2h} (see [12]).

REFERENCES

1. M. Choulli and M. Yamamoto, J. Inverse Ill-Posed Probl. **7**, 241–254 (1999).
2. A. Ashyralyev and D. Agirseven, Nonlinear Anal. Model. Control **19**, 335–349 (2014).
3. A. Ashyralyev and C. Ashyralyyev, Nonlinear Anal. Model. Control **19**, 350–366 (2014).
4. A. Ashyralyev and A. S. Erdogan, Appl. Math. Comput. **226**, 212–228 (2014).
5. C. Ashyralyyev, Filomat **28**, 947–962 (2014).
6. G. Blasio and A. Lorenzi, J. Inverse Ill-Posed Probl. **15**, 709–734 (2007).
7. S. Jator, American Journal of Computational Mathematics **5**, 175–185 (2015).
8. A. Ashyralyev and M. A. Ashyralyyeva, Contemporary Analysis and Applied Mathematics **3**, 88–103 (2015).
9. M. A. Ashyralyyeva and A. Ashyralyyev, AIP Conference Proceedings **1676**, 020024 (2015).
10. M. A. Ashyralyyeva and M. Ashyraliyev, Bulletin of the Karaganda University-Mathematics **91**, 69–74 (2018).
11. M. Ashyralyyeva and M. Ashyraliyev, AIP Conference Proceedings **1997**, 020048 (2018).
12. A. Ashyralyev and P. E. Sobolevskii, *New Difference Schemes for Partial Differential Equations* (Birkhauser Verlag, 2004).

Comparative Analysis of the Weighted Finite Element Method and FEM with Mesh Refinement

Viktor A. Rukavishnikov[a)] and Elena I. Rukavishnikova

Computing Center, Far-Eastern Branch, Russian Academy of Sciences, Kim-Yu-Chen str. 65, Khabarovsk, 680000, Russian Federation

[a)] *Corresponding author: vark0102@mail.ru*

Abstract. In this paper a comparative analysis of the absolute errors of the weighted finite element method and FEM with refined meshes is performed for a model boundary value problem for the Lamé system in an L-shaped domain. For the weighted finite element method an absolute error value is by one or two orders of magnitude less than for the approximate generalized solution obtained by the FEM with graded meshes in the overwhelming majority of nodes.

INTRODUCTION

In [1, 2, 3, 4, 5, 6, 7] the definition of an R_ν-generalized solution was introduced and its differential properties were studied for boundary value problems with a singularity caused by degeneration of the initial data or the presence of reentrant corners at the boundary of the domain. Weighted and weighted vector finite element methods were developed for finding an approximate R_ν-generalized solution [8, 9, 10, 11, 12, 13]. These methods make it possible to find an approximate solution without loss of accuracy regardless of the singularity of the boundary value problem.

The finite element method with mesh refinement to a singularity point for finding an approximate generalized solution of a boundary value problem with a corner singularity with a convergence rate of $O(h)$ is treated in [14, 15, 16]. We performed a comparative numerical analysis of the weighted finite element method and FEM with mesh refinement for finding an approximate solutions of model problems of elasticity theory in the L-shaped domain. A weighted FEM allows one to find a solution with theoretical accuracy on meshes of high dimension. The finite element method with mesh refinement fails at mesh high dimensions and the same calculation conditions [17]. In this paper we carry out a comparative analysis of the absolute errors of these methods for a model boundary value problem for the Lamé system in an L-shaped domain.

PROBLEM STATEMENT. MODEL PROBLEM

Let $\Omega = (-1,1)\times(-1,1)\backslash[0,1]\times[-1,0] \subset R^2$ be a domain with boundary $\partial\Omega$ and $\bar{\Omega} = \Omega\bigcup\partial\Omega$. The boundary $\partial\Omega$ contains reentrant corner $\frac{3\pi}{2}$.

We consider a boundary value problem for the Lamé system with respect to the vector function $\mathbf{u} = (u_1, u_2)$:

$$-\left(2\,\mathbf{div}\left(\mu\varepsilon(\mathbf{u})\right) + \nabla\left(\lambda\,\mathrm{div}\,\mathbf{u}\right)\right) = \mathbf{f}, \quad x\in\Omega, \tag{1}$$

$$u_i = q_i, \quad i = 1,2, \quad x\in\partial\Omega. \tag{2}$$

Here coefficients λ and μ are constants, $\varepsilon(u)$ is a strain tensor with components $\varepsilon_{ij}(\mathbf{u}) = \frac{1}{2}\left(\frac{\partial u_i}{\partial x_j} + \frac{\partial u_j}{\partial x_i}\right)$.

Model problem A. We performed numerical experiments for model problem (1), (2) with coefficients $\mu = 5$, $\lambda = 3$ and an exact solution:

$$u_1 = \cos x_1 \cos^2 x_2 (x_1^2 + x_2^2)^{0.3051},$$
$$u_2 = \cos^2 x_1 \cos x_2 (x_1^2 + x_2^2)^{0.3051}.$$

Singularity order of the u_1, u_2 corresponds to size of the reentrant corner $3\pi/2$ on the domain boundary (see [18]).

International Conference on Analysis and Applied Mathematics (ICAAM 2020)
AIP Conf. Proc. 2325, 020017-1–020017-4; https://doi.org/10.1063/5.0040325
Published by AIP Publishing. 978-0-7354-4069-2/$30.00

THE WEIGHTED FINITE-ELEMENT METHOD

We define a weight function $\rho(x)$ that equals the distance to the origin in $\Omega' = \{x \in \Omega : (x_1^2 + x_2^2)^{1/2} \le \delta < 1\}$ and equals δ for $x \in \bar{\Omega} \backslash \bar{\Omega}'$.

A function $\mathbf{u}_\nu$ is called an R_ν-generalized solution of problem (1), (2) if it satisfies boundary condition (2) almost everywhere on $\partial\Omega$ and for any $\mathbf{v}$ from $\overset{\circ}{\mathbf{W}}{}^1_{2,\nu}(\Omega, \delta)$ the integral identity

$$a(\mathbf{u}_\nu, \mathbf{v}) = l(\mathbf{v})$$

holds for any fixed ν satisfying the inequality $\nu \ge 0$.

Here $a(\mathbf{u}, \mathbf{v}) = (a_1(\mathbf{u}, \mathbf{v}), a_2(\mathbf{u}, \mathbf{v}))$, $l(\mathbf{v}) = (l_1(\mathbf{v}), l_2(\mathbf{v}))$ and

$$a_1(\mathbf{u}, \mathbf{v}) = \int\limits_\Omega \left[(\lambda + 2\mu) \frac{\partial u_1}{\partial x_1} \frac{\partial(\rho^{2\nu} v_1)}{\partial x_1} + \mu \frac{\partial u_1}{\partial x_2} \frac{\partial(\rho^{2\nu} v_1)}{\partial x_2} + \lambda \frac{\partial u_2}{\partial x_2} \frac{\partial(\rho^{2\nu} v_1)}{\partial x_1} + \mu \frac{\partial u_2}{\partial x_1} \frac{\partial(\rho^{2\nu} v_1)}{\partial x_2} \right] dx,$$

$$a_2(\mathbf{u}, \mathbf{v}) = \int\limits_\Omega \left[\lambda \frac{\partial u_1}{\partial x_1} \frac{\partial(\rho^{2\nu} v_2)}{\partial x_2} + \mu \frac{\partial u_1}{\partial x_2} \frac{\partial(\rho^{2\nu} v_2)}{\partial x_1} + (\lambda + 2\mu) \frac{\partial u_2}{\partial x_2} \frac{\partial(\rho^{2\nu} v_2)}{\partial x_2} + \mu \frac{\partial u_2}{\partial x_1} \frac{\partial(\rho^{2\nu} v_2)}{\partial x_1} \right] dx,$$

$$l_1(\mathbf{v}) = \int\limits_\Omega \rho^{2\nu} f_1 v_1 dx, \quad l_2(\mathbf{v}) = \int\limits_\Omega \rho^{2\nu} f_2 v_2 dx.$$

The function $\mathbf{u}_\nu$ is determined from the set $\mathbf{W}^1_{2,\nu}(\Omega, \delta)$. The definition of spaces, sets, the proof of the existence and uniqueness theorem of an R_ν-generalized solution are given in [7].

Comment.

The weight function coincides with the distance to the singular point in her neighborhood. The role of this function is in suppressing of the solution singularity caused by the problem features. Such approach allowed one to decrease the influence of singularity to the accuracy of calculation of approximate solution and to archive the convergence rate $O(h)$ in the weighted norm without mesh refinement towards singularity point.

We construct a weighted finite element method for finding an approximate an R_ν-generalized solution of problem (1), (2). For this purpose, we construct quasi-uniform triangulation of the domain Ω and introduce special weighted basis functions.

The domain Ω is divided into squares by lines parallel to coordinate axis's, with distance equal $1/N$ between them, where N is the number of partitions of segment $[0, 1]$. Each square is subdivided into two triangles by the diagonal. In this case size of the mesh-step $h = \sqrt{2}/N$.

Let P=$\{P_k\}_{k=1}^{k=n}$ is the set of triangulation internal nodes, and $P_1 = \{P_k\}_{k=n+1}^{k=N_1}$ is the set of nodes belonging to the $\partial\Omega$. Each node $P_k \in$ P is associated with a function ψ_k of the form

$$\psi_k(x) = \rho^{\nu^*}(x) \varphi_k(x), \quad k = 1, \ldots, n,$$

where $\varphi_k(x)$ is linear on each finite element and $\varphi_k(P_j) = \delta_{kj}$, $k, j = 1, \ldots, n$, δ_{kj} is the Kronecker delta, and ν^* is a real number.

We introduce the vector set $\mathbf{V}^h = [V^h]^2$, where V^h is the linear span of the system of basis functions $\{\psi_k\}_{k=1}^{k=n}$. Also let $\overset{\circ}{\mathbf{V}}{}^h = \left\{ \mathbf{v} \in \mathbf{V}^h, v_i(P_k)|_{P_k \in \partial\Omega} = 0,\ i = 1, 2 \right\}$.

A function $\mathbf{u}^h_\nu$ in the set V^h satisfying boundary condition (2) in the nodes of the boundary $\partial\Omega$ and the equality

$$a(\mathbf{u}^h_\nu, \mathbf{v}^h) = l(\mathbf{v}^h) \quad \forall \mathbf{v}^h(x) \in \overset{\circ}{\mathbf{V}}{}^h$$

is called the approximate R_ν-generalized solution of problem (1), (2) by the weighted finite element method. Here $\mathbf{u}^h_\nu = (u^h_{\nu,1}, u^h_{\nu,2})$ and

$$u^h_{\nu,1} = \sum_{k=1}^n d_{2k-1} \psi_k, \quad u^h_{\nu,2} = \sum_{k=1}^n d_{2k} \psi_k, \quad d_j = \rho^{-\nu^*}(P_{\left[\frac{j+1}{2}\right]}) c_j, \quad j = 1, \ldots, 2n.$$

In [19], it was shown that convergence rate of the approximate R_ν-generalized solution to the exact one is equal to $O(h)$ for weighted finite element method.

NUMERICAL EXPERIMENTS AND COMPARATIVE ANALYSIS

In this section we present results of absolute errors analysis of finding R_ν-generalized solution by the weighted finite element method and generalized solution by the FEM with graded meshes for model problem A.

Weighted finite element method. For calculations the approximate R_ν-generalized solution we used the weighted finite element method with optimal values of the parameters ν, ν^*, δ. We call as optimal values such intervals of the parameters ν, ν^*, δ for which changing speed of the approximate solution relative error calculated in the weighted norm in not less than theoretical convergence rate $O(h)$ when the mesh in refined. We created the code for numerical analysis of model problem (1), (2) and finding the optimal parameters [20].

FEM with graded meshes. We used for find the generalized solution the finite element method with graded meshes of two kinds (for detailed information about graded meshes, see [15, 21, 22]).

Mesh I. This mesh was built by the following scheme

1. For a given N regular mesh was constructed (see previous section).

2. For each node we determined the level $l = \max_{i=1,2}(|N - [(x_i+1)N]|)$. Here x_i $(i = 1,2)$ are node coordinates on the regular mesh, $[\cdot]$ means integer part of the number.

3. We calculated new coordinates of nodes of the graded mesh by formula $([(x_i+1)N]-N)l^{-1}(l/N)^{1/\kappa}$ $(i = 1,2)$.

Mesh II. The process of constructing this mesh differs from mesh 1 in the way that level l is determined. Here $l = \sum_{i=1}^{2}|N - [(x_i+1)N]|$. For this mesh new coordinates are determined only for nodes with $l \leq N$.

The approximate solution by the finite element method on graded meshes converges to the exact one with the rate of the first order on the mesh step when the value of the parameter κ is less than the order of singularity [15, 21].

In [17] we established that FEM with graded meshes failed on meshes of high dimension N and weighted finite element method stably found approximate solution with theoretical accuracy for large values of N under the same computational conditions. We explain the reason of this failure of FEM with graded meshes by smallness of refined mesh steps in the neighborhood of the singular point.

Calculations were performed for weighted finite element method at $N = 4096$, and for FEM with graded meshes at $N = 1024$ and $\kappa = 0.5$. For each mesh node we calculated the absolute errors $|e_{\nu,1}| = |u_1 - u^h_{\nu,1}|$, $|e_{\nu,2}| = |u_2 - u^h_{\nu,2}|$ and $|e_{1,II}| = |u_1 - u^h_{1,II}|$, $|e_{2,II}| = |u_2 - u^h_{2,II}|$ of approximation the R_ν-generalized solution $\mathbf{u}^h_\nu = (u^h_{\nu,1}, u^h_{\nu,2})$ and of the approximation the generalized solution on mesh II. Table 1 contain number of nodes and its percentages where absolute errors $|e_{1,II}|$, $|e_{2,II}|$, $|e_{\nu,1}|$, $|e_{\nu,2}|$ are not less than given limit values e. We present distribution of the absolute errors $|e_{1,II}|$, $|e_{2,II}|$ and $|e_{\nu,1}|$, $|e_{\nu,2}|$ on Fig. 1.

TABLE 1. Number of nodes, percentage equivalence, where absolute errors $|e_{1,II}|$, $|e_{2,II}|$, $|e_{\nu,1}|$, $|e_{\nu,2}|$ are not less than given limit values.

limit values	$\lvert e_{1,II}\rvert$		$\lvert e_{2,II}\rvert$		$\lvert e_{\nu,1}\rvert$		$\lvert e_{\nu,2}\rvert$	
	%	number	%	number	%	number	%	number
$e = 5e-6$	0.001	6	0.001	6	0.033	4102	0.033	4102
$e = 1e-6$	35.524	278645	35.479	278292	0.764	96075	0.764	96075
$e = 5e-7$	13.631	106920	13.770	108011	2.457	308985	2.457	308985
$e = 1e-7$	33.363	261697	33.377	261808	21.704	2729186	21.704	2729186
$e = 5e-8$	7.020	55066	6.984	54782	12.589	1582976	12.589	1582974
$e = 0$	10.461	82051	10.389	81486	62.454	7853397	62.454	7853399

The numerical results have demonstrated that for the weighted finite element method, an absolute error value is by one or two orders of magnitude less than for the approximate generalized solution obtained by the FEM with graded meshes in the overwhelming majority of nodes.

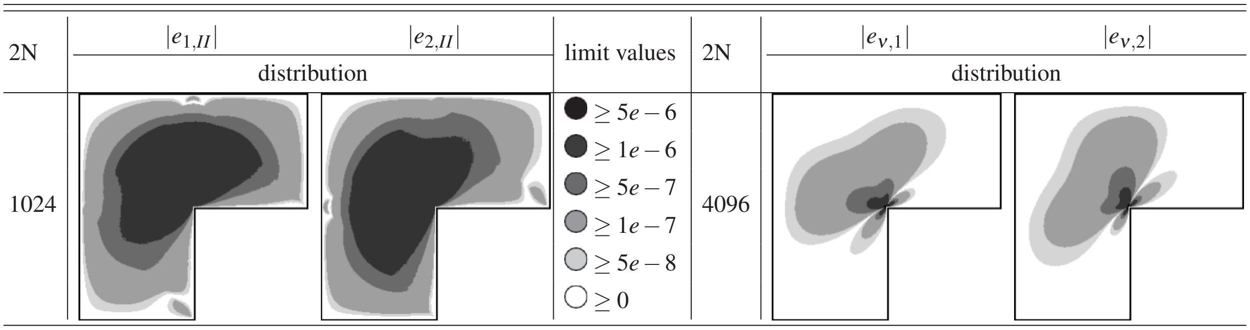

FIGURE 1. Distribution of the absolute errors $|e_{1,II}|$, $|e_{2,II}|$ for the approximate generalized and $|e_{\nu,1}|$, $|e_{\nu,2}|$ for the approximate R_ν-generalized solutions

ACKNOWLEDGMENTS

Computational resources for the numerical experiment were provided by the Shared Facility Center "Data Center of FEB RAS".

REFERENCES

1. V. A. Rukavishnikov, Doklady Akademii Nauk **337**, 447–449 (1994).
2. V. A. Rukavishnikov, Doklady Mathematics **63**, 68–70 (2001).
3. V. A. Rukavishnikov and A. G. Ereklintsev, Differential Equations **41**, 1757–1767 (2005).
4. V. A. Rukavishnikov and E. V. Kuznetsova, Differential Equations **43**, 550–560 (2007).
5. V. A. Rukavishnikov and E. V. Kuznetsova, Differential Equations **45**, 913–917 (2009).
6. V. A. Rukavishnikov, Doklady Mathematics **90**, 562–564 (2014).
7. V. A. Rukavishnikov and E. I. Rukavishnikova, Differential Equations **55**, 832–840 (2019).
8. V. A. Rukavishnikov, Doklady Akademii Nauk SSSR **288**, 1058–1062 (1986).
9. V. A. Rukavishnikov, Russian Journal of Numerical Analysis and Mathematical Modelling **24**, 565–590 (2009).
10. V. A. Rukavishnikov and H. I. Rukavishnikova, Journal of Computational and Applied Mathematics **234**, 2870–2882 (2010).
11. V. A. Rukavishnikov and A. O. Mosolapov, Journal of Computational Physics **231**, 2438–2448 (2012).
12. V. A. Rukavishnikov and S. G. Nikolaev, Doklady Mathematics **88**, 705–709 (2013).
13. V. A. Rukavishnikov and A. V. Rukavishnikov, Journal of Computational and Applied Mathematics **341**, 144–156 (2018).
14. B. Szabó and I. Babuška, *Finite element analysis* (John Wiley & Sons, 1991) 368 p.
15. T. Apel, A.-M. Sändig, and J. R. Whiteman, Mathematical Methods in the Applied Sciences **19**, 63–85 (1996).
16. H. Nguyen-Xuan, G. R. Liu, S. Bordas, S. Natarajan, and T. Rabczuk, Comput Meth Appl Mech Eng **253**, 252–273 (2013).
17. V. A. Rukavishnikov and E. I. Rukavishnikova, in *AIP Conference Proceedings*, Vol. 2116, edited by T. Simos and C. Tsitouras (2019) p. 450042.
18. A. Rössle, Journal of Elasticity **60**, 57–75 (2000).
19. V. A. Rukavishnikov, in *Numerical Mathematics and Advanced Applications ENUMATH 2015*, Lecture Notes in Computational Science and Engineering, Vol. 112, edited by B. Karasözen, M. Manguoğlu, M. Tezer-Sezgin, S. Göktepe, and Ö. Uğur (Springer, Cham, 2016) pp. 411–419.
20. V. A. Rukavishnikov, O. V. Maslov, A. O. Mosolapov, and S. G. Nikolaev, Computational Nanotechnology , 9–19 (2015).
21. L. A. Oganesyan and L. A. Rukhovets, *Variational-difference methods for solving elliptic equations* (Izdatel'stvo Akad. Nauk. Arm. SSR, 1979) (in Russian).
22. G. Raugel, C. R. Acad. Sci. Paris (Sér A) **286**, A791–A794 (1978).

Valuation of Power Generation Projects in the Setting of Kazakhstan

Tynysbek Sh. Kalmenov,[a] Issabek Orazov,[b] Gani A. Besbayev,[c] and Baurzhan Aibek[d]

Institute of Mathematics and Mathematical Modeling, 050010, Almaty, Kazakhstan

[a] *Corresponding author: kalmenov@math.kz*
[b] *Electronic mail: orazov@math.kz*
[c] *Electronic mail: besbayev@math.kz*
[d] *Electronic mail: aibek@math.kz*

Abstract. In this note we characterize the optimal investment strategy for the choice between different types of power production technologies: the coal-fired plants as the representative power generation source for traditional fuels and wind power for the representative renewable source.

INTRODUCTION

This work is devoted to understand the choice between different types of energy production technologies. We focus on coal power plants as a typical source of power generation for traditional fuels. This reflects the fact that natural coal has become the most efficient source of energy production from fossil fuels. The considered renewable energy source is wind. Wind power was the second fastest growing segment in this space (after SPV) and had the second largest share in global electricity production from all renewable energy sources (after hydropower) in 2015. Thus, we consider an operator with a license to build a power plant and who seeks to choose between the construction of a coal power plant or a wind power plant. Since licenses are usually valid for extended periods of time, the timing of the decision to build is flexible. In addition, each of these choices includes the subsequent timing of operations. Therefore, the licensee has a real American-style option on a maximum of two asset values, which in themselves are conditional American-style claims. Some of the fundamental issues that arise in this context are as follows. What is the optimal time frame for making a decision on construction? Under what conditions is it best to invest in the production of energy from renewable sources? Are existing incentive schemes sufficient to stimulate investment in this sector? What is the sensitivity of investments in electricity production in relation to the relevant determinants, for example, price uncertainty, interest rates, incentives and technological parameters.

PRODUCTION FROM TRADITIONAL FUELS: COAL-FIRED PLANT

The operation of a coal-fire plant generates a cash flow equal to the spread between the electricity price and the cost of fuels, in this instance coal. The spread, which is called the spark spread, equals $X = Y - \kappa G$, where Y, G are the respective prices of electricity and coal, and κ is the heat rate, i.e., the amount of coal necessary to generate $1MWh$ of electricity. To simplify the analysis, we model the spark spread directly, assuming that it follows an arithmetic Brownian motion (ABM) with drift under risk-neutral measure (see [3])

$$dX_t = \mu_X dt + \sigma_X dB_t, \quad X_0 = x, \tag{1}$$

where B is a standard Brownian motion, and the parameters μ_X and $\sigma_X > 0$ represent the drift and volatility, respectively. We can rewrite $\mu_X = r - \delta_X$ where δ_X is an implicit dividend yield. The production model assumes that the coal-fired plant can operate indefinitely (infinite horizon) and that it can be in two states: idle (0) and operating (1). There are running cost rates k_0 and k_1 associated with each state, and there are also fixed switching costs c_0 and c_1, to pass from state 0 to 1 and conversely. We also assume that the coal plant has capacity factor $\gamma_g \in (0,1]$. The value of the plant in each state can therefore be described as follows:

$$V_0(x) = \sup_{\tau \geq 0} \mathsf{E}_x \left[-\int_0^\tau e^{-rs} k_0 ds + e^{-r\tau}(V_1(X_\tau) - c_0) \right], \tag{2}$$

International Conference on Analysis and Applied Mathematics (ICAAM 2020)
AIP Conf. Proc. 2325, 020018-1–020018-5; https://doi.org/10.1063/5.0040340
Published by AIP Publishing. 978-0-7354-4069-2/$30.00

$$V_1(x) = \sup_{\zeta \geq 0} \mathsf{E}_x \left[\int_0^{\zeta} e^{-rs}(\gamma_g X_s - k_1) ds + e^{-r\zeta}(V_0(X_\zeta) - c_1) \right] \tag{3}$$

for $x \in \mathbb{R}$. The value of the plant in the idle state, $V_0(x)$ consists in two parts. The first one is the present value of the maintenance cost incurred until operation resumes. The second one is the value created by resuming operations at the future time τ, i.e., the value of the option to resume. The plant maximizes value by choosing the best time τ to resume operations. Likewise, the value $V_1(x)$ of the plant in the operating mode has two components: the value of the net spark spread $X - k_1$ collected while running the plant and the value of idling at the future time ζ, i.e., the value of the option to idle. Value is maximized by choosing the best time ζ to idle. As the timing of the options to operate and idle are endogenous, the two options are American-style. The two values depend on each other. The pair $(V_0(x), V_1(x))$ solves the coupled optimal stopping time problem described above.

Solving the Coal-Fired Plant Problem

The operator of the plant has the possibility of switching back and forth between the two states of operation described above. The optimal switching decisions are determined by two thresholds, $b_0 > b_1$. When the plant is idle, it becomes optimal to turn the system on when X_t hits b_0 from below. When it operates, it becomes optimal to cease production when X_t reaches b_1 from above.

Standard arguments show that the value of idling satisfies the following ODE

$$\frac{\sigma_X^2}{2} V_0''(x) + \mu_X V_0'(x) - rV_0(x) - k_0 = 0 \tag{4}$$

for $x < b_0$. The general solution to this ODE is given by

$$V_0(x) = A_0 e^{\alpha x} + B_0 e^{\widetilde{\alpha} x} - \frac{k_0}{r}, \tag{5}$$

where A_0, B_0 are constants, and $\widetilde{\alpha} < 0 < \alpha$ are the roots of the quadratic equation

$$\frac{\sigma_X^2 \alpha^2}{2} V_0''(x) + \mu_X \alpha - r = 0. \tag{6}$$

As V_0 is bounded, we have that $B_0 = 0$ and thus,

$$V_0(x) = A_0 e^{\alpha x} - \frac{k_0}{r} \tag{7}$$

for $x < b_0$. It is also clear that $V_0(x) = V_1(x) - c_0$ for $x \geq b_0$ and both continuity and smooth pasting conditions hold at b_0.

Likewise, the value of operating satisfies

$$\frac{\sigma_X^2}{2} V_1''(x) + \mu_X V_1'(x) - rV_1(x) + \gamma_g x - k_1 = 0 \tag{8}$$

for $x > b_1$. The solution to this ODE is given by

$$V_1(x) = B_1 e^{\widetilde{\alpha} x} + \frac{\gamma_g x + \gamma_g \mu_X / r - k_1}{r} \tag{9}$$

as V_1 is bounded and where B_1 is some constant. We also have that $V_1(x) = V_0(x) - c_1$ for $x \leq b_1$. Again, continuity and smooth fit conditions are satisfied at b_1.

Given the candidate value functions above and using the continuity and smooth pasting conditions at b_0 and b_1, leads to the system of four algebraic equations with four unknown variables (b_0, b_1, A_0, B_1)

$$A_0 e^{\alpha b_0} - \frac{k_0}{r} = B_1 e^{\widetilde{\alpha} b_0} + \frac{\gamma_g b_0 + \gamma_g \mu_X / r - k_1}{r} - c_0, \tag{10}$$

$$\alpha A_0 e^{\alpha b_0} = \widetilde{\alpha} B_1 e^{\widetilde{\alpha} b_0} + \frac{\gamma_g}{r}, \tag{11}$$

$$A_0 e^{\alpha b_1} - \frac{k_0}{r} - c_1 = B_1 e^{\widetilde{\alpha} b_1} + \frac{\gamma_g b_1 + \gamma_g \mu_X / r - k_1}{r}, \tag{12}$$

$$\alpha A_0 e^{\alpha b_1} = \widetilde{\alpha} B_1 e^{\widetilde{\alpha} b_1} + \frac{\gamma_g}{r}. \tag{13}$$

Clearly, this system has a unique solution and can be solved numerically. The standard verification arguments shows that the solution to this system provides the value functions and optimal operation rules in (2)-(3).

The Value of a Coal-Fired Plant

The value of the coal-fired plant is an increasing convex function of the spark spread as follows

$$V_{cont}(x) = \mathsf{E}_x \left[\int_0^\infty e^{-rs} (\gamma_g X_s - k_1) ds \right] = \frac{\gamma_g x + \gamma_g \mu_X / r - k_1}{r} \tag{14}$$

for $x > 0$. It can be seen that the premium $V_1 - V_{cont}$ due to the operational flexibility and possibility of shutting down is simply $B_1 e^{\widetilde{\alpha} x}$ for $x > b_1$. It has substantial value when the spark spread X is low.

The value function V_1 converges to an affine function as the spark spread goes to infinity. Value increases when the volatility and drift of the spark spread increase, and decreases when the costs of operations and switching increase.

SOLVING WIND PLANT PROBLEM

The profit generated by a wind power plant depends on the price of electricity, the subsidy for generation from renewable and the cost of operating the plant. We assume that the price of electricity follows a geometric Brownian motion process under a risk-neutral measure

$$dY_t = \mu_Y Y_t dt + \sigma_Y Y_t dZ_t,\ Y_0 = y, \tag{15}$$

where Z is a standard Brownian motion positively correlated with B, and the parameters μ_Y and $\sigma_Y > 0$ represent the expected return and the return volatility, respectively. We can also rewrite $\mu_Y = r - \delta_Y$, where $\delta_Y > 0$ is an implicit yield for electricity. The subsidy for clean electricity generation is a premium on top of the market price, assumed to be a constant $s > 0$. The running cost of operations is also constant $k_w > 0$. This cost mainly consists of wages and fixed costs.

The production model assumes that the wind plant can operate indefinitely and that it always operates at capacity level $\gamma_w \in (0,1]$. Its value is the present value of profits

$$W(y) = \mathsf{E}_y \left[\int_0^\infty e^{-rt} (\gamma_w Y_t + \gamma_w s - k_w) dt \right] \tag{16}$$

for $y > 0$. Straightforward computations give

$$W(y) = \frac{\gamma_w}{\delta_Y} y + \frac{\gamma_w s - k_w}{r} \tag{17}$$

for $y > 0$.

INVESTMENTS IN POWER PLANTS

An operator seeking to build a new power plant can choose to build two types of production units, either using traditional fuels (coal-fired) or renewables (wind) (see [1], [2]). The value of a coal-fired plant is $V_g(x) = \max\left\{V^0(x), V^1(x)\right\}$. The value of a wind plant is $W(y)$. The option to choose between the two types of plants has payoff

$$\max\left\{V_g(x) - K_g, W(y) - K_w\right\}, \tag{18}$$

where $K_g > 0$ and $K_w > 0$ represent the sunk costs for a coal-fired system and a wind plant, respectively.

The operator can also choose the timing τ of the investment. The value of the project to build a power plant, either coal-fired or wind-based, is therefore given by

$$V(x,y) = \sup_{0 \le \tau \le \infty} \mathsf{E}_{x,y}\left[e^{-r\tau} \max(V_g(X_\tau) - K_g, W(Y_\tau) - K_w)\right] \tag{19}$$

for $x \in I\!\!R$ and $y > 0$. This is the value of an American option on the maximum of two assets with different strikes, i.e., a dual strike max-option. Moreover, one of the underlying asset prices, namely the price of the coal-fired plant, is itself the maximum between the two values associated with the different states of the system. A priori, the operator could decide to build when the system is in either one of the two possible states.

Optimal Investment in Power Generation

1. *Exercise region*. We now characterize the optimal investment strategy for the operator. First, let us define the investment ($\mathscr{D}$) and continuation ($\mathscr{C}$) regions

$$\mathscr{D} = \{(x,y) \in I\!\!R \times (0,\infty) : V(x,y) = G(x,y)\}, \tag{20}$$

$$\mathscr{C} = \{(x,y) \in I\!\!R \times (0,\infty) : V(x,y) > G(x,y)\} \tag{21}$$

and split the investment region $\mathscr{D}$ into two parts

$$\mathscr{D}_g = \{(x,y) \in \mathscr{D} : G(x,y) = G_1(x)\}, \tag{22}$$

$$\mathscr{D}_w = \{(x,y) \in \mathscr{D} : G(x,y) = G_2(y)\}. \tag{23}$$

In the region $\mathscr{D}_g$, it is optimal to invest in the coal-fired plant; in $\mathscr{D}_w$ the wind plant investment is optimal. As the payoff G is a continuous function, the optimal investment timing rule is given by $\tau_* = \inf\{t \ge 0 : (X_t, Y_t) \in \mathscr{D}\}$.

To gain further insights into the structure of the investment region, we exploit the local time-space formula (see [4]), to obtain,

$$\mathsf{E}_{x,y}\left[e^{-r\tau} \max(V_1(X_\tau) - K_1, W(Y_\tau) - K_w)\right] = G(x,y) + \mathsf{E}_{x,y}\left[\int_0^\tau e^{-rt} H_1(X_t) I(G(X_t,Y_t) = G_1(X_t))dt\right] \tag{24}$$

$$+\mathsf{E}_{x,y}\left[\int_0^\tau e^{-rt} H_2(Y_t) I(G(X_t,Y_t) = G_2(Y_t))dt\right] + \frac{\gamma_w}{2\delta_Y} \mathsf{E}_{x,y}\left[\int_0^\tau e^{-rt} d\ell_t\right]$$

for $(x,y) \in I\!\!R \times (0,\infty)$ and any stopping time τ where ℓ is the local time process that Y spends at the curve $\widehat{y}(x)$, and H_1 and H_2 represent the local gains of waiting to invest into the coal-fired and wind technologies, respectively, which are defined as,

$$H_1(x) = I\!\!L_X G_1(x) - rG_1(x) = -\gamma_g x + k_1 + rK_1 \tag{25}$$

$$H_2(y) = I\!\!L_Y G_2(y) - rG_2(y) = -\gamma_w y - (\gamma_w s - k_w) + rK_w \tag{26}$$

for $(x,y) \in I\!\!R \times (0,\infty)$. As we maximize the left-hand side of (24) over all stopping times, it is clear that the investor should not enter into the coal-fired technology when $X_t < (k_1 + rK_1)/\gamma_g$ as $H_1(X_t) > 0$ and into the wind plant when $Y_t < (rK_w - (\gamma_w s - k_w))/\gamma_w$ as $H_2(Y_t) > 0$. Therefore, $b_X(y) \ge (k_1 + rK_1)/\gamma_g$ for $y > 0$ and $b_Y(x) \ge (rK_w - (\gamma_w s - k_w))/\gamma_w$ for $x \in I\!\!R$. Also, (24) shows that the operator should not invest at all along the curve $\widehat{y}$, i.e., when $Y_t = \widehat{y}(X_t)$, as the local time term dominates the two other terms in dt. In other words, $\{(x,y) \in I\!\!R \times (0,\infty) : x > b_1, y = \widehat{y}(x)\} \in \mathscr{C}$.

Theorem 1 *There exist two boundaries* $b_X : (0,\infty) \to I\!R$ *and* $b_Y : I\!R \to (0,\infty)$ *such that*
(i) The sets $\mathscr{C}$ *and* $\mathscr{D}$ *are given by*

$$\mathscr{D}_g = \{(x,y) \in I\!R \times (0,\infty) : x \geq b_X(y)\}, \tag{27}$$

$$\mathscr{D}_w = \{(x,y) \in I\!R \times (0,\infty) : y \geq b_Y(x)\}, \tag{28}$$

$$\mathscr{C} = \{(x,y) \in I\!R \times (0,\infty) : y < b_Y(x) \ \&\ x < b_X(y)\}. \tag{29}$$

(ii) Both boundaries b_X *and* b_Y *are convex (thus continuous) and increasing functions on* $(0,\infty)$ *and* $I\!R$.
(iii) The limiting values are $b_X(0+) = b_X^g$ *and* $b_Y(-\infty) = b_Y^w$, *where* b_X^g *and* b_Y^w *are the optimal thresholds of standard timing problems for coal-fired and wind plants, respectively,*

$$\sup_{0 \leq \tau \leq \infty} \mathsf{E}_x \left[e^{-r\tau} (V_g(X_\tau) - K_g) \right], \tag{30}$$

$$\sup_{0 \leq \tau \leq \infty} \mathsf{E}_y \left[e^{-r\tau} (W(Y_\tau) - K_w) \right] \tag{31}$$

for $x \in I\!R$ *and* $y > 0$.
(iv) The following inequalities hold: $b_X(y) > \widehat{x}(y)$ *for* $y > \widehat{y}(b_1)$ *and* $b_X(y) > b_X^g$ *for* $y > 0$; $b_Y(x) > \widehat{y}(x)$ *for* $x > b_1$ *and* $b_Y(x) > b_Y^w$ *for* $x \in I\!R$.

Property (i) indicates that the operator should invest in the coal-fired technology when the spark spread x exceeds the boundary $b_X(y)$ and in the wind plant when the price of electricity y exceeds the boundary $b_Y(x)$. Each boundary depends on an underlying state variable: the threshold for investment in the coal-fired (resp. wind) plant depends on the price of electricity (resp. spark spread). Moreover, the investment events determined by the boundaries are mutually exclusive: the boundaries do not cross and the sets $\mathscr{D}_g$ and $\mathscr{D}_w$ do not intersect. Convexity of the boundaries in Property (ii) ensures that the exercise regions are convex as well. Thus, if investment in a given technology is optimal at two point (x_j, y_j), $j = 1,2$, it will also be optimal at any convex combination $\left(x^\lambda, y^\lambda\right) = \lambda\,(x_1,y_1) + (1-\lambda)\,(x_2,y_2)$ for $\lambda \in [0,1]$. Property (iii) establishes a relation between the boundaries $b_X(y), b_Y(x)$ and those when the operator considers an investment in a specific technology. It shows that these boundaries differ, except in extreme circumstances where the spark spread goes to $-\infty$, in which case the project to invest becomes an option to build a wind plant, or where the price of electricity approaches 0 and the project collapses to an option to invest in the coal-fired technology. When both alternatives are considered, Property (iv) elaborates and shows that the thresholds of these single asset options are in fact lower bounds for the investment boundaries in the two asset problem. The selection option adds value to the operator's project ensuring that it is optimal to delay investments relative to the single technology case. Property (iv) also highlights a striking aspect, namely the fact that immediate investment in any technology is always suboptimal along the curve $\widehat{y}(x)$ (or it inverse $\widehat{x}(y)$). This is true irrespective of the size of the spark spread or the price of electricity. Hence, even when the options to invest in single technologies are deep in the money, it may still be optimal to wait before investing when technological choices are factored in.

ACKNOWLEDGMENTS

This research is financially supported by a target program BR05236656 from the Ministry of Science and Education of the Republic of Kazakhstan.

REFERENCES

1. I. Bakke, S. E. Fleten, L. I. Hagfors, V. Hagspiel, and B. Norheim, Journal of Commodity Market **3(1)**, 54–69 (2016).
2. T. K. Boomsma, N. Meade, and S. E. Fleten, European Journal of Operational Research **220(1)**, 225–237 (2012).
3. M. Brennan and E. S. Schwartz, Journal of Business **58(2)**, 135–157 (1985).
4. G. Peskir, Journal of Theoretical Probability **18(3)**, 499–535 (2005).

An Algorithm to Compute the Probability of Ruin of an Insurance Company

Alexey L. Lukashov[1,2,a)]

[1)] *Moscow Institute of Physics and Technology, Moscow, Russian Federation*
[2)] *Saratov State University, Saratov, Russian Federation*

[a)] *Corresponding author: alexey.lukashov@gmail.com*

Abstract. In [1] two-sided bounds were derived for the probability of ruin of an insurance company, whose premium income is represented by an arbitrary increasing real function, the claims are dependent, integer valued r.v.s. and their inter-occurrence times are exponentially, non-identically distributed. Here we give an explicit algorithm to compute that probability.

IGNATOV-KAISHEV STUDIES

In [1] two-sided bounds were derived for the probability of ruin of an insurance company, whose premium income is represented by an arbitrary increasing real function, the claims are dependent, integer valued random variables and their inter-occurrence times are exponentially, non-identically distributed.

More precisely, the following model is considered. It includes the counting process $N_t = \#\{i : \tau_1 + \ldots + \tau_i \leq t\}$, where # denotes the number of elements in the set, and $tau_1, \ldots, \tau_i, \ldots$ are independent, exponentially distributed random variables with mean $E(\tau_i) = 1/\lambda_i, \lambda_i > 0$.

The severities of the successive claims are the integer valued random variables $W_1, W_2, \ldots,$ independent of N_t. The joint distribution of $W_1, W_2, \ldots$ is denoted by

$$P(W_1 = w_1, \ldots, W_i = w_i) = P_{w_1,\ldots,w_i},$$

where $w_i \geq 1, i = 1, 2, \ldots.$

Then the aggregate claims amount at time t will be

$$S_t = \sum_{i=1}^{N_t} W_i$$

and the risk reserve process of an insurance company

$$R_t = h(t) - S_t,$$

where $h(t)$ is a function, representing the premium income. It is supposed to be a nonnegative, increasing, real function, defined on $\mathbb{R}_+$ and such that $\lim_{t\to\infty} h(t) = +\infty$. If $h(t)$ is discontinuous then $h^{-1}(y) = \inf\{z : h(z) \geq y\}$. let us denote $v_i = h^{-1}(i)$, for $i = 0, 1, \ldots$ and the instance of ruin by T, i.e., $T = \inf\{t : t > 0, R_t \leq 0\}$. The probability of non-ruin is then $P(T > x)$. By the formula for the total probability it can by expressed through the conditional probabilities $P(T < x|W_1 = w_1, \ldots, W_n = w_n)$. Here $n = [h(x)] + 1$, where $[h(x)]$ is the integer part of $h(x)$. Furthermore, $k = k(w_1, \ldots, w_n)$ is defined as an integer such that $z_{k-1} \leq x < z_k$, where $z_l = v_{w_1+\ldots+w_l}, l = 1, 2, \ldots.$

Ignatov and Kaishev deduced in [1] a formula for $P(T > x|W_1 = w_1, \ldots, W_n = w_n)$ as a multiple integral. Furthermore, they obtained upper and lower bounds for this integral. In the case of compound Poisson aggregate claims these bounds coincide, hence producing an explicit representation of the survival probability. In [2] that representation was compared with other formulas.

Ignatov-Kaishev formula is as follows (see [1] (formula (18)) :

$$\begin{aligned} P(T > x|W_1 = w_1, \ldots, W_n = w_n) = \lambda_1\lambda_2\ldots\lambda_k \int_0^{+\infty} u^k e^{-u} \\ \times \left(\int_{z_1/u}^{+\infty} \cdots \int_{z_{k-1}/u}^{+\infty} \int_{x/u}^{+\infty} I_{(0,1)}(\lambda_1 y_1 - \lambda_2 y_1 + \lambda_2 y_2 \right. \\ + \ldots - \lambda_k y_{k-1} + \lambda_k y_k) \times I_{(0,\infty)}(\lambda_1 y_1) I_{(0,\infty)}(-\lambda_2 y_1 + \lambda_2 y_2) \ldots \\ \left. \times I_{(0,\infty)}(-\lambda_k y_{k-1} + \lambda_k y_k) dy_1 \ldots dy_k \right) du. \end{aligned} \tag{1}$$

Here $I_X(y)$ is the indicator of the set X.

International Conference on Analysis and Applied Mathematics (ICAAM 2020)
AIP Conf. Proc. 2325, 020019-1–020019-2; https://doi.org/10.1063/5.0040355
Published by AIP Publishing. 978-0-7354-4069-2/$30.00

AN ALGORITHM TO COMPUTE THE NON-RUIN PROBABILITIES USING (1)

First of all we use substitutions $y_j \to uy_j, j = 1, \ldots, k$ and change the order of integration to rewrite (1) as

$$P(T > x | W_1 = w_1, \ldots, W_n = w_n) = \lambda_1 \lambda_2 \ldots \lambda_k \int_{z_1}^{+\infty} e^{-(\lambda_1 - \lambda_2) y_1} \int_{z_2}^{+\infty} I_{(0,\infty)}(-y_1 + y_2) e^{-(\lambda_2 - \lambda_3) y_2} \times \ldots$$
$$\times \int_{z_{k-1}}^{+\infty} I_{(0,\infty)}(-y_{k-2} + y_{k-1}) e^{-(\lambda_{k-1} - \lambda_k) y_{k-1}} \int_{x}^{+\infty} I_{(0,\infty)}(-y_{k-1} + y_k) e^{-\lambda_k y_k} dy_k \ldots dy_1. \quad (2)$$

Put $\lambda_{k+1} = 0$. Now we can transform the integrals in (2) by moving the indicators to lower limits of integrals. The result is

$$P(T > x | W_1 = w_1, \ldots, W_n = w_n) = \lambda_1 \lambda_2 \ldots \lambda_k \int_{z_1}^{+\infty} e^{-(\lambda_1 - \lambda_2) y_1}$$
$$\times \int_{\max(y_1, z_2)}^{+\infty} e^{-(\lambda_2 - \lambda_3) y_2} \times \ldots \int_{\max(y_{k-2}, z_{k-1})}^{+\infty} e^{-(\lambda_{k-1} - \lambda_k) y_{k-1}} \quad (3)$$
$$\times \int_{\max(y_{k-1}, x)}^{+\infty} e^{-(\lambda_k - \lambda_{k+1}) y_k} dy_k \ldots dy_1.$$

Now it is clear that all integrals can be computed explicitly, but the problem is in substitution of lower limits. The algorithm below shows how to do it.

Firstly we consider the case of different λ's, i.e. $\lambda_i \neq \lambda_j$ for $i \neq j, i, j = 1 \ldots, k+1$.

Put $z_k = x, z_{k+1} = +\infty$. The non-ruin probability is computed by the formula

$$P(T > x | W_1 = w_1, \ldots, W_n = w_n) = \lambda_1 \lambda_2 \ldots \lambda_k \sum_w \prod_{s \in w} \sum_{l \in s} \gamma_l. \quad (4)$$

Here the first summation is over all «words» w. Every «word» contains k letters z or y. The first (from the left) letter of a «word» is always z. Every letter z has an index $p \in \{1, \ldots, k\}$, and the sequence of indexes is strictly increasing from the left to the right. If the letter z with the index p is i-th from the left in the «word» w, then the inequality $p \geq i + q$ has to be fulfilled, where q is the amount of letters y, standing in a row after z_p. So every «word» w is made up of «syllables» $s \in w$, where every «syllable» starts from a letter z and contains next letters y, standing in a row (if there is any such letter). Every «syllable» contains one and only one letter z. The «syllable« which starts from z_p in i-th place and contains $q \geq 0$ letters y's, corresponds to the integral

$$\pi_s = \int_{z_p}^{z_{p+1}} e^{-(\lambda_i - \lambda_{i+1}) y_1} \int_{y_1}^{z_{p+1}} e^{-(\lambda_{i+1} - \lambda_{i+2}) y_2} \ldots \int_{y_q}^{z_{p+1}} e^{-(\lambda_{i+q} - \lambda_{i+1+q}) y_{q+1}} dy_{q+1} \ldots dy_1. \quad (5)$$

Every integral π_s can be computed as a sum $\pi_s = \sum_{l \in s} \gamma_l$. Let us describe how to split π_s. For a «syllable» with q letters y's the sum consists of 2^q terms. Every term corresponds to a row of q zeros and units. Here 0 and 1 denote which limit of integration is chosen in substitution. The main observation here is that a substitution of the upper limit gives a constant which can be put ahead of all integrals as a multiplier. Consider a row of the form

$$0, \ldots, 0, 1_{s_1}, 0, \ldots, 0, 1_{s_r}, 0, \ldots, 0,$$

where the index for a unit indicates its position in the row. Also put $s_0 = 0$. The corresponding term γ_l is equal to

$$\gamma_l = (-1)^{r+1} \frac{\left(e^{-\lambda_i - \lambda_{i+s_1}) z_{p+1}} - e^{-(\lambda_i - \lambda_{i+s_1}) z_p}\right) e^{-\left(\lambda_{i+s_1} - \lambda_{i+q+1}\right) z_{p+1}}}{\prod_{j=0}^{r} \prod_{m=s_j}^{s_{j+1}-1} \left(\lambda_{i+m} - \lambda_{i+s_{j+1}}\right)}. \quad (6)$$

The algorithm was realized by the author's graduate student I.V. Diveikin [3]. Also he modified and realized the algorithm for the case of equal λ's (here every "syllable" is computed without splitting to terms).

REFERENCES

1. Z. G. Ignatov and V. K. Kaishev, Scand. Actuarial J. **1**, 46 (2000).
2. Z. G. Ignatov, V. K. Kaishev, and R. S. Krachunov, Insurance Math. Econom. **29**, 375 (2001).
3. I. V. Diveikin, *Probability of Non-ruin for an Insurance Company*, Magister thesis, Saratov State University (2020), in Russian.

On the Alternative Approach to Ψ-fractional Calculus

Mohammad Momenzadeh[a)]

Department of Mathematics, Near East University, Nicosia, Mersin 10, Turkey

[a)]*Corresponding author: mohammad.momenzadeh@neu.edu.tr*

Abstract. The Non-Newtonian calculus is inspired by the homeomorphism from the real line to the open interval that we denote it by $\alpha(x)$. This function modifies the preliminary algebraic operators and the new fractional differintegration formula will be found. On the other hand, the Ψ-fractional calculus was introduced in the aid of generalized Leibniz formula for production of two differentiable functions which has been driven to the similar fractional operators. In this literature the relationship between these two operators are investigated and new interpretation of Ψ-fractional calculus is studied.

INTRODUCTION

The idea of the concerned calculus, which is called Non-Newtonian calculus inspired by an underlying idea of Michael Grossman and Robert Katz to reconsider the preliminary algebraic operations through the homeomorphism from the real line to $I = (0,\infty)$. [1] This function modifies the structure of preliminary algebraic operations as an addition and multiplication. Indeed, if we assume that $y = \alpha(x)$ is the isomorphism in a real field, then we have simply the Newtonian calculus. In fact, the non-Newtonian calculus can be considered as a generalization of Newtonian calculus and generalization is what drives a lot of mathematics. This field of study has been developed in several aspects, theoretical as defining topology based on this function [2] or classifying the functions and introducing the norms [3] and practical approaches and modeling the real world phenomena. [4] One of the remarkable cases of $y = \alpha(x)$ is the case that we substitute exponential function instead of $y = \alpha(x)$ and the result is called multiplicative calculus which is extended to complex numbers. [5] In this calculus we deal with homeomorphism that we list them as follow

$$
\begin{aligned}
a \oplus_\alpha b &= \alpha\left(\alpha^{-1}(a) + \alpha^{-1}(b)\right),\\
a \ominus_\alpha b &= \alpha\left(\alpha^{-1}(a) - \alpha^{-1}(b)\right),\\
a \otimes_\alpha b &= \alpha\left(\alpha^{-1}(a) \times \alpha^{-1}(b)\right),\\
a \oslash_\alpha b &= \alpha\left(\alpha^{-1}(a) / \alpha^{-1}(b)\right).
\end{aligned}
$$

We may consider the addition operator as a function, let say $f : \mathbb{R}^2 \to \mathbb{R}$ which $f(a,b) = a+b$, then $\oplus_\alpha : I^2 \to I$ and $\oplus_\alpha(a,b) = \alpha o f\left(\alpha^{-1}(a), \alpha^{-1}(b)\right)$. This new interpretation of the arithmetics operator modifies the derivative and integral formulae. We call them α-derivative and α-integral that their definitions and corresponding relations to Newtonian calculus can be written as follow:

$$
{}^{\alpha(x)}D(f)(x) = f^{\hat{\alpha}}(x) = \lim_{y\to x}[(f(y) \ominus_\alpha f(x)) \oslash_\alpha (y \ominus_\alpha x)] = \alpha\left(\frac{\alpha^{-1}(f(x))'}{\alpha^{-1}(x)'}\right), \tag{1}
$$

$$
{}^{\alpha(x)}I(f)(x) = \int_a^b f(x)\, d^{\hat{\alpha}}(x) = \lim \bigoplus_{i=1}^{n} {}_\alpha [f(c_i) \otimes_\alpha (x_{i+1} \ominus_\alpha x_i)] = \alpha\left(\int_a^b \alpha^{-1}(f(x))\alpha^{-1}(x)'\, dx\right). \tag{2}
$$

Later on, we will show that this derivative is the natural extension of integral operators to the negative order and for this reason, we refer to both of these operators as differintegration. A bit curious about the fractional interpretation of these operators motivates any researcher to go further. This question in Newtonian calculus is as old as a letter which has been written between L'Hopital and Leibniz in 1695 and assumed as a birthday of fractional calculus. This field of mathematics which deals with the fractional derivative and integral has been developed and studied in both theoretical and practical. The vast range of applications of fractional calculus in the different fields convinced more and more researchers to work in this area. To extend these operators to the fractional case, we have different options. One can start with a derivative and use the Leibniz formula for the derivative and extend the derivative to fractional form. Fortunately, working with non-Newtonian calculi is easy and the formulas seem similar to their famous brotherhood. For instance, assume two differentiable functions $f(x)$ and $g(x)$, then it is easy to see

International Conference on Analysis and Applied Mathematics (ICAAM 2020)
AIP Conf. Proc. 2325, 020020-1–020020-6; https://doi.org/10.1063/5.0040481
Published by AIP Publishing. 978-0-7354-4069-2/$30.00

$$
\begin{aligned}
{}^{\alpha(x)}D^n\left(f(x)\otimes_\alpha h(x)\right) &= \alpha\left(\left(\frac{1}{\alpha^{-1}(x)'}\frac{d}{dx}\right)^n\left(\alpha^{-1}of(x).\alpha^{-1}oh(x)\right)\right) \\
&\bigoplus_{k=0}^{n}{}_\alpha\alpha\left(\frac{n!}{k!(n-k)!}\right)\otimes_\alpha D^k\left(f(x)\right)\otimes_\alpha D^{n-k}\left(h(x)\right) \qquad (3)\\
&= \alpha\left(\sum_{k=0}^{n}\binom{n}{k}\left(\frac{1}{\alpha^{-1}(x)'}\frac{d}{dx}\right)^k\alpha^{-1}of(x)\left(\frac{1}{\alpha^{-1}(x)'}\frac{d}{dx}\right)^{n-k}\alpha^{-1}oh(x)\right). \qquad (4)
\end{aligned}
$$

Wonderfully the allocated non-Newtonian interpretation of Leibniz formula (3), is too close to the generalization of Leibniz formula that was discussed in [6]. In that literature, the generalized formula of a fractional derivative operator was derived from the general Leibniz formula. The idea of generalization was inspired by using $D_{g(z)} = \frac{d}{dg(z)} = \frac{1}{g'(z)}\frac{d}{dz}$ instead of $\frac{d}{dz}$ in the classic format of Leibniz formula. It was assumed that $g(z)$ is a real valued function that is analytic on $g^{-1}(\mathbb{R})$. If we roughly substitute $g(x)$ by $\alpha^{-1}(x)$ then it is easy to see $D_{\alpha^{-1}(x)}o_\alpha Q =^{\alpha(x)} D$, where ${}_\alpha Q(f)(x) = \alpha of(x)$. The generalized Leibniz formula was suggested as [6]

$$
\begin{aligned}
D^n_{g(z)}\left(f(x).g(x)\right) &= \sum_{k=0}^{n}\binom{n}{k}\left(D^k_{g(z)}\right)f(x)\left(D^{n-k}_{g(z)}\right)g(x) \qquad (5)\\
&= \sum_{k=0}^{n}\binom{n}{k}\left(\frac{1}{g(x)'}\frac{d}{dx}\right)^k f(x)\left(\frac{1}{g(x)'}\frac{d}{dx}\right)^{n-k}g(x). \qquad (6)
\end{aligned}
$$

Before any proceeding, we should take care of the $g(z):\mathbb{C}\to\mathbb{R}$ which was assumed to be analytic. Here the restriction of $g^{-1}(z)$ as an analytic function onto $g^{-1}(\mathbb{R})$ was considered which is not necessary to be homeomorphism that is preserved the topological properties. In our assumption, $\alpha(x)$ is a homeomorphism that is differentiable and restricted to the function from the real line to the segment $I=(0,\infty)$. Traditionally, the study of special cases $\alpha(x)=\exp x$ gets more attention than the others. This substitution leads to the calculus which is called bi-αgeometric or bi-αmultiplicative calculus. There are more literatures based on this special case than the general non-Newtonian calculi and their applications in different aspects were considered. $[7-9]$ According to the usage of $g(z)$ in the generalization of Leibniz formula which is reached to the fractional operator that is called Ψ-fractional operator, the given function assumed to be analytic. However, the important point of view in the non-Newtonian calculus was the topological properties and naturally, the function is assumed to be homeomorphism and may suggest being extended to more general function. For example, we might consider $y=\alpha(x)$ as an analytic complex function that is more general and as far as we know, the complex case for $\alpha(x)$ was not considered before. Indeed, the non-Newtonian calculi and its special case multiplicative calculus were developed in the complex plane as an argument of function but not as complex index $y=\alpha(x)$. [5]the previous assumption on $y=\alpha(x)$ deprived us of some special cases of $\alpha(x)$ as $\sqrt[p]{x}$ that leads to an operator which is called Katugampola's operator as an especial case [10].

Since 1970 that Osler has applied $g(z)$ to generalize the fractional operator, this operator has been taken the attention of many researchers and under the name of Ψ-fractional calculus, the properties of this operator were studied.$[11-14]$ The main purpose of the study Ψ-fractional calculus is the property of unification that many different operators can be written in one form, such as let $g^{-1}(z)=\exp z$ then the general operator is changed to Hadamard type, whereas the case $g^{-1}(z)=z$ gives the Riemann operator. However, the Ψ-fractional calculus unifies the range of fractional operators, there is not any obvious reason for this unification. Whereas, the interpretation of fractional operators on non-Newtonian calculus leads to that unification and makes the meaning for each case. For example, the case $\alpha(x)=\exp(x)$ constructs the biα-geometric calculus and Hadamard fractional operator is the related fractional operator of this calculus. In 1892, Hadamard began the publication of a series of articles under the common title [15], that in the third section of this article gave an underlying idea for creating different forms of fractional integral operators. In that section, Hadamard investigated the relationships between coefficients of series with the unit radius of convergent and singularity of function. This operator is compatible with biα-geometric as we will see in this article. The Ψ-fractional calculus and non-Newtonian calculus were developed separately and this literature shows their connections, how the non-Newtonian calculus gives meaning to each case of these operators. Now it is clear why Hadamard fractional operators appear in the application of fractional operators in the study of phenomena that the proportions are more considerable than the differences [16]. This can be seen as an important point, when we see the interpretation of ${}^{\exp(x)}D$ as resiliency where $\frac{1}{\ln(x)'}\frac{d}{dx}\ln f(x)$ is the elasticity in economic.

The rest of the paper is organized as follows: First, in the aid of Cauchy iterated integrals, the fractional integral operator on non-Newtonian calculus is introduced and compared with Ψ-fractional operators. In Section 3, the continuation of these operators is proved and their properties and relations are studied. The Laplace transform on non-Newtonian calculi is introduced in the last section and at the next step the related differential equations are solved.

PRELIMINARY ON FRACTIONAL CALCULUS

The usual starting point to defining a fractional operator could be chosen as Cauchy iterated integrals. In this procedure, the iterated integral is applied to the given function as a solution of differential equations with the natural order. The fractional operators can be considered by extending the natural order to a sufficient general case. The integral operator of non-Newtonian calculus was introduced by (2) which is used in the following formula to construct iterated integrals

$$\begin{aligned} &{}_a^{\alpha(x)}I_x^n(f)(x) = \int_a^x \int_a^{x_1} \cdots \int_a^{x_{n-1}} f(x_n) d^{\hat{\alpha}} x_n d^{\hat{\alpha}} x_{n-1} \cdots d^{\hat{\alpha}} x_1 \rightarrow \\ &{}_a^{\alpha(x)}I_x^\mu(f)(x) = \alpha\left(\frac{1}{\Gamma(\mu)} \int_a^x \left(\alpha^{-1}(x) - \alpha^{-1}(s)\right)^{\mu-1} \alpha^{-1}(f(s)) \alpha^{-1}(s)' \, ds\right). \end{aligned} \tag{7}$$

The formula (7), can be referred to as a definition of fractional integral operator of the order $\mu \in \mathbb{C}\,(Re(\mu) > 0)$ on non-Newtonian calculus. Here, the iterated integrals on non-Newtonian calculus can be interpreted as the Riemann iterated integrals with different scales of grids on Euclidean space. Similar try on Newtonian calculus gives the Riemann-Liouville integral operator, however, the Hadamard integral operator can be derived by taking the iterated integral on the modified form. This method of approach was explained among four different approaches in chapter 2 of [17] which at least guarantees the semigroup properties for these operators. This approach inspired many researchers to generalize the fractional operators. The Riemann-Liouville, Hadamard, Katugampola, and Ψ-fractional integral fractional integral operators can be generated by putting dx, $\frac{dx}{x}$, $x^p dx$ and $\Psi(x)' dx$ in the chain of integration respectively. We put the definitions of these operators in the following definition.

Definition 1 *Let $[a,b]$ be a finite interval on the real line $\mathbb{R}$, then the Riemann-Liouville, Hadamard, Ψ-fractional integral of order $\mu \in \mathbb{C}\,(Re(\mu) > 0)$ are defined respectively by $(x > a)$*

$$\begin{aligned} {}_aI_x^\mu(f)(x) &= \frac{1}{\Gamma(\mu)} \int_a^x (x-s)^{\mu-1} f(s)\, ds, \\ {}_a^HJ_x^\mu(f)(x) &= \frac{1}{\Gamma(\mu)} \int_a^x \left(\ln\frac{x}{s}\right)^{\mu-1} f(s)\, \frac{ds}{s}, \\ {}_aI_{x,\Psi(x)}^\mu(f)(x) &= \cdot\frac{1}{\Gamma(\mu)} \int_a^x (\Psi(x) - \Psi(s))^{\mu-1} f(s) \Psi(s)'\, ds. \end{aligned}$$

The Ψ-fractional operator somehow can be considered as a unification of the Riemann-Liouville and Hadamard fractional integral operator where $\Psi(x) = x$ and $\Psi(x) = \ln x$ respectively, but the nature of this unification is not clear since we give the meaning for each of these operators by related non-Newtonian calculi. The discussion on the domain and the range of the given function leads to different possibilities, one can assume the function with the domain in Newtonian calculus whereas the range is defined as a subset of $\alpha(\mathbb{R})$ in non-Newtonian scales that we can present it by $\alpha(f(x))$. The other case occurs when the domain is collected from the non-Newtonian calculus whereas the range is a real line such that $f(\alpha(x))$ can demonstrate the case. This was discussed in 6.9 of [1] and we assign the following operators to present these functions

$$\begin{aligned} {}_\alpha Q(f)(x) &= \alpha o f(x) = \alpha(f(x)), \\ Q_\alpha(f)(x) &= f o \alpha(x) = f(\alpha(x)). \end{aligned}$$

The immediate consequence of this definition is the following relations between these operators that can be listed as

$$Q_\alpha^{-1} o_{\alpha^{-1}(a)} I_x^\mu o Q_\alpha =_a I^\mu_{x,\alpha^{-1}(x)}, \tag{8}$$

$$_\alpha Q o_a I^\mu_{x,\alpha^{-1}(x)} o_\alpha Q^{-1} =_a^{\alpha(x)} I_x^\mu, \tag{9}$$

$$_\alpha Q o Q_\alpha^{-1} o_{\alpha^{-1}(a)} I_x^\mu o Q_\alpha o_\alpha Q^{-1} =_a^{\alpha(x)} I_x^\mu. \tag{10}$$

Here the convexity of $\alpha(x)$ can make a significant difference. Indeed, at the following lemma, this assumption and restricting ourselves to the probability distribution function derive to the inequality that compares the specific value of Ψ-fractional operator and non-Newtonian one. In the procedure of proof, we used the Jensen inequality in the probability version that was given at Theorem 8.1.3 [18]

Lemma 1 *Let $\alpha(x) : \mathbb{R} \to I = (0,\infty)$ be a differentiable homeomorphism that is convex over the real line. In addition, let $\alpha^{-1} o f(x) : \mathbb{R} \to [0,1]$ be the probability distribution function i.e. $\int_{-\infty}^{+\infty} \alpha^{-1} o f(x) dx = 1$, then for any such functions that the following integrals are defined we can compare Ψ-fractional and non-Newtonian fractional integral operator by*

$$^{\alpha(x)}_{-\infty} I^\mu_\infty f(x) \leq_{-\infty} I^\mu_{\infty,\alpha^{-1}(x)} f(x).$$

Proof. We can start from the improper integral at the left side

$$\begin{aligned}
^{\alpha(x)}_{-\infty} I^\mu_\infty f(x) &= \lim_{b\to\infty} {}^{\alpha(x)}_{-b} I^\mu_b f(x) \\
&= \alpha \left(\lim_{b\to\infty} \int_{-b}^{b} \frac{\left(\alpha^{-1}(x) - \alpha^{-1}(s)\right)^{\mu-1}}{\Gamma(\mu)} \alpha^{-1} o f(s) \alpha^{-1}(s)' \, ds \right) \\
&\leq \int_{-\infty}^{\infty} \frac{\left(\alpha^{-1}(x) - \alpha^{-1}(s)\right)^{\mu-1}}{\Gamma(\mu)} f(s) \alpha^{-1}(s)' \, ds.
\end{aligned}$$

Remark 2 *We will prove continuation of these operators later, now let use that property and tend μ to one which derives to*

$$\alpha \left(\int_{-\infty}^{\infty} \alpha^{-1} o f(s) \alpha^{-1}(s)' \, ds \right) \leq \int_{-\infty}^{\infty} f(s) \alpha^{-1}(s)' \, ds.$$

Our discussion in this section was started by defining the fractional integral operator, furthermore to define the fractional derivative operator we have two options. Since the fractional integral operator was defined, we can assume the corresponding derivative as a combination of the natural order of derivative and fractional order integral. The natural order of the derivative should be $n-\mu$ where n is the smallest integer which is greater than $Re(\mu)$ while the fractional integral order is μ. The sequencing of actions leads to two different fractional derivative operators that are both worth to be considered. If we take the derivative first then the integral, the result is called the Caputo derivative with a more convenient initial value condition in comparison to the other case. Besides, the derivative of the constant function is equal to zero similar to the normal derivative. The second option that we list them as follows, can be written by taking the fractional integral first and then derivative and can be considered as a natural continuation of an integral operator in the sense of the next proposition in the next section. Therefore the fractional derivative operator for Riemann-Liouville, Hadamard, Ψ-fractional and non-Newtonian calculus respectively can be written as follow

$$\begin{aligned}
{}_a D_x^\mu (f)(x) &= \frac{1}{\Gamma(n-\mu)} \left(\frac{d^n}{dx^n} \right) \int_a^x (x-s)^{n-\mu-1} f(s) \, ds, \\
{}^H_a D_x^\mu (f)(x) &= \frac{1}{\Gamma(n-\mu)} \left(x \frac{d}{dx} \right)^n \int_a^x \left(\ln \frac{x}{s} \right)^{n-\mu-1} f(s) \, \frac{ds}{s}, \\
{}_a D^\mu_{x,\Psi(x)} (f)(x) &= \cdot \frac{1}{\Gamma(n-\mu)} \left(\frac{1}{\Psi'(x)} \frac{d}{dx} \right)^n \int_a^x (\Psi(x) - \Psi(s))^{n-\mu-1} f(s) \Psi(s)' \, ds, \\
{}^{\alpha(x)}_a D_x^\mu (f)(x) &= \alpha \left(\frac{1}{\Gamma(n-\mu)} \left(\frac{1}{\alpha^{-1}(x)'} \frac{d}{dx} \right)^n \int_a^x \left(\alpha^{-1}(x) - \alpha^{-1}(s) \right)^{n-\mu-1} \alpha^{-1} o f(s) \alpha^{-1}(s)' \, ds \right).
\end{aligned}$$

It is remarkable that the introduced derivative of non-Newtonian calculus has a meaning and is compatible with the structure of the corresponding calculus and the terms $\left(\alpha^{-1}(x)-\alpha^{-1}(s)\right)$. For instance, if we put $\alpha(x)=\exp x$ that leads to the biα-geometric calculus, then the format of derivative is $\frac{1}{\alpha^{-1}(x)'}\frac{d}{dx}=x\frac{d}{dx}=\delta$ which is the Hadamard derivative operator and it can be seen that $\delta^k\left(\ln^n\left(\frac{x}{s}\right)\right)=\ln^{n-k}\left(\frac{x}{s}\right)$ which is similar to the behavior of $\frac{d}{dx}$ on $(x-s)^n$. Besides, the inherent properties of non-Newtonian calculus help to develop the concepts of Riemann-Liouville operator to any kind of allocated operators immediately. In the next section, we will prove that the defined fractional derivative is the continuation of an integral operator. However, swapping the sequence of action leads to the Caputo derivative that was studied for Ψ-fractional operators in [11]. There are also some possibilities to define the derivative operator by working on the order of integration and derivative that another type of derivative as a Hifler operator is generated by that method. In this literature, we use the above definition for the fractional derivative operator.

PROPERTIES OF FRACTIONAL OPERATORS ON NON-NEWTONIAN CALCULUS

In this section, some principal properties of the introduced operators will be stated. In the first step, the continuation of these operators is considered. Indeed, the allocated fractional derivative is the continuation of a fractional integral operator in the sense of the following proposition. Here, the procedure of proof is very similar to the Riemann-Liouville case which can be found in [19] and is omitted.

Proposition 1 *The operators ${}_a^{\alpha(x)}I_x^\mu$ and ${}_a^{\alpha(x)}D_x^\mu$ are the continuations of each other respect to μ on the respective half line (or half plane in complex case). If $f(x)$ is continuous and $\alpha(x)$ is differentiable homeomorphism (or analytic bijection in the complex case), so that ${}_a^{\alpha(x)}I_x^\mu f(x)$ and ${}_a^{\alpha(x)}D_x^\mu f(x)$ are defined, then they coincide each other at $\mu=0$. In particular, following limits support this statement*

$$\begin{aligned}
&\lim_{\mu\to 0^+}\left({}_a^{\alpha(x)}I_x^\mu f(x)\right)=\lim_{\mu\to 0^+}\left({}_a^{\alpha(x)}D_x^\mu f(x)\right)=f(x),\\
&\lim_{\mu\to n^-}\left({}_a^{\alpha(x)}D_x^\mu f(x)\right)={}^{\alpha(x)}D^n f(x).
\end{aligned}$$

The above proposition determines that the fractional integral and corresponding fractional derivative are the continuations of each other. Because this extension is unique, we refer to these operators as differintegration. Our discussion about fractional integral operator was started by applying Cauchy iterated integral which guarantees that at least the semi-group properties for natural orders are satisfied. However, the classic proof of semi-group properties for Riemann-Liouville operators has some steps that the beta functions made their role there. [19] Besides, the semigroup properties of introduced operators with the small modification in the proof can be reached and we put it as the next proposition.

Proposition 2 *The fractional differintegral operators of non_newtonian calculus have the following semi-group properties.*

$$\begin{aligned}
{}_a^{\alpha(x)}I_x^\mu\left({}_a^{\alpha(x)}I_x^\nu f(x)\right)&={}_a^{\alpha(x)}I_x^{\mu+\nu}f(x) \qquad \mu,\nu>0,\\
{}_a^{\alpha(x)}D_x^\mu\left({}_a^{\alpha(x)}I_x^\nu f(x)\right)&={}_a^{\alpha(x)}D_x^{\mu-\nu}f(x) \qquad \nu>0.
\end{aligned}$$

Proof. We have different options for proof. One may use direct proof in the aid of beta function or we can use the semi-group property of Ψ-fractional operator and (10) that leads to

$${}_a^{\alpha(x)}I_x^\mu\left({}_a^{\alpha(x)}I_x^\nu f(x)\right)=\alpha\left({}_aI^\mu_{x,\alpha^{-1}(x)}\left({}_aI^\nu_{x,\alpha^{-1}(x)}\alpha^{-1}of(x)\right)\right)=\alpha\left({}_aI^{\mu+\nu}_{x,\alpha^{-1}(x)}\alpha^{-1}of(x)\right)={}_a^{\alpha(x)}I_x^{\mu+\nu}f(x).$$

Although the second equation can be proved in a similar way. We should remark that since the derivative is a continuation of integral respect to their order, we can assume that μ is negative in the second equation and still the result is valid. In addition, we remind that these operators are not commutative and if we take the derivative first and integral next, then the results are not the same.

We can take a look at the action of these operators on polynomials of non-Newtonian calculus. The results are similar to the Ψ-fractional with different terminology and can be reached easily by modifying the proof and are written as follow.

Lemma 3 *Let $\nu > 0$ and μ is a complex number with Re$\mu > 0$, then following equations hold true*

$$
{}_{a}^{\alpha(x)}I_{x}^{\mu}\left((t\ominus_{\alpha}a)^{\circledast_{\alpha}(\nu-1)}\right)(x)=\alpha\left(\frac{\Gamma(\nu)}{\Gamma(\nu+\beta)}\right)\otimes_{\alpha}(x\ominus_{\alpha}a)^{\circledast_{\alpha}(\nu+\mu-1)},
$$
$$
{}_{a}^{\alpha(x)}D_{x}^{\mu}\left((t\ominus_{\alpha}a)^{\circledast_{\alpha}(\nu-1)}\right)(x)=\alpha\left(\frac{\Gamma(\nu)}{\Gamma(\nu+\beta)}\right)\otimes_{\alpha}(x\ominus_{\alpha}a)^{\circledast_{\alpha}(\nu-\mu-1)}.
$$

Notation. Here we use the exponential of an expression in non-Newtonian calculus and we denote it by $\circledast_{\alpha}$at the exponent. In fact, the natural extension of production in non-Newtonian calculus can be considered as follow

$$
a^{\circledast_{\alpha}b}=a\otimes_{\alpha}a\otimes_{\alpha}\ldots\otimes_{\alpha}a=\alpha\left(\left(\alpha^{-1}(a)\right)^{b}\right).
$$

In the aid of this notation, the first equation of previous lemma can be written in the notation of Newtonian calculus as follow

$$
\begin{aligned}
{}_{a}^{\alpha(x)}I_{x}^{\mu}\left(\alpha\left(\alpha^{-1}(t)-\alpha^{-1}(a)\right)^{(\nu-1)}\right)(x) &= \alpha\left({}_{a}I^{\mu}_{x,\alpha^{-1}(x)}\left(\left(\alpha^{-1}(t)-\alpha^{-1}(a)\right)^{(\nu-1)}\right)\right)(x)\\
&= \alpha\left(\frac{\Gamma(\nu)}{\Gamma(\nu+\beta)}\left(\alpha^{-1}(t)-\alpha^{-1}(a)\right)^{(\nu+\mu-1)}\right).
\end{aligned}
$$

REFERENCES

1. M. Grossman and R. Katz, *Bigeometric Calculus: A System with a Scale-Free Derivative* (USA, 2006).
2. M. Kirisci, Electronic Journal of Mathematical Analysis and Applications **5(2)**, 156-169 (2017).
3. A. F. Çakmak and F. Başar, Abstract and Applied Analysis **2014 (ID 236124)**, 1-10 (2014).
4. A. E. Bashirov, E. Mısırlı, Y. Tandoğdu, and A. Özyapıcı, Applied Mathematics-A Journal of Chinese Universities **26(4)**, 425-438 (2011).
5. A. E. Bashirov and M. Riza, TWMS Journal of Applied and Engineering Mathematics **1(1)**, 75-85 (2011).
6. T. J. Osler, SIAM Journal on Applied Mathematics **18(3)**, 658-674 (1970).
7. A. E Bashirov and E. M. Kurpınar, and A. Özyapıcı, Journal of Mathematical Analysis and Applications **337(1)**, 36-48 (2008).
8. D. Stanley, Problems, Resources, and Issues in Mathematics Undergraduate Studies **9(4)**, 310-326 (1999).
9. L. Florack and H. van Assen, Journal of Mathematical Imaging and Vision **42(1)**, 64-75 (2012).
10. U. N. Katugampola, Applied Mathematics and Computation **218(3)**, 860-865 (2011).
11. R. Almeida, Communications in Nonlinear Science and Numerical Simulation (**44**), 460-481 (2017).
12. A. Fernandez, M. A. Özarslan, and D. Baleanu, Applied Mathematics and Computation (**354**), 248-265 (2019).
13. J. V. D. C. Sousa and de E. C. Oliveira, Communications in Nonlinear Science and Numerical Simulation (**60**), 72-91 (2018).
14. K. Liu, J. Wang, and D. O'Regan, Journal of Inequalities and Applications **2019(1)**, 27 (2019).
15. J. Hadamard, Gauthier-Villars (1892).
16. A. Marshall, *Marine Concrete* (Springer Science & Business Media, 2013).
17. K. S. Miller and B. Ross, *An introduction to the Fractional Integrals and Derivatives-Theory and Applications* (Wiley, 1993).
18. M. Kuczma, *An Introduction to the Theory of Functional Equations and Inequalities: Cauchy's Equation and Jensen's Inequality* (Springer Science & Business Media, 2009).
19. A. A. Kilbas, H. M. Srivastava, and J. J. Trujillo, *Theory and Applications of Fractional Differential Equations* (Wiley, 2006).
20. N. Yalcin, E. Celik and A. Gokdogan, Optik **127(20)**, 9984-9995 (2016).

On Well-posedness of Source Identification Elliptic Problem with Nonlocal Boundary Conditions

Allaberen Ashyralyev,[1, 2, 3, a)] Charyyar Ashyralyyev,[4, 5, b)] and Viktor G. Zvyagin[6, c)]

[1)] *Department of Mathematics, Near East University, Nicosia, Mersin 10, Turkey*
[2)] *Peoples' Friendship University of Russia (RUDN University), Ul Miklukho Maklaya 6, Moscow 117198, Russia*
[3)] *Institute of Mathematics and Mathematical Modeling, 050010, Almaty,Kazakhstan*
[4)] *Department of Mathematical Engineering, Gumushane University, 29100,Gumushane, Turkey*
[5)] *Department of Computer Technology, TAU, Ashgabat, 744000, Turkmenistan*
[6)] *Voronezh State University, Universitetskaya sq. 1, Voronezh,394018, Russia*

[a)] *Electronic mail: allaberen.ashyralyev@neu.edu.tr*
[b)] *Corresponding author: charyar@gmail.com*
[c)] *Electronic mail: zvg_vsu@mail.ru*

Abstract. We study the well-posedness of the source identification problem for the two dimensional elliptic differential equation with nonlocal boundary conditions. Applying operator approaches, the exact estimates for the solution of this problem in Hölder norms are established.

INTRODUCTION

Theoretical aspects and methods of solutions of source identification problems for partial differential equations have been extensively investigated by many researchers (see [3, 4, 8, 9, 10, 11, 14, 15, 17, 18, 19] and the bibliography herein). Well-posedness of non classical boundary value problems for various differential and difference equations were investigated in a number of publications (see [1-22] and references therein).

In this paper, we study the source identification problem for the two dimensional elliptic differential equation with nonlocal boundary conditions

$$\begin{cases} -\frac{\partial^2 u(y,x)}{\partial y^2} - a(x)\frac{\partial^2 u(y,x)}{\partial x^2} + \delta u(y,x) = f(y,x) + p(x), \\ 0 < y < T, 0 < x < l, \\ u(0,x) = u(T,x), u_y(0,x) = u_y(T,x),\ u(\lambda,x) = \xi(x), 0 \le x \le l, \\ u(y,0) = u(y,l),\ \ u_x(y,0) = u_x(y,l),\ \ 0 \le y \le T, \end{cases} \tag{1}$$

where $a(x)$, $\xi(x)$ and $f(y,x)$ are given sufficiently smooth functions and $a(x) > 0,\ 0 < \lambda < T, \delta > 0$ is a sufficiently large number. Assume that all compatibility conditions are satisfied.

The well-posedness of the source identification problem (1) for the two dimensional elliptic differential equation with nonlocal boundary conditions. Applying operator approaches, the exact estimates for the solution of this problem in Hölder norms are established.

THE MAIN THEOREM ON WELL-POSEDNESS OF PROBLEM (1)

We introduce the Banach spaces $C^\beta[0,l]$ $(0 < \beta < 1)$ of all continuous functions $\varphi(x)$ satisfying a Hölder condition for which the following norms are finite

$$\| \varphi \|_{C^\beta[0,l]} = \| \varphi \|_{C[0,l]} + \sup_{0 \le x < x+\tau \le l} \frac{|\varphi(x+\tau) - \varphi(x)|}{\tau^\beta},$$

where $C[0,l]$ is the space of the all continuous functions $\varphi(x)$ defined on $[0,l]$ with the usual norm

$$\| \varphi \|_{C[0,l]} = \max_{0 \le x \le l} |\varphi(x)|.$$

International Conference on Analysis and Applied Mathematics (ICAAM 2020)
AIP Conf. Proc. 2325, 020021-1–020021-3; https://doi.org/10.1063/5.0040281
Published by AIP Publishing. 978-0-7354-4069-2/$30.00

Theorem 1 *For the solution of the source identification problem (1) the following stability and coercive stability estimates hold:*

$$\|u\|_{C(C^{\beta}[0,l])} \leq M(\beta)\left[\|\xi\|_{C^{\beta}[0,l]} + \|f\|_{C(C^{\beta}[0,l])}\right],$$

$$\|u\|_{C_{0T}^{2+\alpha,\alpha}(C^{\beta}[0,l])} + \|u\|_{C_{0T}^{\alpha,\alpha}(C^{\beta+2}[0,l])} + \|p\|_{C^{\beta}[0,l]}$$

$$\leq \frac{M(\beta)}{\alpha(1-\alpha)}\|f\|_{C_{0T}^{\alpha,\alpha}(C^{\beta}[0,l])} + M(\beta)\|\xi\|_{C^{\beta+2}[0,l]},$$

where $M(\beta)$ is independent of α, $\xi(x)$ and $f(t,x), 0<\alpha<1,\ 0<\beta<1$.Here $C_{0T}^{\alpha,\alpha}(E)$ $(0<\alpha<1)$ is the Banach space obtained by completion of the set of $E-$valued smooth functions $\varphi(t)$ defined on $[0,T]$ with values in E in the norm

$$\|\varphi\|_{C_{0T}^{\alpha,\alpha}(E)} = \|\varphi\|_{C(E)} + \sup_{0\leq t<t+\tau\leq T} \tau^{-\alpha}(T-t)^{\alpha}(t+\tau)^{\alpha}\|\varphi(t+\tau)-\varphi(t)\|_{E},$$

where $C(E)$ stands for the Banach space of all continuous functions $\varphi(t)$ defined on $[0,T]$ with values in E equipped with the norm

$$\|\varphi\|_{C(E)} = \max_{0\leq t\leq T}\|\varphi(t)\|_{E}.$$

Proof. It is known that the differential expression

$$Av(x) = -a(x)v''(x) + \delta v(x) \tag{2}$$

define a positive operator A acting in $C^{\beta}[0,l]$ with domain $C^{\beta+2}[0,l]$ and satisfying the conditions $v(0)=v(l),\ v_x(0)=v_x(l)$. Therefore, source identification problem (1) can be written in abstract form

$$\begin{cases} -u''(t)+Au(t)=f(t)+p, \ \ 0<t<T, \\ \\ u(0)=u(T),\ u'(0)=u'(T), u(\lambda)=\xi \end{cases} \tag{3}$$

in a Banach space E with unknown parameter $p=p(x)$ and unknown abstract function $u(t)=u(t,x)$. Here, element $\xi=\xi(x)$ and smooth abstract function $f(t)=f(t,x)$ defined on $[0,T]$ with values in E are given. Therefore, the proof of Theorem 1 is based on the positivity of the elliptic operator A in $C^{\beta}[0,l]$ [7] and the following theorem on well-posedness of problem (3).

Theorem 2 *Assume that $\xi\in D(A)$ and $f(t)\in C_{01}^{\alpha,\alpha}(E), 0<\alpha<1$. For the solution $\{u(t),p\}$ of source identification problem (3) in $C_{0T}^{\alpha,\alpha}(E)\times E$ the stability and coercive inequality*

$$\|u\|_{C(E)} \leq M\ \left[\|\xi\|_{E} + \|f\|_{C(E)}\right],$$

$$\left\|u''\right\|_{C_{0T}^{\alpha,\alpha}(E)} + \|Au\|_{C_{0T}^{\alpha,\alpha}(E)} + \|p\|_{E} \leq M[\|A\xi\|_{E} + \frac{1}{\alpha(1-\alpha)}\|f\|_{C_{0T}^{\alpha,\alpha}(E)}]$$

are satisfied, where M is independent of α,ξ and $f(t)$.

CONCLUSION

In the current work, the well-posedness of the source identification problem for the two dimensional elliptic differential equation with nonlocal boundary conditions is investigated. The exact estimates for the solution of this problem in Hölder norms are established. In future investigation, absolute stable difference schemes for approximately solution of the source identification problem for the two dimensional elliptic differential equation with nonlocal boundary conditions will be constructed and investigated.

REFERENCES

1. A. Ashyralyev, Numerical Analysis and Optimization **24(1-2)**, 1-15 (2003).
2. A. Ashyralyev, Journal of Mathematical Analysis and Applications **344(1)**, 557-573 (2008).
3. A. Ashyralyev, Ukrainian Mathematical Journal **62(9)**, 1397-1408 (2011).
4. A. Ashyralyev and C. Ashyralyyev, Nonlinear Anal. Model. Control **19(3)**, 350–366 (2014).
5. A. Ashyralyev and F. S. O. Tetikoglu, Math. Method Appl. Sci. **37(17)**, 2663-2676 (2014).
6. A. Ashyralyev and P. E. Sobolevskii, *New Difference Schemes for Partial Differential Equations* (Birkhäuser Verlag, Basel, Boston, Berlin, 2004).
7. A. Ashyralyev and P. E. Sobolevskii, *Well-Posedness of Parabolic Difference Equations* (Birkhäuser Verlag, Basel, Boston, Berlin, 1994).
8. C. Ashyralyyev, Boundary Value Problems **2017:74**, (2017).
9. C. Ashyralyyev, G. Akyuz and M. Dedeturk, Electronic Jourlal of Differential Equations **2017(197)**, 1-16 (2017).
10. C.Ashyralyyev, Numerical Functional Analysis and Optimization **38(10)**, 1226–1243 (2017).
11. C. Ashyralyyev and A. Çay, AIP Conference Proceedings **1997**, 020026 (2018).
12. G. Avalishvili, M. Avalishvili, and D. Gordeziani, Applied Mathematical Letters **24(4)**, 566–571 (2011).
13. G. Berikelashvili and N. Khomeriki, Nonlinear Anal. Model. Control **19(3)**, 367–381 (2014).
14. S. Kabanikhin, *Inverse and Ill-Posed Problems: Theory and Applications* (De Gruyter, Berlin, Germany, 2011).
15. S. Kabanikhin and M. Shishlenin, J. Inverse Ill-Posed Probl. **27(3)**, 453–456 (2019).
16. A. I. Kozhanov, Complex Variables and Elliptic Equations **64(5)**, 741-752 (2019).
17. D. G. Orlovsky, J. Inverse Ill-Posed Probl. **21**, 141-157 (2013).
18. D. Orlovsky and S. Piskarev, Contemporary Analysis and Applied Mathematics **1(2)**, 118-131 (2013).
19. A. Samarskii and P. Vabishchevich, *Numerical Methods for Solving Inverse Problems of Mathematical Physics* (Walter de Gruyter, Berlin, New York, 2007).
20. M. Sapagovas, O. Štikonien, K. Jakubelien, and R. Ciupaila, Boundary Value Problems, **2019:94** (2019).
21. M. Sapagovas, V. Griškonien, and O. Štikonien, Nonlinear Anal., Model. Control **22(4)**, 489–504 (2017).
22. A. L. Skubachevskii, Russian Mathematical Surveys, **71(5)**, 801-906 (2016).

On Periodic Boundary Value Problems with an Inclined Derivative for a Second-Order Elliptic Equation

Batirkhan Kh. Turmetov,[a)] Maira D. Koshanova,[b)] and Moldir A. Muratbekova[c)]

Akhmet Yasawi International Kazakh-Turkish University, Sattarkhanov street 29, 161200, Turkestan, Kazakhstan

[a)]*Corresponding author: turmetovbh@mail.ru*
[b)]*Electronic mail: koshanova-2018@mail.ru*
[c)]*Electronic mail: moldir-1983@mail.ru*

Abstract. In this paper, we study solvability of new classes of nonlocal boundary value problems for second-order elliptic type equation. The considered problems are multidimensional analogues (in the case of circular regions) of classical periodic boundary value problems in rectangular domains. To study the main problem, first, an auxiliary boundary value problem with inclined derivative is considered for the second order elliptic equation. The main problems are solved by reducing them to a sequential solution of the Dirichlet problem and the problem with inclined derivative. Theorems on existence and uniqueness of a solution of the problems are proved.

INTRODUCTION

Let $x=(\tilde{x},x_n)\in R^n, \tilde{x}=(x_1,...,x_{n-1}), \Omega_m=\left\{x\in R^n: |\tilde{x}|^2+|x_n|^m<1\right\}, n\geq 3, m>1, \partial\Omega_m=\left\{x\in R^n: |\tilde{x}|^2+|x_n|^m=1\right\}$ be a boundary of the domain Ω_m.

In the domain Ω_m consider uniformly elliptic operator

$$A\left(x,D\right)) = \frac{\partial^2}{\partial x_n^2}+\sum_{p,q=1}^{n-1} a_{pq}\frac{\partial^2}{\partial x_p \partial x_q}+\sum_{j=1}^{n-1} b_j\frac{\partial}{\partial x_j}+c,$$

where the coefficients a_{pq}, b_j, c depend on only $\tilde{x}=(x_1,x_2,...,x_{n-1})$ and they are smooth enough and $c\leq 0$.

For any point $x\in\Omega_m$ we put in conformity a point $x^*=(x_1,x_2,...,-x_n)$. It is obvious that if $x\in\partial\Omega_m$, then $x^*\in\partial\Omega_m$.

Denote

$$\partial\Omega_m^+=\left\{x\in\partial\Omega_m: x_n\geq 0\right\}, \partial\Omega_m^-=\left\{x\in\partial\Omega_m: x_n\leq 0\right\}, S=\left\{x\in\partial\Omega_m: x_n=0\right\}\equiv\partial\Omega_m^+\cap\partial\Omega_m^-.$$

We introduce the operator $I_*[u](x)=u(z)\mid_{z=x^*}$. Let parameter k take one of the values $k=\pm 1$. In the domain Ω_m we consider the following problem:

$$A(x,D)u(x)=f(x), x\in\Omega, \tag{1}$$

$$u(x)-(-1)^k u(x^*)=g_0(x), x\in\partial\Omega_+, \tag{2}$$

$$\frac{\partial u(x)}{\partial x_n}+(-1)^k\frac{\partial u(x^*)}{\partial x_n}=g_1(x), x\in\partial\Omega_+, \tag{3}$$

$$u(x)=0, x\in S, \tag{4}$$

Here $u(x^*)$ and $\frac{\partial u}{\partial x_n}(x^*)$ mean

$$u\left(x^*\right)=I_*[u](x), \frac{\partial u}{\partial x_n}\left(x^*\right)=I_*\left[\frac{\partial u}{\partial x_n}\right](x).$$

As a solution of the problem (1) - (4) we call a function $u(x)$ from the class $C^2\left(\Omega_m\right)\cap C^1\left(\bar{\Omega}_m\right)$ which satisfies conditions (1) - (4) in the classical sense. Problem (1) - (4) is an analogue of the periodic and antiperiodic problems for equation (1) for circular domains.

International Conference on Analysis and Applied Mathematics (ICAAM 2020)
AIP Conf. Proc. 2325, 020022-1–020022-7; https://doi.org/10.1063/5.0040263
Published by AIP Publishing. 978-0-7354-4069-2/$30.00

It is necessary note to that $\frac{\partial u}{\partial x_n}(x^*) = I_*\left[\frac{\partial u}{\partial x_n}\right](x) \neq \frac{\partial}{\partial x_n} I_*[u](x)$, i.e., operator I_* and differentiation operator $\frac{\partial}{\partial x_n}$ do not commute. Moreover, since

$$\frac{\partial^2 u}{\partial x_n^2}(x^*) = I_*\left[\frac{\partial^2 u}{\partial x_n^2}\right](x) = \frac{\partial^2}{\partial x_n^2} I_*[u](x),$$

the following equality holds

$$A(x,D)u(x^*) \equiv A(x,D)I_*u(x) = I_*A(x,D)u(x). \tag{5}$$

Further, if $x \in S$, then $x = (\tilde{x},0)$ and the corresponding points $x^* = (x_1, x_2, ..., x_{n-1}, 0)$ also belong to the set S. Therefore, $u(x)$ belongs to the class $C^1(\bar{\Omega}_m)$, if the following condition holds:

$$g_0(\tilde{x},0) = u(\tilde{x},0) + (-1)^k u(\tilde{x}^*,0) = (-1)^k \left[u(\tilde{x}^*,0) + (-1)^k u(\tilde{x},0)\right] = (-1)^k g_0(\tilde{x}^*,0), \tilde{x} \in S.$$

However, due to condition (4), equality $u(\tilde{x},0) = 0, \tilde{x} \in S$ holds, and therefore, the last condition can be rewritten in the form $g_0(\tilde{x},0) = g_0(\tilde{x}^*,0) = 0, \tilde{x} \in S$, i.e.,

$$g_0(x) = 0, x \in S. \tag{6}$$

The following condition is also necessary

$$\frac{\partial g_0}{\partial x_j}(x) - (-1)^k \frac{\partial g_0}{\partial x_j}(x^*) = 0, x \in S, j = 1,2,...,n, \tag{7}$$

and

$$g_1(x) + (-1)^k g_1(x^*) = 0, x \in S. \tag{8}$$

Furthermore, we will assume that conditions (6) - (8) are satisfied. Note that similar problems for the Laplace and Poisson equations with normal derivatives of integer and fractional orders were studied in [1-6]. Moreover, in [7] similar problem was studied for a boundary operator with inclined derivative when there is no degeneracy. We also note that degenerate boundary value problems with inclined derivative were studied in [8-12].

UNIQUENESS RESEARCH OF SOLUTION

We give the uniqueness theorem for the solution of problem (1) - (4).

Theorem 1 *Let k take one of the values $k = \pm 1$. If a solution of problem (1)-(4) exists, then it is unique.*

Proof. Let $k = 1$ and $u(x)$ be a solution of the homogenous problem (1) -(4). Then from condition (2) it follows that

$$u(x) = u(x^*) \equiv I_*[u](x), x \in \partial\Omega_m^+.$$

If $x \in \partial\Omega_m^-$, then it is obvious that $x^* \in \partial\Omega_m^+$. Therefore, from the boundary value condition (2) for the points $x \in \partial\Omega_m^-$ we get

$$u(x) = u(x^*) \equiv I_*[u](x), x \in \partial\Omega_m^-.$$

Consequently, for all $x \in \partial\Omega_m$ we have

$$u(x) - u(x^*) = 0, x \in \partial\Omega_m.$$

Denote $v(x) = u(x) - u(x^*)$. Then applying the operator $A(x,D)$ to this function, according to (5), we have

$$A(x,D)v(x) = A(x,D)u(x) - A(x,D)u(x^*) = 0, x \in \Omega_m.$$

Hence, function $v(x)$ is a solution of the following Dirichlet problem:

$$A(x,D)\,v(x)=0, x\in\Omega_m,\; v(x)|_{\partial\Omega_m}=0.$$

Then, due to the uniqueness of the solution of the Dirichlet problem, $v(x)=0, x\in\bar{\Omega}_m$. Therefore $u(x)=u(x^*)\equiv I_*[u](x), x\in\bar{\Omega}_m$. By condition of the problem, $u(x)$ belongs to the class $C^1\left(\bar{\Omega}_m\right)$. Thus, from the condition $u(x)=u(x^*), x\in\bar{\Omega}_m$, due to the equality

$$\frac{\partial}{\partial x_n}I_*[u](x)=\frac{\partial}{\partial x_n}u(x_1,...,x_{n-1},-x_n)=-I_*\left[\frac{\partial}{\partial x_n}u\right](x_1,...,x_{n-1},x_n)\equiv-\frac{\partial u(x^*)}{\partial x_n},$$

we obtain

$$\frac{\partial u}{\partial x_n}(x)=-\frac{\partial u}{\partial x_n}(x^*)\equiv-I_*\left[\frac{\partial u}{\partial x_n}\right](x), x\in\bar{\Omega}_m. \tag{9}$$

On the other hand, by the boundary value condition (3), we have

$$\frac{\partial u}{\partial x_n}(x)=\frac{\partial u}{\partial x_n}(x^*)\equiv I_*\left[\frac{\partial u}{\partial x_n}\right](x), x\in\partial\Omega_m^+,$$

and

$$\frac{\partial u}{\partial x_n}(x)=\frac{\partial u}{\partial x_n}(x^*)\equiv I_*\left[\frac{\partial u}{\partial x_n}\right](x), x\in\partial\Omega_m^-.$$

Consequently, for all points $x\in\partial\Omega_m$ we get

$$\frac{\partial u}{\partial x_n}(x)=\frac{\partial u}{\partial x_n}(x^*)\equiv I_*\left[\frac{\partial u}{\partial x_n}\right](x). \tag{10}$$

Then, adding the left and right sides of equalities (9) and (10), we obtain

$$\frac{\partial u}{\partial x_n}(x)=0, x\in\partial\Omega_m.$$

Therefore, $u(x)$ - solution of the homogeneous problem (1) - (4) is also solution to the following problem

$$A(x,D)\,u(x)=0, x\in\Omega_m,\; \left.\frac{\partial u}{\partial x_n}(x)\right|_{\partial\Omega_m}=0,\; u(x)|_S=0. \tag{11}$$

In [7] it is proved that the solution of the problem (11) is unique and therefore, $u(x)\equiv0, x\in\bar{\Omega}_m$.

Let now $k=2$. In this case, if $u(x)$ is a solution of the homogenous problem (1) - (4), then from condition (2) for all point $x\in\partial\Omega_m^+$ we get

$$u(x)=-u(x^*), x\in\partial\Omega_m^+.$$

In its turn, for points $\partial\Omega_m^-$

$$u(x)=-u(x^*), x\in\partial\Omega_m^-$$

and consequently, for all $x\in\partial\Omega_m$ we have

$$u(x)+u(x^*)=0, x\in\partial\Omega_m.$$

Further, if we denote $v(x)=u(x)+u(x^*)$, then the function $v(x)$ is a solution of the Dirichlet problem:

$$A(x,D)\,v(x)=0, x\in\Omega_m,\; v(x)|_{\partial\Omega_m}=0,$$

and due to the uniqueness of the solution of the Dirichlet problem, $v(x)=0, x\in\bar{\Omega}_m$. Therefore, $u(x)=-u(x^*)\equiv -I_*[u](x), x\in\bar{\Omega}_m$. Then

$$\frac{\partial u}{\partial x_n}(x)=-\frac{\partial u}{\partial x_n}(x^*)\equiv -\frac{\partial}{\partial x_n}I_*[u](x), x\in\bar{\Omega}_m.$$

Further, as in the case $k=1$ from the boundary value condition (3) we obtain:

$$\frac{\partial u}{\partial x_n}(x)=-\frac{\partial u}{\partial x_n}(x^*)\equiv -I_*\left[\frac{\partial}{\partial x_n}u\right](x), x\in\partial\Omega_m^+,$$

$$I_*\left[\frac{\partial}{\partial x_n}u\right](x)\equiv\frac{\partial u}{\partial x_n}(x^*)=-\frac{\partial u}{\partial x_n}(x), x\in\partial\Omega_m^-,$$

and consequently, we have

$$\frac{\partial u}{\partial x_n}(x)=-\frac{\partial u}{\partial x_n}(x^*)\equiv -I_*\left[\frac{\partial}{\partial x_n}u\right](x)=\frac{\partial}{\partial x_n}I_*[u](x), x\in\partial\Omega_m.$$

Hence

$$\frac{\partial u}{\partial x_n}(x)=0, x\in\partial\Omega_m.$$

In this case the function $u(x)$ satisfies conditions of the problem (11). Then $u(x)\equiv 0, x\in\bar{\Omega}_m$. Theorem is proved.

EXISTENCE RESEARCH OF SOLUTION

In this section, we prove theorem on existence and smoothness of a solution of the problem (1) - (4). Consider the following auxiliary problem

$$A(x,D)z(x)=0, x\in\Omega_m, \left.\frac{\partial z}{\partial x_n}(x)\right|_{\partial\Omega_m}=h(x), z(x)|_S=0. \tag{12}$$

In [8] the following proposition is proved.

Lemma 2 *Let $1-\frac{1}{m}<\lambda$, moreover number $\lambda+\frac{1}{m}$ is not integer. For any function $h(x)\in C^{\lambda}(\partial\Omega_m)$ solution of problem (12) exists, unique and belongs to the class $C^{\lambda+\frac{1}{m}}\left(\bar{\Omega}_m\right)$.*

The following statement is true for the main problem.

Theorem 3 *Let k take one of the values $k=\pm 1$, $1-\frac{1}{m}<\lambda<1, f(x)\in C^{\lambda}\left(\bar{\Omega}_m\right),\ g_0(x)\in C^{\lambda+1}(\partial\Omega_m^+), g_1(x)\in C^{\lambda}(\partial\Omega_m^+)$ and the matching conditions (6) - (8) be satisfied. Then solution of the problem (1) - (4) exists, unique and belongs to the class $C^{\lambda+\frac{1}{m}}\left(\bar{\Omega}_m\right)$.*

Proof. Let $k=1$ and $u(x)$ be a solution of the problem (1) - (4). Consider the following function:

$$v(x)=\frac{u(x)-u(x^*)}{2}, w(x)=\frac{u(x)+u(x^*)}{2}. \tag{13}$$

Note that functions $v(x)$ and $w(x)$ have the following properties:

$$v(x)=-v(x^*)\equiv -I_*[v](x); w(x)=w(x^*)\equiv I_*[w](x),$$

$$\frac{\partial v(x)}{\partial x_n} = -\frac{\partial}{\partial x_n} I_*[v](x) = I_*\left[\frac{\partial}{\partial x_n} v\right](x) \equiv \frac{\partial v(x^*)}{\partial x_n},$$

$$\frac{\partial w(x)}{\partial x_n} = \frac{\partial}{\partial x_n} I_*[w](x) = -I_*\left[\frac{\partial}{\partial x_n} w\right](x) \equiv -\frac{\partial w(x^*)}{\partial x_n}.$$

We find the conditions that the functions $v(x)$ and $w(x)$ will satisfy. Applying the operator $A(x,D)$ to the function $v(x)$, we have

$$A(x,D)v(x) = \frac{1}{2}\left[A(x,D)u(x) - A(x,D)u(x^*)\right] = \frac{1}{2}\left[A(x,D)u(x) - I_* A(x,D)u(x)\right]$$

$$= \frac{1}{2}\left[f(x) - f(x^*)\right], x \in \Omega_m.$$

Further, from boundary value condition (2) it follows that

$$v(x)|_{\partial\Omega_m^+} = \frac{1}{2}\left[u(x) - u(x^*)\right]\Big|_{\partial\Omega_m^+} = \frac{1}{2} g_0(x).$$

If the point x belongs to the lower part of the boundary, i.e. $x \in \partial\Omega_m^-$, then the corresponding point x^* belongs to the upper part of the boundary, and therefore, again from the boundary value condition (2), we obtain

$$v(x)|_{\partial\Omega_m^-} = \frac{1}{2}\left[u(x) - u(x^*)\right]\Big|_{\partial\Omega_m^-} = -\frac{1}{2}\left[u(x^*) - u(x)\right]\Big|_{x^*\in\partial\Omega_m^+} = -\frac{1}{2} g_0(x^*).$$

Moreover, condition (4) implies

$$v(x)|_S = \frac{1}{2}\left[u(x) - u(x^*)\right]\Big|_S = 0.$$

Further, making similar actions with respect to the function $w(x)$ from the equality (13), we obtain

$$A(x,D)w(x) = \frac{1}{2}\left[A(x,D)u(x) + A(x,D)u(x^*)\right] = \frac{1}{2}\left[f(x) + f(x^*)\right], x \in \Omega_m,$$

$$\frac{\partial w(x)}{\partial x_n}\Big|_{\partial\Omega_+} = \frac{1}{2}\left[\frac{\partial u(x)}{\partial x_n} + \frac{\partial}{\partial x_n} I_*[u](x)\right]\Big|_{\partial\Omega_+} = \frac{1}{2}\left[\frac{\partial u(x)}{\partial x_n} - I_*\left[\frac{\partial u}{\partial x_n}\right](x)\right]\Big|_{\partial\Omega_+}$$

$$= \frac{1}{2}\left[\frac{\partial u(x)}{\partial x_n} - \frac{\partial u}{\partial x_n}(x^*)\right]\Big|_{\partial\Omega_+} = \frac{1}{2} g_1(x), x \in \partial\Omega_m^+,$$

$$\frac{\partial w(x)}{\partial x_n}\Big|_{\partial\Omega_-} = \frac{1}{2}\left[\frac{\partial u(x)}{\partial x_n} + \frac{\partial}{\partial x_n} I_*[u](x)\right]\Big|_{\partial\Omega_-} = \frac{1}{2}\left[\frac{\partial u(x)}{\partial x_n} - I_*\left[\frac{\partial u}{\partial x_n}\right](x)\right]\Big|_{\partial\Omega_-}$$

$$= \frac{1}{2}\left[\frac{\partial u(x)}{\partial x_n} - \frac{\partial u(x^*)}{\partial x_n}\right]\Big|_{\partial\Omega_-} = -\frac{1}{2}\left[\frac{\partial u(x^*)}{\partial x_n} - \frac{\partial u(x)}{\partial x_n}\right]\Big|_{x^*\in\partial\Omega_+} = -\frac{1}{2} g_1(x^*), x \in \partial\Omega_m^-.$$

Moreover, condition (4) implies

$$w(x)|_S = \frac{1}{2}\left[u(x) + u(x^*)\right]\Big|_S = 0.$$

Denote,

$$f^{\pm}(x) = \frac{1}{2}\left[f(x) \pm f(x^*)\right], 2\tilde{g}_0(x) = \begin{cases} g_0(x), x \in \partial\Omega_m^+ \\ -g_0(x^*), x \in \partial\Omega_m^- \end{cases}, 2\tilde{g}_1(x) = \begin{cases} g_1(x), x \in \partial\Omega_m^+ \\ -g_1(x^*), x \in \partial\Omega_m^- \end{cases}.$$

We research smoothness of these functions. By the condition, $f(x) \in C^{\lambda}\left(\bar{\Omega}_m\right)$. Then it is obvious that the functions $f^{\pm}(x)$ also belong to the class $C^{\lambda}\left(\bar{\Omega}_m\right)$. Further, by the hypothesis of the theorem, the function $g_0(x)$ belongs to the class $C^{\lambda+1}(\partial\Omega_m^+)$ and the matching conditions (6) and (7) are satisfied for it. Then the function $\tilde{g}_0(x)$ belongs to the class $C^{\lambda+1}(\partial\Omega_m)$. Similarly, the function $g_1(x)$ belongs to the class and the matching condition (8) is satisfied for it. Then the function $\tilde{g}_1(x)$ belongs to the class $C^{\lambda}(\partial\Omega_m)$. Thus, if $u(x)$ is a solution of problem (1) - (4), then the functions $v(x)$ and $w(x)$ satisfy conditions of the following problems:

$$A(x,D)\,v(x) = f^{-}(x), x \in \Omega,\ v(x)|_{\partial\Omega} = \tilde{g}_0(x), \tag{14}$$

with the additional condition

$$v(x)|_S = 0 \tag{15}$$

and

$$A(x,D)\,w(x) = f^{+}(x), x \in \Omega_m,\ \frac{\partial w}{\partial x_n}(x)\Big|_{\partial\Omega_m} = \tilde{g}_1(x),\ w(x)|_s = 0. \tag{16}$$

We study the problem (14). We will look for a solution to the problem in the form $v(x) = v_1(x) + v_2(x)$, where functions $v_1(x)$ and $v_2(x)$ satisfy the conditions of the following problems

$$A(x,D)\,v_1(x) = f^{-}(x), x \in \Omega,\ v_1(x)|_{\partial\Omega} = 0, \tag{17}$$

$$A(x,D)\,v_2(x) = 0, x \in \Omega,\ v_2(x)|_{\partial\Omega} = \tilde{g}_0(x). \tag{18}$$

Problems (17) and (18) are classical Dirichlet problems, and for smooth data, solutions to these problems always exist. We need to clarify smoothness of the solutions to these problems. It was proved in [13] that if $0 < \lambda < 1$, $f^{-}(x) \in C^{\lambda}(\bar{\Omega}_m)$, then solution to the problem (17) belongs to the class $C^{\lambda+2}(\bar{\Omega}_m)$. The exact smoothness order of the solution to the problem (18) in the case $\tilde{g}_0(x) \in C^{\lambda+1}(\partial\Omega_m)$ is given in [8] and the order has the form $C^{\lambda+1}(\bar{\Omega}_m)$. In addition, due to the matching condition (6), equality $v_2(x)|_S = 0$ holds. Thus, if $f^{-}(x) \in C^{\lambda}(\bar{\Omega}_m), \tilde{g}_0(x) \in C^{\lambda+1}(\partial\Omega_m)$, then a solution to the problem (14) exists and condition (15) holds for it. Further, we will look for a solution to the problem (16) in the form $w(x) = w_1(x) + w_2(x)$, where the functions $w_1(x)$ and $w_2(x)$ are solutions of the following problems:

$$A(x,D)\,w_1(x) = f^{+}(x),\ \ x \in \Omega_m,\ w_1(x)|_{\partial\Omega_m} = 0, \tag{19}$$

$$A(x,D)\,w_2(x) = 0,\ \ x \in \Omega_m;\ \frac{\partial w_2(x)}{\partial x_n}\Big|_{\partial\Omega_m} = \tilde{g}_1(x) - \frac{\partial w_1(x)}{\partial x_n},\ w_2(x)|_S = 0. \tag{20}$$

As we have already noticed, under the conditions of the theorem and the matching conditions (8), the function $f^{+}(x)$ belongs to the class $C^{\lambda}(\bar{\Omega}_m)$. Then a solution to the problem (19) exists, is unique and belongs to the class $C^{\lambda+2}\left(\bar{\Omega}_m\right)$. Consequently, $\frac{\partial w_1(x)}{\partial x_n} \in C^{\lambda+1}\left(\bar{\Omega}_m\right)$. Further, if $g_1(x) \in C^{\lambda}(\partial\Omega_m^+)$, then the function $\tilde{g}_1(x) - \frac{\partial w_1(\bar{x})}{\partial x_n}$ at least belongs to the class $C^{\lambda}(\partial\Omega_m)$.

With these data, according to Lemma 1, a solution to this problem exists, is unique, and belongs to the class $C^{\lambda+\frac{1}{m}}\left(\bar{\Omega}_m\right)$. Therefore, a solution to the problem (16) exists, is unique and also belongs to the class $C^{\lambda+\frac{1}{m}}\left(\bar{\Omega}_m\right)$. Thus, we constructed the functions $v(x)$ and $w(x)$ from equalities (13). We show that if $v(x)$ and $w(x)$ are solutions to problems (13) and (16), then the function $u(x) = v(x) + w(x)$ satisfies all the conditions of the problem (1) - (4). Indeed, applying the operator $A(x,D)$ to the function $u(x) = v(x) + w(x)$, we have

$$A\left(x,D\right)u(x) = A\left(x,D\right)v(x) + A\left(x,D\right)w(x) = f^{+}(x) + f^{-}(x) = f(x), x \in \Omega.$$

Further, according to the properties of the functions $v(x)$ and $w(x)$, we have

$$u(x) - u(x^*)|_{\partial\Omega_m^+} = v(x) + w(x) - (v(x^*) + w(x^*))|_{\partial\Omega_m^+} = v(x) - v(x^*)|_{\partial\Omega_m^+} = 2v(x)|_{\partial\Omega_m^+} = 2\,\tilde{g}_0\left(x\right)|_{\partial\Omega_m^+} = g_0(x).$$

Similarly,

$$\left.\frac{\partial u(x)}{\partial x_n} - I_*\left[\frac{\partial u}{\partial x_n}\right](x)\right|_{\partial\Omega_m^+} = \left.\frac{\partial v(x)}{\partial x_n} + \frac{\partial w(x)}{\partial x_n} - I_*\left[\frac{\partial v}{\partial x_n}\right](x) - I_*\left[\frac{\partial w}{\partial x_n}\right](x)\right|_{\partial\Omega_m^+} = \left.\frac{\partial w(x)}{\partial x_n} - I_*\left[\frac{\partial w}{\partial x_n}\right](x)\right|_{\partial\Omega_m^+}$$

$$= 2\left.\frac{\partial w(x)}{\partial x_n}\right|_{\partial\Omega_m^+} = 2\,\tilde{g}_0\left(x\right)|_{\partial\Omega_m^+} = g_1(x).$$

Thus, the theorem is proved for the case $k = 1$. The periodic problem ($k = 2$) can be considered in a similar way.Theorem is proved.

ACKNOWLEDGMENTS

This research is financially supported by a grant from the Ministry of Science and Education of the Republic of Kazakhstan, Grant No. AP05131268.

REFERENCES

1. M. A. Sadybekov and B. Kh. Turmetov, Eurasian Mathematical Journal **3(1)**, 143–146 (2012).
2. M. A. Sadybekov and B. Kh. Turmetov, Differential equations **50(2)**, 268 - 273 (2014).
3. M. A. Sadybekov, B. Kh. Turmetov and M. A Muratbekova, AIP Conference Proceedings **1611**, 1 – 6. (2014).
4. M. A. Sadybekov, B. Kh. Turmetov, and B. T. Torebek, Electronic Journal of Differential Equations **2014**, 1 - 14 (2014).
5. B. Kh. Turmetov, M. D. Koshanova, and K. I. Usmanov, Electronic Journal of Differential Equations **2016**, 1–12 (2016).
6. B. Kh. Turmetov, M. D. Koshanova, and K. I. Usmanov, Filomat **32(3)**, 939–946 (2018).
7. B. Turmetov, M. Koshanova, and M. Muratbekova, e-Journal of Analysis and Applied Mathematics **3**, 13 –27 (2020).
8. Sh. A. Alimov, Differ. Uravn. **17(10)**, 1738–17511 (1981).
9. Sh. A. Alimov, Dokl. Akad. Nauk SSSR **252(5)**, 1033–1034 (1980).
10. D. I. Boyarkin, Zhurnal SVMO **18(2)**, 7–10 (2016).
11. K. Zh. Nazarova, B. Kh. Turmetov, and K. I. Usmanov, Zhurnal SVMO **22:1**, 81–93 (2020).
12. P. Popivanov, AIP Conference Proceedings **2159**, 1–10 (2019).
13. D. Gilbarg and N. Trudinger, *Elliptic Partial Differential Equations of Second Order* (Springer-Verlag, Berlin, 1977).

Using the Conjugate Equations Method for Solving Inverse Problems of Mathematical Geophysics and Mathematical Epidemiology

Nurlan Temirbekov[1, 2, a)] and Laura Temirbekova[1, 2, b)]

[1)]*National Engineering Academy of the Republic of Kazakhstan, Almaty, 050010, Kazakhstan*
[2)]*Abai Kazakh National Pedagogical University, Almaty, 050010, Kazakhstan*

[a)]*Electronic mail: temirbekov@rambler.ru*
[b)]*Corresponding author:Laura-nurlan@mail.ru*

Abstract. In this paper, the theory of conjugate equations is used to solve the inverse problem of the continuation of potential fields in the direction of disturbing masses, in the inverse problem of magnetotelluric sounding (MTS), for problems of mathematical epidemiology.

INTRODUCTION

G.I.Marchuk in his work [1] dedicated to conjugate equations and their applications notes that in the XXI century the theory of conjugate equations will play an exceptional role in solving complex systems, thanks to which it will be possible to solve global problems that concern society. To study complex systems and mathematical models, a number of general approaches and principles have been developed. One of them is the principle of duality. In this principle, the concept of the conjugate operator is basic.

In general view, we write the mathematical model of the inverse problem in the operator equation form

$$Au = f \tag{1}$$

with linear operator $A : X \to Y$ and domain $D(A)$, dense in X, i.e. $D(A) = X$. Suppose that one of the goals consideration inverse problems is to minimization of the functional of the coefficient inverse problem

$$J(q,u) = \langle u,q \rangle. \tag{2}$$

For this, we introduce the conjugate operator A^* and consider the conjugate equation

$$A^* u^* = q \tag{3}$$

with element q on the right side defining $J(q,u)$. Then the dual expression for the desired functional has the form

$$J = \langle f,u^* \rangle. \tag{4}$$

Thus, to calculate functional (2), it is necessary to solve the conjugate equation (3) and use formula (4).

In this work, the theory of conjugate equations is used to solve the inverse problem of the continuation of potential fields in the direction of disturbing masses. This problem leads to the solution of the first kind Fredholm integral equation [2] the following view

$$\int_a^b K(x,s)u(s)ds = f(x),\ x \in [a,b] \tag{5}$$

and the corresponding conjugate equation

$$\int_a^b K(s,x)\upsilon_k(s)ds = \alpha_k(x),\ x \in [a,b]. \tag{6}$$

International Conference on Analysis and Applied Mathematics (ICAAM 2020)
AIP Conf. Proc. 2325, 020023-1–020023-5; https://doi.org/10.1063/5.0040264
Published by AIP Publishing. 978-0-7354-4069-2/$30.00

Here $\alpha_k(x)$- known functions, k - number, $\upsilon_k(x)$- solution of the conjugate equation (6), depending on the number k. Multiply (5) on $\upsilon_k(x)$ and integrate by x:

$$\int_a^b \upsilon_k(x) \int_a^b K(x,s)u(s)dsdx = \int_a^b \upsilon_k(x) f(x)dx.$$

Changing the order of integration and taking into account equation (6), we get

$$\int_a^b u(s)\alpha_k(s)ds = \int \upsilon_k(x) f(x)dx. \tag{7}$$

Let $\alpha_k(x)$ - basic functions on a segment $[a,b]$, then the first integral in (7) is k - th coefficient in the expansion of the function $u(x)$ in the Fourier series, i.e. from (7) follows

$$u_k = \int_a^b \upsilon_k f(x)dx,\ u(x) = \sum_{k=1}^{N} u_k \alpha_k(x).$$

The solution to the problem is divided into two stages. At the first stage, the integral equation is solved, in the right hand side of which are a large number of basis functions, while the kernel of integral equation remains the same. At the second stage, the Fourier coefficients are found as an integral of the product of the solution of the conjugate equation and the right hand side of the main integral equation. Then the desired solution is found in the form of the sum of the product of the Fourier coefficients and the basis functions. The optimal number of members of the Fourier series to find an approximate solution is determined from the condition of satisfying the accuracy of the measurement of the input data.

THE INVERSE PROBLEM OF MAGNETOTELLURIC SOUNDING (MTS)

The next considered problem is the inverse MTS problem [3-8]. To solve the inverse MTS problem with an additional condition for the solution, the optimal control method with the duality principle is used. The principle of duality simplifies the procedure for solving the problem. For this, a conjugate equation is introduced with the elements on the right-hand side determining the objective function of the optimal control method. Then, a gradient iterative method is constructed and a numerical solution is found.

Statement of the problem. Consider the direct problem of magnetotelluric sounding (MTS) [3] for the components of the electric and magnetic fields

$$u_{zz} + i\omega\mu_0\sigma(z)u = 0, z \in [0,L], \tag{8}$$

$$(u_z + h_1 u)|_{z=0} = 1, \tag{9}$$

$$(u_z + h_2 u)|_{z=L} = 0, \tag{10}$$

Given additional information

$$u|_{z=0} = f(\omega), \tag{11}$$

we use the theory of conjugate equations to solve the inverse coefficient problem (8) - (11). The coefficient σ is found from the condition of minimum functional

$$J(\sigma) = \int_{\omega_1}^{\omega_2} [u(0,\omega,\sigma) - f(\omega)]^2 d\omega \tag{12}$$

to increment functional (12) we obtain the expression

$$\delta J = \int_0^L \delta\sigma \int_{\omega_1}^{\omega_2} i\psi\omega\mu_0 u d\omega dz, \tag{13}$$

where ψ is solution of the conjugate equation

$$\psi_{zz} + i\mu_0\omega\sigma\psi = 0 \tag{14}$$

with boundary conditions

$$(\psi_z + h_1\psi)_{z=0} = -2[u(0,\omega,\sigma) - f(\omega)], \tag{15}$$

$$(\psi_z + h_2\psi)_{z=L} = 0. \tag{16}$$

Further using (13), a gradient iterative method is constructed.

INVERSE PROBLEM OF MATHEMATICAL EPIDEMIOLOGY

The conjugate equations are also used to solve mathematical epidemiology problems. The paper [9] presents a methodology for the joint use of mathematical models and real data, which is an effective tool for studying complex epidemiological processes and solving practical problems based on it. A significant role here is played conjugate tasks. It is convenient to construct direct and inverse connections between models and daily real data on the distribution of the coronavirus (COVID - 19) and the system organization of computing technologies using variational principles. This approach naturally leads to the combined use of direct and inverse modeling methods. The approach based on the classical Lagrange variational principle using conjugate equations is the most perspective for solving problems of estimating and predicting virus propagation processes.

We considered a modification Kermack-Mckendrick model of mathematical epidemiology

$$\begin{aligned} \frac{dS}{dt} &= -\alpha_E \frac{S(t)E(t)}{N(t)} - \alpha_I \frac{S(t)}{N(t)} + \gamma R(t), \\ \frac{dE}{dt} &= \alpha_E \frac{S(t)E(t)}{N(t)} + \alpha_I \frac{S(t)I(t)}{N(t)} - kE(t) - \rho E(t), \\ \frac{dI}{dt} &= kE(t) - \beta I(t) - \mu I(t), \\ \frac{dR}{dt} &= \beta I(t) + \rho E(t) - \gamma R(t), \\ \frac{dD}{dt} &= \mu I(t) \end{aligned} \tag{17}$$

and

$$\begin{gathered} N(t) = S(t) + E(t) + R(t) + D(t), \\ S(0) = S_0, E(0) = E_0, I(0) = I_0, R(0) = R_0, D(0) = D_0. \end{gathered} \tag{18}$$

The equation parameters have the following values:

$S(t)$ - number of susceptible individuals at a time t;
$E(t)$ - number of people infected without symptoms at a given time t;
$I(t)$ - number of infected individuals at a time t;
$R(t)$ - the number of have been sick individuals at a time t;
$D(t)$ - number of fatalities;
α_I - infection parameter between infected and susceptible populations;
α_E - infection parameter between asymptomatic and susceptible populations;
γ - the speed of re-infection;
k - frequency of symptoms;
ρ - speed of recovery of detected cases;
β - speed of recovery of infected cases;
μ - mortality rate of infected cases.

The inverse problem is to restore parameters $\alpha_I, \alpha_E, \gamma, k, \rho, \beta, \mu, E_0$. The optimization method of conjugate gradients is used for numerical implementation of the inverse problem [9]. Problem (17), (18) with the additional conditions written in the form

$$\frac{dy}{dt} = \mu(t, y, q), \; y(t_0) = y_0, \; y_i(t_k) = f_{ik}. \tag{19}$$

A solution will be found by minimizing the following function

$$J(q, y_0) = \sum_{k=1}^{K} \sum_{i} \omega_i |y_i(t_k; q) - f_{ik}|^2 \to \min_{q, y_0}.$$

The gradient of the functional is determined by the following relation

$$J'(q, y_0) = -\int_{t_0}^{T} \Psi^T(t) \mu_q(y(t), q) dt, \tag{20}$$

where Ψ is the solution to the following conjugate problem

$$\dot{\Psi} = -\mu_y^T(y(t), q)\Psi, \Psi(T) = 0, [\Psi_i]_{t=t_k} = 2\omega_i(y_i(t_k; q) - f_{ik}), \; k = 1, ..., K, \; i \in I \subset \{1, ..., N\}. \tag{21}$$

Consider gradient method to solve the minimization problem by determining approximate solution

$$(q_{n+1}, y_{0_{n+1}}) = (q_n, y_{0_n}) - \alpha_n J'(q_n, y_{0_n}), \; \alpha_n > 0. \tag{22}$$

Kermak-Mackendrick Classic Coronavirus Population Mathematical Model (SIR)

Consider the classic distribution model of the coronavirus COVID-2019 described by systems of nonlinear differential equations. Some coefficients and initial data of the system are unknown or averaged. The inverse problem of identifying model parameters is reduced to minimizing the quadratic target functional (12) and applying the gradient method (14).

$$\begin{gathered} \tfrac{dS}{dt} = -\beta IS, \\ \tfrac{dI}{dt} = \beta IS - \nu I, \\ \tfrac{dR}{dt} = \nu I, \\ S(0) = S_0, I(0) = I_0, R(0) = R_0. \end{gathered} \tag{23}$$

The population is considered constant

$$\frac{dS}{dt} + \frac{dI}{dt} + \frac{dR}{dt} = 0. \tag{24}$$

The intensity of infection of the susceptible, also called the strength of the infection, has the following form:

$$F = \beta I. \tag{25}$$

Parameters of SIR models:

$S(t)$ - the number of susceptible individuals at time t;

$I(t)$ - the number of infected individuals at time t;

$R(t)$ -the number of have been sick individuals at time t;

β-coefficient of contact intensity of individuals followed by infection;

μ-recovery rate of infected individuals. The inverse problem is to find the parameters β, ν from the daily real data S_k, I_k, R_k obtained from official sources.

CONCLUSION

It can be concluded that, the theory of conjugate equations is used to solve the inverse problem of the continuation of potential fields in the direction of disturbing masses, in the inverse problem of magnetotelluric sounding (MTS), for problems of mathematical epidemiology.

REFERENCES

1. G. I. Marchuk, Proceeding of Math. and Mech. UrB RAS **12(1)**, 184–195 (2006).
2. L. N. Temirbekova, AIP Conference Proceedings **1997**, 020072 (2018).
3. A. N. Tikhonov, *Mathematical Geophysics* (Scientific World, Moscow, 1999) p. 476.
4. M. N. Berdichevsky and V. I. Dmitriev, *Models and Methods of Magnetotellurics* (Springer-Verlag, 2008) p. 680.
5. E. Y. Bidaibekov and G. B. Kamalova, Bulletin of Abai KazNPU. Series - Physics and Mathematics **4(64)**, 20–28 (2018).
6. K. M. Zubarev and T. L. Ivanov, Political Youth Magazine **3**, 1–12 (2016).
7. O. V. Kashafutdinov, Political Youth Magazine **3**, www.ict.nsc.ru/ws/YM2004/8565/index.html.
8. P. N. Alexandrov, On the inverse problem of MTS from the position of ideas of M.V. Klibanov, Issues of the theory and practice of geological interpretation of geophysical fields: Materials of the 39-th session of the D. G. Uspensky International Scientific Seminar. Voronezh, January 30 - February 2, 2012.
9. N. M. Temirbekov and L. N. Temirbekova, Proceedings of the Scientific and Technical Society.

On the Solvability of Nonlinear Integral Equations

Akylbek Kerimbekov,[1, a)] Elmira Abdyldaeva,[2, b)] Zhyldyz Asanova,[3, c)] and Alymbek Uraliev[4, d)]

[1)] *Applied Mathematics and Informatics, Kyrgyz-Russian Slavic University, Bishkek, Kyrgyzstan*
[2)] *High Mathematics, Kyrgyz-Turkish Manas University, Bishkek, Kyrgyzstan*
[3)] *Mathematics and Technology of Its Training, Kyrgyz State University, Bishkek, Kyrgyzstan*
[4)] *Differential Equations, Kyrgyz National University, Bishkek, Kyrgyzstan*

[a)] *Corresponding author: akl7@rambler.ru*
[b)] *Electronic mail: efa_69@mail.ru*
[c)] *Electronic mail: zhyldyzasanova73@mail.ru*
[d)] *Electronic mail: ural_alym@mail.ru*

Abstract. The article explores general nonlinear equations with a parameter. Sufficient conditions for the existence of a solution of nonlinear integral equations in the form of the sum of two functions for the individual values of the parameter are found.

INTRODUCTION

Nonlinear integral equations started to be investigated at the beginning of the 20th century. Scientific works [1, 2, 3, 4, 5, 6, 7] of A.Lyapunov (1906), E. Schmidt (1908), P.Levy (1910), G. Bratu (1910), G. Bucht (1912) , A. Collet (1912), H.Gagaj Kian (1912) were a prerequisites for development of nonlinear integral equations theory. New studies of A. Hammerstein, L. Lichtenstein, P. Uryson, R. Iglisch, V. Nemytskii, J. Schauder etc. appeared in this direction later. Theory of nonlinear integral equations was formed in the 30's of the 20th century [1]. After the 1930s, V. Nemytsky, V. Orlich, M. A. Krasnoselsky, Ya.B. Rutitsky, and others made significant contributions to the development of the theory of nonlinear integral equations [2, 3, 4, 5].

Nonlinear integral equations can be used in various fields of science and technology [1, 2, 3, 4, 5, 6, 7, 8, 11, 12, 13, 14, 15, 16] . However, despite a lot of research [6, 7, 8, 11, 12, 13, 14, 15, 16] , bibliography of works [2, 3], analytical methods for solving of nonlinear integral equations are not sufficiently developed.

In the works [9, 10, 17], an analytical method was proposed, developed on the basis of the Lagrange theorem on "finite increments" and allowed finding solutions for individual classes of nonlinear Hammerstein integral equations in the form of a sum of two functions.

PROBLEM STATEMENT AND SOLUTION

Consider the nonlinear integral equation

$$A[\varphi(x)] = \lambda \int_a^b h(x)F[t,\varphi(t)]dt + f(x), \tag{1}$$

where $\varphi(x)$ is an unknown function; $\lambda \in (-\infty,\infty)$ is parameter; $f(x), h(x)$ are given continuous functions, defined at a given interval $[a,b]$; $A[\varphi(x)]$ and $F[x,\varphi(x)]$ are given continuous functions, which have continuous derivatives with respect to a functional variable φ.

We investigate the solvability of the problem where it is required to find the values of parameter λ, for which the equation (1) has a non-trivial solution.

The solution of equation (1) is sought in the form

$$\varphi(x) = \varphi_0(x) + \lambda u(x), \tag{2}$$

where functions $\varphi_0(x), u(x)$, and a parameter λ to be determined. Suppose that function (2) is a solution of equation (1). Then the identity holds

International Conference on Analysis and Applied Mathematics (ICAAM 2020)
AIP Conf. Proc. 2325, 020024-1–020024-4; https://doi.org/10.1063/5.0040547
Published by AIP Publishing. 978-0-7354-4069-2/$30.00

$$A[\varphi_0(x)+\lambda u(x)] = \lambda \int_a^b h(x)F[t,\varphi_0(x)+\lambda u(x)]dt + f(x). \tag{3}$$

Using the Lagrange finite increment formula [9, 10, 17] for the function $A[\varphi(x)]$ and $F[x,\varphi(x)]$ by function variable φ we rewrite identity (3) in the form

$$A[\varphi_0(x)] + A_\varphi[\psi(x)]\lambda u(x) \equiv \lambda h(x) \int_a^b \{F[t,\varphi_0] + F_\varphi[t,\overline{\psi}(t)]\lambda u(x)\}dt + f(x), \tag{4}$$

where $\psi(x)$ and $\overline{\psi}(x)$ functions located between functions $\varphi_0(x)$ and $\varphi_0(x)+\lambda u(x)$. Hence, equating the coefficients at the same degree λ, we have the following inequalities

$$A[\varphi_0(x)] \equiv f(x), \tag{5}$$

$$A_\varphi[\psi(x)]\lambda u(x) \equiv h(x) \int_a^b F[t,\varphi_0(t)]dt, \tag{6}$$

$$\int_a^b F_\varphi[t,\overline{\psi}(t)]u(t)dt \equiv 0. \tag{7}$$

Relations (5) - (7) are necessary conditions for the existence of a solution of equation (1) in the form of a sum (2).It can be shown that they are sufficient.

Theorem 1 *Let the continuous nonlinear functions $A[\varphi(x)]$ and $F[x,\varphi(x)]$ in a functional variable satisfies the Lagrange formula on finite increments. Then, to have a solution in the form of the sum (2) for the nonlinear integral equation (1), it is necessary and sufficient that relations (5) - (7) are satisfied.*

Now we put an algorithm for constructing a solution of the form (2).
1) According to (5), the unknown function $\varphi_0(x)$ defined as a solution of a nonlinear algebraic equation

$$A[\varphi_0(x)] = f(x), \tag{8}$$

If a function $A[\varphi_0(x)]$ nonlinear monotonic function, that $A_\varphi[\varphi_0(x)] \neq 0$ and there is a function $q(\cdot)$ such that equality holds

$$\varphi_0(t) = q[f(x)]. \tag{9}$$

Note that due to the nonlinearity of the function $A[\varphi_0]$, the equation (8) can have several solutions

$$\varphi_{0i}(x) = q_i[f(x)], \;\; i = 1,2,3,...,p \leq \infty,$$

if $A[\varphi(x)]$ is a nonmonotonic function.
2) Further knowing $\varphi_0(x)$ we pass to the definition of an unknown function $u(x)$. Identity (6) according to the equality

$$A_\varphi[\psi(x)]\lambda u(x) = A[\varphi_0(x)+\lambda u(x)] - A[\varphi_0(x)]$$

is rewritten in the form

$$\{A[\varphi_0(x)+\lambda u(x)]-A[\varphi_0(x)]\}\equiv\lambda h(x)\int_a^b F[t,\varphi_0(t)]dt,$$

where $\varphi_0(x)$ an unknown function. This identity means that the unknown function $u(x)$ can be defined as a solution of a nonlinear algebraic equation

$$A[\varphi_0(x)+\lambda u(x)]=f(x)+\lambda h(x)\int_a^b F[t,\varphi_0(t)]dt. \tag{10}$$

Let $A[\varphi]$ monotonic function. Then from the equation (10) we obtain the equality

$$\varphi_0(x)+\lambda u(x)=q[f(x)+\lambda h(x)\int_a^b F[t,\varphi_0(t)]dt].$$

from which we find that

$$u(x)=\frac{1}{\lambda}\{q[f(x)+\lambda h(x)\int_a^b F[t,\varphi_0(t)]dt]-\varphi_0(x)\}. \tag{11}$$

If the function $A[\varphi]$ is not monotonous and has several solutions $q_i(\cdot)$, then equation (10) has several solutions

$$u_i(x)=\frac{1}{\lambda}\{q_i[f(x)+\lambda h(x)\int_a^b F[t,\varphi_0(t)]dt]-q_i[f(x)]\}.i=1,2,3,...,p\leq\infty.$$

3) After unknown functions were found $\varphi_0(x)$ and $u(x)$ we pass to the determination of the values of parameter λ. Identity (7) according to the equality

$$F_\varphi[\overline{\Psi}(t)]\lambda u(t)=F[\varphi_0(t)+\lambda u(t)]-F[\varphi_0(t)]$$

is rewritten in the form

$$\int_a^b\{F[\Phi_0(t)+\lambda u(t)]-F[\varphi_0(t)]\}dt\equiv 0, \tag{12}$$

where $\varphi_0(t)$ and $u(t)$ are known functions. After integration, this identity turns into an algebraic equation with respect to the parameter λ , i.e. has the equation

$$\Phi(\lambda)=0. \tag{13}$$

According to (12) $\Phi'(\lambda)\neq 0$ and equation (13) has at least one root $\lambda=\lambda_0$.

Equation (13) is called the resolvent algebraic equation, and its roots λ_i the resolvent numbers of the nonlinear integral equation (1).

Substituting found functions $\varphi_0(x)$, $u(x)$ and number λ_0 in (2) we obtain the desired solution of the nonlinear integral equation (1) in the form of the sum

$$\varphi(x)=\varphi_0(x)+\lambda_0 u(x). \tag{14}$$

In a similar way, a nonlinear integral equation of the form is solved

$$A[\varphi(x)]=\lambda\int_a^b\sum_{k=1}^m h_k(x)F_k[t,\varphi(t)]dt+f(x), \tag{15}$$

where $h_1(x),...,h_m(x)$ are linearly independent continuous functions. In this case, the resolvent algebraic equations form a system of nonlinear equations

$$\Phi_i(\lambda) = 0, \quad i = 1,2,3,..,m, \tag{16}$$

Let B_i set of roots i-th system of equations (16). Then system (16) has a solution only when the intersection of sets B_i , i.e., set

$$B = \bigcap_{i=1}^{m} B_i,$$

is not empty.

In the works [9]- [10], cases were considered when $A[\varphi(x)] \equiv \varphi(x)$ and examples are given for confirming theoretical conclusions.

REFERENCES

1. N. S. Smirnov, *Introduction to Theory of Nonlinear Integral Equations* (ONTI, Moscow, 1936).
2. E. M. Bogatov and Y. R. Muhin, Iz Vuz. Applied Nonlinear Dynamics (2016).
3. E. M. Bogatov, Scientific Bulletin of Bel SU, Mathematics Series, Physics **46**, 93–106 (2017).
4. F. G. Tricomi, *Integral Equations* (Interscience publishers LTD, London, 1957).
5. M. A. Krasnoselskii, *Topological Methods in the Theory of Nonlinear Integral Equations* (Pergamon Press, Oxford-London-New York-Paris, 1964).
6. A. Jerri, *Introduction to Integral Equations with Applications, Second Edition* (Wiley-Interscience Publication, New York, 1985).
7. M. A. Abdou, Appl. Math. Comput. **146**, 857–871 (2003).
8. S. G. Sardyan, T. E. Terdzhyan, and K. A. Khachatryan, Ukrainian Mathematical Journal **69**, 1107–1122 (2017).
9. A. Kerimbekov, "About the one method of solving nonlinear Fredgolm integral equations," (Issyk-Kul Aurora, Kyrgyzstan, 5-7 June, 2014).
10. A. Kerimbekov, "On a Class of Solutions of the Nonlinear Integral Fredholm Equation," (Birkhauser Switzerland, 2019) pp. 191–197.
11. A. D. Polyanin and A. I. Zhurov, Reports of the Academy of Sciences **419**, 30–34 (2008).
12. M. Dobritouio, Reports of the Academy of Sciences **2**, 403–412 (2008).
13. W. Abdul-Majid, *Linear and Nonlinear Integral Equations: Methods and Applications* (Springer-Verlag, Berlin Heidelberg, 2011) doi: 10.1007/978-3-642-21449-3.
14. K. A. Khachatryan, Journal of Contemporary Mathematical Analysis **46**, 89–100 (2011).
15. M. T. Teryokhin, Bulletin of Russian Academy of Sciences of Natural Sciences **3**, 113–122 (2015).
16. S. N. Askhabov, "Nonlinear integral equations with potential type kernels on a segment," (Moscow, June 23–26, 2003) pp. 5–22.
17. A. Kerimbekov, Vestnik KRSU **16**, 23–26 (2016).

The Riemann-Hilbert Problem for First Order Elliptic Systems on the Plane in the Hardy Space

Alexandre Soldatov[a)]

Moscow Center of Fundamental and Applied Mathematics and Federal Research Center "Computer Science and Control" of RAS, 119333, Moscow, Russia

[a)]*Corresponding author: soldatov48@gmail.com*

Abstract. The Riemann-Hilbert problem for the first order elliptic system is considered in the Hardy-Smirnov space. This system is reduced to an equivalent Fredholm integral system on the boundary in the space L^p.

INTRODUCTION

Let D be a finite domain bounded by a smooth Lyapunov contour $\Gamma \in C^{1,\nu}, 0 < \nu < 1$, which is oriented positively with respect to D. Let all eigenvalues of a matrix $J \in \mathbb{C}^{l\times l}$ lie on the upper half-plane and $G(t)$ be Hölder continuous $l \times l-$ matrix- value function on Γ such that $\det G(t) \neq 0$ for all $t \in \Gamma$. Let us consider the Riemann -Hilbert problem

$$\frac{\partial \phi}{\partial y} - J\frac{\partial \phi}{\partial x} = 0, \quad z = x+iy \in D, \tag{1}$$

$$\mathrm{Re}\; G(t)\phi^+(t) = f(t), \quad t \in \Gamma. \tag{2}$$

The first order elliptic system (1) corresponds to the Cauchy-Riemann system for $J = i$. For Toeplitz matrix J, it was firstly investigated by A. Douglis [1] in the frame of so called hypercomplex numbers. Therefore, the solutions ϕ of the system (1) is called the function analytic in the Douglis sense or shortly Douglis analytic functions. It plays an important role for elliptic systems of second and high order [2, 3]. For general first order elliptic systems, the problem (2) was investigated by many authors [4, 5].

The solution $\phi = (\phi_1, \dots, \phi_l)$ of (1) is a real analytic function and in a neighborhood of each point $z_0 = x_0 + iy_0$, it expands in a generalized Taylor series

$$\phi(z) = \sum_{k=0}^{\infty} \frac{1}{k!}(z-z_0)_J^k \phi^{(k)}(z_0).$$

Here and below, we have accepted the notation $(x+iy)_J = x1 + yJ$, $x, y \in \mathbb{R}$; the writing $(dx+idy)_J = (dx)1 + (dy)J$ for the matrix differential has an analogous meaning.

MAIN RESULTS

We can introduce the generalized Cauchy type integral

$$(I\varphi)(z) = \frac{1}{2\pi i}\int_\Gamma (t-z)_J^{-1} dt_J \varphi(t), \quad z \in D,$$

which gives solutions of (1) and plays the same role as in the usual analytic theory. In particular under the same assumption as in the classical case $J = i$, we have the Cauchy formula $\phi = I\phi^+$ and the Sohotski-Plemel formula $2(I\varphi)^+ = \varphi + S\varphi$, where $S\varphi$ means the corresponding singular integral and the operator I is bounded $C^\mu(\Gamma) \to C^\mu(\overline{D}), 0 < \mu < \nu$.

Analogous to the case of usual analytic function, we can introduce the Hardy-Smirnov space $H^p(D)$ [6].

Theorem 1 *If $\phi \in H^p(D)$, $1 < p < \infty$, then there exist an angular boundary values $\phi^+(t)$ for almost all $t \in \Gamma$, the function ϕ^+ belongs to $L^p(\Gamma)$ and the Cauchy formula holds. Nevertheless the operator I is bounded $L^p(\Gamma) \to H^p(D)$. So we may consider the problem (1), (2) in $H^p(D)$.*

International Conference on Analysis and Applied Mathematics (ICAAM 2020)
AIP Conf. Proc. 2325, 020025-1–020025-3; https://doi.org/10.1063/5.0040860
Published by AIP Publishing. 978-0-7354-4069-2/$30.00

Theorem 2 *The homogeneous problem (1), (2) has a finite number linear independent solutions $\phi_i \in C^\mu(\overline{D})$, $1 \le i \le m$, in the class $H^p(D)$. There exists a finite number linear independent real vector-valued functions $g_i \in C^\mu(\Gamma)$, $1 \le i \le n$, such that the solvability of the inhomogeneous problem in this class is equivalent to orthogonality conditions*

$$(f, g_i) = \int_\Gamma f(t) g_i(t) d_1 t = 0, \quad 1 \le i \le m,$$

where $d_1 t$ denotes the arc lengths.

The index $æ = m - n$ of the problem is given by the formula

$$æ = -\frac{1}{\pi} \arg \det G(t)\big|_\Gamma + l.$$

The same theorem is also valued in infinite domain $D_1 = \mathbb{C} \setminus \overline{D}$ for the problem

$$\operatorname{Im} G(t) \Psi^-(t) = f(t), \quad t \in \Gamma,$$

in the class of Douglis analytic functions $\Psi \in H^p(D_1)$ disappearing on infinity. The corresponding formula of the index $æ_1 = m_1 - n_1$ of this problem is

$$æ_1 = \frac{1}{\pi} \arg \det G(t)\big|_\Gamma - l.$$

Let $\Psi_i, 1 \le i \le m_1$, and $g_i, 1 \le i \le n_1$, be the corresponding functions of this theorem.

Theorem 3 *(a) There exists a finite number linear independent real vector-valued functions $h_i \in C^\mu(\Gamma)$, $1 \le i \le m_1$, and linear independent Douglis analytic functions $H_i \in C^\mu(\overline{D})$, $1 \le i \le n_1$, such that*

$$(h_i, G\Psi_j^-) = \delta_{ij}, \quad 1 \le i, j \le m_1; \quad (\operatorname{Im} GH_i^+, g_j) = \delta_{ij}, \quad 1 \le i, j \le n_1.$$

(b) Each function $\phi \in H^p(D)$ can be uniquely represented by the form

$$\phi = I(G^{-1}\varphi) + \sum\nolimits_{i=1}^{n_1} H_i \xi_i, \quad \xi_i \in \mathbb{R}, \tag{3}$$

where real vector-valued function $\varphi \in L^p(\Gamma)$ satisfies the conditions

$$(\varphi, h_i) = 0, \quad 1 \le i \le m_1. \tag{4}$$

(c) If the function $\phi \in C^\mu(\overline{D})$, then the function $\varphi \in C^\mu(\Gamma)$ in (3).

This theorem is analogue of the corresponding result of N. I. Mushelishvili [7] for usual analytic functions. Using the representation (3) we can reduce the problem (1), (2) to the corresponding equivalent system of singular equations on Γ with respect to an unknown $(\varphi, \xi) \in L^p(\Gamma) \times \mathbb{R}^{n_1}$ satisfying (4). This system is the following:

$$\varphi + K\varphi + 2\sum\nolimits_{i=1}^{n_1} \operatorname{Re}(GH_i^+)\xi_i = 2f \tag{5}$$

with the singular integral operator

$$(K\varphi)(t_0) = \operatorname{Re}\left[\frac{1}{\pi}\int_\Gamma G(t_0)(t - t_0)_J^{-1} G^{-1}(t) dt_J \varphi(t)\right], \quad t_0 \in \Gamma.$$

Let $e(t) = e_1(t) + ie_2(t)$ is the unit tangent vector to Γ at the point t. Then we can represent this operator in the form

$$(K\varphi)(t_0) = \frac{1}{\pi}\int_\Gamma \frac{a(t_0, t)}{|t - t_0|}\varphi(t) d_1 t,$$

where

$$a(t_0, t) = \operatorname{Im}\left[G(t_0)\left(\frac{t - t_0}{|t - t_0|}\right)_J^{-1} e_J(t) G^{-1}(t_0)\right].$$

Lemma 4 *Let $\Gamma \in C^{1,\nu}$ and $G \in C^\nu(\Gamma)$. Then, $a \in C^\nu(\Gamma \times \Gamma)$ and $a(t,t) \equiv 0$.*

This lemma shows that the operator K is compact in the space $L^p(\Gamma)$. So, (4), (5) is the Fredholm integral system.

REFERENCES

1. A. Douglis, Comm. Pure Appl. Math. **6**, 259-289 (1953).
2. A. P. Soldatov, Mathematics of the USSR - Izvestiya **39(2)**, 1033-1061 (1992).
3. A. P. Soldatov, Journal of Mathematical Sciences **132(6)**, 827-882 (2006).
4. B. Bojarski, Ann. Polon. Math. **17**, 281-320 (1966) (in Russian).
5. R. P. Gilbert and J. L. Buchanan, *First Order Elliptic Systems: A Function Theoretic Approach* (Academic Press, 1983).
6. A. P. Soldatov, Doklady Mathematics **76(2)**, 660-664 (2007).
7. N. I. Mushelishvili, *Singular Integral Equations* (Noordhoff, Groningen, 1953).

The Convergence of Approximation Attractors to Attractors for Bingham Model with Periodical Boundary Conditions on Spatial Variables

Allaberen Ashyralyev,[1, 2, 3, a)] Victor Zvyagin,[4, b)] and Mikhail Turbin[4, c)]

[1)]*Department of Mathematics, Near East University, Nicosia, Mersin 10, Turkey*
[2)]*Peoples' Friendship University of Russia (RUDN University), Ul Miklukho Maklaya 6, Moscow 117198, Russian Federation*
[3)]*Institute of Mathematics and Mathematical Modeling, 050010, Almaty,Kazakhstan*
[4)]*Voronezh State University, Universitetskaya sq. 1, Voronezh, 394018, Russian Federation*

[a)]*Electronic mail: allaberen.ashyralyev@neu.edu.tr*
[b)]*Corresponding author: zvg_vsu@mail.ru*
[c)]*Electronic mail: mrmike@mail.ru*

Abstract. The work is devoted to the proof of the convergence of trajectory and global attractors of approximation problems to trajectory and global attractors of the Bingham model on the torus. For research, the theory of trajectory attractors of non-invariant trajectory spaces is used. Namely, the existence of attractors for the Bingham model on a torus, and the existence of attractors for the approximation problem is proved. Then it is shown that the attractors of the approximation problems converge to the attractors of the Bingham model in the sense of the Hausdorff semi-distance in corresponding metric spaces.

INTRODUCTION

The question of the attractor's existence is closely related to theorems on the existence of solutions. An effective method for studying the solvability of fluid dynamic problems and the existence of their attractors is the approximation-topological method. This method was proposed by V. G. Zvyagin and developed by him with his collaborators V. T. Dmitrienko, D. A. Vorotnikov, M. V. Turbin, A. V. Zvyagin and others (see, for example, [1, 2, 3, 4]). It consists of the fact that in the beginning the original initial-boundary-value problem is approximated by some problem with better topological properties. Then, based on the topological degree of completely continuous, or condensing vector fields, or mappings satisfying the alpha condition and a priori estimates of the solutions, the solvability of these approximation problems is established. Approximation equations contain approximation parameters, and these equations move into the original, unperturbed equations as the approximation parameter tends to zero. Once the solvability of the approximation problems is proved, the solvability of the original problem is established using the passage to the limit.

For the solutions to the original problem usually it is possible to obtain some estimates of the dissipative type. Based on them, the trajectory space is constructed, for which the existence of trajectory and global attractors of both the approximation problem and the original problem is proved. Approximation equations have usually more natural properties of continuous dependence of solutions on the right-hand side and initial conditions, i.e. for small changes in the initial conditions and the right-hand side of the equation, a small change in the set of solutions is obtained. The presence of this property makes it possible to apply various approximate methods to find attractors of approximation problems and to study their convergence to attractors of the original system. Such an approach can be useful for the approximate calculation of the attractors for the original problem.

The Bingham fluid motion model is used to describe the motion of visco-plastic media, such as various gels and suspensions. It has been studied in sufficient detail in terms of the solvability of various problems [5, 6, 7, 8, 9]. The next step in the investigation of this model is the study of the qualitative behavior of its solutions. In particular, the study of the behavior of the solutions for the system corresponding to this model at infinity (the existence of its attractors). The notion of the attractor is used to describe the behavior of systems at large time values. Often this behavior also characterizes the process itself, which leads to the relevance of the study of the attractors in the mathematical problems of modern fluid dynamics.

Attractors of the Bingham fluid motion model in the two-dimensional domain were studied by G. A. Seregin in [10]. However, in the three-dimensional case, it was previously not possible to study the attractors of this system. This is due to the fact that for investigation of this problem in the two-dimensional case, the classical theory was used, for which the necessary condition is the uniqueness of the solution to the considered problem. However, for the system of equations for the Bingham model in the three-dimensional case, the uniqueness of weak solutions is not proved yet (as

International Conference on Analysis and Applied Mathematics (ICAAM 2020)
AIP Conf. Proc. 2325, 020026-1–020026-6; https://doi.org/10.1063/5.0040373
Published by AIP Publishing. 978-0-7354-4069-2/$30.00

well as for the Navier-Stokes system). In the paper [11] for an autonomous situation, the existence of trajectory and global attractors in the three-dimensional case is proved under periodic conditions with respect to spatial variables. This was done on the base of the abstract theory of trajectory and global attractors of non-invariant trajectory spaces (see, for example, [1, 4]), in which the uniqueness of solutions is not required. In this paper, we prove the convergence of trajectory and global attractors for approximation problems to trajectory and global attractors of the autonomous Bingham model in the 2D and 3D cases with periodic conditions with respect to spatial variables.

NECESSARY CONCEPTS OF THE ATTRACTORS THEORY

We need some concepts from the theory of attractors for trajectory spaces, which will be given in the first paragraph of this section. In the second paragraph of this section, we also define the concept of convergence of trajectory and global attractors and present some abstract theorems.

Main Concepts of Trajectory Space Attractors Theory

Let E and E_0 be Banach spaces. Suppose that E is continuously embedded in E_0 and that E is reflexive.

Let $C(\mathbb{R}_+;E_0)$ be the space of continuous functions, defined on $\mathbb{R}_+ = [0,+\infty)$ and taking values in E_0. This space is a metric space.

The space $L_\infty(\mathbb{R}_+;E)$ consists of functions u defined almost everywhere on $\mathbb{R}_+$ and taking values in E, for which there is a number $\alpha(u)$ such that $\|u\|_E \leqslant \alpha(u)$ for almost all $t \in \mathbb{R}_+$. The space $L_\infty(\mathbb{R}_+;E)$ is Banach with respect to the norm $\|u\|_{L_\infty(\mathbb{R}_+;E)} = \mathrm{ess\,sup}_{t\in\mathbb{R}_+}\|u(t)\|_E$.

Definition 1 *Consider a nonempty set $\mathscr{H}^+ \subset C(\mathbb{R}_+;E_0)\cap L_\infty^{loc}(\mathbb{R}_+;E)$. The set $\mathscr{H}^+$ is called the trajectory space, and their elements are called trajectories.*

The following theorem takes place (see [12] for details).

Theorem 1 *Let E and E_0 be Banach spaces, and let E be continuously embedded in E_0. If a function u belongs to $L_\infty(0,M;E)$ and it is continuous as a function with values in E_0, then u is weakly continuous as a function with values in E.*

Corollary 1 *The functions of class $C(\mathbb{R}_+;E_0)\cap L_\infty(\mathbb{R}_+;E)$ are weakly continuous with values in E. In particular this implies that their values belong to E for all $t \in \mathbb{R}_+$.*

Consider the translation operators $\mathrm{T}(t)$ $(t \geqslant 0)$, which take a function f to the function $\mathrm{T}(t)f$ defined as follows $\mathrm{T}(t)f(s) = f(s+t)$. The operator $\mathrm{T}(t)$ is linear. It is bounded on $L_\infty(\mathbb{R}_+;E)$ and continuous on $C(\mathbb{R}_+;E_0)$, and there exists $C_t > 0$ such that the inequality $\|\mathrm{T}(t)u\|_{C(\mathbb{R}_+;E_0)} \leq C_t\|u\|_{C(\mathbb{R}_+;E_0)}$ holds for any $u \in C(\mathbb{R}_+;E_0)$.

It can be easily checked that $\mathrm{T}(t_1)\mathrm{T}(t_2) = \mathrm{T}(t_1+t_2)$ for any $t_1,t_2 \geqslant 0$, and that $\mathrm{T}(0)$ is the identity operator. For this reason the family of operators $\{\mathrm{T}(t)\}_{t\geqslant 0}$ is called the *translation semigroup*.

We do not assume the invariance of the space $\mathscr{H}^+$ with respect to the action of the translation semigroup $\{\mathrm{T}(t)\}_{t\geqslant 0}$, that is, the property $\mathrm{T}(t)\mathscr{H}^+ \subset \mathrm{T}(t)$. This condition turns out to be restrictive for applications of this theory in fluid dynamics problems.

Definition 2 *A nonempty set $\mathscr{U} \subset C(\mathbb{R}_+;E_0)\cap L_\infty(\mathbb{R}_+;E)$ is called a minimal trajectory attractor of the trajectory space $\mathscr{H}^+$, if it satisfies the following conditions:*

(i) *$\mathscr{U}$ is compact in $C(\mathbb{R}_+;E_0)$ and bounded in $L_\infty(\mathbb{R}_+;E)$;*

(ii) *the inclusion $\mathrm{T}(t)\mathscr{U} \subset \mathscr{U}$ holds for all $t \geqslant 0$;*

(iii) *$\mathscr{U}$ is an* attracting set, *i.e. for any nonempty set $B \subset \mathscr{H}^+$ bounded with respect to the norm of $L_\infty(\mathbb{R}_+;E)$ we have*

$$\sup_{u\in B}\inf_{v\in\mathscr{U}}\|\mathrm{T}(h)u-v\|_{C(\mathbb{R}_+;E_0)} \to 0 \quad \text{as } h\to\infty;$$

(iv) the set $\mathscr{U}$ is the least with respect to the inclusion, which satisfies conditions (i)–(iii).

Along with the minimal trajectory attractor of the trajectory space $\mathscr{H}^+$, we consider the global attractor of $\mathscr{H}^+$.

Definition 3 *A nonempty set $\mathscr{A} \subset E$ is called the global attractor (in E_0) of the trajectory space $\mathscr{H}^+$ if it satisfies the following conditions:*

(i) $\mathscr{A}$ is compact in E_0 and bounded in E;

(ii) for any nonempty set $B \subset \mathscr{H}^+$ bounded in $L_\infty(\mathbb{R}_+;E)$ the attraction condition *holds:*

$$\sup_{u\in B}\inf_{y\in\mathscr{A}} \|u(t)-y\|_{E_0} \to 0 \quad \text{as } t\to\infty;$$

(iii) $\mathscr{A}$ is contained in any nonempty set that satisfies (i) and (ii).

The concepts of the minimal trajectory attractor of the space $\mathscr{H}^+$ and the global attractor of this space are connected. Namely, the global attractor is a section of the minimum trajectory attractor.

For more details on the theory of attractors for trajectory spaces that do not have the invariance property with respect to the translation semigroup, see in [1, 4].

Convergence of Attractors

In this section we consider the convergence of attractors. Suppose we are given a family of trajectory spaces $\mathscr{H}^+_\lambda \subset C(\mathbb{R}_+;E_0)\cap L_\infty(\mathbb{R}_+;E)$ depending on a parameter λ that ranges over a metric space Λ. Further, suppose that each trajectory space $\mathscr{H}^+_\lambda$ has the minimal trajectory attractor $\mathscr{U}_\lambda$ and the global attractor $\mathscr{A}_\lambda$ (the latter is the section of the former, according to the general theory). We want to describe sufficient conditions for the convergence of $\mathscr{U}_\lambda$ to $\mathscr{U}_{\lambda_0}$ and the convergence of $\mathscr{A}_\lambda$ to $\mathscr{A}_{\lambda_0}$ as $\lambda\to\lambda_0$.

We consider the convergence in the sense of the Hausdorff semi-distance in corresponding metric spaces. Recall that the *Hausdorff semi-distance* from a set A to a set B in a metric space (X,d) is given by the formula

$$h_X(A,B) = \sup_{a\in A}\inf_{b\in B} d(a,b) \equiv \sup_{a\in A}\operatorname{dist}_X(a,B),$$

where $\operatorname{dist}_X(a,B)$ denotes the distance between a point a and a set B. In our case we consider the Hausdorff semi-distances $h_{C(\mathbb{R}_+;E_0)}$ in the space $C(\mathbb{R}_+;E_0)$ and h_{E_0} in the space E_0.

The following proposition offers a sufficient condition for minimal trajectory attractors to converge in the sense of the Hausdorff semi-distance.

Proposition 1 *Suppose that a trajectory space $\mathscr{H}^+_\lambda \subset C(\mathbb{R}_+;E_0)\cap L_\infty(\mathbb{R}_+;E)$ is assigned to every λ belonging to a metric space Λ. Suppose that each space $\mathscr{H}^+_\lambda$ has the minimal trajectory attractor $\mathscr{U}_\lambda$, which is contained in a set $P \subset C(\mathbb{R}_+;E_0)\cap L_\infty(\mathbb{R}_+;E)$, where P is relatively compact in $C(\mathbb{R}_+;E_0)$ and P does not depend on λ. Moreover, suppose that the following condition holds:*

(C) if $\lambda_m\to\lambda_0$, $u_m\in\mathscr{U}_{\lambda_m}$, and $u_m\to u_0$ in $C(\mathbb{R}_+;E_0)$, then $u_0\in\mathscr{U}_{\lambda_0}$.

Then the following limit relation holds

$$h_{C(\mathbb{R}_+;E_0)}(\mathscr{U}_\lambda,\mathscr{U}_{\lambda_0}) = \sup_{u\in\mathscr{U}_\lambda}\inf_{v\in\mathscr{U}_{\lambda_0}} \|u-v\|_{C(\mathbb{R}_+;E_0)} \to 0 \quad \text{as } \lambda\to\lambda_0. \tag{1}$$

The global attractor is a section of the minimal trajectory attractor. Hence, it is not hard to prove that the convergence of minimal trajectory attractors implies the convergence of the global ones. Namely, we have the following assertion.

Proposition 2 *Suppose that a trajectory space $\mathscr{H}^+_\lambda \subset C(\mathbb{R}_+;E_0)\cap L_\infty(\mathbb{R}_+;E)$ is assigned to every λ belonging to a metric space Λ. Suppose that each space $\mathscr{H}^+_\lambda$ possesses the minimal trajectory attractor $\mathscr{U}_\lambda$ and the global attractor $\mathscr{A}_\lambda = \mathscr{U}_\lambda(0)$, and suppose that* (1) *holds. Then the following limit relation holds*

$$h_{E_0}(\mathscr{A}_\lambda,\mathscr{A}_{\lambda_0}) = \sup_{u\in\mathscr{A}_\lambda}\inf_{v\in\mathscr{A}_{\lambda_0}} \|u-v\|_{E_0} \to 0 \quad \text{as } \lambda\to\lambda_0.$$

For more details see [13].

CONVERGENCE OF APPROXIMATION ATTRACTORS TO ATTRACTORS FOR BINGHAM MODEL

In this section, we apply abstract results on the convergence of attractors to the Bingham model.

Bingham Model

The motion of the fluid with constant density, which satisfies the Bingham rheological relation is described by the following system of equations

$$\frac{\partial v}{\partial t}+\sum_{i=1}^{n} v_i \frac{\partial v}{\partial x_i}-\operatorname{Div}\sigma+\operatorname{grad} p=f; \tag{2}$$

$$\operatorname{div} v=0; \tag{3}$$

$$\sigma=\begin{cases} 2\mu\mathscr{E}(v)+\tau^* \frac{\mathscr{E}(v)}{|\mathscr{E}(v)|} & \text{for } |\mathscr{E}(v)|\neq 0,\\ |\sigma|\leqslant\tau^* & \text{for } |\mathscr{E}(v)|=0.\end{cases} \tag{4}$$

Here, $v(x,t)$ and $p(x,t)$ are the velocity vector of the fluid particle and the fluid pressure at the point x in time t. $f(x)$ is the density of external forces at the point x (we suppose that the system is autonomous). $\sigma=(\sigma_{ij})$ is the deviator of the stress tensor; $\mathscr{E}(v)=\frac{1}{2}\left(\nabla v+(\nabla v)^T\right)$ is the strain rate tensor; μ and τ^* are some positive constants.

For system (2)-(4) we consider a periodic problem with respect to spatial variables with the initial condition:

$$v|_{t=0}(x)=a(x),\quad x\in\Omega. \tag{5}$$

In order to give a definition of a weak solution to the considered problem, we give the necessary notations. Let $\Omega=\prod_{i=1}^{n}(0,l_i)\subset\mathbb{R}^n,\ i=\overline{1,n}\ ,n=2,3$. By $(C^\infty_{per})^n$ we denote the space of periodic vector functions with values in $\mathbb{R}^n$ and with periods $l_i, i=\overline{1,n}$. Introduce the set $\Phi=\left\{\phi\in(C^\infty_{per})^n:\int\limits_\Omega\phi\,dx=0,\ \operatorname{div}\phi=0\right\}$. By V^0,V^1, and V^2 we denote the completion of Φ with respect to the norm of $L_2(\Omega)^n, W_2^1(\Omega)^n$, and $W_2^2(\Omega)^n$ respectively. Let $D(A)=V^2$. Let us consider on $D(A)$ the operator $Au=-\pi\Delta u$, where π is the Leray projector. It is possible to show that A is monotone linear self-adjoint operator. For every $\alpha\in\mathbb{R}$ we define A^α, with domain $D(A^\alpha)\subset V^0$. Denote $V^\alpha=D(A^{\alpha/2})$. It can be shown that the operator A is an isomorphism from $V^{\alpha+2}$ into V^α. A detailed definition of spaces, as well as their properties, can be found in [12].

For two matrices $A=(a_{ij}), B=(b_{ij})$ we set $A:B=\sum\limits_{i,j=1}^{n}a_{ij}b_{ij}$.

The results stated below are valid both in the two-dimensional and in the three-dimensional cases. But, since the three-dimensional case is more complicated, we will concentrate on it.

We introduce the following functional space:

$$W=\left\{u:u\in L_2(0,T;V^1)\cap L_\infty(0,T;V^0), u'\in L_2(0,T;V^{-2})\right\}$$

with the norm $\|u\|_W=\|u\|_{L_2(0,T;V^1)}+\|u\|_{L_\infty(0,T;V^0)}+\|u'\|_{L_2(0,T;V^{-2})}$.

Let $a\in V^1, f\in V^0$. We give a definition of a weak solution to the considered problem on a finite interval:

Definition 4 *A pair of functions $(v,\sigma), v\in W, \sigma\in L_2(Q_T)^{n^2}$, is a weak solution to periodic problem for the Bingham model* (2)-(5) *on the time segment $[0,T]$ if for any $\varphi\in V^2$ and almost all $t\in(0,T)$ is satisfies*

$$\langle v',\varphi\rangle-\sum_{i,j=1}^{3}\int\limits_\Omega v_i v_j\frac{\partial\varphi_i}{\partial x_j}dx+\int\limits_\Omega\sigma:\mathscr{E}(\varphi)dx=\int_\Omega f\varphi dx, \tag{6}$$

to rheological relation (4) *and initial condition:*

$$v(0)=a. \tag{7}$$

In the theory of attractors, we are primarily interested in the behavior of the velocity v at infinity. To describe this behavior, we define a weak solution to the Bingham problem on $\mathbb{R}_+$. In this case, we do not consider at infinity the behavior of σ, since it is determined by the behavior of v.

Definition 5 *A function $v \in L_{2,loc}(\mathbb{R}_+;V^1) \cap L_\infty(\mathbb{R}_+;V^0)$, for which there is a time derivative $v' \in L_{2,loc}(\mathbb{R}_+;V^{-2})$, is called a weak solution to Bingham problem* (2)-(5) *on $\mathbb{R}_+$, if for every $T > 0$, there exists $\sigma \in L_2(Q_T)^{n^2}$ such that the pair $(v|_{[0,T]},\ \sigma)$ is the weak solution to Bingham problem* (2)-(5) *on the time segment $[0,T]$.*

Approximation Problem

Consider the following approximation problem for Bingham problem (2)-(4):

$$\frac{\partial v}{\partial t} + \sum_{i=1}^{n} v_i \frac{\partial v}{\partial x_i} - \mathrm{Div}\left(2\mu\mathscr{E}(v) + \tau^* \frac{\mathscr{E}(v)}{\max\{\delta, |\mathscr{E}(v)|\}}\right) - \delta\Delta^3 v + \mathrm{grad}\, p = f; \tag{8}$$

$$\mathrm{div}\, v = 0; \tag{9}$$

$$v|_{t=0}(x) = a(x), \quad x \in \Omega. \tag{10}$$

Let us note that we exclude the unknown σ in the statement of the problem and consider the problem of only finding the velocity v. Let us give a definition of a solution to the approximation problem on a finite interval $[0,T]$. Let $f \in V^0, a \in V^1$.

Definition 6 *A function $v \in W_1 = \{v : v \in L_2(0,T;V^4), v' \in L_2(0,T;V^{-2})\}$ is a solution to approximation problem* (8)-(10) *if for all $\varphi \in V^2$ and almost all $t \in (0,T)$ it satisfies equality*

$$\langle v', \varphi\rangle + \mu \int_\Omega \nabla(v) : \nabla(\varphi)\, dx - \sum_{i,j=1}^{3} \int_\Omega v_i v_j \frac{\partial \varphi_j}{\partial x_i}\, dx + \tau^* \sum_{i,j=1}^{3} \int_\Omega \frac{\mathscr{E}_{ij}(v)\mathscr{E}_{ij}(\varphi)}{max\{\delta, |\mathscr{E}(v)|\}}\, dx + \delta \int_\Omega A^2 v A\varphi\, dx = \int_\Omega f\varphi dx, \tag{11}$$

and initial condition (7).

Definition 7 *A function $v \in L_{2,loc}(\mathbb{R}_+;V^4) \cap L_\infty(\mathbb{R}_+;V^1)$, for which there is a time derivative $v' \in L_{2,loc}(\mathbb{R}_+;V^{-2})$, is called a solution to approximation problem* (8)-(10) *on $\mathbb{R}_+$, if for every $T > 0$ the restriction $v|_{[0,T]}$ is the weak solution to approximation problem* (8)-(10) *on the time segment $[0,T]$.*

Main Result

Let us define trajectory spaces $\mathscr{H}_0^+$ for the original Bingham problem and $\mathscr{H}_\delta^+$ for the approximation problem.

Definition 8 *A function $v \in L_\infty(\mathbb{R}_+;V^0) \cap C(\mathbb{R}_+;V^{-1})$ is called a trajectory to Bingham problem* (2)-(5) *if it is a weak solution of problem* (2)-(5) *on $\mathbb{R}_+$ with certain $a \in V^1$ and satisfies the estimate*

$$\|v\|_{L_\infty(t,t+1;V^0)} + \|v\|_{L_2(t,t+1,V^1)} + \|v'\|_{L_2(t,t+1;V^{-2})} \leqslant R_0(1 + \|v\|^2_{L_\infty(0,1;V^0)} e^{-\alpha t})$$

for almost all $t \geqslant 0$. The set of trajectories is called the trajectory space and denoted $\mathscr{H}_0^+$.

Here R_0 is some positive constant from estimates on solutions to Bingham problem (2)-(5).

Definition 9 *The* trajectory space $\mathscr{H}_\delta^+$ *of approximation problem* (8),(10) *is the set that consists of solutions of approximation problem* (8)-(10) *on $\mathbb{R}_+$ with certain $a \in V^1$ that belong to $L_\infty(\mathbb{R}_+;V^0) \cap C(\mathbb{R}_+;V^{-1})$ and satisfy the estimate*

$$\|v\|_{L_\infty(t,t+1;V^0)} + \|v\|_{L_2(t,t+1,V^1)} + \|v'\|_{L_2(t,t+1;V^{-2})} \leqslant R_0(1 + \|v\|^2_{L_\infty(0,1;V^0)} e^{-\alpha t})$$

for almost all $t \geqslant 0$, as well as functions $\mathrm{T}(h)v$, where v is a solution of approximation problem (8)-(10) *on $\mathbb{R}_+$, $h \geqslant 0$ and $\mathrm{T}(h)v$ satisfy the estimate*

$$\|\mathrm{T}(h)v\|_{L_\infty(t,t+1;V^0)} + \|\mathrm{T}(h)v\|_{L_2(t,t+1,V^1)} + \|\mathrm{T}(h)v'\|_{L_2(t,t+1;V^{-2})} \leqslant R_0(1 + \|v\|^2_{L_\infty(0,1;V^0)} e^{-\alpha t})$$

for almost all $t \geqslant 0$.

The following two lemmas take place.

Lemma 1 *The trajectory space $\mathscr{H}_0^+$ has the minimal trajectory attractor $\mathscr{U}_0$.*

Lemma 2 *The trajectory space $\mathscr{H}_\delta^+$ ($\delta > 0$) has the minimal trajectory attractor $\mathscr{U}_\delta$.*

Theorem 2 *Minimal trajectory attractors $\mathscr{U}_\delta$ of approximation problem* (8)-(10) *converge to the minimal trajectory attractor $\mathscr{U}_0$ of the trajectory space $\mathscr{H}_0^+$ of Bingham problem* (2)-(5) *in the sense of the Hausdorff semi-distance in $C(\mathbb{R}_+;V^{-1})$, i. e.*

$$\sup_{u\in\mathscr{U}_\delta}\inf_{v\in\mathscr{U}_0}\|u-v\|_{C(\mathbb{R}_+;V^{-1})}\to 0 \quad \textit{as } \delta\to 0.$$

Global attractors $\mathscr{A}_\delta$ of approximation problem (8)-(10) *converge to the global attractor $\mathscr{A}_0$ of the trajectory space $\mathscr{H}_0^+$ of Bingham problem* (2)-(5) *in the sense of the Hausdorff semi-distance in the space V^{-1}, i. e.*

$$\sup_{y\in\mathscr{A}_\delta}\inf_{z\in\mathscr{A}_0}\|y-z\|_{V^{-1}}\to 0 \quad \textit{as } \delta\to 0.$$

ACKNOWLEDGMENTS

The work of the first author was financially supported by the Russian Foundation for Basic Research, grant No. 20-01-00051. The work of the second author was supported by the Ministry of Science and Higher Education (project FZGU-2020-0035).

REFERENCES

1. V. G. Zvyagin and D. A. Vorotnikov, *Topological Approximation Methods for Evolutionary Problems of Nonlinear Hydrodynamics* (Walter de Gruyter, 2008).
2. V. G. Zvyagin and M. V. Turbin, *Mathematical Problems in Viscoelastic Hydrodynamics* (Krasand URSS, Russia, 2012) (in Russian).
3. V. G. Zvyagin and M. V. Turbin, Journal of Mathematical Sciences **168**, 157–308 (2010).
4. V. G. Zvyagin and S. K. Kondrat'ev, Russian Mathematical Surveys **69(5)**, 845–913 (2014).
5. V. V. Shelukhin, "Bingham viscoplastic as a limit of non-newtonian fluids," Journal of Mathematical Fluid Mechanic **4**, 109–127 (2002).
6. G. Duvant and J. L. Lions, *Inequalities in Mechanics and Physics* (Springer-Verlag Berlin Heidelberg, 1976).
7. J. U. Kim, Transactions of the American Mathematical Society **304(2)**, 751–770 (1987).
8. V. G. Zvyagin and M. V. Turbin, Doklady Mathematics **99**, 140–142 (2019).
9. V. G. Zvyagin, A. V. Zvyagin, and M. V. Turbin, Journal of Mathematical Sciences **244**, 959–980 (2020).
10. G. A. Seregin, Journal of Mathematical Sciences **70**, 1806–1816 (1994).
11. V. G. Zvyagin and S. V. Kornev, Russian Mathematics **60**, 64–67 (2016).
12. R. Temam, *Infinite-Dimensional Dynamical Systems in Mechanics and Physics* (Springer-Verlag, 1997).
13. V. G. Zvyagin and S. K. Kondratyev, Journal of Fixed Point Theory and Applications **13(2)**, 359–395 (2013).
14. R. Temam, *Navier–Stokes Equations and Nonlinear Functional Analysis: Second Edition* (Society for Industrial and Applied Mathematics, 1995).

Performance-Enhancing of RSA Public Key via Three-Dimensional Hyperchaotic System

Nawras A. Alwan,[1, a)] Ahmed Y. Yousif,[2, b)] and Nadia M.G. Al-Saidi[1, c)]

[1)] *Department of Applied Sciences, University of Technology, Baghdad, Iraq*
[2)] *Information Technology Center, University of Technology, Baghdad, Iraq*

[a)] *Corresponding author: nawrasalwan@gmail.com*
[b)] *Electronic mail: ahmed.y.yousif@uotechnology.edu.iq*
[c)] *Electronic mail: nadia.m.ghanim@uotechnology.edu.iq*

Abstract. Every day the number of attacks increases to break the encryption algorithms. Therefore, it is considered necessary for designing a new algorithm with higher security. Any cryptographic system must have some fundamental features to resist any effective attack, preserve the transmitted information, and robust the statistical characteristics. This article aims to improve the RSA algorithm using a three-dimensional chaotic dynamic system with sophisticated attributes, which proposed for this purpose. It is derived from Memristive's and Sprott's chaotic systems. We call it a 3D-hyperchaotic Memristive Sprott system (3D-HMSS). This new system is adopted in generating keys for the RSA encryption algorithm. Some tests are used to show the efficiency of the proposed cryptosystem.

INTRODUCTION

As communication technology are rapidly developed, the needs for sophisticated techniques play a significant role to provide protection and confidentiality for the transmitted data. Cryptography is the science founded to protect the information and communication through using and developing of mathematical techniques to design hard algorithms against attacks. Several techniques have been presented to improve the traditional methods of encryption and decryption, some of them are based on the of open key space such as Chaos theory [1, 2, 3, 4, 5, 6, 7, 8, 9, 10, 11], Fractal theory [12, 13, 14, 15], and many other fast quantum algorithms. Recently, due to its complexity for producing of random sequences and satisfying of the principle of confusion and diffusion, the chaotic system is highly adopted in cryptography [7]. In this work, a new 3D- chaotic system is proposed we call 3D hyperchaotic Memristive Sprott system (3D-HMSS). It was used to generate pseudo random numbers generator (PRNG). As this generated sequence has high distribution, complex behavior and good ergodicity, it was used to improve the security of RSA cryptosystem. However, a new chaotic RSA (CRSA) system is proposed. The CRSA is applied to encrypt two different types of data, one is extracted from text message and the other from image. The experimental results shows the efficiency of the CRSA.

THE HYPERCHAOTIC MEMRISTIVE SPROTT SYSTEM (3D-HMSS)

In this section, the mathematical structure of the 3D-HMSS is introduced. It was extracted from Memristive [16] and Sprott [17] chaotic systems. This system's electrical circuit is designed to show its behavior, where its chaosity is demonstrated via some dynamical analysis.

Model Description

The description of the 3D-HMSS is given as follows:

$$\begin{aligned} \dot{x} &= b^2 - a(yz), \\ \dot{y} &= (5az+b)x+y, \\ \dot{z} &= y+c(zx), \end{aligned} \tag{1}$$

where x, y, z are state variables, and a, b, c are positive parameters. Figure 1 (a)-(b)shows the phase portrait, where the state variables of the system is (1,1,1), and the parameters are: (a) $a = 10.1, b = 9.2$, $c = 10.7$, and (b) $a = 20, b = 12.2$, $c = 15.7$, respectively.

International Conference on Analysis and Applied Mathematics (ICAAM 2020)
AIP Conf. Proc. 2325, 020027-1–020027-6; https://doi.org/10.1063/5.0040397
Published by AIP Publishing. 978-0-7354-4069-2/$30.00

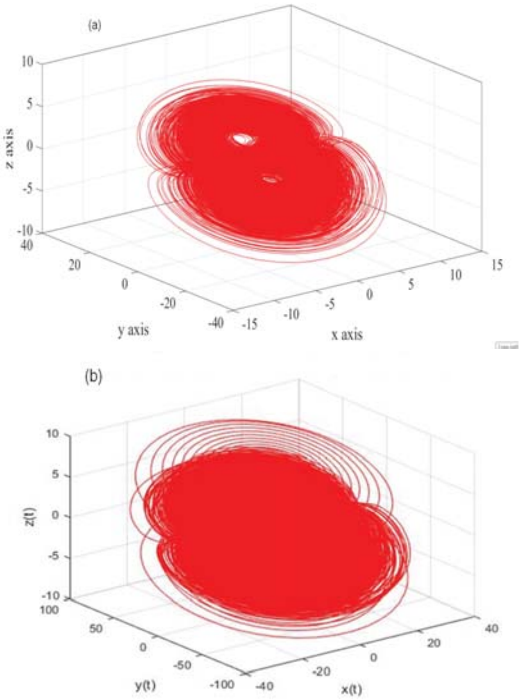

FIGURE 1. Phase portrait of (1) for the initial stats (1,1,1), and the parameters values of a,b and c are: (a) $a = 10.1, b = 9.2$, and $c = 10.7$, and (b) $a = 20, b = 12.2$, and $c = 15.7$, respectively.

Dynamical Analysis of the 3D-HMSS

Our system has several basic properties. First, it has symmetry under the coordinates transform $(x,y,z) \to (-x,-y,z)$, that is mean, the system is under reflection of the z-axis. Therefore, system (1) is symmetric and invariant based on the $z-$axis, which means that if $x = y = 0$ at $t = 0$, then $x = y = 0$ for all $t > 0$. When $t \to \infty$, the orbit tends to the origin on the z-axis. The dissipativity of the system is decided by $\nabla V = \frac{\partial \dot{x}}{\partial x} + \frac{\partial \dot{y}}{\partial y} + \frac{\partial \dot{z}}{\partial z} = 1 + cx;$, which satisfy $1 + cx > 0$. Therefore, it is dissipative, with an exponential contraction rate: $\frac{dV}{dt} = e^{(1+cx)}$. System(1) is a non-Hamiltonian conservative of phase volume, in which the volume element V_0 is contracted by the flow into a volume element $V_0 e^{(1+cx)t}$ in time t. Hence, each volume containing the system trajectory shrinks to zero as $t \to \infty$, and at an exponential rate $1 + cx$. The equilibria points of system (1) can be obtained by setting the right-hand side of (1) equals zero. The equilibria $\left(\frac{-b}{5a^2z^2+abz}, \frac{b^2}{az}, \frac{b^2}{c-5az}\right)$, and $\left(\frac{b}{5a^2z^2+abz}, -(\frac{b^2}{az}), -(\frac{b^2}{c-5az})\right)$ is obtained; where a, b, and $c > 0$. The characteristic equation is obtained from the Jacobian matrix that evaluated at $(x_0; y_0; z_0)$, such that:

$$\lambda^3 - m_1\lambda^2 + m_2\lambda + m_3 = 0, \tag{2}$$

where

$$\begin{aligned} m_1 &= cx + 1, \\ m_2 &= cx - 5ax + 5a^2z^2 + abz + aycz, \\ m_3 &= 5a^2z(cz^2 + y) + acz(x - y) + aby. \end{aligned} \tag{3}$$

One of the essential measures to describe the dynamic behavior is through the Lyapunov exponent's computing, which measures the rates of exponential convergence or divergence of adjacent trajectories of a given system. However, the Lyapunov exponents (LE) for the system (1) is shown in Figure 2.

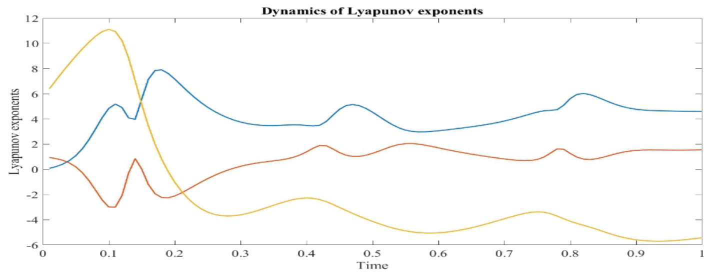

FIGURE 2. The LE of system (1) for the $(x_0, y_0, z_0) = (1, 1, 0.1)$, and $(a, b, c) = (10.1, 5.2, 5.7)$.

The Circuit Design of the 3D-HMSS

Designing the 3D-HMSS circuit using Matlab simulation is shown in Figure 3. The circuit of simulation made up of basic components from gain, add, product, and integrator. Initial values and parameters of (1) are assumed to be $(x_0, y_0, z_0) = (1, 1, 0.1)$, and $(a, b, c) = (1.1, 1.2, 1.2)$. Figure 4 (a,b, and c), shows the simulation results of the attractor of xy, xz, and yz, respectively.

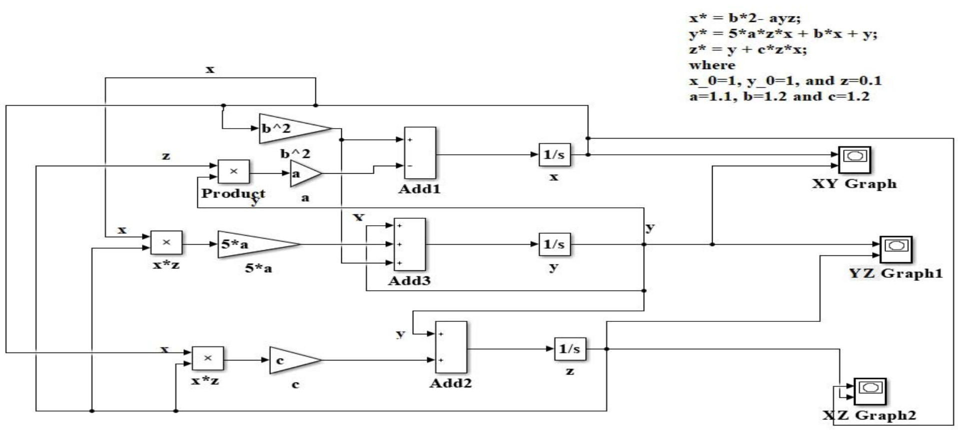

FIGURE 3. Matlab-Simulink Model of the 3D-HMSS

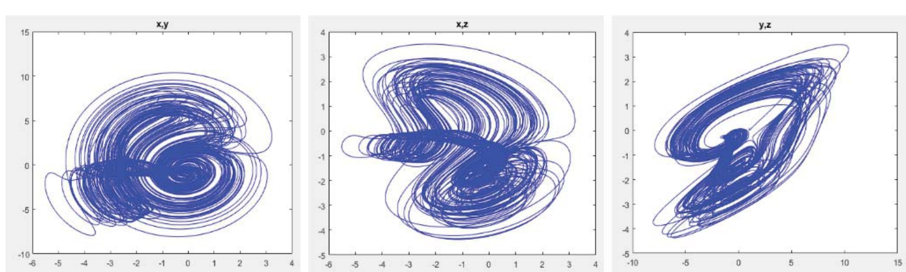

(a) xy phase portrait (b) xz phase portrait (c) yz phase portrait

FIGURE 4. Phase portraits (a) xy, (b) xz, (c) yz of 3D-HMSS

Pseudo-random Number Generator Based on the 3D-HMSS

Encryption is considered one of the processes that used chaotic systems for generating a pseudo-random number generator (PRNG). In this part, a new method to generate PRNG based on a 3D-HMSS has been designed. The NIST tests demonstrate the randomness properties in these sequences to be adopted in the encryption process. However, unlike the other current algorithms to generate PRNG, a new algorithm for generating PRNG is proposed based on the 3D-HMSS. It employs three chaotic attractors xy, xz, and yz with high performance in terms of sensitivity and complexity. It is illustrated in Algorithm 1.

Algorithm 1 PRNS based on 3D-HMSS

Input: The initial values $(x_0, y_0, z_0) = (1, 1, 1)$ of system (1) with the system parameters $(a, b, c) = (10.1, 9.2, 10.7)$.
Output: Three PRNG, namely, XY, XZ, and YZ;
1: Generate the chaotic sequences X, Y, and Z from system (1);
2: Generate Sequences $XY = X + Y$, $XZ = X + Z$, and $YZ = Y + Z$;
3: Convert the floating number XY, XZ, and YZ into a 32 -bit binary.

Additionally, we used NIST-800-22 [18] to assure that the three sequences are random. NIST-800-22 contains 16 different statistical tests. The statistical test results of the generated sequence are shown in Table 1. We select the initial values of the 3D-HMSS to be $(x_0, y_0, z_0) = (1, 1, 1)$, with the parameters $(a, b, c) = (10.1, 9.2, 10.7)$.

TABLE 1. The NIST-800-22 test result of the binary sequences XY, XZ, and YZ.

NIST statistical tests	XY	XZ	YZ	Result
Frequency Test	*0.8615*	*0.1032*	*0.7532*	*Passed*
Block-Frequency Test	*0.1621*	*0.4170*	*0.7325*	*Passed*
Cumulative-Sums Test	*0.9783*	*0.9451*	*0.1032*	*Passed*
Runs Test	*0.4715*	*0.6132*	*0.8319*	*Passed*
Longest-Run Test	*0.7351*	*0.4251*	*0.6322*	*Passed*
Binary Matrix Rank Test	*0.2107*	*0.7191*	*0.7613*	*Passed*
Discrete Fourier Transform Test	*0.5211*	*0.0332*	*0.1198*	*Passed*
Non-Overlapping Templates Test	*0.5315*	*0.4183*	*0.3386*	*Passed*
Overlapping, Templates Test	*0.658*	*0.8641*	*0.2297*	*Passed*
Maurers Universal Statistical Test	*0.1414*	*0.1978*	*0.2157*	*Passed*
Approximate Entropy Test	*0.0517*	*0.7387*	*0.7020*	*Passed*
Random-Excursions Test	*0.9737*	*0.8551*	*0.8211*	*Passed*
Random-Excursions Variant Test	*0.3176*	*0.4365*	*0.6422*	*Passed*
Serial Test-1	*0.2128*	*0.0452*	*0.5357*	*Passed*
Serial Test-2	*0.7131*	*0.6891*	*0.0769*	*Passed*
Linear-Complexity Test	*0.8513*	*0.3167*	*0.6652*	*Passed*

THE CHAOTIC RSA ALGORITHM

Basically, RSA depends on random choosing of two prime numbers p and q. The values n and $\varphi(n)$ are acquired by $p * q$, and $(p-1)*(q-1)$, respectively. a number e is chosen such that, $1 < e < \varphi(\mathrm{n}) \rightarrow \mathrm{gcd}(\mathrm{e}, \varphi(\mathrm{n})) = 1$, then its inverse d is calculated by $e^* d \equiv 1(\bmod \varphi(n))$, where $1 < d < \varphi(n)$. Here, *gcd* refers to the greatest common denominator. These steps represent the key generation phase in the RSA cryptosystem.
The diagram of the CRSA algorithm can be shown in Figure 5. The 3D-HMSS produces PRNG, which is used to develop the CRSA through generation the values of p and q by in Algorithm 1. The resulting sequences are XY, XZ, and YZ. The algorithm's resistance becomes more effective against the attacks when the values of p and q are significant. Algorithm 2 is designed to present the generation, the encryption, and the decryption process of CRSA.

Experimental Results

The proposed CRSA is implemented on two types of messages using Matlab programming language. The first step in the CRSA cryptosystem is generating the PRNG sequence, which is obtained using 3D-HMSS. The CRSA should be

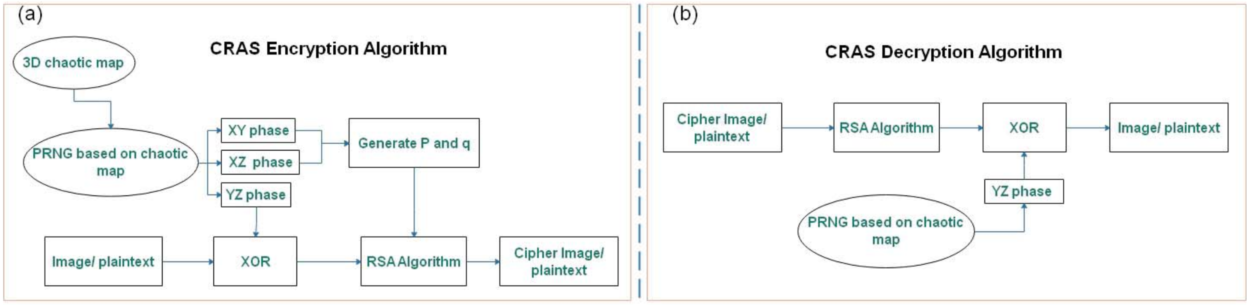

FIGURE 5. Chaotic RSA (a)encryption, (b) decryption

Algorithm 2 CRSA cryptosystem

Input: The Message M; (Original Text).
Output: The Cipher Text C;

KEY GENERATION

1: Use **Algorithm1** to generate p and q as a required size;
2: Compute n and $\varphi(n)$ where $n = p^*q, \varphi(n) = (p-1)^*(q-1)$;
3: Choose e, $1 < e < \varphi(\mathrm{n})$;
4: Compute d such that, $e^*d \equiv 1(\bmod \varphi(n))$;
5: **ENCRYPTION** $C = M^e(\bmod n)$;
6: **DECRYPTION** $M = C^d(\bmod n)$.

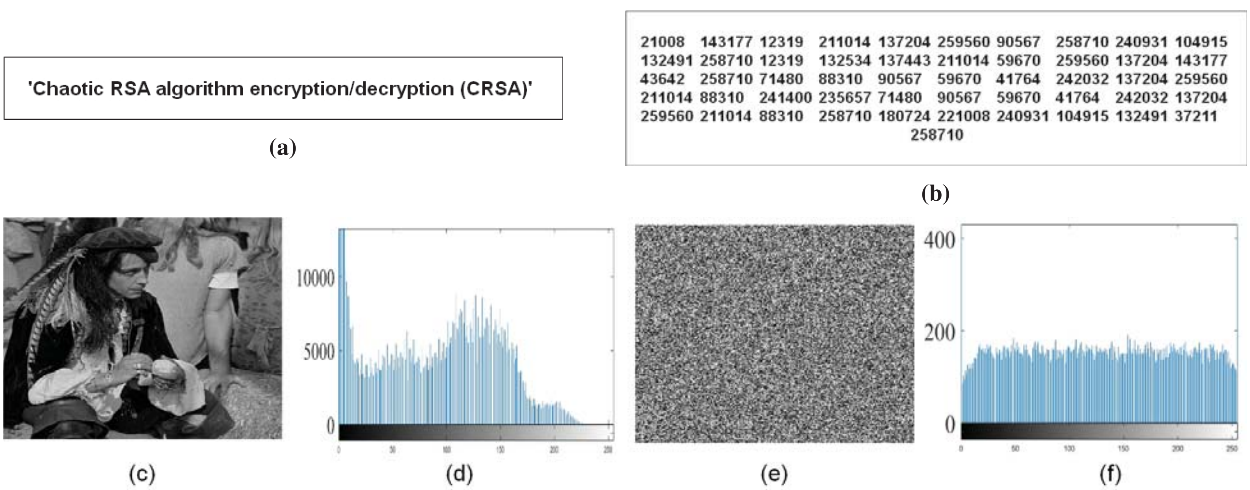

FIGURE 6. The CRSA (a) plaintext, and (b) Cipher of (a); (c) plain image; (d) histogram of (c); (e) encryption of (c); and (f) histogram of (e).

passed through three stages; the key generation, the encryption, and the decryption. To ensure a secure key generation, the sequences should pass the statistical test given in Table (1), to demonstrate the validity of the CRSA. The PRNG is used to assign the prime numbers p and q. In this experiment, we used 3D-HMSS to assign $p = 430201589$, and $q = 284007653$,. Therefore, the module $n = 122180543608760624$ and the value of Euler $\varphi = 122180543608760624$. Hence, the public key is $e = 2746063512000553$ and the private key is $d = 402440341770000$. These keys are used to encrypt two types of data; the plaintext given in Figure 6(a), and the gray image presented in Figure 6(c). The encryption stage is shown in Figure 6(b), and Figure 6(e) represent the cipher image. Before encrypted of the plaintext, it should be converted to a binary number; then, it is XOR'ed with a random series of bits YZ generated by PRNG. Regarding image encryption, it should be converted to binary numbers, then XOR'ed with the random series of bits YZ generated by PRNG. For the decryption stage, this part is generally the reverse operation of the CRSA algorithm.

CONCLUSION

In this paper, an efficient chaotic system (3D-HMSS) is introduced. It has been used to generate a robust PRNG sequence with random statistical features, as shown in Table (1) because, it passes the NIST. However, highly secure, chaotic keys are used to encrypt two types of data (text and image) by the RSA cryptosystem with an improved algorithm designed for this purpose.

REFERENCES

1. G. Makris and I. Antoniou, Cryptography with chaos, in: Proceedings of the 5th Chaotic Modeling and Simulation International Conference, Athens, Greece, 2012, pp. 12-15.
2. A. K. Farhan, R. S. Ali, H. R. Yassein, N. M. G. Al-Saidi, and G. H. Abdul-Majeed, The International Journal of Innovative Computing, Information and Control (IJICIC) **16(1)** (2020).
3. S. B. S. Al Maliky and N. A. Abbas, *Multidisciplinary Perspectives in Cryptology and Information Security* (IGI Global, 2014).
4. U. Cavusoglu, A. Akgul, A. Zengin, and I. Pehlivan, Chaos, Solitons and Fractals **104**, 655-667 (2017).
5. D. Younus, N. M. Al-Saidi, and W. K. Hamoudi, AIP Conference Proceedings **2183(1)**, 090006 (2019).
6. H. Natiq, M. R. M. Said, N. M. Al-Saidi, and A. Kilicman, Entropy **21(1)**, 34.
7. D. S. Ali, N. A. Alwan, and N. M. Al-Saidi, AIP Conference Proceedings **2183(1)**, 080007 (2019).
8. C. Shuai, Z. XianXin, and W. ZhengZhong, Science in China Series F-Information Sciences **51(8)**, 1055-1063 (2008).
9. L. Kocarev and G. Jakimoski, Physics Letters A **289(4-5)**, 199-206 (2001).
10. T. Xiao-Jun, W. Zhu, and Z. Ke, Chinese Physics B **21(2)**, 020506 (2012).
11. A. K. Farhan, R. S. Ali, H. Natiq, and N. M. Al-Saidi, IEEE Access **7**, 124914-124924 (2019).
12. N. M. Al-Saidi and M. R. Md Said, International Journal of Computer Mathematics **88(17)**, 3613-3625 (2011).
13. N. M. Al-Saidi and M. R. M. Said, The European Physical Journal Special Topics, Chaos, Cryptography and Communications **223(8)**, 1647–1662 (2014).
14. N. M. Al-Saidi, International Journal of Applied Mathematics and Informatics **6(4)**, 189-197 (2012).
15. N. M. Al-Saidi and M. R. Said, Journal of Mathematics and Statistics **5(3)**, 183 (2009).
16. H. M. Li, Y. F. Yang, Y. Zhou, C. L. Li, K. Qian, Z. Y. Li, and J. R. Du, Complexity **2019**, Article ID 4647608 (2019).
17. Z. Wei and Q. Yang, Nonlinear Dynamics **68(4)**, 543-554 (2012).
18. A. Rukhin, J. Soto, J. Nechvatal, M. Smid, and E. Barker, A statistical test suite for random and pseudorandom number generators for cryptographic applications, ITL Bulletin, Technical Report(National Institute of Standards and Technology, Gaithersburg, MD,2010), SP800-22; 2001, http://csrc.nist.gov/publications/PubsSPs.html#800-22.

Bright Soliton Solutions for Time Fractional Korteweg-de Vries Equation

Erdoğan Mehmet Özkan[a)] and Ayten Özkan[b)]

Yildiz Technical University, Department of Mathematics, Istanbul, Turkey.

[a)]*Corresponding author: mozkan@yildiz.edu.tr*
[b)]*Electronic mail: uayten@yildiz.edu.tr*

Abstract. In this work, He's semi-inverse variation method and the ansatz method with the modified Riemann-Liouville derivative are used to construct the exact solutions for time fractional Korteweg-de Vries (KdV) equation. The fractional KdV equation is transformed to another non-linear differential equation by travelling wave transformations and then these two methods are applied to find the solution.

INTRODUCTION

Many problems in science and engineering have been modelled by nonlinear partial differential equations. Obtaining the exact solutions of such equations is an important research area. Fractional differential equations (FDEs) have also attracted the attention of researchers in recent years. FDEs have been studied in the literature by researchers to obtain exact solutions with different techniques. In different research studies, several important methods have been used to investigate exact solutions such as the ansatz method, modified simple equation method, the extended trail equation, the first integral, the exp-function and the exp(-$\phi(\varepsilon)$) methods [1, 2, 3]. Some other techniques, like homotopy method [4, 5], generalized Kudryashov method [6, 7], modified Kudryashov and the sine-Gordon expansion approach [8, 9] have been made by some researchers, as well.
KdV equations have examined in a wide spectrum of material science facts as a model for the development and communication of nonlinear waves. The KdV equation was presented by Korteweg and de Vries to define shallow water waves of long wavelength. Afterwards, the KdV equations have also used in other physical situations such as collision-free hydro magnetic waves, stratified internal waves, particle acoustic waves, plasma physics, etc. [10, 11, 12, 13].

THE MODIFIED RIEMANN-LIOUVILLE DERIVATIVE AND METHODOLOGY OF SOLUTION

In [14], $f : R \to R,\ \omega \to f(\omega)$ as a continuous function (not necessarily differentiable), the Jumarie's modified Riemann-Liouville derivative (mRLd) of order α for a continuous function is defined as follows

$$D_\omega^\alpha f(\omega) = \begin{cases} \frac{1}{\Gamma(1-\alpha)} \frac{d}{d\omega} \int_0^\omega \frac{f(\tau)-f(0)}{(\omega-\tau)^\alpha} d\tau, & 0 < \alpha < 1, \\ (f^{(n)}(\omega))^{(\alpha-n)}, & n \le \alpha \le n+1,\ \ n \ge 1, \end{cases} \tag{1}$$

where $\Gamma(.)$ is the Gamma function. Moreover, some important properties of the fractional mRLd are listed as follows [15]:

$$D_\omega^\alpha \omega^\gamma = \frac{\Gamma(1+\gamma)}{\Gamma(1+\gamma-\alpha)}\ ,\gamma > 1, \tag{2}$$

$$D_\omega^\alpha (c) = 0, \tag{3}$$

$$D_\omega^\alpha (af(\omega)+bg(\omega)) = aD_\omega^\alpha f(\omega) + bD_\omega^\alpha g(\omega), \tag{4}$$

where $a \neq 0$, $b \neq 0$, and c are constants.

International Conference on Analysis and Applied Mathematics (ICAAM 2020)
AIP Conf. Proc. 2325, 020028-1–020028-5; https://doi.org/10.1063/5.0040280
Published by AIP Publishing. 978-0-7354-4069-2/$30.00

Now, we will take into account the following nonlinear time FDE of the type

$$H(u, D_t^{\alpha}u, u_x, D_{tt}^{2\alpha}u, u_{xx}, ...) = 0, \quad 0 < \alpha < 1, \tag{5}$$

where u is an unknown function, H is a polynomial of u and its partial fractional derivatives, and α is order of the mRLd of the function $u = u(x,t)$.
The traveling wave transformation is

$$\begin{aligned} &u(x,t) = U(\varepsilon), \\ &\varepsilon = kx - \frac{ct^{\alpha}}{\Gamma(1+\alpha)}, \end{aligned} \tag{6}$$

where $k \neq 0$ and $c \neq 0$ are constants. We use the chain rule

$$\begin{aligned} D_t^{\alpha}u = \sigma_t \frac{\partial U}{\partial \varepsilon} D_t^{\alpha}\varepsilon, \\ D_x^{\alpha}u = \sigma_x \frac{\partial U}{\partial \varepsilon} D_x^{\alpha}\varepsilon, \end{aligned} \tag{7}$$

with σ_t, σ_x are sigma indexes [16] and they can be $\sigma_t = \sigma_x = L$, where L is a constant.
Substituting (6), applying (2) and (7) to (5), we get the following nonlinear ordinary differential equation (ODE)

$$N(U, \frac{dU}{d\varepsilon}, \frac{d^2U}{d\varepsilon^2}, \frac{d^3U}{d\varepsilon^3}, ...) = 0. \tag{8}$$

HE'S SEMI-INVERSE METHOD

We now express He's semi-inverse method for the exact solution of nonlinear time fractional differential equations, established by Jabbari et al [17]. The method consists of the following steps:

1. First, let us convert the given Eq. (5) into Eq. (8) using the above operations.

2. If possible, integrate Eq. (8) term by term one or more times. This yields constant(s) of integration. For simplicity, the integration constant(s) can be set to zero.

3. According to the He's semi-inverse method, we construct the following trial functional

$$J(U) = \int L d\varepsilon \tag{9}$$

   where L is an unknown function of U and its derivatives.

4. By the Ritz method, we can obtain different forms of solitary wave solutions, such as

$$U(\varepsilon) = Asech(B\varepsilon), \;\; U(\varepsilon) = Acsch(B\varepsilon), \;\; U(\varepsilon) = Atanh(B\varepsilon), \;\; U(\varepsilon) = Acoth(B\varepsilon), \tag{10}$$

   and so on, where A and B are constants to be further determined. Substituting Eq.(10) into Eq. (9) and making J stationary with respect to A and B results in

$$\frac{\partial J}{\partial A} = 0, \quad \frac{\partial J}{\partial B} = 0. \tag{11}$$

   Solving system (11), we find A and B. So, the solitary wave solution (10) is well-determined.

APPLICATIONS

We consider the time fractional KdV equation of the form

$$D_t^{\alpha}u + au^2u_x + bu_{xxx} = 0, \quad (t > 0, \;\; 0 < \alpha \leq 1) \tag{12}$$

where a, b are constants [18]. The bright soliton solution will be applied to the solitary wave ansatz method. In order to solve Eq.(12), using the traveling wave transformation (6), we obtain

$$-cLU' + akU^2U' + bk^3U''' = 0.$$

Integrating with respect to ε once and setting the constants of integration to zero, we obtain

$$-cLU + \frac{ak}{3}U^3 + bk^3U'' = 0 \tag{13}$$

with $U' = \frac{dU}{d\varepsilon}$.

APPLICATION OF ANSATZ METHOD TO TIME FRACTIONAL KDV EQUATION

The Bright Soliton Solutions

For the bright soliton solutions, we consider the ansatz

$$U(\varepsilon) = A\text{sech}^p(\theta\varepsilon), \tag{14}$$

where

$$\varepsilon = kx - \frac{ct^{\alpha}}{\Gamma(1+\alpha)}, \tag{15}$$

A is the amplitude of the soliton, θ is the inverse width of the soliton and $p > 0$ for the solitons to exist. It follows from ansatz (14) and (15) that

$$\frac{d^2U}{d\varepsilon^2} = Ap^2\theta^2\text{sech}^p(\varepsilon) - Ap(p+1)\theta^2\text{sech}^{p+2}(\varepsilon), \tag{16}$$

and

$$U^3 = A^3\text{sech}^{3p}(\theta\varepsilon). \tag{17}$$

Substituting the ansatz (14)-(17) into (13), the following equation

$$-cLA\text{sech}^p(\theta\varepsilon) + \frac{ak}{3}A^3\text{sech}^{3p}(\theta\varepsilon) + bk^3\theta^2A\text{sech}^p(\theta\varepsilon) - bk^3\theta^2Ap(p+1)\text{sech}^{p+2}(\theta\varepsilon) = 0 \tag{18}$$

is obtained. From (18), we suppose that the powers $p+2$ and $3p$ are equal and from that p is determined as 1. Now comparing the different powers of $sech(\theta\varepsilon)$, we obtain the following system of algebraic equations

$$\begin{cases} \frac{ak}{3}A^3 - 2bk^3\theta^2A = 0, \\ -cLA + bk^3\theta^2A = 0. \end{cases}$$

Solving this system, we get

$$\begin{aligned}
A^{(1)} &= -\sqrt{\frac{6cL}{ak}}, \qquad \theta^{(1)} = -\sqrt{\frac{cL}{bk^3}}, \\
A^{(2)} &= -\sqrt{\frac{6cL}{ak}}, \qquad \theta^{(2)} = \sqrt{\frac{cL}{bk^3}}, \\
A^{(3)} &= \sqrt{\frac{6cL}{ak}}, \qquad \theta^{(3)} = -\sqrt{\frac{cL}{bk^3}}, \\
A^{(4)} &= \sqrt{\frac{6cL}{ak}}, \qquad \theta^{(4)} = \sqrt{\frac{cL}{bk^3}}.
\end{aligned} \tag{19}$$

Finally, we obtain the bright soliton solutions for the time fractional mKdV equation as follows

$$\begin{aligned}
u_1(x,t) &= -\sqrt{\frac{6cL}{ak}}\ \operatorname{sech}\Big[\Big(-\sqrt{\frac{cL}{bk^3}}\Big)\Big(kx-\frac{ct^\alpha}{\Gamma(1+\alpha)}\Big)\Big],\\
u_2(x,t) &= -\sqrt{\frac{6cL}{ak}}\ \operatorname{sech}\Big[\Big(\sqrt{\frac{cL}{bk^3}}\Big)\Big(kx-\frac{ct^\alpha}{\Gamma(1+\alpha)}\Big)\Big],\\
u_3(x,t) &= \sqrt{\frac{6cL}{ak}}\ \operatorname{sech}\Big[\Big(-\sqrt{\frac{cL}{bk^3}}\Big)\Big(kx-\frac{ct^\alpha}{\Gamma(1+\alpha)}\Big)\Big],\\
u_4(x,t) &= \sqrt{\frac{6cL}{ak}}\ \operatorname{sech}\Big[\Big(\sqrt{\frac{cL}{bk^3}}\Big)\Big(kx-\frac{ct^\alpha}{\Gamma(1+\alpha)}\Big)\Big].
\end{aligned} \tag{20}$$

Application of He's Semi-Inverse Method to Time Fractional KdV Equation

By He's semi-inverse principle [19, 20], from (13) the following variational formula

$$J=\int_0^\infty\Big(\frac{-bk^3}{2}(U')^2-\frac{cL}{2}U^2+\frac{ak}{12}U^4\Big)\,\mathrm{d}\varepsilon. \tag{21}$$

is derived. By a Ritz-like method, we look for a solitary wave solution in the following form

$$U(\varepsilon)=Asech(B\varepsilon), \tag{22}$$

where A and B are unknown constants to be determined later. Substituting Eq.(22) into Eq. (21), we have

$$J=\frac{-bk^3}{6}A^2B-\frac{cL}{2B}A^2+\frac{ak}{18B}A^4. \tag{23}$$

Making J stationary with A and B gives

$$\begin{aligned}
\frac{\partial J}{\partial A} &= \frac{-bk^3}{3}AB-\frac{cL}{B}A+\frac{2ak}{9B}A^3=0,\\
\frac{\partial J}{\partial B} &= \frac{-bk^3}{6}A^2+\frac{cL}{2B^2}A^2-\frac{ak}{18B^2}A^4=0.
\end{aligned} \tag{24}$$

From system (24), we obtain

$$A=\mp\sqrt{\frac{6cL}{ak}},\qquad B=\mp\sqrt{\frac{cL}{bk^3}}. \tag{25}$$

Using travelling wave transformation (6), we have the following bright soliton solutions of the fractional differential Eq.(12)

$$u(x,t)=\mp\sqrt{\frac{6cL}{ak}}\ \operatorname{sech}\Big[\Big(\mp\sqrt{\frac{cL}{bk^3}}\Big)\Big(kx-\frac{ct^\alpha}{\Gamma(1+\alpha)}\Big)\Big]. \tag{26}$$

CONCLUSION

In this study, He's semi-inverse variation method and the ansatz method are applied successfully for finding the bright soliton solutions of the nonlinear fractional KdV equation. It can be concluded from the results that these methods are convenient. Also, when we compare the results found by both methods, it is observed that they are same results. It is clear that other soliton solutions can be found with these methods.

REFERENCES

1. K. Hosseini, P. Mayeli, and R. Ansari, Waves Random Complex Medium **28(3)**, 426–434 (2018).
2. M. Ekici, M. Mirzazadeh, M. Eslami, Q. Zhou, S. Moshokoa, and A. Biswas, Optik **127(22)**, 10659—10669 (2016).
3. Y. Cenesiz, D.Baleanu, A. Kurt, and O.Tasbozan, Waves Random Complex Medium **27(1)**, 103—116 (2017).
4. A. Kurt, O.Tasbozan, and Y. Cenesiz, Bull. Math. Sci. Appl. **17**, 17–23 (2016).
5. O. Iyiola, O. Tasbozan, A. Kurt, and Y. Cenesiz, Chaos, Solitons and Fractals **94**, 1–7 (2017).
6. K. Hosseini, P. Mayeli, and D. Kumar, J. Mod. Opt. **65(3)**, 361—-364 (2018).
7. K. Hosseini, E. Bejarbaneh, A. Bekir, and M. Kaplan, Opt. Quantum Electron. **49(7)**, 241 (2017).
8. K. Hosseini, A. Bekir, M. Kaplan, and O. Guner, Opt. Quantum Electron. **49(11)**, 343 (2017).
9. O. Tasbozan, M. Senol, A. Kurt, and O. Ozkan, Ocean Engineering **161**, 62–68 (2018).
10. D. J. Korteweg and G. de Vries, Philosophical Magazine and Journal of Science **39(240)**, 422–443 (1895).
11. S. Fu, Z.and Liu and S. Liu, Physics Letters A **326(5)**, 364–374 (2004).
12. A. Wazwaz, Commun. Nonlinear Sci. Numer. Simul. **13(2)**, 331–339 (2008).
13. S. Ray, J. Math. Chem. **51(8)**, 2214—-2229 (2013).
14. G. Jumarie, Comput. Math. Appl. **51**, 1367–1376 (2006).
15. G. Jumarie, Appl. Maths. Lett. **22**, 378–385 (2009).
16. J. H. He, S. K. Elegan, and Z. B. Li, Physics Letters A **376**, 257–259 (2012).
17. A. Jabbari, H. Kheiri, and A. Bekir, Comput. Math. Appl. **62**, 2177–2186 (2011).
18. A. Zafar, Nonlinear Engineering **8**, 728—-732 (2019).
19. J. H. He, Int. J. Mod. Phys. B **20(10)**, 1141—-1199 (2006).
20. J. H. He, Chaos, Solitons and Fractals **19(4)**, 847—-851 (2004).

An Approximate Solution of First Derivatives of the Mixed Boundary Value Problem for Laplace's Equation on a Rectangle

Hediye Sarikaya[a)]

Department of Mathematics, Near East University, Nicosia, KKTC, Mersin 10, Turkey

[a)]*Corresponding author: hediye.sarikaya@neu.edu.tr*

Abstract. In a rectangular domain, we discuss about an approximation of the first order derivatives for the solution of the mixed boundary value problem. The boundary values on the sides of the rectangle are supposed to have the second order derivatives satisfying the Hölder condition. Under these conditions for the approximate values of the first derivatives of the solution of mixed boundary problem on a square grid, as the solution of the constructed difference scheme a uniform error estimation of order $O(h)$ (h is the grid size) is obtained. Numerical experiments are illustrated to support the theoretical results.

INTRODUCTION

Laplace equation is an important equation with many applications in engineering fields. The Laplace equation has numerical solutions that have been studied along with many boundary conditions, the most applicable of which is the mixed boundary condition problem. Many of these studies have used classical operators (see [1] and [2]). As well as the solution of the Laplace equation, the derivative of its solution has many applications (see [3]) and many of these solutions were obtained using classical operators (see [4]).

In this study, the mixed boundary value problem of Laplace equation is considered by using 5-point finite difference scheme on a rectangle. A second order finite-difference approximation on square grids is used to obtain numerical solution. The uniform convergence for the approximate solution at the rate of $O(h^2)$ and for the first derivative at the rate of $O(h)$ is proved when the exact solution u belongs to $\widetilde{C}^{2,\lambda}$.

FINITE DIFFERENCE APPROXIMATION

Let $\Pi = \{(x,y) : 0 < x < a, 0 < y < b\}$ be rectangle, a/b be rational, γ_j, $j = 1,2,3,4$, be the sides, including (excluding) the ends, enumerated counterclockwise starting from the side which location on the $x-$axis ($\gamma_0 \equiv \gamma_4, \gamma_1 \equiv \gamma_5$). Denote by s the arc length, measured along γ, and by s_j the value of s at the beginning of γ_j and by $\gamma = \bigcup_{j=1}^{4} \gamma_j$, the boundary of Π, by v_j a parameter taking the values 0 or 1, and $\overline{v}_j = 1 - v_j$.

We consider the following boundary value problem

$$\Delta u = 0 \text{ on } \Pi, \tag{1}$$

$$v_j u + \overline{v}_j u_n^{(1)} = v_j \varphi_j + \overline{v}_j \psi_j \text{ on } \gamma_j, \; j = 1,2,3,4, \tag{2}$$

where $u_n^{(1)}$ is the derivative along the inner normal, φ_j and ψ_j are given functions at the arc length taken along γ,

$$1 \leq \sum_{j=1}^{4} v_j \leq 4, \; v_1 = 1. \tag{3}$$

Definition 1 *We say that the solution u of the problem (1), (2) belongs to* $\widetilde{C}^{k,\lambda}(\overline{\Pi})$, *if*

$$v_j \varphi_j + \overline{v}_j \psi_j \in C^{k,\lambda}(\gamma_j), \; 0 < \lambda < 1, \; j = 1,2,3,4 \tag{4}$$

and at the vertices $A_j = \gamma_{j-1} \cap \gamma_j$ *the conjugation conditions*

$$v_j \varphi_j^{2q+\delta_{\tau-2}} + \overline{v}_j \psi_j^{2q+\delta_\tau} = (-1)^{q+\delta_\tau+\delta_{\tau-1}} (v_{j-1} \varphi_{j-1}^{2q+\delta_{\tau-1}} + \overline{v}_{j-1} \psi_{j-1}^{2q+\delta_\tau}) \tag{5}$$

International Conference on Analysis and Applied Mathematics (ICAAM 2020)
AIP Conf. Proc. 2325, 020029-1–020029-4; https://doi.org/10.1063/5.0040564
Published by AIP Publishing. 978-0-7354-4069-2/$30.00

are satisfied, except may be the case when $q = k/2$ *for* $\tau = 3$, *where* $\tau = \nu_{j-1} + 2\nu_j$, $\delta_w = 1$ *for* $w = 0$; $\delta_w = 0$ *for* $w \neq 0$, $q = 0, 1, ..., Q$, $Q = [(k - \delta_{\tau-1} - \delta_{\tau-2})/2] - \delta_\tau$.

Let $h > 0$, with $a/h \geq 2$, $b/h \geq 2$ be integers. We assign to Π^h a square net on Π, with step h, obtained by the lines $x, y = 0, h, 2h, ...$; γ_j^h be a set of nodes on the interior of γ_j, and let

$$\dot{\gamma}_j^h = \gamma_j \cap \gamma_{j+1},\ \gamma^h = \cup(\gamma_j^h \cup \dot{\gamma}_j^h),\ \overline{\Pi}^h = \Pi^h \cup \gamma^h.$$

Let the operators A, $\boldsymbol{K}$ and $\dot{\boldsymbol{K}}$ be defined as follows:

$$Au(x,y) = \frac{u(x+h,y) + u(x,y+h) + u(x-h,y) + u(x,y-h)}{4} \text{ on } \Pi^h, \tag{6}$$

$$\boldsymbol{K}u(x,y) = \frac{1}{2}u(x + h\sin\frac{j\pi}{2}, y - h\cos\frac{j\pi}{2}) + \frac{1}{4}\sum_{k=0}^{1} u(x + (-1)^k h\cos\frac{j\pi}{2}, y + (-1)^k h\sin\frac{j\pi}{2}) \text{ on } \gamma_j^h,\ j = 1,2,3,4, \tag{7}$$

and

$$\dot{\boldsymbol{K}}u(x,y) = \frac{1}{2}\sum_{k=0}^{1} u(x + h\sin\frac{(j+k)\pi}{2}, y - h\cos\frac{(j+k)\pi}{2}) \text{ on } \dot{\gamma}_j^h,\ j = 1,2,3,4. \tag{8}$$

We consider the classical 5-point finite difference approximations of the problem (1):

$$u_h = Au_h \text{ on } \Pi^h, \tag{9}$$

$$u_h = \nu_j\varphi_j + \bar{\nu}_j(\boldsymbol{K}u_h - \frac{h}{2}\psi_j) \text{ on } \gamma_j^h,\ j = 1,2,3,4, \tag{10}$$

$$u_h = \nu_j\varphi_j + \bar{\nu}_j\nu_{j+1}\varphi_{j+1} + \bar{\nu}_j\bar{\nu}_{j+1}(\dot{\boldsymbol{K}}u_h - \frac{h}{2}(\psi_j + \psi_{j+1})) \text{ on } \dot{\gamma}_j^h,\ j = 1,2,3,4. \tag{11}$$

The system of finite difference equations (9)-(11) which has nonnegative coefficients, with the condition (3) is uniquely solvable.

Theorem 1 *Let* u *the solution of problem (1), (2). If* $u \in \widetilde{C}^{2,\lambda}(\overline{\Pi})$ *the condition (3) holds, then*

$$\max_{\overline{\Pi}^h} |u_h - u| \leq ch^2,$$

where u_h *is the solution of the system (9)-(11).*

The proof of Theorem 1 follows from the Theorem 1 in [1].

APPROXIMATE OF THE FIRST DERIVATIVES

Let u be a solution of problem (1), (2). Let $v = \frac{\partial u}{\partial x}$ and let $\Phi_j = \frac{\partial u}{\partial x}$ on γ_j, $j = 1,2,3,4$, and consider the boundary value problem:

$$\Delta v = 0 \text{ on } \Pi,\ v = \Phi_j \text{ on } \gamma_j,\ j = 1,2,3,4. \tag{12}$$

We define the sets

$$\gamma_{(2^i-1)}^{h+} = \left\{0 \leq x \leq \frac{a}{2},\ y = b(i-1)\right\} \cap \gamma_{(2^i-1)}^h,\ i = 1,2 \tag{13}$$

and

$$\gamma^{h-}_{(2^i-1)} = \left\{\frac{a}{2}+h \le x \le a,\ y = b(i-1)\right\} \cap \gamma^{h}_{(2^i-1)},\ i = 1,2. \tag{14}$$

We define the following operator $\Phi_{ph},\ p = 1,2,3,4,$

$$\Phi_{(2^i-1)h}(u_h) = v_3\frac{\partial u(x,b(i-1))}{\partial x} + \overline{v}_3\frac{1}{h}[-u_h(x,b(i-1)) + u_h(x+h,b(i-1))] \text{ on } \gamma^{h+}_{(2^i-1)}, \tag{15}$$

$$\Phi_{(2^i-1)h}(u_h) = v_3\frac{\partial u(x,b(i-1))}{\partial x} + \overline{v}_3\frac{1}{h}[u_h(x,b(i-1)) - u_h(x-h,b(i-1))] \text{ on } \gamma^{h-}_{(2^i-1)}, \tag{16}$$

$$\Phi_{(2i)h}(u_h) = \overline{v}_{(2i)}\,\psi_{(2i)} + v_{(2i)}\frac{(-1)^{i+1}}{h}[\varphi_{(2i)}((2-i)a) - u_h((2-i)a + (-1)^i h, y)] \text{ on } \gamma^{h}_{(2i)}, \tag{17}$$

where $i = 1,2$ and u_h is the solution of the finite difference problem (9)-(11).
Let v_h be the solution of the following finite difference problem

$$v_h = Av_h \text{ on } \Pi_h,\ v_h = \Phi_{jh} \text{ on } \gamma^h_j,\ j = 1,2,3,4, \tag{18}$$

where Φ_{jh} , $j = 1,2,3,4$, are defined by (15)-(17).

Theorem 2 *The following estimation is true*

$$\max_{(x,y)\in\Pi^h}\left|v_h - \frac{\partial u}{\partial x}\right| \le ch,$$

where u is the solution of the problem (1), v_h is the solution of the finite difference problem (18).

Remark 1 *We have investigated approximations of the first derivative $\frac{\partial u}{\partial x}$. The same results are obtained for the derivative $\frac{\partial u}{\partial y}$, by using the same order forward and backward formulae in the corresponding sides of the rectangular domain.*

NUMERICAL EXAMPLES

Example 1 *Let $\Pi = \{(x,y) : 0 < x, y < 1\}$, and let γ be the boundary of Π. We consider the following problem :*

$$\Delta u = 0 \text{ on } \Pi,\ u = \varphi_j(x,y) \text{ on } \gamma_j,\ j = 1,2,3,\ u^{(1)} = \frac{\partial u(0,y)}{\partial x} = \psi_4(y) \text{ on } \gamma_4,$$

where

$$\varphi_j(x,y) = (x^2+y^2)^{\frac{61}{60}}\cos\left(\frac{61}{30}\arctan\left(\frac{y}{x}\right)\right) \text{ on } \gamma_j,\ j = 1,2,3,$$

and

$$\psi_4(y) = \frac{61}{30}y^{\frac{31}{30}}\sin\left(\frac{61\pi}{60}\right) \text{ on } \gamma_4.$$

Table 1 shows that the order of the solution of the problem given in Example 1 is $O(h^2)$ when the given Neumann condition on the left side and order of the first derivative $O(h)$ when used the first order backward numerical differentiation formula on the right side.

Example 2 *Let $\Pi = \{(x,y) : 0 < x, y < 1\}$, and let γ be the boundary of Π. We consider the following problem :*

$$\Delta u = 0 \text{ on } \Pi,\ u = \varphi(x,y) \text{ on } \gamma_j,\ j = 1,2,3,$$

$$u^{(1)} = \frac{\partial u(x,1)}{\partial y} = \psi_3(y) \text{ on } \gamma_3 \text{ and } u^{(1)} = \frac{\partial u(0,y)}{\partial x} = \psi_4(y) \text{ on } \gamma_4,$$

TABLE 1. The approximate results for the solution and first derivative when $\varphi \in C^{2,\frac{1}{30}}$

h	$\|u_h - u\|$	E_u^m	$\|v_h - v\|$	E_v^m
$\frac{1}{4}$	$3.224E-04$	3.631	$2.641E-01$	1.994
$\frac{1}{8}$	$8.878E-05$	3.879	$1.324E-01$	1.997
$\frac{1}{16}$	$2.289E-05$	3.988	$6.631E-02$	1.999
$\frac{1}{32}$	$5.739E-06$	4.032	$3.318E-02$	1.999
$\frac{1}{64}$	$1.423E-06$	4.040	$1.659E-02$	2.000
$\frac{1}{128}$	$3.523E-07$		$8.299E-03$	

where

$$\varphi_j(x,y) = (x^2+y^2)^{\frac{61}{60}} \cos\left(\frac{61}{30}\arctan\left(\frac{y}{x}\right)\right) \ on\ \gamma_j,\ j=1,2,3,$$

and

$$\psi_3(y) = -\frac{61}{30}\sqrt[60]{x^2+1}\left[x\sin(\frac{61}{30}\arctan(\frac{1}{x}) - \cos(\frac{61}{30}\arctan(\frac{1}{x}))\right] \ on\ \gamma_3,$$

$$\psi_4(y) = \frac{61}{30}y^{\frac{31}{30}}\sin\left(\frac{61\pi}{60}\right) \ on\ \gamma_4.$$

TABLE 2. The approximate results for the solution and first derivative when $\varphi \in C^{2,\frac{1}{30}}$

h	$\|u_h - u\|$	E_u^m	$\|v_h - v\|$	E_v^m
$\frac{1}{4}$	$7.404E-04$	3.999	$2.663E-01$	2.002
$\frac{1}{8}$	$1.851E-04$	4.007	$1.330E-01$	2.001
$\frac{1}{16}$	$4.621E-05$	4.006	$6.647E-02$	2.001
$\frac{1}{32}$	$1.153E-05$	4.004	$3.332E-02$	2.000
$\frac{1}{64}$	$2.881E-06$	4.002	$1.661E-02$	2.000
$\frac{1}{128}$	$7.199E-07$		$8.301E-03$	

Table 2 shows that the order of the solution of the problem given in Example 2 is $O(h^2)$ when the given Neumann condition on the left side and at the top sides and order of the first derivative $O(h)$ when used the first order forward and backward numerical differentiation formula on the right and up sides.

The results which illustrated in Table 1 and Table 2 are the numerical justification of Theorem 1 and Theorem 2.

In Table 1 and Table 2 we have used the following notations:

$\|U_h - U\|_{\overline{\Pi}^h} = \max_{\overline{\Pi}^h}|U_h - U|$ and $E_U^n = \frac{\|U-U_{2-n}\|_{\overline{\Pi}^h}}{\|U-U_{2-(n+1)}\|_{\overline{\Pi}^h}}$, where U be the trace of the exact solution of the continuous problem $\overline{\Pi}^h$, and U_h be its approximate values.

CONCLUSION

The proposed method can be used to obtain the derivative of the solution of the 3D Laplace equation with mixed boundary conditions.

REFERENCES

1. E. A. Volkov, Tr. Mat. Inst. Akad. Nauk SSSR **140**, 68-102 (1976) (English transl. Proc. Steklov Inst.Math. **140(1)**, 68-102 (1979)).
2. A. A. Dosiyev, International Journal of Pure and Applied Mathematics **7(2)**, 223-235 (2003).
3. J. Chmelfk and J. E. Barth, Charged-Particle Optics (vol. 2014 of Proc. SPIE, 2014).
4. A. A. Dosiyev and H. M. Sadeghi, Advances in Difference Equations **1**, 1-11 (2015).

On Strongly Uniformly Paracompact Spaces and Mappings

Meerim Zhanakunova[1, a)] and Bekbolot Kanetov[2, b)]

[1)] *Kuseyin Karasaev Bishkek Humanities University, Bishkek, Kyrgyz Republic*

[2)] *Jusup Balasagyn National University, Bishkek, Kyrgyz Republic*

[a)] *Electronic mail: aelin_jasmin@mail.ru*

[b)] *Corresponding author: bekbolot_kanetov@mail.ru*

Abstract. In this article we study strongly uniformly R-paracompact space and strongly uniformly R-paracompact mappings. In particular, the characterizations of strongly uniformly R-paracompact spaces by using Hausdorff compact extensions and finite additive coverings are obtained.

INTRODUCTION

Throughout this work all uniform spaces are assumed to be Hausdorff, mappings are uniformly continuous.

For coverings α and β of the set X, the symbol $\alpha \succ \beta$ means that the covering α is a refinement of the covering β, i.e. for any $A \in \alpha$ there exists $B \in \beta$ such that $A \subset B$ and, for coverings α and β of a set X, we have: $\alpha \wedge \beta = \{A \bigcap B : A \in \alpha, B \in \beta\}$. The covering α finitely additive if $\alpha^{\angle} = \alpha$, $\alpha^{\angle} = \{\bigcup \alpha_0 : \alpha_0 \subset \alpha \text{ is finite}\}$. $\alpha(x) = \bigcup St(\alpha, x)$, $St(\alpha, x) = \{A \in \alpha : A \ni x\}$, $x \in X$, $\alpha(H) = \bigcup St(\alpha, H)$, $St(\alpha, H) = \{A \in \alpha : A \bigcap H \neq \varnothing\}$, $H \subset X$.

A covering α of the uniform space (X,U) is called uniformly star finite if there exists a uniform covering $\beta \in U$ such that every $\alpha(B)$ meets α only for a finite number of elements of α; a covering α of the uniform space (X,U) is called uniformly locally finite if there exists a uniform covering $\beta \in U$ such that every $B \in \beta$ meets α only for a finite number of elements of α; the covering consisting of the union of countable number of (uniformly) locally finite families is called (uniformly) σ-locally finite; star finitely uniformly σ-locally finite coverings will be called uniformly σ-star finite; a uniform space (X,U) called uniformly R-paracompact, if every open covering has an open uniformly locally finite refinement [1]; a uniform space (X,U) called uniformly B-paracompact, if for each finitely additive open covering γ of (X,U) there exists such sequence uniform covering $\{\alpha_i : i \in N\} \subset U$, that following condition is realized: for each point $x \in X$ there exist such number $i \in N$ and $\Gamma \in \gamma$ that $\alpha_i(x) \subset \Gamma$ (*) [2]; a uniform space (X,U) called uniformly P-paracompact, if for each open cover γ of (X,U) there exists such sequence uniform covering $\{\alpha_i : i \in N\} \subset U$, that the condition (*) is realized [3]; a uniform space (X,U) is called strongly uniformly R-paracompact if every open covering has an open uniformly star finite refinement [2]; a uniform space (X,U) is called strongly uniformly B-paracompact if the space (X,U) is uniformly B-paracompact and (X,U) is strongly paracompact [5]; a uniform space (X,U) is called strongly uniformly P-paracompact if the space (X,U) is uniformly P-paracompact and (X,U) is strongly paracompact [5]; a uniform space (X,U) is called strongly uniformly paracompact, if every open cover of (X,U) has a uniformly σ-star finite open refinement [6].

A uniform space (X,U) is called uniformly B-Lindelöf, if it is both uniformly B-paracompact and $\aleph_0$-bounded [2]; a uniform space (X,U) is called $\aleph_0$-bounded if the uniformity U has a base consisting of countable coverings; a uniform space (X,U) is called uniformly A-Lindelöf, if for each open covering α exist a countable uniformly covering $\beta = \{B_n : n \in N\}$ and $\gamma \in U$ such that $\beta \succ \alpha^{\angle}$ and $\gamma(\bar{B}_n) \subset B_{n+1}$ for any $n \in N$ [7]; a uniform space (X,U) is called uniformly P- Lindelöf, if for each open cover γ of (X,U) there exists such sequence countable uniform covering $\{\alpha_i : i \in N\} \subset U$, that the condition (*) is realized [5]; a uniform space (X,U) is called uniformly R-Lindelöf, if it is both uniformly R-paracompact and $\aleph_0$-bounded; a uniformly continuous mapping $f : (X,U) \to (Y,V)$ of uniform space (X,U) onto a uniform space (Y,V) is called a precompact, if for each $\alpha \in U$ there exist a uniform covering $\beta \in V$ and finite uniform covering $\gamma \in U$, such that $f^{-1}\beta \wedge \gamma \succ \alpha$[2]; a uniformly continuous mapping $f : (X,U) \to (Y,V)$ of uniform space (X,U) onto a uniform space (Y,V) is called a uniformly perfect, if it is both precompact and perfect [2]; a uniformly continuous mapping $f : (X,U) \to (Y,V)$ of uniform space (X,U) onto a uniform space (Y,V) is called a uniformly open, if f maps each open uniform covering $\alpha \in U$ to an open uniform covering $f\alpha \in V$ [2]. For the uniformity U by τ_U we denote the topology generated by the uniformity and symbol U_X means the universal uniformity.

International Conference on Analysis and Applied Mathematics (ICAAM 2020)
AIP Conf. Proc. 2325, 020030-1–020030-5; https://doi.org/10.1063/5.0040268
Published by AIP Publishing. 978-0-7354-4069-2/$30.00

ON STRONGLY UNIFORMLY R-PARACOMPACT SPACES AND STRONGLY UNIFORMLY R-PARACOMPACT MAPPINGS

Let (X,U) be a uniform space.

Proposition 1 *If (X,U) is a strongly uniformly R-paracompact space then the topological space (X,τ_U) is strongly uniformly R-paracompact. Conversely, if (X,τ) is strongly paracompact then the uniform space (X,U_X) is strongly uniformly R-paracompact.*

Proof. Let α be an arbitrary open cover of the space (X,τ_U) . Then for the open covering α exists a uniformly star finite open covering β which is a refinement of it. Let $B\in\beta$ be an arbitrary set. Then exist $L\in\lambda$ such that $B\bigcap L\neq\varnothing$. Then $B\subset\beta(L)$ and the set $\beta(L)$ meets β only for a finite number of elements of β. Hence, β is star finite. Since the space (X,τ_U) is strongly uniformly R-paracompact. Consequently, the space (X,τ_U) is strongly paracompact.

Conversely, if (X,τ) be a strongly uniformly R-paracompact. Then the set of all open coverings forms a base of universal uniformity U_X of the space (X,τ). Thus, (X,U_X) is strongly uniformly R-paracompact.

Theorem 1 *A uniform space (X,U) is strongly uniformly R-paracompact if and only if every finitely additive open covering has an open uniformly star finite refinement.*

Proof. *Necessity*. Let (X,U) be a strongly uniformly R-paracompact space and α be an arbitrary finitely additive open covering of the space (X,U). Then exist uniformly star finite open covering β such that $\beta\succ\alpha$.

Sufficiency. Let α be an arbitrary open covering of the space (X,U). Then open covering $\alpha^{\angle}$ is finitely additive. Let β be an open uniformly star finite covering of the space (X,U) such that $\beta\succ\alpha^{\angle}$. For each $B\in\beta$ choose such $A^{\angle}\in\alpha^{\angle}$that $B\subset A^{\angle}$, where $A^{\angle}=\bigcup\limits_{i=1}^{n}A_i$, $A_i\in\alpha$, $i=1,2,...,n$. Denote $\beta_B=\{A_i\bigcap B: i=1,2,...,n\}$. Then β_B is an open uniformly star finite covering refined in the open covering α. Thus, (X,U) is strongly uniformly R-paracompact.

Theorem 2 *Any closed subspace uniform space (M,U_M) of a strongly uniformly R-paracompact space (X,U) is strongly uniformly R-paracompact.*

Proof. Let α_M be an arbitrary open covering of the subspace (M,U_M). Then there exits open family α of (X,U), such that $\alpha\wedge\{M\}=\alpha_M$. Denote $\beta=\{\alpha,X\backslash M\}$. Obviously the covering β is an open covering of the space (X,U). Then exist uniformly star finite open covering γ such that $\gamma\succ\beta$. Hence $\gamma_M\succ\alpha_M$. Then it is easy to check that γ_M is a uniformly star finite open covering of the space (M,U_M). Thus, (M,U_M) is strongly uniformly R-paracompact.

Theorem 3 *Let (X,U) be a uniform space and bX be a certain compact Hausdorff extension of the space (X,τ_U). A uniform space (X,U) is strongly uniformly R-paracompact if and only if for each compact $K\subset bX\backslash X$ there exist a uniformly star finite coverings α, such that $[A]_{bX}\bigcap K=\varnothing$ for any $A\in\alpha$.*

Proof. *Necessity*. Let (X,U) be a strongly uniformly R-paracompact space and $K\subset bX\backslash X$ be an arbitrary compact. Then for each point $x\in X$ there is a open neighborhood O_x of the bX, such that $[O_x]_{bX}\bigcap K=\varnothing$. Denote $\lambda=\{O_x\bigcap X: x\in X\}$. Obviously λ is open covering of the space (X,U). Let β be a uniformly star finite open covering of the space (X,U), refined in the covering λ, i.e. for any $B\in\beta$ there exists $O_x\bigcap X\in\lambda$ such that $B\subset O_x\bigcap X$. Then $[B]_{bX}\subset[O_x\bigcap X]_{bX}=[O_x]_{bX}$. Consequently, $[B]_{bX}\bigcap K=\varnothing$.

Sufficiency. Let α be an arbitrary finitely additive open covering of the space (X,U). Then for every $A\in\alpha$ exists open subsets $A\in\alpha$ of the bX such that $L_A\bigcap X=A$. Denote $K=bX\backslash\bigcup\{L_A: A\in\alpha\}$. Accordingly to the condition of the theorem, the exists a uniformly star finite coverings β, such that $[B]_{bX}\bigcap K=\varnothing$ for any $B\in\beta$. Since $[B]_{bX}$ is compact, there exist $L_{A_1},L_{A_2},...,L_{A_n}$ of the bX such that $[B]_{bX}\subset\bigcup\limits_{i=1}^{n}L_{A_i}$. Then $B\subset\bigcup\limits_{i=1}^{n}A_i$, $A_i\in\alpha$, $i=1,2,...,n$. Hence, $\alpha_i(x)\subset(\bigcup\limits_{j=1}^{k}L_j)\bigcap X$. By virtue of finitely additiveness of the coverings μ we have $(\bigcup\limits_{j=1}^{k}L_j)\bigcap X\in\mu$. Thus, the uniform space (X,U) is strongly uniformly R-paracompact.

Theorem 4 *A uniform space (X,U) is strongly uniformly R-paracompact if and only if uniform space (X,U) is uniformly R-paracompact and topological space (X,τ_U) is strongly paracompact.*

Proof. *Necessity*. The necessity is obvious.

Sufficiency. Let α be an arbitrary open covering of the space (X,U). By virtue of strongly paracompactness of uniform space (X,τ_U) there exist a open star finite coverings β, such that $\beta \succ \alpha$. Then exist an open uniformly locally finite covering γ refined in the covering β. The covering γ is uniformly locally finite, therefore exists a uniform covering $\lambda \in U$ such that every $L \in \lambda$ meets γ only for a finite number of elements of γ, i.e. the cardinality of the family $St(L,\gamma)$ is finite for each $L \in \lambda$. Let $L \in \lambda$ and $\Gamma \in St(L,\gamma)$. Since $\gamma \succ \beta$, then for any $\Gamma \in \gamma$ there exists $B \in \beta$ such that $\Gamma \subset B$. Due to the star finiteness of the covering β, it follows that the cardinality of the family $St(B,\beta)$ is finite for each $B \in \beta$ and even more so the cardinality of the family $St(\Gamma,\beta)$ is finite for each $\Gamma \in St(L,\gamma)$. Then the cardinality of the family $St(\gamma(L),\beta)$ is finite. Hence, the cardinality of the family $St(L,\beta)$ is finite for each $L \in \lambda$. Then it is easy to check that $St(\beta(L),\beta)$ is finite. Since, every $\beta(L)$ meets β only for a finite number of elements of β. Thus, the uniform space (X,U) is strongly uniformly R-paracompact.

Corollary 1 *Any compact uniform space (X,U) is strongly uniformly R-paracompact.*

Corollary 2 *Any uniformly locally compact uniform space (X,U) is strongly uniformly R-paracompact.*

Corollary 3 *Any uniformly R-paracompact and uniformly B-Lindelöf space (X,U) is strongly uniformly R-paracompact.*

Corollary 4 *Any uniformly R-Lindelöf space (X,U) is strongly uniformly R-paracompact.*

Corollary 5 *Any uniformly R-paracompact and uniformly A-Lindelöf space (X,U) is strongly uniformly R-paracompact.*

Corollary 6 *Any uniformly R-paracompact and uniformly P-Lindelöf space (X,U) is strongly uniformly R-paracompact.*

Corollary 7 *Any uniformly R-paracompact and strongly uniformly P-paracompact space (X,U) is strongly uniformly R-paracompact.*

Corollary 8 *Any uniformly R-Lindelöf space is strongly uniformly B-paracompact.*

Theorem 5 *Any strongly uniformly R-paracompact space is strongly uniformly B-paracompact.*

Proof. Let (X,U) be a strongly uniformly R-paracompact space. Then (X,U) is uniformly B-paracompact and its topological space (X,τ_U) is strongly paracompact. Thus, (X,U) is strongly uniformly B-paracompact.

Theorem 6 *Any strongly uniformly R-paracompact space is strongly uniformly paracompact.*

Proof. Let (X,U) be a strongly uniformly R-paracompact space. Then (X,U) is uniformly paracompact and its topological space (X,τ_U) is strongly paracompact. Thus, (X,U) is strongly uniformly paracompact.

Lemma 7 *A covering α of the uniform space (X,U) uniformly star finite if and only if it is uniformly locally finite and star finite.*

Proof. A uniformly locally finite follows directly from the definition of a uniformly star finite. Now let $A \in \alpha$ be an arbitrary element. Then exist $B \in \beta$ such that $A \bigcap B \neq \varnothing$. Then $A \subset \alpha(B)$ and the set $\alpha(B)$ meets α only for a finite number of elements of α. Hence, α is star finite. Conversely, let α be a uniformly locally finite and star finite covering. Then exists a uniform covering $\beta \in U$ such that every $B \in \beta$ meets α only for a finite number of elements of α i.e. exists $A_{i(B)} \in \alpha$ such that $B \subset \bigcup_{i=1}^{n} A_{i(B)}$. By virtue of the star finite of the covering α , every $A_{i(B)}$ meets α only for a finite number of elements of α. Then $\alpha(B)$ also meets α only for a finite number of elements of α. Thus, the covering α of the uniform space (X,U) uniformly star finite.

Lemma 1 imply the following.

Theorem 8 *A uniform space (X,U) is strongly uniformly R-paracompact if and only if every open covering has an open uniformly locally finite and star finite refinement.*

Lemma 1 and Theorem 2.3.9 [2, p. 155] imply the following theorem.

Theorem 9 *Let $f:(X,U) \to (Y,V)$ be a perfect mapping of a uniform space (X,U) onto a uniform space (Y,V). If (Y,V) is strongly uniformly R-paracompact space then the uniform space (X,U) is also strongly uniformly R-paracompact.*

Corollary 9 *Let $f:(X,U)\to(Y,V)$ be a uniformly perfect mapping of a uniform space (X,U) onto a uniform space (Y,V). If (Y,V) is strongly uniformly R-paracompact space then the uniform space (X,U) is also strongly uniformly R-paracompact.*

Proposition 2.2.15 [2, p. 145] and Exercise 5.3. H (d) [8, p. 487] imply the following theorem.

Theorem 10 *Let $f:(X,U)\to(Y,V)$ be a perfect uniformly open mapping of a uniform space (X,U) onto a uniform space (Y,V). If (X,U) is strongly uniformly R-paracompact space then the uniform space (Y,V) is also strongly uniformly R-paracompact.*

Definition 1 *A uniformly continuous mapping $f:(X,U)\to(Y,V)$ of a uniform space (X,U) onto a uniform space (Y,V) is said to be strongly uniformly R-paracompact, if for each open covering α of the space (X,U) there exist such open covering β of the space (Y,V) and uniformly star finite open covering α of the space (X,U), that the covering $f^{-1}\beta\wedge\alpha$ is refined in a covering λ;*

Proposition 2 *Let $f:(X,U)\to(Y,V)$ be a uniformly continuous mapping of a uniform space (X,U) onto a uniform space (Y,V). If (X,U) is strongly uniformly R-paracompact space then the uniformly continuous mapping f is strongly uniformly R-paracompact.*

Proof. Let (X,U) be a strongly uniformly R-paracompact space and λ be an arbitrary open covering. Then exist such uniformly star finite open covering γ of the space (X,U), that the covering α is refined in a open covering λ. For open covering β of the space (Y,V) we have the covering $f^{-1}\beta\wedge\alpha$ is refined in a covering λ. Consequently, the mapping f is strongly uniformly R-paracompact.

Proposition 3 *If uniformly continuous mapping $f:(X,U)\to(Y,V)$ of a uniform space (X,U) onto a uniform space (Y,V) , $Y=\{y\}$ is strongly uniformly R-paracompact, then the uniform space (X,U) is strongly uniformly R-paracompact.*

Proof. Let f be a strongly uniformly R-paracompact mappings and λ be an arbitrary open covering of the space (X,U). Then exists such open covering β of the space (Y,V) and uniformly star finite open covering α of the space (X,U), that the covering $f^{-1}\beta\wedge\alpha$ is refined in a covering λ. Since $Y=\{y\}$, then $f^{-1}\beta\wedge\alpha=\alpha$. Thus, (X,U) is strongly uniformly R-paracompact.

Lemma 11 *If α and β is uniformly star finite covering of the space (X,U), then covering $\alpha\wedge\beta$ is uniformly star finite covering of the space (X,U).*

Proof. Let α and β be a uniformly star finite covering of the space (X,U). We show the covering $\alpha\wedge\beta$ is also uniformly star finite covering of the space (X,U). Since the coverings α and β is uniformly star finite, there exists such uniform coverings $\mu\in U$ and $\eta\in U$, that $\alpha(M)\subset\bigcup\limits_{i=1}^{n}A_i$, $\beta(N)\subset\bigcup\limits_{j=1}^{m}B_j$, $M\in\mu$, $N\in\eta$. Note that $(\alpha\wedge\beta)(M\bigcap N)\subset\alpha(M)\bigcap\beta(N)\subset\bigcup\limits_{i=1}^{n}\bigcup\limits_{j=1}^{m}(A_i\bigcap B_j)$, $M\bigcap N\in\mu\wedge\eta$. Obviously, $\mu\wedge\eta$ is uniformly covering. Thus, the covering $\alpha\wedge\beta$ is uniformly star finite.

Lemma 12 *Let $f:(X,U)\to(Y,V)$ be a uniformly continuous mapping of a uniform space (X,U) onto a uniform space (Y,V). If β is uniformly star finite open covering of the space (Y,V), then $f^{-1}\beta$ is uniformly star finite open covering of the space (X,U).*

Proof. Let f be a uniformly continuous mapping and β be a uniformly star finite open covering of the space (Y,V). Then exist such uniform covering $\alpha\in V$, that $|St(\alpha(B),\beta)|$ is finite for all $B\in\beta$ i.e. for any $B\in\beta$ exist such elements $B_i\in\beta$, $i=1,2,...,n$, that $\alpha(B)\subset\bigcup\limits_{i=1}^{n}B_i$. Since f is a uniformly continuous mapping, then $f^{-1}\beta$ is open covering of the space $(X,U)$and $f^{-1}\alpha\in U$. Consequently, $f^{-1}\alpha(B)\subset\bigcup\limits_{i=1}^{n}f^{-1}B_i$, $f^{-1}B_i\in f^{-1}\beta$. Thus, the covering $f^{-1}\beta$ is uniformly star finite open covering of the space (X,U).

Theorem 13 *If f and (Y,V) is strongly uniformly R-paracompact, then the uniform space(X,U) is strongly uniformly R-paracompact.*

Proof. Let f and (Y,V) be a strongly uniformly R-paracompact and λ be an arbitrary open covering of the space (X,U). Then exist such open covering β of the space (Y,V) and uniformly star finite open covering α of the space (X,U), that the covering $f^{-1}\beta \wedge \alpha$ is refined in a covering λ. By virtue of the strongly uniformly R-paracompactness of the uniform space (Y,V) exist such uniformly star finite open covering β_0, that the covering β_0 is refined in a covering β. Obviously, $f^{-1}\beta_0 \wedge \alpha \succ f^{-1}\beta \wedge \alpha$. By virtue of Lemma 3 the open covering $f^{-1}\beta_0$ is uniformly star finite. Denote $f^{-1}\beta_0 \wedge \gamma = \delta$. By virtue of Lemma 2 the open covering δ is uniformly star finite. Hence, the space (X,U) is strongly uniformly R-paracompact.

REFERENCES

1. M. D. Rice, Proc. Amer. Math. Soc **62:2**, 359-362 (1977).
2. A. A. Borubaev, *Uniform Topology* (Ilim, Frunze, 2013) (in Russian).
3. D. Buhagiar and B. Pasynkov, Czech Math. J. **46(121)**, 577-586 (1996).
4. B. E. Kanetov, *Some Classes of Uniform Spaces and Uniformly Continuous Mappings* (Bishkek, 2013) (in Russian).
5. B. E. Kanetov and N. A. Baigazieva, AIP Conference Proc. **1997**, 020023 (2018).
6. B. E. Kanetov, D. E. Kanetova, and N. A. Baigazieva, On one property of uniform space, in: Internat. Conf. Topology Appl., Nafpactos, Greece, 2018, pp. 60.
7. L. V. Aparina, Trudy Mosk. Math. Obshestva **57**, 3-15 (1996) (in Russian).
8. R. Engelking, *General Topology* (Mir, Moscow, 1986) (in Russian).

Effective Reproduction Number for North Cyprus Fighting Covid-19

Bilgen Kaymakamzade,[1,2,a)] Evren Hincal,[1,2,b)] Umar T. Mustapha,[1,c)] and Nezihal Gokbulut[1,2,d)]

[1)] *Department of Mathematics, Near East University, Nicosia, Mersin 10, Turkey*
[2)] *Mathematics Research Center, Near East University, Nicosia, Mersin 10, Turkey*

[a)] *Corresponding author: bilgen.kaymakamzade@neu.edu.tr*
[b)] *Electronic mail: evren.hincal@neu.edu.tr*
[c)] *Electronic mail: umartasiumustapha@yahoo.com*
[d)] *Electronic mail: nezihal.gokbulut@neu.edu.tr*

Abstract. The aim of this paper is to show how North Cyprus fights Covid-19 by using the basic reproduction number R_0 and effective reproduction number R_t. According to the Wikipedia page with title Covid-19 pandemic in Northern Cyprus, North Cyprus is the first country in Europe to free from Covid-19. One of the important reasons of this is that the government decided for tackling Covid-19 pandemic by using R_0 and R_t daily. For R_0, we constructed a new SEIR model by using the real data for North Cyprus. From March 11, 2020 to May 15, 2020 R_0, varies from 0.65 to 2.38.

INTRODUCTION

Cyprus is the third largest island located in the Mediterranean region. In the North side of Cyprus, the population is approximately 374 000, and consists mainly of Turkish Cypriots [1, 2]. In Northern Cyprus, the SARS-CoV-2 outbreak started with patient zero on March 9, 2020 [3]. SARS-CoV-2 entered the Northern Cyprus through the routes of Germany and England [4, 5]. We constructed a new SEIR model in order to calculate R_0 and R_t by using the real data for North Cyprus [6].

The basic reproduction number can be defined as the number of cases which are expected to occur on average in a homogeneous population as a result of infection by a single individual. While calculating the basic reproduction number of an infectious disease, the whole population is assumed to be susceptible. The effective reproduction number, R_t, also denoted by R_e, is the number of people in a population who can be infected by an individual at any specific time. The effective reproduction number can be calculated in two ways. We can either use exposed individuals or we can check herd immunity idea. It changes as the population becomes increasingly immunized, either by individual immunity following infection or by vaccination, and also as people die [7, 8].

On May 15, 2020, total of 30,025 tests have been conducted resulting in 108 Covid-19 positive cases in Northern Cyprus, of whom zero patient under treatment. There is no individuals are under quarantine for 26 days due to the risk of carrying the Covid-19, 104 have recovered and 4 deaths have occurred [6].

In this paper, we compare values of R_0 and R_t, as herd immunity, in North Cyprus and by analyzing both we try to find which could be the best parameter for fighting Covid-19 .

THE BASIC REPRODUCTION NUMBER AND EFFECTIVE REPRODUCTION NUMBER

In order to calculate the basic reproduction number in North Cyprus we use the basic SEIR model where S is susceptible, E is expose, I is infected and R is recovery compartment. Herd immunity R_t will be calculated as

$$R_t = 1 - \frac{1}{R_0}. \tag{1}$$

By using the SEIR model,

International Conference on Analysis and Applied Mathematics (ICAAM 2020)
AIP Conf. Proc. 2325, 020031-1–020031-4; https://doi.org/10.1063/5.0040307
Published by AIP Publishing. 978-0-7354-4069-2/$30.00

$$
\begin{cases}
\frac{dS}{dt} = \Pi - \lambda S, \\
\frac{dE}{dt} = \lambda S - (\theta_1 + \theta_2)E, \\
\frac{dQ}{dt} = \theta_1 E - (\delta_1 + \theta_3)Q, \\
\frac{dI_1}{dt} = \theta_2 E + \theta_3 Q - (\delta_2 + \omega + \theta_4 + \alpha_1)I_1, \\
\frac{dI_2}{dt} = \theta_4 I_1 - (\Phi + \alpha_2 + \delta_3)I_2, \\
\frac{dH}{dt} = \omega I_1 + \Phi I_2 - (\delta_4 + \alpha_3)H, \\
\frac{dR}{dt} = \delta_1 Q + \delta_2 I_1 + \delta_3 I_2 + \delta_4 H,
\end{cases}
$$

we calculated R_0 for North Cyprus, where the parameters are given in Table 1 and Table 2. For R_0, we have the following formula

$$
R_0 = \frac{(((b_1 \beta \tau_1 + \beta \tau_2 \theta_3)\,\theta_1 + \beta \tau_2 k_2 \theta_2)\,k_3 + \omega \beta \tau_4\,(\theta_2 k_2 + \theta_3 \theta_1))\,b_2 + \theta_4\,(\beta \tau_4 \varphi + \beta \tau_3 k_3)\,(\theta_2 k_2 + \theta_3 \theta_1)}{k_1 k_2 k_3 b_1 b_2}, \tag{2}
$$

where

$$
k_1 = \theta_1 + \theta_2, k_2 = \delta_1 + \theta_3, k_3 = \delta_4 + \alpha_3, b_1 = \delta_2 + \omega + \theta_4 + \alpha_1, and b_2 = \varphi + \alpha_2 + \delta_3. \tag{3}
$$

R_0 and R_t values for North Cyprus are given in the Figure 1 and Figure 2.

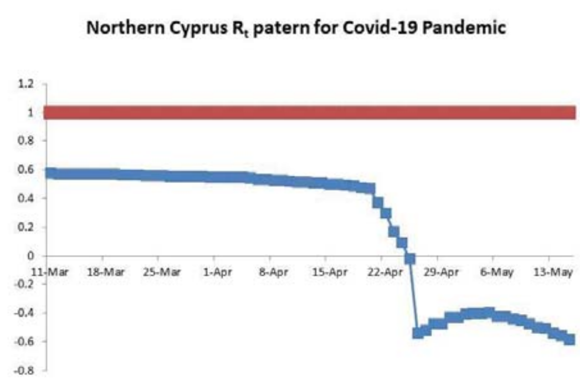

FIGURE 1. R_t values from March 11, 2020 to May 15, 2020.

TABLE 1. Variables for the model

Variables	Descriptions
N	Total population of humans
S	Susceptible humans at the risk of having COVID-19 infection
E	Exposed humans
I_1	Infected humans with moderate infection
I_2	Infected humans with severe infection
Q	Human population under quarantine and isolation
H	Hospitalized humans
R	Recovered humans

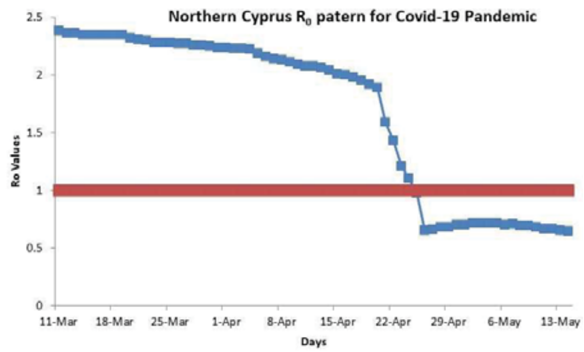

FIGURE 2. R_0 values from March 11, 2020 to May 15, 2020.

TABLE 2. Parameters for the model and basic reproduction number

Parameters	Descriptions
π	Recruitment rate
β	Transmission rate
τ_i (i=1,2,3,4)	Parameters for increase or decrease on infectiousness in humans
θ_i (i=1,2,3,4)	Progression rates
ω	Hospitalization rate from I_1 class
ϕ	Hospitalization rate from I_2 class
α_i (i=1,2,3)	Disease induced death rates
δ_i	Recovery rates

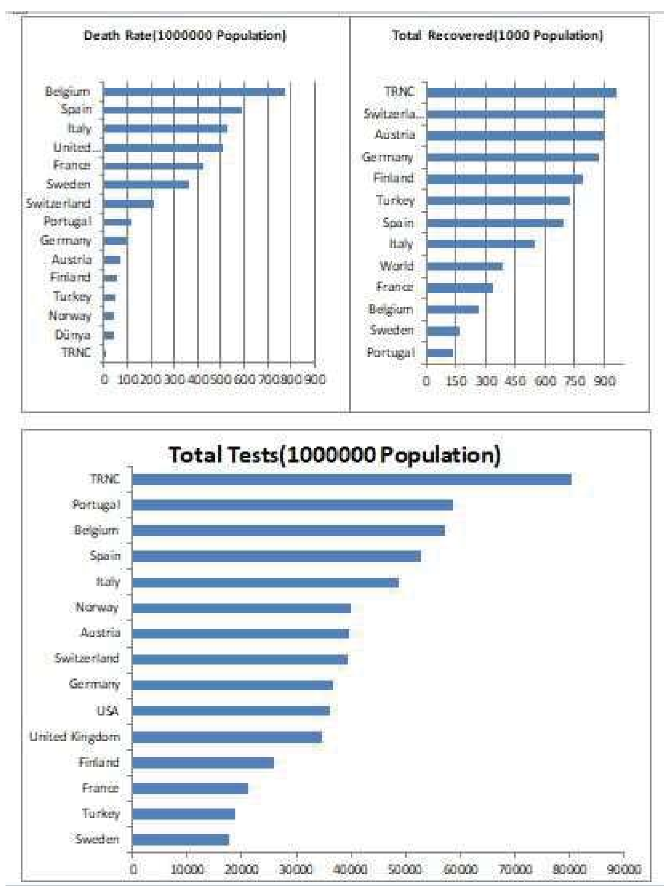

FIGURE 3. North Cyprus and comparison with most crowded countries and world data between March 11, 2020 - May 15, 2020

CONCLUSION

North Cyprus is the first European Country which reached zero Covid-19 cases in 37 days, from March 10, 2020 to April 17, 2020 [9, 10]. We can see that the North Cyprus has the lowest death rate and highest recovery in Europe compare to the other most severe countries in European countries Figure 3.

Between April 17, 2020 - July 1, 2020, no new Covid-19 cases has seen in North Cyprus. In total test with 80,000 tests is the leading country in the Europe between the dates March 11, 2020 - May 15, 2020 Figure 3. North Cyprus SARS-CoV-2 tackling compared with the other European countries. Finally, we have monitored Covid-19 pandemic in North Cyprus with SEIR model R_0 and R_t herd immunity. In North Cyprus R_0 is more effective than R_t, since we don't have enough immune people in North Cyprus. However, we cannot generalize this result.

REFERENCES

1. TRNC State planning Organization - Main site, http://www.devplan.org (accessed 4 April, 2020)
2. N. Kliot and Y. Mansfield, Political Geography **16**, 495–521 (1997).
3. Turkish Republic of Northern Cyprus Ministry of Health, http://saglik.gov.ct.tr/Haberler/DUYURULAR/ArtMID/32470/ArticleID/123665 (accessed 15 May, 2020).
4. Turkish Republic of Northern Cyprus Ministry of Health, http://saglik.gov.ct.tr/Haberler/DUYURULAR/ArtMID/32470/ArticleID/123702 (accessed 15 May, 2020).
5. Turkish Republic of Northern Cyprus Ministry of Health, http://saglik.gov.ct.tr/Haberler/DUYURULAR/ArtMID/32470/ArticleID/124273 (accessed 15 May, 2020).
6. Turkish Republic of Northern Cyprus Ministry of Health, http://saglik.gov.ct.tr (accessed 15 May, 2020).
7. C. P. Farrington and H. J. Whitaker, Biostatistics **4**, 621–632 (2003).
8. H. Nishiura and G. Chowel, Mathematical and Statistical Estimation Approaches in Epidemiology, 103–121 (2009).
9. Covid-19 coronavirus pandemic, http://www.worldometers.info/coronavirus (accessed 19 May, 2020).
10. Coronavirus disease (COVID-19) pandemic, http://www.who.int/emergencies/diseases/novel-coronavirus-2019 (accessed 19 May, 2020).

On the Stability of Second Order of Accuracy Difference Scheme for the Numerical Solution of the Time Delay Telegraph Equation

Allaberen Ashyralyev,[1, 2, 3, a)] Deniz Agirseven,[4, b)] and Koray Turk[4, c)]

[1)] *Department of Mathematics, Near East University, Nicosia, TRNC, Mersin 10, Turkey*
[2)] *Peoples' Friendship University of Russia (RUDN University), 6 Miklukho-Maklaya St, Moscow, 117198, Russian Federation*
[3)] *Institute of Mathematics and Mathematical Modeling, 050010, Almaty, Kazakhstan*
[4)] *Department of Mathematics, Trakya University, Edirne, Turkey*

[a)] *Electronic mail: allaberen.ashyralyev@neu.edu.tr*
[b)] *Electronic mail: denizagirseven@trakya.edu.tr*
[c)] *Corresponding author: korayturk@trakya.edu.tr*

Abstract. In this study, second order of accuracy difference scheme for approximate solution of initial-boundary value problem for time delay telegraph equation with Dirichlet condition is presented. The main theorem on stability of the difference scheme is established. Numerical results are provided.

INTRODUCTION

Telegraph equations with or without delay term arise in many branches of science and engineering, such as hydrodynamics [1], electromagnetic [2], waves in fluids [3], chemistry [4], and applied mathematics [5]. The delay term has received considerable attention in the last decades (see, for examples, [6, 7, 8, 9, 10]). In most cases, the exact solutions cannot be found easily. In numerical methods, the problem of stability has received a great deal of importance and attention. However, the stability theory of difference problems for time delay telegraph equations with delay term have not been studied extensively.

The study is organized as follows. Section 1 is the introduction. In section 2, the initial-boundary value problem for time delay telegraph equation with Dirichlet condition is considered. The second order of accuracy difference scheme for this problem is constructed. The main theorem on stability estimates for the solution of this difference problem is given. In Section 3, numerical results are provided.

THE MAIN THEOREM ON STABILITY

In this section, we consider the initial-boundary value problem for time delay telegraph equation with Dirichlet condition

$$\begin{cases} u_{tt}(t,x)+\alpha u_t(t,x)-(a(x)u_x(t,x))_x+\delta u(t,x)=b\left((-a(x)u_x([t],x))_x+\delta u([t],x)\right), \\ 0<t<\infty,\ 0<x<l, \\ u(0,x)=\varphi(x),\ u_t(0,x)=\psi(x),\ 0\le x\le l, \\ u(t,0)=u(t,l)=0,\ 0\le t<\infty, \end{cases} \tag{1}$$

where $a(x)$, $\varphi(x)$, and $\psi(x)$ are given sufficiently smooth functions. We assume that $a(x)\ge a_0>0$, $(x\in(0,l))$, $a(l)=a(0)$, $\delta>\frac{\alpha^2}{4}$, $\alpha>0$ and $0<b<1$. The discretization of problem (1) is carried out in two steps. In the first step, we define the grid space

$$[0,l]_h=\{x=x_n : x_n=nh,\ 0\le n\le M,\ Mh=l\}.$$

International Conference on Analysis and Applied Mathematics (ICAAM 2020)
AIP Conf. Proc. 2325, 020032-1–020032-4; https://doi.org/10.1063/5.0040279
Published by AIP Publishing. 978-0-7354-4069-2/$30.00

Let $(0,l)_h=[0,l]_h\backslash\{0,l\}$. We introduce the Hilbert spaces $L_{2h}=L_2([0,l]_h)$ and $W_{2h}^1=W_2^1([0,l]_h)$ of the grid functions $\varphi^h(x)=\{\varphi_n\}_0^M$ defined on $[0,l]_h$, equipped with the norms

$$\left\|\varphi^h\right\|_{L_{2h}}=\left(\sum_{x\in[0,l]_h}\left|\varphi^h(x)\right|^2 h\right)^{1/2},$$

$$\left\|\varphi^h\right\|_{W_{2h}^1}=\left\|\varphi^h\right\|_{L_{2h}}+\left(\sum_{x\in[0,l]_h}\left|\varphi_x^h(x)\right|^2 h\right)^{1/2},$$

respectively. To the differential operator A generated by the problem (1), we assign the difference operator A_h^x by the formula

$$A_h^x u^h(x)=\{-(a(x)u_{\bar{x}})_{x,n}+\delta u_n\}_1^{M-1} \tag{2}$$

acting in the space of grid functions $u^h(x)=\{u_n\}_0^M$ satisfying the conditions $u_0=u_M=0$. It is well-known that A_h^x is a self-adjoint positive definite operator in L_{2h}. With the help of A_h^x, we reach the initial value problem

$$\begin{cases}\frac{d^2u^h(t,x)}{dt^2}+\alpha\frac{du^h(t,x)}{dt}+A_h^x u^h(t,x)=bA_h^x u^h([t],x),\\ t>0,\ x\in(0,l)_h,\\ u^h(0,x)=\varphi^h(x),\quad u_t^h(0,x)=\psi^h(x),\ \ x\in[0,l]_h.\end{cases} \tag{3}$$

In the second step, we consider the uniform set of grid points

$$[0,\infty)_\tau=\{t_k:t_k=k\tau,\ 0\le k<\infty,\ N\tau=1\}$$

with step $\tau>0$. We replace (3) with the second order of accuracy difference scheme, and we get

$$\begin{cases}\frac{u_{k+1}^h-2u_k^h+u_{k-1}^h}{\tau^2}+\alpha\frac{u_{k+1}^h-u_{k-1}^h}{2\tau}+\frac{1}{2}A_h^x u_k^h+\frac{1}{4}A_h^x\left(u_{k+1}^h+u_{k-1}^h\right)=bA_h^x u^h_{\left[\frac{k-mN}{N+1}\right]N+mN},\\ N\tau=1,\ (m-1)N+1\le k\le mN-1,\ m=1,2,...,\\ u_0^h=\varphi^h,\quad \left(\left(1+\frac{\alpha\tau}{2}\right)I+\frac{\tau^2}{4}A_h^x\right)\frac{u_1^h-u_0^h}{\tau}=(b-1)\frac{\tau}{2}A_h^x\varphi^h+\psi^h,\\ \left(\left(1+\frac{\alpha\tau}{2}\right)I+\frac{\tau^2}{4}A_h^x\right)\frac{u_{mN+1}^h-u_{mN}^h}{\tau}=(b-1)\frac{\tau}{2}A_h^x u_{mN}^h+\frac{3u_{mN}^h-4u_{mN-1}^h+u_{mN-2}^h}{2\tau},\quad m=1,2,....\end{cases} \tag{4}$$

Theorem 1. For the solution of difference problem (4), the following estimates hold:

$$\max_{1\le k\le N}\left\|u_k^h\right\|_{L_{2h}}\le M_1\left\{\left\|\varphi^h\right\|_{L_{2h}}+\left\|\psi^h\right\|_{L_{2h}}\right\},$$

$$\max_{1\le k\le N}\left\|u_k^h\right\|_{W_{2h}^1}+\max_{1\le k\le N}\left\|\frac{u_k^h-u_{k-1}^h}{\tau}\right\|_{L_{2h}}\le M_2\left\{\left\|\varphi^h\right\|_{W_{2h}^1}+\left\|\psi^h\right\|_{L_{2h}}\right\},$$

$$\max_{mN+1\le k\le(m+1)N}\left\|u_k^h\right\|_{L_{2h}}\le M_3\left\{\max_{(m-1)N\le k\le mN}\left\|u_k^h\right\|_{L_{2h}}+\max_{(m-1)N+1\le k\le mN}\left\|\frac{3u_k^h-4u_{k-1}^h+u_{k-2}^h}{2\tau}\right\|_{L_{2h}}\right\},\ m=1,2,...,$$

$$\max_{mN+1\le k\le(m+1)N}\left\|u_k^h\right\|_{W_{2h}^1}+\max_{mN+1\le k\le(m+1)N}\left\|\frac{u_k^h-u_{k-1}^h}{\tau}\right\|_{L_{2h}}$$
$$\le M_4\left\{\max_{(m-1)N\le k\le mN}\left\|u_k^h\right\|_{W_{2h}^1}+\max_{(m-1)N+1\le k\le mN}\left\|\frac{3u_k^h-4u_{k-1}^h+u_{k-2}^h}{2\tau}\right\|_{L_{2h}}\right\},\ m=1,2,...,$$

where M_1, M_2, M_3 and M_4 do not depend on $\varphi^h(x)$ or $\psi^h(x)$.

NUMERICAL RESULTS

In this section, as a test problem, we consider the initial-boundary value problem

$$\begin{cases} u_{tt}(t,x)+2u_t(t,x)-u_{xx}(t,x)+u(t,x)=0.001\left(-u_{xx}([t],x)+u([t],x)\right), \\ 0<t<\infty,\ 0<x<\pi, \\ u(0,x)=\sin(x),\ u_t(0,x)=-\sin(x),\ 0\le x\le \pi, \\ u(t,0)=u(t,\pi)=0,\ 0\le t<\infty \end{cases} \tag{5}$$

for the time delay telegraph differential equation with Dirichlet condition.

By using step by step method and Fourier series method, it can be shown that the exact solution of the problem (5) is

$$u(t,x)=T_n(t)\sin(x),\ n-1\le t\le n,\ n=1,2,...,$$

where

$$\begin{aligned} T_1(t)&=\frac{999}{1000}e^{-t}\cos(t)-\frac{1}{1000}e^{-t}\sin(t)+\frac{1}{1000}, \\ T_{n+1}(t)&=T_n(n)e^{-t}\cos(t)+\left(T_n(n)+T_n^{'}(n)\right)e^{-t}\sin(t) \\ &\quad+\frac{T_n(n)}{1000}\left(1-e^{-(t-n)}\cos(t-n)-e^{-(t-n)}\sin(t-n)\right),\ n=1,2.... \end{aligned}$$

Using second order of accuracy difference scheme for the approximate solutions of problem (5), we get the following system of equations

$$\begin{cases} \frac{u_{k+1}^n-2u_k^n+u_{k-1}^n}{\tau^2}+2\frac{u_{k+1}^n-u_{k-1}^n}{2\tau}+\frac{1}{2}\left(-\frac{u_k^{n+1}-2u_k^n+u_k^{n-1}}{h^2}+u_k^n\right)+\frac{1}{4}\left(-\frac{u_{k+1}^{n+1}-2u_{k+1}^n+u_{k+1}^{n-1}}{h^2}+u_{k+1}^n\right) \\ +\frac{1}{4}\left(-\frac{u_{k-1}^{n+1}-2u_{k-1}^n+u_{k-1}^{n-1}}{h^2}+u_{k-1}^n\right)=0.001\left(-\frac{u^{n+1}_{\left[\frac{k-mN}{N+1}\right]N+mN}-2u^{n}_{\left[\frac{k-mN}{N+1}\right]N+mN}+u^{n-1}_{\left[\frac{k-mN}{N+1}\right]N+mN}}{h^2}+u^n_{\left[\frac{k-mN}{N+1}\right]N+mN}\right), \\ t_k=k\tau,\ N\tau=1,\ mN+1\le k\le (m+1)N-1,\ m=0,1,2,..., \\ x_n=nh,\ Mh=\pi,\ 1\le n\le M-1, \\ u_0^n=\sin(nh),\ 0\le n\le M, \\ (1+\tau)\frac{u_1^n-u_0^n}{\tau}+\frac{\tau}{4}\left(-\frac{u_1^{n+1}-2u_1^n+u_1^{n-1}}{h^2}+u_1^n\right)+\frac{\tau}{4}\left(-\frac{u_0^{n+1}-2u_0^n+u_0^{n-1}}{h^2}+u_0^n\right) \\ =-0.999\frac{\tau}{2}\left(-\frac{u_0^{n+1}-2u_0^n+u_0^{n-1}}{h^2}+u_0^n\right)-\sin(nh),\ 0\le n\le M, \\ (1+\tau)\frac{u_{mN+1}^n-u_{mN}^n}{\tau}+\frac{\tau}{4}\left(-\frac{u_{mN+1}^{n+1}-2u_{mN+1}^n+u_{mN+1}^{n-1}}{h^2}+u_{mN+1}^n\right)+\frac{\tau}{4}\left(-\frac{u_{mN}^{n+1}-2u_{mN}^n+u_{mN}^{n-1}}{h^2}+u_{mN}^n\right) \\ =-0.999\frac{\tau}{2}\left(-\frac{u_{mN}^{n+1}-2u_{mN}^n+u_{mN}^{n-1}}{h^2}+u_{mN}^n\right)+\frac{3u_{mN}^n-4u_{mN-1}^n+u_{mN-2}^n}{2\tau},\ 0\le n\le M, \\ u_k^0=u_k^M=0,\ mN\le k\le (m+1)N,\ m=0,1,2,.... \end{cases} \tag{6}$$

We find the numerical solutions for different values of N and M. Here, u_k^n represents the numerical solutions of the difference scheme at (t_k, x_n). For $N = M = 40$, $N = M = 80$, $N = M = 160$ in $t \in [0,1]$, $t \in [1,2]$, and $t \in [2,3]$, the errors computed by the following formula are given in Table 1.

$$E_M^N = \max_{\substack{mN+1 \leq k \leq (m+1)N,\ m=0,1,\ldots \\ 0 \leq n \leq M}} \left| u(t_k, x_n) - u_k^n \right|.$$

TABLE 1. Errors of Difference Scheme (6)

	N=M=40	N=M=80	N=M=160
$t \in [0,1]$	0.000067868	0.000016971	0.000004242
$t \in [1,2]$	0.000070234	0.000017619	0.000004412
$t \in [2,3]$	0.000035718	0.000009053	0.000002278

As it is seen in Table 1, the errors in the second order of accuracy difference scheme decrease approximately by a factor of 1/4 when the values of M and N are doubled.

CONCLUSION

In this study, we consider the initial-boundary value problem for delay telegraph equation with Dirichlet condition. The second order of accuracy difference scheme for the numerical solution of this problem is presented. Theorem on stability of this difference scheme is established. Numerical results are given.

ACKNOWLEDGMENTS

We are grateful to the TUBITAK Graduate Scholarship Programme for supporting Koray Turk. The publication has been prepared with the support of the “RUDN University Program 5-100”.

REFERENCES

1. H. Taflove, *Hydrodynamics* (Cambridge University Press, 1993).
2. O. Heaviside, *Electromagnetic Theory* (Cambridge University Press, 2011).
3. J. Lighthill, *Waves in Fluids* (Cambridge University Press, 1978).
4. M. J. Golay, Analytical Chemistry **29**, 928–932 (1957).
5. A. Ashyralyev, D. Agirseven, and K. Turk, AIP Conference Proceedings **1759**, 020022 (2016).
6. A. Ardito and P. Ricciardi, Nonlinear Anal. **4**, 411–414 (1980).
7. O. Arino, *Delay Differential Equations and Applications* (Springer, 2006).
8. G. D. Blasio, Nonlinear Anal.-Theory Appl. **52**, 1–18 (2003).
9. G. Kurulay and H. Ozbay, Appl. Comput. **16**, 48–58 (2017).
10. A. Ashyralyev and D. Agirseven, Mathematics **7**, 1163 (2019).

On a Boundary Value Problem for Systems of Integro-Differential Equations with Involution

Kairat Usmanov,[1, a)] Kulzina Nazarova,[1, b)] and Roza Uteshova[2, 3, c)]

[1)]Akhmet Yassawi University, Sattarkhanov Str. 29, Turkestan, 161200 Kazakhstan
[2)]Institute of Mathematics and Mathematical Modeling, Pushkin Str. 125, Almaty, 050000 Kazakhstan
[3)]International Information Technology University, Manas Str. 34/1, Almaty, 050040 Kazakhstan

[a)]Corresponding author: y_kairat@mail.ru
[b)]Electronic mail: gjnazarova@mail.ru
[c)]Electronic mail: ruteshova1@gmail.com

Abstract. A linear boundary value problem for a system of integro-differential equations with involution is studied by the parameterization method. Sufficient conditions for the existence of a unique solution to the problem are established in terms of coefficients. An algorithm for finding the solution to the problem under consideration is proposed.

INTRODUCTION

On the interval $[0,T]$ we consider the following two-point boundary value problem for the system of integro-differential equations with involution:

$$\frac{dx(t)}{dt} + diag(a_1, a_2, \dots, a_n)\frac{dx(\alpha(t))}{dt} = \int_0^T K(t,s)x(s)ds + f(t), \qquad t \in [0,T], \tag{1}$$

$$Bx(0) + Cx(T) = d, \qquad d \in \mathbb{R}^n, \tag{2}$$

where $K(t,s)$ is a continuous on $[0,T]\times[0,T]$ matrix and $f(t)$ is a n-dimensional vector-function continuous on $[0,T]$.

Here $\alpha(t)$ is a changing orientation homeomorphism $\alpha(t) : [0,T] \to [0,T]$ such that $\alpha^2(t) = \alpha(\alpha(t)) = t$. Such a homeomorphism is called a Carleman shift or deviation of involution. Its properties were studied by G. Litvinchuk [1], N. Karapetyanz and S. Samko [2]. As an example of a deviation with involution on $[0,T]$ we can take the homeomorphism $\alpha(t) = T - t$.

By a solution to problem (1), (2) we mean a vector-function $x(t)$ that is continuous on $[0,T]$ and continuously differentiable on $(0,T)$, satisfies the system of integro-diffferential equations with involution (1) and the boundary condition (2).

In the present paper, problem (1), (2) is studied by the parameterization method [3]. On the basis of this method, we establish necessary and sufficient conditions for the unique solvability of the problem in question and propose an algorithm for finding its solution.

Let us consider equation (1) for $t = \alpha(t)$:

$$\frac{dx(\alpha(t))}{dt} + diag(a_1, a_2, \dots, a_n)\frac{dx(t)}{dt} = \int_0^T K(\alpha(t),s)x(s)ds + f(\alpha(t)), \qquad t \in [0,T].$$

From the system

$$\frac{dx(t)}{dt} + diag(a_1, a_2, \dots, a_n)\frac{dx(\alpha(t))}{dt} = \int_0^T K(t,s)x(s)ds + f(t), \qquad t \in [0,T],$$

$$\frac{dx(\alpha(t))}{dt} + diag(a_1, a_2, \dots, a_n)\frac{dx(t)}{dt} = \int_0^T K(\alpha(t),s)x(s)ds + f(\alpha(t)), \qquad t \in [0,T],$$

International Conference on Analysis and Applied Mathematics (ICAAM 2020)
AIP Conf. Proc. 2325, 020033-1–020033-5; https://doi.org/10.1063/5.0040272
Published by AIP Publishing. 978-0-7354-4069-2/$30.00

we obtain

$$diag(1-a_1^2,1-a_2^2,\dots,1-a_n^2)\frac{dx(t)}{dt}=\int\limits_0^T[K(t,s)-diag(a_1,a_2,\dots,a_n)K(\alpha(t),s)]x(s)ds$$
$$+[f(t)-diag(a_1,a_2,\dots,a_n)f(\alpha(t))].$$

Under assumption that the matrix $diag(1-a_1^2,1-a_2^2,\dots,1-a_n^2)$ is invertible, we can rewrite problem (1), (2) in the form

$$\frac{dx(t)}{dt}=\int\limits_0^T K_1(t,s)x(s)ds+f_1(t), \qquad t\in[0,T], \tag{3}$$

$$Bx(0)+Cx(T)=d, \tag{4}$$

where $K_1(t,s)=diag(1/(1-a_1^2),1/(1-a_2^2),\dots,1/(1-a_n^2))[K(t,s)-diag(a_1,a_2,\dots,a_n)K(\alpha(t),s)]$ and $f_1(t)=diag(1/(1-a_1^2),1/(1-a_2^2),\dots,1/(1-a_n^2))[f(t)-diag(a_1,a_2,\dots,a_n)f(\alpha(t))]$.

METHOD OF INVESTIGATION

Let us divide $[0,T]$ into N equal parts with a step size h: $[0,T)=\bigcup\limits_{r=1}^{N}[(r-1)h,rh)$. We denote by $x_r(t)$ the restriction of the function $x(t)$ to the r-th subinterval, i.e., $x_r(t)=x(t)$ for $t\in[(r-1)h,rh)$. The original problem is then transformed to an equivalent multipoint boundary value problem

$$\frac{dx_r(t)}{dt}=\sum_{j=1}^{N}\int\limits_{(j-1)h}^{jh}K_1(t,s)x_j(s)ds+f_1(t), \qquad t\in[(r-1)h,rh), \qquad r=\overline{1,N}, \tag{5}$$

$$Bx_1(0)+C\lim_{t\to T-0}x_N(t)=d, \tag{6}$$

$$\lim_{t\to sh-0}x_s(t)=x_{s+1}(sh), \qquad s=\overline{1,N-1}. \tag{7}$$

Here (7) are conditions for the continuity of $x(t)$ at the interior partition points $t=sh$, $s=\overline{1,N-1}$.

If $x(t)$ is a solution to problem (3), (4), then the system of its restrictions $x[t]=(x_1(t),x_2(t),\dots,x_N(t))'$ is a solution to multipoint problem (5)-(7). And vice versa, if a system of vector-functions $\widetilde{x}[t]=(\widetilde{x}_1(t),\widetilde{x}_2(t),\dots,\widetilde{x}_N(t))'$ is a solution to problem (5)-(7), then the function $\widetilde{x}(t)$ defined by the equations $\widetilde{x}(t)=\widetilde{x}_r(t)$, $t\in[(r-1)h,rh)$, $r=\overline{1,N}$, and $\widetilde{x}(T)=\lim\limits_{t\to T-0}\widetilde{x}_N(t)$, is a solution to original problem (3), (4).

Let us now introduce parameters λ_r, $r=\overline{1,N}$, that are equal to the values of the functions $x_r(t)$ at the points $t=(r-1)h$. Now, on each subinterval $[(r-1)h,rh)$, $r=\overline{1,N}$, we make the substitution $x_r(t)=u_r(t)+\lambda_r$. The problem (5)-(7) is then reduced to an equivalent multipoint problem with parameters:

$$\frac{du_r(t)}{dt}=\sum_{j=1}^{N}\int\limits_{(j-1)h}^{jh}K_1(t,s)[u_j(s)+\lambda_j]ds+f_1(t), \tag{8}$$

$$u_r[(r-1)h]=0, \qquad t\in[(r-1)h,rh), \qquad r=\overline{1,N}, \tag{9}$$

$$B\lambda_1+C\lambda_N+C\lim_{t\to T-0}u_N(t)=d, \tag{10}$$

$$\lambda_s + \lim_{t \to sh-0} u_s(t) = \lambda_{s+1}, \qquad s = \overline{1, N-1}. \tag{11}$$

Problems (5)-(7) and (8)-(11) are equivalent in the following sense.
If a system of functions $x[t] = (x_1(t), x_2(t), \ldots, x_N(t))'$ is a solution to problem (5)-(7), then the pair $(\lambda, u[t])$ with $\lambda = (x_1(0), x_2(h), \ldots, x_N[(N-1)h])'$ and $u[t] = (x_1(t) - x_1(0), x_2(t) - x_2(h), \ldots, x_N(t) - x_N[(N-1)h])'$ is a solution to problem (8)-(11). Vice versa, if a pair $(\widetilde{\lambda}, \widetilde{u}[t])$ is a solution to (8)-(11), then the system of functions $\widetilde{x}(t) = (\widetilde{\lambda}_1 + \widetilde{u}_1(t), \widetilde{\lambda}_2 + \widetilde{u}_2(t), \ldots, \widetilde{\lambda}_N + \widetilde{u}_N(t))'$ is a solution to problem (5)-(7).

Emergence of initial conditions (9) allows us, for fixed λ_r, to determine $u_r(t)$, $r = \overline{1, N}$, from the system of integral equations

$$u_r(t) = \int\limits_{(r-1)h}^{t} \sum_{j=1}^{N} \int\limits_{(j-1)h}^{jh} K_1(\tau, s)[u_j(s) + \lambda_j] ds d\tau + \int\limits_{(r-1)h}^{t} f_1(\tau) d\tau, \qquad t \in [(r-1)h, rh). \tag{12}$$

By substituting the expressions for $\lim\limits_{t \to T-0} u_N(t)$ and $\lim\limits_{t \to sh-0} u_s(t)$, $s = \overline{1, N}$, obtained from (12), into conditions (10), (11), and multiplying both sides of (10) by $h > 0$, we get the system of linear algebraic equations in unknown parameters λ_r, $r = \overline{1, N}$:

$$\begin{aligned} &hB\lambda_1 + hC\lambda_N + hC \int\limits_{(N-1)h}^{Nh} \sum_{j=1}^{N} \int\limits_{(j-1)h}^{jh} K_1(\tau, s) \lambda_j ds d\tau \\ &= hd - hC \int\limits_{(N-1)h}^{Nh} f_1(\tau) d\tau - hC \int\limits_{(N-1)h}^{Nh} \sum_{j=1}^{N} \int\limits_{(j-1)h}^{jh} K_1(\tau, s) u_j(s) ds d\tau, \end{aligned} \tag{13}$$

$$\begin{aligned} &\lambda_s + \int\limits_{(s-1)h}^{sh} \sum_{j=1}^{N} \int\limits_{(j-1)h}^{jh} K_1(\tau, s) \lambda_j ds d\tau - \lambda_{s+1} \\ &= - \int\limits_{(s-1)h}^{sh} \sum_{j=1}^{N} \int\limits_{(j-1)h}^{jh} K_1(\tau, s) u_j(s) ds d\tau - \int\limits_{(s-1)h}^{sh} f_1(\tau) d\tau, \qquad s = \overline{1, N-1}. \end{aligned} \tag{14}$$

Let us denote by $Q(h)$ the $(nN \times nN)$-matrix corresponding to the left-hand side of system (13),(14). This system thus can be represented in the form

$$Q_h(\lambda) = -F(h) - G(u, h), \qquad \lambda \in \mathbb{R}^{nN}, \tag{15}$$

where

$$F(h) = \Big(-hd + hC \int\limits_{(N-1)h}^{Nh} f_1(\tau) d\tau, \int\limits_{0}^{h} f_1(\tau) d\tau, \ldots, \int\limits_{(N-2)h}^{(N-1)h} f_1(\tau) d\tau \Big)',$$

$$\begin{aligned} G(u, h) = \Big(&hC \int\limits_{(N-1)h}^{Nh} \sum_{j=1}^{N} \int\limits_{(j-1)h}^{jh} K_1(\tau, s) u_j(s) ds d\tau, \\ &\int\limits_{0}^{h} \sum_{j=1}^{N} \int\limits_{(j-1)h}^{jh} K_1(\tau, s) u_j(s) ds d\tau, \ldots, \int\limits_{(N-2)h}^{(N-1)h} \sum_{j=1}^{N} \int\limits_{(j-1)h}^{jh} K_1(\tau, s) u_j(s) ds d\tau \Big)'. \end{aligned}$$

Thus, to find a solution to problem (8)-(11), the pair $(\lambda, u[t])$, we have the system of equations (12),(15). We will find this solution as the limit of the sequence of pairs $(\lambda^{(k)}, u^{(k)}[t])$ according to the following algorithm.

Step 0. (a) Assuming that the matrix $Q(h)$ is invertible, from the equation $Q_h(\lambda) = -F(h)$ we find the initial approximation to the parameter $\lambda^{(0)} = (\lambda_1^{(0)}, \lambda_2^{(0)}, \ldots, \lambda_N^{(0)})' \in \mathbb{R}^{nN}$: $\lambda^{(0)} = -[Q(h)]^{-1}F(h)$.

(b) Substituting $\lambda_r^{(0)}$, $r = \overline{1,N}$, into the right-hand side of the system of integro-differential equations (8) and solving special Cauchy problems with initial conditions (9), we obtain $u^{(0)}[t] = (u_1^{(0)}(t), u_2^{(0)}(t), \ldots, u_N^{(0)}(t))'$.

Step 1. (a) Substituting $u_r^{(0)}(t)$, $r = \overline{1,N}$, into the right-hand side of (15), from the equation $Q_h(\lambda) = -F(h) - G(u^{(0)}, h)$ we determine $\lambda^{(1)} = (\lambda_1^{(1)}, \lambda_2^{(1)}, \ldots, \lambda_N^{(1)})'$.

(b) Substituting $\lambda_r^{(1)}$, $r = \overline{1,N}$, into the right-hand side of (8) and solving special Cauchy problems (8),(9), we obtain $u^{(1)}[t] = (u_1^{(1)}(t), u_2^{(1)}(t), \ldots, u_N^{(1)}(t))'$, and so forth.

Proceeding by the algorithm, in the k-th step we find the pair $(\lambda^{(k)}, u^{(k)}[t])$, $k = 0, 1, 2, \ldots$.

As we said, the unknown functions $u[t] = (u_1(t), u_2(t), \ldots, u_N(t))'$ are determined by solving special Cauchy problems (8),(9) for systems of integro-differential equations. But, unlike the Cauchy problems for ordinary differential equations, special Cauchy problems for integro-differential equations are not always solvable.

RESULTS OF INVESTIGATION

The following theorem provides a sufficient condition for the unique solvability of the special Cauchy problem (8),(9) for fixed values of parameters.

Theorem 1 *Let the step size of the partition $h = T/N$ satisfy the inequality*

$$\delta(h) = \beta T h < 1,$$

where $\beta = \max\limits_{(t,s)\in[0,T]\times[0,T]} \|K_1(t,s)\|$. Then the special Cauchy problem (8),(9) has a unique solution.

Sufficient conditions for the convergence of the algorithm proposed, as well as for the unique solvability of problem (1),(2) are established in the following statement.

Theorem 2 *Let the condition of Theorem 1 be satisfied, the matrix $Q(h)$ be invertible, and the following inequalities hold:*

$$\|[Q(h)]^{-1}\| \le \gamma(h),$$

$$q(h) = \frac{\delta(h)}{1 - \delta(h)} \gamma(h) \max(1, h\|C\|) < 1.$$

Then problem (1),(2) has a unique solution.

The proof of Theorem 2 is similar to that of Theorem 3 in [4] and is carried out by the algorithm proposed above taking into account the specificity of system (1). In [5], the sufficient and necessary conditions were established for the unique solvability of the linear boundary value problem for a system of integro-differential equations

$$\frac{dx}{dt} = \int_0^T K(t,s)x(s)ds + f(t), \qquad t \in [0,T], \tag{16}$$

$$Bx(0) + Cx(T) = d, \qquad d \in \mathbb{R}^n. \tag{17}$$

Theorem 3 *(see [5, p.1216]) Problem (16),(17) is uniquely solvable if and only if there exists $h \in (0, h_0] : Nh = T$ such that the matrix $Q_*(h)$ is invertible.*

Let us now state a corollary of this theorem regarding problem (1),(2).

Corollary 1 *Problem (1),(2) is uniquely solvable if and only if there exists $h \in (0, h_0] : Nh = T$ such that the matrix $Q_*(h)$ is invertible.*

Here h_0 is determined by the condition $q(h_0) = \frac{T}{1+a}\beta h_0 < 1$.

ACKNOWLEDGMENTS

This research has been partially supported by the Ministry of Education and Science of the Republic of Kazakhstan, Grant No. AP 05132486 and the Award "The Best University Teacher 2019".

REFERENCES

1. G. Litvinchuk, *Solvability Theory of Boundary Value Problems and Singular Integral Equations with Shift* (Springer Netherlands, 2000).
2. N. Karapetiants and S. Samko, *Equations with Involutive Operators* (Birkhäuser Basel, 2001).
3. D. Dzhumabaev, J. Comput. Math. Math. Phys. **29:1**, 34-46 (1989).
4. E. Bakirova, *Well-posedness of a Linear Two-Point Boundary Value Problem for Systems of Integro-Differential Equations* (Dissertation Abstract, IMMM, Almaty, 2006).
5. D. S. Dzhumabaev, Comput. Math. Math. Phys. **50**, 1150-1161 (2010).

A Numerical Solution for the Source Identification Telegraph Problem with Neumann Condition

Allaberen Ashyralyev[1, 2, 3, a)] and Haitham Al-Hazaimeh[1, b)]

[1)] *Department of Mathematics, Near East University, Nicosia, Mersin 10, Turkey*

[2)] *Peoples' Friendship University of Russia (RUDN University), 6 Miklukho-Maklaya St,Moscow 117198, Russian Federation*

[3)] *Institute of Mathematics and Mathematical Modeling, 050010, Almaty, Kazakhstan*

[a)] *Electronic mail: allaberen.ashyralyev@neu.edu.tr*

[b)] *Corresponding author: mathmatichhh@gmail.com*

Abstract. In this paper, the source identification problem for the telegraph equation is studied. We propose the first order of accuracy absolute stable difference scheme for the numerical solution of the one-dimensional identification problem for the telegraph equation with the Neumann condition. The obtained numerical results have been compared with the exact solution to verify the accurate nature of our method.

INTRODUCTION

Identification problems play a very important role not only in engineering sciences such as quantum mechanics, but also in mathematical physics, chemical physics, and communication system.

In last years, much attention has been given in the literature to the development, analysis, and implementation of stable methods for the numerical solution of the one-dimensional identification problem for the telegraph equation, and have been studied by many authors (see, e.g., [1-6] and the references given therein).

Direct and inverse boundary value problems for telegraph differential equations have been a major research area in applied mathematics. The solvability of the inverse problems in various formulations with various overdetermination conditions for telegraph and hyperbolic equations were studied in many works (see, e.g., [7-15] and the references given therein).

In particular, the well-posedness of the source identification problem for a telegraph equation with unknown parameter p

$$\left\{ \begin{array}{c} \frac{d^2u(t)}{dt^2} + \alpha \frac{du(t)}{dt} + Au(t) = p + f(t), 0 < t < T, \\ u(0) = \varphi, u'(0) = \psi, u(T) = \zeta \end{array} \right.$$

in a Hilbert space H with the self-adjoint positive definite operator A was proved in [12]. They established stability estimates for the solution of this problem. In applications, three source identification problems for telegraph equations were investigated.

In the present paper, the first order of accuracy absolute stable difference scheme for the numerical solution of the one-dimensional identification problem for the telegraph equation with Neumann condition is presented. Some numerical results are explained.

Finally, some references are introduced at the end. Note that we have computed the numerical results by MATLAB programming.

NUMERICAL ALGORITHM FOR THE SOLUTION OF THE SOURCE IDENTIFICATION TELEGRAPH PROBLEM

In this section, we study the numerical solution of the identification problem

International Conference on Analysis and Applied Mathematics (ICAAM 2020)
AIP Conf. Proc. 2325, 020034-1–020034-5; https://doi.org/10.1063/5.0040419
Published by AIP Publishing. 978-0-7354-4069-2/$30.00

$$\begin{cases} \frac{\partial^2 u(t,x)}{\partial t^2}+2\frac{\partial u(t,x)}{\partial t}-\frac{\partial^2 u(t,x)}{\partial x^2}=p(t)(\cos x+1)-e^{-t}(\cos x+2), \\ x\in(0,\pi), t\in(0,1), \\ u(0,x)=\cos x+1, u_t(0,x)=-(\cos x+1), x\in[0,\pi], \\ u_x(t,0)=u_x(t,\pi)=0, t\in[0,1], \\ \int_0^\pi u(t,x)\,dx=\pi e^{-t}, t\in[0,1] \end{cases} \tag{1}$$

for a telegraph equation. The exact solution pair of this problem is $(u(t,x),p(t))=(e^{-t}(\cos x+1),e^{-t})$.

For the numerical solution of problem (1), we present the following first order of accuracy difference scheme

$$\begin{cases} \frac{u_n^{k+1}-2u_n^k+u_n^{k-1}}{\tau^2}+2\frac{u_n^{k+1}-u_n^k}{\tau}-\frac{u_{n+1}^{k+1}-2u_n^{k+1}+u_{n-1}^{k+1}}{h^2} \\ =p_k(\cos x_n+1)-e^{-t_{k+1}}(\cos x_n+2), \\ t_k=k\tau, x_n=nh, 1\leqslant k\leqslant N-1, 1\leqslant n\leqslant M-1, \\ u_n^0=1+\cos x_n, \frac{u_n^1-u_n^0}{\tau}=-(1+\cos x_n), 0\leqslant n\leqslant M, Mh=\pi, N\tau=1, \\ u_0^{k+1}=u_1^{k+1}, u_{M-1}^{k+1}=u_M^{k+1}, \sum_{i=1}^{M-1}u_i^{k+1}h=\pi e^{-t_{k+1}}, -1\leqslant k\leqslant N-1. \end{cases} \tag{2}$$

Algorithm for obtaining the solution of identification problem (2), $\{u_k\}_{k=0}^N=\left\{\left\{u_n^k\right\}_{k=0}^N\right\}_{n=0}^M$ and $\{p_k\}_{k=1}^{N-1}$, contain three stages. Now, let us define

$$u_n^k=w_n^k+\eta_k(\cos x_n+1), 0\le k\le N, 0\le n\le M. \tag{3}$$

Applying difference scheme (2) and the formula (3), we obtain

$$\eta_{k+1}=\frac{\pi e^{-t_{k+1}}-\sum_{i=1}^{M-1}w_i^{k+1}h}{\sum_{i=1}^{M-1}(\cos x_i+1)h}, -1\le k\le N-1, \tag{4}$$

and the difference scheme

$$\begin{cases} \frac{w_n^{k+1}-2w_n^k+w_n^{k-1}}{\tau^2}+2\frac{w_n^{k+1}-w_n^k}{\tau}-\frac{w_{n+1}^{k+1}-2w_n^{k+1}+w_{n-1}^{k+1}}{h^2} \\ +\frac{\sum_{i=1}^{M-1}w_i^{k+1}h}{\sum_{i=1}^{M-1}(\cos x_i+1)h}\cos x_n\frac{2(\cos h-1)}{h^2}-2\frac{\sum_{i=1}^{M-1}\frac{w_i^{k+1}-w_i^k}{\tau}h}{\sum_{i=1}^{M-1}(\cos x_i+1)h}(\cos x_n+1) \\ =-\frac{2\pi\frac{e^{-t_{k+1}}-e^{-t_k}}{\tau}}{\sum_{i=1}^{M-1}(\cos x_i+1)h}(\cos x_n+1)+\frac{\pi e^{-t_{k+1}}}{\sum_{i=1}^{M-1}(\cos x_i+1)h}\frac{2(\cos h-1)}{h^2}\cos x_n-e^{-t_{k+1}}(\cos x_n+2), \\ 1\leqslant k\leqslant N-1, 1\leqslant n\leqslant M-1, \\ w_n^0=1+\cos x_n, \frac{w_n^1-w_n^0}{\tau}=-(1+\cos x_n), 0\leqslant n\leqslant M, \\ w_0^{k+1}=w_1^{k+1}, w_{M-1}^{k+1}=w_M^{k+1}, -1\leqslant k\leqslant N-1. \end{cases} \tag{5}$$

In the first stage, we find numerical solution $\left\{\left\{w_n^k\right\}_{k=0}^N\right\}_{n=0}^M$ to the corresponding first order of accuracy difference scheme (5). For obtaining the solution of difference scheme (5), we will write it in the matrix form as

$$\begin{cases} Aw^{k+1}+Bw^{k}+Cw^{k-1}=f^{k}, 1\leqslant k\leqslant N-1, \\ w^{0}=\{\cos x_{n}+1\}_{n=0}^{M}, w^{1}=(1-\tau)\{\cos x_{n}+1\}_{n=0}^{M}, \end{cases} \tag{6}$$

where A,B,C are $(M+1)\times(M+1)$ square matrices, $w^{s}, s=k,k\pm 1, f^{k}$ are $(M+1)\times 1$ column matrices, and

$$A=\begin{bmatrix} 1 & -1 & 0 & 0 & \cdots & 0 & 0 & 0 & 0 \\ b & a+c_1 & b+c_1 & c_1 & \cdots & c_1 & c_1 & c_1 & 0 \\ 0 & b+c_2 & a+c_2 & b+c_2 & \cdots & c_2 & c_2 & c_2 & 0 \\ 0 & c_3 & b+c_3 & a+c_3 & \cdots & c_3 & c_3 & c_3 & 0 \\ \vdots & \vdots & \vdots & \vdots & \ddots & \vdots & \vdots & \vdots & \vdots \\ 0 & c_{M-3} & c_{M-3} & c_{M-3} & \cdots & a+c_{M-3} & b+c_{M-3} & c_{M-3} & 0 \\ 0 & c_{M-2} & c_{M-2} & c_{M-2} & \cdots & b+c_{M-2} & a+c_{M-2} & b+c_{M-2} & 0 \\ 0 & c_{M-1} & c_{M-1} & c_{M-1} & \cdots & c_{M-1} & b+c_{M-1} & a+c_{M-1} & b \\ 0 & 0 & 0 & 0 & \cdots & 0 & 0 & -1 & 1 \end{bmatrix}_{(M+1)\times(M+1)},$$

,

$$B=\begin{bmatrix} 0 & 0 & 0 & 0 & \cdots & 0 & 0 & 0 & 0 \\ 0 & e+z_1 & z_1 & z_1 & \cdots & z_1 & z_1 & z_1 & 0 \\ 0 & z_2 & e+z_2 & z_2 & \cdots & z_2 & z_2 & z_2 & 0 \\ 0 & z_3 & z_3 & e+z_3 & \cdots & z_3 & z_3 & z_3 & 0 \\ \vdots & \vdots & \vdots & \vdots & \ddots & \vdots & \vdots & \vdots & \vdots \\ 0 & z_{M-3} & z_{M-3} & z_{M-3} & \cdots & e+z_{M-3} & z_{M-3} & z_{M-3} & 0 \\ 0 & z_{M-2} & z_{M-2} & z_{M-2} & \cdots & z_{M-2} & e+z_{M-2} & z_{M-2} & 0 \\ 0 & z_{M-1} & z_{M-1} & z_{M-1} & \cdots & z_{M-1} & z_{M-1} & e+z_{M-1} & 0 \\ 0 & 0 & 0 & 0 & \cdots & 0 & 0 & 0 & 0 \end{bmatrix}_{(M+1)\times(M+1)},$$

,

$$C=\begin{bmatrix} 0 & 0 & \cdots & 0 & 0 \\ 0 & g & \cdots & 0 & 0 \\ \vdots & \vdots & \ddots & \vdots & \vdots \\ 0 & 0 & \cdots & g & 0 \\ 0 & 0 & \cdots & 0 & 0 \end{bmatrix}_{(M+1)\times(M+1)},$$

,

$$f^{k}=\begin{bmatrix} 0 \\ f(t_k,x_1) \\ . \\ f(t_k,x_{M-1}) \\ 0 \end{bmatrix}_{(M+1)\times 1}, w^{s}=\begin{bmatrix} w_0^s \\ w_1^s \\ . \\ w_{M-1}^s \\ w_M^s \end{bmatrix},$$

for $s=k,k\pm 1$. Here,

$$a=\frac{1}{\tau^2}+\frac{2}{\tau}+\frac{2}{h^2}, b=-\frac{1}{h^2}, c_n=\frac{h}{d}\cos x_n\left[\frac{2(\cosh-1)}{h^2}-\frac{2}{\tau}\right],$$

$$d=\sum_{i=1}^{M-1}\left(\cos x_i+1\right)h, e=-\frac{2}{\tau^2}-\frac{2}{\tau}, g=\frac{1}{\tau^2}, z_n=\frac{2h}{d\tau}\left(\cos x_n+1\right),$$

$$f\left(t_k,x_n\right)=-\frac{2\pi\frac{e^{-t}k+1-e^{-t_k}}{\tau}}{\sum_{i=1}^{M-1}\left(\cos x_i+1\right)h}\left(\cos x_n+1\right)+\frac{\pi e^{-t_{k+1}}}{\sum_{i=1}^{M-1}\left(\cos x_i+1\right)h}\frac{2(\cos h-1)}{h^2}\cos x_n-e^{-t_{k+1}}\left(\cos x_n+2\right),$$

$$1\leq k\leq N-1, 1\leq n\leq M-1.$$

So, we have the initial value problem for the first order difference equation (2) with respect to k with matrix coefficients A,B and C. Since $w^0$and $w^1$are given, we can obtain the solution$\left\{\left\{w_n^k\right\}_{k=0}^N\right\}_{n=0}^M$ of (6) by direct formula

$$w^{k+1}=A^{-1}\left(f^k-Bw^k-Cw^{k-1}\right), k=1,...,N-1.$$

In the second stage, applying formulas

$$p_k=\frac{\eta_{k+1}-2\eta_k+\eta_{k-1}}{\tau^2}, 1\leq k\leq N-1. \tag{7}$$

and (4), we can obtain $\{p_k\}_{k=1}^{N-1}$. Finally, in the third stage, we obtain $\left\{\left\{u_n^k\right\}_{k=0}^N\right\}_{n=0}^M$ by formulas (3) and (4). The errors are computed by

$$E_u=\max_{0\leqslant k\leqslant N}\left(\sum_{n=0}^M\left|u\left(t_k,x_n\right)-u_n^k\right|^2h\right)^{\frac{1}{2}},$$

$$E_p=\max_{1\leqslant k\leqslant N-1}\left|p\left(t_k\right)-p_k\right|,$$

where $u\left(t,x\right)$ and $p(t)$ represent the exact solutions, u_n^k represent the numerical solutions at $\left(t_k,x_n\right)$, and p_k represent the numerical solutions at t_k. The numerical results are given in the following table:

TABLE 1. Error analysis

$Error$	$N=M=20$	$N=M=40$	$N=M=80$	$N=M=160$
E_u	0.1180	0,0609	0.0309	0.015
E_p	0.3528	0.1780	0.0893	0.0447

As it is seen in Table 1, if N and M are doubled, the value of errors between the exact solution and approximate solution decreases by a factor of approximately $1/2$ for first order difference scheme (2).

REFERENCES

1. A. Ashyralyev and C. Ashyralyyev, Nonlinear Anal. Model. Control **19(3)**, 350–366 (2014).
2. M. Dehghan, Applied Mathematical Modelling **25**, 743–754 (2001).
3. A. Ashyralyev and A. S. Erdogan, Applied Mathematics and Computation **226**, 212–228 (2014).
4. C. Ashyralyyev, Filomat **28(5)**, 947–962 (2014).
5. S. Jator, American J. of Computational Mathematics **5(2)**, 175–185 (2015).
6. A. Ashyralyev and F. Emharab, Journal of Inverse and Ill-Posed Problems **27(3)**, 301–315 (2019).
7. A. Ashyralyev and F. Dal, Applied Mathematics and Computation **217(9)**, 4654–4664 (2011).
8. Z. Direk and M. Ashyraliyev, Advances in Difference Equations **2014(132)** (2014).
9. T. S. Kalmenov and D. Suragan, Electronic Journal of Differential Equations **2014(48)**, 1–6 (2014).
10. A. Ashyralyev and D. Agirseven, Mathematics **7(12)**, 1163 (2019).

11. F. F. Ivanauskas, Y. A. Novitski, and M. P. Sapagovas, Differential Equations **49(7)**, 849–856 (2013).
12. A. Ashyralyev and F. Cekic, Book Series: Springer Proceedings in Mathematics & Statistics **164**, 39–50 (2016).
13. A. Ashyralyev and P. E. Sobolevskii, New Difference Schemes for Partial Differential Equations (Birkhäuser Verlag, Basel, Boston, Berlin, 2004).
14. A. Ashyralyev and A. Al-Hammouri, AIP Conference Proceedings **2183(1)**, 070008 (2019).
15. T. S. Kalmenov and D. Suragan, Electronic Journal of Differential Equations **2014(48)**, 1–6 (2014).

Multivariate Stochastic Mechanisms and Information Measures in Population Growth Processes

Petras Rupšys[a)]

Vytautas Magnus University, Agriculture Academy, Universiteto g. 20-214, Akademija, Kaunas district. LT – 53361, Lithuania

[a)]Corresponding author: petras.rupsys@vdu.lt

Abstract. Stochastic differential equations (SDEs) have been intensively used to analyze data from physics, finance, engineering, medicine, biology, and forestry. This study proposes general mixed effect parameters (fixed and random) multivariate SDE model of a population growth which includes random forces governing the dynamic of multivariate distribution of tree size variables. The dynamic of the multivariate probability density function of the size variables in a population is described by mixed effect parameters Gompertz type SDE. The advantages of the multivariate SDE model are that it does not need to choose many different equations to be tried, it relates the size variables dynamic against the time dimension, and considers the underlying covariance structure driving changes in the size variables. SDE model allows us a better understanding of processes driving the dynamic of natural phenomena. The new derived multivariate probability density function and its marginal univariate, bivariate, trivariate, conditional univariate, bivariate, trivariate, and much more distributions can be applied for the modeling of population attributes such as the mean value, quantiles and much more. This study introduces general multivariate mutual information measures based on the differential entropy to capture multivariate interactions between size variables. The purpose of the present study is therefore to experimentally confirm the effectiveness of using multivariate information measures to reconstruct multivariate interactions in size variables. The study of information sharing amongst size variables is illustrated using a dataset of the Scots pine (Pinus Sylvestris L.) stands measurements in Lithuania.

INTRODUCTION

In the last decades the theory of population growth treats the size variables of the population as stochastic continuous random vector that own a particular distribution. Traditionally, a dynamic model of a population is processed by deterministic and stochastic components that operate simultaneously. Noise term as a substantial component is generally introduced using a stochastic Brownian motion process. Stochastic excitations are mathematically represented by complex stochastic differential equations of the Itô type [1]. Stochastic differential equations (SDEs) were developed at the beginning of the twentieth century to quantify aspects of stochastic processes. The pioneering work of Bachelier [2] was primarily motivated by problems associated with introducing a mathematical model of Brownian motion and its use for valuing stock options. Subsequent paper by Einstein [3] helped to clarify the ability of so-called Brownian molecular motion to quantify the molecular kinetic theory of heat and bodies of a microscopically visible size. The modern theory of SDE has gradually been developed into an attractive approach for applications [4, 5]. Although applications of stochastic calculus theory can be highly technical, but the fundamental concepts of the SDEs theory are not difficult to understand. Moreover, they are profound in the sense that they apply to situations in which commonly used models produce unsatisfactory results. Fundamental SDEs theory is defined on random variables. The universality of the SDEs accounts for the wide range of applications of the theory including human population, forestry, engineering, and biology [5-8]. The fundamental advantage of stochastic

International Conference on Analysis and Applied Mathematics (ICAAM 2020)
AIP Conf. Proc. 2325, 020035-1–020035-6; https://doi.org/10.1063/5.0040284
Published by AIP Publishing. 978-0-7354-4069-2/$30.00

dynamical models over deterministic models is that they combine both deterministic and stochastic elements of dynamic, where the stochasticity is affected by the outside random fluctuations in population size variables.

The fixed effect parameters univariate and bivariate Gompertz type SDEs are in-depth examined for modeling [9-11]. In many cases a real-life process involves several random variables by a system of fixed- and mixed effect parameters SDE [12-15]. This paper focused on: 1) to present different aspects of the mixed effect parameters Gompertz type SDE models that may be applicable; 2) to derive the essential characteristics of these models; 3) to discuss the corresponding computational issues. Another goal is to study in a general way the interaction information measures of cross comparisons of all marginal and conditional distributions by using the Shannon type differential entropy [16-18]. Results are illustrated using sample dataset from Scots pine tree stands in Lithuania. Moreover, the mixed effect parameters are estimated by developed approximated maximum likelihood procedure. All results are implemented in the symbolic algebra system MAPLE.

MATERIALS AND METHODS

SDE Framework

Let us consider n-variate reducible SDE of the Gompertz type to study the multivariate distribution problem of the population size variables. This equation results in an exact probability density function which parameters can be estimated by an approximated maximum likelihood procedure based on discrete time observations. The mixed effect parameters Gompertz-type SDE that describes the development of the population size variables is defined in the following form

$$dX^i(t) = A(X^i(t))dt + D(X^i(t))B^{\frac{1}{2}} \cdot dW(t), \; i = 1, \ldots, M, \tag{1}$$

here: M is the total number of individuals used for model fitting, t is the time, $X(t) = (X_1(t), \ldots, X_n(t))^T$, $t \in [t_0; T]$, $t_0 \geq 0$, $X(t_0) = x_0 = (x_{10}, \ldots, x_{n0}))^T$, $x_{10} > 0$, …, $x_{n0} > 0$, $W^i(t) = \left(W_1^i(t), \ldots, W_n^i(t)\right)^T$ are independent n-variate Brownian motions, φ_j^i, i=1, ..., M; j=1, ..., n are independent and normally distributed random variables with zero mean and constant variances ($\varphi_j^i \sim N\left(0; \sigma_j^2\right)$), $\theta \equiv \{\alpha_1, \ldots, \alpha_n, \beta_1, \ldots, \beta_n, B, \sigma_1, \ldots, \sigma_n\}$ is a set of fixed effect parameters to be estimated, the drift vector $A(x)$ and diffusion matrix G(x) are defined, respectively

$$A(x) = \left(\left(\left(\alpha_1 + \varphi_1^i\right) - \beta_1 \ln(x_1)\right) x_1, \ldots, \left(\left(\alpha_n + \varphi_n^i\right) - \beta_n \ln(x_n)\right) x_n\right)^T, \tag{2}$$

$$G(x) = \left(D(x)B^{\frac{1}{2}}\right)\left(D(x)B^{\frac{1}{2}}\right)^T = \begin{pmatrix} x_1 & \cdots & 0 \\ \vdots & & \vdots \\ 0 & \cdots & x_n \end{pmatrix} \begin{pmatrix} \sigma_{11} & \cdots & \sigma_{1n} \\ \vdots & & \vdots \\ \sigma_{1n} & \cdots & \sigma_{nn} \end{pmatrix} \begin{pmatrix} x_1 & \cdots & 0 \\ \vdots & & \vdots \\ 0 & \cdots & x_n \end{pmatrix}. \tag{3}$$

$$B = \begin{pmatrix} \sigma_{11} & \cdots & \sigma_{1n} \\ \vdots & & \vdots \\ \sigma_{1n} & \cdots & \sigma_{nn} \end{pmatrix}, D(x) = \begin{pmatrix} x_1 & \cdots & 0 \\ \vdots & & \vdots \\ 0 & \cdots & x_n \end{pmatrix},$$

Using the Itô [1] formula and transformation $Y^i(t) = \ln(X^i(t))$, Eq. (1) can be converted into a well-studied n-variate Ornstein-Uhlenbeck process [19]. Therefore, the conditional stochastic process $X(t)|X(t_0) = x_0$ has the n-variate lognormal distribution $LN_n(\mu^i(t);\; \Sigma(t))$ with the mean vector

$$\mu^i(t) = \left(\ln\left(x_{j0}\right) e^{-\beta_j(t-t_0)} + \frac{\alpha_j + \varphi_j^i}{\beta_j}\left(1 - e^{-\beta_j(t-t_0)}\right), j = 1 \ldots n\right)^T, \tag{4}$$

the variance-covariance matrix

$$\Sigma(t) = \left(\frac{1 - e^{-\left(\beta_i + \beta_j\right)(t-t_0)}}{\beta_i + \beta_j} \sigma_{ij}\right)_{1 \leq i,j \leq n}, \tag{5}$$

and the probability density function

$$f\left(x_1, \ldots, x_n, t \middle| \theta, \varphi_1^i, \ldots, \varphi_n^i\right) = (2\pi)^{-\frac{n}{2}} |\Sigma_{G3}(t)|^{-\frac{1}{2}} (x_1 \cdot \ldots \cdot x_n)^{-1} \cdot \exp\left(-\frac{1}{2}\Omega^i(x_1, \ldots, x_n, t)\right), \tag{6}$$

$$\Omega^i(x_1,\dots,x_n,t) = \left(ln(x_j) - \mu_j^i(t),\ j=1,\dots,n\right)(\Sigma(t))^{-1}\left(ln(x_j) - \mu_j^i(t),\ j=1,\dots,n\right)^T. \tag{7}$$

According to the lognormal distribution of the random vector $\left(X^i(t)\middle|X^i(t_0)=x_0\right)$, the univariate marginal process $\left(X_j^i(t)\middle|X_j^i(t_0)=x_{j0}\right)$ (j=1,…,n), and m-variate sub-marginal processes $\left(X_{j_s}^i(t)\middle|X_{j_s}^i(t_0)=x_{j_s0}, s=1,\dots,m\right)$ (m=1, …., n-1) are also lognormal distributed, respectively, $LN_1\left(\mu_j^i(t);\ v_{jj}(t)\right)$ and $LN_m(\mu^{i,m}(t);\ \Sigma^m(t))$, where

$$\mu^{i,m}(t) = \left(ln(x_{j_s0})\, e^{-\beta_{j_s}(t-t_0)} + \frac{\alpha_{j_s}+\varphi_{j_s}^i}{\beta_{j_s}}\left(1-e^{-\beta_{j_s}(t-t_0)}\right), s=1,\dots,m\right)^T \tag{8}$$

$$\Sigma^m(t) = \left(\frac{1-e^{-\left(\beta_{i_s}+\beta_{j_s}\right)(t-t_0)}}{\beta_{i_s}+\beta_{j_s}}\sigma_{i_s j_s}\right)_{1\le s\le m} \tag{9}$$

The univariate marginal mean, median, mode, p-quantile (0<p<1) and variance trajectories $m_j^i(t)$, $me_j^i(t)$, $mo_j^i(t)$, $mq_j^i(t,p)$ and $w_j(t)$, $1\le j\le n$ are defined, respectively, by

$$m_j^i(t) \equiv E\left(X_j^i(t)\middle|X_j^i(t_0)=x_{j0}\right) = exp\left(\mu_j^i(t) + \frac{1}{2}v_{jj}(t)\right), \tag{10}$$

$$me_j^i(t) \equiv Median\left(X_j^i(t)\middle|X_j^i(t_0)=x_{j0}\right) = exp\left(\mu_j^i(t)\right), \tag{11}$$

$$mo_j^i(t) \equiv Mode\left(X_j^i(t)\middle|X_j^i(t_0)=x_{j0}\right) = exp\left(\mu_j^i(t) - v_{jj}(t)\right), \tag{12}$$

$$mq_j^i(t,p) \equiv Quantile\left(X_j^i(t)\middle|X_j^i(t_0)=x_{j0}\right) = exp\left(\mu_j^i(t) + \sqrt{v_{jj}(t)}\Phi^{-1}(p)\right), \tag{13}$$

$$w_j^i(t) \equiv Var\left(X_j^i(t)\middle|X_j^i(t_0)=x_{j0}\right) = exp\left(2\mu_j^i(t) + v_{jj}(t)\right)\cdot\left(exp\left(v_{jj}(t)\right)-1\right), \tag{14}$$

where: $\Phi^{-1}(\cdot)$is the inverse of standard normal distribution function.

The conditional distribution of $\left(X_j^i(t)\middle|X_j^i(t_0)=x_{j0}\right)$ (j=1, …., n) at a given $\left(X_{j_1}^i(t)=x_{j_1},\dots,X_{j_m}^i(t)=x_{j_m}\right)$, $1\le m\le n-1$ is a univariate lognormal $LN_1\left(\eta_j^i(t,x^m);\ \lambda_j(t)\right)$ with the mean, $\eta_j^i(t,x^m)$, $x^m=\left(x_{j_1},\dots,x_{j_m}\right)^T$, and variance, $\lambda_j(t)$ computed in the following forms

$$\eta_m^i(t,x^m) = \mu_j^i(t) + \Sigma_{jm}(t)[\Sigma_{mm}(t)]^{-1}(ln(x^m) - \mu^{i,m}(t)), \tag{15}$$

$$\lambda_j(t) = v_{jj}(t) - \Sigma_{jm}(t)[\Sigma_{mm}(t)]^{-1}\left(\Sigma_{jm}(t)\right)^T, \tag{16}$$

$$\Sigma_{jm}(t) = (v_{jj_1}(t) \quad \cdots \quad v_{jj_m}(t)), \tag{17}$$

$$\Sigma_{mm}(t) = \begin{pmatrix} v_{j_1j_1}(t) & \cdots & v_{j_1j_m}(t) \\ \vdots & & \vdots \\ v_{j_1j_m}(t) & \cdots & v_{j_mj_m}(t) \end{pmatrix} \tag{18}$$

The univariate conditional mean, median, mode, p-quantile (0<p<1) and variance trajectories $m_j^i(t,x^m)$, $me_j^i(t,x^m)$, $mo_j^i(t,x^m)$, $mq_j^i(t,x^m,p)$ and $w_j(t,x^m)$, $1\le j\le n$ are defined, respectively, by

$$m_j^i(t,x^m) \equiv E\left(X_j^i(t)\middle|X_j^i(t_0)=x_{j0}, X_{j_1}^i(t)=x_{j_1},\dots,X_{j_m}^i(t)=x_{j_m}\right) = exp\left(\eta_j^i(t,x^m) + \frac{1}{2}\lambda_j(t)\right), \tag{19}$$

$$me_j^i(t, x^m) \equiv Median\left(X_j^i(t) \middle| X_j^i(t_0) = x_{j0}, X_{j_1}^i(t) = x_{j_1}, \ldots, X_{j_m}^i(t) = x_{j_m}\right) = exp\left(\eta_j^i(t, x^m)\right), \tag{20}$$

$$mo_j^i(t, x^m) \equiv Mode\left(X_j^i(t) \middle| X_j^i(t_0) = x_{j0}, X_{j_1}^i(t) = x_{j_1}, \ldots, X_{j_m}^i(t) = x_{j_m}\right) = exp\left(\eta_j^i(t, x^m) - \lambda_j(t)\right) \tag{21}$$

$$mq_j^i(t, x^m, p) \equiv Quantile\left(X_j^i(t) \middle| X_j^i(t_0) = x_{j0}, X_{j_1}^i(t) = x_{j_1}, \ldots, X_{j_m}^i(t) = x_{j_m}\right)$$
$$= exp\left(\eta_j^i(t, x^m) + \sqrt{\lambda_j(t)}\Phi^{-1}(p)\right), \tag{22}$$

$$w_j^i(t, x^m) \equiv Var\left(X_j^i(t) \middle| X_j^i(t_0) = x_{j0}, X_{j_1}^i(t) = x_{j_1}, \ldots, X_{j_m}^i(t) = x_{j_m}\right)$$
$$= exp\left(2\eta_j^i(t, x^m) + \lambda_j(t)\right) \cdot \left(exp\left(\lambda_j(t)\right) - 1\right). \tag{23}$$

Information Interaction Measures

Population modeling is concerned with complex systems in which there are many diverse interactions, and can provide a way of understanding how size variables change over time or their multiple dependencies. The central issue in population models is the prediction of the size variables structure of individuals by modeling size distributions and the detection of multivariable dependencies of diverse kinds. Characterization the dynamic of the joint probability distribution of the size variables is the base of describing the mathematical dependency among the size variables. Shannon entropy [16] is a measure of the amount of uncertainty associated with a random variable X. Uncertainty is something which is realizable but is unknown. The Shannon entropy of a continuous random variable, X, with probability density function p(x) is defined as [20]

$$H(X) \equiv -\int_{-\infty}^{+\infty} p(x)\, ln\left(p(x)\right) dx \tag{24}$$

For the fixed effect scenario we assume that the random effects, φ_i, $i = 1, \ldots, M$, are equal its mean value $E(\varphi_i) = 0$, $\mu_j^i(t) \equiv \mu_j(t)$, $1 \leq j \leq n$. Therefore, the expressions of differential entropies (measured in nats) for univariate, m-variate ($2 \leq m \leq n$) diffusions take the following forms

$$H(X_j, t) \equiv -\int_0^{+\infty} f\left(x_j, t \middle| \hat{\theta}, 0\right) ln\left(f\left(x_j, t \middle| \hat{\theta}, 0\right)\right) dx_j = \frac{1}{2} ln\left(2\pi e v_{jj}(t)\right) + \mu_j(t), \tag{25}$$

$$H(X^m, t) \equiv -\int_{R_+^m} f\left(x^m, t \middle| \hat{\theta}, 0\right) ln\left(f\left(x^m, t \middle| \hat{\theta}, 0\right)\right) dx^m = \frac{1}{2} ln(|\Sigma^m(t)|) + \frac{m}{2} ln(2\pi e) + \sum_{s=1}^{m} \mu_{j_s}(t) \tag{26}$$

Information measures can be used to explore the presence or absence of statistical interaction between size variables. The simplest information theory measure between two variables is described by the difference between the entropy and the conditional entropy, which is named as the interaction (mutual) information and defines the information contained in one size variable about another in the following form

$$I(X_i, X_j, t) = H(X_i, t) + H(X_j, t) - H(X_i, X_j, t),\ 1 \leq i, j \leq n. \tag{27}$$

The author expects that the future development of information theory could address the concept of causality [21] that is commonly understandable as the capacity of one variable to influence another. The process of choosing between models can be performed using the normalized information measure defined as

$$NI = \frac{I(X_i, X_j, t)}{max\left(H(X_i, t), H(X_j, t)\right)},\ 1 \leq i, j \leq n. \tag{28}$$

Data and Parameter Estimators

The data used were obtained from Scots pine (Pinus sylvestris L.) stands in Lithuania [14]. The observed dataset of the diameter (D), total height (H), crown base height (CH), and crown width (CW) was obtained from the Institute of Forest Management and Wood Science at Vytautas Magnus University. The mixed effect (fixed and random) parameters of the SDE (1), were estimated using a new developed two-step approximated maximum log-likelihood procedure.

TABLE 1. Estimates of parameters.

Parameters of the drift term									
α_1	β_1	α_2	β_2	α_3	β_3	α_4	β_4		
17.5866	5.7033	17.5797	5.7879	10.4525	3.8980	6.6614	5.5462	0.6427	0.3816
Parameters of the diffusion term									
σ_{11}	σ_{12}	σ_{13}	σ_{14}	σ_{22}	σ_{23}	σ_{24}	σ_{33}	σ_{34}	σ_{44}
0.6119	0.2490	0.1092	0.5772	0.1702	0.1101	0.1765	0.1403	0.0009	1.0623
Parameters of the random effect									
σ_1	σ_2	σ_3	σ_4						
1.4052	1.3291	1.1244	0.9799						

DISCUSSION

To illustrate that the sample datasets of Scots pine trees do indeed follow the new developed mixed effect parameters marginal bivariate probability density function defined by Eq. (6) the contour plots are presented in Figure 1 for two different stands. Figure 1 shows that the marginal bivariate mixed effect parameters distribution well capture the forthcoming values from the observed dataset for both forest stands.

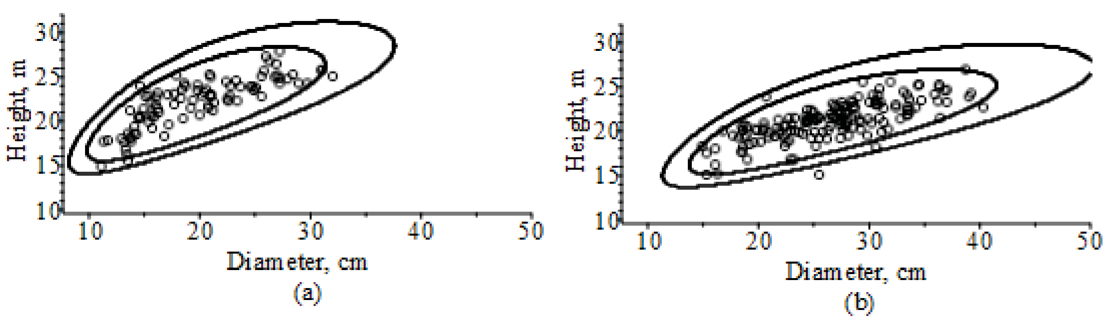

FIGURE 1. Contour plots (levels: 10^{-3}, 10^{-4}) of the estimated (see Table 1) bivariate lognormal probability density function defined by Eq. (6): (a) the first forest stand (55 years of age); (b) the second forest stand (94 years of age).

Traditionally, the used statistical metrics for goodness-of-fit linear and nonlinear regression models mostly reflect only fitting criteria (not goodness of fit). Modeling of the dynamics of the tree size variables requires better understanding which predictor exerts primary control on response tree size variable. Therefore, for the ranging of the all developed models is advisable to use normalized interaction measures defined by Eq. (28). Figure 2 shows the dynamics of the bivariate normalized information measure for the tree diameter (with predictors: height, crown base height and crown width), and two different forest stands. The higher normalized information measure value of the bivariate normalized information measure (Eq. (28)) shows stronger relationship. Hence, for the quantifying tree diameter relationship against a single predictor variable it must be the height, as the corresponding bivariate normalized information curve are on the top of the others. Eventually, for the quantifying of tree diameter relationship the worst predictor variable must be the crown base height.

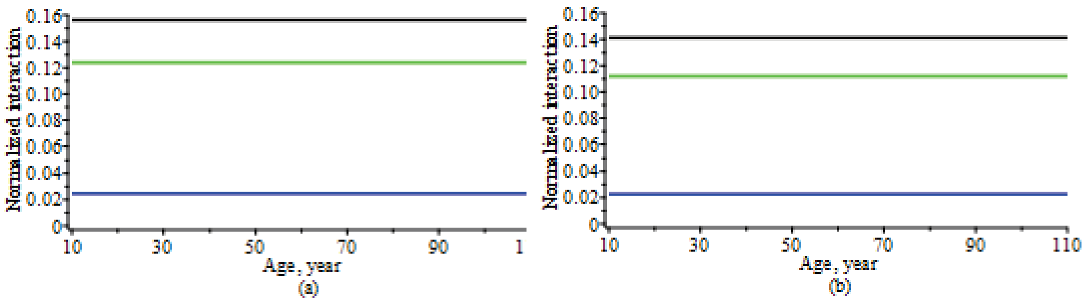

FIGURE 2. Dynamics of bivariate normalized information (Eq. 28): (a) the first forest stand (55 years of age); (b) the second forest stand (94 years of age); black color – height as a predictor for diameter; blue color – crown base height as a predictor for diameter; green color – crown width as a predictor for diameter.

REFERENCES

1. K. Itô, Jap. J. Math. **18**, 261–301 (1942).
2. L. Bachelier, Annales Scientifiques de l'École Normale Supérieure **3(17)**, 21–86 (1900).
3. A. Einstein, Annalen der Physik **17(8)**, 549–560 (1905).
4. E. J. Allen, *Modeling with Itô Stochastic Differential Equations,* Mathematical Modeling, Theory and Applications, Vol. 22. (Dordrecht: Springer, 2007).
5. B. Øksendal, *Stochastic Differential Equations: An Introduction with Applications*, 5th edition. (Berlin: Springer-Verlag, 2003).
6. E. Petrauskas, E. Bartkevičius, P. Rupšys and R. Memgaudas, Baltic For. **19**, 43–151 (2013).
7. P. Rupšys and E. Petrauskas, Sci. Rep. **7**, 12154 (2017).
8. J. Cresson and S. Sonner, Stoch. Anal. Appl. **36**, 224–239 (2018).
9. R. Gutiérrez, R. Gutiérrez-Sánchez, and A Nafidi, Res. Risk Assess. **22**, 55–66 (2008).
10. N. Cufaro Petroni, S. De Martino, and S. De Siena, arXiv:2002.06409 [math.PR] (2020).
11. G. Ascione and E. Pirozzi, Mathematics **8**, 60 (2020).
12. P. Rupšys and E. Petrauskas, J. Forest Res. Jap. **24**, 16–26 (2019).
13. P. Román-Román, J. J. Serrano-Pérez, and F. Torres-Ruiz, Mathematics **7**, 541 (2019).
14. P. Rupšys and E. Petrauskas, Forests **8**, 479 (2017).
15. E. Petrauskas, P. Rupšys, M. Narmontas, M. Aleinikovas, L. Beniušienė, and B. Šilinskas, Algorithms **13**, 94 (2020).
16. C. E. Shannon, Bell. Syst. Tech. J. **27**, 379–423 (1948)
17. P. Rupšys, AIP Conference Proceedings **2164**, 060017 (2019).
18. P. Rupšys, Mathematics **7**, 761 (2019).
19. G. E. Uhlenbeck and L. S. Ornstein, Phys. Rev. **36**, 823–841 (1930).
20. A. Lazo and P. Rathie, IEEE T. Inform. Theory **24(1)**, 120–122 (1978).
21. N. Wiener, “The Theory of Prediction,” in *Modern Mathematics for Engineers*, edited by E. F. Beckenbach (McGraw-Hill, New York, 1956), pp. 165–190.

Evaluation of Total Artificial Heart Using Multi-Criteria Decision Analysis

Ali Denker,[1, a)] Abdullah Almasri,[2, b)] and Dilber Uzun Ozsahin[3, c)]

[1)]*Department of Mathematics, Near East University, Nicosia, TRNC, Turkey*
[2)]*Department of Biomedical Engineering, Near East University, Nicosia, TRNC, Turkey*
[3)]*Experimental Health Sciences Research Centre, Near East University, Nicosia, TRNC, Turkey*

[a)]*Corresponding author: ali.denker@neu.edu.tr*
[b)]*Electronic mail: Syria-me2@hotmail.com*
[c)]*Electronic mail: dilber.uzun@neu.edu.tr*

Abstract. Heart failure is a condition that affects a great part of the world population. A heart transplant is one of the alternatives to survive heart failure. Since the organ donors are very limited and the wait list for the organ is very long it is difficult to find the organ. A viable alternative until the organ becomes available is the total artificial heart (TAH) and ventricle assisting devices. The total artificial heart is used to bridge the time to heart transplants. There are different types of artificial hearts. In this paper, we compared the various TAH devices by creating a database, and by using a simulation we determined which device is the best out in the market. We used Fuzzy Promethee as the methodology. It is observed that with pneumatic (SynCardia) TAHs as a bridge to transplant, promising results have been achieved, but still, they are not free of problems. Nevertheless, implantable total artificial hearts have a long way to go if they are to replace the natural heart permanently, made for destination therapy. So far, the only device that is commercially approved is SynCardia TAH, it's the only one in the market for patient use.

INTRODUCTION

The artificial heart may sound like science fiction, but for over 35 years they have been in clinical use to help patients with end-stage heart failure. An artificial heart is a medical device that is used to span the time to cardiac transplantation, or to replace the heart indefinitely if heart transplantation is not feasible. Plenty of problems and difficulties facing the manufacture of an artificial heart that can meet the minimum level of needs of the body to the blood. By looking at the history of the development of the artificial heart, it will be observed that the natural heart was completely dispensed at the beginning but after a while the method will be proved to be a failure which led to the death of the patient.Then a new generation of artificial hearts emerged in which the atria were maintained while pumps were installed to replace the ventricles [1]. The newest generations of the artificial heart have tended to preserve the entire heart and develop the mechanism to help ventricles contract. The problem of the heart transplant is the availability of the donor. As the number of patients suffering from heart diseases increased over the years, the global organ donors are limited [2].

MATERIAL AND METHODS

The decision making real-life challenges have multiple competing objectives and requirements to be addressed concurrently. For example, the contrast needed to strike a balance between the efficiency, safety, and cost of the total artificial heart. Different contradictions in the choosing of materials exist between material properties and efficiency metrics. We have several multi-criteria decision-making methods such as TOPSIS (Technique for Order Preference by Similarity to Ideal Solution), ELECTRE (ELimination Et Choix Traduisant la REalité), VIKOR (Vise Kriterijumska Optimizacija I Kompromisno Resenje) and PROMETHEE (Preference Ranking Organization Method for Enrichment Evaluations). In this paper, we will focus on Fuzzy Promethee. Fuzzy promethee method blends the promethee method with fuzzy logic [3].

Fuzzy logic helps decision-makers to evaluate the method even in the unclear context and transform the linguistic variable into the statistical variable in real-world situations. Hence, we can compare the fuzzy value in the Fuzzy Promethee method. The fuzzy promethee method was discussed in detail in the study conducted by Ozsahin, et al. in 2017 [4, 5]. They compared several nuclear medicine imaging devices using the Fuzzy Promethee method. The same method is used in this study to analyze the techniques for the total artificial heart.

Basic capabilities allow continuous monitoring of the right and left ventricular cardiac outputs. The right and left atrial lines provide estimates of the ventricular right and left filling pressures. An arterial line helps in the assessment

International Conference on Analysis and Applied Mathematics (ICAAM 2020)
AIP Conf. Proc. 2325, 020036-1–020036-5; https://doi.org/10.1063/5.0040596
Published by AIP Publishing. 978-0-7354-4069-2/$30.00

of blood pressure and artery structural resistance. The cardiac output sensor and diagnostic panel produce those measurements. The key role of the COMDU system is to help the consumer to visualize the flows associated with ventricular right and left filling and to track the pressure curves produced as blood is expelled from the ventricles [6].

Hemodynamic variables such as the flow (cardiac output) and press details [aortic pressure (LAP) and pulmonary artery pressure (RAP)] are required for secure closed-loop operation. For the pressure and ventricular production, we used two non-invasive hemodynamic estimators. The number alluded to in LAP is [7]:

$$\text{Pneumatic energy input} = \int LAP(t).flow(t)dt + friction = LAP.SV_1 + friction,$$

where t is the time of measurement, and LAP and SVl are the mean amount of LAP and left stroke, respectively. A mean LAP estimator may be set from this equation [8].

Estimates of the ventricular output were generated by using computational fluid dynamics techniques. Essentially, the ventricular output is found using the method of finite volume to solve the fully incompressible, three-dimensional Navier–Stokes equations in conjunction with the blood flow simulation model k-ÿ turbulence. Reynolds averaged equations in Cartesian rectangular coordinates are the governing equations used for analyzation. The Reynolds-averaged continuity and momentum equations of the tensor forms are given as follows [9]:

$$\frac{\partial}{\partial x_j}\left(\rho u_j\right) = 0,$$

$$\frac{\partial}{\partial t}\left(\rho u_i\right) + \frac{\partial}{\partial x_j}\left(\rho u_j u_i\right) = -\frac{\partial p}{\partial x_i} + \frac{\partial}{\partial x_j}\left(\mu_{eff}\left(\frac{\partial u_i}{\partial x_j}\right)\right),$$

where u_i is the x_i directional velocity component, p is static pressure, ρ is the fluid density and μ_{eff} is viscosity. In the present analysis, the $k-\varepsilon$ turbulent model along with the wall function is adopted to identify essential parameters including tension from Reynolds, turbulent energy flux, and viscous job fluctuating [9].

The ventricular output estimators estimate the ventricular output to the left and right for each cycle (heart-beat). As control operation is done (say, every five beats or more), if the cardiac output is less than the fixed value, inlet air pressure decreases along with a higher heart rate if necessary. Meanwhile, the controlled output is tested and adjusted by adjusting the systolic ratio, if required. When the cardiac output exceeds the fixed value, the inlet air pressure will be reduced, and the controlled output will be tested. The ventricular output estimator measures the ventricular output for each heart-beat, while the control operation is usually done every five (or more) beats and can be modified in the system to keep the control mode constant. Additionally, a limitation was imposed on the beat length variability. If the difference in the systolic period between two adjacent beats was more than 96 ms, the most recent estimate result was discarded to maintain the stability of beat to beat. By using a Fuzzy Promethee and knowledge-based control scheme as follows, the below control scheme (**TABLE 1**) can be accomplished [11, 12].

TABLE 1. The information about the TAH devices.

Device	Energy source	Volume, ml	Weight, g	Cost, $	Status
SynCardia	Pneumatic	400	160	350,000	Commercially used
Carmat	Electro-hydraulic	750	900	218,000	Clinical test
AbioCor	Electromechanical	800	1090	250,000	Late stage of trails
ReinHeart	Electromechanical	550	940	Not estimated	Early stage of trails
BiVACOR	Electrmagnetical	350	512	Not estimated	Early stage of trails

1. If CO is less than CO_{set}, then raise inlet air pressure.
2. Change the right ventricular systolic ratio to sustain a good output at any control operation.

For this research, the criteria are used for linear choice and field of indifference. The function of Preference is defined as follows [13]:

$$P_j(t_j) = \begin{cases} 0, & t_j \leq g_j, \\ (\| t_j \| - g_j)/(r_j - g_j), & g_j < t_j \leq r_j, \\ 1, & t_j > r_j. \end{cases}$$

where $t_j = q_{ij} - q_{kj}$ denote the disparity in a choice between pairs in alternatives on criterion $k_j.r_j$ and g_j is choice and the level of indifference, respectively.

Using the function of preference, we will obtain the degree of preference for a pair of alternatives on each criterion. To achieve the average degree of preference $D(M_i, M_k)$, the degree of choice will be aggregated according to the formula [7]:

$$D(M_i, M_k) = \sum_{j}^{n} \omega_j P_j(M_i, M_k),$$

where ω_j stands for the weight of g_j.

The SynCardia TAH is the only commercially used device. It has 2 sizes 70 cc 400 ml (BSA) $\geq 1.7m^2$ and for 50cc (BSA) $\leq 1.85m^2$ [13]. The 70 cc is used for males and the 50cc is used for women and adolescence. One of the advantages is a small size and lightweight device (160 g) [13]. The device is simple in which it does not have any complicated batteries and electronics [14]. It provides an individual pumping on both sides; for optimal ejection and filling. One of the drawbacks is that it's a bridge to transplant instead of destination therapy.

However, the fuzzy scale of the linguistic data used for the TAH devices is given as seen in Table 2. The Yager index has been applied for the defuzzification of the triangular fuzzy numbers, which are assigned to the linguistic data.

TABLE 2. The triangular fuzzy scale of the linguistic data

Linguistic scale for evaluation	Triangular fuzzy scale
Very High (VH)	(0.75, 1, 1)
High (H)	(0.50, 0.75, 1)
Medium (M)	(0.25, 0.50, 0.75)
Low (L)	(0, 0.25, 0.50)
Very Low (VL)	(0, 0, 0.25)

Furthermore, the life time, advantage, practicability, approvals and durability of the TAH devices are maximized while weight, size and the disadvantages of the TAH devices are minimized. And the importance weights of the criteria are selected equally. The decision maker also could get different ranking results based on the priority of the criteria.

RESULT AND DISCUSSION

In this paper the different TAH devices based on several criteria such as practicability, lifetime, weight, advantage, disadvantage, approvals, size, and durability. As shown in figure 1, the ranking of the devices starting from the left as the best and ending to the right as the worst.

TABLE 3. The ranking of the devices.

Rank	Phi	Phi+	Phi-
1-SynCardia	0,0798	0,1685	0,0887
2-Carmat	0,0707	0,1647	0,0940
3-BiVACOR	0,0239	0,1340	0,1101
4-AbioCor	-0,0006	0,1263	0,1269
5-ReinHeart	-0,1738	0,0283	0,2021

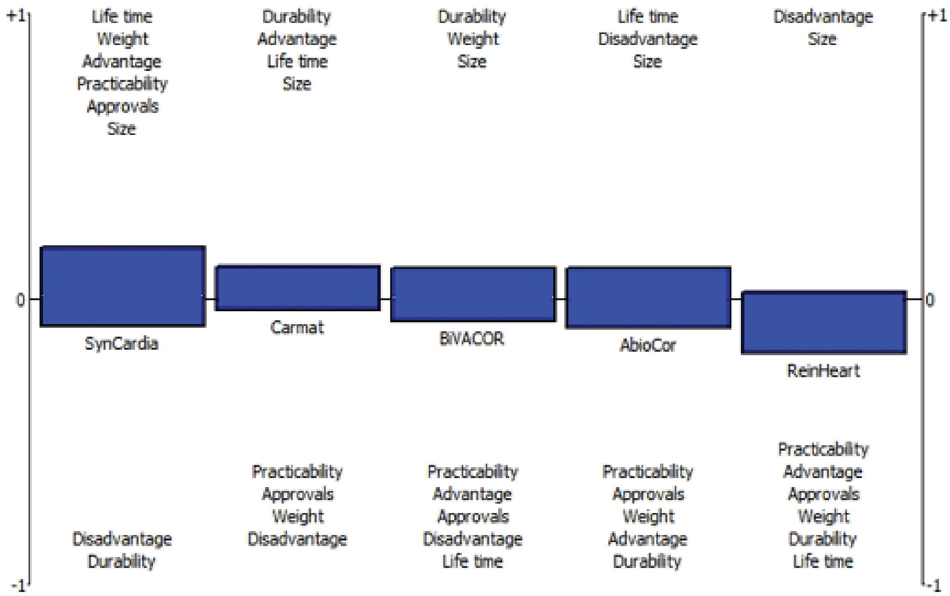

FIGURE 1. The chart compares the TAH devices based on several criteria

The Syncardia TAH is still the only satisfactory TAH despite the pneumatic drive. For addition, there is a larger capacity of ReinHeart TAH pump machine. The surgical procedure is much more complex, together with the additional implantable components. On the other side, pericardium and lungs may not occupy the empty gap between the Syncardia ventricles. This may become a source of infection due to clot and debris accumulation.

The TET system's outer coil may be misaligned or detached. The internal battery provides power for up to 45 minutes in the case of disconnection. Without the additional equipment, we agree that this length is appropriate for the patient's body treatment. The expected service period of up to 12h for two external battery packs is equivalent to the state of the art LVAD(Left Ventricular Assist Device) and TAH devices [20]. Nevertheless,implantable total artificial hearts have a long way to go if they are to replace the natural heart permanently, made for destination therapy. Problems such as management of anti-coagulation, size, energy, biocompatibility, and durability continue to be a challenge. TAH is currently used as a bridge to transplantation instead of destination therapy. The AbioCor is in the process of being approved by the Food and Drug Administration (FDA), but complications on its atrial attachments associated with thromboembolic events and thrombus formation must be resolved before market and professional approval is received. Other devices like Carmat TAH solved the thromboembolic events by having a membrane that is made of bovine pericardial tissue treated fabric but it's still undergoing feasibility studies. So far, the only device that is commercially approved is SynCardia TAH, it's the only one in the market for patient use. Bioengineering research offers promising alternatives for optimizing the hemodynamics of TAH and achieving a high degree of natural heart physiological and functional mimicry. TAH research remains an open avenue for creative minds, carrying forward a bright future.

CONCLUSION

The pneumatic driver generates high noise that can interrupt the patient and the surrounding people. SynCardia TAH has several approvals such as FDA, Health Canada, and European CE mark. Carmat is still undergoing feasibility studies [16]. The device is biocompatible since the membrane and valves are obtained from bovine. It makes the patients less dependent on anti-coagulation drugs. The device has sensors to track the pressure. The information is delivered to the internal control system to modify the flow rate, for example when patient exercise [17]. The system is self-regulated, based on the need of the patient. As in SynCardia TAH, it's not completely implanted in the patient's body; carrying the driver all the time can impair the patient's mobility [15]. BiVACOR is in the early stage of animal trails. It has intelligent controllers to adjust the action of the pump to alter the condition of the user. The device is highly durable since the device life is up to more than 10 years [18]. The Abiocor lack trans-corporeal wires or tubing in which greatly reduces the risk of infection and increases the mobility of patients. It has a large device size in which it does not suit children and women. The durability and bio compatibility of the device are uncertain and can cause thrombosis and mortality threats. The TET device (Transcutaneous Energy Transmission) uses about 40% of the external battery capacity, which allows the patient to carry heavy portable batteries. The internal battery has a short life, which must be replaced every 1-2 years, requires surgery. Reinheart is in the early stage of animal trails. The complete unit pump configuration and fixed ventricles solved the problem of the space between the ventricles that may not be filled by the lung and pericardium. The use of the transcutaneous energy transmission system to power the inserted battery reduces the risk of permanent skin incisions causing infections. The device requires a complex surgical procedure. The patient is connected to an external drive which limits his mobility. The external battery allows the patient to disconnect the outer coil of TET system for 45 minutes only.

Although complete implantability and the TET system are encouraging, the TAH system also needs to be tested in 90-day animal testing. The Syncardia TAH is still the only satisfactory TAH despite the pneumatic drive. Also, there is a larger capacity of the Reinheart TAH pump machine. The surgical procedure is much more complex, together with the additional implantable components. On the other side, the pericardium and lungs may not occupy the empty gap between the Syncardia ventricles. This may become a source of infection due to clot and debris accumulation [19].

REFERENCES

1. R. Kormos and L. Miller, *Mechanical Circulatory Support* (Elsevier, Saunders, 2012).
2. J. G. Copeland, M. M. Levinson, T. B. Icenogle, et. al., JAMA **256(21)**, 2991-2995 (1986).
3. M. Behzadian, R. B. Kazamzadeh, et. al., Europen Journal of Operational Research **200(1)**, 198-215 (2010).
4. I. Ozsahin, T. Sharif, D. Ozsahin, and B. Uzun, Journal of Instrumentation **14**, C01019 (2019).
5. I. Ozsahin, D. Ozsahin, M. Maisaini, and G. Mok, World Cancer Research Journal **6**, e1315 (2019).
6. A. Snyder, G. Rosenberg, D. Landis, W. Weiss and W. Pierce, World Cancer Research Journal, pp. 167-190(1986).
7. I. Ozsahin, B. Uzun, N. Isa, G. Mok and D. Ozsahin, "Comparative Analysis of the Common Scintillation Crystals Used in Nuclear Medicine Imaging Devices", IEEE Xplore, (2018).
8. C. Kwan-Gett, M. Crosby, A. Schoenberg, S. Jacobsen and W. Kolff, "Control systems for artificial hearts", (1968).
9. B. McInnis, J. Wang, and G. Goodwin, "Adaptive control system for the artificial heart", IEEE Frontiers Eng Health Care Mag, (1982).
10. M. Maisaini, B. Uzun, I. Ozsahin and D. Uzun, "Evaluating Lung Cancer Treatment Techniques Using Fuzzy PROMETHEE Approach", International Conference on Theory and Applications of Fuzzy Systems and Soft Computing.
11. S. Takatani, T. Tanaka, T. Nakatani, H. Takano, T. Akutsu, H. Kohno, H. Nudeshima, and A. Takahashi, Trans. Amer. Soc. Artif. Intern. Organs **31(1)**, 45-49 (1985).
12. D. Ozsahin, N. Isa, B. Uzun and I. Ozsahin, "Effective analysis of image reconstruction algorithms in nuclear medicine using fuzzy PROMETHEE", IEEE Xplore, (2018).
13. D. Uzun and et. al., "Evaluating cancer treatment alternatives using Fuzzy PROMETHEE", International Journal of Advanced Computer Science and Applications, **8**, (2017).
14. BiVACOR. Technology. BiVACOR, "TAH", https://bivacor.com/(accessed 20 Dec. 2019).
15. S. J. Sonntag, T. A. S. Kaufmann, M. R. Büsen, M. Laumen, F. Graf, T. Linde, and U. Steinseifer, Int. J. Artif Organs **37(3)**, 241-252 (2014).
16. SynCardia, https://syncardia.com/patients/patient-resources/how-does-the-total-artificial-heart-work/ (accessed 20 Dec. 2019).
17. S. Sale and N. Smedira, Best Pract. Res. Clin. Anaesthesiol **26(2)**, 147-165 (2012).
18. The Carmat Prosthesis, "Total Artificial Heart", https://www.carmatsa.com/en/our-product/"/(accessed 20 Dec. 2019).
19. S. Young, "A new kind of artificial heart that combines synthetic and biological materials", MIT Technologiocal Review, 2013.
20. S. J. Sonntag, T. A. S. Kaufmann, M. R. Büsen, M. Laumen, T. Linde, T. Schmitz-Rode, and U. Steinseifer, J. Fluids Struct. **38**, 187-204 (2013).

On the Stability of Solution of the Parabolic Differential Equation with Time Involution

Allaberen Ashyralyev[1, 2, 3, a)] and Amer Ahmed[1, b)]

[1)]Department of Mathematics, Near East University, Nicosia, Mersin 10, Turkey
[2)]Peoples' Friendship University of Russia (RUDN University), 6 Miklukho-Maklaya St,Moscow 117198, Russian Federation
[3)]Institute of Mathematics and Mathematical Modeling, 050010, Almaty,Kazakhstan

[a)]Electronic mail: allaberen.ashyralyev@neu.edu.tr
[b)]Corresponding author: amermzory81@gmail.com

Abstract. The initial value problem for the parabolic type involutory partial differential equation is studied. Applying Green's function of space operator generated by the differential problem, we get formula for solution of this problem. The theorem on stability estimates for the solution of this problem with involution is established.

INTRODUCTION

In an experiment measuring the population growth of a species of water fleas, Nesbit (1997), used a delay differential equation model in his study. In simplified form his population equation was (see, [1, 2])

$$N'(t) = aN(t-d) + bN(t).$$

He got into a difficulty with this model because he did not have a reasonable history function to carry out the solution of this equation. To overcome this roadblock he proposed to solve a "time reversal" problem in which he sought the solution to an involutory differential equation that is neither a delay differential equation, nor a functional differential equation. He used a "time reversal" equation to get the juvenile population prior to the beginning time $t = 0$. The time reversal problem is a special case of a type of equation called an involutory differential equation. These are defined as equations of the form

$$y'(t) = f(t, y(t), y(u(t))), t \in I, y(t_0) = y_0. \tag{1}$$

Here $u(t)$ is involution function, that is $u(u(t)) = t$, and t_0 is a fixed point of u. For the "time reversal" problem, we have the simplest involutory differential equation, one in which the deviating argument is $u(t) = -t$. This function is involution since $u(u(t)) = u(-t) = -(-t) = t$.

Differential equations with involution appear in mathematical models of ecology, biology, and population dynamics (see, e.g, [3, 4, 5] and the reference given therein). In recent decades, one-dimensional partial differential equations with involution have been investigated by many scientific in papers (see, e.g. [6, 7, 8, 9, 10, 11] and the references given therein). In the study [6], the mixed problem of one dimensional parabolic equation with involution in x was investigated. Applying operator tools, the stability and coercive stability estimates in Hölder norms for the solution of this problem were established. In the paper [7], a mixed problem for two dimensional elliptic equation with involution was studied. This problem was reduced to boundary value problem for the abstract elliptic equation in Hilbert space with a self-adjoint positive definite operator. Operator tools permit us to obtain stability and coercive stability estimates in Holder norms, in one variable, for the solution. In the paper [8], a stable difference scheme for approximate solution of an elliptic equations with involution was constructed. Theorem on stability and almost coercive stability and coercive stability of this difference scheme was established. The theoretical statements for statements for the solution of this difference scheme were supported by the results of the numerical experiment. In the paper [9], a mixed problem of one dimensional hyperbolic equation with the involution in x was investigated. The stability estimates in maximum norm in t for the solution of this problem are established. In the paper [11], the theory of the basis property of eigenfunctions of second order differential operators with involution was investigated, on this basis the Fourier method was justified for solving direct and inverse problems for one dimensional parabolic equations with involution in x. The applied value of these results in their importance in the study of several mathematical models containing partial differential equations with involution in space variable. The existence and uniqueness of the solution

International Conference on Analysis and Applied Mathematics (ICAAM 2020)
AIP Conf. Proc. 2325, 020037-1–020037-6; https://doi.org/10.1063/5.0040395
Published by AIP Publishing. 978-0-7354-4069-2/$30.00

of a mixed problem for a parabolic equation with an involution in x in the form of a Fourier series were established. The classes of solvability of ill-posed problems for a parabolic equation with involution in x were considered. The questions of solvability of inverse problems for the heat equation and their fractional analogues were investigated. Solvability of inverse problems for a parabolic equation with an involution in x was proved.

As it mention before we need the values of unknown function at previous time for solving delay differential equations. There, there is important to study parabolic type differential equations with time involution. Noted that partial differential equations with time involution are not investigated before as well.

Our goal in this paper is to investigate the stability of the solution of the initial value problem for the parabolic type involutory partial differential equation

$$\begin{cases} \frac{\partial v(t,x)}{\partial t} - \frac{\partial^2 v(t,x)}{\partial x^2} - b\frac{\partial^2 v(-t,x)}{\partial x^2} = f(t,x), \\ t,x \in I = (-\infty,\infty), \\ v(0,x) = \varphi(x), x \in I = (-\infty,\infty). \end{cases} \tag{2}$$

Here $f(t,x)\,(t,x \in I)$ and $\varphi(x)$ are given smooth functions and $|b| > 1$. Applying Green's function of space operator generated by problem (2), we get formula for solution of this problem. The theorem on stability of the solution of this problem under the condition $|b| > 1$ is established.

It is well-known that, methods of finding Green's function of operator with involution and without involution are different. Therefore, we obtain formula of solution of problem (2) involving the Green's function of operator with involution.

Problem (2) can be written as abstract initial value problem

$$\begin{cases} \frac{dv(t)}{dt} + Av(t) + bAv(-t) = f(t), t \in I \\ \\ v(0) = \varphi \end{cases} \tag{3}$$

in a Hilbert space $H = L_2(I)$ of all square integrable functions $\psi(x)$ defined on I equipped with the norm

$$\|\psi\|_{L_2(I)} = \left\{ \int_{-\infty}^{\infty} \psi^2(x)\,dx \right\}^{1/2}.$$

Here, positive operator A defined by the formula

$$Au = -u''(x)$$

with domain $D(A) = \{u : u(x), u''(x) \in L_2(I)\}$, $f(t) = f(t,x)$ and $v(t) = v(t,x)$ are known and unknown abstract functions with values in $L_2(I)$ and $\varphi = \varphi(x)$ is the unknown element of $L_2(I)$. Now, we will obtain the initial value problem for the second order differential equation equivalent to problem (3) under smoothness conditions of solution.

Using initial condition and equation in problem (2), we get

$$v(0) = \varphi, v'(0) = f(0) - (1+b)A\varphi. \tag{4}$$

Differentiating equation (2), we get

$$v''(t) = bAv'(-t) - Av'(t) + f'(t). \tag{5}$$

Substituting $-t$ for t into equation (2), we get

$$v'(-t) = -bAv(t) - Av(-t) + f(-t). \tag{6}$$

Using these equations, we can eliminate $v(-t)$ and $v'(-t)$ terms. Actually, using equations (5) and (6), we get

$$v''(t) = -b^2A^2v(t) - bA^2v(-t) + bAf(-t) - Av'(t) + f'(t).$$

Using that and equation (2), we get

$$v''(t) = -b^2A^2v(t) + A\left[v'(t) + Av(t) - f(t)\right] + bAf(-t) - Av'(t) + f'(t)$$

or

$$v''(t) + \left(b^2-1\right)A^2v(t) = -Af(t) + bAf(-t) + f'(t). \tag{7}$$

So, we get the initial value problem (4) and (7) for the second order differential equation in a Hilbert $H = L_2(I)$. It is easy to see that

$$\frac{d^2v(t)}{dt^2} + \left(b^2-1\right)A^2v(t) = \left(\frac{d}{dt} + i\sqrt{b^2-1}A\right)\left(\frac{d}{dt} - i\sqrt{b^2-1}A\right)v(t).$$

Therefore, problem (4) and (7) can be written as abstract initial value problem

$$\begin{cases} \frac{d}{dt}v(t) + \sqrt{b^2-1}iAv(t) = u(t), v(0) = \varphi, \\ \frac{d}{dt}u(t) - \sqrt{b^2-1}iAu(t) = F(t), \\ F(t) = -Af(t) + bAf(-t) + f'(t), t \in I, \\ u(0) = f(0) - (1+b)A\varphi + i\sqrt{b^2-1}A\varphi \end{cases} \tag{8}$$

for the system of first order abstract differential equations in a Hilbert $H = L_2(I)$. Integrating these equations, we can write

$$\begin{cases} v(t) = e^{-i\sqrt{b^2-1}tA}\varphi + \int\limits_0^t e^{-i\sqrt{b^2-1}(t-y)A}u(y)\,dy, \\ u(t) = e^{i\sqrt{b^2-1}tA}\left[f(0) - (1+b)A\varphi + i\sqrt{b^2-1}A\varphi\right] \\ +\int\limits_0^t e^{i\sqrt{b^2-1}(t-s)A}\left[-Af(s) + bAf(-s) + f'(s)\right]ds. \end{cases} \tag{9}$$

Therefore,

$$v(t) = e^{-i\sqrt{b^2-1}tA}\varphi + \int\limits_0^t e^{-i\sqrt{b^2-1}(t-2y)A}dy\left[f(0) - (1+b)A\varphi + i\sqrt{b^2-1}A\varphi\right]$$

$$+\int\limits_0^t e^{-i\sqrt{b^2-1}(t-y)A}\int\limits_0^y e^{i\sqrt{b^2-1}(y-s)A}\left[-Af(s) + bAf(-s) + f'(s)\right]dsdy.$$

Making the change of the order of integration and integration by parts, we can write

$$v(t) = \frac{1}{2}\left(e^{i\sqrt{b^2-1}tA} + e^{-i\sqrt{b^2-1}tA}\right)\varphi - \frac{1+b}{2\sqrt{b^2-1}}\left(e^{i\sqrt{b^2-1}tA} - e^{-i\sqrt{b^2-1}tA}\right)\varphi$$

$$+\frac{1}{2i\sqrt{b^2-1}}\int\limits_0^t\left(e^{i\sqrt{b^2-1}(t-s)A} - e^{-i\sqrt{b^2-1}(t-s)A}\right)\left[-f(s) + bf(-s)\right]ds \tag{10}$$

$$-\frac{1}{2}\int\limits_0^t\left(e^{i\sqrt{b^2-1}(t-s)A} + e^{-i\sqrt{b^2-1}(t-s)A}\right)f(s)ds.$$

THE MAIN THEOREM ON STABILITY

Theorem 1 *Assume that* $|b| > 1$ *and* $\varphi(x) \in W_2^2(I)$ *and* $f(t,x), f_t(t,x) \in C(I, L_2(I))$. *Then, for solutions of problem (2) we have following stability estimates*

$$\sup_{t\in I} \|v(t)\|_{L_2(I)} \leq M_1 \left[\|\varphi\|_{L_2(I)} + \int_{-\infty}^{\infty} \|f(y)\|_{L_2(I)}\, dy \right], \tag{11}$$

$$\sup_{t\in I} \|v_t(t)\|_{L_2(I)} + \sup_{t\in I} \|v(t)\|_{W_2^2(I)} \tag{12}$$

$$\leq M_1 \left[\|\varphi\|_{W_2^2(I)} + \|f(0)\|_{L_2(I)} + \int_{-\infty}^{\infty} \left\|f'(y)\right\|_{L_2(I)} dy \right],$$

where M_1 *does not depend on* $\varphi(x)$ *and* $f(t,x)$. *Here,* $W_2^2(I)$ *is the Sobolev space of all square integrable functions* $\psi(x)$ *defined on* I *equipped with the norm*

$$\|\psi\|_{W_2^2(I)} = \left\{ \int_{-\infty}^{\infty} \left[\psi^2(x) + \psi_{xx}^2(x) \right] dx \right\}^{1/2},$$

$C(I, L_2(I))$ *is the Banach space of all continuous bounded in* t *and square integrable in* x *functions* $f(t,x)$ *equipped with the norm*

$$\|f\|_{C(I,L_2(I))} = \sup_{t\in I} \|f(t)\|_{L_2(I)} = \left\{ \int_{-\infty}^{\infty} f^2(t,x)\, dx \right\}^{1/2}.$$

Proof. For the self-adjoint positive definite operator A and $t \in I$, we have the following estimate

$$\left\| e^{i\sqrt{b^2-1}tA} \right\|_{H\to H} \leqslant 1. \tag{13}$$

Applying formula (10), triangle inequality and estimate (13), we get

$$\|v(t)\|_H \leq \|\varphi\|_H + \frac{|1+b|}{\sqrt{b^2-1}} \|\varphi\|_H$$

$$+ \left(1 + \frac{1+|b|}{\sqrt{b^2-1}}\right) \int_{-\infty}^{\infty} \|f(s)\|_H\, ds$$

for any $t \in I$. From that it follows estimate (11). Applying formula (10), we get

$$Av(t) = \frac{1}{2}\left(e^{i\sqrt{b^2-1}tA} + e^{-i\sqrt{b^2-1}tA}\right) A\varphi - \frac{1+b}{2\sqrt{b^2-1}} \left(e^{i\sqrt{b^2-1}tA} - e^{-i\sqrt{b^2-1}tA}\right) A\varphi$$

$$-\frac{1}{(b^2-1)}\left[f(t) - bf(-t)\right] + \frac{1}{2(1+b)}\left(e^{i\sqrt{b^2-1}tA} + e^{-i\sqrt{b^2-1}tA}\right) f(0)$$

$$+\frac{1}{2i(b^2-1)} \int_0^t \left(e^{i\sqrt{b^2-1}(t-s)A} + e^{-i\sqrt{b^2-1}(t-s)A}\right) \left[-f'(s) - bf'(-s)\right] ds \tag{14}$$

$$+\frac{1}{2i\sqrt{b^2-1}}\left(e^{i\sqrt{b^2-1}tA}-e^{-i\sqrt{b^2-1}tA}\right)f(0)$$

$$+\frac{1}{2i\sqrt{b^2-1}}\int_0^t\left(e^{i\sqrt{b^2-1}(t-s)A}-e^{-i\sqrt{b^2-1}(t-s)A}\right)f'(s)ds.$$

Applying formula (14), triangle inequality and estimate (13), we get

$$\|Av(t)\|_H\le\|A\varphi\|_H+\frac{|1+b|}{\sqrt{b^2-1}}\|A\varphi\|_H$$

$$+\left[\frac{1+|b|}{b^2-1}+\frac{1}{1+b}+\frac{1}{\sqrt{b^2-1}}\right]\|f(0)\|_H$$

$$+\left(\frac{1}{\sqrt{b^2-1}}+\frac{2(1+|b|)}{b^2-1}\right)\int_{-\infty}^{\infty}\left\|f'(s)\right\|_H ds$$

for any $t\in I$. From that it follows estimate

$$\sup_{t\in I}\|v(t)\|_{W_2^2(I)}$$

$$\le M_1\left[\|\varphi\|_{W_2^2(I)}+\|f(0)\|_{L_2(I)}+\int_{-\infty}^{\infty}\left\|f'(y)\right\|_{L_2(I)}dy\right].$$

In the same manner, we can prove that

$$\sup_{t\in I}\|v_t(t)\|_{L_2(I)}$$

$$\le M_1\left[\|\varphi\|_{W_2^2(I)}+\|f(0)\|_{L_2(I)}+\int_{-\infty}^{\infty}\left\|f'(y)\right\|_{L_2(I)}dy\right].$$

This completes the proof of Theorem 1.

Applying this approach we can obtain same stability estimates for the solution of the initial boundary value problem for the involutory parabolic type differential equation

$$\begin{cases}\frac{\partial v(t,x)}{\partial t}-\frac{\partial^2 v(t,x)}{\partial x^2}-b\frac{\partial^2 v\left(\frac{t_0}{2}-t,x\right)}{\partial x^2}=f(t,x),\\ t,x\in I=(-\infty,\infty),\\ v\left(\frac{t_0}{2},x\right)=\varphi(x),x\in I=(-\infty,\infty).\end{cases}$$

CONCLUSION

In the present paper, the initial value problem for the parabolic type involutory partial differential equation is investigated. Applying Green's function of space operator generated by this problem with time involution, we get formula for solution of this problem. The theorem on stability of the linear problem with time involution is proved. Moreover, applying the result of the monograph [12], the absolute stable difference schemes for the numerical solution of the initial value problem (2) for parabolic type involutory linear partial differential equations can be constructed and investigated.

REFERENCES

1. C. E. Falbo, Journal of Interdisciplinary Mathematics **6(3)**, 279–289 (2003).
2. R. M. Nesbit, "Delay differential equations for structured populations," (Springer, Boston, MA, 1997) pp. 89–118.
3. D. Przeworska-Rolewicz, *Equations with Transformed Argument: Algebraic Approach* (North-Holland, Amsterdam, 1997).
4. J. Wiener, *Generalized Solutions of Functional Differential Equations* (World Scientific, 1993).
5. A.Cabada and F. Tojo, *Differential Equations with Involution's* (Atlantis Press, 2015).
6. A. Ashyralyev and A. M. Sarsenbi, Numerical Functional Analysis and Optimization **38(10)**, 1295–1304 (2017).
7. A. Ashyralyev and A. M. Sarsenbi, Electronic Journal of Differential Equations **248**, 8 (2015).
8. A. Ashyralyev and B. Karabaeva, AIP Conf. Proc **1759**, 020111 (1983).
9. A. Ashyralyev and A. M. Sarsenbi, Springer Proceedings in Mathematics and Statistics **216**, 204–212 (2017).
10. A. A. Sarsenbi, *Well-Posedness of Mixed Problems for Parabolic type with Involution*, Phd thesis, CSU, Kazakhstan (2019).
11. A. Ashyralyev and T. Abbas, AIP Conf. Proc. **2183**, 070015 (2019).
12. A. Ashyralyev and P. E. Sobolevskii, *New Difference Schemes for Partial Differential Equations* (Birkhäuser Verlag, Basel, Boston, Berlin, 2004).

Determining the Awareness of Users Towards E-Signature: A Scale Development Study

Nuriye Sancar[1, 2, a)] and Nadire Cavus[2, 3, b)]

[1)]*Department of Mathematics, Near East University, Nicosia, TRNC, Turkey*
[2)]*Computer Information Systems Research and Technology Centre, Near East University, Nicosia, TRNC, Turkey*
[3)]*Department of Computer Information Systems, Near East University, Nicosia, TRNC, Turkey*

[a)]*Corresponding author: nuriye.sancar@neu.edu.tr*
[b)]*Electronic mail: nadire.cavus@neu.edu.tr*

Abstract. The necessity of e-signature has been accepting by all organizations like finance, education, business. With the effect of this, the popularity has been increasing day by day especially uncertainty times such as the Covid-19 pandemic. However, there is a missing gap in the literature about e-signature studies. The literature review showed that the studies on e-signature awareness and the benefits of e-signature usage in any organization or/and the person are not enough. For this reason, the purpose of the study is to develop a valid and reliable scale to use in scientific studies to understand the awareness of users towards e-signature. Therefore, both validity and reliability of scale have been investigated. Through the exploratory factor analysis, the AoE-sign scale has 16 items and 2 subfactors which are "Awareness" and "Benefits". The factor analysis results indicated that Cronbach Alpha for Awareness was .888, for Benefits was .790 and for the overall scale was .889. Consequently, the study results demonstrated that the AoE-sign scale is reliable and valid tool and the developed scale could be used by top-level managers, in developing countries such as Cyprus, to be able to understand the awareness level of users. Moreover, they can organize staff training on e-signature to make it possible to use e-signature efficiently in the organizations.

INTRODUCTION

Digital transformation is affecting all sectors all over the world. The results of the scientific researches showed that new technologies made human life more easy, fast and secure than traditional tools and methods. In today's information society, all organizations' aim is to increase their competitiveness, and move quickly [1]. In order for the transactions to be carried out, it brings out the need for urgent approvals of the authorized person just on the needed time. For this reason, approval processes, namely the signature process, also need to be digitalized. Digital signatures usage has some benefits for the user such as increasing the speed of transactions [2] as well as and increasing security [3] and reducing costs [4]. For this purpose, free and commercial digital signature software such as DocuSign, PandaDoc, SignEasy, etc. were developed to create, manage, and sign documents online from anywhere, anytime on any device like laptop, PC, smart phones etc. However, to adopt and use digital signature software, the user must know that they will facilitate the importance and benefits for their life. For this reason, it is very important to determine the awareness of users towards e-signature. However, when the literature was examined, it was determined that the scale studies prepared in this direction were not sufficient. For this reason, the scale named AoE-sign, has been developed in this study to understand the awareness of users towards e-signature. The literature indicated that the reliability and validity studies must be investigated to develop a quality scale. The aim of this study is to develop a valid and reliable scale for understanding the awareness of users towards e-signature. Thus, the process of this current study was constructed to investigate the reliability and validity of the scale for the awareness of users towards e-signature (AoE-sign).

MATERIAL AND METHODS

The process of this study was described in details in this part. Participants (n = 278) (53.2% (male), 46.8% (female)) were determined by convenience sampling and were voluntarily participating where n is number of participants. All participants were between the ages of 18 and 35 years.

Data Analysis

SPSS 23 software was used in the analysis process. In this process, Exploratory factor analysis(EFA) was used to investigate the characteristics of the scale for the construct validity. For the evaluation of the reliability of the scale, Cronbach's alpha and Sperman-Brown coefficient were calculated as internal consistency coefficients. Moreover, item analysis was applied with corrected item-total correlation and Cronbach's alpha if item deleted.

International Conference on Analysis and Applied Mathematics (ICAAM 2020)
AIP Conf. Proc. 2325, 020038-1–020038-4; https://doi.org/10.1063/5.0040408
Published by AIP Publishing. 978-0-7354-4069-2/$30.00

Exploratory Factor Analysis

Factor analysis is a technique used to determine whether a number of variables (or items) $X_1, X_2, \ldots, X_p$ are linearly correlated to a lower number of factors $F_1, F_2, \ldots, F_k$,where $k < p$. The logic is that there are underlying factors and some variables can be measures of the identical factors. In this method, the variables are linear combinations of the underlying factors. Factor analysis utilizes mathematical procedures to facilitate correlated measures to explore model in a group of variables [5].

In the factor analysis model, it is assumed that there are p variables and k factors ,where k<p. In this model, the variables $X_1, X_2, \ldots, X_p$, taken from a population with mean vector μ and variance matrix $\sum$. For each variable X_i, the factor analysis model is defined as:

$$X_1 = \mu_1 + \lambda_{11} F_1 + \lambda_{12} F_2 + \cdots + \lambda_{1k} F_k + e_1,$$

$$X_2 = \mu_2 + \lambda_{21} F_1 + \lambda_{22} F_2 + \cdots + \lambda_{2k} F_k + e_2,$$

$$\cdots$$

$$X_p = \mu_p + \lambda_{p1} F_1 + \lambda_{p2} F_2 + \cdots + \lambda_{pk} F_k + e_p,$$

where F_k are factors and e_p are error terms. In the model, the λ_{ij} s are factor loadings that shows the contribution of the common factor j on the variable i. The model assumes that the $e_i s$ are independent and $E(e_i) = 0$ and $Var(e_i) = \psi_i$. And another assumption is about the factors. The factors $F_j s$ are independent and $E(F_j) = 0$ and $Var(F_j) = 1$. And additionally, $Cov(F_i, F_j) = 0, Cov(e_i, F_j) = 0, and Cov(e_i, e_j) = 0$. According to these assumptions, $Var(X_i)$ is obtained as

$$Var(X_i) = \sum_{m=1}^{k} \lambda_{im}^{k} + \psi_i. \tag{1}$$

From the Equation (1), it is seen that $Var(X_i)$ has two parts: The first part, $Var(X_i) = \sum_{m=1}^{k} \lambda_{im}^{k}$ is the communality (or common variance) of the variable. It is the proportion of the variance of each variable that is accounted by the factors. It is denoted by h^2 and defined as the total of square of the factor loadings for the variable. The second part of $Var(X_i)$, ψ_i is residual variance, the variance of the error term e_i.
The factor analysis model can also be defined as matrix form as in Equation (2):

$$x = \mu + \Lambda F + e, \tag{2}$$

where $X = (X_1, X_2, \ldots, X_p)'$, $\mu = (\mu_1, \mu_2, \ldots, \mu_p)'$, $F = (F_1, F_2, \ldots, F_k)'$, $e = (e_1, e_2, \ldots, e_p)'$ and $\Lambda = (\lambda_{ij})$ with $i = 1, 2, \ldots, p$ and $j = 1, 2, \ldots, k$. And covariance matrix is defined as

$$Var(X) = \Lambda \Lambda' + \psi, \tag{3}$$

where $\Psi = diag(\psi_1, \psi_2, \ldots., \psi_p)$. There are several methods for estimation of the factor loadings Λ and communalities in factor analysis. These are principal component method, principal factor solution, and maximum likelihood method. The most commonly preferred method is the principal component method. This method investigates the values of factor loadings by estimating the total common variance (or communality) fairly close to the sum of the oberved variances. Principal components are described as linear combinations of the variables, factors are described as linear combinations of the underlying variables. The principal component method is used to obtain the sample covariance matrix S from a sample of data and after achieve an estimator $\hat{\Lambda}$. The sample covariance matrix $S \approx \hat{\Lambda}\hat{\Lambda}'$ is defined in the form of singular value decomposition (SVD) as in Equation (4):

$$S = CKC' = CK^{(1/2)} K^{(1/2)} C', \tag{4}$$

where C is an orthogonal matrix of eigenvectors of S and $K = diag(\theta_1, \theta_2, \ldots, \theta_p)$ represents diagonal matrix of eigenvalues $\theta_1, \theta_2, \ldots, \theta_p$ of S. In $SVD, CK^{(1/2)}$ is matrix with order pxp. However, $\hat{\Lambda}$ is order of pxk. Thus, the first k columns of $CK^{(1/2)}$ to describe $\hat{\Lambda}$ with $\theta_1 > \theta_2 > \cdots > \theta_k$. There are several ways to choose the number of factors. Some of these ways are exploring the number of eigenvalues higher than the mean eigenvalue or plotting a scree plot. Factor analysis may not be suitable for all data structures. The suitability of the data for factor analysis can be examined with the Kaiser-Meyer-Olkin (KMO) coefficient and Barlett sphericity test. The KMO coefficient gives information about whether the data matrix is suitable for factor analysis and the suitability of the data structure for factor extraction as the measure of the adequecy of sampling. The KMO index is calculated as

$$KMO = \frac{\sum_i \sum_{i \neq j} {r_{ij}}^2}{\sum_i \sum_{i \neq j} {r_{ij}}^2 + \sum_i \sum_{i \neq j} {b_{ij}}^2}, \tag{5}$$

where the correlation matrix is R= (r_{ij}), the inverse of the correlation matrix $R^{(-1)} = (g_{ij})$, and partial correlarion matrix is $B = (b_{ij})$, $b_{ij} = \frac{-g_{ij}}{\sqrt{(g_{ij} * g_{ij})}}$. For factorability, KMO is expected to be higher than 0.60. Approach of KMO values to zero indicates that there exist high partial correlations when compared to total correlations.
Barlett sphericity test examines whether there is a relationship between variables on the basis of partial correlations. If the calculated chi-square statistic is significant, then it is an indicator that the data matrix is suitable. The significant test result can also be seen as an indicator of the normality of the scores. The Barlett's test statistic is calculated by:

$$\chi^2 = -\left(n - 1 - \frac{2p+5}{6}\right) x \ln \left|R\right| \tag{6}$$

with $\left[px\frac{(p-1)}{2}\right]$ number of degrees of freedom where p is the number of variables.
The researcher can be subjected to an axis rotation to provide dependence, clarity, and significance in interpretation of k important factors obtained by applying a factor analysis technique [6]. There are two types of rotation approaches, orthogonal and oblique. In orthogonal rotation, factors are rotated by the same angle without changing the position of the axes. In oblique rotation, which is based on the idea that the factors are related to each other, the rotation is done at different angles. There are different techniques for the orthogonal rotation such as varimax, quartimax and for oblique rotation such as oblimin, promax.
Another important point in factor analysis is the quality of the factor model, in other words, its reliability. There are numerious criteria for the reliability of the factor model. The internal consistency reliability is commonly provided by Cronbach's alpha coefficient (α) [7]. Cronbach's alpha usually increases if the correlations between the variables increase. Therefore, this coefficient measures the internal consistency of the test or scale. For the given $X_1, \ldots, X_p$ and $X_t = \sum_{j=1}^{p} X_j$, Cronbach's alpha coefficient is obtained as

$$\alpha = \frac{p}{p-1}\left(1 - \frac{\sum_{j=1}^{p} var(X_j)}{var(X_t)}\right). \tag{7}$$

It is a generally accepted rule that Cronbach's alpha coefficient is 0.70 and above for the internal consistency.

RESULTS

EFA was performed to explore the underlying factor structure of the scale using principal-components analysis with oblimin rotation. In EFA, the factors of the scale were determined based on eigenvalues>1 and scree-plot. The factorability of the 20 items of the scale was investigated. KMO measure of sampling adequacy and Bartlett's test of sphericity were computed to ensure that the characteristics of the data were suitable for the factor analysis. KMO was .890, indicating that sample size is sufficient for the analysis. Bartlett's test of sphericity result was significant (χ^2=1793;df=120; p $<$ 0.001), indicating that the data has multivariate normal distribution and is appropriate for the analysis. This research took 0.4 as the threshold value of factor loadings and factor loadings lower than 0.4 were not used. Any item with communality values lower than 0.2 were removed from the analysis (Child 2006). One item was removed, as the factor loading was low, at 0.31. It is also seen that 3 items had relatively high load values in both factors according to EFA results obtained. It was deemed appropriate to exclude these items, which have high load values in both factors. The remaining 16 items were clustered under two factors based on the number of eigenvalues that are higher than or equal to 1.0. The variance explained by these two factors for the scale is 50.483%. The eigenvalues showed that the first factor, which was determined to be important, explained 38.225% of the total variance regarding the scale, and 12.258% of the variance was explained by the second factor. Similarly, scree plot analysis results supported a two factor solution. When the items are examined in the first factor and the second factor, respectively, subfactor 1 with 9 items was renamed “awareness” and “benefit” for subfactor 2 with 7 items. Item factor loadings ranged from .433 to .838 and communalities ranged from 0.312 to 0.649. The Cronbach’s alpha of the overall 16-item AoE-sign scale was 0.889 indicating good internal consistency. Both AoE-sign subscales indicated good internal consistency with Cronbach’s alpha value of 0.888 (awareness; 9 items) to 0.790 (benefits; 7 items). It was observed that the corrected item-total corelation ranged between 0.353 and 0.680, for all items in the AoE-sign scale. The corrected item-total correlation values of the items in the scale were observed to be higher than the threshold value, 0.3 (expected to be higher than 0.3). Also, the corrected item-total correlation of overall items were above 0.3 for both subscales. In addition, Cronbach’s Alpha value found when the items in the scale were deleted separately were not greater than the Cronbach’s alpha of the overall 16-items of 0.889. At the same time, there was no increase in Cronbach’s alpha value by removing any item for both subscales. These results of item analysis indicated that overall 16-items should remain in AoE-sign scale. These findings can be interpreted as the items in the scale have high validity and are items aimed at measuring the same behavior.

CONCLUSION

In the digitalizing world, the need for e-signature usage is increasing day by day and even its use has become a necessity. Everyday, many documents need to be signed and the business process should be shaped. It is difficult to reach the authorized person by manual to obtain their approval, i.e., their signature. It is even seen that there are problems in the work-flow due to this. For this reason, there is an urgent necessity for business users to create awareness about e-signature and to ensure that those who do not use digital signature use it with the necessary assistance. For this purpose, a developed scale consists of 16 items, through EFA, the “Scale for the Awareness of Users towards E-Signature” was validated in two factors: “Awareness,” and “benefits”. The developed scale is suitable for developing countries like Cyprus. The results of the analysis showed that the reliability and validity of this scale met all the necessary criteria. Therefore, the AoE-sign scale can be scientifically used to identify the level of the users’ awareness of e-signature. In the future, we are planning to use the AoE-sign scale in the study to investigate the users’ who are working at the different sectors in different countries all around the world, awareness towards e-signature.

ACKNOWLEDGMENTS

The researchers would like to express their sincere thanks to Hamza Wahab who help to collect data for this study.

REFERENCES

1. S. Aydın, H. Çam and N. Alıpour, Journal of Economics Bibliography, **5(4)**, 238-252 (2018).
2. E. Paul, "What is digital signature-how it works, benefits, objectives, concept" (2017).
3. R. Publico, "Why you should adopt digital signatures for your paperless office" (2017).
4. J. Lunttila, "Digital signature: Adoption, technology, costs & benefits", Master thesis, Lappeenranta-Lahti University of Technology, Lut School of Business and Management (2019).
5. D. Child, *The Essentials of Factor Analysis* (Continuum International Publishing Group, New York, NY, 2006).
6. Ş. Büyüköztürk, *Sosyal Bilimler İçin Veri Analizi El Kitabı* (Pegem Akademi, Ankara, 2018) (in Turkish).
7. L. Cronbach, Psychometrika **16**, 297–334 (1951).

Existence and Uniqueness of Solution of Fractional Order Covid-19 Model

Evren Hincal,[1, 2, a)] Sultan Hamed Alsaadi,[1, b)] and Nezihal Gokbulut[2, c)]

[1)] *Department of Mathematics, Near East University, Nicosia, Mersin 10, Turkey*
[2)] *Mathematics Research Center, Near East University, Nicosia, Mersin 10, Turkey*

[a)] *Corresponding author: evren.hincal@neu.edu.tr*
[b)] *Electronic mail: alsaad99@hotmail.com*
[c)] *Electronic mail: nezihal.gokbulut@neu.edu.tr*

Abstract. In this paper, a fractional order mathematical model is constructed to study the dynamics of coronavirus. The model consists of a system of eight non-linear fractional order differential equations in Caputo sense. Existence and uniqueness of the solution of the model are studied.

INTRODUCTION

Some epidemic diseases are capable of producing large number of infections starting from a fewer ones, an example of such diseases is Covid-19 [1]. Coronavirus disease is an inspiratory and zoonotic disease, caused by a virus of the coronaviridae family which originated in the city of Wuhan China on December 01, 2019 [2]. The virus strain is severe acute respiratory syndrome coronavirus 2 (SARS-CoV-2), resulting in fever, coughing, breathing difficulties, fatigue, and myalgia. It may transform into pneumonia of high intensity.
We need modelling approach to understand the exact dynamics of the disease. This is what motivates this research. It is important to note that, in the classical order model, the state of epidemic model does not depend on its history. However, in real life memory plays a vital role in studying the pattern of spread of any epidemic disease. It was found that the waiting times between doctor visits for a patient follow a power law model [4]. It is worth to know that Caputo fractional time derivative is a consequence of power law [5]. When dealing with real world problem Caputo fractional-order derivatives allows traditional initial and boundary conditions. Furthermore, due to its non-local behavior and its ability to change at every instant of time Caputo fractional-order gives better result than the integer order.
The aim of this research is to study existence and uniqueness of solution of fractional order epidemic model that investigates the dynamics of Covid-19. Based on the memorability nature of Caputo fractional-order derivatives, this model can be fitted with data reasonably well.

FORMULATION OF THE MODEL

Let the total population be $N(t)$. The population is divided into eight compartments, namely; susceptible population $S(t)$, exposed population $E(t)$, asymptomatic infective population $I_A(t)$, symptomatic infective population $I_S(t)$, isolated infective population $I_I(t)$, hospitalized infective population $I_H(t)$, recovered population $R(t)$, and dead individuals $D(t)$. The dynamics of this population is represented by the following system of fractional order differential equations (FODE) and the meaning of parameters is given in Table 1.

$$\begin{cases} {}^{C}\mathscr{D}^{\upsilon}_{0^+}S(t) = -\beta S(\alpha I_A + \xi I_I + I_S), \\ {}^{C}\mathscr{D}^{\upsilon}_{0^+}E(t) = \beta S(\alpha I_A + \xi I_I + I_S) - kE, \\ {}^{C}\mathscr{D}^{\upsilon}_{0^+}I_A(t) = (1-p)kE - \gamma_A I_A, \\ {}^{C}\mathscr{D}^{\upsilon}_{0^+}I_S(t) = pkE - qI_S, \\ {}^{C}\mathscr{D}^{\upsilon}_{0^+}I_I(t) = q(1-\Psi)I_S - (\gamma_S + \mu_S)I_I, \\ {}^{C}\mathscr{D}^{\upsilon}_{0^+}I_H(t) = q\Psi I_S - (\gamma_H + \mu_H)I_H, \\ {}^{C}\mathscr{D}^{\upsilon}_{0^+}R(t) = \gamma_A + \gamma_S + \gamma_H, \\ {}^{C}\mathscr{D}^{\upsilon}_{0^+}D(t) = \mu_S)I_S + \mu_H I_H. \end{cases} \tag{1}$$

International Conference on Analysis and Applied Mathematics (ICAAM 2020)
AIP Conf. Proc. 2325, 020039-1–020039-4; https://doi.org/10.1063/5.0040302
Published by AIP Publishing. 978-0-7354-4069-2/$30.00

TABLE 1. Description of the parameters.

Parameters	Descriptions
β	effective contact rate
α	reduction of infectiousness in asymptomatic people
ξ	reduction of infectiousness in isolated people
k	progression from exposed to infectious class
p	proportion of asymptomatic cases
q	progression from asymptomatic unaware to self-isolated
Ψ	proportion of hospitalized people
$\gamma_A, \gamma_S, \gamma_H$	recovery rate for asymptomatic, symptomatic and hospitalized individuals respectively
μ_S, μ_H	mortality rate in isolated and hospitalized classes

EXISTENCE AND UNIQUENESS RESULTS

The theory of existence and uniqueness of solutions is one of the most dominant fields in the theory of fractional-order differential equations. The theory has recently attracted the attention of many researchers, we are referring to [6] and the references therein for some of the recent growth.

In this section, we discuss the existence and uniqueness of solution of the proposed model using fixed point theorems. Let us reformulate the proposed model (1) in the subsequent form

$$\begin{cases} {}^{C}\mathscr{D}^{\upsilon}_{0^+}S(t) = \Theta_1(t,S,E,I_A,I_S,I_I,I_H,R,D), \\ {}^{C}\mathscr{D}^{\upsilon}_{0^+}E(t) = \Theta_2(t,S,E,I_A,I_S,I_I,I_H,R,D), \\ {}^{C}\mathscr{D}^{\upsilon}_{0^+}I_A(t) = \Theta_3(t,S,E,I_A,I_S,I_I,I_H,R,D), \\ {}^{C}\mathscr{D}^{\upsilon}_{0^+}I_S(t) = \Theta_4(t,S,E,I_A,I_S,I_I,I_H,R,D), \\ {}^{C}\mathscr{D}^{\upsilon}_{0^+}I_I(t) = \Theta_5(t,S,E,I_A,I_S,I_I,I_H,R,D), \\ {}^{C}\mathscr{D}^{\upsilon}_{0^+}I_H(t) = \Theta_6(t,S,E,I_A,I_S,I_I,I_H,R,D), \\ {}^{C}\mathscr{D}^{\upsilon}_{0^+}R(t) = \Theta_7(t,S,E,I_A,I_S,I_I,I_H,R,D), \\ {}^{C}\mathscr{D}^{\upsilon}_{0^+}D(t) = \Theta_8(t,S,E,I_A,I_S,I_I,I_H,R,D), \end{cases} \tag{2}$$

where

$$\begin{aligned} \Theta_1(t,S,E,I_A,I_S,I_I,I_H,R,D) &= -\beta S(\alpha I_A + \xi I_I + I_S), \\ \Theta_2(t,S,E,I_A,I_S,I_I,I_H,R,D) &= \beta S(\alpha I_A + \xi I_I + I_S) - kE, \\ \Theta_3(t,S,E,I_A,I_S,I_I,I_H,R,D) &= (1-p)kE - \gamma_A I_A, \\ \Theta_4(t,S,E,I_A,I_S,I_I,I_H,R,D) &= pkE - qI_S, \\ \Theta_5(t,S,E,I_A,I_S,I_I,I_H,R,D) &= q(1-\Psi)I_S - (\gamma_S + \mu_S)I_I, \\ \Theta_6(t,S,E,I_A,I_S,I_I,I_H,R,D) &= q\Psi I_S - (\gamma_H + \mu_H)I_H, \\ \Theta_7(t,S,E,I_A,I_S,I_I,I_H,R,D) &= \gamma_A + \gamma_S + \gamma_H, \\ \Theta_8(t,S,E,I_A,I_S,I_I,I_H,R,D) &= \mu_S)I_S + \mu_H I_H. \end{aligned} \tag{3}$$

Thus, the proposed model (1) takes the form

$$\begin{gathered} {}^{C}\mathscr{D}^{\alpha}_{0}\Phi(t) = \mathscr{K}(t,\Phi(t)); \quad t \in J = [0,b], 0 < \alpha \leq 1, \\ \Phi(0) = \Phi_0 \geq 0, \end{gathered} \tag{4}$$

on condition that

$$\begin{gathered} \Phi(t) = (S,E,I_A,I_S,I_I,I_H,R,D)^T, \\ \Phi(0) = (S_0,S_0,I_{A0},I_{S0},I_{I0},I_{H0},R_0,D_0)^T, \\ \mathscr{K}(t,\Phi(t)) = (\Theta_i(t,S,E,I_A,I_S,I_I,I_H,R,D))^T, \ \ i = 1,\cdots,8, \end{gathered} \tag{5}$$

where $(\cdot)^T$ represents the transpose operation. In view of Theorem in [10], problem (5) is given by

$$\Phi(t) = \Phi_0 + \mathscr{J}^{\upsilon}_{0^+}\mathscr{K}(t,\Phi(t)) = \Phi_0 + \frac{1}{\Gamma(\upsilon)}\int_0^t (t-\tau)^{\upsilon-1}\mathscr{K}(\tau,\Phi(\tau))d\tau. \tag{6}$$

Let $\mathbb{E} = C([0,b];\mathbb{R})$ denotes the Banach space of all continuous functions from $[0,b]$ to R endowed with the norm defined by

$$\|\Phi\| = \sup_{t\in J}|\Phi(t)|,$$

where
$|\Phi(t)| = |S(t)|+|E(t)|+|I_A(t)|+|I_S(t)|+|I_I(t)|+|I_H(t)|+|R(t)|+|D(t)|$ and $S,E,I_A,I_S,I_I,I_H,R,D \in C([0,b])$.

Theorem 1 *Suppose that the function $\mathscr{K} \in C([J,\mathbb{R}])$ and maps bounded subset of $J\times\mathbb{R}^8$ into relatively compact subsets of $\mathbb{R}$. In addition, there exists constant $\mathscr{L}_{\mathscr{K}} > 0$ such that (A_1) $|\mathscr{K}(t,\Phi_1(t)) - \mathscr{K}(t,\Phi_2(t))| \leq \mathscr{L}_{\mathscr{K}}|\Phi_1(t) - \Phi_2(t)|$; for all $t \in J$ and each $\Phi_1,\Phi_2 \in C([\mathscr{J},\mathbb{R}])$. Then the integral equation (6) which is equivalent with the proposed model (1) has a unique solution provided that $\Omega\mathscr{L}_{\mathscr{K}} < 1$, where $\Omega = \frac{b^{\upsilon}}{\Gamma(\upsilon+1)}$.*

Proof. Consider the operator $P : \mathbb{E} \to \mathbb{E}$ defined by

$$(P\Phi)(t) = \Phi_0 + \frac{1}{\Gamma(\upsilon)}\int_0^t (t-\tau)^{\upsilon-1}\mathscr{K}(\tau,\Phi(\tau))d\tau. \tag{7}$$

Obviously, the operator P is well defined and the unique solution of model (1) is just the fixed point of P. Indeed, let us take $\sup_{t\in J}\|\mathscr{K}(t,0)\| = M_1$ and $\kappa \geq \|\Phi_0\| + \Omega M_1$. Thus, it is enough to show that $P\mathbb{H}_\kappa \subset \mathbb{H}_\kappa$, where the set $\mathbb{H}_\kappa = \{\Phi \in \mathbb{E} : \|\Phi\| \leq \kappa\}$, is closed and convex. Now, for any $\Phi \in \mathbb{H}_\kappa$, yields

$$\begin{aligned}
|(P\Phi)(t)| &\leq |\Phi_0| + \frac{1}{\Gamma(\upsilon)}\int_0^t (t-\tau)^{\upsilon-1}|\mathscr{K}(\tau,\Phi(\tau))|d\tau \\
&\leq \Phi_0 + \frac{1}{\Gamma(\upsilon)}\int_0^t (t-\tau)^{\upsilon-1}\left[|\mathscr{K}(\tau,\Phi(\tau)) - \mathscr{K}(\tau,0)| + |\mathscr{K}(\tau,0)|\right]d\tau \\
&\leq \Phi_0 + \frac{(\mathscr{L}_{\mathscr{K}}\kappa + M_1)}{\Gamma(\upsilon)}\int_0^t (t-\tau)^{\upsilon-1}d\tau \leq \Phi_0 + \frac{(\mathscr{L}_{\mathscr{K}}\kappa + M_1)}{\Gamma(\upsilon+1)}b^{\upsilon} \leq \Phi_0 + \Omega(\mathscr{L}_{\mathscr{K}}\kappa + M_1) \leq \kappa.
\end{aligned} \tag{8}$$

Hence, the results follow. Also, given any $\Phi_1,\Phi_2 \in \mathbb{E}$, we get

$$\begin{aligned}
|(P\Phi_1)(t) - (P\Phi_2)(t)| &\leq \frac{1}{\Gamma(\upsilon)}\int_0^t (t-\tau)^{\upsilon-1}|\mathscr{K}(\tau,\Phi_1(\tau)) - \mathscr{K}(\tau,\Phi_2(\tau))|d\tau \\
&\leq \frac{\mathscr{L}_{\mathscr{K}}}{\Gamma(\upsilon)}\int_0^t (t-\tau)^{\upsilon-1}|\Phi_1(\tau) - \Phi_2(\tau)|d\tau \leq \Omega\mathscr{L}_{\mathscr{K}}|\Phi_1(t) - \Phi_2(t)|,
\end{aligned} \tag{9}$$

which implies that $\|(P\Phi_1) - (P\Phi_2)\| \leq \Omega\mathscr{L}_{\mathscr{K}}\|\Phi_1 - \Phi_2\|$. Therefore, as a consequence of Banach contraction principle, proposed model (1) possess a unique solution.

Next, we prove the existence of solutions of the proposed model (1) by employing the concept of well-known Krasnoselskii's fixed point theorem.

Theorem 2 *Let $M \neq \emptyset$ be a closed, bounded and convex subset of a Banach Space $\mathbb{E}$. Let P_1,P_2 be two operators that obey the given relations*

- *$P_1\Phi_1 + P_2\Phi_2 \in M$, whenever $\Phi_1,\Phi_2 \in M$;*
- *P_1 is compact and continuous;*
- *P_2 is a contraction mapping.*

Then there exists $u \in M$ such that $u = P_1u + P_2u$ [7].

Theorem 3 *Suppose that the function $\mathscr{K} : \mathscr{J}\times\mathbb{R}^8 \to \mathbb{R}$ is continuous and satisfies condition (A_1). In addition, assume that (A_2) $|\mathscr{K}(t,\Phi)| \leq \psi(t)$, for all $(t,\Phi) \in J\times\mathbb{R}^8$ and $\psi \in C([0,b],\mathbb{R}_+)$.*
Then the proposed model (1) has at least one solution provided

$$\mathscr{L}_K\|\Phi_1(t_0) - \Phi_2(t_0)\| < 1.$$

Proof. Setting $\sup_{t\in J}|\psi(t)| = \|\psi\|$ and $\eta \geq \|\Phi_0\| + \Omega\|\psi\|$, we consider $\mathbf{B}_\eta = \{\Phi \in \mathbb{E} : \|\Phi\| \leq \eta\}$. Consider the operators P_1, P_2 on $\mathbf{B}_\eta$ defined by

$$(P_1\Phi)(t) = \frac{1}{\Gamma(\upsilon)}\int_0^t (t-\tau)^{\upsilon-1}\mathscr{K}(\tau,\Phi(\tau))d\tau t \in J,$$

and

$$(P_2\Phi)(t) = \Phi(t_0), t \in J.$$

Thus, for any $\Phi_1, \Phi_2 \in \mathbf{B}_\eta$, yields

$$\|(P_1\Phi_1)(t) + (P_2\Phi_2)(t)\| \leq \|\Phi_0\| + \frac{1}{\Gamma(\upsilon)}\int_0^t (t-\tau)^{\upsilon-1}\|\mathscr{K}(\tau,\Phi_1(\tau))\|d\tau \leq \|\Phi_0\| + \Omega\|\psi\| \leq \eta < \infty. \tag{10}$$

Hence, $(P_1\Phi_1 + P_2\Phi_2) \in \mathbf{B}_\eta$.
Next, we prove the contraction of the operator P_2.
Obviously, given any $t \in J$ and $\Phi_1, \Phi_2 \in \mathbf{B}_\eta$, gives

$$\|(P_2\Phi_1)(t) - (P_2\Phi_2)(t)\| \leq \|\Phi_1(t_0) - \Phi_2(t_0)\|. \tag{11}$$

Since the function $\mathscr{K}$ is continuous, the operator P_1 is also continuous. Moreover, for any $t \in J$ and $\Phi_1 \in \mathbf{B}_\eta$,

$$\|P_1\Phi\| \leq \Omega\|\psi\| < +\infty$$

implies that P_1 is uniformly bounded. Finally, we show that the operator P_1 is compact. Define $\sup_{(t,\Phi)\in J\times\mathbf{B}_\eta}|\mathscr{K}(t,\Phi(t))| = \mathscr{K}^*$, gives

$$\begin{aligned}
|(P_1\Phi)(t_2) - (P_1\Phi)(t_2)| &= \frac{1}{\Gamma(\upsilon)}\bigg|\int_0^{t_1}[(t_2-\tau)^{\upsilon-1} - (t_1-\tau)^{\upsilon-1}]\mathscr{K}(\tau,\Phi(\tau))d\tau \\
&\quad + \int_{t_1}^{t_2}(t_2-\tau)^{\upsilon-1}\mathscr{K}(\tau,\Phi(\tau))d\tau\bigg| \\
&\leq \frac{\mathscr{K}^*}{\Gamma(\upsilon)}[2(t_2-t_1)^\upsilon + (t_2^\upsilon - t_1^\upsilon)] \to 0 \quad as \quad t_2 \to t_1.
\end{aligned} \tag{12}$$

Thus, P_1 is equicontinuous and so is relatively compact on $\mathbf{B}_\eta$. Hence, as consequences of Arzelá Ascoli theorem, P_1 is compact on $\mathbf{B}_\eta$. Since all the hypotheses of Theorem [7] are true, proposed model (1) has at least one solution.

CONCLUSION

In conclusion, this paper consists of a system of eight non–linear fractional order differential equations in Caputo sense. The existence and uniqueness of solution of the proposed model using fixed point theorems is discussed.

REFERENCES

1. S. W. Youdom, R. Tahar, and L. K. Basco, Malaria **16**, 311 (2017).
2. N. Wurtz, A. Pascual, A. M. Jauffre, et al., Malaria **11**, 146 (2012).
3. O. Izevbekhai, B. Adeagbo, A. Olagunju, and O. Bolaji, Transactions of the Royal Society of Tropical Medicine & Hygiene **111**, 90–96 (2017).
4. W. Pongtavornpinyo, S. Yeung, I. M. Hastings, et al., Malaris **7**, 229 (2008).
5. L. Esteva, A. B. Gumel, and C. V. De-Leon, Mathematical and Computer Modelling **50**, 611–630 (2009).
6. J. Tumwiine, S. D. Musekwa, and F. Nyabadza, ISRN Biomathematics **2014**, 1–12 (2014).
7. M. M. Meerschaert and A. Sikorskii, Stochastic Models for Fractional Calculus, De Gruyter Studies in Mathematics vol. 43.

$O(h^8 |\ln h|)$ Order of Accurate Difference Method for Solving the Dirichlet Problem for Laplace's Equation on a Rectangle with Boundary Values in $C^{k,1}$

Hediye Sarikaya[a] and Adiguzel A. Dosiyev[b]

Department of Mathematics, Near East University, Nicosia, TRNC, Mersin 10, Turkey

[a]*Corresponding author: hediye.sarikaya@neu.edu.tr*
[b]*Electronic mail: adiguzel.dosiyev@neu.edu.tr*

Abstract. A three stage (9-point, 5-point and 5-point) difference method for solving the Dirichlet problem for Laplace's equation on a rectangle is proposed and justified. It is proved that the proposed difference solution converges uniformly to the exact solution of order $O(h^8 |\ln h|)$, h is the mesh size, when the boundary functions are from $C^{9,1}$. Numerical experiment is illustrated to support the analysis made.

INTRODUCTION

In many versions of the domain decomposition, composite grids, and combined methods in solving Laplace's boundary value problems the obtained system of equations is separated into a fixed number of subsystems, each of which is adequate for the difference equations on a rectangle. Therefore, the detailed error analysis for the classical finite difference or finite element methods for the problems in rectangular domains becomes important.

In [1] for 5-point, and in [2] for 9-point solution for the convergence order $O(h^2)$ and $O(h^6)$ are obtained by requiring minimum smoothness of the functions given on the sides of the boundary in Hölder classes $C^{k,\lambda}$, $0 < \lambda < 1$, for $k = 2$, and $k = 6$, respectively. In [3] it is proved that for the 5-point solution the error in maximum norm is of order $O(h^2(|\ln h| + 1))$, when the boundary function is from $C^{1,1}$. In [4], for the classical 9-point scheme on square grids in solving the Dirichlet problem for Laplace's equation on rectangles it was proved that the order of accuracy in maximum norm is $O(h^6(|\ln h| + 1))$,when the given boundary functions are from $C^{5,1}$. These requirements on the boundary functions cannot be lowered in Hölder classes $C^{k,\lambda}$.

In this paper a three-stage difference method which was announced in [5] for the solution of the Dirichlet problem for Laplace's equation on a rectangular domain is justified, when the boundary functions are from the classes $C^{9,1}$. By using at the first stage the 9-point, and at the second and third stages the 5-point scheme the obtained approximate solution converges of order $O(h^8(|\ln h| + 1))$ Numerical experiment is illustrated to support the analysis made.

DIFFERENTIAL AND DIFFERENCE DIRICHLET PROBLEMS

Let $\Pi = \{(x, y) : 0 < x < a,\ 0 < y < b\}$ be rectangle, a/b be rational, $\gamma_j(\gamma_j'),\ j = 1, 2, 3, 4$, be the sides, including (excluding) the ends, enumerated counterclockwise starting from the left side ($\gamma_0 \equiv \gamma_4$, $\gamma_1 \equiv \gamma_5$) and let $\gamma = \cup_{j=1}^{4} \gamma_j$ be the boundary of Π. Denote by s the arc length, measured along γ, and by s_j the value of s at the beginning of γ_j. We say that $f \in C^{k,\lambda}(D)$, if f has kth derivatives on D satisfying a Hölder condition with exponent $\lambda \in (0, 1]$, which is a Lipschitz condition when $\lambda = 1$.
We consider the boundary value problem

$$\Delta u = 0 \text{ on } \Pi,\ u = \varphi_j(s) \text{ on } \gamma_j,\quad j = 1, 2, 3, 4, \tag{1}$$

where $\Delta \equiv \partial^2/\partial x^2 + \partial^2/\partial y^2$, φ_j, $j = 1, 2, 3, 4$ are given functions of s. Assume that

$$\varphi_j \in C^{9,1}(\gamma_j),\ 0 < \lambda < 1,\ j = 1, 2, 3, 4, \tag{2}$$

$$\varphi_j^{(2q)}(s_j) = (-1)^q \varphi_{j-1}^{(2q)}(s_j),\ q = 0, \ldots, 4. \tag{3}$$

Lemma 1 *Under the conditions (2) and (3) the solution u of the Dirichlet problem (1) belongs to the class $C^{9,\lambda}(\overline{\Pi})$, $0 < \lambda < 1$.*

International Conference on Analysis and Applied Mathematics (ICAAM 2020)
AIP Conf. Proc. 2325, 020040-1–020040-4; https://doi.org/10.1063/5.0040565
Published by AIP Publishing. 978-0-7354-4069-2/$30.00

Lemma 2 *The following type of partial derivatives of the solution u to problem* (1) *satisfy the next inequality*

$$\max_{0\le p\le 5}\sup_{(x,y)\in\Pi}\left|\frac{\partial^{10}u}{\partial x^{2p}\partial y^{10-2p}}\right|<\infty. \tag{4}$$

We introduce the functions w^m, $m=4,8$ on $\overline{\Pi}$ as

$$w^m=w^m(x,y)=\frac{\partial^m u(x,y)}{\partial x^m}, \tag{5}$$

where u is the solution to Dirichlet problem (1).

From Lemma 1 it follows that, for each of $m=4,8$ the function (5) is the solution of the boundary value problem

$$\Delta w^m=0 \ \text{ on } \Pi, \tag{6}$$
$$w^m=\Psi_k^m=\Psi_k^m(y) \ \text{ on } \gamma_k, \ \ k=1,3, \tag{7}$$
$$w^m=\Psi_l^m=\Psi_l^m(x) \ \text{ on } \gamma_l, \ \ l=2,4, \tag{8}$$

where

$$\Psi_k^m(y)=\frac{d^m\varphi_k}{dy^m},\ k=1,3,\ \ \Psi_l^m(x)=\frac{d^m\varphi_l}{dx^m},\ l=2,4. \tag{9}$$

Furthermore, as it follows from Lemma 2 the following $(10-m)$-th order derivatives are bounded on Π :

$$\max_{0\le p\le(10-m)/2}\sup_{(x,y)\in\Pi}\left|\frac{\partial^{10-m}w^m}{\partial x^{2p}\partial y^{10-m-2p}}\right|<\infty,\ m=4,8. \tag{10}$$

ERROR ESTIMATION FOR THE FINITE DIFFERENCE SOLUTION

Let $h>0$, and $a/h\ge 8$, $b/h\ge 8$ be integers. We assign Π^h a square grid on Π with step size h, obtained by the lines $x,y=0,h,2h,\ldots$. Let γ_j^h be a set of nodes on the interior of γ_j, and let

$$\gamma^h=\bigcup_{j=1}^{4}\gamma_j^h,\ \dot{\gamma}_j=\gamma_{j-1}\cap\gamma_j,\ \overline{\gamma}^h=\bigcup_{j=1}^{4}(\gamma_j^h\cup\dot{\gamma}_j),\ \overline{\Pi}^h=\Pi^h\cup\overline{\gamma}^h.$$

Let the operator $\mathfrak{B}^p$, $p\in\{0,1\}$ be defined as follows:

$$\begin{aligned}\mathfrak{B}^p u(x,y)=&\frac{1}{5-p}\{u(x+h,y)+u(x-h,y)+u(x,y+h)+u(x,y-h)\}\\&+\frac{1-p}{20}\{u(x+h,y+h)+u(x-h,y+h)+u(x+h,y-h)\\&+u(x-h,y-h)\}.\end{aligned} \tag{11}$$

We consider for the approximation of problems (6)-(8) the following system of difference equations:

$$w_h^4=\mathfrak{B}^0 w_h^4 \ \text{ on } \Pi^h,\ w_h^4=\Psi_j^4 \ \text{ on } \gamma_j^h\cup\dot{\gamma}_j,\ j=1,2,3,4; \tag{12}$$

$$w_h^8=\mathfrak{B}^1 w_h^8 \ \text{ on } \Pi^h,\ w_h^8=\Psi_j^8 \ \text{ on } \gamma_j^h,\ j=1,2,3,4. \tag{13}$$

By the maximum principle, problems (12) and (13) have the unique solution.

In what follows and for simplicity $c,c_0,c_1,\ldots$ denote the positive constants independent of h and the nearest factor, the identical notation is allowable for various constants.

Let ϖ be a solution of the problem

$$\Delta\varpi = 0 \;\text{ on } \Pi,\; \varpi = \theta_{p,j}(s) \;\text{ on } \gamma_j, \;\; j = 1,2,3,4, \tag{14}$$

where $\theta_{p,j},\; j = 1,2,3,4$ are given functions and

$$\theta_{p,j} \in C^{2^{3-p},\lambda}(\gamma_j),\; 0 < \lambda < 1,\; j = 1,2,3,4, \tag{15}$$

$$\theta_{p,j}^{(2q)}(s_j) = (-1)^q \theta_{p,j-1}^{(2q)}(s_j),\; q = 0,..,3-2p;\; p \in \{0,1\}. \tag{16}$$

The proofs of the following Lemmas 3 and 4 are curried out by analogy with the proof of Theorem 3.1 in [4].

Lemma 3 *The estimation holds*

$$\max_{(x,y)\varepsilon\Pi} |\mathfrak{B}^p\varpi - \varpi| \le ch^{2^{3-p}}(|\ln h| + 1),\; where\; p \in \{0,1\} \tag{17}$$

and ϖ is the solution of problem (14)-(16) on $\overline{\Pi}^h$.

Lemma 4 *The estimation holds*

$$\max_{\overline{\Pi}^h} |w_h^m - w^m| \le ch^{10-m}(|\ln h| + 1),\; m \in \{4,8\}, \tag{18}$$

where w_h^4 and w_h^8 is a solution of system (12) *and* (13) *respectively; w^m are the traces of the functions* (5) *on $\overline{\Pi}^h$.*

Let w_h^4 and w_h^8 be a solution of the difference problem (12) and (13) respectively. We approximate the solution of the given Dirichlet problem (1) on the grid $\overline{\Pi}^h$ as a solution u_h of the following difference problem

$$u_h = \mathfrak{B}^1 u_h - \frac{h^4}{4!} w_h^4 - \frac{h^8}{8!} w_h^8 \;\text{ on } \Pi^h,\;\; u_h = \varphi_j \;\text{ on } \gamma_j^h,\; j = 1,2,3,4. \tag{19}$$

By virtue of (19) and Lemmas 3-4 the following Theorem is proved:

Theorem 5 *On Π^h, the pointwise estimation is true*

$$\max_{\overline{\Pi}^h} |u_h - u| \le ch^8(|\ln h| + 1), \tag{20}$$

where u is the trace of the exact solution of problem (1) *on Π^h, u_h is the solution to system* (19).

NUMERICAL RESULTS

Let $\Pi = \{(x,y) : 0 < x < 1,\; 0 < y < 1\}$, and let γ be the boundary of Π. We consider the following problem :

$$\Delta u = 0 \;\text{ on } \Pi,\, u = \varphi(x,y) \;\text{ on } \gamma_j,\; j = 1,2,3,4,$$

where

$$\varphi(x,y) = (x^{10} - 45x^8y^2 + 210x^6y^4 - 210x^4y^6 + 45x^2y^8 - y^{10})\tan^{-1}\left(\frac{y}{x}\right)$$
$$+(10x^9y - 120x^7y^3 + 252x^5y^5 - 120x^3y^7 + 10xy^9)\ln\sqrt{x^2+y^2}.$$

We denote by $\|U_h - U\|_{\overline{\Pi}^h} = \max_{\overline{\Pi}^h} |U_h - U|$ and by $E_U^n = \frac{\|U - U_{2^{-n}}\|_{\overline{\Pi}^h}}{\left\|U - U_{2^{-(n+1)}}\right\|_{\overline{\Pi}^h}}$, where U is the trace of the exact solution of the continuous problem on $\overline{\Pi}^h$, and U_h is its approximate values.

TABLE 1. Results by the proposed method

$h=2^{-n}$	$\left\|w_h^4-w^4\right\|_{\overline{\Pi}^h}$	$E^n_{w^4}$	$\left\|w_h^8-w^8\right\|_{\overline{\Pi}^h}$	$E^n_{w^8}$	$\left\|u_h-u\right\|_{\overline{\Pi}^h}$	E^n_u
2^{-3}	$1.083E-08$	62.632	$2.045E-02$	3.694	$1.404E-12$	250.578
2^{-4}	$1.729E-10$	62.844	$5.535E-03$	3.872	$5.604E-15$	256.146
2^{-5}	$2.751E-12$	63.495	$1.430E-03$	3.936	$2.188E-17$	256.037
2^{-6}	$4.333E-14$	63.761	$3.632E-04$	3.968	$8.545E-20$	256.059
2^{-7}	$6.796E-16$		$9.154E-05$		$3.337E-22$	

CONCLUSION

A three stage method in solving the Dirichlet problem for Laplace's equation in a rectangle is proposed and justified. It is assumed that the boundary functions on the sides are from $C^{9,1}$ and at the vertices satisfy the compatibility conditions for the even order derivatives up to eighth order, which result from the Laplace equation. Under these conditions, the constructed approximate solution by this method converges to the exact solution in the uniform metric of order $O(h^8\,|\ln h|)$.

The proposed method can be applied when the boundary functions are from the classes $C^{k,1}$ (see [4]), and can be generalized for the Laplace and Poisson equations on a multidimensional parallelepiped, which will be investigated in sequential papers.

Furthermore, this method can be used to obtain a highly accurate approximation in the different type of domain decomposition methods (see [1, 6, 7, 8, 9]).

REFERENCES

1. E. A. Volkov, Trudy Mat. Inst. Steklov. **140**, 68-102 (1976).
2. A. A. Dosiyev, Intern. Journal of Pure and Appl. Math. **7(2)**, 229-241 (2003).
3. E. A. Volkov, Proc. Steklov Inst. Math. **105**, 54-78 (1969).
4. A. A. Dosiyev, Mediterranean Journal of Mathematics **8(3)**, 451-462 (2011).
5. A. A. Dosiyev and H. Sarikaya, AIP Conference Proceedings **1880**, 040006 (2017).
6. A. A. Dosiyev, Comp. Maths Math. Phys. **42(6)**, 832-849 (2002).
7. A. A. Dosiyev, SIAM Journal on Numerical Analysis **42(1)**, 153-178 (2004).
8. A. A. Dosiyev, S. Buranay Cival, and D. Subasi, Computers and Mathematics with Applications **64**, 616-632 (2012).
9. A. A. Dosiyev, Journal of Computational and Applied Mathematics **259**, 14-23 (2014).

The Fictitious Domain Method for the Navier-Stokes Equations in Natural Variables

Zhadra Zhaksylykova,[1, a)] Nurlan Temirbekov,[2, b)] and Yerzhan Malgazhdarov[3, c)]

[1)] Abai Kazakh National Pedagogical University, 050000 Almaty, Kazakhstan
[2)] National Engineering Academy of the Republic of Kazakhstan, 050000 Almaty, Kazakhstan
[3)] S. Amanzholov East Kazakhstan State University, 070002 Ust-Kamenogorsk, Kazakhstan

[a)] Corresponding author: zhaksylykova0507@mail.ru
[b)] Electronic mail: temirbekov@rambler.ru
[c)] Electronic mail: malgazhdarov_e@mail.ru

Abstract. In this paper, we consider a variant of the fictitious domain method associated with the modification of nonlinear terms in a fictitious subdomain. The model problem shows the effectiveness of using this modification. The proposed version of the method is used to solve the problem of an arbitrary region and to set a boundary condition for pressure. A numerical solution is implemented and the results of numerical results are given.

INTRODUCTION

The method of fictitious domains is widely used for the numerical solution of mathematical physics problems in an arbitrary domain [1, 2]. A. N. Konovalov [2] constructed a theory of fictitious domains method to solve the problem of an arbitrary domain in the numerical implementation of discrete models. On its basis, a new class of locally-bilateral approximations in direct and spectral problems was created.

The works of A. N. Bugrov, Sh. S. Smagulov were dedicated to the fictitious domain method for the Navier-Stokes equations [3]. In the work of Sh. S. Smagulov and M. K. Orunkhanov was proposed a method of fictitious domains for the equations of hydrodynamics in multiply connected domains [4].

In work [5], one version of the fictitious domain method was proposed for the Navier – Stokes equations of a viscous incompressible fluid in a variable velocity and pressure field. Moreover, at the boundary of the auxiliary region, a boundary condition is set for pressure with a zero value. This condition makes it possible to obtain the Dirichlet problem for pressure for the Poisson equation, for which with the help of known methods can be developed iterative difference schemes.

The works of R. Glowinski, T-W. Pan, J. Periaux [6] consider a family of a region-division method based on the explicit use of the Lagrange multiplier defined on the actual boundary. The proposed technique associated with genuine boundary conditions is common for modeling inviscid incompressible potential flows. According to the proposed methodology, the initial differential problem is posed with the optimal control problem with a saddle point, and for the numerical implementation iterative method of conjugate gradients is used.

In work [7], for the numerical simulation of the suspension concentration, the method of fictitious regions without Lagrange multipliers is used. To distinguish between the areas occupied by the liquid and the solid particles, the boundary is tracked as a function. The particle indicator function is constructed using the Heaviside function. Further, the Heaviside function in a small vicinity (proportionally to the grid step) around the boundary is approximated using the hyperbolic tangent. Such a continuous function provides smooth change, increasing numerical accuracy and reliability.

In this paper considered one version of the method of fictitious domains associated with the modification of nonlinear terms in the fictitious subdomain. The model problem shows the effectiveness of using such a modification. The proposed version of the method is used to solve the problem of an arbitrary region and to set the boundary condition for pressure.

FORMULATION OF THE PROBLEM

In a limited area $\Omega \subset \mathbb{R}^2$ with curved border S consider the initial-boundary-value problem for the unsteady flow of a viscous incompressible fluid. The problem is reduced to solving a system of non-linear Navier-Stokes equations in

International Conference on Analysis and Applied Mathematics (ICAAM 2020)
AIP Conf. Proc. 2325, 020041-1–020041-5; https://doi.org/10.1063/5.0040727
Published by AIP Publishing. 978-0-7354-4069-2/$30.00

velocity-pressure variables

$$\frac{\partial v}{\partial t} + (v \cdot \nabla) v = \mu \Delta v - \nabla p + f, \tag{1}$$

$$\operatorname{div} v = 0, \tag{2}$$

$$v\Big|_{t=0} = v_0(x), \;\; v\Big|_S = 0. \tag{3}$$

The auxiliary problem corresponding to the method of fictitious domains reduces to solving a system of nonlinear equations with variable coefficients in $D = D_1 \cup \Omega$ with boundary S:

$$\frac{\partial v^\varepsilon}{\partial t} + (v^\varepsilon \cdot \nabla)(a^\varepsilon v^\varepsilon) = \operatorname{div}(\mu^\varepsilon \nabla v^\varepsilon) - \nabla p^\varepsilon + f, \tag{4}$$

$$\operatorname{div} v^\varepsilon = 0, \tag{5}$$

$$v^\varepsilon\Big|_{t=0} = 0, \;\; v^\varepsilon \cdot \tau\Big|_{S_1} = 0, \;\; p^\varepsilon\Big|_{S_1} = 0, \tag{6}$$

with the terms of the agreement on the border S

$$\left[\left(a^\varepsilon v^\varepsilon(\delta v^\varepsilon) - \mu^\varepsilon \nabla v^\varepsilon - p^\varepsilon \cdot \delta\right) n\right]\big|_S = 0, \;\; [v^\varepsilon]\big|_S = 0 \tag{7}$$

where τ - tangent vector to the border S_1, $[\cdot]$ defines a jump when crossing through S, δ - metric tensor, n - normal to the border S, f - is continued in D_1, keeping the norm $L_2(\Omega)$.

$$\mu^\varepsilon = \begin{cases} \mu, & \text{in } \Omega, \\ \frac{\mu}{\varepsilon^2}, & \text{in } D_1, \end{cases} \tag{8}$$

$$a^\varepsilon = \begin{cases} 1, & \text{in } \Omega, \\ \frac{1}{\varepsilon^2}, & \text{in } D. \end{cases} \tag{9}$$

Condition (7) is obtained after a preliminary transformation of nonlinear terms

$$(v^\varepsilon \cdot \nabla)(a^\varepsilon v^\varepsilon) = (v^\varepsilon \cdot \nabla)(a^\varepsilon v^\varepsilon) + a^\varepsilon v^\varepsilon(\nabla \cdot v^\varepsilon) = \nabla \cdot \left(a^\varepsilon v^\varepsilon(\delta v^\varepsilon)\right). \tag{10}$$

Introduce the set of infinitely differentiable solenoidal in D vector functions $v(x)$, with tangent components that vanish on the S_1, $M(D) = \{v(x) \in C^\infty(D),\ \operatorname{div} v = 0,\ v(x) \cdot \tau(x) = 0,\ x \in S_1\}$.

Spaces obtained by closure $M(D)$ in norms $L_2(D)$ and $\mathring{W}_2^1(D)$ is defined accordingly through their conjugate spaces $V^*(D)$, $V_1^*(D)$.

A definition of generalized solutions to problem is given (4)-(7), a lemma is proved for a v^ε function from a $L_2(0,T;V_1(D)) \cap L_\infty(0,T;L_2(D))$ class, and numerical calculations are presented.

To illustrate the advantages of the proposed approach, considered the numerical solution of the auxiliary problem (4)-(7).

As the region under consideration, took a curved channel with solid boundaries (figure 1). A region D_1 - is a fictitious region, Ω - is a physical region.

For the numerical implementation of auxiliary problem (4)-(7), used the finite difference method and the splitting scheme for physical processes [8]. The solution domain is covered by the so-called MAC-grid [9], which provides approximation with the second order of accuracy in space and the first order in time.

In the numerical implementation were set the pressure values and zero values of the tangent component of the fluid velocity at the inlet and outlet of the computational domain. On the «solid» boundaries, the pressure values are set in the form of linear functions and the tangential component of the velocity is equal to zero.

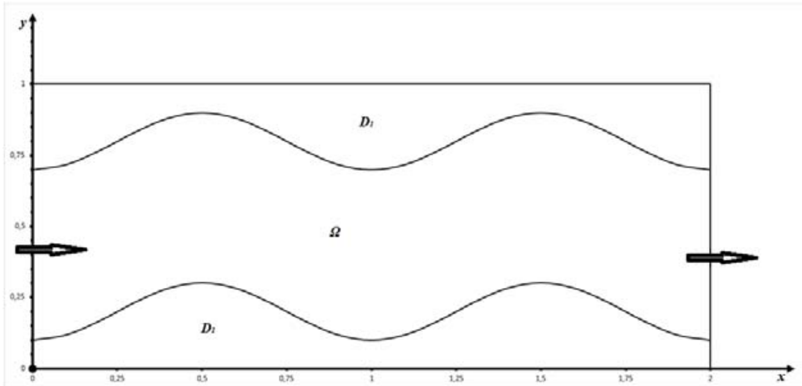

FIGURE 1. Schematic representation of the area under consideration

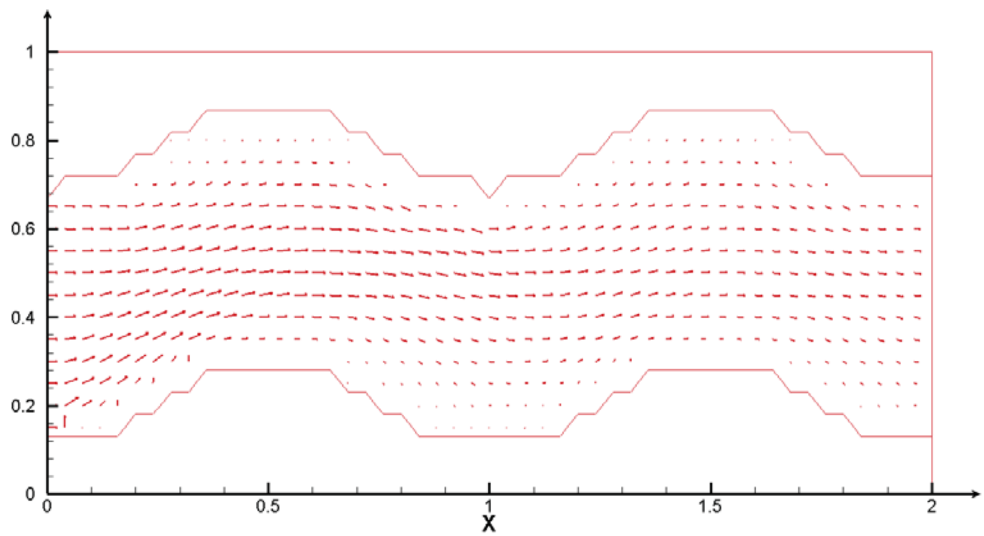

FIGURE 2. Fields of the velocity vector

For numerical implementation, a 50x20 grid and the following dimensionless parameter values were used:

$$0 < x_i < 2,\ 0 < y_i < 1,\ \tau = 0.001,\ \mu = \frac{1}{\mathrm{Re}} = 0.001,\ \varepsilon = 10^{-5}.$$

The upper and lower solid curved boundaries are described by the equations

$$y_1 = 0.2 - 0.1\cos(2\pi x),\ \ y_2 = 0.8 - 0.1\cos(2\pi x).$$

The isolines of the stream function show the vorticities of the flow at the folds of the boundary, which arise at flowing around smooth bodies, the boundary layer of the stream directly adjacent to the streamlined body is inhibited more strongly than the layers removed from the boundary. This leads to a reduction to zero of the tangential friction on the streamlined surface, separation of the flow from it and the formation of a return flow behind the separation line (figure 3). On the reverse side of the bend of the boundary, a mixture of the oncoming flow and the return flow, i.e. the formation of vortex movements.

From the Figure 4 it can be seen that during the flow on convex bends the velocity component is positive, and negative on concave bends. And on the next convex bend, the shapes of the velocity profiles are repeated. And where the fictitious region, the velocity profiles have values close to zero.

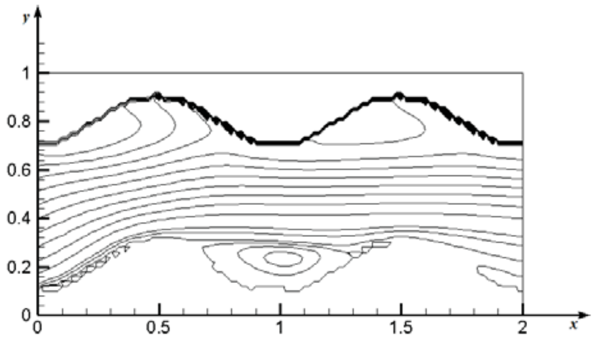

FIGURE 3. Isolines of the current function

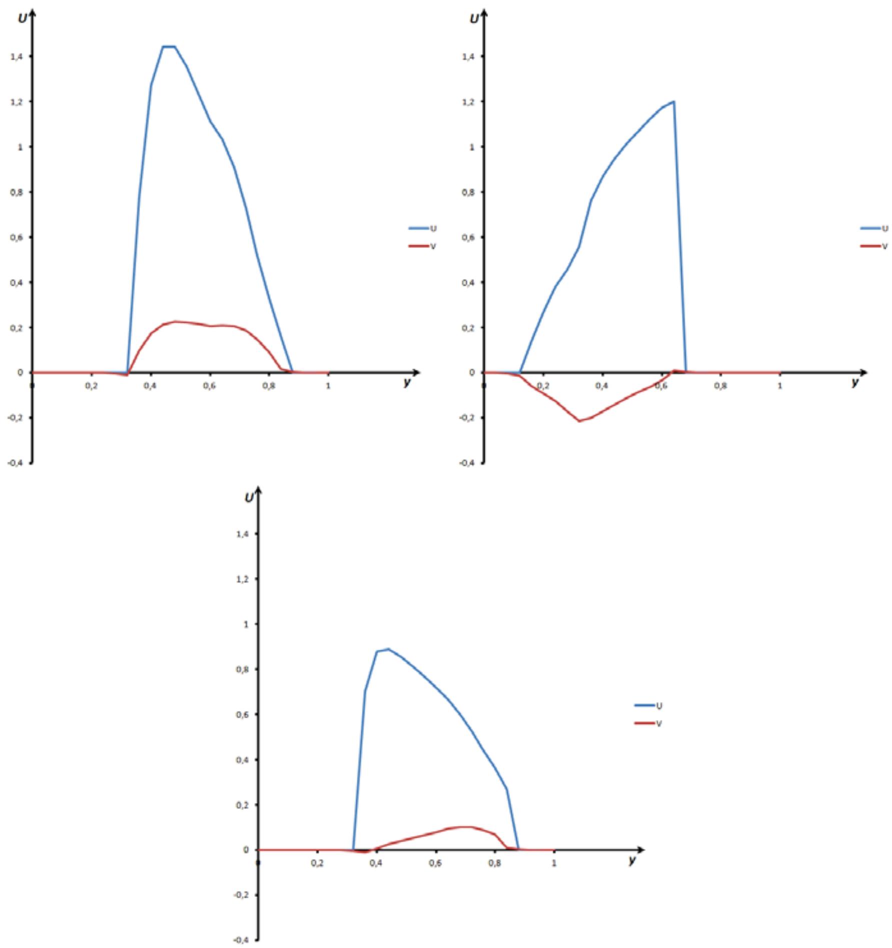

FIGURE 4. The velocity profile in sections a) at $x = 0.5$; b) at $x = 1.0$; c) at $x = 1.5$

REFERENCES

1. P. Vabishchevich, *Metod fiktivnykh oblastey dlya zadachi matematicheskoy fiziki* (Publishing House of Moscow State University, 1991) p. 156.
2. A. Konovalov, *Zadachi fil'tratsii mnogofaznoy neszhimaemoy zhidkosti* (World Scientific, 1994) p. 173.
3. A. Bugrov and S. Smagulov, Matematicheskie modeli techenii zhidkosti , 79–89 (1978).
4. S. Smagulov and M. Orunkhanov, DAN SSR **260**, 1078–1082 (1981).
5. S. Smagulov, N. Danaev, and N. Temirbekov, Doklady Akademii Nauk Rossii **374**, 333–335 (2000).

6. G. Chai, J. Su, L. Wang, C. Yu, Y. Zhang, and Z. Gu, Advances in Mathematical Physics **2019**, 18 (2019).
7. O. Belotserkovskiy, V. Gushchin, and S. V.V., Zh. vychisl. matem. i matem. fiz. **15**, 197–207 (1975).
8. P. Rouch, *Vychislitel'naya gidrodinamika* (Mir, 1980) p. 616.
9. K. Khazimov, G. Bora, B. Urmashev, M. Khazimov, and Z. Khazimov, International Journal of Engineering and Innovative Technology (IJEIT) **4 (1)**, 251–261 (2014).
10. R. Glowinski, T.-W. Pan, and J. Periaux, Computer Methods in Applied Mechanics and Enginering **111**, 283–303 (1994).
11. S. Gallier, E. Lemaire, L. Lobry, and F. Peters, Journal of Computational Physics **256**, 367–387 (2014).
12. N. Temirbekov, Y. Malgazhdarov, and S. Tokanova, Journal of Theoretical and Applied Information **88 (3)**, 441–448 (2016).
13. A. Temirbekov and W. Wójcik, International Journal of Electronics and Telecommunications **60 (3)**, 219–223 (2014).
14. A. Temirbekov, AIP Conference Proceedings **1759**, 020053.
15. A. Temirbekov, B. Urmashev, and K. Gromaszek, International Journal of Electronics and Telecommunications **64 (3)**, 391–396 (2018).

The Effects of Maths Anxiety on Mathematical Modelling

Bilgen Kaymakamzade[1, 2, a)] and Meryem Cumhur[1, b)]

[1)] *Department of Mathematics, Near East University, Nicosia, Mersin 10, Turkey*
[2)] *Mathematics Research Center, Near East University, Nicosia, Mersin 10, Turkey*

[a)] *Corresponding author: bilgen.kaymakamzade@neu.edu.tr*
[b)] *Electronic mail: meryem.cumhur@neu.edu.tr*

Abstract. Some factors related to students maths anxiety are perceived to be important for academic failure. Such of these factors and some other factors contribute immensely to the problem of mathematics achievement that is spreading among students of Economics and Administrative Sciences. Considering such a problem as a maths anxiety, we propose a mathematical model to study how this problem is spread in the Faculty. We have discussed about basic properties of the system. Basic reproduction numbers are calculated. Our numerical findings are illustrated through computer simultaneous using MATLAB, which show the reliability of our model from the practical point of view. Students' math-anxiety implications of our analytical findings are addressed critically. The model analysis reveals that all of the students start to show better maths achievement on the positive way during the semester (approximately 3,5 months). The sensitivity analysis of the parameters of the model shows that reducing maths anxiety by focusing positive change of behaviour in relation to the teaching of maths and the teachers' way of teaching is an effective on students' achievement of maths.

INTRODUCTION

Mathematics is an agent in people's understanding the world and life better and raising ideas. Therefore, in all the reforms in education today, the most important target is to create a system to help learners learn better by understanding mathematics. However, one of the factors affecting this target negatively is the anxiety learners experience in mathematics [1]. Anxiety is a feeling and experience an individual goes through at certain times. This feeling affects life negatively and many times causes uneasiness, leading to a feeling of fear of weak performance [2]. Mathematics anxiety is defined as an experience of negative feelings. It affects numerical and mathematical thoughts negatively. It is true that anxiety affects performance in mathematics. It has been observed that individuals with anxiety experience exhibited low performance, were less self-confident and less motivated in basic tasks, mental calculations, and mathematics problems [3]. As Ahmed [4] argues, anxiety is one of the most common among academic anxiety types at school. It can be defined as "a feeling of strain and nervousness hindering manipulation and solution of numbers".

In recent development, mathematical model of epidemics has sufficiently proved to be reliable and successfully applied to the different settings consisting of social problems such as use of drugs, computer viruses, and global ideas [5, 10]. Indeed, a simple epidemic model of SIR type was proposed in [6] to get insights on how alcoholic drinking spread and how it can be limited. In [16, 18] found out that variables such as type of high school, teachers' attitude, lack of self-confidence and motivation, stress experienced in maths classes and disappointment increased anxiety.

The significance of this study is that it dealt with the key variables in the anxiety university students experience, evaluate their features and the steps to be taken to prevent anxiety about mathematics. However, this study is motivated by students of the faculty of Economics and Administrative Sciences against the pasted results for the second semester 2018/2019 academic-year. Such an act indicates that there is a need to take appropriate measure to lessen maths anxiety. To address such a problem, we propose a deterministic mathematical model of SIR type to get insights on how to overcome the problem.

The remaining part of the paper is organized as follows: In Section 2, we formulate the model. The model is rigorously analyzed in Section 3. In Section 4, we provide a concluding remarks.

MODEL DESCRIPTION

We divide the faculty students of their primary, elementary and high school maths average levels into 3 different classes: W, average students; B, below average students; and A, above average students. We have choose these definitions in relation to academic performance since primary to high school. The students population, N is assumed to be constant. Note that cohort replacement plays an important role on contagion among students regarding academic calender but that is not considered here for simplicity. The model is given by the following system of non-linear ordinary differential equations:

International Conference on Analysis and Applied Mathematics (ICAAM 2020)
AIP Conf. Proc. 2325, 020042-1–020042-4; https://doi.org/10.1063/5.0040308
Published by AIP Publishing. 978-0-7354-4069-2/$30.00

TABLE 1. Parameters for the model and basic reproduction number

Parameters	Descriptions
μ	Participant rate from Faculty of Economics and Administrative Sciences
β_1	Transmission rate of weak students to above average students
β_2	Transmission rate of weak students to below average students
p	Fraction (proportion) of average students
γ, τ	Rates of positive change of behavior in relation to the teaching of maths and the teachers' way of teaching

$$\begin{cases} \frac{dW}{dt} &= \mu - p(\tau+\gamma)\beta_1 AW - (1-p)(\tau+\gamma)\beta_2 BW - \mu A, \\ \frac{dB}{dt} &= (1-p)(\tau+\gamma)\beta_2 BW - \mu B, \\ \frac{dA}{dt} &= p(\tau+\gamma)\beta_1 AW - \mu A. \end{cases} \tag{1}$$

The parameters given in the Table I.

Equilibrium Points

Equating the equations in (1) to zero and solving simultaneously we find the following three equilibrium points.
1.Problem-free equilibrium,

$$E_0 = (1,0,0),$$

always exists.
2.Below weak students-free equilibrium,

$$E_1 = (\frac{\mu}{\beta_1 p(\tau+\gamma)}, \frac{\beta_1 p(\tau+\gamma)-\mu}{\beta_1 p(\tau+\gamma)}, 0),$$

exists when $R_0^A > 1$.
3.Above weak-students-free equilibrium,

$$E_2 = (\frac{\mu}{\beta_1 p(\tau+\gamma)}, \frac{\beta_1 p(\tau+\gamma)-\mu}{\beta_1 p(\tau+\gamma)}, 0),$$

exists when $R_0^B > 1$.

Threshold Parameters

The threshold parameter is denoted by R_0 and it is usually called the basic reproduction number. In this paper we use next generation of matrix method to find R_0 and we found two threshold parameters

$$R_0^A = \frac{\beta_1 p(\tau+\gamma)}{\mu} \tag{2}$$

and

$$R_0^B = \frac{\beta_2(1-p)(\tau+\gamma)}{\mu}. \tag{3}$$

GLOBAL STABILITY ANALYSIS OF THE EQUILIBRIA

In this section, stability analysis of the two equilibrium points is obtained by the use of Lyapunov function. The conditions for the global stability of the equilibria in each case depends on the magnitude of the basic reproduction ratio R_0. Hence we have the following theorems and their proofs.

Theorem 1 *The problem free equilibrium is globally asymptotically stable when* $R_0^A < 1$ *and* $R_0^B < 1$.

Proof. We construct the following Lyapunov function

$$V = (W - W_0 ln(W)) + A + B + 1, \tag{4}$$

which is positive definite at the disease free equilibrium point. By the derivative of Eq. 4, we have

$$\begin{aligned} V' &= 1 - A' + B' + W'\frac{W}{W_0} \\ &= \mu W_0 (2 - \frac{W}{W_0} - \frac{W_0}{W}) + (p(\tau+\gamma)\beta_1 W_0 - \mu)A + ((1-p)(\tau+\gamma)\beta_2 W_0 - \mu)B. \end{aligned}$$

Relation between geometric and arithmetic means we have $2 - \frac{W}{W_0} - \frac{W_0}{W} < 0$. Hence, $V' \leq 0$ when $R_0^A < 1$ and $R_0^B < 1$. Therefore, the problem free equilibrium is globally asymptotically stable when $R_0^A < 1$ and $R_0^B < 1$.

Theorem 2 *Below average students-free equilibrium* E_1 *is globally asymptotically stable when* $R_0^B < 1$.

Proof. We construct the following Lyapunov function

$$V = (W - W_1 \ln(W)) + (A - A_1 \ln(A)) + B + C, \tag{5}$$

where

$$C = -[W_1 - W_1 \ln(W_1) + A_1 - A_1 \ln(A_1)].$$

Here, V is positive definite at the below average student free equilibrium point. From the derivative of Eq. 5, we get

$$\begin{aligned} V' &= W'(1 - \frac{W}{W_1}) + (1 - \frac{A}{A_1})A' + B' \\ &= \mu W_0 (2 - \frac{W}{W_1} - \frac{W_1}{W}) + ((1-p)(\tau+\gamma)\beta_2 W_0 - \mu)B. \end{aligned}$$

By the relation between geometric and arithmetic means $2 - \frac{W}{W_1} - \frac{W_1}{W} < 0$. Therefore, if $R_0^B < 1$, then we have $V' < 0$. Hence, below average students-free equilibrium E_1 is globally asymptotically stable when $R_0^B < 1$.

Theorem 3 *Above average students-free equilibrium* E_1 *is globally asymptotically stable when* $R_0^A < 1$.

Proof. We construct the following Lyapunov function

$$V = (W - W_2 \ln(W)) + A + (B - B_2 \ln(B)) + C, \tag{6}$$

where

$$C = -[W_2 - W_2 \ln(W_2) + B_2 - B_2 \ln(B_1)].$$

Here, V is positive definite at the above average student free equilibrium point. The derivative of Eq. 6 is less than zero when $R_0^A < 1$. Hence, above average students-free equilibrium E_2 is globally asymptotically stable when $R_0^A < 1$.

CONCLUSION

We present a modelling of mathematical anxiety as a three-dimensional in Economics and Administrative Sciences. The proposed model is analyzed and the analysis reveals that the dynamics of such a problem is determined by the basic reproduction numbers $R_0^A$and R_0^B . The model analysis reveals that all of the students start to show better maths achievement on the positive way during the semester (approximately 3,5 months).

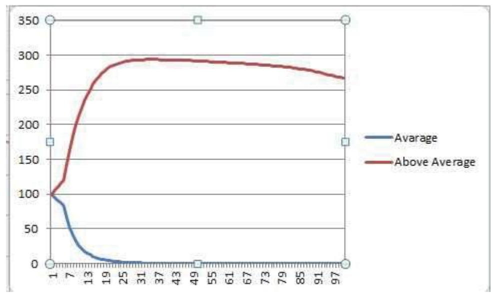

FIGURE 1. R_t values from March 11, 2020 to May 15, 2020.

The simulation with given in Fig. 1 shows that reducing maths anxiety by focusing positive change of behaviour in relation to the teaching of maths and the teachers' way of teaching is an effective on students' achievement of maths. In conclusion, the proposed model suggests that reducing maths anxiety by focusing positive change of behaviour in relation to the teaching of maths and the teachers' way of teaching is an effective on students' achievement of maths.

REFERENCES

1. M. Peker and M. Ulu, International Journal of Instruction **11**, 249-264 (2018).
2. S. Köse, Ş.K. Yılmaz, and S. Göktaş, Journal of Psychatric Nursing **9**, 105-111 (2018).
3. H. M. Sokolowski, Z. Hawes, and I. Lyons, Cognition **182**, 193-212 (2019).
4. W. Ahmed, Journal of Adolescence **67**, 158-166 (2018).
5. W. O. Kermack and A. G. Mckendrick, Proceeding of Royal Society London **1927**, 700-721 (2018).
6. B. Benedict, SIAM News **40**, (2007).
7. L. M. A. Bettencourt, A. Cintrón-Arias, D. I. Kaiser, and C. Castillo-Chávez, Phys. A. **364**, 513-536 (2006).
8. B. González, E. Huerta-Sánchez, A. Ortiz-Nieves, et al., J. Math. Psychol. **47**, 515-526 (2003).
9. A. Noymer, The Journal of Mathematical Sociology **25**, 299-323 (2001).
10. J. R. C. Piqueira, B. F. Navarro, and L. H. A. Moneteiro, The Journal of Mathematical Sociology **1**, 31-34 (2000).
11. H. W. Hethcote, SIAM Rev. **42**, 599-653 (2000).
12. p. Van den Driessche and J. Wanmough, Math. Biosci. **180**, 29-48 (2000).
13. L. Perko, *Differential Equations and Dynamical Systems* (Springer-Verlag, 2001).
14. N. Chitnis, J. M. Hyman, and J. M. Cushing, Bull. Math. Biol. **70**, 1272-1296 (2008).
15. B. Buonomo and D. Lacitignola, Nonlinear Anal. Modell. Control. **16**, 30-46 (2011).
16. I. M. McDonough and G. Ramirez, Learning and Individual Differences **64**, 33-42 (2018).
17. Z. Wang, N. Shakeshaft, and K. Schofield, PLOS ONE **13**, e0192072 (2018).
18. M. J. Justica-Galiano, British Journal of Educational Psychology **87**, 573-589 (2017).

On Solvability of the Nonlinear Optimization Problem with the Limitations on the Control

Akylbek Kerimbekov[1, a)] and Saltanat Doulbekova[2, b)]

[1)]Applied Mathematics and Informatics, Kyrgyz-Russian Slavic University, Bishkek, Kyrgyzstan
[2)]Applied Mathematics and Informatics, Kyrgyz-Russian Slavic University, Bishkek, Kyrgyzstan

[a)]Corresponding author: akl7@rambler.ru
[b)]Electronic mail: doulbekova25@mail.ru

Abstract. In this article the solvability of the problem of optimal control of oscillatory processes described by the integro-differential equation with the Fredholm operator, with given control limitation is investigated.
It is established that the desired control is among the solutions of the nonlinear Fredholm integral equation of the first kind. Sufficient conditions for the existence of a solution of nonlinear optimization problem are found.

OPTIMIZATION PROBLEM STATEMENT

The article investigates the unique solvability of nonlinear optimization problem of oscillatory processes (see [1,2]), where it is necessary to minimize the integral functional

$$J[u]=\int_0^1 [V(T,x)-\xi(x)]^2dx+\beta\int_0^T p[t,u(t)]dt, \beta>0 \tag{1}$$

on the set of solutions of boundary value problem

$$V_{tt}=V_{xx}+\lambda\int_0^T K(t,\tau)V(\tau,x)d\tau+g(t,x)f[u(t)],\ \ 0<x<1,\ 0<t\leq T,$$

$$V(0,x)=\psi_1,\ V_t(0,x)=\psi_2,\ \ 0<x<1, \tag{2}$$

$$V_x(t,0)=0, V_x(t,1)=0,\ 0<t<T.$$

Here the control $u(t)$ is an element of a Hilbert space $H(0,T)$, i.e., $u(t)\in H(0,T)$; $f[u(t)]\in H(0,T)$ is external influence function, which is nonlinear and monotonic with respect to the functional variable $u(t)$ i.e.,

$$f_u[u(t)]\neq 0,\ \forall t\in[0,T], \tag{3}$$

where functions $p[t,u(t)]\in H(0,T)$, $\xi(x)\in H(0,1)$, $g(t,x)\in H(Q)$, $Q=(0,1)\times(0,T)$, $\psi_1(x)\in H_1(0,1)$, $\psi_2(x)\in H(0,1)$, $K(t,\tau)\in H(D)$, $D=(0,T)\times(0,T)$ and number

$$K_0=\int_0^T\int_0^T K^2(t,\tau)d\tau dt$$

are considered as given, λ is a parameter, $H_1(0,1)$ is the first order Sobolev space, T is fixed time point.

In this task, the desired control $u^0(t)\in H(0,T)$ is searched among the elements of the set

$$M=\{u(t)\in H(0,T)|\ f_u[u(t)]\neq 0,\ p_u[t,u(t)]=0\} \tag{4}$$

which minimizes the functional (1) together with the corresponding solution $V(t,x)$ of the boundary value problem (2).

International Conference on Analysis and Applied Mathematics (ICAAM 2020)
AIP Conf. Proc. 2325, 020043-1–020043-4; https://doi.org/10.1063/5.0040550
Published by AIP Publishing. 978-0-7354-4069-2/$30.00

OPTIMIZATION PROBLEM SOLUTION

Generalized solution $V(t,x) \in H(Q)$ of boundary value problem (2) is constructed, which for each $u(t) \in H(0,T)$ and valid condition (3), is uniquely determined by the formula

$$V(t,x) = \sum_{n=1}^{\infty} \left[\lambda \int_0^t R_n(t,s,\lambda) q(s) ds + q(t) \right] z_n(x), \tag{5}$$

where $R(t,s,\lambda)$ is resolvent of kernel

$$K_n(t,s) = \frac{1}{\lambda} \int_0^t sin\lambda_n(t-\tau) K(\tau,s) d\tau, \ K(0,s) = 0$$

of integral equation

$$V_n(t) = \lambda \int_0^T K_n(t,s) V_n(s) ds + q_n(t), \tag{6}$$

$$q_n(t) = \psi_{1n} cos\lambda_n t + \frac{\psi_{2n}}{\lambda_n} sin\lambda_n t + \frac{1}{\lambda_n} \int_0^t g_n f[u(\tau)] sin\lambda_n(t-\tau) d\tau.$$

In formulas (5) and (6), $z_n(x) = \sqrt{2} cos\lambda_n x$ is orthonormal system of eigenfunctions of the boundary value problem

$$z_n''(x) + \lambda_n^2 z_n = 0, \ z'(0) = 0, \ z'(1) = 0, \ \lambda_n = n\pi, \ n = 1,2,3,...,$$

resolvent $R(t,s,\lambda)$ is a continuous function which exists for parameter values satisfying inequality

$$|\lambda| < \frac{\lambda_1}{\sqrt{K_0 T^2}},$$

$$\int_0^T R^2(t,s,\lambda) ds < \frac{K_0 T}{\left(\lambda_n - |\lambda| \sqrt{K_0 T^2}\right)^2}, \tag{7}$$

$g_n(t), \ \psi_{1n}, \ \psi_{2n}$ are Fourier coefficients, accordingly of functions $g(t,x), \ \psi_1(x), \ \psi_2(x)$.

Calculating the increment functional (1) we obtain the relation

$$\Delta J[u(t)] = J[u(t) + \Delta u(t)] - J[u(t)] = -\int_0^T \Delta\Pi[t, V(t,x), \omega(t,x)] dx f[u(t)] + \int_0^T \Delta V^2(T,x) dx,$$

where

$$\Pi[t, V(t,x), \omega(t,x)] = \int_0^1 g(t,x) \omega(t,x) dx f[u(t)] - \beta p[t, u(t)],$$

$$\Delta\Pi[\cdot, u(t)] = \Pi[\cdot, u(t) + \Delta u(t)] - \Pi[\cdot, u(t)].$$

The set of valid values of control is an open set. Therefore, we have the following optimality conditions in the form of the equality

$$\int_0^1 g(t,x) \omega(t,x) dx f_u[u(t)] - \beta p_u[t, u(t)] = 0 \tag{8}$$

and in the form of differential inequality

$$\int_0^1 g(t,x), \omega(t,x) f_{uu}[u(t)] dx - \beta p_{uu}[t, u(t)] < 0, \tag{9}$$

where $\omega(t,x)$ is a generalized solution of the conjugate boundary value problem

$$\begin{gathered}\omega_{tt}=\omega_{xx}+\lambda\int_0^T K(\tau,t)\omega(\tau,x)d\tau,\ \ 0<x<1,\ 0<t<T,\\ \omega(T,x)=0,\ \omega_t(T,x)-2[V(T,x)-\xi(x)]=0,\ \ 0<x<1,\\ \omega_x(t,0)=0,\ \omega_x(t,1)=0,\ \ 0\le t<T\end{gathered}\tag{10}$$

and has a form

$$\omega(t,x)=-2\sum_{n=1}^{\infty}\left[\lambda\int_0^T C_n(s,t,\lambda)y_n(s)ds+y_n(t)\right]z_n(x).\tag{11}$$

Here $C_n(s,t,\lambda)$ is a resolvent of kernel

$$B_n(s,t)=\frac{1}{\lambda_n}\int_0^T sin\lambda_n(\tau-t)K(\tau,s)d\tau,\ B_n(s,T)=0,$$

of integral equation

$$\omega_n(t)=\lambda\int_0^T B_n(s,t)\omega_n(s)ds+y_n(t),\tag{12}$$

$$y_n(t)=\frac{2}{\lambda_n}[V_n(T)-\xi_n]\,sin\lambda_n(T-t),\tag{13}$$

where ξ_n are Fourier coefficients of the function $\xi(x)$.

On the set M the optimality conditions (8), (9) takes the form

$$\int_0^1 g(t,x)\omega(t,x)dx=0,\tag{14}$$

$$p_{uu}[t,u(t)]>0.\tag{15}$$

According to (11), equality (14) has the form

$$\sum_{n=1}^{\infty}g_n(t)\left[\lambda\int_0^T C_n(s,t,\lambda)y_n(s)ds+y_n(t)\right]=0,$$

which, taking into account (13), we rewrite in the form

$$2\sum_{n=1}^{\infty}g_n(t)\frac{1}{\lambda_n}\left[sin\lambda_n(T-t)+\lambda\int_0^T C_n(s,t,\lambda)sin\lambda_n(T-s)ds\right](V_n(T)-\xi_n)=0.$$

This equality is valid only if $V_n(T)-\xi_n=0$, i.e., only when

$$V(T,x)=\xi(x).\tag{16}$$

Therefore, we find only those controls, for which equality (16) takes place. Taking into account (5) and (6) we rewrite the equality (16) in the form

$$\int_0^T G_n(t,\lambda)f[u(t)]dt=\psi_n(T,\lambda),\ n=1,2,3,...,\tag{17}$$

where

$$G_n(t,\lambda)=\frac{g_n(t)}{\lambda_n}\left[sin\lambda_n(T-t)+\lambda\int_0^T R_n(T,s,\lambda)sin\lambda_n(s-t)ds\right],\tag{18}$$

$$\psi_n(T,\lambda) = \xi_n - \psi_{1n}\left[cos\lambda_n T + \lambda\int_0^T R_n(T,s,\lambda)cos\lambda_n(s)ds\right] - \frac{\psi_{2n}}{\lambda_n}\left[sin\lambda_n T + \lambda\int_0^T R_n(T,s,\lambda)sin\lambda_n(s)ds\right] \quad (19)$$

Now we investigate the system of nonlinear integral equations (17). We introduce the following notation

$$f[u(t)] = \nu(t). \quad (20)$$

Note that, by (3), the function $u(t)$ is uniquely defined, i.e. there is a such $\varphi(\cdot)$ function, that the equality

$$u(t) = \varphi[\nu(t)] \quad (21)$$

takes place. According to (20), we rewrite the system (17) in the form

$$\int_0^T G_n(t,\lambda)\nu(t)dt = \psi_n(T,\lambda),\ n = 1,2,3,... \quad (22)$$

and in

$$G[\nu] = h \quad (23)$$

operator form, where

$$G[\nu] = \int_0^T G_n(t,\lambda)\nu(t)dt,\ h = \{\psi_1(T,\lambda),...,\psi_n(T,\lambda),...\},$$
$$G(t) = \{G_1(t,\lambda),...,G_n(t,\lambda),...\}.$$

It is proved that the operator equation (23) has a solution in a form

$$\nu(t,\gamma) = \sum_{n,j=1}^{\infty} G_n(t,\lambda)\alpha_n + \gamma$$
$$= \sum_{n,j=1}^{\infty} G_n(t,\lambda)\sum_{k=1}^{\infty}\varepsilon_{nk}(t,\lambda)\left[\psi_k(T,\lambda) - \int_0^T G_k(t,\lambda)dt\cdot\gamma\right] + \gamma, \quad (24)$$

in

$$\ell_2 = \{b = (b_1,...,b_n,...)|\ \|b\|_{\ \ell_2} = \sum_{k=1}^{\infty} b_n^2 < \infty\}$$

Hilbert space. Here γ is arbitrary constant. Substituting this solution into (21), we obtain the solution of the system of nonlinear Fredholm integral equations of the first kind (17)

$$u(t,\gamma) = \varphi[\nu(t,\gamma)] \quad (25)$$

On each of these controls the equality (16) takes place.

Now from the optimality conditions $p_u[t,u(t)] = 0,\ p_{uu}[t,u(t)] > 0$ we find a control $u = u^*(t) \in H(0,T)$. The question now arises - is $u^*(t)$ included in controls family (25)? It is established that there is a unique γ_0 value at which the equality

$$u(t,\gamma_0) = u^*(t)$$

takes place. Thus, it is stated that on the set M there is a unique $u^0 = u^*(t)$ element that minimizes functional (1) and equality (16) is valid.

REFERENCES

1. E. F. Abdyldaeva and A. K. Kerimbekov, FILOMAT **33**, 1369–1379 (2019).
2. E. F. A. A. K. Kerimbekov, Eurasian Mathematical Journal **6**, 18–40 (2015).

Mobile App Evaluation Application with AHP Method Based on Interval Type-2 Fuzzy Sets

Büsra Meniz[a)] and Fatma Tiryaki[b)]

Department of Mathematics, Yildiz Technical University, 34210 Istanbul, Turkey

[a)] *Corresponding author: bmeniz@yildiz.edu.tr*
[b)] *Electronic mail: ftiryaki@yildiz.edu.tr*

Abstract. In the present article the Analytic Hierarchy Process (AHP) method, which has an important place among multi-criteria decision making methods, will be used in the solution. In addition, the group decision making will be applied as it will be beneficial to the result that there will be more than one decision maker. The method will be handled with the Interval Type-2 Fuzzy Sets (IT2FSs) that have high success in handling uncertainties.

INTRODUCTION

Nowadays, there are many applications for smart phones that are widely used. These phone applications created initially with small-scale sources. They grow with the investments of developers and appeal to a wider population. However, not every application may have a high level of success. Therefore, which application the investor will support is an important decision making problem. A hierarchy of goal, criteria, sub-criteria and alternatives has been created for this decision making problem.

The selection and classification of criteria in decision-making problems and the creation of a hierarchy are the first and the most important stage of the solution. It is also important to weigh the selected criteria correctly and measure the alternatives according to these weights. For this, it is necessary to choose the most appropriate decision making tool depending on the type of problem. Among the multi-criteria decision making methods, AHP method is very successful in criterion weighting. AHP method was developed by Saaty [1]. Saaty sampled the problem of choosing a school as the first application. Fuzzy sets, which allow uncertain situations to be taken into account, were proposed by Zadeh [2]. The first adaptation of the AHP method to fuzzy numbers was made by Laarhoven and Pedrycz [3]. Its full adaptation to fuzzy numbers was made by Buckley [4]. Regarding uncertainty, Zadeh [5] further expanded the existing fuzzy set theory and introduced type-2 fuzzy sets into the literature. Then Mendel, John and Liu [6] added the concept of spacing to type-2 fuzzy sets. Interval type-2 fuzzy numbers, a special case of IT2FSs, were used by Chen [7] for the first time in decision making. Thus, Kahraman et al. [8] was able to adapt the AHP methodology to the interval type-2 fuzzy numbers. In this application, AHP method based on IT2FSs will be applied to an investment problem together with the group decision making.

PRELIMINARIES

An interval type-2 fuzzy number can be defined by the upper membership function and the lower membership function. Accordingly, the Interval Type-2 Trapezoidal Fuzzy Number (IT2TrFN) can be represented by

$$\tilde{\tilde{A}}_i = \left(\left(a_{i1}^U, a_{i2}^U, a_{i3}^U, a_{i4}^U; H_1\left(\tilde{A}_i^U\right), H_2\left(\tilde{A}_i^U\right)\right), \left(a_{i1}^L, a_{i2}^L, a_{i3}^L, a_{i4}^L; H_1\left(\tilde{A}_i^L\right), H_2\left(\tilde{A}_i^L\right)\right)\right). \tag{1}$$

The sum of two IT2TrFN is calculated by

$$\begin{aligned}\tilde{\tilde{A}}_1 \oplus \tilde{\tilde{A}}_2 = &\left(a_{11}^U + a_{21}^U, a_{12}^U + a_{22}^U, a_{13}^U + a_{23}^U, a_{14}^U + a_{24}^U; \min\left(H_1\left(\tilde{A}_1^U\right), H_1\left(\tilde{A}_2^U\right)\right), \min\left(H_2\left(\tilde{A}_1^U\right), H_2\left(\tilde{A}_2^U\right)\right)\right), \\ &\left(a_{11}^L + a_{21}^L, a_{12}^L + a_{22}^L, a_{13}^L + a_{23}^L, a_{14}^L + a_{24}^L; \min\left(H_1\left(\tilde{A}_1^L\right), H_1\left(\tilde{A}_2^L\right)\right), \min\left(H_2\left(\tilde{A}_1^L\right), H_2\left(\tilde{A}_2^L\right)\right)\right).\end{aligned} \tag{2}$$

The multiplication of two IT2TrFN is calculated by

$$\begin{aligned}\tilde{\tilde{A}}_1 \otimes \tilde{\tilde{A}}_2 = &\left(a_{11}^U \times a_{21}^U, a_{12}^U \times a_{22}^U, a_{13}^U \times a_{23}^U, a_{14}^U \times a_{24}^U; \min\left(H_1\left(\tilde{A}_1^U\right), H_1\left(\tilde{A}_2^U\right)\right), \min\left(H_2\left(\tilde{A}_1^U\right), H_2\left(\tilde{A}_2^U\right)\right)\right), \\ &\left(a_{11}^L \times a_{21}^L, a_{12}^L \times a_{22}^L, a_{13}^L \times a_{23}^L, a_{14}^L \times a_{24}^L; \min\left(H_1\left(\tilde{A}_1^L\right), H_1\left(\tilde{A}_2^L\right)\right), \min\left(H_2\left(\tilde{A}_1^L\right), H_2\left(\tilde{A}_2^L\right)\right)\right).\end{aligned} \tag{3}$$

International Conference on Analysis and Applied Mathematics (ICAAM 2020)
AIP Conf. Proc. 2325, 020044-1–020044-6; https://doi.org/10.1063/5.0040267
Published by AIP Publishing. 978-0-7354-4069-2/$30.00

The inverse of an IT2TrFN is calculated by

$$\tilde{\tilde{A}}^{-1} = 1/\tilde{\tilde{A}} = \left(\left(\frac{1}{a_4^U}, \frac{1}{a_3^U}, \frac{1}{a_2^U}, \frac{1}{a_1^U}; H_1\left(a_2^U\right), H_2\left(a_3^U\right)\right), \left(\frac{1}{a_4^L}, \frac{1}{a_3^L}, \frac{1}{a_2^L}, \frac{1}{a_1^L}; H_1\left(a_2^L\right), H_2\left(a_3^L\right)\right)\right). \quad (4)$$

The n-th root of an IT2TrFN is calculated by

$$\tilde{\tilde{A}}^{1/n} = \left(\left(\sqrt[n]{a_1^U}, \sqrt[n]{a_2^U}, \sqrt[n]{a_3^U}, \sqrt[n]{a_4^U}; H_1\left(\tilde{A}^U\right), H_2\left(\tilde{A}^U\right)\right), \left(\sqrt[n]{a_1^L}, \sqrt[n]{a_2^L}, \sqrt[n]{a_3^L}, \sqrt[n]{a_4^L}; H_1\left(\tilde{A}^L\right), H_2\left(\tilde{A}^L\right)\right)\right). \quad (5)$$

AHP METHODOLOGY

In this section we introduce the methodology:

Step 1. The components at each level of the hierarchy, which show the structure of the problem, are compared pairwise by decision-makers according to the level above, and pairwise comparison matrices are created using Equation (4)

$$\tilde{\tilde{A}} = \begin{bmatrix} \tilde{\tilde{1}} & \tilde{\tilde{a}}_{12} & \dots & \tilde{\tilde{a}}_{1n} \\ \tilde{\tilde{a}}_{21} & \tilde{\tilde{1}} & \dots & \tilde{\tilde{a}}_{2n} \\ \vdots & \vdots & \ddots & \vdots \\ \tilde{\tilde{a}}_{n1} & \tilde{\tilde{a}}_{n2} & \dots & \tilde{\tilde{1}} \end{bmatrix} = \begin{bmatrix} \tilde{\tilde{1}} & \tilde{\tilde{a}}_{12} & \dots & \tilde{\tilde{a}}_{1n} \\ 1/\tilde{\tilde{a}}_{12} & \tilde{\tilde{1}} & \dots & \tilde{\tilde{a}}_{2n} \\ \vdots & \vdots & \ddots & \vdots \\ 1/\tilde{\tilde{a}}_{1n} & 1/\tilde{\tilde{a}}_{2n} & \dots & \tilde{\tilde{1}} \end{bmatrix}.$$

Step 2. Consistency analysis is performed for all fuzzy pairwise comparison matrices created in Step 1. For this, the consistencies of the crisp pairwise comparison matrices obtained by defuzzifying the pairwise comparison matrices are calculated. If the matrices are not consistent, re-evaluation is asked from decision makers.
Step 3. Fuzzy pairwise comparison matrices that created separately for each decision maker are aggregated with geometric mean using Equations (3) and (5).
Step 4. In pairwise comparison matrices, the geometric mean of each row is again calculated using Equations (3) and (5). Then the weights obtained are normalized and fuzzy normalized weights are found.
Step 5. Fuzzy utility values of alternatives are obtained by multiplication of fuzzy weights and geometric mean of rows by using Eq. (3).
Step 6. The final rankings of alternatives are found by defuzzifying and normalizing the fuzzy utility values.

APPLICATION

In practice, a hierarchy was created by gathering the criteria taken from [9, 10, 11]. Also, evaluations were made with 4 alternatives. The hierarchical structure of the problem is illustrated by Figure 1. Comparisons were made with a group of 3 decision makers.
Step 1. Decision makers were asked to compare criteria, sub-criteria and alternatives in pairs. Thus, fuzzy pairwise comparison matrices are created with the help of linguistic variables. The interval type-2 trapezoidal fuzzy number equivalents of linguistic variables are given in Table 1. Pairwise comparisons are shown in Tables 2–17.

TABLE 1. Fuzzy scales of linguistic variables

Linguistic variables	Interval type-2 fuzzy set
Absolutely Strong (AS)	(7,8,9,9;1,1),(7.2,8.2,8.8,9;0.8,0.8)
Very Strong (VS)	(5,6,8,9;1,1),(5.2,6.2,7.8,8.8;0.8,0.8)
Fairly Strong (FS)	(3,4,6,7;1,1),(3.2,4.2,5.8,6.8;0.8,0.8)
Slightly Strong (SS)	(1,2,4,5;1,1),(1.2,2.2,3.8,4.8;0.8,0.8)
Exactly Equal (E)	(1,1,1,1;1,1),(1,1,1,1;1,1)
If factor i has one of the above linguistic variables assigned to it when compared with factor j, the j has the reciprocal value when compared with i	Reciprocals of above

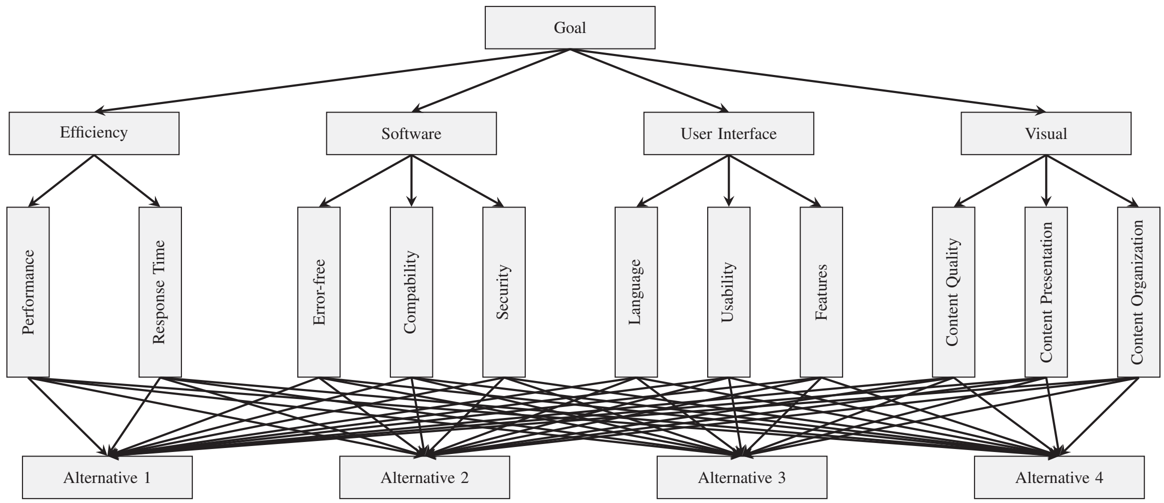

FIGURE 1. The hierarchical structure of the problem

TABLE 2. Pairwise comparisons of efficiency

	P	R
P	(E,E,E)	(E,1/SS,SS)
R	(E,SS,1/SS)	(E,E,E)

TABLE 3. Pairwise comparisons of software

	E	C	S
E	(E,E,E)	(VS,SS,E)	(1/VS,1/FS,1/AS)
C	(1/VS,1/SS,E)	(E,E,E)	(1/AS,1/AS,1/AS)
S	(VS,FS,AS)	(AS,AS,AS)	(E,E,E)

TABLE 4. Pairwise comparisons of user interface

	L	U	F
L	(E,E,E)	(SS,1/FS,1/FS)	(FS,1/AS,1/FS)
U	(1/SS,FS,FS)	(E,E,E)	(SS,1/FS,E)
F	(1/FS,AS,FS)	(1/SS,FS,E)	(E,E,E)

TABLE 5. Pairwise comparisons of visual

	Q	P	O
Q	(E,E,E)	(SS,1/SS,VS)	(FS,1/AS,VS)
P	(1/SS,SS,1/VS)	(E,E,E)	(SS,1/VS,E)
O	(1/FS,AS,1/VS)	(1/SS,VS,E)	(E,E,E)

TABLE 6. Pairwise comparisons of main criteria

	E	S	U	V
E	(E,E,E)	(E,E,E)	(AS,AS,VS)	(VS,AS,VS)
S	(E,E,E)	(E,E,E)	(AS,AS,VS)	(VS,AS,VS)
U	(1/AS,1/AS,1/VS)	(1/AS,1/AS,1/VS)	(E,E,E)	(1/SS,E,E)
V	(1/VS,1/AS,1/VS)	(1/VS,1/AS,1/VS)	(E,E,E)	(E,E,E)

TABLE 7. Pairwise comparisons of alternatives w.r.t performance

	A1	A2	A3	A4
A1	(E,E,E)	(AS,VS,AS)	(FS,SS,FS)	(AS,E,SS)
A2	(1/AS,1/VS,1/AS)	(E,E,E)	(1/SS,1/FS,1/FS)	(E,1/VS,1/VS)
A3	(1/FS,1/SS,1/FS)	(SS,FS,FS)	(E,E,E)	(SS,1/SS,1/SS)
A4	(1/AS,E,1/SS)	(E,VS,VS)	(1/SS,SS,SS)	(E,E,E)

TABLE 8. Pairwise comparisons of alternatives w.r.t response time

	A1	A2	A3	A4
A1	(E,E,E)	(FS,VS,SS)	(E,E,SS)	(SS,SS,SS)
A2	(1/FS,1/VS,1/SS)	(E,E,E)	(1/FS,1/VS,E)	(1/SS,1/FS,E)
A3	(E,E,1/SS)	(FS,VS,E)	(E,E,E)	(SS,SS,E)
A4	(1/SS,1/SS,1/SS)	(SS,FS,E)	(1/SS,1/SS,E)	(E,E,E)

TABLE 9. Pairwise comparisons of alternatives w.r.t error-free

	A1	A2	A3	A4
A1	(E,E,E)	(SS,FS,E)	(E,E,VS)	(1/SS,E,FS)
A2	(1/SS,1/FS,E)	(E,E,E)	(1/SS,1/FS,VS)	(1/FS,1/FS,FS)
A3	(E,E,1/VS)	(SS,FS,1/VS)	(E,E,E)	(1/SS,E,1/SS)
A4	(SS,E,1/FS)	(FS,FS,1/FS)	(SS,E,SS)	(E,E,E)

TABLE 10. Pairwise comparisons of alternatives w.r.t compability

	A1	A2	A3	A4
A1	(E,E,E)	(SS,SS,1/SS)	(1/SS,E,1/SS)	(1/SS,AS,1/FS)
A2	(1/SS,1/SS,SS)	(E,E,E)	(1/FS,1/SS,E)	(1/FS,FS,1/SS)
A3	(SS,E,SS)	(FS,SS,E)	(E,E,E)	(E,AS,1/SS)
A4	(SS,1/AS,FS)	(FS,1/FS,SS)	(E,1/AS,SS)	(E,E,E)

TABLE 11. Pairwise comparisons of alternatives w.r.t security

	A1	A2	A3	A4
A1	(E,E,E)	(FS,VS,E)	(FS,E,1/FS)	(SS,E,1/AS)
A2	(1/FS,1/VS,E)	(E,E,E)	(E,1/VS,1/FS)	(1/SS,1/VS,1/AS)
A3	(1/FS,E,FS)	(E,VS,FS)	(E,E,E)	(1/SS,E,1/SS)
A4	(1/SS,E,AS)	(SS,VS,AS)	(SS,E,SS)	(E,E,E)

TABLE 12. Pairwise comparisons of alternatives w.r.t language

	A1	A2	A3	A4
A1	(E,E,E)	(FS,SS,SS)	(E,FS,FS)	(E,E,SS)
A2	(1/FS,1/SS,1/SS)	(E,E,E)	(1/FS,SS,SS)	(1/FS,1/SS,E)
A3	(E,1/FS,1/FS)	(FS,1/SS,1/SS)	(E,E,E)	(E,1/FS,1/SS)
A4	(E,E,1/SS)	(FS,SS,E)	(E,FS,SS)	(E,E,E)

TABLE 13. Pairwise comparisons of alternatives w.r.t usability

	A1	A2	A3	A4
A1	(E,E,E)	(VS,AS,AS)	(VS,VS,FS)	(FS,SS,SS)
A2	(1/VS,1/AS,1/AS)	(E,E,E)	(E,1/SS,1/FS)	(1/SS,1/VS,1/VS)
A3	(1/VS,1/VS,1/FS)	(E,SS,FS)	(E,E,E)	(1/SS,1/FS,1/SS)
A4	(1/FS,1/SS,1/SS)	(SS,VS,VS)	(SS,FS,SS)	(E,E,E)

TABLE 14. Pairwise comparisons of alternatives w.r.t features

	A1	A2	A3	A4
A1	(E,E,E)	(E,FS,FS)	(E,E,SS)	(1/FS,1/SS,1/SS)
A2	(E,1/FS,1/FS)	(E,E,E)	(E,1/FS,1/SS)	(1/FS,1/AS,1/AS)
A3	(E,E,1/SS)	(E,FS,SS)	(E,E,E)	(1/FS,1/SS,1/VS)
A4	(FS,SS,SS)	(FS,AS,AS)	(FS,SS,VS)	(E,E,E)

TABLE 15. Pairwise comparisons of alternatives w.r.t content quality

	A1	A2	A3	A4
A1	(E,E,E)	(SS,FS,1/FS)	(FS,SS,1/AS)	(FS,1/SS,1/VS)
A2	(1/SS,1/FS,FS)	(E,E,E)	(SS,1/SS,1/FS)	(SS,1/AS,1/SS)
A3	(1/FS,1/SS,AS)	(1/SS,SS,FS)	(E,E,E)	(E,1/VS,SS)
A4	(1/FS,SS,VS)	(1/SS,AS,SS)	(E,VS,1/SS)	(E,E,E)

TABLE 16. Pairwise comparisons of alternatives w.r.t content presentation

	A1	A2	A3	A4
A1	(E,E,E)	(SS,VS,FS)	(SS,1/SS,1/FS)	(1/SS,E,1/FS)
A2	(1/SS,1/VS,1/FS)	(E,E,E)	(E,1/AS,1/AS)	(1/VS,1/VS,1/AS)
A3	(1/SS,SS,FS)	(E,AS,AS)	(E,E,E)	(1/VS,1/SS,E)
A4	(SS,E,FS)	(VS,VS,AS)	(VS,1/SS,AS)	(E,E,E)

TABLE 17. Pairwise comparisons of alternatives w.r.t content organization

	A1	A2	A3	A4
A1	(E,E,E)	(VS,AS,AS)	(FS,SS,E)	(VS,E,SS)
A2	(1/VS,1/AS,1/AS)	(E,E,E)	(1/SS,1/FS,1/AS)	(E,1/AS,1/VS)
A3	(1/FS,1/SS,E)	(SS,FS,AS)	(E,E,E)	(SS,1/SS,SS)
A4	(1/VS,E,1/SS)	(E,AS,VS)	(1/SS,SS,1/SS)	(E,E,E)

Step 2. Consistency analysis was performed for all pairwise comparison matrices. Matrices have been found to be consistent.
Step 3. Geometric means of pairwise comparison matrices created separately for each decision maker were taken.
Step 4. Weights of criteria and alternatives were calculated and normalized. The results obtained are shown in Tables 18, 19 and 20.

TABLE 18. Fuzzy weights of main criteria

Efficiency	(0.353, 0.398, 0.490, 0.546; 1,1), (0.362, 0.409, 0.477, 0.534; 0.8 0.8)	User Interface	(0.042, 0.045, 0.059, 0.072; 1,1), (0.043, 0.047, 0.056, 0.069; 0.8 0.8)
Software	(0.353, 0.398, 0.490, 0.546; 1,1), (0.362, 0.409, 0.477, 0.534; 0.8 0.8)	Visual	(0.048, 0.055, 0.073, 0.088; 1,1), (0.049, 0.057, 0.071, 0.084; 0.8 0.8)

TABLE 19. Fuzzy weights of sub-criteria

Performance	(0.103, 0.158, 0.309, 0.467; 1,1), (0.114, 0.170, 0.286, 0.424; 0.8 0.8)	Usability	(0.008, 0.013, 0.029, 0.049; 1,1), (0.009, 0.014, 0.026, 0.044; 0.8 0.8)
Response Time	(0.103, 0.158, 0.309, 0.467; 1,1), (0.114, 0.170, 0.286, 0.424; 0.8 0.8)	Features	(0.010, 0.015, 0.032, 0.053; 1,1), (0.011, 0.016, 0.029, 0.047; 0.8 0.8)
Error-free	(0.037, 0.050, 0.087, 0.120; 1,1), (0.040, 0.054, 0.082, 0.113; 0.8 0.8)	Content Quality	(0.012, 0.019, 0.044, 0.072; 1,1), (0.013, 0.021, 0.040, 0.065; 0.8 0.8)
Compability	(0.020, 0.024, 0.040, 0.058; 1,1), (0.020, 0.026, 0.037, 0.053; 0.8 0.8)	Content Presentation	(0.006, 0.009, 0.022, 0.037; 1,1), (0.006, 0.010, 0.020, 0.033; 0.8 0.8)
Security	(0.204, 0.270, 0.437, 0.558; 1,1), (0.216, 0.288, 0.410, 0.530; 0.8 0.8)	Content Organization	(0.009, 0.013, 0.028, 0.045; 1,1), (0.009, 0.014, 0.025, 0.40; 0.8 0.8)
Language	(0.004, 0.006, 0.015, 0.025; 1,1), (0.005, 0.007, 0.013, 0.022; 0.8 0.8)		

TABLE 20. Fuzzy weights of alternatives

Performance	
Alternative 1	(0.307, 0.438, 0.732, 0.964; 1,1), (0.334, 0.465, 0.693, 0.906; 0.8 0.8)
Alternative 2	(0.034, 0.043, 0.070, 0.103; 1,1), (0.036, 0.045, 0.066, 0.094; 0.8 0.8)
Alternative 3	(0.079, 0.117, 0.237, 0.386; 1,1), (0.087, 0.126, 0.219, 0.343; 0.8 0.8)
Alternative 4	(0.114, 0.158, 0.279, 0.411; 1,1), (0.123, 0.168, 0.262, 0.375; 0.8 0.8)
Response Time	
Alternative 1	(0.191, 0.313, 0.604, 0.853; 1,1), (0.216, 0.338, 0.568, 0.790; 0.8 0.8)
Alternative 2	(0.049, 0.064, 0.114, 0.179; 1,1), (0.052, 0.068, 0.107, 0.161; 0.8 0.8)
Alternative 3	(0.167, 0.235, 0.403, 0.570; 1,1), (0.181, 0.248, 0.381, 0.525; 0.8 0.8)
Alternative 4	(0.085, 0.120, 0.239, 0.415; 1,1), (0.092, 0.128, 0.220, 0.362; 0.8 0.8)
Error-free	
Alternative 1	(0.213, 0.284, 0.455, 0.602; 1,1), (0.228, 0.299, 0.434, 0.565; 0.8 0.8)
Alternative 2	(0.089, 0.117, 0.207, 0.310; 1,1), (0.094, 0.123, 0.194, 0.282; 0.8 0.8)

Alternative 3	(0.103, 0.137, 0.231, 0.326; 1,1), (0.110, 0.144, 0.218, 0.300; 0.8 0.8)
Alternative 4	(0.154, 0.229, 0.405, 0.549; 1,1), (0.169, 0.244, 0.384, 0.512; 0.8 0.8)
Compability	
Alternative 1	(0.097, 0.146, 0.298, 0.497; 1,1), (0.106, 0.157, 0.274, 0.438; 0.8 0.8)
Alternative 2	(0.076, 0.112, 0.228, 0.388; 1,1), (0.083, 0.120, 0.210, 0.341; 0.8 0.8)
Alternative 3	(0.186, 0.285, 0.518, 0.732; 1,1), (0.207, 0.305, 0.487, 0.675; 0.8 0.8)
Alternative 4	(0.117, 0.180, 0.334, 0.473; 1,1), (0.130, 0.194, 0.314, 0.437; 0.8 0.8)
Security	
Alternative 1	(0.160, 0.209, 0.322, 0.414; 1,1), (0.170, 0.219, 0.308, 0.392; 0.8 0.8)
Alternative 2	(0.050, 0.061, 0.096, 0.133; 1,1), (0.052, 0.064, 0.091, 0.123; 0.8 0.8)
Alternative 3	(0.147, 0.188, 0.304, 0.426; 1,1), (0.155, 0.197, 0.288, 0.393; 0.8 0.8)
Alternative 4	(0.228, 0.327, 0.547, 0.729; 1,1), (0.249, 0.347, 0.519, 0.683; 0.8 0.8)
Language	
Alternative 1	(0.214, 0.320, 0.559, 0.753; 1,1), (0.236, 0.340, 0.530, 0.705; 0.8 0.8)
Alternative 2	(0.067, 0.096, 0.189, 0.307; 1,1), (0.072, 0.102, 0.175, 0.273; 0.8 0.8)
Alternative 3	(0.073, 0.096, 0.174, 0.276; 1,1), (0.077, 0.101, 0.162, 0.247; 0.8 0.8)
Alternative 4	(0.171, 0.239, 0.405, 0.560; 1,1), (0.185, 0.253, 0.383, 0.519; 0.8 0.8)
Usability	
Alternative 1	(0.305, 0.446, 0.801, 1.103; 1,1), (0.333, 0.477, 0.754, 1.027; 0.8 0.8)
Alternative 2	(0.032, 0.040, 0.069, 0.107; 1,1), (0.033, 0.042, 0.065, 0.097; 0.8 0.8)
Alternative 3	(0.051, 0.070, 0.133, 0.209; 1,1), (0.055, 0.075, 0.123, 0.187; 0.8 0.8)
Alternative 4	(0.114, 0.175, 0.358, 0.565; 1,1), (0.126, 0.189, 0.332, 0.508; 0.8 0.8)
Features	
Alternative 1	(0.108, 0.144, 0.255, 0.382; 1,1), (0.115, 0.152, 0.239, 0.347; 0.8 0.8)
Alternative 2	(0.043, 0.053, 0.089, 0.132; 1,1), (0.045, 0.056, 0.084, 0.121; 0.8 0.8)
Alternative 3	(0.082, 0.108, 0.189, 0.284; 1,1), (0.087, 0.114, 0.177, 0.258; 0.8 0.8)
Alternative 4	(0.287, 0.437, 0.808, 1.116; 1,1), (0.317, 0.469, 0.758, 1.039; 0.8 0.8)
Content Quality	
Alternative 1	(0.111, 0.173, 0.343, 0.512; 1,1), (0.123, 0.186, 0.320, 0.467; 0.8 0.8)
Alternative 2	(0.072, 0.111, 0.234, 0.386; 1,1), (0.080, 0.120, 0.216, 0.343; 0.8 0.8)
Alternative 3	(0.114, 0.175, 0.343, 0.523; 1,1), (0.126, 0.188, 0.319, 0.473; 0.8 0.8)
Alternative 4	(0.164, 0.250, 0.486, 0.733; 1,1), (0.181, 0.268, 0.452, 0.665; 0.8 0.8)
Content Presentation	
Alternative 1	(0.104, 0.149, 0.277, 0.412; 1,1), (0.113, 0.159, 0.259, 0.376; 0.8 0.8)
Alternative 2	(0.037, 0.045, 0.072, 0.100; 1,1), (0.039, 0.048, 0.068, 0.093; 0.8 0.8)
Alternative 3	(0.166, 0.232, 0.387, 0.520; 1,1), (0.179, 0.246, 0.366, 0.486; 0.8 0.8)
Alternative 4	(0.253, 0.343, 0.560, 0.750; 1,1), (0.271, 0.361, 0.531, 0.701; 0.8 0.8)
Content Organization	
Alternative 1	(0.285, 0.398, 0.646, 0.838; 1,1), (0.309, 0.422, 0.614, 0.790; 0.8 0.8)
Alternative 2	(0.035, 0.043, 0.067, 0.095; 1,1), (0.037, 0.045, 0.063, 0.088; 0.8 0.8)
Alternative 3	(0.120, 0.180, 0.338, 0.504; 1,1), (0.132, 0.193, 0.316, 0.459; 0.8 0.8)
Alternative 4	(0.108, 0.144, 0.251, 0.377; 1,1), (0.115, 0.152, 0.235, 0.342; 0.8 0.8)

Step 5. Fuzzy utility values were calculated. The values found are shown in Table 21.

TABLE 21. Fuzzy utility values of alternatives

Alternative 1	(0.103, 0.213, 0.686, 1.367; 1,1), (0.122, 0.244, 0.602, 1.168; 0.8 0.8)
Alternative 2	(0.026, 0.047, 0.148, 0.323; 1,1), (0.030, 0.053, 0.129, 0.269; 0.8 0.8)
Alternative 3	(0.068, 0.132, 0.418, 0.880; 1,1), (0.079, 0.149, 0.366, 0.740; 0.8 0.8)
Alternative 4	(0.084, 0.169, 0.533, 1.087; 1,1), (0.099, 0.193, 0.466, 0.920; 0.8 0.8)

Step 6. The calculated fuzzy utility values were defuzzified and then normalized. The defuzzified utility values and normalized utility values are shown in 22.

As a result, the order of alternatives was obtained as Alternative 1 $\succ$ Alternative 4 $\succ$ Alternative 3 $\succ$ Alternative 2.

TABLE 22. Defuzzified utility values and normalized utility values

Alternative	Defuzzified utility value	Normalized utility value
Alternative 1	0.542	0.378
Alternative 2	0.124	0.086
Alternative 3	0.341	0.238
Alternative 4	0.427	0.298

CONCLUSION

In this study, mobile applications were evaluated. AHP method was used to see which of the applications are superior. In order to increase the effectiveness of the decision-making method, the method was based on IT2FSs. A hierarchy including sub-criteria was created for modeling of the problem. Also, group decision making technique was used for the effectiveness of the decision. Thus, the most superior alternative has been found.

REFERENCES

1. T. L. Saaty, *The Analytic Hierarchy Process* (New York: McGraw-Hill, 1980).
2. L. A. Zadeh, Information and control **8**, 338–353 (1965).
3. P. J. Van Laarhoven and W. Pedrycz, Fuzzy sets and Systems **11**, 229–241 (1983).
4. J. J. Buckley, Fuzzy sets and systems **17**, 233–247 (1985).
5. L. A. Zadeh, Information sciences **8**, 199–249 (1975).
6. J. M. Mendel, R. I. John, and F. Liu, IEEE transactions on fuzzy systems **14**, 808–821 (2006).
7. C.-T. Chen, Fuzzy sets and systems **114**, 1–9 (2000).
8. C. Kahraman, B. Öztayşi, İ. U. Sarı, and E. Turanoğlu, Knowledge-Based Systems **59**, 48–57 (2014).
9. S. Basaran and O. J. Aduradola, International Journal of Advanced Computer Science and Applications **9**, 99–107 (2018).
10. U. Buse, G. Şeyda, E. Tamer, and E. ÖZCAN, İstanbul İktisat Dergisi **70**, 113–139 (2020).
11. M. Pandey, R. Litoriya, and P. Pandey, Wireless Personal Communications **108**, 683–710 (2019).

An Approximate Method for Telegraph Equations

Dounia Belakroum[a)]

Department of Mathematics, University of Mentouri Brothers , Constantine, Algeria

[a)]*Corresponding author: belakroum05@yahoo.fr*

Abstract. In this paper, the Sinc-Galerkin method is applied to construct the numerical solution of telegraph equation with variable coefficients. This study shows that the Sinc-Galerkin method is a very effective and powerful tool in solving such problems numerically.

INTRODUCTION

A lot of attention has been given to the Sinc-Galerkin method and its efficiency has been proved for both linear and nonlinear partial differential equations [1, 2, 3, 4, 5, 6]. In [1] author proposed an application of Sinc-Galerkin method for solving space fractional boundary value problems. Numerical solution of time-dependent partial differential equations is proposed by authors of [2, 3, 4].
The purpose of this work is to introduce a numerical approach based on Sinc function for the approximate solution of a telegraph equation with variable coefficients.

THE SINC-GALERKIN METHOD

Consider the following telegraph equation with variable coefficients

$$\frac{\partial^2 u}{\partial t^2} + a(x)\frac{\partial u}{\partial t} + b(x)u - \frac{\partial^2 u}{\partial x^2} = f(x,t) \tag{1}$$

for all $(x,t) \in (0,1) \times (0,+\infty)$. Subject to the initial and boundary conditions

$$u(x,0) = u_t(x,0) = 0,\ u(0,t) = u(1,t) = 0,$$

where a and b are analytic on $[0,1]$. We shall assume that u and f are analytic with respect to x in a neighbourhood of $[0,1]$ and that u and f are analytic with respect to t in $[0,+\infty]$.
We consider Sinc approximation by the formula

$$u(x,t) = \sum_{i=-N}^{N}\sum_{j=-N}^{N} u_{i,j} S_{i,j}(x,t), \tag{2}$$

where

$$\begin{aligned} S_{i,j}(x,t) &= S_i(x)S_j(t) \\ &= [S(i,h_x))o\phi(x)][S(j,h_t)o\psi(t)] \end{aligned}$$

and

$$\phi(x) = ln\left(\frac{x}{1-x}\right),\ \ \psi(t) = ln(t).$$

We define the inner product denoted $<,>$ of two analytic functions f and g by

$$< f,g >= \int_0^1\int_0^1 f(x,t)g(x,t)W(x,t)dxdt,$$

where $w(x,y)$ is weight function given by

$$W(x,y) = w(x)v(t) = [\frac{1}{\phi'(x)^{1/2}}][\psi'(t)]^{-1/2}.$$

International Conference on Analysis and Applied Mathematics (ICAAM 2020)
AIP Conf. Proc. 2325, 020045-1–020045-3; https://doi.org/10.1063/5.0040591
Published by AIP Publishing. 978-0-7354-4069-2/$30.00

The unknown coefficients $u_{i,j}$ in (2) can be determined by the orthogonality the residual with respect to the Sinc basis functions $S_{i,j}(x,y)$. This yields the discrete Galerkin system

$$< Lu_{N_x,N_t} - f(x,t), S_{kl} >= 0, \qquad -N_x \le k \le N_x, \quad -N_t \le l \le N_t, \tag{3}$$

where

$$Lu:\; u \longrightarrow \frac{\partial^2 u}{\partial t^2} + a(x)\frac{\partial u}{\partial t} + b(x)u - \frac{\partial^2 u}{\partial x^2}.$$

MAIN RESULTS

Theorem 1
The following relations hold:

$$< f(x,t), \mathscr{S}_k\mathscr{S}_l > \approx h_t\, h_x \frac{w(x_k)\, f(x_k,t_l)\, v(t_l)}{\phi'(x_k)\,\psi'(t_l)}, \tag{4}$$

$$< b(x)u, \mathscr{S}_k\mathscr{S}_l > \approx h_t\, h_x \frac{w(x_k)\, b(x_k)\, u(x_k,t_l)\, v(t_l)}{\phi'(x_k)\,\psi'(t_l)}, \tag{5}$$

$$< \frac{\partial^2 u}{\partial x^2}, \mathscr{S}_k\mathscr{S}_l > \approx h_t\, h_x \frac{v(t_k)}{\psi'(t_l)} \sum_{i=-N_x}^{N_x} \sum_{j=0}^{2} \frac{u(x_i,t_l)}{\phi'(x_i)} \left[\frac{1}{h_x^j}\, \delta_{ki}^{(j)} \rho_j\right], \tag{6}$$

$$< \frac{\partial^2 u}{\partial t^2}, \mathscr{S}_k\mathscr{S}_l > \approx h_t\, h_x \frac{w(x_k)}{\phi'(x_k)} \sum_{j=-N_t}^{N_t} \sum_{i=0}^{2} \frac{u(x_k,t_j)}{\psi'(t_j)} \left[\frac{1}{h_t^i}\, \delta_{lj}^{(i)} \eta_i\right], \tag{7}$$

$$< a(x)\frac{\partial u}{\partial t}, \mathscr{S}_k\mathscr{S}_l > \approx h_x\, h_t \frac{a(x_k)\, w(x_k)}{\phi'(x_k)} \sum_{j=-N_t}^{N_t} \sum_{i=0}^{1} \frac{u(x_k,t_j)}{\psi'(t_j)} \left[\frac{1}{h_t^i} \delta_{lj}^{(i)} \mu_i\right] \tag{8}$$

for some functions ρ_j, μ_i, ν_j to be determined. Consequently, we have a linear system of $(2n+1)$ equations of the $(2n+1)$ unknown coefficients.

APPLICATION

In this section, we consider numerical examples to test the efficiency of the new scheme for solving the telegraph equation. The following computations and graphical representations were prepared by using Maple. We consider the following example

$$\begin{cases} \dfrac{\partial^2}{\partial t^2}u(x,t) + (1-x)\dfrac{\partial}{\partial t}u(x,t) + \sqrt{x}u(x,t) = \dfrac{\partial^2}{\partial x^2}u(x,t) + f(x,t), \\ u(0,t) = u(1,t) = 0, \\ u(x,0) = u_t(x,0) = 0, \end{cases} \tag{9}$$

where $a(x) = 1-x$, $b(x) = x^{1/2}$,

$$f(x,t) = te^{-t}x^{5/2}(1-x)^{5/2}(6-6t+t^2) + t^2e^{-t}x^{5/2}(1-x)^{7/2}(3-t)$$

$$+t^3e^{-t}x^{1/2}(1-x)^{1/2}[(1-x)^2(x^{5/2} - 15/4) + x((25/2)(1-x) - (15/4)x].$$

The exact solution is given by

$$u(x,t) = t^3e^{-t}x^{5/2}(1-x)^{5/2}.$$

TABLE 1. Numerical results at $t = 2.45$

x	Exact(x,t)	Apprx(x,t)	Err(x,t)
0.30	0.00308377757554	0.00312781372528	0.0000440361497052
0.60	0.0358100458207	0.0362585654039	0.000448519583086
0.90	0.0256463171905	0.0259687181574	0.000322400966537

We will choose

$$\phi(x) = \ln(\frac{x}{1-x}),\ \psi(t) = \ln(t), \overline{W}(x,t) = w(x)v(t) = \frac{1}{\sqrt{\phi(x)}}\frac{1}{\sqrt{\psi(t)}},$$

$$N_x = N_t = 12;\ h = s = \frac{2}{\sqrt{N}}, x_k = \frac{e^{kh}}{1+e^{kh}}, t_j = e^{js}, N = 12.$$

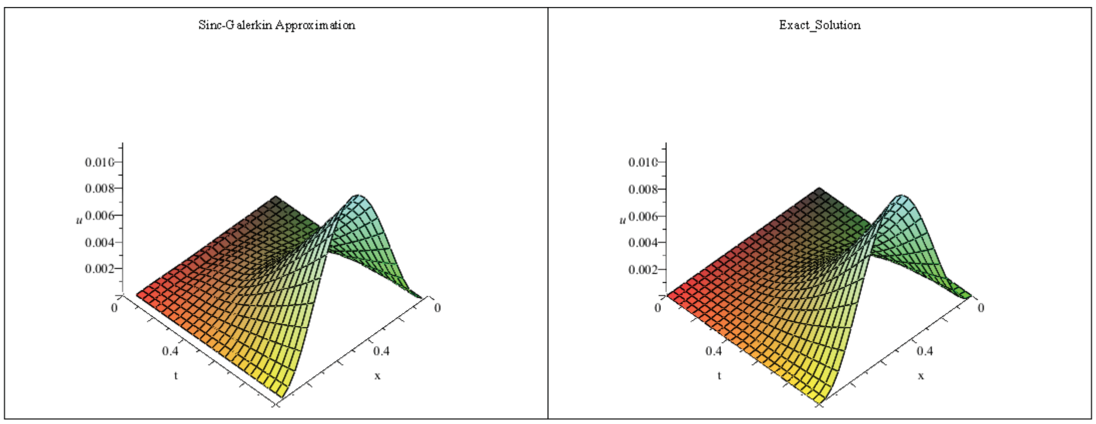

FIGURE 1. Exact and approximate solutions

REFERENCES

1. S. Alkan and A. Secer, Mathematical Problems in Engineering **2015**, Article ID 217348 (2015).
2. M. El-Gamel, Numerical Algorithms **77(2)**, 517-533 (2018).
3. K. M. McArthur, K. L. Bowers, and J. Lund, Numerical Methods for Partial Differential Equations **3(3)**, 169-185(1987).
4. A. Secer, An International Journal of Optimization and Control: Theories and Applications **8(2)**, 250-258 (2018).
5. F. Stenger, *Numerical Methods Based on Sinc and Analytic Functions* (Springer, New York, 1993).
6. D. Trif, Seminar on Fixed Point Theory Cluj-Napoca **3**, 173-182 (2002).

Measuring the Effectiveness of Biochemical Autoanalyser and Laser Device in Detection of WSLs Around Orthodontic Brackets

Selda Lale[a)]

Department of Orthodontics, Near East University Faculty of Dentistry, Nicosia, Mersin 10, Turkey

[a)]*Corresponding author: selda.lale@neu.edu.tr*

Abstract. This study used two quantitative methods to investigate the efficacy of different methods in preventing enamel demineralization around orthodontic brackets under similar in vitro conditions. The study included 90 extracted bovine incisors randomized into six groups: fluoride toothpaste(FT), non-fluoride toothpaste(NFT), fluoride varnish plus fluoride toothpaste(FV+FT), casein phosphopeptide–amorphous calcium phosphate(CPP-ACP) varnish plus fluoride toothpaste(CPP-ACP+FT), medical mineral gel plus non-fluoride toothpaste(MMG+NFT), and no intervention(control). All groups were subjected to a pH cycle. The buccal surfaces were assessed with a DIAGNOdent pen(DD) at baseline(T0) and the 19th day(T1). For each group, the mean Ca^{2+} loss was also measured by the colorimetric method. The current study focused on the assessment of total mineral loss using DD and colorimetric methods.

INTRODUCTION

Preventing demineralization has become a vital issue during orthodontic therapy. A clinical study found that when high-dose FV (6% NaF and CaF) was applied around the orthodontic bracket, the mean demineralization depth was approximately 40% lower than in the control group [1]. Recently, a more advanced FV has been developed: MI Varnish (GC, Tokyo, Japan), with added CPP-ACP (5%) [2]. Self-applied agents under the guidance of dentists, such as gel systems, require close cooperation from patients. R.O.C.S. Medical Minerals Gel (DRC-Group, Russia) is a newcomer in the field of prevention and treatment of caries. Its mechanism of action is based on the release of bioavailable calcium, phosphate, and magnesium; the system is indicated to treat early carious lesions through remineralization [3].

Early diagnosis of WSLs is of great importance because it helps clinicians take preventive steps to monitor the process of demineralization before lesions progress. One reliable and efficient method that can be used intraorally is the DIAGNOdent pen (DD; KaVo, Biberach, Germany). DD has been used widely both in vivo and in vitro for detecting enamel demineralization [4, 5]. This portable handheld instrument also uses fluorescence laser to distinguish between carious and healthy tooth structure by measuring reflected laser fluorescence from the tooth surface [6, 7].

While our previous study [8] observed the path of demineralization for treatment materials using visual assessment and colorimetric method at certain time points, the current study focused on the assessment of total mineral loss using DD and colorimetric methods for 19 days. The present study aimed to investigate the preventive effect of the medical mineral gel (MMG) and compare it with that of two types of varnish (FV and CPP-ACP varnish) using DD and evaluate the results with colorimetric method measurements. We hypothesized that the results of DD and colorimetric measurements would be parallel.

MATERIALS AND METHODS

Ninety incisor teeth were collected and selected from the mandibles of 15, three-year-old freshly slaughtered bovines. All teeth was stored in a 0.1% thymol solution at $4°C$. To standardize the exposed enamel surface, a window of 4 x 6 mm^2 was created and placed $5mm$ gingivally at the incisal edge and in the clinical crown's mesiodistal middle. All the teeth were painted on all surfaces except the window area with a thin coat of acid-resistant nail polish. Metal lower incisor brackets (3M Unitek, MN, USA) were bonded in the center of the exposed region with a light-curing resin composite cement (Transbond XT, M Unitek, MN, USA) [8].

International Conference on Analysis and Applied Mathematics (ICAAM 2020)
AIP Conf. Proc. 2325, 020046-1–020046-5; https://doi.org/10.1063/5.0040350
Published by AIP Publishing. 978-0-7354-4069-2/$30.00

DIAGNOdent Pen Assessment

The detailed description of the visual assessment, conducted in accordance with the scoring criteria established by Ekstrand et al. [9], has been fully described in our previous investigation [8]. Only lesions scoring 1 according to those criteria were included in the study.

In addition to visual evaluation, at the beginning (T0) and the 19th day (T1) of the experiment, the enamel around the brackets of each tooth was evaluated using DD as we can see in Table 1 and Figure 1.

TABLE 1. DIAGNOdent Scale.

Display Value	Clinical Situation
0-10	Sound tooth enamel
11-20	Outer-half demineralized enamel
21-30	Inner-half demineralized enamel
30+	Dentinal caries

FIGURE 1. Baseline measurements for the teeth to be included in the study with DD.

Treatment Groups and Cycling Procedure

Table 2 shows the treatment groups and materials applied in each group.

Determination of Demineralization

In the current study, the total average calcium loss during the experiment period, as shown in Table 3, was considered for each group, to compare the results with DD readings at day 19.

TABLE 2. In this table, the treatment groups, materials applied and experimental procedure for each group are shown.

Groups	Materials	Procedure
No intervention (control)	–	Received no treatment
Fluoride toothpaste(FT)	Colgate Total (14450ppmF-) Colgate-Palmolive Company, NY, USA	Brushed with FT for 2 sec per tooth
Non-fluoride toothpaste(NFT)	R.O.C.S. Pro Brackets & Ortho, 'DRC-Group' Company, Russia	Brushed with NFT for 2 sec per tooth
Fluoride varnish plus fluoride toothpaste(FV+FT)	Bifluorid 12 (6%NaF), Voco, Cux-haven, Germany+Colgate Total, Colgate-Palmolive Company, NY, USA	Bifluorid 12 varnish was applied once at the beginning of the experiment and brushed with FT for 2 sec per tooth
CPP-ACP varnish plus fluoride toothpaste(CPP-ACP+FT)	MI Varnish (CPP-ACP (5%)), GC, Tokyo, Japan+Colgate Total, Colgate-Palmolive Company, NY, USA	MI Varnish was applied once at the beginning of the experiment and brushed with FT for 2 sec per tooth
Medical minerals gel plus non-fluoride toothpaste(MMG+NFT)	R.O.C.S. Medical Minerals; 'DRC-Group' company, Russia+R.O.C.S. Pro Brackets&Ortho, 'DRC-Group' Company, Russia	R.O.C.S. Medical Minerals gel was applied daily 30 min before next demineralization cyle and brushed with NFT

TABLE 3. Ca(mg/dL) over time by group. Calcium dissolution (mg/dL)-(Mean±St.Dev.)

Day	MEG+NFT	FT	FV+FT	CPP-ACP+FT	NFT	CONTROL
1	0.314±0.07	0.557±0.14	0.157±0.08	0.014±0.04	0.486±0.21	0.929±0.15
2	0.357±0.08	0.643±0.14	0.486±0.12	0.043±0.05	0.586±0.23	0.943±0.21
3	0.329±0.11	0.700±0.10	0.586±0.09	0.100±0.08	0.586±0.20	0.914±0.23
4	0.362±0.11	0.705±0.11	0.590±0.10	0.076±0.10	0.762±0.19	0.948±0.26
5	0.419±0.07	0.719±0.11	0.590±0.15	0.148±0.09	0.719±0.11	0.919±0.22
6	0.490±0.10	0.733±0.12	0.676±0.15	0.148±0.11	0.833±0.15	1.019±0.20
7	0.533±0.12	0.705±0.21	0.619±0.17	0.162±0.11	0.790±0.14	0.962±0.16
8	0.562±0.11	0.805±0.23	0.748±0.19	0.219±0.12	0.976±0.15	1.062±0.11
9	0.590±0.13	0.833±0.19	0.790±0.15	0.233±0.12	0.962±0.18	1.190±0.17
10	0.586±0.16	0.929±0.28	0.771±0.21	0.200±0.13	0.914±0.21	1.171±0.21
11	0.605±0.15	0.790±0.19	0.762±0.18	0.205±0.11	0.933±0.16	1.148±0.19
12	0.586±0.12	0.886±0.15	0.786±0.27	0.214±0.09	0.943±0.19	1.114±0.20
13	0.600±0.13	0.814±0.16	0.786±0.20	0.243±0.10	0.871±0.23	1.114±0.09
14	0.600±0.14	0.886±0.15	0.800±0.22	0.243±0.13	0.929±0.24	1.086±0.20
15	0.571±0.17	0.814±0.17	0.771±0.21	0.243±0.11	0.929±0.21	1.000±0.12
16	0.414±0.13	0.757±0.33	0.700±0.26	0.029±0.11	0.771±0.25	0.986±0.17
17	0.719±0.17	1.090±0.20	1.019±0.24	0.376±0.13	1.005±0.28	1.176±0.20
18	0.671±0.17	1.129±0.29	0.986±0.19	0.314±0.17	0.971±0.28	1.143±0.16
19	0.543±0.14	0.957±0.24	0.800±0.15	0.271±0.15	0.886±0.13	0.943±0.19

TABLE 4. Diagnodent Pen readings at day 1 and 19.

Groups	MEG+NFT	FT	FV+FT	CPP-ACP+FT	NFT	CONTROL
Day 1	3,43	3,57	3,43	3	3,43	3,29
Day 19	10,3	11,7	9,57	3	12,71	14

STATISTICAL EVALUATIONS

Ca Loss Measurements

Repeated analysis of variance results yielded a significant F statistic ($F[5,36] = 36.394, P < 0.001$), suggesting significant differences between groups. A post hoc Bonferroni test revealed significant differences between groups [11, 12] which can be seen in Table 5. A power analysis was conducted using the Wilcoxon test data to ensure that the sample size and the magnitude of the observed effect were sufficient. The statistical analysis was performed using SPSS software (version 24.0.1, SPSS, Chicago, IL, USA).

TABLE 5. Statistical analysis of Ca loss measurements according to groups. In below table, cell entries are p-values. Bold values denote $p < 0.05$.

Group	MEG+NFT	FT	FV+FT	CPP-ACP+FT	NFT	CONTROL
MEG+NFT	-	**0.001**	0.869	**0.001**	**0.001**	**0.000**
FT	**0.001**	-	0.183	**0.000**	1.000	0.086
FV+FT	0.869	0.183	-	**0.000**	0.249	**0.000**
CPP-ACP+FT	**0.001**	**0.000**	0.000	-	0.000	**0.000**
NFT	**0.001**	1.000	0.249	**0.000**	-	0.062
CONTROL	**0.000**	0.086	**0.000**	**0.000**	0.062	-

DIAGNOdent Pen Measurements

Descriptive statistics were calculated. The Kolmogorov–Smirnov test was used to test data normality. All six groups were statistically compared with a Bonferroni test to detect differences between groups. Wilcoxon comparison tests were performed to identify significance between T0 and T1. The results were considered significant at $p = 0.05$. The statistical analysis was performed using SPSS software (version 24.0.1, SPSS, Chicago, Ill).

TABLE 6. Statistical analysis of DIAGNOdent Pen measurements according to groups. In below table, cell entries are p-values. Bold values denote $p < 0.05$.

Group	MEG+NFT	FT	FV+FT	CPP-ACP+FT	NFT	CONTROL
MEG+NFT	-	0.088	1	**0.000**	**0.000**	**0.000**
FT	0.088	-	**0.001**	**0.000**	0.716	**0.001**
FV+FT	1	**0.001**	-	**0.000**	**0.000**	**0.000**
CPP-ACP+FT	**0.000**	**0.000**	**0.000**	-	**0.000**	**0.000**
NFT	**0.000**	0.716	**0.000**	**0.000**	-	0.185
CONTROL	**0.000**	**0.001**	**0.000**	**0.000**	0.185	-

RESULTS

The initial DD readings for all groups were not statistically different from each other ($P > 0.05$). A statistically significant difference was found in demineralization over time for all groups except for the CPP-ACP+FT group ($P < 0.05$). The results of the Ca^{+2} loss measurements confirm the findings of the DD readings and indicate that the extent of prevention in the CPP-ACP+ FT group was significantly higher than all other groups.

No statistical difference was found between the FV+FT and MMG+NFT groups for either method at day 19 ($P > 0.05$). However, considering the numerical data obtained from DD measurements, while the FV+FT group showed less demineralization than the MMG+NFT group, the numerical values of the Ca^{+2} loss findings showed the opposite for these groups.

The difference between FT and NFT was not significant for either measurement method.

CONCLUSION

The findings of this 19-day in vitro study indicate that:

1. A clinical advantage was seen in the daily use of MMG and the one-time application of 5% FV as a protective agent during orthodontic treatment compared to no treatment.
2. One-time application of the CPP-ACP varnish as an adjunct to the FT was significantly the most protective treatment against demineralization.
3. Both toothpastes (fluoride and non-fluoride) had a weak preventive effect.

In addition to the contribution of our previous research on various preventive approaches, the current study provides an idea of the validity of the laser fluorescence approach for early detection of WSLs in routine clinical applications. Although DD measures with accuracy, it may be helpful to support with another method such as visual evaluation, so as not to overlook the WSLs during their formation.

REFERENCES

1. N. Farhadian, A. Miresmaeili, B. Eslami, and S. Mehrabi, American Journal of Orthodontics and Dentofacial Orthopedics **133(4)**, 95–98 (2008).
2. P. Rechmann, S. Bekmezian, B. M. Rechmann, et al., Clinical Oral Investigations **22(6)**, 2229–2239 (2018).
3. A. A. Kunin, I. A. Belenova, and T. V. Kupets, EPMA **5(Suppl 1)**, A122 (2014).
4. S. Comert and A. A. Oz, American Journal of Orthodontics and Dentofacial Orthopedics **157(1)**, 67–72 (2020).
5. M. M. Alabdullah, A. Nabawia, M. A. Ajaj, and H. Saltaji, European Journal of Orthodontics **39(6)**, 634–640 (2017).
6. A. V. Sichani, S. Javadinejad, and R. Ghafari, Dental Research Journal **13(4)**, 327 (2016).
7. V. Virajsilp, A. Thearontree, D. Paiboonwarachat, and S. Aryatawong, Pediatric Dentistry **27(6)**, 493–499 (2005).
8. S. Lale, H. Solak, E. Hincal, and L. Vahdettin, Biomed Res. Int. **2020**, (2020).
9. K. Ekstrand, D. Ricketts, and E. Kidd, Caries Research **31(3)**, 224–231 (1997).
10. P. Matheus, C. Demito, P. Scheibel, et al., Odonto **18**, 31–39 (2010).
11. H. Motulsk, Intuitive Biostatistics: A Nonmathematical Guide to Statistical Thinking (4th ed., Oxford University Press, 2013).
12. M. J. Campbell, D. Machin, and S. J. Walters, Medical Statistics: A Textbook for the Health Sciences (4th ed., Wiley, 2007).

Modelling Job Satisfaction Using a Logistic Regression Model

Behiye Cavusoglu,[a] Kemal Cek,[b] and Serife Z. Eyupoglu[c]

Department of Economics, Near East University, 99138, Nicosia, TRNC, Mersin 10, Turkey

[a] *Corresponding author: behiye.cavusoglu@neu.edu.tr*
[b] *Electronic mail: kemal.cek@neu.edu.tr*
[c] *Electronic mail: serife.eyupoglu@neu.edu.tr*

Abstract. Employee satisfaction plays an important role in the effective operation of any type of organization. The study aimed to investigate the explanatory factors influencing job satisfaction and model the satisfaction of employees (teachers) using logistic regression. Analysis results indicated that current workplace experience had a positive influence on teacher job satisfaction. However, as the teachers' education level and their overall years of experience in teaching increased their satisfaction levels decreased.

INTRODUCTION

An important factor influencing the efficiency and effectiveness of any organization is employees' job satisfaction. In an educational context, teachers' job satisfaction contribute to the school performance and to the teachers' performance ([1, 2]). Teacher job satisfaction is an important research topic as teachers with high levels of job satisfaction can provide higher teaching quality and better support for the students [3]. According to [4], teachers' job satisfaction can be described as the association between teachers and their teaching duties. Thus, individual factors about teachers play an important role in their job satisfaction [5].

This study investigates the effect of demographical factors on the job satisfaction of teachers working in Turkish Republic of Northern Cyprus (TRNC). Logistic regression approach is adopted to test the influence of gender, age, education, overall experience in teaching, experience at their current workplace (school), and marital status on job satisfaction.

PRELIMINARY INFORMATION

Job Satisfaction

Job satisfaction is the positive perceptions and emotions of employees towards their work regarding their expectations from their work [5]. Initially, [6] separated factors which determine job satisfaction as hygiene (extrinsic) and motivational (intrinsic) factors. The extrinsic factors are supervision, co-workers, salary, and working conditions. The intrinsic factors are recognition, achievement, progression, and work itself [7]. These factors have been proven to be significant factors of job satisfaction and they influence the employee performance. Job satisfaction is a crucial aspect in todays' organizations to achieve efficiency and better employee performance amongst the company [8]. In other words, unsatisfied employees may cause unfavourable performance outcomes.

Demographics and Job Satisfaction

Studies have been conducted in relation to demographic factors and the job satisfaction relationship and studies have indicated mixed results. Some studies have found that female teachers tend to show stronger job satisfaction than male teachers ([1, 9]). According to [10], being employed as a respectful teacher in schools can be the major source of job satisfaction in developing countries. In contrast, [11] concluded that male teachers showed a higher level of job satisfaction than female teachers. In addition, marital status can affect the job satisfaction of employees. For instance, [12] indicated that job satisfaction can be positively influenced by marital status. It was reported by [13] that level of experience and job ranks had an effect on job satisfaction. These findings are in line with [14] who found that age, gender, education, and experience had an impact on job satisfaction. However, several studies found that age, gender, education, and marital status do not have a significant effect on job satisfaction ([13, 15]). The study conducted by

International Conference on Analysis and Applied Mathematics (ICAAM 2020)
AIP Conf. Proc. 2325, 020047-1–020047-6; https://doi.org/10.1063/5.0040383
Published by AIP Publishing. 978-0-7354-4069-2/$30.00

[16] supported these findings that mixed results on the relationship between experience and job satisfaction of teachers is that country-specific factors can play an important role.

Logistic Regression Analysis

Logistic regression analysis (LRA) extends the techniques of multiple regression analysis to research situations in which the outcome variable is categorical [17]. In practice, situations involving categorical outcomes are quite common. The Multiple Regression model is applicable when the outcome variable, Y, is continuous, but is not appropriate for situations in which Y is categorical. For example, if Y takes on the value 1 for "success" and 0 for "failure," the multiple regression equation would not result in predicted values restricted to exactly 1 or 0. The model for logistic regression analysis is a more realistic representation of the situation when an outcome variable is categorical. The model for logistic regression analysis assumes that the outcome variable, Y, is categorical (e.g., dichotomous), but LRA does not model this outcome variable directly. Rather, LRA is based on probabilities associated with the values of Y ([18], [19]).
For theoretical, mathematical reasons, LRA is based on a linear model for the natural logarithm of the odds (i.e., the log-odds) in favor of $Y = 1$. Dependent variable Y becomes a binary variable taking a categorical value of 1 if individual/household satisfied from his/her job or taking a value of 0 otherwise.
Linear Probability Model can produce predicted probabilities more than 1 and/or less than 0 which causes statistics problem. Such outcome simply doesn't make sense. Since the probability of satisfaction cannot exceed 1 or 0.
In developing the logistic function following two conditions must be met.

1. The probability function must be positive (since $p \geq 0$).
2. The probability function must be less than 1 (since $p \leq 1$).

We need to constrain p such that $0 \leq p \leq 1$. The formula can be given by

$$p = \frac{e^{\alpha+\beta x}}{1+e^{\alpha+\beta x}} \tag{1}$$

satisfies these two conditions. Exponential of any number $+$ or $-$ is always $+$ any number divided by another that slightly greater than it will always result in a value less than 1. Adding 1 to denominator is always satisfies the condition of bound 0 and 1. The logistic function is nonlinear. Fortunately, by performing some algebra we can rewrite the logistic expression to obtain the following function, which is the logistic regression model. $\ln(\frac{p}{1-p}) = \alpha + \beta X$ is the natural log of odds ratio. P is the probability of satisfaction, $1 - P$ is the probability of dissatisfaction. The term $(\frac{p}{1-p})$ is called the 'odds ratio'. Odds ratio increase as the likelihood of non-approval in the nominator (P) is increases. In the logit model;
Probability of Satisfaction $= P(Y = 1) = P = \frac{e^{\alpha+\beta x}}{1+e^{\alpha+\beta x}}$
Probability of Dissatisfied $= P(Y = 0) = P = 1 - \frac{e^{\alpha+\beta x}}{1+e^{\alpha+\beta x}}$
Odds ratio;

$$\frac{p}{1-p} = \frac{\frac{e^{\alpha+\beta x}}{1+e^{\alpha+\beta x}}}{1 - \frac{e^{\alpha+\beta x}}{1+e^{\alpha+\beta x}}}. \tag{2}$$

Theorem 1 *The odd ratio measures the probability that $Y = 1$ relative to the probability that $Y = 0$.*

Proof. $\lambda = \alpha + \beta x$, then,

$$\frac{p}{1-p} = \frac{\frac{e^{\lambda}}{1-e^{\lambda}}}{1 - \frac{e^{\lambda}}{1-e^{\lambda}}}. \tag{3}$$

Therefore;

$$\frac{p}{1-p} = e^{\lambda} = e^{\alpha+\beta}. \tag{4}$$

By taking the natural logarithm of both sides, we find the logistic regression model as

$$\ln\left(\frac{p}{1-p}\right). \tag{5}$$

For the estimation of parameters of the logistic regression model maximum likelihood estimation method has been used. After running the regression model, we calculate the estimated probability, i.e., the probability of satisfaction:

$$\hat{E}p = \frac{e^{\hat{a}o+\hat{a}1X}}{1+e^{\hat{a}o+\hat{a}1X}}, \tag{6}$$

where the $\hat{a}0$ and $\hat{a}1$ are estimates from the regression [20].

AN APPLICATION: THE INFLUENCE OF DEMOGRAPHIC VARIABLES ON JOB SATISFACTION

The study aims to investigate the explanatory factors influencing job satisfaction and model the satisfaction of employees using Logistic regression. In order to test the proposed model it was necessary to compile job satisfaction data from middle school teachers in the Turkish Republic of Northern Cyprus (TRNC). The short-form Minnesota Satisfaction Questionnaire (MSQ) [21] was utilized. The short-form MSQ consists of 20 items/facets of the job (such as ability utilization, compensation, responsibility, and recognition) and the aggregate of these 20 facets measures overall job satisfaction. Teachers were asked to express the extent of their satisfaction with each of the 20 facets of their job on a five-point Likert scale ranging from 1 (very dissatisfied) to 5 (very satisfied). A total of 165 teachers agreed to complete the questionnaire and the data collection process took place in April 2019.
To analyze data, a Binary Logistic Regression Method was used and regression coefficients are estimated to predict the probability of the outcome of interest. To conduct the binary logistic regression, the degrees of satisfaction were recoded with the value of "not satisfied" = 0 and "satisfied" = 1. The study used 6 explanatory variable which are age, marital status, education, experience, current experience, and gender. These variables are used as a proxy for job satisfaction. The functional form of the model is:

$$Y = \alpha + \beta_1 X_1 + \beta_2 X_2 + \cdots + \beta_6 X_6 + \varepsilon, \tag{7}$$

where: X_1: Age, X_2: Current Experience, X_3 : Education, X_4: Experience, X_5: Gender, X_6: MStatus $Y = 1$: if satisfied, 0: otherwise.
Therefore, Y becomes a binary variable taking a categorical values of 1 if individual/household satisfied his/her job and 0 if not. Here the Y-intercept (i.e., the expected value of Y when all X's are set to 0), β_j is a multiple (partial) regression coefficient (i.e., the expected change in Y per unit change in X_j assuming all other $X's$ are held constant) and ε is the error of prediction. If error is omitted, the resulting model represents the expected, or predicted, value of Y:

$$E(Y|X_1,\cdots,X_\varphi) = Y^{'} = \alpha + \alpha + \sum_{j-1}^{\varphi} \beta_j X_j. \tag{8}$$

Data analysis was carried out with E-views 11 software. Diagnostics test was imposed and all of the tests are statistically significant. In the Logit model usual statistical tests cannot be used because the dependent variable is not continuous, thus the testing the model would be biased. There are other test that can be used to test the significance and reliability of the model, such as Wald test and Goodness of Fit test. The statistical significance of individual regression coefficients is tested using the Wald chi-square statistics (Table 1). According to the Table 1, current experience, education and experience variables were significant predictors ($p > .05$) of job satisfaction, intercept term, age, gender and marital status are not significant predictors ($p > .05$).

TABLE 1. Wald Test

	Chi-square	Probability
Constant	0.1819	0.6697
Education	4.5648	0.0326*
Current Experience	4.7923	0.0286*
Age	0.522709	0.4697
Experience	3.9759	0.0462*
Gender	0.182173	0.6695
MStatus	0.027912	0.8673

TABLE 2. Goodness-of-Fit Evaluation for Binary Specification. Andrews and Hosmer-Lemeshow Tests

H-L Statistic	10.5858	Prob. Chi-Sq(8)	0.4263

To check the goodness of fit of the logistic regression model Hosmer - Lemeshaw test performed [22]. According to the test result H-L test statistics value is 10.5858 with a p-value of 0.4263, suggesting that the model is a fit to the data well. In other words the hypothesis of a good model fit to the data is not rejected. So, the test is significant (Table 2).

Logistic regression analysis was carried out by the Logistic procedure in E-views 11 software. The results can be seen in Table 3.
According to the model, the log of the odds of job satisfaction is positively related to Age ($p < .05$), Current Experience ($p < .05$), Gender ($p < .05$), and MStatus ($p < .05$). The log of odds of job satisfaction is negatively related to Education ($p < .05$) and Experience ($p < .05$). If the coefficients are substituted with the numerical values obtained from the regression output, the following result is obtained:

$$\ln\left(\frac{p}{1-p}\right) = -0.5227 + 0.3168X_1 + 0.4955X_2 - 0.1032X_3 - .1217X_4 + 0.2108X_5 + 0.0713_6. \tag{9}$$

However, these variables cannot be interpreted in the same way as the OLS method. The most appropriate way to interpret the regression output is by explaining the odds ratio and the marginal effect. Equation (9) states that the log of the odds ratio is a linear function of the coefficients and variables, where the overall equation known as logit (log of the odds ratio). The odds ratio of job satisfaction shows the probability that a person satisfied with their job to the probability that they are not satisfied with their job. For a logistic regression the relationship between the odds ratio and the regression coefficient is the exponential function of the coefficient can be seen as below:

$$\ln\left(\frac{p}{1-p}\right) = e^{(-0.5227+0.3168X_1+0.4955X_2-0.1032X_3+-.1217X_4+0.2108X_5+0.0713_6)}. \tag{10}$$

According to the odds ratio, the impact of each variable is multiplicative. For each one unit increase in explanatory variable, the predicted odds are increased by a factor of exponential of the odds ratio. For example, each one-unit increase (decrease) in given predictor, the estimated odds are increased (decrease) by an exponential factor. The results can be expressed in terms of probabilities by use of the logistic function.
The database is used for the purpose of illustration. The outcome variable is satisfied (1) and dissatisfied (0). Three statistically significant explanatory variables are used in three different scenarios. In each scenario only one variable is changed (doubled)(see Table 4).

Scenario 1 assumes that the experience of teachers in their current workplace doubles while the other predictors are held constant. Expected probability, which is shown by p-hat, exhibits that if the current workplace experience doubles then the probability that the teachers are satisfied with their job increases by 69.6 %. On the other hand, scenario 2 assumes the education level of the teachers doubles while the other predictors are held constant. As a result, the expected probability of 0,397 shows that the probability that teachers are satisfied with their job decreases by 39.7%. Finally, scenario 3 assumes that the overall experience of teachers gained from teaching doubled while the other predictors are held constant. As a result, the probability that teachers are satisfied with their job decreases by 37.9%.

TABLE 3. Logistic Regression Results. Here, Dependent Variable: SAT_UNSAT, Method: ML - Binary Logit (Newton-Raphson / Marquardt steps), Date: 07/03/20, Time: 21:32, Sample: 1 135, Included observations: 133, Convergence achieved after 4 iterations, and Coefficient covariance computed using observed Hessian

Variable	Coefficient	Std. Error	z-Statistic	Prob.
C	-0.522781	1.225500	-0.426585	0.0697
AGE	0.316896	0.438315	1.722986	0.0497
CURRENT EXPERIENCE	0.495578	0.226379	2.189150	0.0286
EDUCATION	-0.103256	0.453137	2.227869	0.0197
EXPERIENCE	-0.121798	0.285009	2.427349	0.0091
GENDER	0.210829	0.493956	1.426818	0.0395
MSTATUS	0.071326	0.426927	1.167069	0.0773
McFadden R-squared	0.468148	Mean dependent var	0.789474	
S.D. dependent var	0.509224	S.E. of regression	0.402321	
Akaike info criterion	0.959855	Sum squared resid	20.39464	
Schwarz criterion	1.011979	Log likelihood	-13.48037	
Hannan-Quinn criter.	0.921672	Deviance	26.9607	
Restr. deviance	36.8977	Restr. log likelihood	-28.44887	
LR statistic	19.93702	Avg. log likelihood	-0.477296	
Prob(LR statistic)	0.007330			
Obs with Dep=0	28	Total obs	133	
Obs with Dep=1	105			

TABLE 4. Application- Predicted Probabilities

	CURRENT EXPERIENCE	EDUCATION	EXPERIENCE
Coefficients	0.495578	-0.103256	-0.121798
Scenario 1	2	1	1
Current Experience Doubled	$\ln\left(\frac{p}{1-p}\right)=\frac{e^{0,8423}}{e^{0,8423}+1}$		
p-hat	0,6960		
Scenario 2	1	2	1
Education Doubled		$\ln\left(\frac{p}{1-p}\right)=\frac{e^{0,248}}{e^{0,248}+1}$	
p-hat		0,397	
Scenario 3	1	1	2
Education Doubled			$\ln\left(\frac{p}{1-p}\right)=\frac{e^{0,225}}{e^{0,225}+1}$
p-hat			0,397

CONCLUSION

The study aimed to investigate the explanatory factors (demographical) influencing job satisfaction and model the satisfaction of school teachers using logistic regression. Among the demographical factors examined were age, gender, years of experience teaching, years of experience at the current school, and education. The results of the analysis conducted indicated that current workplace experience had a positive influence on teacher job satisfaction. However, results also indicated that as the education level and the overall years of experience in teaching increases the satisfaction levels of teachers decrease.

ACKNOWLEDGEMENTS

The publication has been prepared with the support of the Near East University, Nicosia, Turkey.

REFERENCES

1. W. Magee, Sex Roles **69**, 308-322 (2013).
2. M. E. Menon and A. A. Reppa, School Leadership and Management **31(5)**, 435-450 (2011).

3. M. Kunter, U. Klusmann, J. Baumert, D. Richter, T. Voss, and A. Hachfeld, Journal of Educational Psychology **105(3)**, 805-820 (2013).
4. M. Zembylas and E. Papanastasiou, Journal of Educational Administration **42**, 357-374 (2004).
5. P. E. Spector, *Job Satisfaction: Application, Assessment, Causes, and Consequences* (Sage Publications, California, 1997).
6. F. B. Herzberg, M. Mausner, and B. B. Snyderman, *The Motivation to Work* (John Wiley and Sons, New York, 1959).
7. F. B. Herzberg, *Work and the Nature of Man* (World Publishing Company, Cleveland, OH, 1966).
8. R. W. Rowden, Human Resource Development Quarterly **13**, 407-425 (2020).
9. A. Aydin, S. Uysal, and Y. Sarier, Procedia-Social and Behavioral Sciences **46**, 356-362 (2012).
10. A. Turanli, *The Analysis of the Relationship Between Teacher's Job Satisfaction and Organizational Commitment*, PhD thesis, Dokuz Eylul University (2007).
11. H. Joo, T. Kim, J. Nam, and S. Lee, The Journal of Educational Administration **31(1)**, 133-157 (2013).
12. L. Hagedorn, *What Contributes to Job Satisfaction Among Faculty and Staff?* (New Directions for Institutional Research, Jossey-Bass, 2000).
13. T. Oshagbemi, International Journal of Social Economics **30(12)**, 1210-1232 (2003).
14. N. Malik, International Journal of Academic Research **3(1)**, 267-272 (2011).
15. E. P. Paul and S. K. Phua, Journal of Higher Education Policy and Management **33(2)**, 141- 151 (2011).
16. S. Kukla-Acevedo, The Journal of Educational Research **102(6)**, 443-452 (2009).
17. B. Efron, Journal of the American Statistical Association **70**, 892-898 (1975).
18. D. R. Cox and E. J. Snell, *The Analysis of Binary Data* (2nd ed., Chapman and Hall, London, 1989).
19. D. W. Jr. Hosmer and S. Lemeshow, *Applied Logistic Regression* (2nd ed., Wiley, New York, 2000).
20. C. Y. Peng and T. S. H. So, A Primer Understanding Statistics **1(1)**, 31-70 (2002).
21. D. J. Weiss, R. V. Dawis, G. W. England, and L. H. Lofquist, *Manual for the Minnesota Satisfaction Questionnaire* (The University of Minnesota Press, Minneapolis, MN, 1967).
22. D. W. Hosmer, S. Lemeshow, Communications in Statistics-Theory and Methods **9(10)**, 1043-1069 (1980).

A Fractional-Order Two-Strain Epidemic Model with Two Vaccinations

Bilgen Kaymakamzade,[1,2,a] Evren Hincal,[1,2,b] and David Amilo[1,c]

[1] *Department of Mathematics, Near East University, Nicosia, Mersin 10, Turkey*
[2] *Mathematics Research Center, Near East University, Nicosia, Mersin 10, Turkey*

[a] *Corresponding author: bilgen.kaymakamzade@neu.edu.tr*
[b] *Electronic mail: evren.hincal@neu.edu.tr*
[c] *Electronic mail: 20185133@neu.edu.tr*

Abstract. In this research paper, we extended an existing SIR epidemic integer model containing two strains and two vaccinations by using a system of fractional ordinary differential equations in the sense of Caputo derivative of order $\sigma \in (0,1]$. Four equilibrium points were established which are disease free equilibrium, strain1 disease free equilibrium, strain2 disease free equilibrium and endemic equilibrium. Explicit analysis of the equilibrium points of the model was given by applying fractional calculus and Routh-Hurwitz criterion. Stability analysis of the equilibrium points was carried out by employing the Jacobian matrix. Numerical simulations were iterated to support the analytic results. It was shown that when both of the reproduction numbers R_1 and R_2 are less than one, the disease die out over time and while it persist in relation to the thriving strain when either of them is greater than one. We also studied the effect of vaccine. With the fractional order technique, the memory effect of the system is made visible and hence easier to predict.

INTRODUCTION

Mathematical models are needed for understanding the dynamics of epidemic models [2]. Many authors [3] have tried to work on a fractional order epidemic model for influenza dynamics by applying the reimbursements of the fractional-order concept to influenza dynamic. Here the purpose is to postulate conditions under which the epidemic can be contained. Other scientists like [4] and [5] have adopted the fractional-order unification on influenza dynamics and have even extended it to an SIRC model. Fractional calculus techniques allows memory effects which gives a better insight in the history of spread of a disease.

Influenza, also known as flu, is a communicable disease caused by the influenza virus that is transmitted via airborne droplets and attacks the respiratory system [1]. Some of its common symptoms include: fevers sore throat, coughing, running noses and headache. Vaccines and antiviral drugs have been formulated and recommended by the World Health Organization(WHO) and Centers for Disease Control and Prevention(CDC) for curbing and controlling the disease. It is estimated that, between 2018 and 2019, over 35 million people living in the United State of America(USA) have shown related symptomatic illness from the influenza virus.

In 2018, [6] constructed two strain epidemic model with two vaccines where the second strain is the mutation of the first strain. In our work, we extended the model which is given in [6] by adding fractional derivative.

THE FRACTIONAL MODEL ANALYSIS

Adding fractional-order σ as the order of the differential equation on the model in paper [6], we arrive at the following system

$$\begin{cases} \frac{d^\sigma S(t)}{dt^\sigma} = \wedge - (\beta_1 I_1 + \beta_2 I_2 + \lambda) S, \\ \frac{d^\sigma V_1(t)}{dt^\sigma} = r_1 S - (k_1 I_2 + \mu) V_1, \\ \frac{d^\sigma V_2(t)}{dt^\sigma} = r_2 S - (k_2 I_1 + \mu) V_2, \\ \frac{d^\sigma I_1(t)}{dt^\sigma} = (k_2 V_2 + \beta_1 S) I_1 - \alpha_1 I_1, \\ \frac{d^\sigma I_2(t)}{dt^\sigma} = (k_1 V_1 + \beta_2 S) I_2 - \alpha_2 I_2, \end{cases} \tag{1}$$

where $\sigma \in (0,1]$ is the order of the fractional derivative, $\lambda = r_1 + r_2 + \mu$, $\alpha_1 = \mu + v_1 + \gamma_1$, and $\alpha_2 = \mu + v_2 + \gamma_2$. Here it is assumed that there is a constant recruitment into susceptible class through birth and immigration and there is no double infection. The average life expectancy is μ and d_i $(i = 1,2)$ are infection death rates of strain 1 and 2,

International Conference on Analysis and Applied Mathematics (ICAAM 2020)
AIP Conf. Proc. 2325, 020048-1–020048-5; https://doi.org/10.1063/5.0040309
Published by AIP Publishing. 978-0-7354-4069-2/$30.00

respectively. The average time spent in class I_1 and I_2 until becoming recovered are $1/\gamma_1$ and $1/\gamma_2$, respectively. The susceptible individuals are vaccinated with constant rate r_1 for strain 1 and r_2 for strain 2. The vaccinated individual V_1 can also be infected by strain 2 at a rate k_1 and the vaccinated individual V_2 can also be infected by strain 1 at a rate k_2. β_1 and β_2 are transmission coefficients of susceptible individuals to strain 1 and strain 2, respectively. The variables and parameters are positive.

The fractional derivative of the model is in the sense of Caputo as Caputo technique. This technique is often used in real life application as it allows initial values for the fractional differential equations with Caputo derivatives similar to the integer order differential equations.

The biological feasible region of the model is given by

$$\varphi = \left\{ \left(S, V_1, V_2, I_1, I_2, R \in R_+^6 : 0 \leq N \leq \frac{\wedge}{\mu} \right) \right\}.$$

Observe that all parameters used are non-negative. So, since the system is bounded for given any initial condition, the solution is defined for any time $t \geq 0$ and it remains in the region. Therefore, the region φ is positively invariant.

Basic Reproduction Ratio and Local Stability Analysis

The equilibrium points are computed in the paper [6] and the disease free equilibrium point is obtained as follows:

$$E_0 = \left(\tfrac{\wedge}{\lambda}, \tfrac{\wedge r_1}{\mu\lambda}, \tfrac{\wedge r_2}{\mu\lambda}, 0, 0 \right).$$

By using the next generation matrix

$$G = FV^{-1} = \begin{pmatrix} \frac{k_2 V_2^0 + \beta_1 S^0}{\alpha_1} & 0 \\ 0 & \frac{k_1 V_1^0 + \beta_2 S^0}{\alpha_2} \end{pmatrix},$$

the reproduction number obtained as $R_0 = max\{R_1, R_2\}$ where $R_1 = \frac{k_2 r_2 \wedge}{\alpha_1 \mu \lambda} + \frac{\beta_1 \wedge}{\alpha_1 \lambda}$ and $R_2 = \frac{k_1 r_1 \wedge}{\alpha_2 \mu \lambda} + \frac{\beta_2 \wedge}{\alpha_2 \lambda}$.
Details of the equilibrium dynamics and reproduction number are in [6].

Theorem 1 *The disease-free equilibrium E_0 is locally asymptotically stable if $R_1 < 1$ and $R_2 < 1$.*

Proof. Evaluating the Jacobian matrix of model (1) at the disease free equilibrium E_0, we get

$$\begin{pmatrix} -\lambda & 0 & 0 & \frac{-\beta_1 \wedge}{\lambda} & \frac{-\beta_2 S}{\lambda} \\ r_1 & -\mu & 0 & 0 & \frac{-k_1 r_1 \wedge}{\mu\lambda} \\ r_2 & 0 & -\mu & \frac{-k_2 r_2 \wedge}{\mu\lambda} & 0 \\ 0 & 0 & 0 & \frac{k_2 r_2 \wedge}{\mu\lambda} + \frac{\beta_1 \wedge}{\lambda} - \alpha_1 & 0 \\ 0 & 0 & 0 & 0 & \frac{k_1 r_1 \wedge}{\mu\lambda} + \frac{\beta_2 \wedge}{\lambda} - \alpha_2 \end{pmatrix}.$$

Solving for the eigenvalues we arrive at

$$(-\lambda - p)(-\mu - p)(-\mu - p)\left[\left(\frac{k_2 r_2 \wedge}{\mu\lambda} + \frac{\beta_1 \wedge}{\lambda} - \alpha_1 \right) - p \right] \left[\left(\frac{k_1 r_1 \wedge}{\mu\lambda} + \frac{\beta_2 \wedge}{\lambda} - \alpha_2 \right) - p \right] = 0. \tag{2}$$

Further solving and simplifying (2), we get that $p_1 = -\lambda, p_2 = p_3 = -\mu$, and the quadratic $p^2 + a_1 p + a_2 = 0$, where $a_1 = (\alpha_1(-R_1 + 1) + \alpha_2(-R_2 + 1))$ and $a_2 = (\alpha_1(R_1 - 1)\alpha_2(R_2 - 1))$.
Observe that a_1 and a_2 will be positive only when the conditions $R_1 < 1$ and $R_2 < 1$ hold. So, by Routh-Hurwitz criterion, all eigenvalues are negative $\left(|arg\lambda_j| = \pi > \frac{\sigma\pi}{2}, j = 1, 2, \ldots, 5\right)$ if we have $R_1 < 1$ and $R_2 < 1$. Therefore, the disease-free equilibrium E_0 is locally asymptotically stable for $\sigma \in (0, 1]$ if $R_1 < 1$ and $R_2 < 1$.

Theorem 2 *The Strain 1 disease equilibrium E_1 is locally asymptotically stable if $R_1 < 1$.*

Proof. The eigenvalues of the Jacobian matrix at the point E_1 are found,
$p_1 = -\beta_1 I_1 + \lambda, p_2 = -k_1 I_2 + \mu, p_3 = -\mu$ and the quadratic $p^2 + a_1 p + a_2 = 0$,
where
$a_1 = \left(\frac{-\alpha_2\lambda}{\beta_2 I_2+\lambda}\left(\frac{k_1 r_1 \wedge}{\alpha_2\lambda(k_1 I_2+\mu)} + \frac{\beta_2\wedge}{\alpha_2\lambda} - 1 - \frac{\beta_2 I_2}{\lambda}\right)\right) + \left(\frac{-\alpha_1\lambda}{\beta_2 I_2+\lambda}\left(R_1 - 1 - \frac{\beta_2 I_2}{\lambda}\right)\right)$
and
$a_2 = \left(\frac{\alpha_2\lambda}{\beta_2 I_2+\lambda}\left(\frac{k_1 r_1 \wedge}{\alpha_2\lambda(k_1 I_2+\mu)} + \frac{\beta_2\wedge}{\alpha_2\lambda} - 1 - \frac{\beta_2 I_2}{\lambda}\right)\right) + \left(\frac{\alpha_1\lambda}{\beta_2 I_2+\lambda}\left(R_1 - 1 - \frac{\beta_2 I_2}{\lambda}\right)\right).$
Here, a_1 and a_2 will only be positive when $R_1 < 1$. So, by Routh-Hurwitz criterion, all eigenvalues are negative $\left(|arg\lambda_j| = \pi > \frac{\sigma\pi}{2}, j = 1, 2, \ldots, 5\right)$ at the equilibrium point E_1 if $R_1 < 1$. Therefore, the strain 1 disease equilibrium E_1 is locally asymptotically stable for $\sigma \in (0, 1]$ if $R_1 < 1$.

Theorem 3 *The Strain2 disease equilibrium E_2 is locally asymptotically stable if $R_2 < 1$.*

Proof. The proof is similar with the proof of Theorem 2.

NUMERICAL SIMULATIONS OF THE FRACTIONAL MODEL

Numerical simulations were carried out to support the analytic results that we obtained. In these simulations, we used the MATLAB code fde12.m which implements the Predictor-Corrector Method [7]. Parameters were calculated and adopted from previous studies [8]. In this study, the assumed initial conditions are as follows: $(S(t), V_1(t), V_2(t), I_1(t), I_2(t)) = (200, 133, 133, 2, 2)$ with a time prospect of 100 days and varying values of the order of the derivative between 0 and 1.

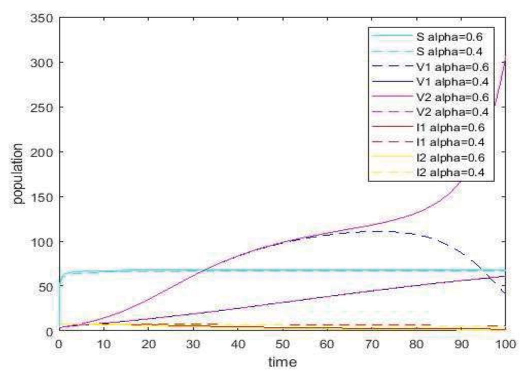

FIGURE 1. Disease free equilibrium E_0. Here both strains die out. Parameter values are: $\wedge = 200, \lambda = 0.01, r_1 = 0.3, r_2 = 0.3, \mu = 0.02, \alpha_1 = 0.0003, \alpha_2 = 0.0003, \beta_1 = 0.00001, \beta_2 = 0.00001, k_1 = 0.07, k_2 = 0.09$ and order of the derivative is 0.6 and 0.4 simultaneously

CONCLUSION

In this paper, we have investigated a fractional order two strain epidemic model with two vaccinations as a generalization of the integer order model proposed by [6]. The reproduction number R_0 has been computed and used to prove the stability equilibrium of the fractional-order model of the seasonal influenza disease. Analytically and numerically, the disease free equilibrium is locally asymptotically stable when $R_1 < 1$ and $R_2 < 1$ which implies that the disease will die out in the population over a period of time. Also, the strain1 disease free equilibrium locally asymptotically stable if $R_1 < 1$ and $R_2 > 1$ while the strain2 disease free equilibrium locally asymptotically stable if $R_1 > 1$ and $R_2 < 1$. Therefore, to evade a pandemic of the disease, it is sufficient to shrink the threshold value of the reproduction number below 1 by dropping the occurrence of the recruitment rate or by possibly vaccinating the entire population if

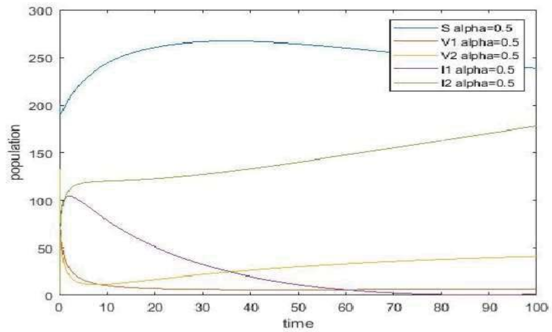

FIGURE 2. Strain1 disease free equilibrium E_1. Parameter values are: $\wedge = 20, \lambda = 0.5, r_1 = 0.3, r_2 = 0.3, \mu = 0.02, \alpha_1 = 0.0721, \alpha_2 = 0.0719, \beta_1 = 0.0000001, \beta_2 = 0.0000001, k_1 = 0.0089, k_2 = 0.0099$ and order of the derivative is 0.5

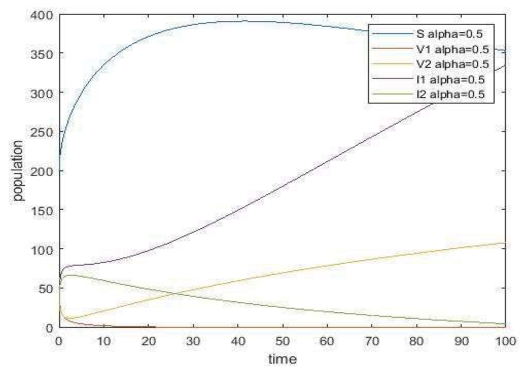

FIGURE 3. Strain2 disease free equilibrium E_2. Parameter values are: $\wedge = 43, \lambda = 0.0001, r_1 = 0.03, r_2 = 0.003, \mu = 0.02, \alpha_1 = 0.000001, \alpha_2 = 0.01, \beta_1 = 0.00001, \beta_2 = 0.001, k_1 = 0.0089, k_2 = 0.0099$ and order of the derivative is 0.5

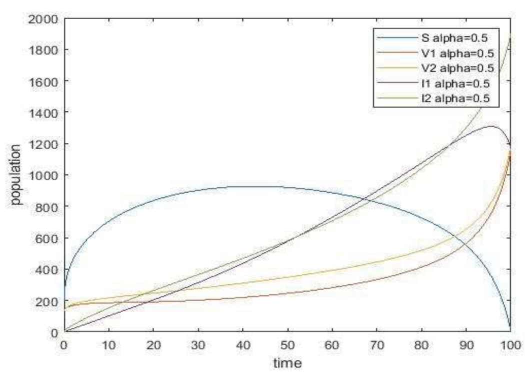

FIGURE 4. Endemic equilibrium E_3. Parameter values are: $\wedge = 200, \lambda = 0.01, r_1 = 0.3, r_2 = 0.3, \mu = 0.02, \alpha_1 = 0.0003, \alpha_2 = 0.0003, \beta_1 = 0.001, \beta_2 = 0.001, k_1 = 0.0089, k_2 = 0.009$ and order of the derivative is 0.5

the vaccines are effective and safe, as many flu vaccines cause neurological disorder.
More so, from the numerical simulations, the memory effect can clearly be appreciated, deduced from incorporating the fractional order on the system as compared to the integer order; where the values of the fractional order were varied between 0 and 1. In Figure 1, we see a transitional memory effect from the order of the derivative as it increases from 0.4 to 0.6 and approaches 1; the disease eventually die out over time, with its description in stages.The 0.5 order of

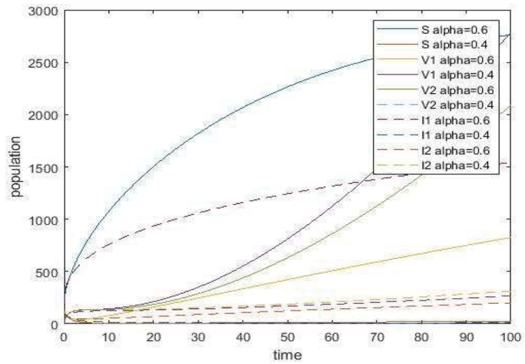

FIGURE 5. Endemic effect of vaccine. Parameter values are: $\wedge = 200, \lambda = 0.03, r_1 = 0.3, r_2 = 0.3, \mu = 0.02, \alpha_1 = 0.0009, \alpha_2 = 0.0007, \beta_1 = 0.00003, \beta_2 = 0.00003, k_1 = 0.003, k_2 = 0.003$ and order of the derivative is 0.6 and 0.4 simultaneously

derivative as used through Figure 2 to Figure 4 gives a faster convergence of result as compared to that of the integer. Figure 5 in one view give us a detailed history of the behaviour of the disease as the vaccines are lowered with respect to the order of the derivative between 0.4 and 0.6. So, with the fractional system, we can have a clearer picture of the dispositions of the disease, giving an insight of how the parameters gradually changes the behaviour of the disease over time.

ACKNOWLEDGEMENTS

We wish to acknowledge the support of Near East University.

REFERENCES

1. B. Kaymakamzade, I. A. Baba, and E. Hincal, Procedia Computer Science **102**, 333-341 (2016).
2. F. Brauer and C. Castillo-Chavez, Mathematical Models in Population Biology and Epidemiology (2nd ed., Springer, 2012).
3. Y. Li, Y. Chen, and I. Podlubny, Computers & Mathematics with Applications **59(5)**, 1810–1821 (2010).
4. M. El-Shahed and A. Alsaedi, Mathematical Problems in Engineering, (2011).
5. N. Aguila-Camacho, M. A. Duarte-Mermoud, and J. A. Gallegos, Communications in Nonlinear Science and Numerical Simulation **19(9)**, 2951–2957 (2014).
6. I. A. Baba, B. Kaymakamzade, and E. Hincal, Springer **106**, 342–348 (2018).
7. R. Garrappa, Mathematics and Computer in Simulation **110**, 96–112 (2015).
8. X. Ye and C. Xu, Mathematical Methods in the Applied Sciences **42(14)**, 4765–4779 (2019).

Optimisation of Multi Robots Hunting Game

Bashir Abdullahi Baba[1, 2, a)] and Bulent Bilgehan[3, b)]

[1)] *Department of Electrical Engineering, Near East University, Nicosia, TRNC, Turkey*
[2)] *Department of Computer Science, Sule Lamido University, Jigawa State, Nigeria*
[3)] *Department of Mathematics, Near East University, Nicosia, TRNC, Turkey*

[a)] *Corresponding author: bashirabdullahi.baba@neu.edu.tr, bashirbabaabdullahi@jsu.edu.ng*
[b)] *Electronic mail: bulent.bilgehan@neu.edu.tr*

Abstract. This paper presents Multi-robot co-operative hunting behavior using Differential game approach. Two robots were used as pursuers while another robot is used as evader, the two robots (pursuers) try to search and surround the prey (evader) robot. The aim of the game is for the two robots to detect the evader at the minimum possible time while at the same time the evader dodged the pursuer to the maximum possible time. Differential game approach was used to construct the problem using system of ordinary differential equation. We give the required conditions for the two pursuers to catch the evader. It was also shown that the evader maximize the capture time, while the pursuers minimize the capture time.

INTRODUCTION

Multi-robot systems consist of group of robots that are working together to achieve a common goal. These systems are designed to work in a way that the common purpose of the overall system can be achieved. Cooperative control laws are mostly used to control these systems. In the analysis of these systems, it is important to first model the cooperative behavior of the system [1, 2]. There are two most essentials models, first is a mathematical model which gives all the necessary properties required for computer simulations of the robot, secondly is another model that gives all the tools required in multi-robot system analysis and maintaining the important aspects of the system operation.

Differential game is an area in applied mathematics which is attracting more attention of researchers because of its application in solving practical problems in the fields of engineering, behavioral biology, economics, missile guidance, mention but few. It was first introduced by Rufus Isaacs [3], as “the homicidal chauffeur game” one of the games analyzed. The fundamental concepts of differential games were given in [3,4]. Pursuit evasion differential game is one of the many types of differential games that are in literature. It consists of two players, called pursuer and evader, with contradictory aims [5-10].

In this paper Multi-robots co-operative hunting game was studied using Differential game approach, in which two robots $(R_1\ and\ R_2)$, were used as Pursers and another robot (E), was used as Evader. The objective here from the pursuers' point of view is for the two pursuers to catch the evader at the minimum possible time while from the evader's point of view is to maximize the time taken for the capture. The problem was represented mathematically and the condition for the termination of the game was given and proved.

FORMULATING THE PROBLEM

In this work, multi-robot system consists of identical reactive robots interacting implicitly with each other and also working together to achieve a common goal. These robots act as pursuers, P_i for $i = 1,2$, searching for a single prey, another robot E (the evader). The cooperative pursuit is a very challenging task for the multi-robot system. The performance of the task has significance for multi-robot collaborative behaviors.

Method of Hunting

There are three behaviors of the hunting: searching, following, and surrounding. First, the pursuers will search the evader with group of sensors (searching). If the evader comes into detecting area, the pursuers will follow it based on one of the tracking algorithms (following). The pursuers will then move to the ambient region of the evader whenever possible (surrounding). This will be repeated until the evader is captured.

International Conference on Analysis and Applied Mathematics (ICAAM 2020)
AIP Conf. Proc. 2325, 020049-1–020049-3; https://doi.org/10.1063/5.0040282
Published by AIP Publishing. 978-0-7354-4069-2/$30.00

If one pursuer detects an evader, it will follow it and wait for the other pursuer to cooperate with it. If there is no other pursuer detecting the robot within a certain period, the pursuer will go ahead and capture the evader. On the other hand, when another searching robot detects the same evader, the team will go together and capture the evader .

MATHEMATICAL FORMULATION OF THE PROBLEM

Consider an evader E and two robots pursuers R_1 and R_2 with simple motion dynamics and constant speeds S_E, S_{R1} and S_{R2}, respectively. Thus, the controls of E, R_1 and R_2 are their respective instantaneous headings ϕ, ψ_1, and ψ_2. The states of E, R_1 and R_2 are defined by their Cartesian coordinates in the realistic plane.
$X_E = (x_E, y_E),\ X_{R_1} = (x_{R_1}, y_{R_1}),\ \ and\ X_{R_2} = (x_{R_2}, y_{R_2})$, respectively.
Thus, the complete state of the hunting is defined as:

$$X = (x_E, y_E, x_{R_1}, y_{R_1}, x_{R_2}, y_{R_2}) \in \mathrm{R}^6.$$

The evader's control variable is the instantaneous heading angle, $U_E = \phi$. While R_1 *and* R_2 affect the state of the hunting by choosing their states instantaneous respective headings ψ_1, *and* ψ_2, so the pursuers control variable is $U_R = \{\psi_1, \psi_2\}$. The normalized dynamics in the realistic plane $(\dot{X} = f(x, U_R, U_E))$ are specified by the system of ordinary differential equations:

$$\begin{aligned} \dot{x}_E &= cos\phi, & \dot{y}_E &= sin\phi, \\ \dot{x}_{R_1} &= \beta_1 cos\psi_1, & \dot{y}_{R_1} &= \beta_1 sin\psi_1, \\ \dot{x}_{R_2} &= \beta_2 cos\psi_2, & \dot{y}_{R_2} &= \beta_2 sin\psi_2. \end{aligned}$$

Here, $\beta_1 = \frac{S_{R_1}}{S_E} > 1$ and $\beta_2 = \frac{S_{R_2}}{S_E} > 1$ are the normalized speeds of the two pursuers (robots) and they are not necessarily the same.
The initial state is:

$$X_0 = (x_{E0}, y_{E0},\ x_{R_{10}}, y_{R_{10}},\ x_{R_{20}}, y_{R_{20}}) = X(t_0).$$

The hunting (game) ends at t_f when the state of the system satisfies one of the following conditions:

a) $x_{R_1} = x_E$, $y_{R_1} = y_E$,
b) $x_{R_2} = x_E$, $y_{R_2} = y_E$,
c) Both a) and b)

The terminal state is:

$$X_f = (x_{Ef}, y_{Ef},\ x_{R_{1f}}, y_{R_{1f}},\ x_{R_{2f}}, y_{R_{2f}}) = X(t_f).$$

The evader tries to maximize the capture time, while the pursuers try to minimize the capture time together, hence the performance functional is:

$$\min_{(\psi_1,\psi_2)} \max_{\phi} \int_0^{t_f} dt.$$

ANALYSIS OF THE GAME

Let us introduce the co-states as follows:

$$\lambda = (\lambda_{xE}, \lambda_{yE},\ \lambda_{xR_1}, \lambda_{yR_1},\ \lambda_{xR_2}, \lambda_{yR_2}) \in \mathrm{R}^6.$$

Then the Hamiltonian of the differential game is:

$$H = 1 + \lambda_{xE} cos\phi + \lambda_{yE} sin\phi + \beta_1 \lambda_{xR_1} cos\psi_1 + \beta_1 \lambda_{yR_1} sin\psi_1 + \beta_2 \lambda_{xR_2} cos\psi_2 + \beta_2 \lambda_{yR_2} sin\psi_2.$$

Then, the optimal control inputs are obtained by:

$$\min_{(\psi_1,\psi_2)} \max_{\phi} H \equiv 0.$$

The optimal controls headings $E,\ R_1\ and\ R_2$ are characterized as follows:

$$\begin{aligned} cos\phi^* &= \frac{\lambda_{xE}}{\sqrt{\lambda_{xE}^2+\lambda_{yE}^2}}, & sin\phi^* &= \frac{\lambda_{yE}}{\sqrt{\lambda_{xE}^2+\lambda_{yE}^2}}, \\ \cos\psi_1^* &= \frac{-\lambda_{xR1}}{\sqrt{\lambda_{xR_1}^2+\lambda_{yR_1}^2}}, & sin\psi_1^* &= \frac{-\lambda_{yR1}}{\sqrt{\lambda_{xR_1}^2+\lambda_{yR_1}^2}}, \\ \cos\psi_2^* &= \frac{-\lambda_{xR2}}{\sqrt{\lambda_{xR_2}^2+\lambda_{yR_2}^2}}, & sin\psi_2^* &= \frac{-\lambda_{yR2}}{\sqrt{\lambda_{xR_2}^2+\lambda_{yR_2}^2}}. \end{aligned}$$

In addition the co-state dynamic can be obtained using the following formula

$$\dot{\lambda} = -\frac{\partial H}{\partial x}.$$

Hence,

$$\dot{\lambda_{xE}} = \dot{\lambda_{yE}} = \dot{\lambda_{xR_1}} = \dot{\lambda_{yR_1}} = \dot{\lambda_{xR_2}} = \dot{\lambda_{yR_2}} = 0.$$

This implies, all co-states and optimal control inputs are constants, which means the robots optimal trajectories must be straight lines.

CONCLUSION

Multi robots hunting game was discussed using differential game approach. The evolution of robot collective behaviors represent the transition between different states of the robots. The two robots hunting game consist of two pursuers and a single evader robot. The optimal trajectory of the robots is found to be a straight line, when the two pursuers minimized the capture time and at the same time the evader maximized the time, this condition was stated and proved.

REFERENCES

1. P. Stone and M. Veloso, Autonomous Robots **8(3)**, 345–383 (2000).
2. S. Schaal and C. G. Atkeson, IEEE Robotics & Automation Magazine **17(2)**, 20–29 (2010).
3. Isaacs, R. Differential Games. In *Mathematical Theory with Applications to Warfare and Pursuit, Control and Optimization* (Courier Corporation: North Chelmsford, MA, USA, 1999).
4. L. D. Berkovitz, *A Survey of Differential Games, Mathematical Theory of Control* (Academic Press: New York, NY, USA, 1967), pp. 373–385.
5. G. I. Ibragimov, Differ. Equations **41**, 627–635 (2005).
6. G. I. Ibragimov, Adv. Math. **14**, 14–26 (2004).
7. G. Ibragimov, A. Azamov, and M. Khakestari, AZIAM J. **52**, 59–75 (2011).
8. G. I. Ibragimov, F. Massimiliano, K. Atamurat, and P. Antonio, Dyn. Games Appl. **8**, 352–378 (2018).
9. G. I. Ibragimov, M. Salimi, and M. Amini, Eur. J. Oper. Res. **218**, 505–511 (2012).
10. W. J. Leong and G. I. Ibragimov, Far East J. Appl. Math. **33**, 205–214 (2008).

Estimating Covid-19 Deaths by Using Binomial Model

Evren Hincal,[1, 2, a)] Bilgen Kaymakamzade,[1, 2, b)] Fatma Nese Suren,[1, c)] and Nezihal Gokbulut[1, 2, d)]

[1)] *Department of Mathematics, Near East University, Nicosia, Mersin 10, Turkey*
[2)] *Mathematics Research Center, Near East University, Nicosia, Mersin 10, Turkey*

[a)] *Corresponding author: evren.hincal@neu.edu.tr*
[b)] *Electronic mail: bilgen.kaymakamzade@neu.edu.tr*
[c)] *Electronic mail: nesesuren@gmail.com*
[d)] *Electronic mail: nezihal.gokbulut@neu.edu.tr*

Abstract. Coronavirus disease 2019, also known as Covid-19, is an infectious disease that has infected more than nineteen million people all around the world. This virus is a member of coronavirus family but it is the most mortal one. It has named as 2019-nCoV by World Health Organization(WHO) after Chinese Center for Disease Control and Prevention(CDC) discovered a new coronavirus from a swab sample of a patient. As we know this pandemic started December 2019 in China, and it is still spreading and causing deaths all around the world. In this paper, we aimed to estimate the right size of epidemic. For that purpose, we chose 10 countries, which are affected by, and still fighting with this disease, to forecast the upcoming death rates by using the previous week deaths. These 10 countries are Argentina, Austria, Brazil, France, Iran, Italy, Sweden, Turkey, United Kingdom, and United States of America. We used the death data of WHO with assumption that data is accurate. For this estimation, firstly, we used the assumption that the reported death delay distributed according to a gamma distribution. Then, we used a binomial distribution for assumption of deaths. This binomial formula led us to find a posterior distribution which is an extension of Bayes' theorem for death ratio. Lastly, we compared our estimations with real data.

INTRODUCTION

Covid-19 is the infectious disease that has occurred by the most recently discovered coronavirus, SARS-CoV-2. In December 2019, this disease began in Wuhan, China [1, 2]. The name Covid-19 was given by WHO, when CDC discovered a new coronavirus from the throat swab sample of a patient [3, 4]. Now, it is a pandemic, affecting countries worldwide. People can catch this disease from the ones who are already infected. Covid-19 can be transmitted through small droplets when an infected person coughs, sneezes or speaks [1]. Symptoms of this disease are very similar with the symptoms of influenza such as fever, headache, dry cough and tiredness. However, viruses are very different and behave very differently [5]. In addition to being a very fatal disease, it has been observed that it affects individuals with elderly and chronic diseases more [6].

The Covid-19 has spread and became an outbreak quickly in countries all around the world. As of 18^{th} of August, more than 22,070,411 coronavirus cases have been reported with approximately 777,766 deaths, worldwide [7]. In many countries obligation to wear mask and rubber gloves are introduced by some governments [8]. Closure of airports, lockdown, quarantine for the suspected individuals are some of the restrictions that has been taken by some governments [9, 10].

In this paper, our main aim is to forecast the deaths for 10 countries which are Argentina, Austria, Brazil, France, Iran, Italy, Sweden, Turkey, United Kingdom, and United States of America. For that purpose, we tried to estimate the death rates of these 10 countries by using many distributions which are gamma distribution, binomial distribution and posterior distribution as an extension of Bayes' theorem.

For a continuous random variable X, gamma distribution with positive parameters α and λ, shown by $X \sim \Gamma(\alpha, \lambda)$. In order to use gamma distribution for X, its probability density function should be given by

$$f_X(x) = \begin{cases} \frac{\lambda^{\alpha} x^{\alpha-1} e^{-\lambda x}}{\Gamma(\alpha)}, & x > 0, \\ 0, & otherwise. \end{cases} \tag{1}$$

Binomial distribution has two parameters that are generally represented by n and p. Here, in an experiment, number of independent trials is shown by n and probability of success is shown by p. In other words, binomial distribution is used when an event has two possible outcomes, success or failure. For a random variable X, binomial distribution is presented by $X \sim Bin(n, p)$ [11, 12].

Bayes' theorem, for events $A_1, A_2, \ldots, A_n$ and B, is given by the following equation:

International Conference on Analysis and Applied Mathematics (ICAAM 2020)
AIP Conf. Proc. 2325, 020050-1–020050-4; https://doi.org/10.1063/5.0040303
Published by AIP Publishing. 978-0-7354-4069-2/$30.00

$$P(A_i|B) = \frac{P(B|A_i)P(A_i)}{\sum_{j=1}^{n} P(B|A_j)P(A_j)}, \tag{2}$$

where $i = 1, \ldots, n$. Here $P(A_i)$ and $P(B)$ are the probabilities of occurrence of events A_i and B, respectively. Also, $P(A_i|B)$ is a conditional probability; when B is true, the occurring likelihood of event A_i. Similarly, $P(B|A_i)$ is a conditional probability; the occurring likelihood of event B, when A_i is true. In our work, we used posterior distribution which is an extension of Bayes' theorem that is used when an evidence about the event is taken into the consideration [13, 14].

In our work, the higher quality of data for the countries means more accurate results for death rates [15]. This will give us a chance to see how the control measures are effective for these countries. Here, we shouldn't forget the rapidly changing data for death rates as a result of Covid-19 infection [2].

The results presented in this paper do not explicitly model the various interventions and control efforts put in place by countries. Our predictions of transmissibility reflect the epidemiological situation during the infection of Covid-19 fatalities. For this reason, the impact of controls on predictive transmissibility will have a significant effect with a delay between transmission and death.

In the continuation of this paper, at first we mentioned about our objectives. Then, we introduced our statistical model and the table that consists of expected and occurred death rates in the countries which we chose. Lastly, we give our results with discussion part.

OBJECTIVES

Our main objective in this study is to estimate the right size of epidemic. For the forecasting what we did is using the previous week death numbers to estimate the coming week numbers. Our assumptions are very important for this work in order to get accurate results. During this work, we assumed that the statistics of deaths due to Covid-19 , for the countries that we have studied, are purely reported. For the death delay cases gamma distribution used for mean as 10 and standard deviations as 2.5. After, we used binomial distribution for the number of deaths. By using the formula obtained from binomial distribution, we found posterior distribution for the ratio of deaths to reported cases in each country.

STATISTICAL MODEL

Let $D_{i,t}$ be the number of deaths in any country i at time t. Let $I^r_{i,t}$ be the reported number of cases in the country i at time t and $I^r_{i,t}$ be the appropriate number of cases. We assume that the reporting to death delay δ is distributed according to a gamma distribution with mean μ and standard deviation σ. That is,

$$\delta \sim \Gamma(\mu, \sigma). \tag{3}$$

Let $r_{i,t}$ be the ratio of deaths to reported cases in the country i at time t. We assume that deaths are distributed according to a Binomial Distribution. Thus,

$$D_{i,t} \sim Binom\left(\int_0^\infty \Gamma(x|\mu,\sigma) I^r_{i,t-x} dx, r_{i,\mu}\right). \tag{4}$$

The above binomial formula will allow us to find a posterior distribution for $r_{i,t}$. Case error value is defined as:

$$\rho_{i,t} = \frac{FR}{r_{i,t}}. \tag{5}$$

Hence, a posterior distribution for $\rho_{i,t}$ could be obtained by using the posterior distribution for $r_{i,t}$ and the posterior distribution for $FR(2)$.

For the time period over which we have data on deaths, up to time $t-\mu$, we use the posterior distribution of FR to obtain $I_{i,t}^{appropriate}$. The appropriate number of cases in a location l at time t is the sum cases that did not die and the number of deaths is

$$I_{i,t}^{appropriate} \sim D_{i,t-\mu} + NBin(D_{i,t-\mu}, FR). \tag{6}$$

In this formulation, the negative binomial is parameterised as $NBin(n,p)$ where n is the number of failure(that is, death), and p is the probability of observing a failure.

For the time period which we do not have information about deaths, that is after time $t-\mu$, we use the posterior distribution of case ascertainment to obtain

$$I_{i,t}^{appropriate} \sim I_{i,t}^{r} + NBin(I_{i,t}^{r}, \rho_{i,t}). \tag{7}$$

In order to calculate the estimated number of deaths, we believe in the reported cases and we use

$$\int_0^\infty \Gamma(x|\mu,\sigma) I_{i,t-x}^{r} dx. \tag{8}$$

Since the recorded cases in the following week might die within the same week, that is, for $x \in \{0,7\}$, $\Gamma(x|\mu,\sigma) > 0$, we predicted new registered cases in the following week by using a sample from a gamma distribution with mean and standard deviation by predicting from the number of observed cases in the last week. Because this assumes no increase or decrease in the following week, this is controlled by the assumption which is appropriately a null-hypothesis scenario as it does not affect our results completely given the contribution to deaths due to those being very small (that is, less than 1.5%).

We attain the estimated number of deaths as:

$$D_{i,t} \sim Binom\left(\int_0^\infty \Gamma(x|\mu,\sigma) I_{i,t-x}^{r} dx, r_{i,\mu}\right), \tag{9}$$

where $r_{i,\mu}$ is the estimated ratio of deaths to reported cases for the last week of data, and

$$\int_0^\infty \Gamma(x|\mu,\sigma) I_{i,t-x}^{r} dx, r_{i,\mu} dx \tag{10}$$

relies on observed reported cases up to the last day with available and estimated reported cases as described above.

TABLE OF EXPECTED AND OCCURRED DEATH RATES

As we mentioned before, we tried to estimate death rates of 10 countries which are; Argentina, Austria, Brazil, France, Iran, Italy, Sweden, Turkey, United Kingdom and United States of America. We can see the actual death rates and estimated death rates in Table 1, detailed.

TABLE 1. In the following table, O.C. denotes the number of occurred cases, D(25%) denotes death rates with 25 percent, D(50%) denotes death rates with 50 percent, D(75%) denotes death rates with 75 percent. E.D(25%), E.D.(50%), E.D.(75%) denote expected death rates with 25, 50 and 75 percent, respectively. These expected rates are found by using the distributions explained that are explained in below section

No.	Country	O.C.	D(25%)	D(50%)	D(75%)	E.D.(25%)	E.D.(50%)	E.D.(75%)
1	Argentina	3548	0.041	0.051	0.1	0.214	0.269	0.344
2	Austria	267	0.019	0.035	0.1	0.231	0.395	0.742
3	Brazil	114256	0.094	0.096	0.1	0.127	0.143	0.159
4	France	2515	0.127	0.136	0.1	0.089	0.101	0.115
5	Iran	15129	0.034	0.035	0	0.315	0.364	0.419
6	Italy	4567	0.121	0.129	0.1	0.094	0.107	0.122
7	Sweden	3511	0.072	0.081	0.1	0.147	0.171	0.199
8	Turkey	7619	0.016	0.018	0	0.631	0.749	0.889
9	United Kingdom	15084	0.074	0.077	0.1	0.159	0.179	0.201
10	United States of America	154786	0.05	0.051	0.1	0.242	0.27	0.301

RESULTS AND DISCUSSION

When we look at the table, we can easily see the difference between expected death rates and actual death rates which are taken from World Health Organization. In infectious diseases, binomial distribution is a very effective model to determine the size of the pandemic and unrecorded patients. So, governments can use this statistical model to identify the real patient number and take precautions. If we make decisions for the future of the countries by using these expected rates, then this means more restrictions should be taken, which may affect public psychologically and also economy of the countries.

In infectious diseases, pure data is very important in order to take right and quick decisions for public health. By using pure data many statistics or modelling can be prepared to see the infectiousness or effects of the pandemic. So, we can conclude that inaccurate or doctored data may change progression of disease, negatively.

ACKNOWLEDGEMENTS

The publication has been prepared with the support of Mathematical Research Center.

REFERENCES

1. World Health Organization, Q&A on coronaviruses (Covid-19), https://www.who.int/emergencies/ diseases/novel-coronavirus-2019/question-and-answers-hub/q-a-detail/q-a-coronaviruses (accessed 17 April, 2020).
2. R. Verity, L. C. Okell, et al., The Lancet **20**, 669–677 (2020).
3. N. Chen, M. Zhou, et al., The Lancet **395**, 507–513 (2020).
4. Identifying the source of the outbreak, https://www.cdc.gov/coronavirus/2019-ncov/cases-updates/about-epidemiology/identifying-source-outbreak.html (accessed 1 July, 2020).
5. H. Pham, "On Estimating the Number of Deaths Related to Covid-19", MDPI, 10 (2020).
6. A. Clark, M. Jit, et al., The Lancet **15**, (2020).
7. Covid-19 coronavirus pandemic, https://www.worldometers.info/coronavirus/ (accessed 18 August 2020).
8. J. Howarda, A. Huangb, A. W. Rimoint, et al., "Face Masks Against covid-19: An evidence review", Preprints 2020 **30**, 9(2020).
9. M. Chinazzi, J.T. Davis, et al., Science **368**, 395–400 (2020).
10. L. L. Martin Kahanec and J. S. Marcus, The impact of COVID-19 restrictions on individual mobility, https://www.bruegel.org/2020/05/the-impact-of-covid-19-restrictions-on-individual-mobility/ (accessed 5 May 2020).
11. S. M. Ross, A First Course in Probability, (Pearson, Upper Saddle River, New Jersey 07458, 2010) Chap. 5, pp. 215–216, 8th ed.
12. A. T. Andrea Viti and L. Bertolaccini, Journal of Thoracic Disease **7**, E7–E10 (2015).
13. B. Efron, Science **340**, 1177–1178 (2013).
14. S. M. Ross, A First Course in Probability, (Pearson, Upper Saddle River, New Jersey 07458, 2010) Chap. 3, pp. 65–74, 8th ed.
15. C. F. D. Control and P. (CDC), The CDC Field Epidemiology Manual, (Oxford University Press, 2018) Chap. 4, pp. 53–69, 1st ed.

On the Solutions of the Radial Schrödinger Equation Using Symmetry Methods

Kismet Kasapoglu[a)]

Trakya University, Department of Mathematics, Edirne, Turkey

[a)]*Corresponding author: kismetkasapoglu@trakya.edu.tr*

Abstract. In this study, the solutions of a radial Schrödinger equation which has got the potential $V(r) = 0$ are found by using symmetries. These solutions are compared with the classical solution of the equation.

INTRODUCTION

Time independent Schrödinger equation has a number of important physical applications in quantum mechanics. Using separation of variables in spherical coordinates to this equation, we obtain the radial Schrödinger equation as

$$\frac{d}{dr}(r^2\frac{dR(r)}{dr}) + \frac{2mr^2}{\hbar^2}[E - V(r) - \frac{l(l+1)\hbar^2}{2mr^2}]R(r) = 0 \quad l = 0,1,2,..., \tag{1}$$

where E and V are the total and potential energies, respectively, m is the mass of particle, $\hbar$ is the reduced planck constant [1, 2].

For a confining potential

$$V(r) = \begin{cases} 0, & \mathrm{r} \leq a, \\ \infty, & \mathrm{r} > a \end{cases} \tag{2}$$

at the GaAs/AlAs quantum dot of confining particle with infinite sphere potential with radius a and $\frac{2mE}{\hbar^2} = k^2$, $k \neq 0$, in the special case $l = 0$, the equation (1) becomes

$$\frac{d^2R}{dr^2} + \frac{2}{r}\frac{dR}{dr} + k^2R = 0. \tag{3}$$

The normalized radial solution of the equation (3) is

$$R = \begin{cases} \sqrt{\frac{2}{a}}\frac{sinkr}{r}, & \mathrm{r} < a, \\ 0, & \mathrm{r} \geq a \end{cases} \tag{4}$$

[1, 2].

In this study , the solutions of the equation (3) found with symmetry are compared with the series solution (4) of the equation (3).

GENERAL THEORY OF LIE SYMMETRIES

In the Lie group theory which was developed by Sophus Lie , the order of differential equations can be reduced with the help of symmetry groups and by using these symmetries their analytical solutions can be obtained. The Lie point symmetry of the differential equation

$$y^{(n)} = w(x,y,y',y'',\ldots,y^{(n-1)}) \tag{5}$$

is found by determining the functions $\xi(x,y)$ and $\eta(x,y)$ from symmetry condition

$$\mathbf{X}w = \eta^n \quad (mody^{(n)} = w), \tag{6}$$

International Conference on Analysis and Applied Mathematics (ICAAM 2020)
AIP Conf. Proc. 2325, 020051-1–020051-4; https://doi.org/10.1063/5.0040368
Published by AIP Publishing. 978-0-7354-4069-2/$30.00

where the symmetry generator is

$$\mathbf{X} = \xi(x,y)\frac{\partial}{\partial x} + \eta(x,y)\frac{\partial}{\partial y} + \eta'\frac{\partial}{\partial y'} + \cdots + \eta^{(n)}\frac{\partial}{\partial y^{(n)}} \tag{7}$$

and

$$\eta^{(n)} = \frac{d\eta^{(n-1)}}{dx} - y^{(n)}\frac{d\xi}{dx} \tag{8}$$

[3, 4, 5].

In fact , the symmetry condition (6) is a differential equation for the functions $\xi(x,y)$ and $\eta(x,y)$, that is linear for both functions. Moreover, since $\xi(x,y)$ and $\eta(x,y)$ are functions of x and y, it will split into many partial differential equations whose solutions can be found. We have to determine functions of $\xi(x,y)$ and $\eta(x,y)$ from these partial differential equations. The differential equation (5) can be solved with normal form of the generator which is constructed with the functions $s(x,y)$ and $t(x,y)$

If a second order differential equation admits two-parameter group (G_2), then there exist two generators $\mathbf{X_1}$ and $\mathbf{X_2}$ and their commutator is a linear combination of these two generators

$$[\mathbf{X_1}, \mathbf{X_2}] = a_1\mathbf{X_1} + a_2\mathbf{X_2}, \tag{9}$$

where a_1 and a_2 are structure constants. If both of the structure constants are zero, then the group is abelian, if at least one of them is not zero, then group is not abelian. In a second order differential equation there are two generators, the suitable coordinates $s(x,y)$ and $t(x,y)$ which reduce the equation to a first order differential equation can be obtained [3, 4, 5].

THE SOLUTION WITH SYMMETRY OF RADIAL SCHRÖDINGER EQUATION FOR A PARTICLE CONFINING QUANTUM DOT WITH RADIUS a

Let apply theory of Lie symmetry to the radial Schrödinger equation. If we take $R = y$, $r = x$, $b = -k^2$ in the equation (3), then the equation (3) is

$$y'' = -\frac{2}{x}y' + by \tag{10}$$

and the symmetry condition of the equation (10) from (6) is

$$\begin{aligned} &-\xi_{,yy}y'^3 + (\frac{4}{x}\xi_{,y} + \eta_{,yy} - 2\xi_{,xy})y'^2 + (\frac{2}{x}\xi_{,x} - 3by\xi_{,y} - \frac{2}{x^2}\xi \\ &+2\eta_{,xy} - \xi_{,xx})y' + (b\eta_{,y} - 2b\xi_{,x})y - b\eta + \frac{2}{x}\eta_{,x} + \eta_{,xx} = 0. \end{aligned} \tag{11}$$

In order to hold the condition (11), we get

$$\xi_{,yy} = 0, \tag{12}$$

$$\frac{4}{x}\xi_{,y} + \eta_{,yy} - 2\xi_{,xy} = 0, \tag{13}$$

$$\frac{2}{x}\xi_{,x} - 3by\xi_{,y} - \frac{2}{x^2}\xi + 2\eta_{,xy} - \xi_{,xx} = 0, \tag{14}$$

$$(b\eta_{,y} - 2b\xi_{,x})y - b\eta + \frac{2}{x}\eta_{,x} + \eta_{,xx} = 0. \tag{15}$$

The functions $\xi(x,y)$ and $\eta(x,y)$ from these equations are determined as follows

$$\xi(x,y) = \alpha + \beta e^{2\sqrt{b}x} + \gamma e^{-2\sqrt{b}x}, \tag{16}$$

$$\eta(x,y) = [\beta(\sqrt{b} - \frac{1}{x})e^{2\sqrt{b}x} - \gamma(\sqrt{b} + \frac{1}{x})e^{-2\sqrt{b}x,} - \frac{\alpha}{x} + \nu]y \tag{17}$$

where α, β, γ and ν are arbitrary constants. In that case, infinitesimal generator of the equation (10) is

$$\mathbf{X} = \left[\alpha + \beta e^{2\sqrt{b}x} + \gamma e^{-2\sqrt{b}x}\right]\frac{\partial}{\partial x}$$
$$+\left[\beta(\sqrt{b} - \frac{1}{x})e^{2\sqrt{b}x} - \gamma(\sqrt{b} + \frac{1}{x})e^{-2\sqrt{b}x} - \frac{\alpha}{x} + \nu\right]y\frac{\partial}{\partial y}. \tag{18}$$

By making arbitrary choices for arbitrary constants α, β, γ, ν in the generator (18), basis generators of the equation (10) are found as

$$\mathbf{X}_1 = \frac{\partial}{\partial x} - \frac{y}{x}\frac{\partial}{\partial y}, \tag{19}$$
$$\mathbf{X}_2 = y\frac{\partial}{\partial y}, \tag{20}$$
$$\mathbf{X}_3 = e^{2\sqrt{b}x}\frac{\partial}{\partial x} + (\sqrt{b} - \frac{1}{x})e^{2\sqrt{b}x}y\frac{\partial}{\partial y}, \tag{21}$$
$$\mathbf{X}_4 = e^{-2\sqrt{b}x}\frac{\partial}{\partial x} - (\sqrt{b} + \frac{1}{x})e^{-2\sqrt{b}x}y\frac{\partial}{\partial y}. \tag{22}$$

They satisfy the commutator relations for $i,j = 1,2,3,4$, $[\mathbf{X}_i, \mathbf{X}_j] = -[\mathbf{X}_j, \mathbf{X}_i]$,$[\mathbf{X}_i, \mathbf{X}_i] = 0$, $[\mathbf{X}_i, \mathbf{X}_2] = 0$ and $[\mathbf{X}_i, \mathbf{X}_j] \neq 0$, for $i,j \neq 2$, $i \neq j$ [6].

By taking the generators $\mathbf{X}_1$ and $\mathbf{X}_2$, let determine coordinates $s(x,y)$ and $t(x,y)$ which reduce the equation (10) to first order differential equation. The commutator of the generators $\mathbf{X}_1$ and $\mathbf{X}_2$ is $[\mathbf{X}_1, \mathbf{X}_2] = 0$ (the group is abelian). Therefore normal forms of generators are

$$\mathbf{X}_1 = \frac{\partial}{\partial x} - \frac{y}{x}\frac{\partial}{\partial y} = \frac{\partial}{\partial s}, \tag{23}$$
$$\mathbf{X}_2 = y\frac{\partial}{\partial y} = \frac{\partial}{\partial t}. \tag{24}$$

If the normal forms (23),(24) are applied to $t(x,y)$and $s(x,y)$, respectively, then we have

$$t = t(x,y) = \ln xy, \tag{25}$$
$$s = s(x,y) = x. \tag{26}$$

By using of the coordinates (25) and (26), the equation (10) is written as

$$s'' = s' - bs'^3 \quad s = s(t). \tag{27}$$

The solution of the differential equation (27) is

$$s = \frac{1}{\sqrt{b}}\ln[\sqrt{1 + bc_1e^{2t}} + \sqrt{bc_1e^{2t}}] + c_2, \tag{28}$$

where c_1 and c_2 are integration constants. In that case, for $c_2 = 0$, the solution of equation (10) is

$$y = \frac{1}{k\sqrt{c_1}}\frac{\sin kx}{x}. \tag{29}$$

When this solution is normalized, the normalization constant is $c_1 = \frac{a^3}{2\pi^2}$ and it is equivalent to the series solution (4) of the radial Schrödinger equation for $V(r) = 0$ [6].

Let study for the non-abelian situation, for example we consider the generators $\mathbf{X}_1$ and $\mathbf{X}_4$, commutator of these generators is $[\mathbf{X}_1, \mathbf{X}_4] \neq 0$. From (9), the structure constants are $a_1 = 2\sqrt{b}$, $a_2 = 0$ for $[\mathbf{X}_4, \mathbf{X}_1] = 2\sqrt{b}\mathbf{X}_4$. If these transformations

$$\widetilde{\mathbf{X}}_1 = a_1\mathbf{X}_1, \tag{30}$$
$$\widetilde{\mathbf{X}}_2 = \frac{1}{a_1}\mathbf{X}_4 \tag{31}$$

are applied with the generators $\mathbf{X}_1$ and $\mathbf{X}_4$, we have $[\widetilde{\mathbf{X}}_1, \widetilde{\mathbf{X}}_2] = \widetilde{\mathbf{X}}_1$. In that case, the normal forms of the generators (30) and (31) are

$$\widetilde{\mathbf{X}}_1 = 2\sqrt{b}e^{-2\sqrt{bx}}\frac{\partial}{\partial x} - 2\sqrt{b}(\sqrt{b}+\frac{1}{x})e^{-2\sqrt{bx}}y\frac{\partial}{\partial y} = \frac{\partial}{\partial s}, \tag{32}$$

$$\widetilde{\mathbf{X}}_2 = \frac{1}{2\sqrt{b}}\frac{\partial}{\partial x} - \frac{1}{2\sqrt{bx}}y\frac{\partial}{\partial y} = t\frac{\partial}{\partial t} + s\frac{\partial}{\partial s}. \tag{33}$$

If the normal forms (32), (33) are applied to $t(x,y)$ and $s(x,y)$, respectively, then we have

$$t = t(x,y) = x^2y^2e^{2\sqrt{bx}}, \tag{34}$$

$$s = s(x,y) = \frac{e^{2\sqrt{bx}}}{4b} + x^2y^2e^{2\sqrt{bx}}. \tag{35}$$

By using of the coordinates (34) and (35), the equation (10) is written as

$$s'' + \frac{s'}{2t} = \frac{1}{2t} \tag{36}$$

and the solution of the differential equation (36) is

$$s = 2c_3t^{1/2} + t + c_4, \tag{37}$$

where c_3 and c_4 are integration constants. For $c_4 = -\frac{1}{4k^2}$, in the coordinate (x,y), the solution of equation (10) is

$$y = \frac{-i}{2k^2c_3}\frac{\sin kx}{x}, \tag{38}$$

when this solution is normalized, the normalization constant is $c_3 = \frac{a^{\frac{5}{2}}}{2\sqrt{2}\pi^2}$ and it is equivalent to the series solution (4) of the Radial Schrödinger equation for $V(r) = 0$ [6].

CONCLUSION

Finally, for abelian and non-abelian situations, the solution of the radial Schrödinger equation for $V(r) = 0$ by using Lie symmetry has been obtained analytically, without making any approximation. This solution is compatible with the series solution of the equation.

ACKNOWLEDGMENTS

The study is taken from PHD thesis entitled "The Solutions of Special Radial Schrödinger Equation by Using Appropriate Symmetries, Kismet Kasapoglu, 2016".

REFERENCES

1. F.A.Brezin and M. Shubin, *The Schrödinger Equation Mathematics and Its Applications* (Kluwer Academic Publishers Groups, 1991).
2. B. Karaoğlu, *Kuantum Mekaniğine Giriş* (Bilgitek yayıncılık, 1994).
3. H. Stephani, *Differential Equations. Their Solution Using Symmetries* (Cambridge University Press, 1994).
4. F. Oliveri, Symmetry **2**, 658–706 (2010).
5. J. Strarrett, Mathematical Association of America **114**, 778–792 (2007).
6. K.Kasapoğlu, *The Solutions of Special Radial Schrödinger Equation by Using Appropriate Symmetries*, Phd dissertation, Trakya University (2016).

Hamiltonian System Related to the Casimir Operator of the Group SO(3,2) for Parabolic Coordinates

Yasemin Isik[a)] and Mehmet Sezgin[b)]

Department of Mathematics, Faculty of Science, Trakya University, Edirne, Turkey

[a)]*Corresponding author: isikyasemin1@gmail.com*
[b)]*Electronic mail: msezgin22@yahoo.com*

Abstract. The generators of the quasi-regular representation of the group SO(3,2) are obtained for parabolic coordinates. By the generators, the expression of the quadratic Casimir operator is presented. From the relation between the Casimir operator and Hamiltonian, the corresponding physical system is expressed, and its exact solution is given.

INTRODUCTION

The concept of symmetry plays an important role in science, and especially in physics, it appears as group theory in terms of mathematics. Since the paper of Sophus Lie who introduced Lie groups to the scientific world [1], applications of the theory have attracted a great deal of attention [2, 3, 4, 5, 6]. Among Lie group theory applications to physics, Casimir operator has significant importance [7]. In addition to expressing quantities such as angular momentum, elementary particle mass, spin, etc., Casimir operator also offers a physical system corresponding to the group owing to its relation with Hamiltonian [8, 9].

In this paper, we are interested in studying the Casimir operator of the group SO(3,2), so-called 3+2 de Sitter group [10, 11, 12, 13]. In literature, there are several works on the quadratic Casimir operator (or Laplace-Beltrami operator) of the group for certain cases. For instance, Hannabuss used the group theoretical method to construct a plausible wave equation for particles of spin in the de Sitter spaces [14], and Wickramasekara studied Casimir operator of the group as a spectrum generating algebra to obtain the mass-spin spectra of hadrons [15]. In Elçin and Dane's work [16], the authors discussed the quantum integrable systems related to the group via Laplace-Beltrami operator for different coordinates. On the other hand, in the recent paper [17], the author considered the Casimir operator in the spherical coordinates of the homogeneous space on which the group SO(3,2) acts. Using the Casimir operator, the author constructed the eigenvalue problem leading us to the required Hamiltonian system and thus gave the exact solution of the Schrödinger equation by virtue of the group approach. For this study, however, we aim to give the expression of the Casimir operator of the group SO(3,2) for parabolic coordinates by following the same process in [17].

The paper is organized as follows. In the second section, all required notations and results for the group SO(3,2) are listed. The generators of the quasi-regular representation and the Casimir operator of the group in Cartesian coordinates are obtained. In the third section, the generators and then the Casimir operator are expressed for parabolic coordinates. Finally, the eigenvalue problem of the Casimir operator is reduced to the corresponding Hamiltonian system and its exact solution is given.

SO(3,2) GROUP STRUCTURE

The real five-dimensional vector space equipped with the bilinear form

$$[x,y] = -x_1y_1 - x_2y_2 - x_3y_3 + x_4y_4 + x_5y_5, \quad x,y \in \mathbb{R}^5$$

is called the pseudo-Euclidean space $\mathbb{R}^5_{3,2}$. The set of linear transformations of the space preserving distances between points forms the group SO(3,2). The equality $[x,y] = -x_1^2 - x_2^2 - x_3^2 + x_4^2 + x_5^2 = 1$ defines the hyperboloid H_+ in $R^5_{3,2}$. H_+ is the homogeneous space on which SO(3,2) group acts.

We shall denote the one-parameter subgroups of the group SO(3,2) consisting of rotations and hyperbolic rotations in the plane by $\{g_{ij}(t)\}, 1 \le i < j \le 3$ or $4 \le i < j \le 5$ and $\{g_{ij}(t)\}, 1 \le i \le 3 < j \le 5$, respectively. Therefore, we have the rotations $g_{12}(\theta), g_{13}(\varphi), g_{23}(\psi), g_{45}(\phi)$ and hyperbolic rotations $g_{14}(\alpha), g_{15}(\beta), g_{24}(\tau), g_{25}(\mu), g_{34}(\nu)$,

International Conference on Analysis and Applied Mathematics (ICAAM 2020)
AIP Conf. Proc. 2325, 020052-1–020052-5; https://doi.org/10.1063/5.0040363
Published by AIP Publishing. 978-0-7354-4069-2/$30.00

$g_{35}(t),\ \theta,\varphi,\psi,\phi\in[0,2\pi),\ \alpha,\beta,\tau,\mu,\nu,t\in(-\infty,\infty)$ [18]. The tangent matrices to these one-parameter subgroups at the identity element form a basis of the Lie algebra $\mathfrak{so}$(3,2) of the group SO(3,2).

In this paper, we shall consider the quasi-regular representation T of the group

$$T(g)f(x)=f(xg),\qquad g\in SO(3,2),\ x\in H_+,$$

where $f(x)$ is a square-integrable function on the hyperboloid with the invariant measure $dx=dx_1dx_2dx_3dx_4/|x_5|$. The generators J_{ij} of the representation T of the one-parameter subgroups g_{ij} are defined by

$$J_{ij}=\frac{d}{dt}T(g_{ij}(t))|_{t=0}\ .$$

In this case, the generators corresponding to the rotations are

$$\begin{aligned}
J_{12}&=-x_2\frac{\partial}{\partial x_1}+x_1\frac{\partial}{\partial x_2},\\
J_{13}&=-x_3\frac{\partial}{\partial x_1}+x_1\frac{\partial}{\partial x_3},\\
J_{23}&=-x_3\frac{\partial}{\partial x_2}+x_2\frac{\partial}{\partial x_3},\\
J_{45}&=-x_5\frac{\partial}{\partial x_4}
\end{aligned}\tag{1}$$

and, the generators corresponding to the hyperbolic rotations are

$$\begin{aligned}
J_{14}&=x_4\frac{\partial}{\partial x_1}+x_1\frac{\partial}{\partial x_4},\\
J_{24}&=x_4\frac{\partial}{\partial x_2}+x_2\frac{\partial}{\partial x_4},\\
J_{34}&=x_4\frac{\partial}{\partial x_3}+x_3\frac{\partial}{\partial x_4},\\
J_{15}=x_5\frac{\partial}{\partial x_1},\qquad J_{25}&=x_5\frac{\partial}{\partial x_2},\quad J_{35}=x_5\frac{\partial}{\partial x_3}\ .
\end{aligned}\tag{2}$$

Identifying $I_i\equiv\varepsilon_{ijk}J_{jk},\ S_i\equiv J_{i4},\ i=1,2,3$ and $J_{j5}\equiv K_j,\ j=1,2,3,4,$ these generators satisfy the following set of commutation relations:

$$\begin{gathered}
[I_i,I_j]=\varepsilon_{ijk}I_k,\quad [I_i,S_j]=\varepsilon_{ijk}S_k,\quad [S_i,S_j]=-\varepsilon_{ijk}I_k,\\
[I_i,K_j]=\varepsilon_{ijk}K_k,\quad [S_i,K_j]=-\delta_{ij}K_0,\quad [S_i,K_4]=-K_i,\\
[I_i,K_4]=[K_i,K_j]=[K_i,K_4]=0,
\end{gathered}$$

where ε_{ijk} , δ_{ij} denote Levi-Civita symbol and Kronecker delta symbol, respectively. SO(3,2) group is of rank two, and therefore it possesses two Casimir operators constructed by these generators: second-order and fourth-order Casimir operators [15]. However, we are interested only in the quadratic (second-order) Casimir operator for the group here. The general form of the quadratic Casimir operator for SO(3,2) is the element

$$\boldsymbol{C}=[\,J_{12}^2+J_{13}^2+J_{23}^2+J_{45}^2\,]\;-\;[\,J_{14}^2+J_{15}^2+J_{24}^2+J_{25}^2+J_{34}^2+J_{35}^2\,]\tag{3}$$

of the universal enveloping algebra $\mathfrak{U}(\mathfrak{so}(3,2))$ such that $[C,J_{ij}]=0$ [18].

HAMILTONIAN SYSTEM RELATED TO THE CASIMIR OPERATOR

Choosing different parameterizations of the homogeneous space of the group leads one to different Casimir operator realizations and thus different Hamiltonian systems with various potentials. For this study, we shall consider parabolic coordinates on the hyperboloid H_+ which can be expressed by

$$
\begin{aligned}
x_1 &= \sinh(\alpha) + \frac{1}{2}t^2 e^{\alpha}, \\
x_2 &= t_1 e^{\alpha}, \\
x_3 &= t_2 e^{\alpha}, \\
x_4 &= \cosh(\alpha) - \frac{1}{2}t^2 e^{\alpha}, \\
x_5 &= t_3 e^{\alpha},
\end{aligned}
\tag{4}
$$

where $-\infty < \alpha, t_1, t_2, t_3 < \infty$, $t^2 = -t_1^2 - t_2^2 + t_3^2$ [18, 19]. In this case, the generators (1) - (2) from the previous section become

$$
\begin{aligned}
J_{12} &= t_1\Big(-\frac{\partial}{\partial\alpha} + t_2\frac{\partial}{\partial t_2} + t_3\frac{\partial}{\partial t_3}\Big) + \Big[\sinh\alpha\, e^{-\alpha} + \frac{1}{2}(t_1^2 - t_2^2 + t_3^2)\Big]\frac{\partial}{\partial t_1}\,, \\
J_{13} &= t_2\Big(-\frac{\partial}{\partial\alpha} + t_1\frac{\partial}{\partial t_1} + t_3\frac{\partial}{\partial t_3}\Big) + \Big[\sinh\alpha\, e^{-\alpha} + \frac{1}{2}(-t_1^2 + t_2^2 + t_3^2)\Big]\frac{\partial}{\partial t_2}\,, \\
J_{23} &= -t_2\frac{\partial}{\partial t_1} + t_1\frac{\partial}{\partial t_2}, \\
J_{45} &= t_3\Big(-\frac{\partial}{\partial\alpha} + t_1\frac{\partial}{\partial t_1} + t_2\frac{\partial}{\partial t_2}\Big) + \Big[\cosh\alpha\, e^{-\alpha} + \frac{1}{2}(t_1^2 + t_2^2 + t_3^2)\Big]\frac{\partial}{\partial t_3}\,, \\
J_{14} &= \frac{\partial}{\partial\alpha} - t_1\frac{\partial}{\partial t_1} - t_2\frac{\partial}{\partial t_2} - t_3\frac{\partial}{\partial t_3}, \\
J_{15} &= t_3\Big(\frac{\partial}{\partial\alpha} - t_1\frac{\partial}{\partial t_1} - t_2\frac{\partial}{\partial t_2}\Big) + \Big[\sinh\alpha\, e^{-\alpha} - \frac{1}{2}(t_1^2 + t_2^2 + t_3^2)\Big]\frac{\partial}{\partial t_3}\,, \\
J_{24} &= t_1\Big(\frac{\partial}{\partial\alpha} - t_2\frac{\partial}{\partial t_2} - t_3\frac{\partial}{\partial t_3}\Big) + \Big[\cosh\alpha\, e^{-\alpha} - \frac{1}{2}(t_1^2 - t_2^2 + t_3^2)\Big]\frac{\partial}{\partial t_1}\,, \\
J_{25} &= t_3\frac{\partial}{\partial t_1} + t_1\frac{\partial}{\partial t_3}, \\
J_{34} &= t_2\Big(\frac{\partial}{\partial\alpha} - t_1\frac{\partial}{\partial t_1} - t_3\frac{\partial}{\partial t_3}\Big) + \Big[\cosh\alpha\, e^{-\alpha} - \frac{1}{2}(-t_1^2 + t_2^2 + t_3^2)\Big]\frac{\partial}{\partial t_2}\,, \\
J_{35} &= t_3\frac{\partial}{\partial t_2} + t_2\frac{\partial}{\partial t_3}\,.
\end{aligned}
$$

Therefore, the Casimir operator (3) can be written as follows

$$
\boldsymbol{C} = -\frac{\partial^2}{\partial\alpha^2} - 3\,\frac{\partial}{\partial\alpha} - e^{-2\alpha}\left(\frac{\partial^2}{\partial t_1^2} + \frac{\partial^2}{\partial t_2^2} - \frac{\partial^2}{\partial t_3^2}\right). \tag{5}
$$

The expression (5) is in agreement with the general expression of the Casimir operator for the parabolic coordinates described in [20]. Now let us give the eigenvalue equation

$$
\boldsymbol{C} f(x) = -\sigma(\sigma+3) f(x),
$$

or

$$
\left[-\frac{\partial^2}{\partial\alpha^2} - 3\,\frac{\partial}{\partial\alpha} - e^{-2\alpha}\left(\frac{\partial^2}{\partial t_1^2} + \frac{\partial^2}{\partial t_2^2} - \frac{\partial^2}{\partial t_3^2}\right)\right] f(x) = -\sigma(\sigma+3) f(x), \tag{6}
$$

where $\sigma(\sigma+3)$, $\sigma \in \mathbb{C}$ is the eigenvalue of the Casimir operator for the group SO(3,2) [18]. In order to solve the eigenvalue problem (6), the separation of variables method can be used. Setting the solution as

$$
f(\alpha, t_1, t_2, t_3) = A(\alpha)\, e^{-i\kappa t_1}\, e^{-i\lambda t_2}\, e^{-i\eta t_3}, \tag{7}
$$

where κ, λ, η are integers or half-integers, leads us to the differential equation

$$
\frac{d^2A}{d\alpha^2} + 3\,\frac{dA}{d\alpha} - (\kappa^2 + \lambda^2 - \eta^2)\, e^{-2\alpha} A = \sigma(\sigma+3) A\,. \tag{8}
$$

As a general quantum problem, physicists deal with the Schrödinger equation

$$H\Psi = E\Psi$$

for a given Hamiltonian H. Starting from a Lie group, however, the group theory approach allows one to end up with a corresponding physical system with certain potential and energy spectrum [21, 22]. In order to illustrate this fact, we put

$$A(\alpha) = e^{-3\alpha/2}\,\Psi(\alpha) \tag{9}$$

into Eq. (8) . Then we get the time-independent Schrödinger equation

$$H\,\Psi = \left[-\frac{d^2}{d\alpha^2} + (\kappa^2+\lambda^2-\eta^2)\,e^{-2\alpha}\right]\Psi = -\left(\sigma+\frac{3}{2}\right)^2\Psi \tag{10}$$

with the exponential potential

$$V(\alpha) = (\kappa^2+\lambda^2-\eta^2)\,e^{-2\alpha} \tag{11}$$

and the energy spectrum $E = -\left(\sigma+3/2\right)^2$. Making the substitution

$$z = e^{-\alpha} \tag{12}$$

into Eq.(10) , we arrive at the equation

$$z^2\,\frac{d^2\Psi}{dz^2} + z\,\frac{d\Psi}{dz} + \left[(\eta^2-\kappa^2-\lambda^2)\,z^2 - \left(\sigma+\frac{3}{2}\right)^2\right]\Psi = 0\,. \tag{13}$$

For $\eta^2-\kappa^2-\lambda^2 > 0$, Eq.(13) is called Bessel equation, one of whose particular solutions is in the form

$$\Psi(z) = J_{(\sigma+3/2)}\left(\sqrt{\eta^2-\kappa^2-\lambda^2}\,z\right),$$

where $\left(\sigma+3/2\right)$ is not an integer [23]. Considering the substitution (12), the wave function of the Schrödinger equation can be given as follows

$$\Psi(\alpha) = N\,J_{(\sigma+3/2)}\left(\sqrt{\eta^2-\kappa^2-\lambda^2}\,e^{-\alpha}\right), \tag{14}$$

where N is the normalization constant. From the transformation (9), the solution of Eq. (8) becomes

$$A(\alpha) = e^{-3\alpha/2}\,J_{(\sigma+3/2)}\left(\sqrt{\eta^2-\kappa^2-\lambda^2}\,e^{-\alpha}\right).$$

Finally, the solution of the eigenvalue problem of (6) is in the form

$$f(\alpha,t_1,t_2,t_3) = e^{-3\alpha/2}\,e^{-i(\kappa t_1+\lambda t_2+\eta t_3)}\,J_{(\sigma+3/2)}\left(\sqrt{\eta^2-\kappa^2-\lambda^2}\,e^{-\alpha}\right).$$

CONCLUSION

In this paper, we illustrate an application regarding the group SO(3,2) of group theoretical approach to physics. From the well-known fact that choosing different parameterizations one can obtain various Hamiltonian systems with the same energy spectrum, we consider the parabolic coordinates for the group. Thus, we arrive at the Hamiltonian system with exponential-type potential and given the energy spectrum of the system. In a future publication, we aim to discuss the Eq.(10) in detail for the potential (11).

REFERENCES

1. S. Lie, Arch. Math. **6**, 328 (1881).
2. W. Pauli, Z. Phys. **36**, 336 (1926).
3. A. O. Barut, Phys. Rev. **135**, B839 (1964).
4. A. M. Perelomov and V. S. Popov, Math. USSR Izv. **2**, 1313 (1968).
5. E. G. Kalnins and W. Miller, Jr., J. Math. Phys. **16**, 2507 (1975).
6. J. Wu and Y. Alhassid, J. Math. Phys. **31**, 557 (1990).
7. H. Casimir, Proc. Roy. Akad. Amst. **34**, 844 (1931).
8. G. Racah, Z. Phys. **36**, 336 (1950).
9. I. M. Gelfand, Mat. Sb. **26**, 103 (1950).
10. P. A. M. Dirac, Ann. Math. **36**, 657 (1935).
11. F. Gürsey, *Group Theoretical Concepts and Methods in Elementary Particle Physics: Lectures*, Vol. 1 (Gordon and Breach, New York, 1964).
12. J. B. Erhman, Math. Proc. Camb. Phil. Soc. **53**, 290 (1957).
13. N. T. Evans, J. Math. Phys. **8**, 170 (1967).
14. K. C. Hannabuss, J. Phys. A: Gen. Phys. **2**, 274 (1969).
15. S. Wickramasekara, Int. J. Teor. Phys. **36**, 2409 (1977).
16. E. Elçin and C. Dane, Trakya Univ. J. Sci. **8**, 35 (2007).
17. M. Sezgin, Far East J. App. Math. **62**, 37 (2012).
18. N. J. Vilenkin and A. U. Klimyk, *Representations of Lie Groups and Special Functions*, Vol. 2 (Kluwer Academic Publishers, The Netherland, 1993).
19. M. Sezgin, A. Y. Verdiyev, and Y. A. Verdiyev, J. Math. Phys. **39**, 1910 (1998).
20. N. J. Vilenkin, *Special Functions and the Theory of Group Representations*, Vol. 22 (American Mathematical Society, USA, 1968).
21. P. Levay, J. Phys. A: Math. Gen. **28**, 5919 (1995).
22. D. Petrosyan and G. S. Pogosyan, Non. Phen. Com. Sys. **17**, 405 (2014).
23. H. Bateman, *Higher Transcendental Functions*, Vol. 2 (McGraw-Hill Book Company, Inc, USA, 1953).

Domain of Generalized Riesz Difference Operator of Fractional Order in Maddox's Space $\ell(p)$

Taja Yaying[a)]

Department of Mathematics, Dera Natung Govt. College, Itanagar-791113, Arunachal Pradesh, India

[a)] *Corresponding author: tajayaying20@gmail.com*

Abstract. Let $\Gamma(x)$ denotes the gamma function of a real number $x \notin \{0,-1,-2,\ldots\}$. Then the backward difference matrix Δ^{Bq} of fractional order q is defined as

$$(\Delta^{Bq}v)_i = \int_{l=0}^{\infty}(-1)^l \frac{\Gamma(q+1)}{l!\Gamma(q-l+1)} v_{i-l}.$$

In this paper we introduce paranormed Riesz difference sequence space $\mathbf{r}^t(\Delta^{Bq})$ of fractional order q obtained by the domain of generalized difference operator $R^t\Delta^{Bq}$ in Maddox's space $\ell(p)$. We investigate certain topological properties and obtain the Schauder basis of the space $\mathbf{r}^t(\Delta^{Bq})$. We also obtain the $\alpha-$, $\beta-$ and $\gamma-$duals and characterize certain matrix classes related to the space $\mathbf{r}^t(\Delta^{Bq})$.

INTRODUCTION

Throughout the article $\Gamma(x)$ will denote the gamma function of a real number $x \notin \{0,-1,-2,\ldots\}$. It is defined as $\Gamma(x) = \int_0^\infty t^{x-1}e^{-t}dt$. Clearly $\Gamma(x+1) = x!$ for $x \in \mathbb{N}_0$. Also $\Gamma(x+1) = x\Gamma(x)$ for any real number $x \notin \{0,-1,-2,\ldots\}$. Here and in the rest of the paper, the notation $\mathbb{N}_0 = \{0,1,2,\ldots\}$ and w denotes the space of all real valued sequences. Any linear subspace of w is called sequence space. Let ℓ_p, ℓ_∞, c and c_0 denote the spaces of all absolutely p-summable, bounded, convergent and null sequences, respectively. Moreover, bs and cs will denote the spaces of all bounded and convergent series, respectively. Throughout the paper, we shall use the notation that the summation symbol without limit runs from 0 to ∞.

Definition 1 *A linear topological space V over the real field $\mathbb{R}$ is said to be a paranormed space if there exists a subadditive function $g : V \to \mathbb{R}$ such that $g(\theta) = 0$, $g(\mathbf{v}) = g(-\mathbf{v})$ and the scalar multiplication is continuous, i.e. $|\xi_i - \xi| \to 0$ and $g(v_i - \mathbf{v}) \to 0$ for all $\xi \in \mathbb{R}$ and $\mathbf{v} \in V$, where $\theta \in V$ is the zero vector.*

Let $p = (p_i)$ be a bounded sequence of strictly positive real numbers with $M = \max\{1,H\}$ where $H = \sup_i p_i$. Then, Maddox [21] defined the sequence space $\ell(p) = \{\mathbf{v} = (v_i) \in w : \sum_i |v_i|^{p_i} < \infty\}$, which is a complete space paranormed by $g(\mathbf{v}) = \left(\sum_i |v_i|^{p_i}\right)^{\frac{1}{M}}$.

Let $\lambda = (\lambda_{ij})$ be an infinite matrix of real entries. By λ_i, we denote the sequence in the i^{th} row of the matrix λ. The matrix λ is called a matrix mapping from sequence space V to sequence space W if $\lambda-$transforms of the sequence $\mathbf{v} = (v_i)$ i.e. $\lambda\mathbf{v} = \{(\lambda\mathbf{v})_i\}$ exists and belongs to W for all $\mathbf{v} \in V$ where

$$(\lambda\mathbf{v})_i = \sum_j \lambda_{ij}v_j,\ (i \in \mathbb{N}_0). \tag{1}$$

Let $(V : W)$ denotes the class of all such matrices that map from V to W. In other words, $\lambda \in (V : W)$ if and only if the series on the R.H.S. of the equation (1) converges for each $i \in \mathbb{N}_0$ and $\mathbf{v} \in V$ such that $\lambda\mathbf{v} \in W$ for all $\mathbf{v} \in V$.

Define the sequence space V_λ by

$$V_\lambda = \{\mathbf{v} \in w : \lambda\mathbf{v} \in V\}. \tag{2}$$

Then V_λ is called the matrix domain of λ in the space V.

The $\alpha-$, $\beta-$ and $\gamma-$duals of the subset $V \subset w$ are defined by $V^\alpha = \{\mathbf{t} = (t_i) \in w : \mathbf{tv} = (t_iv_i) \in \ell_1$ for all $\mathbf{v} \in V\}$, $V^\beta = \{\mathbf{t} = (t_i) \in w : \mathbf{tv} = (t_iv_i) \in cs$ for all $\mathbf{v} \in V\}$ and $V^\gamma = \{\mathbf{t} = (t_i) \in w : \mathbf{tv} = (t_iv_i) \in bs$ for all $\mathbf{v} \in V\}$, respectively.

The domains $c_0(\Delta^F)$, $c(\Delta^F)$ and $\ell_\infty(\Delta^F)$ of the forward difference matrix Δ^F are introduced by Kızmaz [17]. Since then several other authors [13, 14, 15, 18] generalized the notion of forward and backward difference operator Δ^F and Δ^B and studied difference spaces of integer order. The difference sequence spaces of integer order were further generalized by Baliarsingh [8]. Aftermore, several authors [7, 9, 10, 12, 16] studied difference spaces of fractional order.

International Conference on Analysis and Applied Mathematics (ICAAM 2020)
AIP Conf. Proc. 2325, 020053-1–020053-5; https://doi.org/10.1063/5.0040346
Published by AIP Publishing. 978-0-7354-4069-2/$30.00

Definition 2 *[7] Let $q>0$ be a proper fraction. Then backward difference operator Δ^{Bq} of fractional order q is defined as* $(\Delta^{Bq}\mathbf{v})_i=\sum_l(-1)^l\frac{\Gamma(q+1)}{l!(q-l+1)}v_{i-l}$.

The difference operator Δ^{Bq} can also be expressed in the form of triangle as follows:

$$(\Delta^{Bq})_{ij}=\begin{cases}(-1)^{i-j}\frac{\Gamma(q+1)}{(i-j)!\Gamma(q-i+j+1)} & (0\leq j\leq i),\\ 0 & (j>i).\end{cases}$$

Now we give the definition and notation regarding the Riesz mean matrix.

Definition 3 *Let (t_k) be a sequence of positive numbers and define $T_i=\sum_{l=0}^i t_l$, $i\in\mathbb{N}_0$. Then the Riesz mean matrix $R^t=(r^t_{ij})$ is defined as*

$$r^t_{ij}=\begin{cases}\frac{t_j}{T_i} & (0\leq j\leq i),\\ 0 & (j>i).\end{cases}$$

Malkowsky [3] introduced the sequence spaces $\mathbf{r}^t_\infty$, $\mathbf{r}^t_c$ and $\mathbf{r}^t_0$ as the set of all sequences whose R^t- transforms are in the spaces ℓ_∞, c and c_0, respectively. Altay and Başar [1] studied the sequence space $\mathbf{r}^t(p)$ defined by $\mathbf{r}^t(p)=\left\{v=(v_j)\in w:\sum_{i\in\mathbb{N}_0}\left|\frac{1}{T_i}\sum_{j=0}^i t_jv_j\right|^{p_i}<\infty\right\}$, where $p=(p_j)$ is a bounded sequence of positive real numbers. Afterthen, several authors studied and generalized Riesz spaces [2, 4, 5, 6]. Recently Yaying [11] introduced the paranormed Riesz difference sequence spaces $\mathbf{r}^t_\infty(p,\Delta^{Bq})$, $\mathbf{r}^t_c(p,\Delta^{Bq})$ and $\mathbf{r}^t_0(p,\Delta^{Bq})$ as the set of all sequences whose $R^t\Delta^{Bq}-$transforms are in the spaces $\ell_\infty(p)$, $c(p)$ and $c_0(p)$, respectively.

PARANORMED RIESZ DIFFERENCE SEQUENCE SPACE $\mathbf{r}^t(p,\Delta^{Bq})$ OF FRACTIONAL ORDER

Before constructing the sequence space $\mathbf{r}^t(p,\Delta^{Bq})$, we recall certain notions and definitions which can be found in [11]:

Definition 4 *[11] Let $q>0$ be a proper fraction. Then the product matrix $R^t\Delta^{Bq}$ of Riesz mean R^t and the difference operator Δ^{Bq} is defined as follows:*

$$\left(R^t\Delta^{Bq}\right)_{ij}=\begin{cases}\sum\limits_{l=j}^{i}(-1)^{l-j}\frac{\Gamma(q+1)}{(l-j)!\Gamma(q-l+j+1)}\frac{t_l}{T_i} & (0\leq j\leq i),\\ 0 & (j>i).\end{cases}$$

In the rest of the paper, for brevity, we shall denote $R^t\Delta^{Bq}$ by $\mathscr{R}$.

Definition 5 *[11] (Lemma 2.1) The inverse of the product matrix $\mathscr{R}=R^t\Delta^{Bq}$ is given by:*

$$\left(R^t\Delta^{Bq}\right)^{-1}_{ij}=\begin{cases}(-1)^{i-j}\sum\limits_{l=j}^{j+1}\frac{\Gamma(-q+1)}{(i-l)!\Gamma(-\alpha-i+l+1)}\frac{T_j}{t_l} & (0\leq j<i),\\ \frac{T_i}{t_i} & (j=i),\\ 0 & (j>i).\end{cases}$$

Let us define the $R^t\Delta^{Bq}=\mathscr{R}-$transforms of a sequence $\mathbf{v}=(v_j)$ as follows:

$$u_i=(\mathscr{R}\mathbf{v})_i=\sum_{j=0}^{i-1}\left[\sum_{l=j}^{i}(-1)^{l-j}\frac{\Gamma(q+1)}{(l-j)!\Gamma(q-l+j+1)}\frac{t_l}{T_i}\right]v_j+\frac{t_i}{Q_i}v_i,\quad(i\in\mathbb{N}_0).\tag{3}$$

Now we introduce paranormed Riesz difference sequence space $\mathbf{r}^t(p,\Delta^{Bq})$ of fractional order q as follows:

$$\mathbf{r}^t(p,\Delta^{Bq})=\{\mathbf{v}=(v_i)\in w:\mathscr{R}\mathbf{v}\in\ell(p)\}=\left\{\mathbf{v}=(v_i)\in w:\sum_i|(\mathscr{R}\mathbf{v})_i|^{p_i}<\infty\right\}.$$

The above sequence space can be expressed in the notation of (2) by $\mathbf{r}^t(p,\Delta^{Bq})=(\ell(p))_{R^t\Delta^{Bq}}=(\ell(p))_{\mathscr{R}}$. The sequence space $\mathbf{r}^t(p,\Delta^q)$ may be reduced to the following classes of sequence spaces in the special case of q:

1. If $q=0$ then the sequence space $\mathbf{r}^t(p,\Delta^{Bq})$ reduces to $\mathbf{r}^t(p)$ as defined by Altay and Başar [1].
2. If $q=1$ then the sequence space $\mathbf{r}^t(p,\Delta^{Bq})$ reduces to $\mathbf{r}^t(p,\Delta^{B})$ where $(\Delta^{B}\mathbf{v})_j = v_j - v_{j-1}$.
3. If $q=m\in\mathbb{N}$ then the sequence space $\mathbf{r}^t(p,\Delta^{Bq})$ reduces to $\mathbf{r}^t(p,\Delta^{Bm})$ where $(\Delta^{Bm}\mathbf{v})_j = \sum\limits_{l=0}^{m}(-1)^l\binom{m}{l}v_{j-l}$ (see [18]).

Theorem 1 *The sequence space $\boldsymbol{r}^t(p,\Delta^{Bq})$ is a complete linear metric space paranormed by $\mathscr{P}_q$ defined by*

$$\mathscr{P}_q\boldsymbol{v} = \|\mathscr{R}\boldsymbol{v}\|_{\ell(p)} = \left(\sum_i\left|\sum_{j=0}^{i-1}\left[\sum_{l=j}^{i}(-1)^{l-j}\frac{\Gamma(q+1)}{(l-j)!\Gamma(q-l+j+1)}\frac{t_l}{T_i}\right]v_j+\frac{t_i}{T_i}v_i\right|^{p_i}\right)^{\frac{1}{M}} \text{ with } 0<p_i\le H<\infty. \quad (4)$$

Theorem 2 *The Riesz difference sequence space $\boldsymbol{r}^t(p,\Delta^{Bq})$ is linearly isomorphic to $\ell(p)$ where $0<p_i\le H<\infty$.*

We now construct sequence of points in the space $\mathbf{r}^t(p,\Delta^{Bq})$ which will form the Schauder basis for that space. First we recall the definition of Schauder basis for a normed space $(V,\|\cdot\|)$.

Definition 6 *A sequence $\boldsymbol{v}=(v_j)$ of a normed space $(V,\|\cdot\|)$ is called a Schauder basis of the space V if for every $v\in V$ there exists a unique sequence of scalars (a_j) such that $\lim\limits_{i\to\infty}\left\|v-\sum_{j=0}^{i}a_jv_j\right\|=0$.*

Theorem 3 *Let $\mathscr{R}_j(t)=(\mathscr{R}\boldsymbol{v})_j$ for all $j\in\mathbb{N}_0$ where $\mathscr{R}=R^t\Delta^{Bq}$ and $0<p_j\le H<\infty$. Define the sequence $b^{(j)}(t)=(b_i^{(j)}(t))$ of the elements of the space $\boldsymbol{r}^t(p,\Delta^{Bq})$ for every fixed $j\in\mathbb{N}_0$ by*

$$b_i^{(j)}(t)=\begin{cases}\sum\limits_{l=j}^{j+1}(-1)^{i-j}\frac{\Gamma(-q+1)}{(i-l)!\Gamma(-q-i+l+1)}\frac{T_j}{t_l} & (j<i),\\ \frac{T_j}{t_j} & (j=i),\\ 0 & (j>i).\end{cases}$$

Then, the sequence $\{b^{(j)}(t)\}$ is basis for the space $\boldsymbol{r}^t(p,\Delta^{Bq})$ and every $\boldsymbol{v}\in\boldsymbol{r}^t(p,\Delta^{Bq})$ has a unique representation of the form $\boldsymbol{v}=\sum_j\mathscr{R}_j(t)b^{(j)}(t)$.

$\alpha-$, $\beta-$ AND $\gamma-$DUALS

In this section we obtain the $\alpha-$, $\beta-$ and $\gamma-$duals of $\mathbf{r}^t(p,\Delta^{Bq})$. Throughout $\mathscr{F}$ will denote the collection of all finite subsets of $\mathbb{N}_0$ and $s_j=\frac{p_j}{p_j-1}$ for all $j\in\mathbb{N}_0$.

Theorem 4 *Let $1<p_j\le H<\infty$ for every $j\in N_0$. Define the set*

$$\mathscr{D}_1(p)=\bigcup_{B>1}\left\{\boldsymbol{a}=(a_j)\in w:\sup_{I\in\mathscr{F}}\sum_j\left|\sum_{i\in I}\left[\sum_{l=j}^{j+1}(-1)^{i-j}\frac{\Gamma(-q+1)}{(i-l)!\Gamma(-q-i+l+1)}\frac{T_j}{t_l}a_j+\frac{T_i}{t_i}a_i\right]B^{-1}\right|^{s_j}<\infty\right\} \text{ and}$$
$$\mathscr{D}_2(p)=\bigcup_{B>1}\left\{\boldsymbol{a}=(a_k)\in w:\sum_j\left|\Delta^{Bq}\left(\frac{a_j}{t_j}\right)T_jB^{-1}\right|^{s_j}<\infty \text{ and } \left\{\left(\frac{a_j}{t_j}T_jB^{-1}\right)^{s_j}\right\}\in\ell_\infty\right\},$$

where $\Delta^{Bq}\left(\frac{a_j}{t_j}\right)=\frac{a_j}{t_j}+\sum_{l=j+1}^{i}(-1)^{l-j}a_l\sum_{m=j}^{j+1}\frac{\Gamma(-q+1)}{(l-m)!\Gamma(-\alpha-l+m+1)t_m}$.

Then $\left[\boldsymbol{r}^t(p,\Delta^{Bq})\right]^{\alpha}=\mathscr{D}_1(p)$, $\left[\boldsymbol{r}^t(p,\Delta^{Bq})\right]^{\beta}=\mathscr{D}_2(p)$ and $\left[\boldsymbol{r}^t(p,\Delta^{Bq})\right]^{\gamma}=\mathscr{D}_2(p)$.

Theorem 5 *Let $0 < p_j \le 1$ for every $j \in \mathbb{N}_0$. Define the sets $\mathscr{D}_3(p)$ and $\mathscr{D}_4(p)$ as follows:*

$$\mathscr{D}_3(p) = \left\{ \boldsymbol{a} = (a_j) \in w : \sup_{I \in \mathscr{F}} \sup_{j \in \mathbb{N}_0} \left| \sum_{i \in I} \left[\sum_{l=j}^{j+1} (-1)^{i-j} \frac{\Gamma(-q+1)}{(i-l)!\Gamma(-q-i+l+1)} \frac{T_j}{t_l} a_j + \frac{T_i}{t_i} a_i \right] B^{-1} \right|^{p_j} < \infty \right\} \text{ and}$$

$$\mathscr{D}_4(p) = \left\{ \boldsymbol{a} = (a_j) \in w : \sup_{j \in \mathbb{N}_0} \left| \Delta^{Bq} \left(\frac{a_j}{t_j} \right) T_j \right|^{p_j} < \infty \text{ and } \sup_{j \in \mathbb{N}_0} \left| \frac{a_j}{t_j} T_j \right|^{p_j} < \infty \right\}.$$

Then $\left[\boldsymbol{r}^t(p,\Delta^{Bq})\right]^{\alpha} = \mathscr{D}_3(p)$, $\left[\boldsymbol{r}^t(p,\Delta^{Bq})\right]^{\beta} = \left[\boldsymbol{r}^t(p,\Delta^{Bq})\right]^{\gamma} = \mathscr{D}_4(p)$.

MATRIX TRANSFORMATIONS

In this section, we characterize certain matrix transformations from the space $\mathbf{r}^t(p,\Delta^{Bq})$ to space $W. \in \{\ell_\infty, c, c_0\}$. Before we proceed, we note down the following results:

Lemma 1 *[19] (Theorem 5.1.0)*

(a) Let $1 < p_j \le H < \infty$ for every $j \in \mathbb{N}_0$. Then $\lambda \in (\ell(p), \ell_1)$ if and only if there exists an integer $B > 1$ such that

$$\sup_{I \in \mathscr{F}} \sum_j \left| \sum_{i \in I} \lambda_{ij} B^{-1} \right|^{s_j} < \infty. \tag{5}$$

(b) Let $0 < p_j \le 1$ for every $j \in \mathbb{N}_0$. Then $\lambda \in (\ell(p), \ell_1)$ if and only if

$$\sup_{I \in \mathscr{F}} \sup_{j \in \mathbb{N}_0} \left| \sum_{i \in I} \lambda_{ij} \right|^{p_j} < \infty. \tag{6}$$

Lemma 2 [20] *(Theorem 1)*

(a) Let $1 < p_j \le H < \infty$ for every $j \in \mathbb{N}_0$. Then $\lambda \in (\ell(p), \ell_\infty)$ if and only if there exists an integer $B > 1$ such that

$$\sup_{i \in \mathbb{N}_0} \sum_j \left| \lambda_{ij} B^{-1} \right|^{s_j} < \infty. \tag{7}$$

(b) Let $0 < p_j \le 1$ for every $j \in \mathbb{N}_0$. Then $\lambda \in (\ell(p), \ell_\infty)$ if and only if

$$\sup_{i,j \in \mathbb{N}_0} \left| \lambda_{ij} \right|^{p_j} < \infty. \tag{8}$$

Lemma 3 [20] *(Theorem 1) Let $0 < p_j \le H < \infty$ for every $j \in \mathbb{N}_0$. Then $\lambda \in (\ell(p), c)$ if and only if (7), (8) hold, and*

$$\lim_{i \to \infty} \lambda_{ij} = \alpha_j \text{ for } j \in \mathbb{N}_0 \tag{9}$$

also holds.

Theorem 6 *Let W be any given FK-space. Then $\lambda \in (\boldsymbol{r}^t(p,\Delta^{Bq}), W)$ if and only if $\lambda_i \in \left[\boldsymbol{r}^t(p,\Delta^{Bq})\right]^{\beta}$ for all $i \in \mathbb{N}_0$ and $\tilde{\lambda} \in (\ell(p), W)$, where $\tilde{\lambda}_{ij} = \left(\frac{\lambda_{ij}}{t_j} + \sum_{l=j+1}^{\infty} (-1)^{l-j} \lambda_{il} \sum_{m=j}^{j+1} \frac{\Gamma(-q+1)}{(l-m)!\Gamma(-q-l+m+1) q_m} \right) T_j$ for all $i, j \in \mathbb{N}_0$.*

Corollary 1 *Let $\lambda = (\lambda_{ij})$ be an infinite matrix. Then we have the following results:*

(a) $\lambda \in (\boldsymbol{r}^t(p,\Delta^{Bq}) : \ell_\infty)$ if and only if $\lambda_i \in \left[\boldsymbol{r}^t(p,\Delta^{Bq})\right]^{\beta}$ for all $i \in \mathbb{N}_0$ and (7) and (8) hold with $\tilde{\lambda}_{ij}$ instead of λ_{ij}.

(b) $\lambda \in (\boldsymbol{r}^t(p,\Delta^{Bq}) : c)$ if and only if $\lambda_i \in \left[\boldsymbol{r}^t(p,\Delta^{Bq})\right]^{\beta}$ for all $i \in \mathbb{N}_0$, and (7), (8) and (9) hold with $\tilde{\lambda}_{ij}$ instead of λ_{ij}.

(c) $\lambda \in (\boldsymbol{r}^t(p,\Delta^{Bq}) : c_0)$ if and only if $\lambda_i \in \left[\boldsymbol{r}^t(p,\Delta^{Bq})\right]^{\beta}$ for all $i \in \mathbb{N}_0$, and (7), (8) and (9) hold with $\tilde{\lambda}_{ij}$ instead of λ_{ij} and $\beta_j = 0$ for all $j \in \mathbb{N}_0$.

ACKNOWLEDGEMENT

The research of author is supported by Science and Engineering Research Board (SERB), New Delhi, India under the grant EEQ/2019/000082.

REFERENCES

1. B. Altay and F. Başar, Southeast Asian Bull. Math. **26**, 701-715 (2002).
2. B. Altay and F. Başar, Southeast Asian Bull. Math. **30**, 591-608 (2006).
3. E. Malkowsky, Mat. Vesnik **49**, 187-196 (1997).
4. M. Başarir and M. Öztürk, Rend. Circ. Mat. Palermo **57(2)**, 377-389 (2008).
5. M. Başarir, Filomat **24(4)**, 35-52 (2010).
6. M. Başarir and M. Kayikçi, J. Inequal. Appl. **2009**, Article ID 385029 (2009).
7. P. Baliarsingh and S. Dutta, Bol. Soc. Paran. Mat. **33**, 49-57 (2015).
8. P. Baliarsingh, Appl. Math. Comput. **219**, 9737-9742 (2013).
9. J. Meng and L. Mei, J. Inequal. Appl. **2018**, Article number: 274 (2018).
10. T. Yaying and B. Hazarika, Math. Slovaca **69(4)**, 901-918 (2019).
11. T. Yaying, Kragujevac J. Math. **46(2)**, 175-191 (2022).
12. S. Dutta and P. Baliarsingh, J. Egypt. Math. Soc. **22**, 249-253 (2014).
13. M. Et and R. Çolak, Soochow J. Math. **21**, 377-386 (1995).
14. M. Et and A. Esi, Bull. Malays. Math. Sci. Soc. **231**, 25-32 (2000).
15. M. Et and M. Basarir, Periodica Math. Hungar. **35**, 169-175 (1997).
16. H. Furkan, J. Egypt Math. Soc. **25(1)**, 37-42 (2017).
17. H. Kizmaz, Can. Math. Bull. **24**, 169-176 (1981).
18. E. Malkowsky and S. D. Parashar, Analysis **17**, 87-97 (1997).
19. K. G. Grosse-Erdmann, J. Math. Anal. Appl. **180**, 223-238 (1993).
20. C. G. Lascarides and I. J. Maddox, Proc. Camb. Phil. Soc. **68**, 99-104 (1970).
21. I. J. Maddox, Quart. J. Math. Oxford Ser. **18(2)**, 345-355 (1967).

A Fourth Order Accurate Difference Method for Solving the Second Order Elliptic Equation with Integral Boundary Condition

Rifat Reis[a)] and Adiguzel A. Dosiyev[b)]

Department of Mathematics, Near East University, Nicosia, TRNC, Mersin 10, Turkey

[a)]*Corresponding author: rifat.reis@neu.edu.tr*
[b)]*Electronic mail: adiguzel.dosiyev@neu.edu.tr*

Abstract. A uniform estimation of order $O(h^4)$, for the convergence of the finite difference solution for the general second order elliptic equation with nonlocal integral boundary condition is obtained where h is the mesh step.

INTRODUCTION

A highly accurate method is one of the powerful tools for reducing the number of unknowns, which is the main problem in the numerical solution of differential equations to get reasonable results. In [1, 2, 3] the fourth order difference schemes were constructed and justified by solving several local test problems.

In this paper, a convergence of order $O(h^4)$, h is the step mesh, in the uniform metric for the solution of the finite difference problem constructed for the local Dirichlet problem by schemes [1, 2] for $h \leq h_0$, (h_0 is a fixed real number), is proved. Then, for the second-order linear elliptic equations with nonlocal integral boundary condition the finite difference problem which is related to the scheme given in [1, 2] are proposed and justified It is verified that the uniform estimate of the error of the approximate solution is order of $O(h^4)$, when the boundary functions have a sixth derivative satisfying a Holder condition.

NONLOCAL BOUNDARY VALUE PROBLEM

Let $R = \{(x,y) : 0 < x < \beta_1, 0 < y < \beta_2\}$be an open rectangle, γ^m, $m = 1,2,3,4$, be its sides including the endpoints, numbered in the clockwise direction, beginning with the side lying on the y-axis and let $\gamma = \cup_{m=1}^{4} \gamma^m$ be the boundary of R and $\overline{R} = R \cup \gamma$. Let C^0 denote the linear space of continuous functions of one variable x on the interval $[0, \beta_1]$ of x-axis, and vanish at the points $x = 0$ and $x = \beta_1$. For the function $f \in C^0$ we define the norm

$$\|f\|_{C^0} = \max_{0 \leq x \leq \beta_1} |f(x)|.$$

Consider the nonlocal boundary value problem on R

$$Lu = 0 \text{ on } R,\ u = 0 \text{ on } \gamma^1 \cup \gamma^3,\ u = \tau \text{ on } \gamma^2, \tag{1}$$

$$u(x,0) = \alpha \int_{\xi}^{\beta_2} u(x,y)dy + \mu(x), \quad 0 < x < \beta_1, 0 < \xi < \beta_2, \tag{2}$$

where

$$Lu = \frac{\partial^2 u}{\partial x^2} + \frac{\partial^2 u}{\partial y^2} + a(x,y)\frac{\partial u}{\partial x} + b(x,y)\frac{\partial u}{\partial y} + c(x,y)u,$$

a, b and c are given functions with $b(x,y) \geq 0$ and $c(x,y) \leq 0$; $\tau = \tau(x)$ and $\mu = \mu(x)$ are given functions from C^0 and α is a given constant with $|\alpha| < \frac{1}{\beta_2 - \xi}$.

Let U be a solution of the following multilevel nonlocal boundary value problem

$$LU = 0 \text{ on } R,\ U = \tau \text{ on } \gamma^2,\ U = 0 \text{ on } \gamma^1 \cup \gamma^3\ ,$$

$$U(x,0) = \alpha \sum_{k=1}^{M} \rho_k . U(x, \eta_k) + \mu(x), \quad 0 \leq x \leq \beta_1,$$

International Conference on Analysis and Applied Mathematics (ICAAM 2020)
AIP Conf. Proc. 2325, 020054-1–020054-5; https://doi.org/10.1063/5.0040375
Published by AIP Publishing. 978-0-7354-4069-2/$30.00

where $\rho_1=\rho_M=\frac{h}{3}$, $\rho_j=\frac{h}{3}\left(3+(-1)^j\right)$ for $j=2,3,...,M-1$, $\eta_j=\xi+(j-1)h$, $j=1,2,...,M$, $h=\frac{\beta_1}{N}$, $(M-1)h+\xi=\beta_2$ and $\frac{\xi}{h}$ is an integer.

We represent U as

$$U(x,y)=V(x,y)+W(x,y),$$

where V is the solution of the problem

$$LV=0 \text{ on } R,\ V=\tau \text{ on } \gamma^2,\ V=0 \text{ on } \gamma/\gamma^2,$$

and W is the solution of the problem

$$LW=0 \text{ on } R,\ W=0 \text{ on } \gamma/\gamma^4,\ W=f \text{ on } \gamma^4,$$

with an unknown function f from C^0.

We define the operator B_i from C^0 to C^0 as follows

$$B_i f(x)=W(x,\eta_i),\ i=1,2,...,M. \tag{3}$$

It is verified that

$$\|B_i f\|_{C^0}<\left(1-\frac{\xi+(i-1)h}{\beta_2}\right)\|f\|_{C^0},\quad i=1,2,...,M,$$

and

$$0<|B_M|<|B_{M-1}|<...<|B_1|<1.$$

We set

$$\varphi_k(x)=V(x,\eta_k) \text{ for } k=1,2,...,M,$$

and

$$\varphi=\alpha\sum_{k=1}^{M}\rho_k\varphi_k.$$

Consider the sequence in C^0

$$\psi_i^0=0,\ \psi_i^n=B_i\left(\varphi+\mu+\alpha\sum_{k=1}^{M}\rho_k\psi_k^{n-1}\right),$$
$$i=1,2,...,M;\ \ n=1,2,....$$

The limit of the sequence is found as a solution of the following nonlinear equations

$$\psi_i=B_i\left(\varphi+\mu+\alpha\sum_{k=1}^{M}\rho_k\psi_k\right),\ i=1,2,...,M.$$

Therefore, the function f in (3) is defined by

$$f=\varphi+\mu+\alpha\sum_{k=1}^{M}\rho_k\psi_k,$$

FINITE-DIFFERENCE EQUATIONS

We define a square mesh with the mesh size $h = \frac{\beta_1}{N} = \frac{\beta_2}{M^*}$, $N, M^* > 2$ are integers, constructed with the lines $x, y = h, 2h, \ldots$. Let D_h be the set of nodes of this square grid, $R_h = R \cap D_h$, $\overline{R}_h = \overline{R} \cap D_h$ and $\gamma_h^m = \gamma^m \cap D_h$, $m = 1,2,3,4$. It is assumed that $h \leq h_0$, where

$$h_0 = \frac{1}{2} \max \left\{ \max\left(|a| + |b|\right), \max\left(\sqrt{\frac{1}{2}\frac{\partial a}{\partial x} + a^2} + \sqrt{\frac{1}{2}\left(\frac{\partial b}{\partial y}\right) + b^2} \right), \max\left(\frac{\frac{1}{2}\frac{\partial b}{\partial y} + b^2 - c}{b} \right) \right\}.$$

Let

$$[0, \beta_1]_h = \left\{ x = x_i,\ x_i = ih,\ i = 0, 1, \ldots, N,\ h = \frac{\beta_1}{N} \right\}$$

be the set of points divided by the step size h on $[0, \beta_1]$.
We represent the difference operator obtained by [1], [2] in the form

$$\begin{aligned}
L_h u \equiv\ & e^{f_1} \left[\frac{5}{6} - \frac{1}{12} h^2 \left(\frac{1}{2} \left(\frac{\partial a}{\partial x} \right)_1 + \frac{1}{4} a_1^2 - c_1 \right) \right] u(x+h, y) \\
& + e^{g_2} \left[\frac{5}{6} - \frac{1}{12} h^2 \left(\frac{1}{2} \left(\frac{\partial b}{\partial y} \right)_2 + \frac{1}{4} b_2^2 - c_2 \right) \right] u(x, y+h) \\
& + e^{f_3} \left[\frac{5}{6} - \frac{1}{12} h^2 \left(\frac{1}{2} \left(\frac{\partial a}{\partial x} \right)_3 + \frac{1}{4} a_3^2 - c_3 \right) \right] u(x-h, y) \\
& + e^{g_4} \left[\frac{5}{6} - \frac{1}{12} h^2 \left(\frac{1}{2} \left(\frac{\partial b}{\partial y} \right)_4 + \frac{1}{4} b_4^2 - c_4 \right) \right] u(x, y-h) \\
& + \frac{1}{12} \left[e^{f_1} \left(1 - \frac{hb_1}{2} \right) + e^{g_4} \left(1 + \frac{ha_4}{2} \right) \right] u(x+h, y-h) \\
& + \frac{1}{12} \left[e^{f_3} \left(1 + \frac{hb_3}{2} \right) + e^{g_2} \left(1 - \frac{ha_2}{2} \right) \right] u(x-h, y+h) \\
& + \frac{1}{12} \left[e^{f_3} \left(1 - \frac{hb_3}{2} \right) + e^{g_4} \left(1 - \frac{ha_4}{2} \right) \right] u(x-h, y-h) \\
& + \frac{1}{12} \left[e^{f_1} \left(1 + \frac{hb_1}{2} \right) + e^{g_2} \left(1 + \frac{ha_2}{2} \right) \right] u(x+h, y+h) \\
& - \left[e^{\frac{ah}{2}} \left(1 - \frac{1}{12} h^2 \left(\frac{1}{2} \left(\frac{\partial a}{\partial x} \right)_1 + \frac{1}{4} a_1^2 \right) \right) + e^{\frac{bh}{2}} \left(1 - \frac{1}{12} h^2 \left(\frac{1}{2} \left(\frac{\partial b}{\partial y} \right)_2 + \frac{1}{4} b_2^2 \right) \right) \right. \\
& \left. + e^{\frac{-ah}{2}} \left(1 - \frac{1}{12} h^2 \left(\frac{1}{2} \left(\frac{\partial a}{\partial x} \right)_3 + \frac{1}{4} a_3^2 \right) \right) + e^{\frac{-bh}{2}} \left(1 - \frac{1}{12} h^2 \left(\frac{1}{2} \left(\frac{\partial b}{\partial y} \right)_4 + \frac{1}{4} b_4^2 \right) \right) - \frac{5}{6} h^2 c_0 \right] u(x, y). \quad (4)
\end{aligned}$$

APPROXIMATION OF THE NONLOCAL BOUNDARY VALUE PROBLEM BY FINITE-DIFFERENCE METHOD

We say that $F \in C^{k,\lambda}(E)$, if F has k-th derivatives on E satisfying the Hölder condition with exponent λ.

We assume that $\tau(x) \in C^{6,\lambda}\left(\gamma^2\right)$, $\mu(x) \in C^{6,\lambda}\left(\gamma^4\right)$ in (1) and (2), respectively. Denote by C_h^0 the linear space of grid functions defined on $[0, \beta_1]_h$ that vanish at $x = 0$ and $x = \beta_1$. The norm of a function $f_h \in C_h^0$ is defined as

$$\|f_h\|_{C_h^0} = \max_{x \in [0, \beta_1]_h} |f_h|.$$

Let L_h be operator defined in (4). and let v_h be a solution of following the system of grid equations

$$L_h v_h = 0 \text{ on } R_h, \quad v_h = \tau_h \text{ on } \gamma_h^2, \quad v_h = 0 \text{ on } \gamma_h / \gamma_h^2,$$

where τ_h is the trace of τ on γ_h^2 and we define

$$\widetilde{\varphi}_{i,h}(x) = v_h(x, \eta_i),\ i = 1, 2, ..., M.$$

Let w_h be a solution of the finite difference problem

$$L_h w_h = 0 \text{ on } R_h,\ \ w_h = 0 \text{ on } \gamma_h / \gamma_h^4,\ \ w_h = \widetilde{f}_h \text{ on } \gamma_h^4, \tag{5}$$

where $f_h \in C_h^0$, is an arbitrary function.

Let B_i^h be a linear operator from C_h^0 to C_h^0 defined as

$$B_i^h f_h(x) = w_h(x, \eta_i),\ i = 1, 2, ..., M,$$

where w_h is the solution of the problem (5).

Everywhere, for all estimations, the all constants $c_1, c_2, ...,$ are independent of h.

The following all statements are proved whenever the one of the following conditions satisfy:

(i) a, b, c are arbitrary constants.

(ii) a and b are single variable functions depends on x and y, respectively.

Lemma 1 *The following estimate remains true*

$$\left\| B_i^h f_h(x) \right\|_{C_h^0} \leq \| f_h \|_{C_h^0} \left(1 - \frac{\xi +_{(i-1)h}}{\beta_2} \right),\ i = 1, 2, ..., M.$$

By [2], we have,

$$\max_{R_h} |L_h (v_h - V_h)| \leq c_1 h^4. \tag{6}$$

By virtue of maximum principle and (6), it follows that

$$\max_{(x,y)\in \overline{R}_h} |v_h - V_h| \leq c_2 h^4.$$

We define the function

$$\widetilde{f}_h = \widetilde{\varphi}_h + \mu_h + \alpha \sum_{k=1}^{M} \rho_k \widetilde{\psi}_{k,h},$$

where μ_h is the trace of μ defined in (2) on $[0, \beta_1]_h$ and $\widetilde{\psi}_{k,h} \in C_h^0, k = 1, 2, ..., M,$ are the solution of the system of equations

$$\widetilde{\psi}_{i,h} = B_i^h \left(\widetilde{\varphi}_h + \mu_h + \alpha \sum_{k=1}^{M} \rho_k \widetilde{\psi}_{k,h} \right),\ i = 1, 2, ..., M. \tag{7}$$

The solution of the system (7) are sought by using the fixed point iteration:

$$\begin{aligned} &\widetilde{\psi}_{i,h}^0 = 0, \quad \widetilde{\psi}_{i,h}^n = B_i^h \left(\widetilde{\varphi}_h + \mu_h + \alpha \sum_{k=1}^{M} \rho_k \widetilde{\psi}_{k,h}^{n-1} \right), \\ &i = 1, 2, ..., M; \quad n = 1, 2, ... \,. \end{aligned} \tag{8}$$

By using the $n-th$ iteration $\widetilde{\psi}_{i,h}^n$, $n \geq 1$ of (8), we define the function

$$\widetilde{f}_h^n = \widetilde{\varphi}_h + \mu_h + \alpha \sum_{k=1}^{M} \rho_k \widetilde{\psi}_{k,h}^n.$$

Hence, we define (see [4], [5], [6]), for the approximate solution of the nonlocal problem (1), (2), the following difference problem

$$\widetilde{u}_h^n = B_h \widetilde{u}_h^n \ \text{ on } R_h,\ \ \widetilde{u}_h^n = \tau_h \ \text{ on } \gamma_h^2,\ \ \widetilde{u}_h^n = 0 \ \text{ on } \gamma_h^1 \cup \gamma_h^3, \tag{9}$$

$$\widetilde{u}_h^n = \widetilde{f}_h^n \ \text{ on } \gamma_h^4. \tag{10}$$

Theorem 2 *The estimation holds*

$$\max_{(x,y)\in\overline{R}_h} |\widetilde{u}_h^n - u| \leq c_3 h^4 + q_0 \frac{q_1^{n+1}}{1-q_1} c_4, \tag{11}$$

where $\widetilde{u}_h^n$ *is a solution of problem* (9), (10), u *is the exact solution of nonlocal boundary value problem* (1), (2), $q_0 = |\alpha| \sum_{k=1}^{M} \rho_k < 1$ and $q_1 = 1 - \frac{\xi}{\beta_2}$.

Remark 3 *In* (11) *the right-hand side is* $O\left(h^4\right)$, *when*

$$n = \max\left\{\left[\frac{\ln h^4(1-q_1)}{\ln q_1}\right], 1\right\},$$

where $[a]$ *is the integer part of* a.

CONCLUSION

The proposed method can be used for getting numerical solution for different types of nonlocal problem for general elliptic equations. Also, it can be developed to obtain higher order as $O(h^p)$, $p > 4$, uniform estimate of the error of the approximate solution.

REFERENCES

1. S. C. R. Dennis and J. D. Hudson, J. Inst. Maths. Applics. **23**, 43-51 (1979).
2. S. C. R. Dennis and J. D. Hudson, J. Inst. Maths. Applics. **26**, 369-379 (1980).
3. M. M. Gupta, "A fourth order finite difference scheme for two-dimensional elliptic equations," in *Scientific Computing*, edited by R. S. Stepleman et al. (North Holland, Amsterdam, 1983) pp. 147-154.
4. E. A. Volkov and A. A. Dosiyev, Mediterr. J. Math. **13**, 3589-3604 (2016).
5. A. A. Dosiyev, J. Comput. Appl. Math. **354**, 587-596 (2019).
6. A. A. Dosiyev and R. Reis, Adv. Diff. Equ. **2019**, Article number: 340 (2019).

On Uniformly Lindelöf Spaces

Bekbolot Kanetov[1, a)] and Meerim Zhanakunova[2, b)]

[1)] *Jusup Balasagyn National University, Bishkek, Kyrgyz Republic*
[2)] *Kuseyin Karasaev Bishkek Humanities University, Bishkek, Kyrgyz Republic*

[a)] *Corresponding author: bekbolot_kanetov@mail.ru*
[b)] *Electronic mail: aelin_jasmin@mail.ru*

Abstract. As we know the Lindelöfness play an important role in the General Topology. Therefore, the finding of uniform analogues of Lindelöfness is an important and interesting problem in the theory of Uniform Topology. For example, uniform *B*-Lindelöfness in the sense of A. A. Borubaev [1], uniform *A*-Lindelöfness in the sense of L.V. Aparina [2], uniform *I*- Lindelöfness in the sense of D. R. Isbell [3].

In this article we show a new approach to the definition of a uniform analog of Lindelöfness. We introduce and study uniform *R*-Lindelöf and uniform Lindelöf spaces.

INTRODUCTION

Throughout this work all uniform spaces are assumed to be Hausdorff and mappings are uniformly continuous.

For coverings α and β of the set X, the symbol $\alpha \succ \beta$ means that the covering α is a refinement of the covering β, i.e. for any $A \in \alpha$ there exists $B \in \beta$ such that $A \subset B$ and, for coverings α and β of a set X, we have: $\alpha \wedge \beta = \{A \bigcap B : A \in \alpha, B \in \beta\}$. The covering α finitely additive if $\alpha^{\angle} = \alpha$, $\alpha^{\angle} = \{\bigcup \alpha_0 : \alpha_0 \subset \alpha \text{ is finite}\}$. $\alpha(x) = \bigcup St(\alpha, x)$, $St(\alpha, x) = \{A \in \alpha : A \ni x\}$, $x \in X$, $\alpha(H) = \bigcup St(\alpha, H)$, $St(\alpha, H) = \{A \in \alpha : A \bigcap H \neq \varnothing\}$, $H \subset X$.

A uniform space (X,U) is called $\aleph_0$-bounded if the uniformity U has a base consisting of countable coverings; a uniform space (X,U) is called τ-bounded if the uniformity U has a base consisting of coverings of cardinality $\leq \tau$ [1], if $\tau \leq \aleph_0$, then the uniform space (X,U) is called uniformly *I*-Lindelöf [3]; a uniform space (X,U) is called uniformly *B*-Lindelöf, if it is both uniformly *B*-paracompact and $\aleph_0$-bounded [1]; a uniform space (X,U) is called uniformly *A*-Lindelöf, if for each open covering α exist a countable uniformly covering $\beta = \{B_n : n \in N\}$ and $\gamma \in U$ such that $\beta \succ \alpha^{\angle}$ and $\gamma(\bar{B}_n) \subset B_{n+1}$ for any $n \in N$ [2]; a uniformly continuous mapping $f : (X,U) \to (Y,V)$ of uniform space (X,U) onto a uniform space (Y,V) is called a precompact, if for each $\alpha \in U$ there exist a uniform covering $\beta \in V$ and finite uniform covering $\gamma \in U$, such that $f^{-1}\beta \wedge \gamma \succ \alpha$[1]; a uniformly continuous mapping $f : (X,U) \to (Y,V)$ of uniform space (X,U) onto a uniform space (Y,V) is called a uniformly perfect, if it is both precompact and perfect [1]; a uniformly continuous mapping $f : (X,U) \to (Y,V)$ of uniform space (X,U) onto a uniform space (Y,V) is called a uniformly open, if f maps each open uniform covering $\alpha \in U$ to an open uniform covering $f\alpha \in V$ [1]; a continuous mapping $f : X \to Y$ of topological space to a topological space called ω-mapping, if for each point $y \in Y$ there exist such neighborhood O_y and $W \in \omega$, that $f^{-1}O_y \subset W$ [1]; a uniform space (X,U) called uniformly *R*-paracompact, if every open covering has an open uniformly locally finite refinement [4]; a uniform space (X,U) called uniformly *B*-paracompact, if for each finitely additive open covering γ of (X,U) there exists such sequence uniform covering $\{\alpha_i : i \in N\} \subset U$, that following condition is realized: for each point $x \in X$ there exist such number $i \in N$ and $\Gamma \in \gamma$ that $\alpha_i(x) \subset \Gamma$ (*) [1]; a uniform space (X,U) called uniformly *P*-paracompact, if for each open cover γ of (X,U) there exists such sequence uniform covering $\{\alpha_i : i \in N\} \subset U$, that the condition (*) is realized [5]; a uniform space (X,U) is called uniformly *P*-Lindelöf, if for each open cover γ of (X,U) there exists such sequence countable uniform covering $\{\alpha_i : i \in N\} \subset U$, that the condition (*) is realized [6]; a uniform space (X,U) is called uniformly locally compact, if there exists a uniform covering $\alpha \in U$ consisting of compact subsets; a uniform space (X,U) is called uniformly locally Lindelöf [1], if there exists such uniform covering $\alpha \in U$ that the closures of all its elements are Lindelöf [5]; a uniform space (X,U) is called strongly uniformly *R*-paracompact if every open covering has an open uniformly star finite refinement. For the uniformity U by τ_U we denote the topology generated by the uniformity.

UNIFORMLY *R*-LINDELÖF SPACES AND THEIR GENERALIZATIONS

Let (X,U) be a uniform space.

Definition 1 *A uniform space (X,U) is said to be uniformly R-Lindelöf, if it is both uniformly R-paracompact and $\aleph_0$-bounded.*

International Conference on Analysis and Applied Mathematics (ICAAM 2020)
AIP Conf. Proc. 2325, 020055-1–020055-5; https://doi.org/10.1063/5.0040273
Published by AIP Publishing. 978-0-7354-4069-2/$30.00

Proposition 1 *If (X,U) is a uniformly R-Lindelöf space then the topological space (X,τ_U) is uniformly R-Lindelöf. Conversely, if (X,τ) is Lindelöf then the uniform space (X,U_X) is uniformly R-Lindelöf.*

Proof. Let α be an arbitrary open cover of the space (X,τ_U) . Then for the open covering α exists a uniformly locally finite open covering β which is a refinement of it. Since the space (X,U) is $\aleph_0$-bounded, there exists a countable cover λ such that for any $i \in N$ we have that $L_i \subset \bigcup_{j=1}^{k} A_j$. Then system $\{L_i \bigcap A_j\}$, $i = 1,2,...,n,\ j = 1,2,...,k$ forms a countable open covering which is refinement in covering α. Consequently, the space (X,τ_U) is Lindelöf.

Conversely, if (X,τ) is Lindelöf, then the system of all open coverings forms a base of universal uniformity U_X of the space (X,τ). It follows from this that (X,U_X) is uniformly R-Lindelöf.

Proposition 2 *Any compact space is uniformly R-Lindelöf.*

Proof. Since any compact uniform space is precompact, it is all the more $\aleph_0$-bounded. It is clear that every compact space is uniform R-paracompact. Concequently, the uniform space (X,U) is uniformly R-Lindelöf.

Proposition 3 *Each closed subspace of a uniformly R-Lindelöf space is uniformly R-Lindelöf.*

Proposition 4 *Any uniformly R-Lindelöf space is uniformly locally Lindelöf.*

Proposition 5 *Any uniformly locally compact and $\aleph_0$-bounded space is uniformly R-Lindelöf.*

Proposition 6 *Any uniformly R-Lindelöf space is uniformly B-Lindelöf.*

Proof. Let (X,U) be a uniformly R-Lindelöf space. As is known, every uniformly R-paracompact space is uniformly B-paracompact [1]. Hence, the uniform space is uniformly B-Lindelöf.

Theorem 1 *Any uniformly R-Lindelöf space is strongly uniformly R-paracompact.*

Proof. Let (X,U) be a uniformly R-Lindelöf space. Then from the fact that a space (X,U) is strongly uniformly R-paracompact if and only if it is uniformly R-paracompact and the space (X,τ_U) is strongly paracompact it follows that is strongly uniformly R-paracompact.

Proposition 7 *Any uniformly R-Lindelöf space is complete.*

Theorem 2 *Let $f : (X,U) \to (Y,V)$ be a uniformly perfect mapping of a uniform space (X,U) onto a uniform space (Y,V). Then uniformly R-Lindelöf space converse both to direction of image and to one of preimage.*

Proof. If a space (X,U) is $\aleph_0$-bounded, then its uniformly continuous image (Y,V) is also $\aleph_0$-bounded. Let a uniform space (X,U) is uniformly R-paracompact. Then by Theorem 2.3.9 [1, p. 155] we have the space (Y,V) is uniformly R-paracompact. Thus the uniform space (Y,V) is uniformly R-Lindelöf. Conversely, let the space (Y,V) is $\aleph_0$-bounded. Let $\alpha \in U$ be an arbitrary uniformly covering. Then by virtue of the perfectness of the mappings f there exist such a countable covering $\beta \in V$ and finite covering $\gamma \in U$ that $f^{-1}\beta \wedge \gamma \succ f^{-1}\alpha$. But the covering $f^{-1}\beta \wedge \gamma$ is countable. Therefore the space (X,U) is $\aleph_0$-bounded. The uniformly R-paracompactness of the space (X,U) follows from Theorem 2.3.9. [1, p. 155] Thus, (X,U) is uniformly R-Lindelöf.

Theorem 3 *Let $f : (X,U) \to (Y,V)$ be a uniformly open mapping of a uniform space (X,U) onto a uniform space (Y,V). If (X,U) is uniformly R-Lindelöf space then the uniform space (Y,V) is also uniformly R-Lindelöf.*

Proof. Let f be a uniformly open mapping of a uniform space (X,U) onto a uniform space (Y,V) and α be an arbitrary finite additive open covering. Then $f^{-1}\alpha$ is a finite additive open covering of the space (X,U) and by the criterion of uniformly R-paracompactness we have $f^{-1}\alpha \in U$. By virtue of the uniformly openness of the mapping f we have $\alpha \in V$. Hence, (Y,V) is uniformly R-paracompact. If a space (X,U) is $\aleph_0$-bounded, then (Y,V) is also $\aleph_0$-bounded. Consequently, the space (Y,V) is uniformly R-Lindelöf.

Definition 2 *A uniformly continuous mapping $f : (X,U) \to (Y,V)$ of a uniform space (X,U) onto a uniform space (Y,V) is said to be uniformly R-Lindelöf, if the following conditions is realized:*

1. *For each open covering α of the space (X,U) there exist such open covering β of the space (Y,V) and uniformly locally finite open covering γ of the space (X,U), that the covering $f^{-1}\beta \wedge \gamma$ is refined in a covering α;*

2. *For each $\lambda \in U$ there exist such $\eta \in V$ and countable covering $\mu \in U$, that the covering $f^{-1}\eta \wedge \mu$ is refined in a covering λ.*

Proposition 8 *Let $f : (X,U) \to (Y,V)$ be a uniformly continuous mapping of a uniform space (X,U) onto a uniform space (Y,V). If (X,U) is uniformly R-Lindelöf space then the uniformly continuous mapping f is uniformly R-Lindelöf.*

Proof. Let (X,U) be a uniformly R-Lindelöf space and α be an arbitrary open covering. Then exist such uniformly locally finite open covering γ of the space (X,U), that the covering γ is refined in a covering α. For open covering β of the space (Y,V) we have the covering $f^{-1}\beta \wedge \gamma$ is refined in a covering α. Let $\lambda \in U$ be an arbitrary uniform covering. By virtue of the $\aleph_0$-boundedness of the uniform space (X,U) exist such countable uniform covering $\mu \in U$, that the covering μ is refined in a covering λ. Then for uniform covering $\eta \in V$ we have that the uniform covering $f^{-1}\eta \wedge \mu$ is refined in a uniform covering λ. Consequently, the mapping f is uniformly R-Lindelöf.

Proposition 9 *If uniformly continuous mapping $f : (X,U) \to (Y,V)$ of a uniform space (X,U) onto a uniform space (Y,V) , $Y = \{y\}$ is uniformly R-Lindelöf, then the uniform space (X,U) is uniformly R-Lindelöf.*

Proof. Let f be a uniformly R-Lindelöf mapping and α be an arbitrary open covering of the space (X,U). Then the uniformly R-Lindelöfness of the mapping f implies there exists such open covering β of the space (Y,V) and uniformly locally finite open covering γ of the space (X,U), that the covering $f^{-1}\beta \wedge \gamma$ is refined in a covering α. Since $Y = \{y\}$, then $f^{-1}\beta \wedge \gamma = \gamma$. Let $\lambda \in U$ be an arbitrary uniform covering. Then exist such $\eta \in V$ and countable covering $\mu \in U$, that the covering $f^{-1}\eta \wedge \mu$ is refined in a covering λ. It's clear that $f^{-1}\eta \wedge \mu = \mu$. Hence, the space (X,U) is uniformly R-Lindelöf.

Lemma 1 *If α and β is uniformly locally finite covering of the space (X,U), then covering $\alpha \wedge \beta$ is uniformly locally finite covering of the space (X,U).*

Proof. Let α and β be a uniformly locally finite covering of the space (X,U).

We show the covering $\alpha \wedge \beta$ is also uniformly locally finite covering of the space (X,U). Since the coverings α and β is uniformly locally finite, there exists such uniform coverings $\mu \in U$ and $\eta \in U$, that $M \subset \bigcup_{i=1}^{n} A_i$, $N \subset \bigcup_{j=1}^{m} B_j$, $M \in \mu$, $N \in \eta$. Note that $M \bigcap N \subset \bigcup_{i=1}^{n} \bigcup_{j=1}^{m} (A_i \bigcap B_j)$, $M \bigcap N \in \mu \wedge \eta$. Obviously, $\mu \wedge \eta$ is uniformly covering. Thus, the covering $\alpha \wedge \beta$ is uniformly locally finite.

Lemma 2 *Let $f : (X,U) \to (Y,V)$ be a uniformly continuous mapping of a uniform space (X,U) onto a uniform space (Y,V). If β is uniformly locally finite open covering of the space (Y,V), then $f^{-1}\beta$ is uniformly locally finite open covering of the space (X,U).*

Proof. Let f be a uniformly continuous mapping of a uniform space (X,U) onto a uniform space (Y,V) and β be a uniformly locally finite open covering of the space (Y,V). Then exist such uniform covering $\alpha \in V$, that $|St(A,\beta)|$ is finite for all $B \in \beta$ i.e. for any $A \in \alpha$ exist such elements $B_i \in \beta$, $i = 1,2,...,n$, that $A \subset \bigcup_{i=1}^{n} B_i$. Consequently,$f^{-1}A \subset \bigcup_{i=1}^{n} f^{-1}B_i$, $f^{-1}A \in f^{-1}\alpha$, $f^{-1}B_i \in f^{-1}\beta$. Note, $f^{-1}\alpha \in U$ and $f^{-1}\beta$ is open covering of the uniform space (X,U). Thus, the covering $f^{-1}\beta$ is uniformly locally finite open covering of the space (X,U).

Theorem 4 *If f and (Y,V) is uniformly R-Lindelöf, then the uniform space (X,U) is uniformly R-Lindelöf.*

Proof. Let f and (Y,V) be a uniformly R-Lindelöf and α be an arbitrary open covering of the space (X,U). Then exist such open covering β of the space (Y,V) and uniformly locally finite open covering γ of the space (X,U), that the covering $f^{-1}\beta \wedge \gamma$ is refined in a covering α. By virtue of the uniformly R-Lindelöfness of the uniform space (Y,V) exist such uniformly locally finite open covering β_0, that the covering β_0 is refined in a covering β. Then $f^{-1}\beta_0 \wedge \gamma \succ f^{-1}\beta \wedge \gamma$. By virtue of Lemma 2 the open covering $f^{-1}\beta_0$ is uniformly locally finite. Denote $f^{-1}\beta_0 \wedge \gamma = \delta$. By virtue of Lemma 1 the open covering δ is uniformly locally finite. Let $\lambda \in U$ be an arbitrary uniform covering. Then exist such $\eta \in V$ and countable covering $\mu \in U$, that the covering $f^{-1}\eta \wedge \mu$ is refined in a covering λ. By virtue of the uniformly R-Lindelöfness of the uniform space (Y,V) exist such countable covering $\eta_0 \in V$, that the covering η_0 is refined in a covering η. Therefore $f^{-1}\eta_0 \wedge \mu \succ f^{-1}\eta \wedge \mu$. Denote $f^{-1}\eta_0 \wedge \mu = \omega$. Obviously, the covering $f^{-1}\eta_0$ and ω is countable. Hence, the space (X,U) is uniformly R-Lindelöf.

Definition 3 *A uniform space (X,U) is said to be uniformly Lindelöf, if for each finitely additive open covering γ of (X,U) there exists such a sequence of countable uniform coverings $\{\alpha_i : i \in N\} \subset U$, with property (*).*

Proposition 10 *Any uniformly R-Lindelöf space is uniformly Lindelöf.*

Proposition 11 *Any separable metrizable uniform apace (X,U) is uniformly Lindelöf.*

Proposition 12 *If (X,U) is uniformly Lindelöf space then the topological space (X,τ_U) is Lindelöf. Conversely, if (X,τ) is Lindelöf then the uniform space (X,U_X) is uniformly Lindelöf, where U_X is a universally uniformities of the space (X,τ).*

Proposition 13 *Each closed subspace of a uniformly Lindelöf space (X,U) is uniformly Lindelöf.*

Proposition 14 *Any uniformly Lindelöf space is uniformly locally Lindelöf.*

Proposition 15 *Any uniformly P -Lindelöf space is uniformly Lindelöf.*

Proposition 16 *Any compact uniform space is uniformly Lindelöf.*

Theorem 5 *Let (X,U) be a uniform space and bX be a certain compact Hausdorff extension of the space (X,τ_U). Then the following conditions are equivalent:*

1. *A uniform space (X,U) is uniformly Lindelöf.*
2. *For each compact $K \subset bX \backslash X$ there exist a sequence of countable uniformly coverings $\{\alpha_i\} \subset U$, realizing the condition: for each point $x \in X$ there exists such number $n \in N$, that $[\alpha_i(x)]_{bX} \bigcap K = \varnothing$.*

Proof. $1 \Rightarrow 2$. Let (X,U) be a uniformly Lindelöf space, bX be a certain compact Hausdorff extension of the space (X,τ_U) and $K \subset bX\backslash X$ be an arbitrary compact. Denote as λ the set of all such open subsets L of compact bX, that $[L]_{bX} \bigcap K = \varnothing$. Then it is easy to check that $\mu = \{L \bigcap X : L \in \lambda\}$ is finitely additive open covering of the space (X,U). By the condition 1, for the covering μ exists sequence of countable uniformly coverings $\{\alpha_i\}$, such that for each point $x \in X$ exist such number $i \in N$, that $\alpha_i(x) \subset L \bigcap X$ for each $L \in \lambda$. Consequently, $[\alpha_i(x)]_{bX} \bigcap K = \varnothing$.

$2 \Rightarrow 1$. Let μ be an arbitrary finitely additive open covering of the space (X,U). There exists such family λ of open subsets of the bX, that $\mu = \{L \bigcap X : L \in \lambda\}$. Denote $K = bX \backslash \bigcup\{L : L \in \lambda\}$. Consequently, for the compact $K \subset bX\backslash X$ there exist such sequence of countable uniformly coverings $\{\alpha_i\}$, that for each point $x \in X$ there exists such number $i \in N$, that $[\alpha_i(x)]_{bX} \bigcap K = \varnothing$. Then there exist such $\{L_1, L_2, ..., L_k\} \subset \lambda$, that $[\alpha_i(x)]_{bX} \subset \bigcup\limits_{j=1}^{k} L_j$. Hence, $\alpha_i(x) \subset (\bigcup\limits_{j=1}^{k} L_j) \bigcap X$. By virtue of finitely additiveness of coverings μ we have $(\bigcup\limits_{j=1}^{k} L_j) \bigcap X \in \mu$. Thus, the uniform space (X,U) is uniformly Lindelöf.

Theorem 6 *The uniform space (X,U) is uniformly Lindelöf if and only if for each finitely additive open covering ω of the space (X,U) there exists a uniformly continuous ω -mapping f of the uniform space (X,U) onto a separable metrizable uniform space (Y,V) .*

Proof. *Necessity*. Let (X,U) be a uniformly Lindelöf space and ω be a finitely additive open covering of the space (X,U). Then for a covering ω there exists a normal sequence of the countable coverings $\{\alpha_i\} \subset U$, realizing the property (*). For sequence $\{\alpha_i\} \subset U$, there exists separable pseudometric d on X, such that $\alpha_{i+1}(x) \subset \{y : d(x,y) < \frac{1}{2^{i+1}}\} \subset \alpha_i(x)$, for all $x \in X$, $i \in N$. Introduce the relation of equivalence: $x \sim y$ if $d(x,y) = 0$, for any $x, y \in X$. Let Y_ω be the factor set of the set X relative to the equivalence relation " $\sim$ " and $f : X \to Y_\omega$ is natural projection. Denote $\rho(y_1,y_2) = d(f^{-1}y_1, f^{-1}y_2)$ for all $y_1, y_2 \in Y$. It is easy to check that ρ is a separable metric. Let V_ω be a uniformity on Y_ω induced by the separable metric ρ. The mapping $f : (X,U) \to (Y_\omega, V_\omega)$ is a uniformly continuous.

Let $y \in Y$ be an arbitrary point and $x \in f^{-1}y$. Then there exist such number $i \in N$ and $L \in \omega$, that $\alpha_i(x) \subset L$. Denote $O_y = \{y^* \in Y : \rho(y, y^*) < \frac{1}{2^{i+1}}\}$. Then $f^{-1}O_y \subset \{x \in X : \rho(x, y) \leq \frac{1}{2^{i+1}}\} \subset \alpha_i(x) \subset L$. Hence, f is a ω-mapping.

Sufficiency. Let ω be an arbitrary finitely additive open covering of the space (X,U) and $f : (X,U) \to (Y_\omega, V_\omega)$ be a uniformly continuous ω -mapping of the uniform space (X,U) onto a separable metrizable uniform space (Y_ω, V_ω). Then exists a base consisting of countable coverings $\{\gamma_i\} \subset V_\omega$. Then $\{f^{-1}\gamma_i\} \subset U$. It is easy to check that the sequence countable uniformly coverings $\{f^{-1}\gamma_i\}$ realizes the condition (*). Thus, the space (X,U) is uniformly Lindelöf.

REFERENCES

1. A.A. Borubaev, *Uniform Topology* (Ilim, Frunze, 2013) (in Russian).
2. L.V. Aparina, Trudy Mosk. Math. Obshestva **57**, 3-15 (1996) (in Russian).
3. J. R. Isbell, *Uniform Spaces* (American Mathematical Society, Providence, 1964).
4. M. D. Rice, Proc. Amer. Math. Soc **62(2)**, 359-362 (1977).
5. D. Buhagiar and B. Pasynkov, Czech Math. J. **46(121)**, 577-586 (1996).
6. B. E. Kanetov, AIP Conference Proc. **1997**, 020085 (2018).

Mathematical Modeling for the Course of COVID-19 Pandemics in Libya

Zafer Cakir[1, a)] and Hasan Basri Savas[2, b)]

[1)] *Faculty of Education, Alanya Alaaddin Keykubat University, Antalya, Turkey*
[2)] *Faculty of Medicine, Alanya Alaaddin Keykubat University, Antalya, Turkey*

[a)] *Corresponding author: zafer.cakir@alanya.edu.tr*
[b)] *Electronic mail: hasan.savas@alanya.edu.tr*

Abstract. In this study, it was aimed to determine the course of COVID-19 infection in Libya with a new modified mathematical modeling and to show the possible number of cases and deaths in the upcoming period. We performed detailed analyzes with the help of the analytical solution of the time-dependent logistics model that we obtained. The results obtained separately on a total and daily basis were shown graphically. In the last part, it is emphasized how important individual and public precautions in order to decrease the spread rate of the disease and to be better controlled.

INTRODUCTION

There are many studies modeling the spread of the COVID-19 pandemic in different countries (see, e.g., [1, 2, 3, 4] and the references given therein). The disease known as COVID-19, caused by a new type of coronavirus, first appeared in China at the end of 2019. Due to COVID-19, which spread all over the world in a very short time, the World Health Organization declared a pandemic. It caused over 21 million cases and nearly 769 thousand deaths before the completion of a year. The most important factor in determining the number of cases is the efficient laboratory tests. In the diagnosis of the disease, antibody and PCR tests in the laboratory, direct radiography and MRI in imaging, acute respiratory tract infection findings in the clinic can be considered. In radiological imaging, involvement in the lung and ground glass appearance are typical. In addition, typical viral infection findings are seen in blood analysis such as hemogram, routine biochemistry. If patients can be diagnosed and isolated, then the spread of the disease can be partially prevented. Individuals who are elderly, have chronic diseases, have a weak immune system, have poor nutrition, are under severe stress, and do not pay attention to hygiene are at more severe risk.

The first COVID-19 case in Libya was seen in the middle of February 2020, and 7738 cases have been reached to date. The number of deaths caused by COVID-19 in Libya has been 145 until today [5]. In this study, it was aimed to determine the course of COVID-19 infection in Libya with a new modified mathematical modeling and to show the possible number of cases and deaths in the upcoming period.

DESCRIPTION OF MATHEMATICAL MODEL

The population distribution, socioeconomic situation, social reflexes, individual sensitivities, public health service delivery quality and individuals' level of access to health services vary. Therefore, in creating a model for the course of the disease, in addition to the initial conditions, it requires improvements to accommodate these situations. In this study, the logistic model was revised specifically for the "corona pandemic" to include the time-variable and considered in the form of "the spreading rate of the disease; is directly proportional with the multiplication of the numbers of those who have caught the disease and those who have not".

Meanings corresponding to used variables and parameters similar to our previous studies [1, 2]. Let the initial $(t=0)$ number of patients be $M(0)=M_0$, the number of patients at a time $t=t_1$ be $M(t_1)=M_1$ and the number of individuals who are open to the disease be P. The purpose of the study is, based on real case and death data from August 1 to August 15, 2020; to determine the course of COVID-19 pandemic in Libya in August, September, October, November, December. In the model given in [6], to take the right-hand side as a function of the time variable t, and with the help of a modified mathematical model to be more compatible with actual data, to obtain more reliable data regarding the course of the disease in the progression of time. For this, by using the expression $\delta=\delta(t)=0.9k\sqrt[10]{t}$ dependent on the t-time variable, we are proposing the following initial value problem (IVP):

$$\frac{dM}{dt}=\delta M(P-M),\ (t>0),\ M(0)=M_0,\ M(t_1)=M_1. \tag{1}$$

International Conference on Analysis and Applied Mathematics (ICAAM 2020)
AIP Conf. Proc. 2325, 020056-1–020056-4; https://doi.org/10.1063/5.0040372
Published by AIP Publishing. 978-0-7354-4069-2/$30.00

Solving problem (1) we get,

$$M(t) = \frac{Pc}{c + e^{-\beta t^{0.9}}}, \tag{2}$$

where $c = \dfrac{M_0}{P - M_0}$ and $\beta = t_1^{-0.9} \ln\left(\dfrac{M_1}{c(P - M_1)}\right)$.

APPLICATION OF MATHEMATICAL MODELING

Here using solution (2), we give a detailed analysis the course of COVID-19 pandemic for next 4.5 months in Libya. For this aim, we take the potential number of individuals open to getting the disease is $P = 50000$. We chose the date 01 August 2020 as $t = 0$, $M(0) = M_0 = 3691$ patients; $t_1 = 14$ as 15 August 2020 with $M(t_1) = M(14) = M_1 = 7738$ patients, let us assess the figure below where we may observe the behavior of the spread (approximate number of cases) in a 150-day future time interval ahead of us.

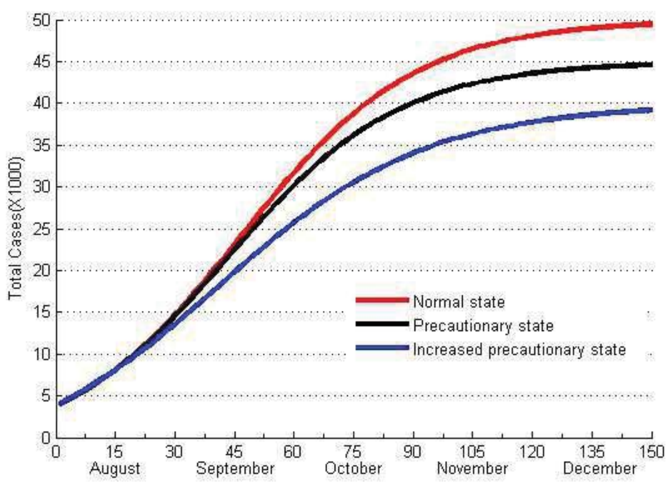

FIGURE 1. Total cases from August 01 to December 30 2020

The red curve in Figure 1 shows that if the current course continues, the total number of cases will increase rapidly, increasing more slowly from mid-October and has the potential to exceed 50000 at the end of December 2020. The black curve says that if the measures are slightly increased, the number of cases can decrease to around 44000 by the end of 2020. We understand from the solution expressed with the blue curve that the number of positive cases could be between 30000-40000 by the end of the year, if the measures are strictly implemented both in individual and public spheres.

Figure 2 shows the number of cases on a daily basis. Accordingly, from the item a) corresponding to the current situation, it can be said that the highest numbers on a daily basis will occur in September and the daily number of cases will reach a peak value of around 600 in mid-September. If the measures are increased a little, it is possible to reduce the peak value in mid-September to 500 figures from item b). From item c), which corresponds to the excessive increase in measures, it is understood that the number of daily cases may decrease to 400. In this case, it is clear that hospital health services can be provided more comfortably without exceeding the capacity.

From the red graph in Figure 3, it is predicted that together with the number of cases, the total deaths have also increased and may reach 2500 at the end of 2020 according to the normal course. It is understood from the black and blue charts that the total number of deaths may remain below 2000, depending on the increasing in measures, the quality and capacity of health services, accessibility of health services, personal hygiene-social distance practices, and the intensity of travel within the country.

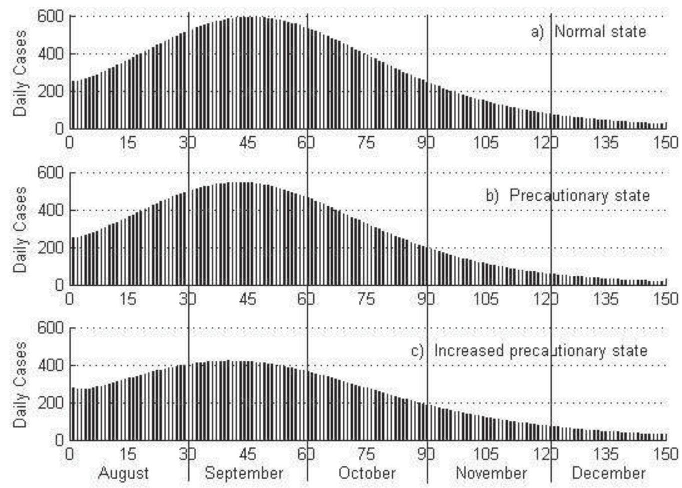

FIGURE 2. Changing in the daily number of cases according to the prevention levels

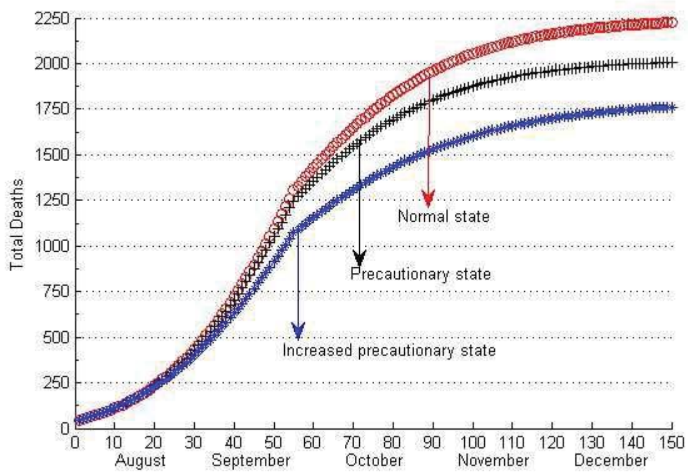

FIGURE 3. The total number of deaths in the 5-month period

In the light of the data in item a in Figure 4, if the current situation continues, it is expected that the daily deaths will reach the highest number and be around 30 at the end of September. From the points b) and c), it is seen that there will be a decrease in the number of daily deaths depending on the seriousness of the implementation of individual and public measures. According to the data obtained from the solution of the problem (if there is no nonlinear case), daily deaths are expected to occur below 10 by the end of 2020.

CONCLUSION

According to our research results, the most important factor that will determine the course of the COVID19 pandemic in Libya is compliance with the measures. Taking the measures effectively and applying them adequately individually and publicly will significantly reduce the number of cases and deaths. Significant measures should be taken against COVID19 by the end of September. In the diagnosis, relatively inexpensive and practical direct radiography, Computed Tomography, hemogram, routine biochemical tests should also be used. Individual hygiene, natural and healthy nutrition, a life suitable for exercise and mobility, avoiding stress, social isolation, using masks are very important

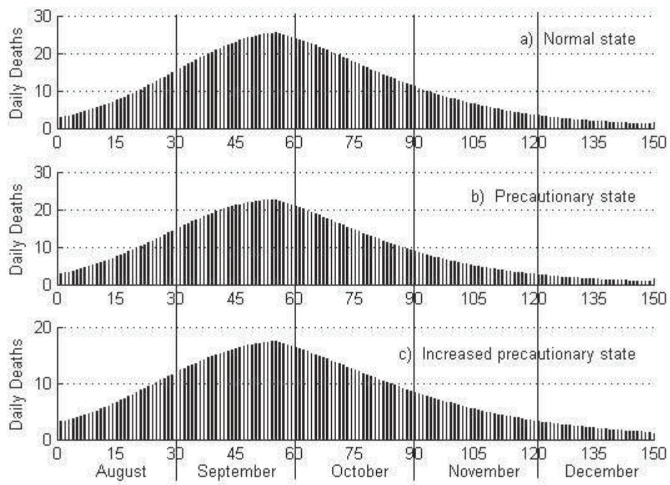

FIGURE 4. Daily deaths

and will reduce the number of cases. Regular intake of antioxidant or immune-enhancing items such as vitamin C, probiotics, zinc, selenium with diet will reduce the frequency of infection. It is very important to take measures that cover the entire population, and the efficiency and capacity of health services in public, the correct application of PCR tests (see, e.g., [7, 8, 9, 10]).

REFERENCES

1. Z. Cakir and H. B. Savas, Electron. J. Gen. Med. **17**, 1–4 (2020).
2. Z. Cakir and H. B. Savas, Ortadogu Tip Derg. **12**, 206–210 (2020).
3. A. Issanov, Y. Amanbek, A. Abbay, S. Adambekov, M. Aljofan, A. Kashkynbayev, and A. Gaipov, Electron J. Gen. Med. **17** (2020).
4. Z. Kristóf, Central European Journal of Educational Research **2**, 84–92 (2020).
5. Worldometers, *Web page: https://www.worldometers.info/coronavirus/ Date of access:16.08.2020* (Worldometers, 2020).
6. C. H. Edwards and D. E. Penney, *Differential Equations and Boundary Value Problems: Computing and Modeling* (Pearson Prentice Hall, 2008).
7. T. Y. Hu, M. Frieman, and J. Wolfram, Nature Nanotechnology **12**, 247–249 (2020).
8. F. Gultekin, M. Naziroglu, H. B. Savas, and B. Cig, Metab. Brain Dis. **33**, 1761–1774 (2018).
9. H. B. Savas and F. Gultekin, J. Ann. Eu. Med. **5**, 50–52 (2017).
10. H. B. Savas, O. Yuksel, H. S. Aloglu, Z. Oner, E. D. Ozer, and F. Gultekin, Cell Membranes and Free Radical Research **5**, 252–255 (2013).

Numerical Solution to the Second Order of Accuracy Difference Scheme for the Source Identification Elliptic-Telegraph Problem

Allaberen Ashyralyev[1, 2, 3, a)] and Ahmad Al-Hammouri[1, b)]

[1)]Department of Mathematics, Near East University, Nicosia, Mersin 10, Turkey
[2)]Peoples' Friendship University of Russia (RUDN University), 6 Miklukho-Maklaya St, Moscow 117198, Russian Federation
[3)]Institute of Mathematics and Mathematical Modeling, 050010, Almaty, Kazakhstan

[a)]Electronic mail: allaberen.ashyralyev@neu.edu.tr
[b)]Corresponding author: alhammouri.math@gmail.com

Abstract. In the present paper, source identification problem for the elliptic-telegraph equation is investigated. The second order of accuracy absolute stable difference scheme for the numerical solution of the one-dimensional identification problem for the elliptic-telegraph equation with the Dirichlet condition is presented. Some numerical results are provided.

INTRODUCTION

Identification problems take an important place in applied sciences and engineering applications, and have been studied by many authors (see, e.g., [1-5] and the references given therein).

Direct and inverse boundary value problems for elliptic-telegraph differential equations have been a major research area in many branches of science and engineering particularly in applied mathematics. The solvability of the inverse problems in various formulations with various overdetermination conditions for telegraph and hyperbolic equations were studied in many works (see, e.g., [7-15] and the references given therein).

In particular, it is well-known that several identification problems for elliptic-telegraph equations can be reduced to the space source identification problem for the elliptic-telegraph equation

$$\begin{cases} u_{tt}(t)+\alpha u_t(t)+Au(t)=p+f(t), 0<t<1, \\ -u_{tt}(t)+Au(t)=p+g(t), -1<t<0, \\ u(-1)=\psi, u(1)=\xi, u(0)=\varphi, u_t(0^+)=u_t(0^-) \end{cases} \tag{1}$$

in a Hilbert space H with the self-adjoint positive definite operator $A\geq\delta I$ $(\delta>0)$. Here, p is the unknown parameter. They established stability estimates for the solution of this problem. In the paper [6], the stability of the identification problem (1) was studied.

The present paper is devoted to study the second order of accuracy absolute stable difference scheme for the numerical solution of the one-dimensional identification problem for the elliptic-telegraph equation with Dirichlet condition. Numerical results are obtained.

THE NUMERICAL ALGORITHM

Source identification problem with the Dirichlet condition

$$\begin{cases} \frac{\partial^2 u(t,x)}{\partial t^2}+2\frac{\partial u(t,x)}{\partial t}-\frac{\partial^2 u(t,x)}{\partial x^2}=p(x)-\sin x, x\in(0,\pi), t\in(0,1), \\ -\frac{\partial^2 u(t,x)}{\partial t^2}-\frac{\partial^2 u(t,x)}{\partial x^2}+u(t,x)=p(x)-\sin x, x\in(0,\pi), t\in(-1,0), \\ u(0,x)=\sin x, u(-1,x)=e\sin x,\ u(1,x)=e^{-1}\sin x, x\in[0,\pi], \\ u(t,0)=0, u(t,\pi)=0, t\in[-1,1] \end{cases} \tag{2}$$

for the elliptic-telegraph equation is considered. The exact solution pair of this problem is

$$(u(t,x),p(x))=\left(e^{-t}\sin x,\sin x\right), 0\leq x\leq\pi, -1\leq t\leq 1.$$

International Conference on Analysis and Applied Mathematics (ICAAM 2020)
AIP Conf. Proc. 2325, 020057-1–020057-5; https://doi.org/10.1063/5.0040389
Published by AIP Publishing. 978-0-7354-4069-2/$30.00

Here, we denote the set $[-1,1]_\tau \times [0,\pi]_h$ of all grid points

$$[-1,1]_\tau \times [0,\pi]_h = \{(t_k, x_n) : t_k = k\tau, -N \le k \le N,\ N\tau = 1, x_n = nh, 0 \le n \le M, Mh = \pi\}.$$

The solution of source identification problem (2) can be written as

$$u(t,x) = \omega(t,x) + q(x), \tag{3}$$

where $q(x)$ is the solution of the problem

$$-q''(x) = p(x), 0 < x < \pi, q(0) = q(\pi) = 0, \tag{4}$$

and the function $\omega(t,x)$ is the solution of the nonlocal boundary value problem

$$\begin{cases} \frac{\partial^2 \omega(t,x)}{\partial t^2} + 2\frac{\partial \omega(t,x)}{\partial t} - \frac{\partial^2 \omega(t,x)}{\partial x^2} = -\sin x, x \in (0,\pi), t \in (0,1), \\ -\frac{\partial^2 \omega(t,x)}{\partial t^2} - \frac{\partial^2 \omega(t,x)}{\partial x^2} = -\sin x, x \in (0,\pi), t \in (-1,0), \\ \omega(0,x) - \omega(-1,x) = (1-e)\sin x, \omega(0,x) - \omega(-1,x) = \left(1 - e^{-1}\right)\sin x, x \in [0,\pi], \\ \omega(t,0) = 0, \omega(t,\pi) = 0, t \in [-1,1]. \end{cases} \tag{5}$$

Taking into account all of the above, the following numerical algorithm can be used for the approximate solutions of the identification problem (2):
1. Search the approximate solution of the nonlocal boundary value problem (5).
2. Find approximate the source $p(x)$ by using formula

$$p(x) = e^{-1}\sin x + \omega_{xx}(1,x). \tag{6}$$

3. Obtain the approximate value of $q(x)$ by formula (4).
4. Find the approximate solutions of source identification problem (2) by formula (3).

Moreover, for approximate solution of identification problem (2), we construct the second order of accuracy difference scheme in t

$$\begin{cases} \frac{u_n^{k+1} - 2u_n^k + u_n^{k-1}}{\tau^2} + 2\frac{u_n^{k+1} - u_n^{k-1}}{2\tau} - \frac{1}{2}\left(\frac{u_{n+1}^{k+1} - 2u_n^{k+1} + u_{n-1}^{k+1}}{h^2} + \frac{u_{n+1}^{k-1} - 2u_n^{k-1} + u_{n-1}^{k-1}}{h^2}\right) \\ = p_n - \sin x_n, 1 \le k \le N-1, 1 \le n \le M-1, \\ -\frac{u_n^{k+1} - 2u_n^k + u_n^{k-1}}{\tau^2} - \frac{u_{n+1}^k - 2u_n^k + u_{n-1}^k}{h^2} \\ = p_n - \sin x_n, -N+1 \le k \le -1, 1 \le n \le M-1, \\ -3u_n^0 + 4u_n^1 - u_n^2 = 3u_n^0 - 4u_n^{-1} + u_n^{-2}, 0 \leqslant n \leqslant M, \\ u_n^0 = 0, u_n^{-N} = (e-1)\sin x_n, u_n^N = \left(e^{-1} - 1\right)\sin x_n, 0 \leqslant n \leqslant M, \\ u_0^k = u_M^k = 0, -N \le k \le N. \end{cases} \tag{7}$$

In the first step, we will obtain $\left\{\left\{\omega_n^k\right\}_{k=-N}^{N}\right\}_{n=0}^{M}$ as solution of nonlocal boundary value problem

$$\begin{cases} \frac{\omega_n^{k+1} - 2\omega_n^k + \omega_n^{k-1}}{\tau^2} + 2\frac{\omega_n^{k+1} - \omega_n^{k-1}}{2\tau} - \frac{1}{2}\left(\frac{\omega_{n+1}^{k+1} - 2\omega_n^{k+1} + \omega_{n-1}^{k+1}}{h^2} + \frac{\omega_{n+1}^{k-1} - 2\omega_n^{k-1} + \omega_{n-1}^{k-1}}{h^2}\right) \\ = p_n - \sin x_n, 1 \le k \le N-1, 1 \le n \le M-1, \\ -\frac{\omega_n^{k+1} - 2\omega_n^k + \omega_n^{k-1}}{\tau^2} - \frac{\omega_{n+1}^k - 2\omega_n^k + \omega_{n-1}^k}{h^2} \\ = p_n - \sin x_n, -N+1 \le k \le -1, 1 \le n \le M-1, \\ -3\omega_n^0 + 4\omega_n^1 - \omega_n^2 = 3\omega_n^0 - 4\omega_n^{-1} + \omega_n^{-2}, 0 \leqslant n \leqslant M, \\ \omega_n^0 = 0, \omega_n^{-N} = (e-1)\sin x_n, \omega_n^N = \left(e^{-1} - 1\right)\sin x_n, 0 \leqslant n \leqslant M, \\ \omega_0^k = \omega_M^k = 0, -N \le k \le N. \end{cases} \tag{8}$$

Here, ω_k^n denotes the numerical approximation of $\omega(t,x)$ at (t_k, x_n). For obtaining the solution of DS (8), we can write it in the matrix form as

$$\begin{cases} A\omega_{n+1} + B\omega_n + C\omega_{n-1} = F_n, 1 \le n \le M-1, \\ \omega_0 = \omega_M = 0, \end{cases} \tag{9}$$

where A,B,C are $(2N+1)\times(2N+1)$ square, and $F_n,\omega_s, s=n,n\pm1$ are $(2N+1)\times 1$ column matrices

$$A=C=\begin{bmatrix}
0&0&0&\cdots&0&0&0&0&0&0&\cdots&0&0&0\\
0&0&0&\cdots&0&0&t&0&t&0&\cdots&0&0&0\\
0&0&0&\cdots&0&0&0&t&0&t&\cdots&0&0&0\\
\vdots&\vdots&\vdots&\ddots&\vdots&\vdots&\vdots&\vdots&\vdots&\vdots&\ddots&\vdots&\vdots&\vdots\\
0&0&0&\cdots&0&0&0&0&0&0&\cdots&t&0&0\\
0&0&0&\cdots&0&0&0&0&0&0&\cdots&0&t&0\\
0&0&0&\cdots&0&0&0&0&0&0&\cdots&t&0&t\\
0&0&0&\cdots&0&0&0&0&0&0&\cdots&0&0&0\\
0&b&0&\cdots&0&0&0&0&0&0&\cdots&0&0&0\\
0&0&b&\cdots&0&0&0&0&0&0&\cdots&0&0&0\\
\vdots&\vdots&\vdots&\ddots&\vdots&\vdots&\vdots&\vdots&\vdots&\vdots&\ddots&\vdots&\vdots&\vdots\\
0&0&0&\cdots&b&0&0&0&0&0&\cdots&0&0&0\\
0&0&0&\cdots&0&b&0&0&0&0&\cdots&0&0&0\\
0&0&0&\cdots&0&0&0&0&0&0&\cdots&0&0&0
\end{bmatrix}_{(2N+1)\times(2N+1)}$$

with $A_{N+i,i}=b$ and $A_{i,N+i-1}=A_{i,N+i+1}=t$ for $i=2,...,N$.

$$B=\begin{bmatrix}
-1&0&0&\cdots&0&0&1&0&0&0&\cdots&0&0&0\\
0&0&0&\cdots&0&0&d&c&a&0&\cdots&0&0&0\\
0&0&0&\cdots&0&0&0&d&c&a&\cdots&0&0&0\\
\vdots&\vdots&\vdots&\ddots&\vdots&\vdots&\vdots&\vdots&\vdots&\vdots&\ddots&\vdots&\vdots&\vdots\\
0&0&0&\cdots&0&0&0&0&0&0&\cdots&a&0&0\\
0&0&0&\cdots&0&0&0&0&0&0&\cdots&c&a&0\\
0&0&0&\cdots&0&0&0&0&0&0&\cdots&d&c&a\\
0&0&0&\cdots&-1&4&-6&4&-1&0&\cdots&0&0&0\\
g&j&g&\cdots&0&0&0&0&0&0&\cdots&0&0&0\\
0&g&j&\cdots&0&0&0&0&0&0&\cdots&0&0&0\\
\vdots&\vdots&\vdots&\ddots&\vdots&\vdots&\vdots&\vdots&\vdots&\vdots&\ddots&\vdots&\vdots&\vdots\\
0&0&0&\cdots&j&g&0&0&0&0&\cdots&0&0&0\\
0&0&0&\cdots&g&j&g&0&0&0&\cdots&0&0&0\\
0&0&0&\cdots&0&0&1&0&0&0&\cdots&0&0&-1
\end{bmatrix}_{(2N+1)\times(2N+1)},$$

with $B_{N+i,i}=j, B_{N+i,i-1}=B_{N+i,i+1}=g$, and $B_{i,N+i-1}=d, B_{i,N+i}=c, B_{i,N+i+1}=a$ for $i=2,...,N$.

$$F_n=\begin{bmatrix}(1-e^{1})\sin x_n\\-\sin x_n\\\vdots\\-\sin x_n\\0\\-\sin x_n\\\vdots\\-\sin x_n\\(1-e^{-1})\sin x_n\end{bmatrix}_{(2N+1)\times1},\omega_s=\begin{bmatrix}\omega_s^1\\\omega_s^2\\\vdots\\\omega_s^{N-1}\\\omega_s^{N}\\\omega_s^{N+1}\\\vdots\\\omega_s^{2N}\\\omega_s^{2N+1}\end{bmatrix}_{(2N+1)\times1}.$$

Here,

$$a=\tfrac{1}{\tau^2}+\tfrac{1}{\tau}+\tfrac{1}{h^2}, b=-\tfrac{1}{h^2}, c=-\tfrac{2}{\tau^2}, t=-\tfrac{1}{2h^2},$$
$$d=\tfrac{1}{\tau^2}-\tfrac{1}{\tau}+\tfrac{1}{h^2}, g=-\tfrac{1}{\tau^2}, z=\tfrac{2}{\tau^2}+\tfrac{2}{h^2}.$$

For the solution of the matrix equation (9), we use the modified Gauss elimination method. We seek a solution of the matrix equation (9) by the following form

$$\omega_n=\alpha_{n+1}\omega_{n+1}+\beta_{n+1},\ n=M-1,...,1,0, \tag{10}$$

TABLE 1. Error analysis

	$N=M=20$	$N=M=40$	$N=M=80$	$N=M=160$
$\|E_{\omega}\|_{\infty}$	0.0054	0.0014	$3.4447e-04$	$8.6605e-05$
$\|E_{p}\|_{\infty}$	0.0028	$7.2547e-04$	$1.8454e-04$	$4.6572e-05$
$\|E_{u}\|_{\infty}$	$7.5025e-04$	$1.9041e-04$	$4.7966e-05$	$1.2041e-05$

where α_n $(1 \le n \le M-1)$ are $(2N+1)\times(2N+1)$ square matrices and β_n $(1 \le n \le M-1)$ are $(2N+1)\times 1$ column vectors, calculated as

$$\begin{cases} \alpha_{n+1} = -Q_n A,\ \beta_{n+1} = Q_n(DF_n - C\beta_n), \\ Q_n = (B + C\alpha_n)^{-1},\ n = 1,2,\ldots,M-1. \end{cases}$$

Here, D and α_1 are identity $(2N+1)\times(2N+1)$ square matrix, and β_1 is $(2N+1)\times 1$ column vector with zero elements.

In the second step, using (6), we get

$$p_n = \frac{\omega_{n+1}^{2N+1} - 2\omega_n^{2N+1} + \omega_{n-1}^{2N+1}}{h^2} - e^{-1}\frac{\sin x_{n+1} - 2\sin x_n + \sin x_{n-1}}{h^2}, 1 \le n \le M-1.$$

In the third step, using (4), we get

$$-\frac{q_{n+1} - 2q_n + q_{n-1}}{h^2} = p_n, 1 \le n \le M-1, q_0 = q_M = 0. \tag{11}$$

In the fourth step, using (3), we obtain

$$u_n^k = \omega_n^k + q_n, n = 0,1,\ldots,M, k = -N,\ldots,N. \tag{12}$$

Finally, we compute the error between the exact solution and numerical solution by

$$\begin{cases} \|E_\omega\|_\infty = \max\limits_{-N\le k\le N, 0\le n\le M} \left|\omega(t_k,x_n) - \omega_n^k\right|, \\ \|E_u\|_\infty = \max\limits_{-N\le k\le N, 0\le n\le M} \left|u(t_k,x_n) - u_n^k\right|, \\ \|E_p\|_\infty = \max\limits_{-N\le k\le N, 0\le n\le M} \left|p(x_n) - p_n\right|, \end{cases}$$

where $\omega(t,x), u(t,x), p(x)$ represent the exact solutions, ω_n^k and u_n^k represent the numerical solutions at (t_k,x_n), and p_n represent the numerical solutions at x_n. The numerical results are given in the Table 1. As it is seen in Table 1, if N and M are doubled, the values of errors decrease by a factor of approximately $1/4$.

ACKNOWLEDGMENTS

The authors would like to thank Prof. A.L. Skubachevskii for his valuable comments and suggestions to improve the quality of the present paper. The publication has been prepared with the support of the “RUDN University Program 5-100”.

REFERENCES

1. A. Ashyralyev and C. Ashyralyyev, Nonlinear Anal. Model. Control **19(3)**, 350–366 (2014).
2. M. Dehghan, Applied Mathematical Modelling **25**, 743–754 (2001).
3. A. Ashyralyev and A. S. Erdogan, Applied Mathematics and Computation **226**, 212–228 (2014).
4. C. Ashyralyyev, Filomat **28(5)**, 947–962 (2014).
5. S. Jator, American J. of Computational Mathematics **5(2)**, 175–185 (2015).

6. A. Ashyralyev and A. Al-Hammouri, AIP Conference Proceedings **2183(1)**, 070008 (2019).
7. M. Choulli and M. Yamamoto, Journal of Inverse and III-posed Problems **7(3)**, 241–254 (1999).
8. G. D. Blasio and A. Lorenzi, Journal of Inverse and Ill-Posed Problems **15(7)**, 709–734 (2007).
9. Z. Direk and M. Ashyraliyev, Advances in Difference Equations **2014(132)** (2014).
10. T. S. Kalmenov and D. Suragan, Electronic Journal of Differential **2014(48)**, 1–6 (2014).
11. A. Ashyralyev and F. Cekic, Book Series: Springer Proceedings in Mathematics & Statistics **164**, 39–50 (2016).
12. A. Ashyralyev and P. E. Sobolevskii, *New Difference Schemes for Partial Differential Equations* (Birkhäuser Verlag, Basel, Boston, Berlin, 2004).
13. A. Ashyralyev and F. Özger, Mathematical Methods in the Applied **37(4)**, 524–545 (2013).
14. M. B. A. Mansour, Communications in Mathematical Sciences **4(4)**, 731–739 (2006).
15. A. Ashyralyev, G. Judakova, and P. E. Sobolevskii, Abstract and Applied Analysis **2006(ID 14816)**, 1–16 (2006).

Mathematical Modelling of HIV Infection with the Effect of Horizontal and Vertical Transmissions

Evren Hincal,[1,2,a)] Bilgen Kaymakamzade,[1,2,b)] Umar T. Mustapha,[1,3,c)] Salisu M. Muhammad,[1,d)] and Nezihal Gokbulut[1,2,e)]

[1)] *Department of Mathematics, Near East University, Nicosia, Mersin 10, Turkey*
[2)] *Mathematics Research Center, Near East University, Nicosia, Mersin 10, Turkey*
[3)] *Department of Mathematics, Federal University Dutse, Dutse, Nigeria*

[a)] *Corresponding author: evren.hincal@neu.edu.tr*
[b)] *Electronic mail: bilgen.kaymakamzade@neu.edu.tr*
[c)] *Electronic mail: umartasiumustapha@yahoo.com*
[d)] *Electronic mail: salisumuhammadmuhammad@gmail.com*
[e)] *Electronic mail: nezihal.gokbulut@neu.edu.tr*

Abstract. In this study, we developed a mathematical model to study the transmission dynamics of HIV infection and analyzed the effect of horizontal and vertical transmission in Turkey. We fit the model by using confirmed HIV cases of both vertical and horizontal transmission between 2011 and 2018. By using the next generation operator, we obtained the basic reproduction number of the model which shows whether the disease persists or dies out in time. Further, the most sensitive parameters, that are efficient for the control of the infection, obtained by using forward normalized sensitivity index. The results obtained with the aid of mesh and contour plots.

INTRODUCTION

Human Immuno-deficiency Virus(HIV) intends to reduce or destroy the human defense mechanisms to prevent fighting with infections or any other diseases and the progression of this virus occurred as a result of infecting the CD4+ T-cells of the organism [1, 2]. CD4+ T-cells shows how active and functioning the immune system is [3, 4]. HIV is the virus that causes Acquired Immune Deficiency Syndrome(AIDS), which is the most advanced phase of the HIV infection [5].

HIV can be transmitted through direct contact with contaminated blood products, such as syringes or needles, contaminated transfusion, unprotected sexual intercourse, and breastfeeding or as a vertical transmission during birth [6]. It was discovered in United States of America in the early 1980s. In 2014, it was reported that the number of people that are living with HIV was 35 million [5]. In 2015, with 150000 newly infected children, 1.8 million children were living with HIV according to the UNAIDS and 110000 children died because of AIDS-related diseases [7]. This data shows that AIDS has become one of the major death causes. In each day about 1500 children get newly infected [8].

Several mathematical models have been developed and used to gain insight into the transmission dynamics of HIV in human population (see, for instance, [2, 5, 7, 9, 10] and some of the references therein). However, none of these studies the dynamics of HIV transmission with effect of both vertical and horizontal transmission. The purpose of the current study is to design, and analyse, a new realistic model (which extends some of the aforementioned studies in the literature) for HIV transmission dynamics.

In this paper, first the epidemic model is developed and analyzed. Then, model fitting is presented. After that we showed the sensitivity analysis. Lastly, we presented the concluding remarks.

MODEL FORMULATION

We proposed a mathematical model to monitor the dynamics of both vertical and horizontal transmissions of HIV infections at a time t. The total population $N(t)$ is divided into four different classes as susceptible adults $S(t)$, infected adults $I(t)$, new born child with no HIV infection $C(t)$, and new born child with HIV infection $I_c(t)$.

We constructed the following system.

International Conference on Analysis and Applied Mathematics (ICAAM 2020)
AIP Conf. Proc. 2325, 020058-1–020058-5; https://doi.org/10.1063/5.0040304
Published by AIP Publishing. 978-0-7354-4069-2/$30.00

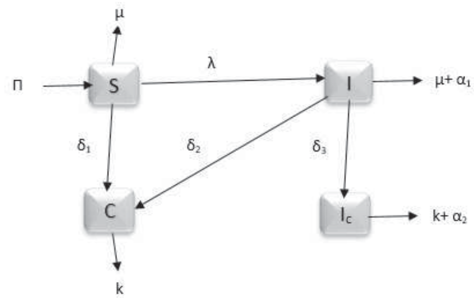

FIGURE 1. Flow diagram of the model

$$
\begin{cases}
\frac{dS}{dt} &= \Pi - \lambda S - (\delta_1 + \mu)S, \\
\frac{dI}{dt} &= \lambda S - (\mu + \alpha_1 + \delta_2 + \delta_3)I, \\
\frac{dC}{dt} &= \delta_1 S + \delta_2 I - \mu C, \\
\frac{dI_c}{dt} &= \delta_3 I - (\mu + \alpha_2)I_c,
\end{cases}
\tag{1}
$$

where $\lambda = \frac{\beta I}{N}$ is the force of infection.

TABLE 1. Variables of the model

Variables	Descriptions
N	Total human population
$S(t)$	Susceptible Adults(Both female and male)
$I(t)$	Infected Adults with HIV(Both female and male)
$C(t)$	New born child
I_c	New born child with HIV infection

TABLE 2. Parameters of the model

Parameters	Descriptions
ϕ	Recruitment rate of both adults and new born children
β	Transmission or successful contact rate
α_1	HIV induced mortality rate of an adult
α_2	HIV induced mortality rate of a new born child
μ	Natural death for adults
k	Natural death for new born children
$\delta_j (j = 1,2,3)$	Progression rates

FUNDAMENTAL PROPERTIES OF THE MODEL

In this section, we will state the theorems that we used.

Theorem 1 *Suppose that, initially the data $S(0) > 0, I(0) > 0, C(0) > 0, I_c(0) > 0$. Then the solutions of the model (S, I, C, I_c) are positive for all time $t > 0$, moreover,*

$$\lim_{t\to\infty}\sup N(t) \leq \frac{\Pi}{\mu}, where, N = S+I+C+I_c.$$

Theorem 2 *The solutions of the system (1) are said to be feasible for all* $0 \leq t$ *whenever they enter the invariant region* Ω.

Disease-free Equilibrium(DFE) and Local Stability

The disease-free equilibrium of model (1) exists and can be obtained by setting the R.H.S of the system (1) to zero as

$$\chi^0 = (S,I,C,I_c) = \left(\frac{\Pi}{\mu},0,0,0\right).$$

By using the next generation method [12], we calculated the basic reproduction as

$$R_0 = \frac{\beta}{\alpha_1+\delta_2+\delta_3+\mu}. \tag{2}$$

Endemic Equilibrium

The endemic equilibrium (EE) of the model exist only when $I \neq 0$, $C \neq 0$, and $I_c \neq 0$. This means that there exists a persistence of the HIV infection in the populace, and it is denoted by $\chi^* = (S^*,I^*,C^*,I_c^*)$. In our model, EE calculated as $\chi^* = (S^*,I^*,C^*,I_c^*) = \left(\frac{\pi}{\lambda+\mu-\alpha_1}, \frac{\lambda\pi}{(\mu-\delta_3-\delta_2+\alpha_1)(\lambda+\mu-\alpha_1)}, \frac{\pi(\lambda\delta_2+\mu\delta_1+\alpha_1\delta_1-\delta_1\delta_2-\delta_1\delta_3)}{\mu(\mu-\delta_3-\delta_2+\alpha_1)(\lambda+\mu-\alpha_1)}, \frac{\delta_3\lambda\pi}{(\mu-\delta_3-\delta_2+\alpha_1)(\mu+\alpha_2)(\lambda+\mu-\alpha_1)}\right)$.

MODEL FITTING

This section explains the fitting of parameters involved in (1) based upon the real cases of HIV(CD4+) in Turkey for both vertical and horizontal cases between 2011 and 2018. The objective function yields to relatively small error having the value 0.000009. The Figure 2 shows the real HIV(CD+4) cases by black cycles whereas the best fitted curve of the model is shown by the black solid line. The biological parameters included in the model are listed in Table 3 along with their best estimated values obtained via least-squares technique. These parameters have finally produced the value of the basic reproduction number equivalent to $R_0 = 1.23$.

TABLE 3. Values of the parameters of the proposed HIV model

Parameters	Values	Source
Π	35	Estimated
β	0.0071	Estimated
α_1	0.000129	Fitted
α_2	0.000234	Fitted
μ	0.0052	[2]
k	0.0092	[7]
δ_1	0.00011	Fitted
δ_2	0.00000011	Fitted
δ_3	0.00044	Fitted

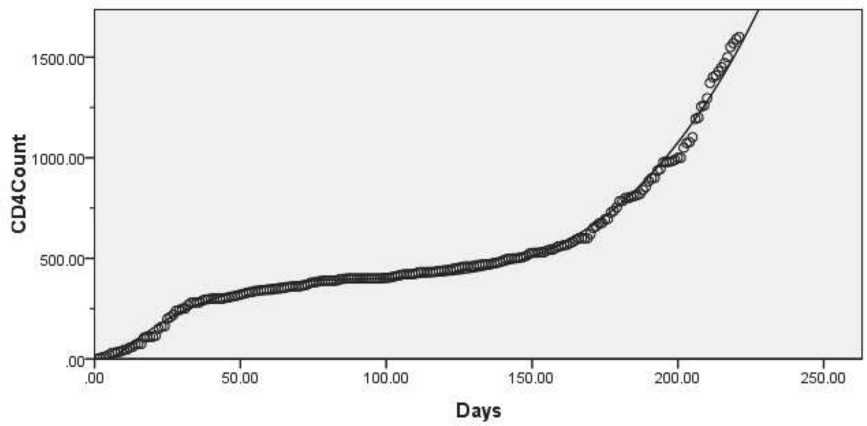

FIGURE 2. Data fitting for the real cases of TB(CD4+) in Turkey for both vertical and horizontal cases from 2011 to 2018

SENSITIVITY ANALYSIS

In this section we used the local sensitivity analysis method to outline the sensitivity of the R_0 to certain key associated parameters of the proposed HIV model. R_0 was obtained and described as a parameter-dependent output of the model and the severity indicator of the HIV infection, the main way of curtailing and spreading the HIV infection in the population is to lower this reproduction number below unity. Therefore, it became crucially important to investigate the relationship between the parameters of the model and R_0. Our main concern here is to explain the sensitivity of R_0 with respect to the significant parameters used in the model (1). The set of input parameters relative to R_0 is $\sigma = \{\beta, \mu, \delta_1, \delta_2, \delta_3, \alpha_1, \}$.

Typically, if a model has different parameters, variations in parameters might not always affect the outcome due to variance in the sensitivity of the parameters. So, those with positive sign are considered as highly and proportionally sensitive for increasing the value of R_0 while those with negative sign are sensitive for the decrease of R_0 value and the other category are neutrally sensitive (with zero relative sensitivity) [11, 13]. We denote the normalized local sensitivity index of the output R_0 with respect to a parameter (γ) by $\Omega_{\gamma}^{R_0}$, where $\gamma \in \sigma$. Using the above definition, we compute the following indices for the output R_0 with respect to every parameter presented in Table 3.

TABLE 4. Forward Normalized Sensitivity Indices

Parameters	Elasticity Indices	Values of the Elasticity Index
β	$\Omega_{\beta}^{R_0}$	1.000
μ	$\Omega_{\mu}^{R_0}$	-0.002
δ_2	$\Omega_{\delta_2}^{R_0}$	-0.285
δ_3	$\Omega_{\delta_3}^{R_0}$	-0.585
α_1	$\Omega_{\alpha_1}^{R_0}$	-0.109

CONCLUSION

In this study, we developed a mathematical model to study the transmission dynamics of HIV infection and analyzed the effect of horizontal and vertical transmission in Turkey. We fit the model with the use of confirmed HIV cases of both vertical and horizontal transmission from 2011 to 2018. Using the next generation operator, we obtained the R_0 of the model which shows whether the disease persist or dies out in time. Further analysis shows that, the model is locally asymptotically stable when $R_0 < 1$ and unstable when $R_0 > 1$. The most sensitive parameters that are efficient

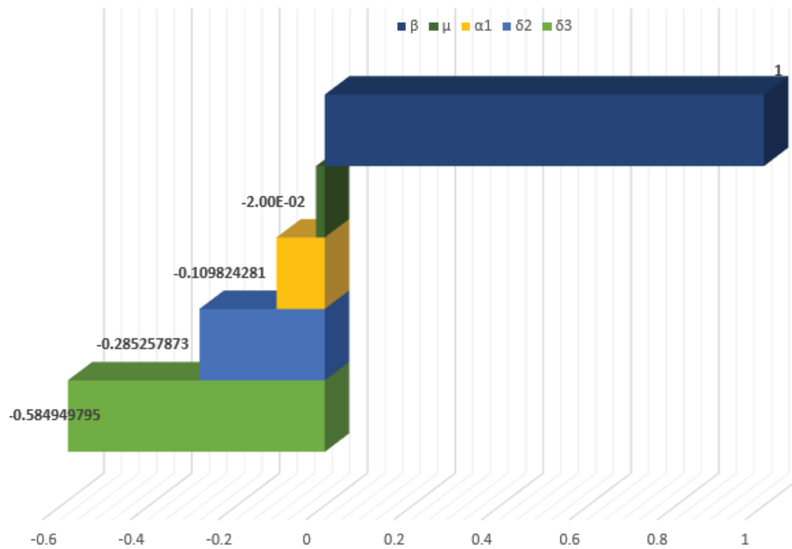

FIGURE 3. Plot diagram for elasticity index values

for the control of the infection obtained by using forward normalized sensitivity index. The results obtained with the aid of mesh and contour plots, which shows that decreasing the values of transmission rate, disease induced mortality rates and progression rate play a significant role in controlling the spread of HIV transmission.

REFERENCES

1. O. M. Ogunlaran and S. C. O. Noutschie, BioMed Research International **2016**, 6 (2016).
2. E. H. Elbasha and A. B. Gumel, Bull Math Biol. **68**, 577-614 (2006).
3. S. D. Hove-Musekwaa and F. Nyabadza, Computational and Mathematical Methods in Medicine **10**, 287-305 (2009).
4. R. P. Duffin and R. H. Tullis, Journal of Theoretical Medicine **4(4)**, 215-221 (2002).
5. S. Al-Sheikh, F. Musali, and M. Alsomi, International Mathematical Forum **6**, 3251-3273 (2011).
6. G. Kockaya et. al., Farmeconomia Health Economics and Therapautic Pathways 2016 **17(1)**, 13-17 (2016).
7. M. Mahy et. al., AIDS **31**, S13-S22 (2017).
8. UNAIDS website, https://www.unaids.org/sites/default/files/media_asset/FactSheet_Children_en.pdf (accessed 18 September, 2020).
9. D. Y. Melesse and A. B. Gumel, Journal of Mathematical Analysis and Applications **366(1)**, 202-217 (2010).
10. F. T. Saad, T. Sanlidag, E. Hincal, M. Sayan, I. A. Baba, B. Kaymakamzade, 13th International Conference on Theory and Application of Fuzzy Systems and Soft Computing, 830-839 (2019).
11. T. Turanyi, Journal of Mathematical Chemistry **5(3)**, 203–248 (1990).
12. P. van den Driessche and J. Wanmough, Math Biosci **180**, 29-48 (2000).
13. J. Wu, R. Dhingra, M. Gambhir, and J. V. Remais, Journal of the Royal Society Interface **10(86)**, (2013).

Convergence of High-Precision Finite Element Method Schemes for Two-Temperature Plasma Equation

Mirsaid Aripov,[1, a)] Dauletbay Utebaev,[2, b)] and Zhusipbay Nurullaev[2, c)]

[1)]*Mirzo Ulugbek National University of Uzbekistan, Tashkent, Uzbekistan*
[2)]*Berdakh Karakalpak State University, Nukus, Uzbekistan*

[a)]*Corresponding author: mirsaidaripov@mail.ru*
[b)]*Electronic mail: dutebaev_56@mail.ru*
[c)]*Electronic mail: njusipbay@mail.ru*

Abstract. In this paper, difference schemes of the high-order finite element method for the Sobolev type equation are constructed and investigated. In particular, boundary value problems for the two-temperature plasma equation are considered. A high order of accuracy of the scheme is achieved by special sampling of time and space variables. The stability and convergence of the constructed algorithms are proved. A priori estimates are obtained in various norms, which are used later to obtain estimates of the accuracy of the scheme under weak assumptions about the smoothness of solutions to differential problems.

INTRODUCTION

The solution of complex applied problems requires the creation of more accurate numerical algorithms or improving existing ones. It manifests itself especially in the study of complex non-stationary processes, for example, as boundary value problems for linear partial differential equations that are unsolvable with respect to the highest time derivative, which are called Sobolev type equations. These are problems of geophysics, oceanology, atmospheric physics, physics of magnetically ordered structures, related to wave propagation in media with strong dispersion, and many others [1, 2, 3, 4, 5, 6].

This paper deals with the construction and research of difference schemes of increased accuracy of boundary value problems for the non-stationary equation of two-temperature plasma.

PROBLEM STATEMENT

The equation describing low-frequency electronic magneto-sound waves has the form [3]:

$$\frac{\partial^2}{\partial t^2}\Delta_2\Phi_e+\frac{u_{A_e}^2}{c^2}\frac{\partial^2}{\partial t^2}\left(\Delta_3\Phi_e-\frac{1}{r_{D_e}^2}\Phi_e\right)+\omega_{B_e}^2\frac{\partial^2\Phi_e}{\partial x_3^2}=\frac{u_{A_e}^2}{c^2}divF(x,t). \tag{1}$$

The equation describing low-frequency ion magneto-sound waves has the form

$$\frac{\partial^2}{\partial t^2}\Delta_2\Phi_i+\frac{u_{A_i}^2}{c^2}\frac{\partial^2}{\partial t^2}\left(\Delta_3\Phi_i-\frac{1}{r_{D_i}^2}\Phi_i\right)+\omega_{B_i}^2\frac{\partial^2\Phi_i}{\partial x_3^2}=\frac{u_{A_i}^2}{c^2}divF(x,t). \tag{2}$$

Here $\Phi_e(x,t)$ are electric fields of electrons, $\Phi_i(x,t)$ are electric fields of ions, $\Delta_p u = div\left(|\nabla u|^{p-2}\nabla u\right)$ is pseudolaplacian, $r_{D_e}^2=T_e^2/(4\pi e^2 n_0)$ is square of the electronic Debye radius, $r_{D_i}^2=T_i^2/(4\pi e^2 n_0)$ is square ionic radius of debye,$u_{A_e}=B_0/(4\pi n_0 M)$ is alfven speed for electrons, $u_{A_i}=B_0/(4\pi n_0 M)$ is alfven speed for ions, $\omega_{B_e}=eB_0/(mc)$, $\omega_{B_i}=ZeB_0/(Mc)$ are the Larmor frequencies of electrons and ions (m and M their mass, respectively), c is the speed of light in a vacuum, Z is the ratio of the charges of an ion and an electron, B_0 is an external constant magnetic field, n_0 is the unperturbed particle density, e is absolute value of the electron charge, T_e is electron temperature, T_i is the temperature of the ions.

Initial conditions for (1) and (2) are, respectively,

$$\left.\frac{\partial^k}{\partial t^k}\Phi_e(x,t)\right|_{t=0}=0,\ k=0,1,\ \left.\frac{\partial^k}{\partial t^k}\Phi_i(x,t)\right|_{t=0}=0,\ k=0,1. \tag{3}$$

In addition, some boundary conditions are added to the above equations.

International Conference on Analysis and Applied Mathematics (ICAAM 2020)
AIP Conf. Proc. 2325, 020059-1–020059-6; https://doi.org/10.1063/5.0041303
Published by AIP Publishing. 978-0-7354-4069-2/$30.00

The existence and uniqueness of solutions to such problems were considered in [1, 2, 3].

Equations (1), (2) are written in the following general form:

$$\frac{\partial^2}{\partial t^2}\left(\Delta_3 u-\rho^2 u\right)+\omega^2\frac{\partial^2}{\partial t^2}\left(\Delta_2 u\right)+\theta^2\Delta_1 u=f(x,t),\ (x,t)\in Q_T, \tag{4}$$

where $\rho^2, \omega^2, \theta^2$ are const >0, depending on debye's radius or from the alfven-speed, ω^2 is Langmuir's frequency, $\Omega=\{0<x_k<l_k, k=1,2,3\}$, $Q_T=\{(x,t): x\in\Omega, t\in(0,T]\}$, $\Delta_3=\partial^2/\partial x_1^2+\partial^2/\partial x_2^2+\partial^2/\partial x_3^2, \Delta_2=\partial^2/\partial x_1^2+\partial^2/\partial x_2^2, \Delta_1=\partial^2/\partial x_3^2, f(x,t)$ are the right-hand parts (1), (2), correspondingly.

Equation (4) is supplemented with the following initial and boundary conditions:

$$u(x,t)\bigg|_{\partial\Omega}=0, \forall t\in[0,t],\ u(x,0)=u_0(x),\ \frac{\partial u(x,0)}{\partial x}=u_1(x). \tag{5}$$

We formulate a generalized statement of the problem (4), (5). Let us call the function a generalized solution of the problem $u(x,t)$, which at each $t\in(0,T]$ belongs to $H=\{u\in W_2^1(\Omega), u=0, x\in G=\partial\Omega\}$, has a derivative $\frac{\partial^2 u}{\partial t^2}\in W_2^1(\Omega)$ and almost everywhere for everyone $t\in(0,T]$ fulfil the relations:

$$a_3\left(\frac{d^2u(t)}{dt^2},v\right)+a_2\left(\frac{d^2u(t)}{dt^2},v\right)+a_1\left(u(t),v\right)=\left(f(t),v\right), \tag{6}$$

$$(u(0)-u_0,v)=0,\ \left(\frac{du}{dt}(0)-u_1,v\right)=0,\ \forall v(x)\in H. \tag{7}$$

Here

$$a_3(u,v)=\int_\Omega\sum_{k=1}^{3}\left(u_{x_k}v_{x_k}-\rho^2 uv\right)dx,\ a_2(u,v)=\omega^2\int_\Omega\sum_{k=1}^{2}u_{x_k}v_{x_k}dx,\ a_1(u,v)=\theta^2\int_\Omega u_{x_3}v_{x_3}dx;$$

$u=u(t)$ is the function of abstract argument $t\in[0,T]$ with the meaning in H.

We denote $\|u\|_1=\sqrt{\int_\Omega\left(\sum_{k=1}^3\left(u_{x_k}\right)^2+u^2\right)dx}$ norm in H. It is obvious that $0\le a_1(u,u)\le C_1\|u\|_1^2, 0\le a_2(u,u)\le C_2\|u\|_1^2, c_3\|u\|_1^2\le a_3(u,u)\le C_3\|u\|_1^2$, where C_1, C_2, C_3, c_3 are positive constants that depend on θ, ρ, ω.

DISCRETIZATION BY SPACE AND TIME

We discretize the problem by spatial variables using the finite element method. Let $H_h\subset H$ multiple view elements $v_h=\sum_{m=1}^M a_m\Phi_m(x)$. Here $\{\Phi_m=\Phi_m(x)\}_{m=1}^M$ is a basis of piecewise polynomial functions that are a polynomial of degree p on each finite element [7, 8].

We give an example of a basis based on polynomials of the third degree. Let us introduce a partition of the area Ω on $M=N_1*N_2*N_3$ parallelepipeds:

$$\Omega_{ijk}=\{(i-1)h_1\le x_1\le ih_1, (j-1)h_2\le x_2\le jh_2, (k-1)h_3\le x_3\le kh_3\},$$

$i=\overline{1,N_1}, j=\overline{1,N_2}, k=\overline{1,N_3}, h_s=l_s/N_s, s=1,2,3.$

Let us choose a system of basic functions:

$$\Phi_{ijk}(x_1,x_2,x_3)=\phi_i(x_1)\phi_j(x_2)\phi_k(x_3), i=\overline{1,N_1}, j=\overline{1,N_2}, k=\overline{1,N_3},$$

where $\phi_l(x)$ is a basic function based on B_3 - spline [7]. In this case $p=3$.

Let us set for (6), (7) a semi-discrete problem for $t\in[0,T]$:

$$a_3\left(\frac{d^2u_h(t)}{dt^2},v_h\right)+a_2\left(\frac{d^2u_h(t)}{dt^2},v_h\right)+a_1\left(u_h(t),v_h\right)=\left(f(t),v_h\right), \tag{8}$$

$$(u_h(0)-u_0,v_h)=0,\ \left(\frac{du_h}{dt}(0)-u_1,v_h\right)=0,\ \forall v_h(x)\in H_h. \tag{9}$$

The problem (8), (9) corresponds to the Cauchy problem:

$$D\frac{d^2u_h(t)}{dt^2}+Au_h(t)=f_h(t),\ u_h(0)=u_{0,h},\ \frac{du_h}{dt}(0)=u_{1,h}. \tag{10}$$

Operators D,A operate from H_h to H_h. They correspond to the stiffness matrix $D=(a_3(\phi_l,\phi_m)+(a_2(\phi_l,\phi_m))_{l,m=1}^{M}$ and $A=(a_1(\phi_l,\phi_m))_{l,m=1}^{M}$. Besides that, $u_{k,h}=P_hu_k(x), k=0,1$, where P_h is an operator of the form $P_hH=H_h$.

We approximate the problem (10) in time with the difference scheme [9]:

$$D_\gamma\dot{y}_t+Ay^{(0.5)}=\phi_1,\ D_\alpha y_t-D_\beta\dot{y}^{(0.5)}=\phi_2,\ y^0=u_0,\ \dot{y}^0=u_1. \tag{11}$$

Here $y=y^n=y(t_n),\ \dot{y}=\dot{y}^n=\frac{dy}{dt}(t_n),\ D_\gamma=D-\gamma\tau^2A,\ D_\beta=D-\beta\tau^2A,\ y_t=\left(y^{n+1}-y^n\right)/\tau,\ \dot{y}_t=\left(\dot{y}^{n+1}-\dot{y}^n\right)/\tau,$ $y^{(0.5)}=\left(y^{n+1}+y^n\right)/2,\ \dot{y}^{(0.5)}=\left(\dot{y}^{n+1}+\dot{y}^n\right)/2,\ y^n,\dot{y}^n\in H_h,\ n=0,1,\ldots$ Further $\Phi_k=\int_0^1 f(t_n+\tau\xi)v_k(\xi)d\xi,\ k=1,2,\ \xi=(t-t_n)/\tau,\ v_1(\xi)=1,\ v_2(\xi)=s_1v_2^{(1)}(\xi)+s_2v_2^{(2)}(\xi),\ v_2^{(1)}(\xi)=\tau(\xi-1/2),\ v_2^{(2)}(\xi)=\tau(\xi^3-3\xi^2/2+\xi/2),\ s_1=180\beta-40\alpha,\ s_2=1680\beta-280\alpha.$

Parameters α,β,γ subject to the condition of the fourth order of approximation

$$\alpha+\beta=\gamma+1/6. \tag{12}$$

ACCURACY RESEARCH OF DISCRETIZATION IN SPACE-BASED SAMPLING

Theorem 1. *Let $u(x,t),\frac{\partial u}{\partial t}(x,t)\in C\left([0,T];W_2^{p+1}(\Omega)\cap H\right)$. If space is narrowed H_h on a separate finite element is a polynomial of degree p, then for solving the problem (6), (7) there is an accuracy estimation*

$$\|u(x,t)-u_h(x,t)\|_1\le Mh^k\left(\max_{t'}\|\frac{\partial u}{\partial t}(x,t')\|_{k+1}+\sqrt{\int_0^t\|\frac{\partial u}{\partial t}(x,t')\|_{k+1}^2dt'}+\sqrt{\int_0^t\|u(x,t')\|_{k+1}^2dt'}\right),$$

$\forall t\in[0,T], M=M(T,\rho,\theta,\omega)>0.$

Proof. Integrate identities (6), (7) and (8), (9) by t from t_n till $t_{n+1}=t_n+\tau$. Applying the integration formula in parts and subtracting both obtained identities, we get:

$$\int_{t_n}^{t_{n+1}}[-a_3(\dot{u}-\dot{u}_h,\dot{v}_h)+a_2(\dot{u}-\dot{u}_h,\dot{v}_h)+a_1(u-u_h,v_h)]dt$$
$$+a_3(\dot{u}-\dot{u}_h,v_h)\big|_{t_n}^{t_{n+1}}+a_2(\dot{u}-\dot{u}_h,v_h)\big|_{t_n}^{t_{n+1}}=0,\forall v_h(x)\in H_h. \tag{13}$$

Denote $e_h=u-u_I,\xi_h=u_I-u_h,z_h=u-u_h=e_h+\xi_h$, where $u_I=P_hu(x,t)$. Choose $v_h(t)=-\int_t^s\xi_h(t')dt'\in H_h,t<s;v_h(t)=0,t\ge s$. It is clear that $\dot{v}_h(t)=\xi_h(t)$.

Enter the function $w_h(t)=\int_0^t\xi_h(t')dt'\in H_h,t<s;w_h(t)=0,t\ge s$, which is related to other functions in this way:$\dot{w}_h(t)=\xi_h(t),v_h(t)=w_h(t)-w_h(s)$. Taking into consideration $(\dot{\xi}_h,\xi_h)=0.5\frac{d}{dt}(\xi_h,\xi_h),a_k(\dot{v}_h,v_h)=0.5\frac{d}{dt}a_k(v_h,v_h)$, $k=1,2,3$ and $\xi_h(0)=0,v_h(s)=0,v_h(0)=w_h(s)$, with summation (13) by $n=\overline{0,m-1}$, where number m corresponds to a point in time $s=m\tau$, we get the following energy identity:

$$0.5a_3(\xi_h,\xi_h)(s)+0.5a_2(\xi_h,\xi_h)(s)+0.5a_1(w_h,w_h)(s)=-a_3(\dot{e}_h(0),w_h(s))$$
$$-a_2(\dot{e}_h(0),w_h(s))-\int_0^s[a_3(\dot{e}_h,\xi_h)+a_2(\dot{e}_h,\xi_h)-a_1(e_h,w_h(t)-w_h(s))]dt.$$

Evaluating the terms on the right-hand side using ε - inequality and taking into account Grönwall's lemma, we estimate

$$a_3(\xi_h,\xi_h)(s)+a_2(\xi_h,\xi_h)(s)+a_1(w_h,w_h)(s)\le M(a_3(\dot{e}_h(0),\dot{e}_h(0))+a_2(\dot{e}_h(0),\dot{e}_h(0))$$
$$+\int_0^s a_3(\dot{e}_h,\dot{e}_h)dt+\int_0^s a_2(\dot{e}_h,\dot{e}_h)dt+\int_0^s a_1(e_h,e_h)dt),$$

where M is permanent. From here, since $0\le a_1(u,u)\le C_1\|u\|_1^2$, we have:

$$\|\xi_h(s)\|_1^2\le M\left(\|\dot{e}_h(0)\|_1^2+\int_0^s\|\dot{e}_h(t)\|_1^2dt+\int_0^s\|e_h(t)\|_1^2\right). \tag{14}$$

For the solution $u(x,t), \dot{u}(x,t) \in W_2^{k+1}(\Omega), \forall t \in [0,T]$ there are assessments [8]: $\|e_h(t)\|_1 \le Mh^k\|u(t)\|_{k+1}, \|\dot{e}_h(t)\|_1 \le Mh^k\|\dot{u}(t)\|_{k+1}$. Therefore, based on (14) and the triangle inequality $\|z_h\| \le \|e_h\| + \|\xi_h\|$ there is a statement of the theorem. ■

ACCURACY RESEARCH OF DISCRETIZATION IN TIME

Theorem 2. *Let $D^* = D > 0, A^* = A > 0$. Apart from that, let the approximation (12) and stability conditions be met*

$$D - \mu\tau^2 A \ge \varepsilon D,\ \forall \varepsilon \in (0,1),\ \mu = \max\{\alpha, \beta\gamma, 0\}. \tag{15}$$

Then for the solution of the scheme (11) approximating the solution of the problem (10) such that $\frac{d^4u_h}{dt^4}(t) \in C[0,T]$, the accuracy score is correct

$$\|u_h(t) - y(t)\|_1 \le M\tau^3\sqrt{\int_0^t \|\frac{d^4u_h}{dt^4}(t')\|_1^2 dt'}.$$

Proof. Let $y = y(x,t) \in H_h^\tau = H_h \otimes H_\tau$. As usual we denote $e_\tau = y - u_\tau, \xi_\tau = u_\tau - u_h, \zeta_\tau = y - u_h = e_\tau + \xi_\tau$, where

$$u_\tau(t) = u_h^n\phi_{00}^n(t) + \dot{u}_h^n\phi_{10}^n(t) + u_h^{n+1}\phi_{01}^n(t) + \dot{u}_h^{n+1}\phi_{11}^n(t).$$

Being that $\zeta_\tau(t) = \xi_\tau(t) + e_\tau(t)$, then for $v_\tau(t) = -\int_t^s \xi_\tau(t)dt', t < s; v_\tau(t) = 0, t \ge s$ we get the energy identity:

$$\begin{aligned} &0.5a_3(\xi_\tau, \xi_\tau)(s) + 0.5a_2(\xi_\tau, \xi_\tau)(0) + 0.5a_1(v_\tau, v_\tau)(0) \\ &= a_3(\dot{e}_\tau, v_\tau)(0) + a_2(\dot{e}_\tau, v_\tau)(0) + \int_0^s [a_3(\dot{e}_\tau, \xi_\tau) + a_2(\dot{e}_\tau, \xi_\tau) - a_1(e_\tau, v_\tau)]dt. \end{aligned}$$

Denote $w_\tau(t) = \int_0^t \xi_\tau(t')dt', t < s, w_\tau(t) = 0, t \ge s$ and note, that $\dot{e}_\tau(0) = \dot{u}_h(0) - \dot{u}_\tau(0) = u_{1,h} - u_{1,h} = 0$. Then from the last identity we get the main energy identity for the error $\xi_\tau(t)$:

$$\begin{aligned} &0.5a_3(\xi_\tau, \xi_\tau)(s) + 0.5a_2(\xi_\tau, \xi_\tau)(s) + 0.5a_1(w_\tau, w_\tau)(s) \\ &= \int_0^s [a_3(\dot{e}_\tau, \xi_\tau) + a_2(\dot{e}_\tau, \xi_\tau) - a_1(e_\tau, w_\tau(t) - w_\tau(s))]dt. \end{aligned}$$

From this identity we get an estimate

$$\|\xi_\tau(s)\|_1^2 \le M\left(\int_0^s \|\dot{e}_\tau(t)\|_1^2 dt + \int_0^s \|e_\tau(t)\|_1^2 dt\right).$$

The linear and bounded functions $\dot{e}_\tau(t), e_\tau(t)$ vanish on polynomials up to the third degree including the variable t. Then, based on the Bramble-Hilbert lemma [10], for example, we have

$$\int_0^s \|e_\tau(t')\|_1^2 dt' \le M^2\tau^8 \int_0^s \|\frac{d^4u_h}{dt^4}(t)\|_1^2 dt.$$

However

$$\int_0^s \|\dot{e}_\tau(t')\|_1^2 dt' \le M^2\tau^6 \int_0^s \|\frac{d^4u_h}{dt^4}(t)\|_1^2 dt.$$

From here, given $\|y - u_h\| \le \|e_\tau\| + \|\xi_\tau\|$, we get a statement of the theorem. ■

ON THE CONVERGENCE OF THE SCHEME

Note that in the evaluation of Theorem 2, the error depends on the solution $u_h(t)$ of semi-discrete problem (10),whereas it is desirable to have smoothness requirements for solving the original problem (4). To do this, use the estimate [8]:

$$\|u_h\|_k = \|u-u+u_h\|_k \leq \|u\|_k + \|u-u_h\|_k \leq \|u\|_k + Ch|u|_{k+1} \leq \overline{C}\|u\|_{k+1}, k=0,1.$$

Constant $\overline{C}$ does not depend on h.

Therefore, the estimate in Theorem 2 will take the form

$$\|u_h(t)-y(t)\|_1 \leq M\tau^3\sqrt{\int_0^t \|\frac{\partial^4 u}{\partial t^4}(x,t')\|_2^2 dt'}.$$

Based on Theorems 1 and 2, a statement takes place.

Theorem 3. *Let the conditions of Theorem 2 will be fulfilled. Then for the solution of the scheme (11) approximating the solution of the problem (4) such that $u(x,t)$, $\frac{\partial u}{\partial t}(x,t) \in C\{[0,T];W_2^2(\Omega)\}$, $\frac{\partial^4 u}{\partial t^4}(x,t) \in C\{[0,T];W_2^2(\Omega)\}$, the accuracy estimation is correct:*

$$\|u(x,t)-y(x,t)\|_1 \leq M\Bigg\{h^k\left(\max_t \|\frac{\partial u}{\partial t}(x,t)\|_{k+1} + \sqrt{\int_0^t \|u(x,t')\|_{k+1}^2 dt'}\right)$$
$$+\tau^3\sqrt{\int_0^t \|\frac{\partial^4 u}{\partial t^4}(x,t')\|_2^2 dt'}\Bigg\}, \forall t \in [0,T], M=M(T,\rho,\theta,\omega_0)>0.$$

When selecting on each finite element of the space of a polynomial of degree $k=3$ we obtain the third order of accuracy for both steps h,τ.

Make sure that the stability condition (15) holds. Let us represent the operators of the scheme (11) as

$$D=(1+\omega^2)(A_1+A_2)+A_3+\rho^2 E, A=\theta^2 A_3,$$

where operators $A_k \geq 0$ correspond to the stiffness matrix $A_k=(b_k(\phi_l,\phi_m))_{l,m=1}^M$ with the bilinear form $b_k(u,v)=\int_\Omega \left(u_{x_k},v_{x_k}\right)dx$. Condition (15) takes the form

$$(1-\varepsilon)[(1+\omega^2)(A_1+A_2)+A_3+\rho^2 E]-\mu\tau^2\theta^2 A_3 \geq 0.$$

To fulfill it, it is sufficient that

$$\tau^2 \leq \frac{1-\varepsilon}{\mu\theta^2}, \text{ where } 0<\varepsilon<1.$$

The last condition is interesting because the time step is not related to the space step and is determined by the parameters of the problem. For scheme parameters (11), for instance, at $\alpha=1/8, \beta=1/24$ we have $\mu=1/8$. So finally $\tau \leq \frac{2\sqrt{2(1-\varepsilon)}}{\theta}$.

ALGORITHM FOR IMPLEMENTING THE SCHEME

To implement the scheme (11), it is necessary to solve a system of two equations with respect to unknowns $\hat{y},\hat{\dot{y}}$:

$$m_{11}\hat{y}+m_{12}\hat{\dot{y}}=\Phi_1,\ m_{21}\hat{y}+m_{22}\hat{\dot{y}}=\Phi_2, \quad (16)$$

$$m_{11}=D-\tau^2\gamma A, m_{12}=0.5\tau A, m_{21}=-0.5\tau(D-\beta\tau^2 A), m_{22}=D-\alpha\tau^2 A,$$

$$\Phi_1=\tau\phi_1-0.5\tau Ay+(D-\tau^2\gamma A)\dot{y}, \Phi_2=\tau\phi_2+(D-\alpha\tau^2 A)y+0.5\tau(D-\beta\tau^2 A)\dot{y}.$$

The parameters α, β, γ are subject to the fourth-order approximation condition of the scheme (11). Further, for definiteness, $\alpha = 1/8, \beta = 1/24, \gamma = 1/12$.

With the exception of (11) $\hat{\dot{y}}$, we get the equation for finding $\hat{y}$:

$$C\hat{y} = F, \tag{17}$$

where $C = m_{22}m_{11} - m_{12}m_{21} = D^2 - (\alpha + \gamma - 1/4)\tau^2 AD + (\alpha\gamma - \beta/4)\tau^4 A^2, F = m_{12}\Phi_2 - m_{22}\Phi_1$.

The first algorithm for implementing the scheme (16) consists of directly solving the equation (17), and then calculating $\hat{\dot{y}}$ from the first equation in (16):

$$(D - \tau^2\gamma A)\hat{\dot{y}} = \Phi_1 - 0.5\tau A\hat{y}.$$

The second algorithm for implementing the scheme (16) is reduced to solving two equations at each step in time:

$$Cy^{n+1} = F_1, C\dot{y}^{n+1} = F_2,$$

where $C = D^2 - (\alpha - 1/6)\tau^2 AD + (\alpha/12 - \beta/4)\tau^4 A^2$, and the right-hand parts F_1, F_2 calculated by known $y^n, \dot{y}^n$ and ϕ_1, ϕ_2.

The matrix C is factorized $C = C_1C_2 = (D - \sigma_1 A)(D - \sigma_2 A)$, where σ_1, σ_2 are the roots of the equation $\sigma^2 + (\alpha + \gamma - 1/4)\sigma + (\alpha\gamma - \beta/4) = 0$.

For $\alpha = 1/8, \beta = 1/24$, for example, we have $\sigma_1 = -1/24, \sigma_2 = 0$. Then there will be this

$$y^{n+1} = C^{-1}F_1 = C_2^{-1}C_1^{-1}F_1, \dot{y}^{n+1} = C_2^{-1}C_1^{-1}F_2.$$

For matrix inversion C_1, C_2 the direct square root method is applied once at the initial point in time. On the other layers, the solution is found by multiplying the matrix $C^{-1} = C_2^{-1}C_1^{-1}$ on the vector F_1, F_2.

REMARK

The scheme (11) has certain advantages over other schemes: a) a scheme of high order of accuracy (above two); b) in addition to the solution itself, at the same time its derivative (speed) is found with the same accuracy; c) using the interpolation representation

$$y(t) = y^n\phi_{00}^n(t) + \dot{y}^n\phi_{10}^n(t) + y^{n+1}\phi_{01}^n(t) + \dot{y}^{n+1}\phi_{11}^n(t), \phi_{00}^n(t) = 2\xi^3 - 3\xi^2 + 1, \phi_{01}^n(t) = 3\xi^2 + 2\xi^3,$$

$$\phi_{10}^n(t) = \tau(\xi^3 - 2\xi^2 + \xi), \phi_{11}^n(t) = \tau(\xi^3 - \xi^2),$$

if necessary, we can obtain a solution and its derivative at any time; d) since the schemes are two-layer, it is possible to use a variable pitch without loss of accuracy; e) the scheme is conditionally stable and requires 4 times more arithmetic operations than usual, but this scheme for achieving a certain accuracy allows you to choose large steps in time.

REFERENCES

1. S. A. Gabov, *New Problems of Mathematical Theory of Waves* (Moscow: Nauka, 1998).
2. S. A. Gabov and A. G. Sveshnikov, *Linear Problems of the Theory of Non-Stationary Internal Waves* (Moscow: Nauka, 1990).
3. A. G. Sveshnikov, A. B. Alshin, M. O. Korpusov, and Y. D. Pletner, *Linear and Nonlinear Equations of the Sobolev type* (Moscow: FIZMATLIT, 2007).
4. M. N. Moskalkov and D. Utebaev, Mathematical Models and Computer Simulations **3**, 264–271 (2012).
5. M. N. Moskalkov and D. Utebaev, Journal Computation and Applied Mathematics **2**, 97–104 (2010).
6. M. N. Moskalkov and D. Utebaev, Cybernetics and Systems Analysis **47**, 459–465 (2011).
7. G. I. Marchuk and V. I. Agoshkov, *Introduction to Projection-Grid Methods* (Moscow: Nauka, 1981).
8. A. Quarteroni and A. Valli, *Numerical Approximation of Partial Differential Equations* (Berlin: Springer-Verlag, 1994).
9. M. N. Moskalkov and D. Utebaev, Journal Computation and Applied Mathematics **92**, 70–76 (2005).
10. P. Ciarlet, *The Finite Element Method for Elliptic Problems* (Oxford, 1978).

Chatterjea-Type Fixed Point Theorem on Cone Rectangular Metric Spaces with Banach Algebras

Abba Auwalu[1, 2, a)] and Ali Denker[2, b)]

[1)] *Sule Lamido University Kafin Hausa, Nigeria*
[2)] *Near East University, Nicosia, Turkey*

[a)] *Electronic mail: abba.auwalu@slu.edu.ng, abba.auwalu@neu.edu.tr*
[b)] *Corresponding author: ali.denker@neu.edu.tr, adenker63@gmail.com*

Abstract. In this paper, we shall establish the existence and uniqueness of fixed point of a Chatterjea - type contraction in Cone rectangular metric spaces over Banach algebras. We shall further give an example to illustrate our main results. Our results extend and generalize some results in the literature.

INTRODUCTION AND PRELIMINARIES

In 1972, Chatterjea [1] proved the following fixed point theorem:

Theorem 1 ([1]) *Let (K,η) be a complete metric space. Suppose that the mapping $J : K \to K$ satisfies the following contractive condition*

$$\eta(Jy,Jz) \preccurlyeq \gamma[\eta(Jy,z)+\eta(Jz,y)], \text{ for all } y,z \in K, \tag{1}$$

where $0 \leq \gamma < 1/2$ is a constant. Then J has a unique fixed point in K.

The following definitions and Lemmas will be needed in the sequel.

Definition 1 ([2]) *A Banach algebra B is a real Banach space in which an operation of multiplication is defined subject to the following properties, for all $x,y,z \in B$, $\lambda \in \mathbb{R}$:*
(1) $(xy)z = x(yz)$; (2) $x(y+z) = xy+xz$ *and* $(x+y)z = xz+yz$;
(3) $\lambda(xy) = (\lambda x)y = x(\lambda y)$; (4) $\|xy\| \leq \|x\|\,\|y\|$.

Definition 2 ([4]) *A subset C of Banach algebra B is called a cone if:*
(1) *C is nonempty, closed and* $\{\theta,e\} \subset C$;
(2) $k_1C+k_2C \subset C$ *for all nonnegative real numbers* k_1,k_2;
(3) $C^2 = CC \subset C$; (4) $C\cap(-C) = \{\theta\}$, *where θ and e denote the zero and unit elements of the Banach algebra B, respectively.*
For a given cone $C \subset B$, we write $y \preccurlyeq z$ if and only if $z-y \in C$, where $\preccurlyeq$ is a partial order relation defined on C. We shall write $y \prec z$ to indicate that $y \preccurlyeq z$ but $y \neq z$, while $y \ll z$ will stand for $z-y \in intC$, where intC denotes the interior of C. If $intC \neq \varnothing$ then C is called a solid cone.

The cone C is called normal if there is a number N such that, for all $y,z \in B$,

$$\theta \preccurlyeq y \preccurlyeq z \Longrightarrow \|y\| \leq N\|z\|.$$

Definition 3 ([5]) *Let S be a solid cone in a Banach algebra B. A sequence $\{y_i\} \subset S$ is said to be a c-sequence if for each $\theta \ll c$ there exists $n_0 \in \mathbb{N}$ such that $y_i \ll c$ for all $i > n_0$.*

Lemma 1 ([5]) *Let S be a solid cone in a Banach algebra B and $\{y_i\} \subset S$ be a sequence with $\|y_i\| \to 0$ $(i \to \infty)$, then for each $\theta \ll c$, there exists $n_0 \in \mathbb{N}$ such that for all $i > n_0$, we have $y_i \ll c$.*

Lemma 2 ([2]) *Let B be a Banach algebra with a unit element e and $\gamma \in B$. If the spectral radius $\delta(\gamma)$ of γ is less than one, i.e. $\delta(\gamma) = \lim_{n\to\infty}\|\gamma^n\|^{\frac{1}{n}} = inf_{n\in\mathbb{N}}\|\gamma^n\|^{\frac{1}{n}} < 1$, then $(e-\gamma)$ is invertible in B. Moreover, $(e-\gamma)^{-1} = \sum_{j=0}^{\infty}\gamma^j$.*

Lemma 3 ([5]) *If the spectral radius $\delta(\gamma) < 1$, then*
(1) $\|\gamma^i\| \to 0$ $(i \to \infty)$
(2) $\delta[(e-\gamma)^{-1}] \leq [1-\delta(\gamma)]^{-1}$.

International Conference on Analysis and Applied Mathematics (ICAAM 2020)
AIP Conf. Proc. 2325, 020060-1–020060-6; https://doi.org/10.1063/5.0040595
Published by AIP Publishing. 978-0-7354-4069-2/$30.00

Lemma 4 ([7]) *Let B be a real Banach algebra with a solid cone S. For $a,b,c,\gamma \in S$, if*
(1) $a \preccurlyeq b \ll c$, *then* $a \ll c$. (2) $\theta \preccurlyeq a \ll c$, *for each* $\theta \ll c$, *then* $a = \theta$. (3) $a \preccurlyeq \gamma a$ *and* $\delta(\gamma) < 1$, *then* $a = \theta$.

Definition 4 ([4]) *Let $\mathscr{X}$ be a nonempty set and B be a Banach algebra. Suppose that the mapping $\rho : \mathscr{X} \times \mathscr{X} \to B$ satisfies, $\forall x,y,z \in \mathscr{X}$, the following conditions:*
(C_1) $\theta \preccurlyeq \rho(x,y)$ *and* $\rho(x,y) = \theta \Leftrightarrow x = y$;
(C_2) $\rho(x,y) = \rho(y,x)$;
(C_3) $\rho(x,y) \preccurlyeq \rho(x,z) + \rho(z,y)$ *(Triangle inequality).*
Then ρ is called a cone metric on $\mathscr{X}$, and $(\mathscr{X}, \rho)$ is a cone metric space over Banach algebra B.

Remark 1 *A metric space is a cone metric space over Banach algebra B where by $B = \mathbb{R}$ and $C = [0,+\infty)$. The converse is not true (e.g. see [*3, 4, 6*]).*

Definition 5 ([7]) *Let K be a nonempty set and B be a Banach algebra. Suppose that $\eta : K \times K \to B$ is a mapping satisfying, $\forall x,y,u,v \in K$, $x \neq u, u \neq v, v \neq y$, the following conditions:*
(R_1) $\theta \preccurlyeq \eta(x,y)$ *and* $\eta(x,y) = \theta \Leftrightarrow x = y$;
(R_2) $\eta(x,y) = \eta(y,x)$;
(R_3) $\eta(x,y) \preccurlyeq \eta(x,u) + \eta(u,v) + \eta(v,y)$ *(Rectangular inequality).*
Then η is called a cone rectangular metric on K, and (K,η) is called a cone rectangular metric space over Banach algebra B.

Remark 2 *A cone metric space over Banach algebra B is a cone rectangular metric space over Banach algebra B. The converse is not true (see [*7*]).*

Definition 6 ([7]) *Let (K,η) be a cone rectangular metric space over Banach algebra B, $y \in K$ and $\{y_i\}$ be a sequence in (K,η). Then we say*
(1) $\{y_i\}$ *converges to y if, for each $c \in B$ with $\theta \ll c$, there is a natural number n_0 such that $\eta(y_i, y) \ll c$ for all $i \geq n_0$. We denote this by $y_i \to y$ $(i \to \infty)$.*
(2) $\{y_i\}$ *is a Cauchy sequence if, for each $c \in B$ with $\theta \ll c$, there is a natural number n_0 which is independent of j such that $\eta(y_i, y_{i+j}) \ll c$ for all $i \geq n_0$.*
(3) (K,η) *is said to be complete if every Cauchy sequence is convergent.*

Lemma 5 ([8]) *Let (K,η) be a complete cone rectangular metric space over Banach algebra B, S be the underlying solid cone and $\{y_i\}$ be a sequence in (K,η). If $\{y_i\}$ converges to $y \in K$, then*
(1) $\{\rho(y_i, y)\}$ *is a c-sequence.* (2) *for any* $j \in \mathbb{N}$, $\{\rho(y_i, y_{i+j})\}$ *is a c-sequence.*

Lemma 6 ([5]) *Let B be a Banach algebra with a solid cone S and let $\{\alpha_n\}$ and $\{\beta_n\}$ be sequences in S. If $\{\alpha_n\}$ and $\{\beta_n\}$ are c-sequences and $k_1, k_2 \in S$ then $\{k_1\alpha_n + k_2\beta_n\}$ is also a c-sequence.*

Lemma 7 ([7]) *Let $\{y_i\}$ be a Cauchy sequence in a cone rectangular metric space (K,η) over Banach algebra B such that $y_i \neq y_j$ whenever $i \neq j$. If $y, z \notin \{y_i : i \in \mathbb{N}\}$ and $\{y_i\}$ converges to both y and z, then $y = z$.*

MAIN RESULTS

Theorem 2 *Let (K,η) be a complete cone rectangular metric space over Banach algebra B with a unit element e and S be a solid cone in B. Suppose that the mapping $J : K \to K$ satisfies the Chatterjea - type contraction* (1)*, where $\gamma \in S$ such that the spectral radius $\delta(\gamma) < 1/2$. Then*
(I) *J has a unique fixed point in K.*
(II) *For any point $y_0 \in K$, the iterative sequence $\{J^i y_0\}$ $(i \in \mathbb{N})$ converges to the fixed point.*

Proof. To show part (I); we firstly show that the mapping J has at most one fixed point, say $y_* \in K$. Now, suppose that y_* and y^* are both fixed point of the mapping J. That is; $y_* = Jy_*$ and $y^* = Jy^*$. From (1) it follows that

$$\begin{aligned}
\eta(y_*, y^*) &= \eta(Jy_*, Jy^*) \\
&\preccurlyeq \gamma\big[\eta(Jy_*, y^*) + \eta(Jy^*, y_*)\big] \\
&= \gamma\big[\eta(y_*, y^*) + \eta(y^*, y_*)\big]. \\
\therefore \quad \eta(y_*, y^*) &\preccurlyeq 2\gamma\eta(y_*, y^*).
\end{aligned}$$

Since $\delta(\gamma) < 1/2$, it follows that $\delta(2\gamma) < 1$, and using Lemma 4(3), we have that $\eta(y_*, y^*) = \theta$. Hence $y_* = y^*$ i.e. the fixed point of J, if it exists, is unique.
Next, we prove the existence of the fixed point y_* in K and show part (II). By choosing an arbitrary point $y_0 \in K$, we define a sequence $\{y_i\}$ in (K, η) as follows: $Jy_0 = y_1, Jy_1 = J^2y_0 = y_2, \cdots, Jy_i = J^{i+1}y_0 = y_{i+1}, \cdots$. That is,

$$Jy_i = y_{i+1}, \text{ for all } i \in \mathbb{N}. \tag{2}$$

Suppose $y_j = y_{j+1}$ for some $j \in \mathbb{N}$, then $y_* := y_j = Jy_j$ is a fixed point of J and the result is proved. Hence, we assume that $y_i \neq y_{i+1}$ for all $i \in \mathbb{N}$. We shall show that $\{Jy_i\}$ is a Cauchy sequence in (K, η). By using (1), (2) and Rectangular inequality, we have that

$$\begin{aligned}
\eta(y_i, y_{i+1}) &= \eta(Jy_{i-1}, Jy_i) \\
&\preccurlyeq \gamma\big[\eta(Jy_{i-1}, y_i) + \eta(Jy_i, y_{i-1})\big] \\
&= \gamma\eta(Jy_{i-1}, y_i) + \gamma\eta(y_{i+1}, y_{i-1}) \\
&\preccurlyeq \gamma\eta(Jy_{i-1}, y_i) + \gamma\big[\eta(y_{i+1}, y_i) + \eta(y_i, Jy_{i-1}) + \eta(Jy_{i-1}, y_{i-1})\big] \\
&= 2\gamma\eta(Jy_{i-1}, y_i) + \gamma\big[\eta(y_{i+1}, y_i) + \eta(Jy_{i-1}, y_{i-1})\big] \\
&\preccurlyeq 2\gamma\eta(y_i, y_i) + \gamma\big[\eta(y_{i+1}, y_i) + \eta(y_i, y_{i-1})\big] \\
(e-\gamma)\eta(y_i, y_{i+1}) &\preccurlyeq \gamma\eta(y_{i-1}, y_i). \\
\therefore\ \ \eta(y_i, y_{i+1}) &\preccurlyeq (e-\gamma)^{-1}\gamma\eta(y_{i-1}, y_i) = \lambda\eta(y_{i-1}, y_i),
\end{aligned} \tag{3}$$

where $\lambda = (e-\gamma)^{-1}\gamma \in B$. Hence, from (2) and (3), we obtain that

$$\begin{aligned}
\eta(y_i, y_{i+1}) &\preccurlyeq \lambda\eta(y_{i-1}, y_i) = \lambda\eta(Jy_{i-2}, Jy_{i-1}) \\
&\preccurlyeq \lambda^2\eta(y_{i-2}, y_{i-1}) = \lambda^2\eta(Jy_{i-3}, Jy_{i-2}) \\
&\preccurlyeq \lambda^3\eta(y_{i-3}, y_{i-2}) \\
&\ \vdots \\
&\preccurlyeq \lambda^i\eta(y_0, y_1) \text{ for all } i \in \mathbb{N}.
\end{aligned} \tag{4}$$

Similarly, by using (1), (2) and (4), we have that

$$\begin{aligned}
\eta(y_i, y_{i+2}) &= \eta(Jy_{i-1}, Jy_{i+1}) \\
&\preccurlyeq \gamma\big[\eta(Jy_{i-1}, y_{i+1}) + \eta(Jy_{i+1}, y_{i-1})\big] \\
&\preccurlyeq \gamma\eta(y_i, y_{i+1}) + \gamma\big[\eta(y_{i+2}, y_{i+1}) + \eta(y_{i+1}, y_i) + \eta(y_i, y_{i-1})\big] \\
&\preccurlyeq \gamma\big[\lambda^i\eta(y_0, y_1) + \lambda^{i+1}\eta(y_0, y_1) + \cdots + \lambda^{i+4}\eta(y_0, y_1)\big] \\
&\preccurlyeq \gamma\lambda^i\left(\sum_{n=0}^{\infty}\lambda^n\right)\eta(y_0, y_1) \\
&\preccurlyeq \gamma\lambda^i\big(e-\lambda\big)^{-1}\eta(y_0, y_1), \text{ for all } i \in \mathbb{N}.
\end{aligned} \tag{5}$$

Now, for the sequence $\{Jy_i\}$, we consider $\eta(Jy_i, Jy_{i+j})$ in two cases:

Case 1. If j is odd, say $j = 2n+1$ $(n \in \mathbb{N})$, then it follows that

$$\begin{aligned}
\eta(y_i, y_{i+2n+1}) &\preccurlyeq \eta(y_{i+2n}, y_{i+2n+1}) + \eta(y_{i+2n-1}, y_{i+2n}) + \eta(y_i, y_{i+2n-1}) \\
&\preccurlyeq \eta(y_{i+2n}, y_{i+2n+1}) + \eta(y_{i+2n-1}, y_{i+2n}) + \eta(y_{i+2n-2}, y_{i+2n-1}) \\
&\quad + \eta(y_{i+2n-3}, y_{i+2n-2}) + \eta(y_i, y_{i+2n-3}) \\
&\preccurlyeq \eta(y_{i+2n}, y_{i+2n+1}) + \eta(y_{i+2n-1}, y_{i+2n}) + \eta(y_{i+2n-2}, y_{i+2n-1}) \\
&\quad + \cdots + \eta(y_{i+1}, y_{i+2}) + \eta(y_i, y_{i+1}) \\
&\preccurlyeq \lambda^{i+2n}\eta(y_0, y_1) + \lambda^{i+2n-1}\eta(y_0, y_1) + \lambda^{i+2n-2}\eta(y_0, y_1) \\
&\quad + \cdots + \lambda^{i+1}\eta(y_0, y_1) + \lambda^{i}\eta(y_0, y_1) \\
&\preccurlyeq \lambda^i \left(\sum_{n=0}^{\infty} \lambda^n \right) \eta(y_0, y_1) \\
&\preccurlyeq \lambda^i (e-\lambda)^{-1} \eta(y_0, y_1).
\end{aligned}$$

By Lemma 3 and the fact that $\delta(\gamma) < 1/2$, it follows that

$$\begin{aligned}
\delta[(e-\lambda)^{-1}\gamma] &\preccurlyeq \delta[(e-\lambda)^{-1}]\delta(\gamma) \\
&\preccurlyeq [1-\delta(\lambda)]^{-1}\delta(\gamma) \\
&\preccurlyeq 1.
\end{aligned}$$

Then $\|\lambda^i (e-\lambda)^{-1}\eta(y_0, y_1)\| \le \|\lambda^i\| \, \|(e-\lambda)^{-1}\eta(y_0, y_1)\| \to 0$ $(i \to \infty)$ and by Lemma 1 for any $c \in B$ with $\theta \ll c$, there exists $n_1 \in \mathbb{N}$ such that

$$\eta(y_i, y_{i+2n+1}) \preccurlyeq \lambda^i (e-\lambda)^{-1}\eta(y_0, y_1) \ll c, \text{ for all } i > n_1.$$

Therefore, by using Lemma 4(1), we have that

$$\eta(y_i, y_{i+2n+1}) \ll c, \text{ for all } i > n_1. \tag{6}$$

Case 2. If j is even, say $j = 2n$ $(n \in \mathbb{N})$, then it follows that

$$\begin{aligned}
\eta(y_i, y_{i+2n}) &\preccurlyeq \eta(y_{i+2n-1}, y_{i+2n}) + \eta(y_{i+2n-1}, y_{i+2n-2}) + \eta(y_i, y_{i+2n-2}) \\
&\preccurlyeq \eta(y_{i+2n-1}, y_{i+2n}) + \eta(y_{i+2n-2}, y_{i+2n-1}) + \eta(y_{i+2n-3}, y_{i+2n-2}) \\
&\quad + \eta(y_{i+2j-3}, y_{i+2n-4}) + \eta(y_i, y_{i+2n-4}) \\
&\preccurlyeq \eta(y_{i+2n-1}, y_{i+2n}) + \eta(y_{i+2n-2}, y_{i+2n-1}) + \eta(y_{i+2n-3}, y_{i+2n-2}) \\
&\quad + \cdots + \eta(y_{i+3}, y_{i+2}) + \eta(y_i, y_{i+2}) \\
&\preccurlyeq \lambda^{i+2n-1}\eta(y_0, y_1) + \lambda^{i+2n-2}\eta(y_0, y_1) + \lambda^{i+2n-3}\eta(y_0, y_1) \\
&\quad + \cdots + \lambda^{i+2}\eta(y_0, y_1) + \gamma\lambda^i (e-\lambda)^{-1}\eta(y_0, y_1) \\
&\preccurlyeq \lambda^{i+2} \left(\sum_{n=0}^{\infty} \lambda^n \right) \eta(y_0, y_1) + \gamma\lambda^i (e-\lambda)^{-1}\eta(y_0, y_1) \\
\therefore \quad \eta(y_i, y_{i+2n+1}) &\preccurlyeq \lambda^i (e-\lambda)^{-1} \left(\gamma + \lambda^2\right) \eta(y_0, y_1).
\end{aligned}$$

In similar fashion, we have that $\|\lambda^i (e-\lambda)^{-1} \left(\gamma + \lambda^2\right) \eta(y_0, y_1)\| \to 0$ $(i \to \infty)$, and for any $c \in B$ with $\theta \ll c$, there exists $n_2 \in \mathbb{N}$ such that

$$\eta(y_i, y_{i+2n}) \preccurlyeq \lambda^i (e-\lambda)^{-1} \left(\gamma + \lambda^2\right) \eta(y_0, y_1) \ll c, \text{ for all } i > n_2.$$

Therefore, by using Lemma 4(1), we have that

$$\eta(y_i, y_{i+2n}) \ll c, \text{ for all } i > n_2. \tag{7}$$

Let $n_0 := \max\{n_1, n_2\}$, hence, from (6) and (7), we have that

$$\eta(y_i, y_{i+n}) \ll c, \text{ for all } i \ge n_0,$$

which implies, by Definition 6(2), that $\{y_i\}$ is a Cauchy sequence in (K,η) and since (K,η) is complete, the sequence $\{y_i\}$ converges i.e. there exists y_* in K such that $y_i \to y_*$ $(i\to\infty)$. Now, using (1) and (2), we have

$$\begin{aligned}\eta(y_*,Jy_*) &\preccurlyeq \eta(y_*,y_i)+\eta(y_i,Jy_i)+\eta(Jy_i,Jy_*)\\ &\preccurlyeq \eta(y_*,y_i)+\eta(y_i,y_{i+1})+\gamma\big[\eta(Jy_i,y_*)+\eta(Jy_*,y_i)\big]\\ &\preccurlyeq \eta(y_*,y_i)+\eta(y_i,y_{i+1})+\gamma\eta(y_{i+1},y_*)+\gamma\eta(Jy_*,y_i).\end{aligned}$$

Using Lemma 5 and Lemma 6; $\{\eta(y_*,y_i)\}$, $\{\eta(y_i,y_{i+1})\}$, $\eta(y_{i+1},y_*)$, $\eta(Jy_*,y_i)$ and $\{\eta(y_*,y_i)+\eta(y_i,y_{i+1})+\gamma\eta(y_{i+1},y_*)+\gamma\eta(Jy_*,y_i)\}$ are c-sequences. Therefore, for any $c\in B$ with $\theta \ll c$, there exists $n_0\in\mathbb{N}$ such that

$$\eta(y_*,Jy_*) \preccurlyeq \eta(y_*,y_i)+\eta(y_i,y_{i+1})+\gamma\eta(y_{i+1},y_*)+\gamma\eta(Jy_*,y_i) \ll c, \text{ for all } i>n_0, \tag{8}$$

which implies, by part (1) and (2) of Lemma 4, that $\eta(y_*,Jy_*)=\theta$. Hence, $y_*=Jy_*$. Thus, y_* is a fixed point of J.

Example 1 *Let $B=C^1_{\mathbb{R}}[0,1]$ and define a norm on B by*

$$\|y\| = \|y\|_\infty + \|y'\|_\infty \text{ for } y\in B.$$

Define multiplication in B as just pointwise multiplication. Then B is a real Banach algebra with unit element $e=1$. The set $S=\{y\in B : y(t)\geq 0, t\in[0,1]\}$ is a non-normal cone in B.
Let $K=\{1,2,3,4\}$. Define $\eta : K\times K\to B$ by

$$\eta(y,z)=\begin{cases}0, & \text{if } y=z;\\ 3e^t, & \text{if } y,z\in\{1,2\} \text{ and } y\neq z;\\ e^t, & \text{otherwise.}\end{cases}$$

Then (K,η) is a cone rectangular metric space over Banach algebra B but not cone metric space because it lacks the triangular property.
Now, let $J: K\to K$ be a mapping define by

$$Jy=\begin{cases}1/4, & \text{if } 0\leq y<1;\\ 1/8, & \text{if } y=1.\end{cases}$$

Then the mapping K is a Chatterjea - type contraction (1) *with $\gamma=\frac{1}{7}$. Moreover, J satisfies all the conditions of Theorem 2 and $y_*=1/4$ is the unique fixed point of J.*

Corollary 1 ([5]) *Let (K,η) be a complete cone metric space over a Banach algebra B and S be a solid cone in B. Suppose that the mapping $J: K\to K$ satisfies the contractive condition* (1)*, where $\gamma\in S$ such that the spectral radius $\delta(\gamma)<1/2$. Then J has a unique fixed point in K. And for any $y\in K$, iterative sequence $\{J^i y\}$ converges to the fixed point.*

Proof. The result follows from Remark 2 and Theorem 2.

Corollary 2 ([4]) *Let (K,η) be a complete cone metric space over a Banach algebra B and S be a normal cone. Suppose that the mapping $J: K\to K$ satisfies the contractive condition* (1)*, where $\gamma\in S$ such that $\delta(\gamma)<1/2$. Then J has a unique fixed point in K. And for any $y\in K$, iterative sequence $\{J^i y\}$ converges to the fixed point.*

Proof. The result follows from Remark 2 and Corollary 1.

Corollary 3 ([3]) *Let (K,η) be a complete cone metric space, S be a normal cone in B. Suppose that the mapping $J: K\to K$ satisfies the contractive condition* (1)*, where $\gamma\in S$ such that $0\leq\gamma<1/2$ is a constant. Then J has a unique fixed point in K. And for any $y\in K$, iterative sequence $\{J^i y\}$ converges to the fixed point.*

Proof. The result follows from Remark 2 and Corollary 2.

Corollary 4 ([1]) *Let (K,η) be a complete metric. Suppose that the mapping $J: K\to K$ satisfies the contractive condition* (1)*, where $0\leq\gamma<1/2$ is a constant. Then J has a unique fixed point in K.*

Proof. The result follows from Remark 1 and Corollary 3.

CONCLUSION

The aim of this paper is to introduce a new Chatterjea- type contraction mappings on cone rectangular metric spaces over Banach algebras and establish the existence and uniqueness of fixed point for such mappings. Our results extend and generalize some results in [1, 3, 4, 5, 6] and others in the literature. Moreover, an example to illustrate the main results is also presented.

REFERENCES

1. S. K. Chatterjea, Rend. Acad. Bulgare Sci. **25**, 727 - 730 (1972).
2. W. Rudin, Functional Analysis (McGraw-Hill, New York, 1991).
3. L. G. Huang and X. Zhang, J. Math. Anal. Appl. **332**, 1468 - 1476 (2007).
4. L. Hao and X. Shaoyuan, Fixed Point Theory Appl. **320**, 1 - 10 (2013).
5. S. Xu, S. Radenović, Fixed Point Theory Appl. **102**, 1 - 12 (2014).
6. A. Auwalu, AIP Conf. Proc. **1997**, 020004 (2018).
7. S. Shukla, S. Balasubramanian, and M. Pavlovic, Bull. Mal. Math. Sci. Soc. **39**, 1529 - 1539 (2016).
8. A. Auwalu and A. Denker, Cone rectangular metric spaces over Banach algebras and fixed point results of T-contraction mappings, Fourth International Conference on Analysis and Applied Mathematics (ICAAM), Nicosia - Cyprus, 6 - 9 September, 2018.

Interpolation of Data in $\mathbb{R}^3$ using Quartic Triangular Bézier Surfaces

Krassimira Vlachkova[a)] and Krum Radev[b)]

Faculty of Mathematics and Informatics, Sofia University "St. Kliment Ohridski", 1164 Sofia, Bulgaria

[a)]*Corresponding author: krassivl@fmi.uni-sofia.bg*
[b)]*Electronic mail: kvradev@uni-sofia.bg*

Abstract. We consider the problem of interpolation of scattered data in $\mathbb{R}^3$ and propose a solution based on Nielson's minimum norm network and triangular Bézier patches. Our algorithm applies splitting to all triangles of an associated triangulation and constructs G^1-continuous bivariate interpolant consisting of quartic triangular Bézier patches. The algorithm is computationally simple and produces visually pleasant smooth surfaces. We have created a software package for implementation, 3D visualization and comparison of our algorithm and the known Shirman and Séquin's method which is also based on splitting and quartic triangular Bézier patches. The results of our numerical experiments are presented and analysed.

INTRODUCTION

Interpolation of data points in $\mathbb{R}^3$ by smooth surface is an important problem in applied mathematics which finds applications in various areas such as medicine, architecture, archeology, computer graphics, bioinformatics, scientific visualization, etc. In general the problem can be formulated as follows: Given a set of points $\mathbf{d}_i = (x_i, y_i, z_i) \in \mathbb{R}^3$, $i = 1, \ldots, n$, find a bivariate function $F(x, y)$ defined in a certain domain D containing points $\mathbf{v}_i = (x_i, y_i)$, such that F possesses continuous partial derivatives up to a given order and $F(x_i, y_i) = z_i$.

Various methods for solving this problem were proposed and applied, see [1, 2, 3, 4]. A standard approach to solve the problem consists of two steps, see [1]:

1. Construct a triangulation $T = T(\mathbf{v}_1, \ldots, \mathbf{v}_n)$;
2. For every triangle in T construct a surface (patch) which interpolates the data at the three vertices of T.

The interpolation surface constructed in Step 2 is usually polynomial or piecewise polynomial. Typically, the patches are computed with a priori prescribed normal vectors at the data points. G^1 or G^2 smoothness of the resulting surface is achieved either by increasing the degree of the patches, or by the so called *splitting*. Splitting was originally proposed by Clough and Tocher [5] and further developed by Percell [6] and Farin [7] for solving different problems. In practice using patches of least degree and splitting is preferable since it is computationally simple and efficient.

Shirman and Séquin [8, 9] construct a G^1 smooth surface consisting of quartic triangular Bézier surfaces (TBS). Their method assumes that the normal vectors at points $\mathbf{d}_i$, $i = 1, \ldots, n$, are given as part of the input. Shirman and Séquin construct a smooth cubic curve network defined on the edges of T, first, and then degree elevate it to quartic. This increases the degrees of freedom and allows them to connect smoothly the adjacent Bézier patches. Next, they apply splitting where for each triangle in T a macro-patch consisting of three quartic Bézier sub-patches is constructed. To compute the inner Bézier control points closest to the boundary of the macro-patch, Shirman and Séquin use a method proposed by Chiyokura and Kimura [10, 11]. The interpolation surfaces constructed by Shirman and Séquin's algorithm often suffer from unwanted bulges, tilts, and shears as pointed out by the authors in [12] and more recently by Hettinga and Kosinka in [13].

Nielson [14] proposes a method which computes a smooth interpolation curve network defined on the edges of T so as to satisfy an extremal property and then extends it to a smooth interpolation surface using an appropriate *blending* method based on convex combination schemes. The interpolation curve network is called *minimum norm network* (MNN) and is cubic. Nielson's interpolant is a rational function on every triangle in T. A significant advantage of Nielson's method is that the normal vectors at the data points are obtained through the computation of the MNN.

In this paper we propose an algorithm for interpolation of data in $\mathbb{R}^3$ which improves on Shirman and Séquin's approach in two ways. First, we use Nielson's MNN and second, we apply different strategy for computation of the control points. During the computation of control points closest to the boundary of a macro-patch we adopt additional criteria so that to avoid unwanted distortions and twists which appear in surfaces constructed by Shirman and Séquin's method. As a result, the quality of the resulting surfaces is improved. Furthermore, Shirman and Séquin impose an additional condition that the three quartic curves defined on the common edges of the three sub-patches are degree

International Conference on Analysis and Applied Mathematics (ICAAM 2020)
AIP Conf. Proc. 2325, 020061-1–020061-6; https://doi.org/10.1063/5.0040457
Published by AIP Publishing. 978-0-7354-4069-2/$30.00

elevated cubic curves. This condition is not necessary to obtain G^1-continuity across the common edges of the sub-patches. We apply different criterion for choosing the inner points of the sub-patches and believe that our choice would facilitate the construction of macro-patches that are convex in addition.

We implemented a software package for construction and 3D visualization of interpolation surfaces obtained by both Shirman and Séquin's algorithm and our algorithm. We tested the two algorithms extensively using data of increasing complexity and analysed the results with respect to different criteria.

RELATED WORK

Let $n \geq 3$ be an integer and $\mathbf{d}_i := (x_i, y_i, z_i),\ i = 1, \ldots, n$ be different points in $\mathbb{R}^3$. We call this set of points *data* and assume that the projections $\mathbf{v}_i := (x_i, y_i)$ onto the plane Oxy are different and non-collinear.

A *triangulation* T of points $\mathbf{v}_i$ is a collection of non-overlapping, non-degenerate closed triangles in Oxy such that the set of the vertices of the triangles coincides with the set of points $\mathbf{v}_i$. Hereafter we assume that a triangulation T of the points $\mathbf{v}_i,\ i = 1, \ldots, n$, is given and fixed.

Nielson's MNN

Furthermore, for the sake of simplicity, we assume that the domain D formed by the union of the triangles in T is connected. In general D is a collection of polygons with holes.

The set of the edges in T is denoted by E. If there is an edge between $\mathbf{v}_i$ and $\mathbf{v}_j$ in E, it will be referred to by e_{ij} or simply by e if no ambiguity arises.

A *curve network* is a collection of real-valued univariate functions $\{f_e\}_{e \in E}$ defined on the edges in E. With any real-valued bivariate function F defined on D we naturally associate the curve network defined as the restriction of F on the edges in E, i.e. for $e = e_{ij} \in E$,

$$f_e(t) := F\left(\left(1 - \frac{t}{\|e\|}\right)x_i + \frac{t}{\|e\|}\,x_j,\ \left(1 - \frac{t}{\|e\|}\right)y_i + \frac{t}{\|e\|}\,y_j\right), \text{ where } 0 \leq t \leq \|e\| \text{ and } \|e\| = \sqrt{(x_i - x_j)^2 + (y_i - y_j)^2}. \quad (1)$$

Furthermore, according to the context F will denote either a real-valued bivariate function or a curve network defined by (1). We introduce the following class of *smooth interpolants* defined on D

$$\mathscr{F} := \left\{F(x,y) \in C(D) \,|\, F(x_i, y_i) = z_i,\ i = 1, \ldots, n,\ \partial F/\partial x, \partial F/\partial y \in C(D),\ f_e' \in AC,\ f_e'' \in L^2,\ e \in E\right\}$$

and the corresponding class of so-called *smooth interpolation curve networks*

$$\mathscr{C}(E) := \left\{F_{|E} = \{f_e\}_{e \in E} \mid F(x,y) \in \mathscr{F}\right\},$$

where $C(D)$ is the class of bivariate continuous functions defined in D, AC is the class of univariate absolutely continuous functions defined in $[0, \|e\|]$, and L^2 is the class of univariate functions defined in $[0, \|e\|]$ whose second power is Lebesgue integrable.

The smoothness of the interpolation curve network $F \in \mathscr{C}(E)$ geometrically means that at each point $\mathbf{d}_i$ there is a *tangent plane* to F, where a plane is *tangent* to the curve network at a point $\mathbf{d}_i$ if it contains the tangent vectors at $\mathbf{d}_i$ of the curves incident to $\mathbf{d}_i$.

The L^2-norm is defined in $\mathscr{C}(E)$ by $\|F\|_{L^2(T)} := \|F\| = \left(\sum_{e \in E} \int_0^{\|e\|} |f_e(t)|^2 dt\right)^{1/2}$. We denote the networks of the second derivative of F by $F'' := \{f_e''\}_{e \in E}$ and consider the following extremal problem:

$$(\mathbf{P}) \qquad \textit{Find } F^* \in \mathscr{C}(E) \ \textit{ such that } \|F^{*\prime\prime}\| = \inf_{F \in \mathscr{C}(E)} \|F''\|.$$

Nielson [14] showed that $(\mathbf{P})$ possesses a unique solution (MNN). The MNN is obtained by solving a linear system of equations.

Shirman and Séquin's method

This method assumes that the normal vectors at the data points $\mathbf{d}_i$, $i = 1, \ldots, n$, are given a priori. First, Shirman and Séquin construct smooth interpolation cubic curve network defined on the edges of T which is compatible with the normal vectors given and degree elevate it to quartic. Then, for each triangle in T they apply splitting procedure which constructs three triangular Bézier patches (sub-patches) that possess a common vertex and form a G^1-continuous polynomial surface (macro-patch) defined in the triangle. The Bézier patches are computed through computation of their control points as shown in Fig. 1**a.** We use the following notation.

■ vertices of the sub-patches;
● inner control points on the boundary of the macro-patch;
□ inner control points of the three inner boundary curves of the sub-patches;
○ inner control points of the sub-patches.

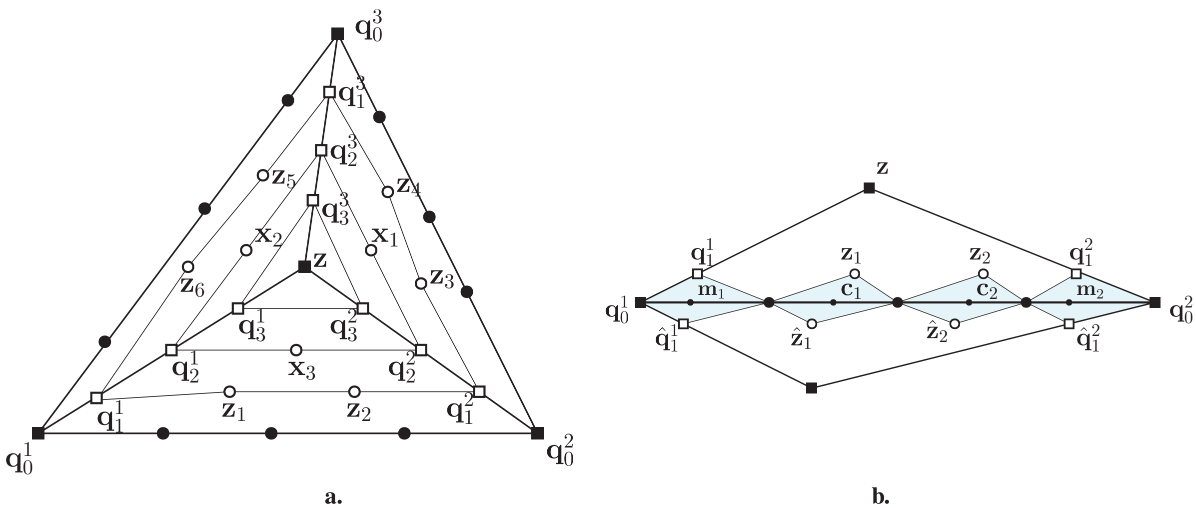

FIGURE 1. a. Construction of a G^1-continuous Bézier macro-patch by splitting to three sub-patches; **b.** A sufficient condition for G^1 continuity between $\mathscr{T}$ and its neighbouring patch is that the four shaded quadrilaterals are planar

Shirman and Séquin's Algorithm 1 below takes a triangle in T and the degree-elevated quartic boundary control points of the corresponding macro-patch and computes 19 control points of the three G^1-continuous quartic Bézier sub-patches.

Algorithm 1

Step 1. Compute the control points closest to the boundary of the macro-patch :
1.1 Points $\mathbf{q}_1^i$, $i = 1, 2, 3,$ are centers of the three small triangles with vertices ●■●.
1.2 Then points $\mathbf{z}_i$, $i = 1, \ldots, 6,$ are computed using Chiyokura and Kimura's method [10, 11].

Step 2. Compute points $\mathbf{q}_2^1 = \frac{1}{3}(\mathbf{q}_1^1 + \mathbf{z}_1 + \mathbf{z}_6)$, $\mathbf{q}_2^2 = \frac{1}{3}(\mathbf{q}_1^2 + \mathbf{z}_2 + \mathbf{z}_3)$, $\mathbf{q}_2^3 = \frac{1}{3}(\mathbf{q}_1^3 + \mathbf{z}_4 + \mathbf{z}_5)$.

Step 3. Compute points $\mathbf{p}_i = 2\mathbf{q}_2^i - \frac{4}{3}\mathbf{q}_1^i + \frac{1}{3}\mathbf{q}_0^i$, $i = 1, 2, 3$.

Step 4. Compute the splitting point $\mathbf{z} = \frac{1}{3}(\mathbf{p}_1 + \mathbf{p}_2 + \mathbf{p}_3)$.

Step 5. Compute points $\mathbf{q}_3^i = \frac{3}{4}\mathbf{p}_i + \frac{1}{4}\mathbf{z}$, $i = 1, 2, 3$.

Step 6. Compute points $\mathbf{x}_1 = \frac{3}{2}(-\mathbf{q}_3^1 + \mathbf{q}_3^2 + \mathbf{q}_3^3) - \frac{1}{2}(-\mathbf{q}_2^1 + \mathbf{q}_2^2 + \mathbf{q}_2^3)$, $\mathbf{x}_2 = \frac{3}{2}(\mathbf{q}_3^1 - \mathbf{q}_3^2 + \mathbf{q}_3^3) - \frac{1}{2}(\mathbf{q}_2^1 - \mathbf{q}_2^2 + \mathbf{q}_2^3)$,
$\mathbf{x}_3 = \frac{3}{2}(\mathbf{q}_3^1 + \mathbf{q}_3^2 - \mathbf{q}_3^3) - \frac{1}{2}(\mathbf{q}_2^1 + \mathbf{q}_2^2 - \mathbf{q}_2^3)$.

OUR ALGORITHM

In this section we propose our algorithm to construct G^1-continuous interpolation surface consisting of quartic TBP. First, we compute the MNN and then degree elevate it to quartic. Then for each triangle in T we apply splitting and construct three triangular Bézier sub-patches with a common vertex which form a G^1-continuous macro-patch defined in the triangle.

Let τ be a triangle in T and $\mathscr{T}$ be the corresponding macro-patch. We compute the control points of the three Bézier sub-patches of $\mathscr{T}$ consecutively in four layers as shown in Fig. 1**a.** The first layer consists of inner control points closest to the boundary of $\mathscr{T}$. The last fourth layer contains of single point $\mathbf{z}$. This point $\mathbf{z}$ is the splitting point and will be computed as a center of the triangle with vertices in the previous third layer.

Computing the control points in the first layer. There are three points of type □ and six points of type ○ in this layer, see Fig. 1**a.** First, we compute points of type □ as centers of the three small triangles with vertices ●■● on the boundary of the macro-patch. Then we compute the points $\mathbf{z}_i$, $i = 1,2$, of type ○ as follows.

Let the corresponding edge of τ be inner for T and $\hat{\mathbf{q}}_1^i$, $\hat{\mathbf{z}}_i$, $i = 1,2$, be the corresponding control points of the neighbouring patch, see Fig. 1**b.** A sufficient condition for G^1 continuity between the two patches is that the four shaded quadrilaterals in Fig. 1**b.** are planar. We compute the following points.

$$\begin{aligned}&\mathbf{z}_i' = \mathbf{q}_1^1 + \mathbf{c}_i - \mathbf{m}_1,\ \hat{\mathbf{z}}_i' = \hat{\mathbf{q}}_1^1 + \mathbf{c}_i - \mathbf{m}_1,\ \mathbf{z}_i'' = \mathbf{q}_1^2 + \mathbf{c}_i - \mathbf{m}_2,\ \hat{\mathbf{z}}_i'' = \hat{\mathbf{q}}_1^2 + \mathbf{c}_i - \mathbf{m}_2,\\ &\mathbf{a}_i = (1-\frac{i}{3})\mathbf{z}_i' + \frac{i}{3}\mathbf{z}_i'',\ \hat{\mathbf{a}}_i = (1-\frac{i}{3})\hat{\mathbf{z}}_i' + \frac{i}{3}\hat{\mathbf{z}}_i'',\ i = 1,2,\end{aligned} \tag{2}$$

where $\mathbf{c}_i$, $i = 1,2$, are control points of the cubic curve defined on the common edge of τ and its neighbouring triangle, and $\mathbf{m}_i$, $i = 1,2$, are the intersection points of the diagonals of the quadrilaterals $\mathbf{q}_0^1\mathbf{q}_1^1\bullet\hat{\mathbf{q}}_1^1$ and $\bullet\mathbf{q}_1^2\mathbf{q}_0^2\hat{\mathbf{q}}_1^2$, respectively, as shown in Fig. 1**b.**

Let $\mathbf{z}_i = (\xi_i, \eta_i, \zeta_i)$ and $\hat{\mathbf{z}}_i = (\hat{\xi}_i, \hat{\eta}_i, \hat{\zeta}_i)$. We choose ξ_i, η_i and $\hat{\xi}_i, \hat{\eta}_i$ to be equal to the corresponding coordinates of $\mathbf{a}_i$ and $\hat{\mathbf{a}}_i$, respectively, $i = 1,2$. In this way the projections of $\mathbf{z}_i$, $i = 1,2$, onto Oxy lie inside τ. Hence, we avoid unwanted twisting and tilting of the patch. We compute the third coordinates ζ_i, $\hat{\zeta}_i$ so that $\zeta_i = \hat{\zeta}_i$ and $\mathbf{z}_i$, $\hat{\mathbf{z}}_i$, $\mathbf{c}_i$ to be collinear, $i = 1,2$. In this way we avoid unwanted oscillations between the adjacent patches.

In the case where the corresponding edge of τ is boundary for T, i.e. there is no neighbouring patch of $\mathscr{T}$, we compute $\mathbf{z}_i$, $i = 1,2$ as follows.

$$\mathbf{r}_i' = \mathbf{q}_1^1 - \mathbf{q}_0^1 + \mathbf{c}_i,\ \mathbf{r}_i'' = \mathbf{q}_1^2 - \mathbf{q}_0^2 + \mathbf{c}_i,\ \mathbf{z}_i = (1-\frac{i}{3})\mathbf{r}_i' + \frac{i}{3}\mathbf{r}_i'',\ i = 1,2. \tag{3}$$

The rest of the points $\mathbf{z}_i$, $i = 3,\ldots,6$, are computed analogously.

Computing the control points in the second and third layers. Now we already know the control points of type ■ and type ● on the boundary of the macro-patch and control points □,○ in the first layer. Let us consider an inner boundary curve, e.g. the curve with control points $\mathbf{q}_i^1, \mathbf{z}$, $i = 0,\ldots,3$, see Fig. 1**a.** We have to compute the remaining control points so as to satisfy the G^1-continuity conditions across that curve. Hence, $\mathbf{q}_2^1$ is a center of the triangle $\mathbf{z}_1\mathbf{q}_1^1\mathbf{z}_6$, and $\mathbf{q}_3^1$ is a center of the triangle $\mathbf{x}_3\mathbf{q}_2^1\mathbf{x}_2$. Now suppose that we know points $\mathbf{x}_1$,$\mathbf{x}_2$,$\mathbf{x}_3$ in the second layer. Then points $\mathbf{q}_3^1$,$\mathbf{q}_3^2$,$\mathbf{q}_3^3$ in the third layer are

$$\mathbf{q}_3^1 = (\mathbf{q}_2^1 + \mathbf{x}_2 + \mathbf{x}_3)/3,\ \mathbf{q}_3^2 = (\mathbf{q}_2^2 + \mathbf{x}_1 + \mathbf{x}_3)/3,\ \mathbf{q}_3^3 = (\mathbf{q}_2^3 + \mathbf{x}_1 + \mathbf{x}_2)/3.$$

Finally, the splitting point is $\mathbf{z} := \frac{1}{3}(\mathbf{q}_3^1 + \mathbf{q}_3^2 + \mathbf{q}_3^3)$.

It remains to compute the three points $\mathbf{x}_1$,$\mathbf{x}_2$,$\mathbf{x}_3$. They provide three degrees of freedom which can be used for example to control the shape of the surface. In [8, 9] Shirman and Séquin use the condition that the three quartic curves defined on the inner edges are degree elevated cubic curves as it is for the boundary curves of the macro-patch. This condition is not necessary for G^1-continuity between two sub-patches and hence we do not need to impose it. We compute points $\mathbf{x}_1$,$\mathbf{x}_2$,$\mathbf{x}_3$ as mid-points of the edges of the triangle $\mathbf{q}_2^1\mathbf{q}_2^2\mathbf{q}_2^3$ as follows.

$$\mathbf{x}_1 = (\mathbf{q}_2^2 + \mathbf{q}_2^3)/2,\ \mathbf{x}_2 = (\mathbf{q}_2^1 + \mathbf{q}_2^3)/2,\ \mathbf{x}_3 = (\mathbf{q}_2^1 + \mathbf{q}_2^2)/2.$$

Then the control points in second, third, and fourth layers become co-planar. We believe that this choice of $\mathbf{x}_1$,$\mathbf{x}_2$,$\mathbf{x}_3$ will be useful when we try to construct a simple macro-patch which is convex in addition.

Algorithm 2 below takes a triangle τ in T and the degree-elevated quartic boundary control points of the corresponding patch $\mathscr{T}$ and computes 19 control points of the three G^1-continuous quartic Bézier sub-patches.

Algorithm 2

Step 1.	Compute the control points in the first layer:
	1.1 Points of type □ are centers of the three small triangles with vertices ●■●.
	1.2 Then points of type ○ are computed as described in (2) and (3).
Step 2.	Compute the control points in the second layer:
	2.1 Points of type □ are centers of the three small triangles with vertices ○□○ in the first layer.
	2.2 Then points of type ○ are mid-points of the segments with vertices of type □ in the second layer.
Step 3.	Compute the control points in the third layer: The three points of type □ are centers of the small triangles with vertices ○□○ in the second layer.
Step 4.	Compute the splitting point of type ■ as a center of the triangle with vertices □ in the third layer.

EXAMPLE

We implemented our Algorithm 2 as a web application using HTML, JavaScript, and the open source library `Plotly` [15]. The advantages of using `Plotly` are the options to display the coordinate system and the coordinates of the points when the cursor is placed on them, and to control the surfaces displayed. To demonstrate the results of our work we present here a simple example that clearly shows the typical differences between the surfaces produced by Shirman and Séquin's and our algorithms. As input for both algorithms we use the MNN for the data given.

Example 1 We consider data obtained from a regular triangular pyramid. We have $N = 4$, $\mathbf{v}_1 = (-1/2, -\sqrt{3}/6)$, $\mathbf{v}_2 = (1/2, -\sqrt{3}/6)$, $\mathbf{v}_3 = (0, \sqrt{3}/3)$, $\mathbf{v}_4 = (0, 0)$, and $z_i = 0$, $i = 1, 2, 3$, $z_4 = -1$. The corresponding MNN is shown in Fig. 3. The triangulation and the corresponding Shirman and Séquin's surface are shown in Fig. 3**a.** The surface generated by our Algorithm 2 and the triangulation are shown in Fig. 3**b.**

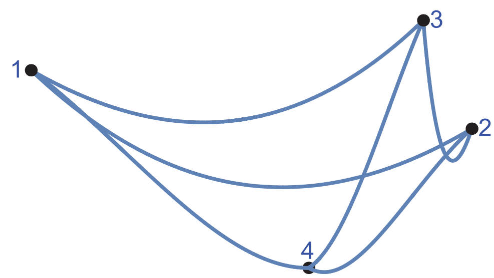

FIGURE 2. The MNN for the data in Example 1

CONCLUSION AND FUTURE WORK

In this paper we have proposed a method for constructing a G^1-continuous interpolation surface that consists of triangular quartic Bézier patches based on the MNN construction on the edges of the underlying triangulation. We have tested our method extensively and have witnessed various advantages over the existing methods. A promising approach for further improvement is to identify a smaller, possibly minimal, subset of T where splitting is to be done so that a smooth interpolant can be constructed. It is known that splitting decreases the smoothness of the resulting surface and hence, it would be advantageous to minimize the number of triangles where splitting is done.

ACKNOWLEDGMENTS

This research was supported by Sofia University Science Fund Grant No. 80-10-171/2020, and by European Regional Development Fund and the Operational Program “Science and Education for Smart Growth" under Contract BG05M2OP001-1.001-0004 (2018-2023).

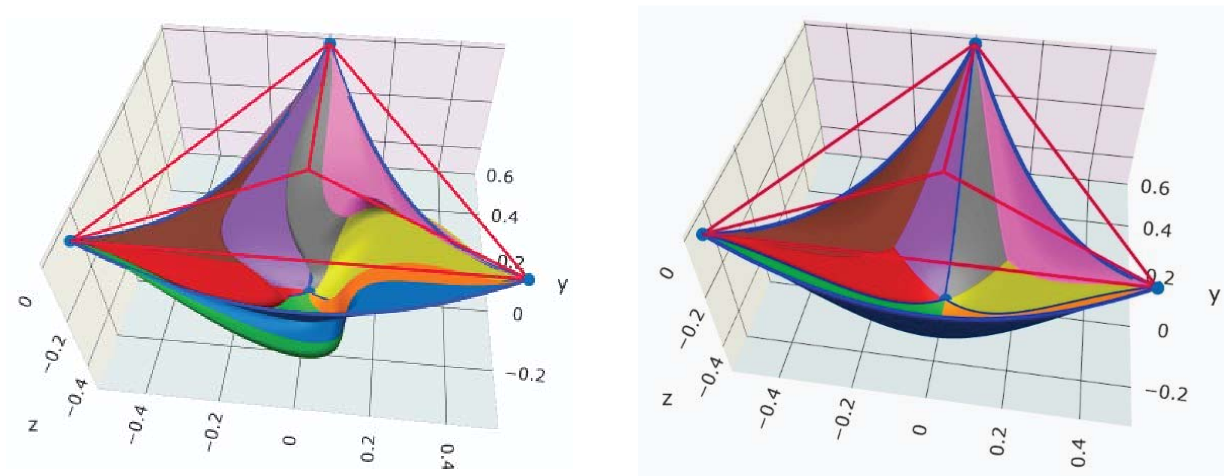

a. **b.**

FIGURE 3. Comparison of the two surfaces for the data in Example 1: **a.** The surface generated using Algorithm 1 (Shirman and Séquin); **b.** The surface generated using our Algorithm 2

REFERENCES

1. S. Mann, C. Loop, M. Lounsbery, D. Meyers, J. Painter, T. DeRose, and K. Sloan, "A survey of parametric scattered data fitting using triangular interpolants," in *Curve and Surface Design*, edited by H. Hagen (SIAM, Philadelphia, 1992) pp. 145–172.
2. T. K. Dey, *Curve and Surface Reconstruction: Algorithms with Mathematical Analysis*, Cambridge Monographs on Applied and Computational Mathematics (Cambridge University Press, 2006).
3. K. Anjyo, J. Lewis, and F. Pighin, "Scattered data interpolation for computer graphics, SIGGRAPH 2014 course notes," `http://olm.co.jp/rd/research_event/scattered-data-interpolation-for-computer-graphics` (Last accessed June 20, 2020).
4. M. Berger, A. Tagliasacchi, L. Seversky, P. Alliez, G. Guennebaud, J. Levine, A. Sharf, and C. Silva, Comput. Graph. Forum **36**, 301–329 (2017).
5. R. Clough and J. Tocher, "Finite elements stiffness matrices for analysis of plate bending," in *Proceedings of the 1st Conference on Matrix Methods in Structural Mechanics*, Vol. 66–80 (Wright-Patterson A. F. B., Ohio, 1965) pp. 515–545.
6. P. Percell, SIAM J. Numer. Anal. **13**, 100–103 (1976).
7. G. Farin, Comput. Aided Geom. Des. **2**, 19–27 (1985).
8. L. Shirman and C. Séquin, Comput. Aided Geom. Des. **4**, 279–295 (1987).
9. L. Shirman and C. Séquin, Comput. Aided Geom. Des. **8**, 217–221 (1991).
10. H. Chiyokura and F. Kimura, "Design of solids with free-form surfaces," in *SIGGRAPH '83 Proceedings of the 10th annual conference on Computer graphics and interactive techniques*, Vol. 17, edited by P. P. Tanner (ACM, New York, 1983) pp. 289–298.
11. H. Chiyokura, "Localized surface interpolation method for irregular meshes," in *Advanced Computer Graphics, Proceedings of Computer Graphics Tokyo'86*, Vol. 66–80, edited by T. Kunii (Springer, Tokyo, 1986) pp. 3–19.
12. L. Shirman and C. Séquin, Comput. Aided Geom. Des. **7**, 375–388 (1990).
13. G. Hettinga and J. Kosinka, Comput. Aided Geom. Des. **62**, 166–180 (2018).
14. G. Nielson, Math. Comput. **40**, 253–271 (1983).
15. "Plotly.js," `https://plot.ly/javascript` (Last accessed June 20, 2020).

Study of Initial Boundary Value Problem for Two-Dimensional Differential Equation with Fractional Time Derivative in the Sense of Caputo

Nurlana Alimbekova,[1, a)] Abdumauvlen Berdyshev,[1, b)] and Dossan Baigereyev[2, c)]

[1)] *Abai Kazakh National Pedagogical University, 050000 Almaty, Kazakhstan*
[2)] *S. Amanzholov East Kazakhstan State University, 070002 Ust-Kamenogorsk Kazakhstan*

[a)] *Electronic mail: ernur_09.83@mail.ru*
[b)] *Electronic mail: berdyshev@mail.ru*
[c)] *Corresponding author: dbaigereyev@gmail.com*

Abstract. In this paper, we study an initial boundary value problem for a two-dimensional differential equation with a fractional time derivative in the sense of Caputo. This equation is of great applied importance in modeling flow processes and anomalous dispersion. The uniqueness and continuous dependence of the solution on the input data in differential form is proved. A computationally effective implicit scheme with weights is proposed. A priori estimates are obtained for the solution of the problem under the assumption that a solution exists in the class of sufficiently smooth functions. These estimates imply the uniqueness of the solution and the stability of the scheme with respect to the initial data and the right-hand side of the equation. The convergence of the approximate solution to the solution of the differential problem with the second order both in time and space variables is proved. The results of computational experiments confirming the reliability of theoretical analysis are presented.

INTRODUCTION

Partial differential equations with a fractional derivative are of great importance in science and industry. One of the recent and important practical applications of fractional differential equations is the modeling of physical diffusion processes in media with fractal geometry and memory. This direction, in turn, prompted the interest of researchers of underground flows of multiphase fluids in fractured porous media. Numerous studies have shown that these mathematical models provide a more accurate and realistic description of the processes taking place in such complex media. Therefore, the development of analytical and numerical methods in the theory of fractional differential equations is an urgent and important problem.

In this paper, we study a two-dimensional convection-diffusion equation with a fractional time derivative in the sense of Caputo. Determination of the saturation field in the multiphase flow problem in fractured porous media with fractal fracture geometry is reduced to solving this type of equation. This direction appeared relatively recently in the theory of multiphase flows and continues its development [1, 2, 3]. In [4], the classical equations describing the motion of a fluid in a porous medium are rewritten taking into account the formalism of memory using a fractional derivative in the sense of Caputo. In [5], fractional derivatives of various orders in the sense of Caputo with a variable lower limit in fractured and matrix regions are used.

The study of the existence and uniqueness of solving problems for equations with a fractional derivative has been the subject of many papers [6, 7, 8, 9, 10]. The papers [7, 9, 11, 12, 13, 14] are devoted to the development of numerical methods for solving boundary value problems for equations with a fractional derivative.

In this paper, a priori estimate is obtained which implies the uniqueness of the solution. Then we propose an implicit second-order approximation scheme with respect to time and spatial variables. The stability of the proposed scheme as well as convergence with an order equal to the approximation order is proved. The results obtained are confirmed by numerical calculations carried out for two test problems.

FORMULATION OF THE PROBLEM

The paper is devoted to the study of the following problem for the fractional partial differential equation:

$$\frac{\partial^\alpha u}{\partial t^\alpha} = Ku + Du + f(x,t), \;\; x = (x_1, x_2) \in \Omega = (0,1) \times (0,1), \;\; 0 < t < 1, \tag{1}$$

International Conference on Analysis and Applied Mathematics (ICAAM 2020)
AIP Conf. Proc. 2325, 020062-1–020062-6; https://doi.org/10.1063/5.0040517
Published by AIP Publishing. 978-0-7354-4069-2/$30.00

$$u(x,0)=\rho(x),\ u\Big|_{\partial\Omega}=0, \tag{2}$$

where $0<\alpha<1$, $K=K_1+K_2$, $D=D_1+D_2$, $K_m u=q_m\dfrac{\partial u}{\partial x_m}$, $D_m u=\dfrac{\partial}{\partial x_m}\left(k_m\dfrac{\partial u}{\partial x_m}\right)$.

The fractional derivative is defined as $\dfrac{\partial^\alpha u}{\partial t^\alpha}=\dfrac{1}{\Gamma(1-\alpha)}\int\limits_0^t\dfrac{u_\tau(x,\tau)}{(t-\tau)^\alpha}d\tau$.

Assume that the coefficients and the right-hand side of the equation (1) satisfy the conditions

$$k_m(x,t)\in C^{1,0}\left(\overline{Q}_T\right),\ q_m(x,t),\ f(x,t)\in C\left(\overline{Q}_T\right), \tag{3}$$

$$c_1\le k_m(x,t)\le c_2,\quad |q_m(x,t)|\le c_2,\quad c_1>0,\ c_2>0,\ 2c_1>c_2^2. \tag{4}$$

Suppose that there exists a solution to the problem (1)-(2) in the class of sufficiently smooth functions.

UNIQUENESS OF THE SOLUTION

Standard L^2-norms and dot products as well as the following norms are used:

$$\|\nabla u\|^2_{L^2(\overline{Q}_T)}=\left\|\frac{\partial u}{\partial x_1}\right\|^2_{L^2(\overline{Q}_T)}+\left\|\frac{\partial u}{\partial x_2}\right\|^2_{L^2(\overline{Q}_T)},\quad \|u\|^2_*=\int_0^1\int_\Omega D_{0t}^{-\alpha}\|u\|^2_{L^2(\Omega)}\,dx\,dt,$$

where $u,\ \upsilon$ are functions defined on $\overline{Q}_T$; $D_{0t}^{-\alpha}$ is the fractional integration operator:

$$D_{0t}^{-\alpha}u=\frac{1}{\Gamma(\alpha)}\int_0^t\frac{u(x,\tau)}{(t-\tau)^{1-\alpha}}d\tau,\quad 0<\alpha<1.$$

Lemma 1 *The following estimate is valid for any absolute continuous function $y(t)$ on $[0,T]$:*

$$y\frac{\partial^\alpha y}{\partial t^\alpha}\ge\frac{1}{2}\frac{\partial^\alpha y^2}{\partial t^\alpha},\quad 0<\alpha<1.$$

Lemma 2 *[15]. Let a nonnegative absolutely continuous function $y(t)$ satisfy the inequality*

$$\frac{\partial^\alpha y(t)}{\partial t^\alpha}\le\gamma_1 y(t)+\gamma_2(t),\ 0\le\alpha\le 1$$

for almost every $t\in[0,T]$, where $\gamma_1>0$, $\gamma_2(t)$ is a summable non-negative function on $[0,T]$. Then

$$y(t)\le y(0)E_\alpha\left(\gamma_1 t^\alpha\right)+\Gamma(\alpha)E_{\alpha,\alpha}\left(\gamma_1 t^\alpha\right)D_{0t}^{-\alpha}\gamma_2(t),$$

where $E_\alpha(z)$, $E_{\alpha,\mu}(z)$ are Mittag-Leffler functions.

Using the properties of a definite integral and the boundedness of the functions $E_\alpha(t^\alpha)$ and $E_{\alpha,\alpha}(t^\alpha)$ at $0\le t\le 1$, one can show that under the conditions of Lemma 2, the non-negative absolutely continuous function $y(x,t)$ satisfies the inequality

$$\|y\|^2_{L^2(\overline{Q}_T)}\le M_1\|y(x,0)\|^2_{L^2(\overline{Q}_T)}+M_2\|\gamma_2\|^2_*. \tag{5}$$

The following theorem is proved using Lemma 1 and Lemma 2.

Theorem 1 *If $u(x,t)\in C^{2,0}(Q_T)\cap C^{1,0}\left(\overline{Q}_T\right)$, $\dfrac{\partial^\alpha u}{\partial t^\alpha}(x,t)\in C\left(\overline{Q}_T\right)$ and the conditions (3)-(4) hold, then the following a priori estimate holds for the solution of the problem (1)-(2):*

$$\|u(x,t)\|^2_{L^2(\overline{Q}_T)}\le M_1\|u(x,0)\|^2_{L^2(\overline{Q}_T)}+M_2\|f(x,t)\|^2_*,\quad M_1,M_2>0,$$

which implies uniqueness and continuous dependence of the solution of (1)-(2) on the input data.

FORMULATION OF THE DIFFERENCE PROBLEM

Introduce a uniform mesh $\overline{\omega}_{h\tau}$ in $\overline{Q}_T$ with the mesh size h in the spatial variables and τ in time. Associate the implicit scheme of the approximation order $O\left(h^2+\tau^2\right)$ with weights to the differential problem (1)-(2) on $\overline{\omega}_{h\tau}$:

$$\Delta^{\alpha}_{0t_{n+\sigma}} y_{ij} = \Theta y_{ij} + \Psi y_{ij} + \varphi^n_{ij}, \quad y^0_{ij} = \rho_{ij}, \quad y^{(\sigma)}\Big|_{\gamma_h} = 0, \quad n > 0, \tag{6}$$

where $\Theta = \Theta_1 + \Theta_2$, $\Psi = \Psi_1 + \Psi_2$,

$$\Theta_m y_{ij} = 0.5\left(\eta_{m,ij} - \left|\eta_{m,ij}\right|\right)\xi_{m,ij} y^{(\sigma)}_{\bar{x}_m,ij} + 0.5\left(\eta^{+1_m}_{m,ij} + \left|\eta^{+1_m}_{m,ij}\right|\right)\xi^{+1_m}_{m,ij} y^{(\sigma)}_{x_m,ij}, \quad \Psi_m y_{ij} = \left(\xi_m y^{(\sigma)}_{\bar{x}_m}\right)_{x_m,ij},$$

$\Delta^{\alpha}_{0t_{n+\sigma}} y$ is the discrete analogue of a fractional Caputo derivative of order α, $0<\alpha<1$ [10]:

$$\Delta^{\alpha}_{0t_{n+\sigma}} y = \frac{\tau^{1-\alpha}}{\Gamma(2-\alpha)} \sum_{s=0}^{n} g^{\alpha,\sigma}_{n-s} y^s_t;$$

where γ_h is the set of boundary nodes of $\overline{\omega}_h$; the coefficients $g^{\alpha,\sigma}_s$ are determined as [9]

$$g^{\alpha,\sigma}_0 = A^{\alpha,\sigma}_0 \text{ when } n=0; \; g^{\alpha,\sigma}_s = \begin{cases} A^{\alpha,\sigma}_0 + B^{\alpha,\sigma}_1, & s=0, \\ A^{\alpha,\sigma}_s + B^{\alpha,\sigma}_{s+1} - B^{\alpha,\sigma}_s, & 1 \le s \le n-1, \quad \text{when } n>0, \\ A^{\alpha,\sigma}_n - B^{\alpha,\sigma}_n, & s=n, \end{cases}$$

$$A^{\alpha,\sigma}_0 = \begin{cases} \sigma^{1-\alpha}, & s=0, \\ (s+\sigma)^{1-\alpha} - (s-1+\sigma)^{1-\alpha}, & s \ge 1, \end{cases}, \quad \xi^n_{1,ij} = k\left(x_{i-\frac{1}{2},j}, t^{n+\sigma}\right), \; \xi^n_{2,ij} = k\left(x_{i,j-\frac{1}{2}}, t^{n+\sigma}\right),$$

$$B^{\alpha,\sigma}_s = \frac{1}{2-\alpha}\left[(s+\sigma)^{2-\alpha} - (s-1+\sigma)^{2-\alpha}\right] - \frac{1}{2}\left[(s+\sigma)^{1-\alpha} + (s-1+\sigma)^{1-\alpha}\right], \; s \ge 1,$$

$$\eta^n_{m,ij} = \frac{q_m\left(x_{ij}, t^{n+\sigma}\right)}{k_m\left(x_{ij}, t^{n+\sigma}\right)}, \; \varphi^n_{ij} = f\left(x_{ij}, t^{n+\sigma}\right), \; \sigma = 1 - \frac{\alpha}{2}, \; g^{\alpha,\sigma}_s > 0, \; y^{(\sigma)} = \sigma y^{n+1} + (1-\sigma) y^n.$$

In addition, the notation from [16, 17, 18] is used.

STABILITY AND CONVERGENCE OF THE DIFFERENCE SCHEME

Lemma 3 *[15]. The following inequality holds for any function y defined on $\overline{\omega}_{h\tau}$:*

$$y^{(\sigma)} \Delta^{\alpha}_{0t_{n+\sigma}} y \ge \frac{1}{2} \Delta^{\alpha}_{0t_{n+\sigma}} y^2.$$

Lemma 4 *The following inequality holds for the solution of the problem (6) under the conditions (4):*

$$\Delta^{\alpha}_{0t_{n+\sigma}} \|y\|^2 + c_1 \left\|\nabla y^{(\sigma)}\right\|^2 \le \mu_1 \left\|y^{(\sigma)}\right\|^2 + \|\varphi\|^2.$$

This lemma is proved using Lemma 3, the difference analogue of the Green's theorem and conditions (4).

Lemma 5 *[9]. Let non-negative sequences y^n and φ^n, $n = 0, 1, 2,...$ satisfy the inequality*

$$\Delta^{\alpha}_{0t_{n+\sigma}} y^n \le \lambda_1 y^{n+1} + \lambda_2 y^n + \varphi^n, \;\; n \ge 1,$$

where $\lambda_1 \ge 0$, $\lambda_2 \ge 0$ are some constants. Then there exists a constant t_0 such that the following inequality holds under the condition $\tau \le t_0$: $y^{n+1} \le 2\left(y^0 + \frac{(t^n)^{\alpha}}{\Gamma(1+\alpha)} \max_{0\le m\le n} \varphi^m\right) E_{\alpha}\left(2\lambda \left(t^n\right)^{\alpha}\right)$, $\lambda = \lambda_1 + \frac{\lambda_2}{2+2^{1-\alpha}}$.

The following theorem is proved based on Lemmas 4 and 5.

Theorem 2 *Under the conditions (4), there exists t_0 such that the following estimate holds for the solution of the problem (6) for $\tau \leq t_0$:*

$$\left\|y^{n+1}\right\|^2 \leq \mu_2 \left(\left\|y^0\right\|^2 + \frac{(t^n)^\alpha}{\Gamma(1+\alpha)} \max_{0\leq m\leq n} \|\varphi^m\|^2\right),$$

which implies the uniqueness and stability of the difference scheme (6) according to the initial data and the right-hand side.

Theorem 3 *Under the conditions of Theorem 2, the solution of (6) converges to the solution of the differential problem (1)-(2) with the second order both in spatial variable and time.*

IMPLEMENTATION OF THE DIFFERENCE SCHEME

The following two-step alternating directions method is used to solve (6):

$$\frac{g_0^{\alpha,\sigma}\left(u_{i,j}^{n+\frac{1}{2}} - u_{i,j}^n\right)}{\tau^\alpha \Gamma(2-\alpha)} + \frac{1}{\tau^\alpha \Gamma(2-\alpha)} \sum_{s=0}^{n-1} g_{n-s}^{\alpha,\sigma}\left(u_{i,j}^{s+1} - u_{i,j}^s\right) = \sigma\left(\Theta_1 + \Psi_1\right) u_{i,j}^{n+\frac{1}{2}} + (1-\sigma)\left(\Theta_2 + \Psi_2\right) u_{i,j}^n, \quad (7)$$

$$\frac{g_0^{\alpha,\sigma}\left(u_{i,j}^{n+1} - u_{i,j}^{n+\frac{1}{2}}\right)}{\tau^\alpha \Gamma(2-\alpha)} + \frac{1}{\tau^\alpha \Gamma(2-\alpha)} \sum_{s=0}^{n-1} g_{n-s}^{\alpha,\sigma}\left(u_{i,j}^{s+1} - u_{i,j}^s\right) = \sigma\left(\Theta_1 + \Psi_1\right) u_{i,j}^{n+\frac{1}{2}} + (1-\sigma)\left(\Theta_2 + \Psi_2\right) u_{i,j}^{n+1}. \quad (8)$$

The solution process is reduced to the sequential solution of systems of equations with tridiagonal matrices at each time layer that are solved with the Thomas algorithm. Direct check shows that the stability condition for the Thomas algorithm is satisfied. The accuracy of the method (6) is verified on a number of computational experiments.

Problem 1. Consider the equation (1) with the right-hand side

$$\begin{aligned} f(x,y,t) = &-\frac{18x^2y^2\left(1-x^2\right)\left(1-y^2\right)t^{3-\alpha}}{\Gamma(1-\alpha)(\alpha-3)(\alpha-2)(\alpha-1)} - 6y^2\left(1-y^2\right)t^3\left(-2x^3-6x^2+x+1\right) \\ &-6x^2\left(1-x^2\right)t^3\left(-2y^3-6y^2+y+1\right) \end{aligned}$$

and initial condition $u(x,y,0) \equiv 0$. The exact solution to this problem is $u(x,y,t) = 3x^2y^2t^3\left(1-x^2\right)\left(1-y^2\right)$.

The value of the time step is chosen to be $\tau = 10^{-5}$ when analyzing the dependence of the error order on the spatial step. The step value in the spatial variable h varies between $h = 10^{-2}$ and $h = 10^{-5}$. The value of the spatial step is chosen equal to $h = 10^{-4}$ when analyzing the dependence of the order of error on the time step. The time step value varies between $\tau = 10^{-5}$ and $\tau = 10^{-8}$. The order of the fractional derivative is chosen to be $\alpha = 0.15$, $\alpha = 0.5$ and $\alpha = 0.85$.

Tables 1 and 2 show the error values for various values of the parameters σ, h and τ. Figure 1 (left) shows an approximate solution to the problem on a layer $n = 1000$ at $\alpha = 0.85$.

Problem 2. Consider the equation (1) with the right-hand side

$$\begin{aligned} f(x,y,t) = &-\frac{6x^2y^2\left(x^2-1\right)\left(1-y^2\right)t^{3-\alpha}}{\Gamma(1-\alpha)(\alpha-3)(\alpha-2)(\alpha-1)} - (x+y)t^3 6y^2\left(1-y^2\right)\left(-2x^3-6x^2+x+1\right) \\ &-6x^2\left(1-x^2\right)t^3\left(-2y^3-6y^2+y+1\right) \end{aligned}$$

and the initial condition $u(x,y,0) \equiv 0$. The exact solution to this problem is $u(x,y,t) = x^2y^2t^3\left(x^2-1\right)\left(1-y^2\right)$.

Tables 3 and 4 show the error values for various values of the parameters σ, h and τ. Figure 1 (right) shows the approximate solution of the problem on the layer $n = 1000$ at $\alpha = 0.85$. It follows from results given in Tables 1 and 3 that the error is a value of the order of $O\left(h^2\right)$. Similarly, it follows from results given in Tables 2 and 4 that the error is an order of magnitude $O\left(\tau^2\right)$. Thus, computational experiments have confirmed that the difference scheme converges with the second order both in spatial variables and time.

TABLE 1. Error analysis for Problem 1

Mesh size	$\alpha = 0.15$	$\alpha = 0.5$	$\alpha = 0.85$
$h = 1/100$	$1.374858 \cdot 10^{-7}$	$1.098641 \cdot 10^{-7}$	$5.933419 \cdot 10^{-8}$
$h = 1/500$	$5.557511 \cdot 10^{-9}$	$4.585992 \cdot 10^{-9}$	$2.634147 \cdot 10^{-9}$
$h = 1/1000$	$1.430960 \cdot 10^{-9}$	$1.297898 \cdot 10^{-9}$	$8.675095 \cdot 10^{-10}$
$h = 1/2000$	$4.004706 \cdot 10^{-10}$	$4.850132 \cdot 10^{-10}$	$4.320614 \cdot 10^{-10}$
$h = 1/5000$	$1.147281 \cdot 10^{-10}$	$2.657353 \cdot 10^{-10}$	$3.123288 \cdot 10^{-10}$
$h = 1/10000$	$7.063983 \cdot 10^{-11}$	$2.355103 \cdot 10^{-10}$	$2.960129 \cdot 10^{-10}$

TABLE 2. Error analysis for Problem 1

Mesh size	$\alpha = 0.15$	$\alpha = 0.5$	$\alpha = 0.85$
$\tau = 10^{-5}$	$1.386493 \cdot 10^{-9}$	$1.297898 \cdot 10^{-9}$	$8.675095 \cdot 10^{-10}$
$\tau = 10^{-6}$	$1.155476 \cdot 10^{-11}$	$8.650119 \cdot 10^{-12}$	$2.399971 \cdot 10^{-12}$
$\tau = 10^{-7}$	$8.692040 \cdot 10^{-14}$	$4.623733 \cdot 10^{-14}$	$4.631788 \cdot 10^{-15}$
$\tau = 10^{-8}$	$5.877397 \cdot 10^{-16}$	$2.145534 \cdot 10^{-16}$	$7.503443 \cdot 10^{-18}$

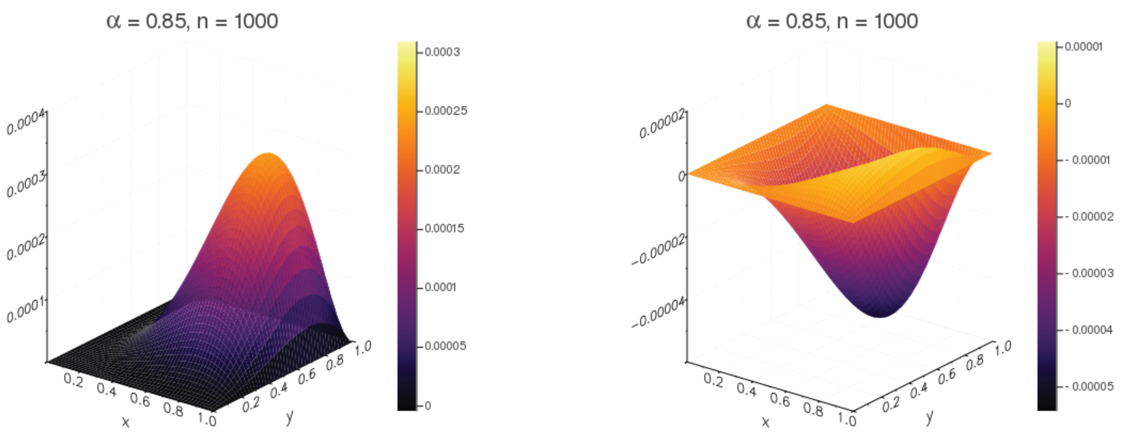

FIGURE 1. Approximate solution of the Problem 1 (left) and Problem 2 (right) at $\alpha = 0.85$

TABLE 3. Error analysis for Problem 2

Mesh size	$\alpha = 0.15$	$\alpha = 0.5$	$\alpha = 0.85$
$h = 1/100$	$3.283814 \cdot 10^{-7}$	$2.846682 \cdot 10^{-7}$	$1.552110 \cdot 10^{-7}$
$h = 1/500$	$1.451361 \cdot 10^{-8}$	$1.199802 \cdot 10^{-9}$	$6.984047 \cdot 10^{-9}$
$h = 1/1000$	$3.767931 \cdot 10^{-9}$	$3.487531 \cdot 10^{-9}$	$2.356834 \cdot 10^{-9}$
$h = 1/2000$	$1.085025 \cdot 10^{-9}$	$1.378421 \cdot 10^{-9}$	$1.205480 \cdot 10^{-9}$
$h = 1/5000$	$3.428998 \cdot 10^{-10}$	$8.026266 \cdot 10^{-10}$	$8.855067 \cdot 10^{-10}$
$h = 1/10000$	$2.404071 \cdot 10^{-10}$	$7.222409 \cdot 10^{-10}$	$8.399404 \cdot 10^{-10}$

TABLE 4. Error analysis for Problem 2

Mesh size	$\alpha = 0.15$	$\alpha = 0.5$	$\alpha = 0.85$
$\tau = 10^{-5}$	$3.709663 \cdot 10^{-9}$	$3.487531 \cdot 10^{-9}$	$2.356834 \cdot 10^{-9}$
$\tau = 10^{-6}$	$3.151834 \cdot 10^{-12}$	$2.440338 \cdot 10^{-12}$	$8.282573 \cdot 10^{-12}$
$\tau = 10^{-7}$	$2.468931 \cdot 10^{-15}$	$1.448078 \cdot 10^{-15}$	$2.613030 \cdot 10^{-16}$
$\tau = 10^{-8}$	$1.786572 \cdot 10^{-18}$	$7.579424 \cdot 10^{-19}$	$1.613023 \cdot 10^{-19}$

CONCLUSION

Thus, the implicit finite difference scheme is constructed for the fractional differential equation with variable coefficients containing the fractional time derivative in the sense of Caputo. The stability and error estimation of the difference scheme are established. Empirical convergence agrees well with theoretical estimates. The results obtained can find application in the numerical solution of other equations containing a fractional time derivative.

ACKNOWLEDGMENTS

The work was supported by the Ministry of Education and Science of the Republic of Kazakhstan (Grant No. AP08053189).

REFERENCES

1. E. Di Giuseppe, M. Moroni, and M. Caputo, Transport in Porous Media **83**, 479–500 (2010).
2. R. K. Gazizov and S. Y. Lukaschuk, Vestnik UGATU **21**, 104–112 (2017).
3. O. D. Abiola, H. M. Enamul, M. Kaseem, and A. A. Sidqi, Computers and Mathematics with Applications **73**, 1385–1402 (2017).
4. M. Caputo, Water Resources Research **36**, 693–705 (2000).
5. W. Zhong, C. Li, and J. Kou, Advances in Mathematical Physics **2013**, 1–7 (2013).
6. A. Berdyshev, A. Cabada, and B. Turmetov, Applied Mathematical Modelling **4**, 4548–4569 (2015).
7. A. Berdyshev, B. Eshmatov, and B. Kadirkulov, Electronic Journal of Differential Equations (2016).
8. P. Agarwal, A. Berdyshev, and E. Karimov, Results in Mathematics (2017).
9. A. A. Alikhanov, Journal of Computational Physics **280**, 424–438 (2015).
10. M. K. Beshtokov, Matematicheskie trudy **21**, 72–101 (2018).
11. M. Beshtokov, Ufimskii Mathematicheskii Zhurnal **11**, 36–55 (2019).
12. A. Kanwal, C. Phang, and U. Iqbal, Computation **6**, 1–12 (2018).
13. V. F. Morales-Delgado, J. F. Gomez-Aguilar, and M. A. Taneco-Hemandez, Revista Mexicana de Fisica **65**, 82–88 (2019).
14. F. Liu, P. Zhuang, and K. Burrage, Computers and Mathematics with Applications **64**, 2990–3007 (2012).
15. A. A. Alikhanov, Differential Equations **46**, 660–666 (2010).
16. W. Wójcik, N. Temirbekov, and D. Baigereyev, Przeglad Elektrotechniczny **92 (7)**, 24–31 (2016).
17. B. Zhumagulov, N. Temirbekov, and D. Baigereyev, AIP Conference Proceedings **1880 (060001)**, 1–10 (2017).
18. A. N. Temirbekov, B. A. Urmashev, and K. Gromaszek, International Journal of Electronics and Telecommunications **64 (3)**, 391–396 (2018).

Parallel CUDA Implementation of a Numerical Algorithm for Solving the Navier-Stokes Equations Using the Pressure Uniqueness Condition

Almas Temirbekov,[1, a)] Dossan Baigereyev,[2, b)] Nurlan Temirbekov,[1, 3, 4, c)] Baidaulet Urmashev,[1, d)] and Aidana Amantayeva[1, e)]

[1)]*Al-Farabi Kazakh National University, 050040 Almaty, Republic of Kazakhstan*
[2)]*S. Amanzholov East Kazakhstan State University, 070002 Ust-Kamenogorsk, Republic of Kazakhstan*
[3)]*National Engineering Academy of the Republic of Kazakhstan, 050010 Almaty, Republic of Kazakhstan*
[4)]*Kazakhstan Engineering Technological University, 050060 Almaty, Republic of Kazakhstan*

[a)]*Electronic mail: almas.temirbekov@kaznu.kz*
[b)]*Corresponding author: dbaigereyev@gmail.com*
[c)]*Electronic mail: temirbekov@rambler.ru*
[d)]*Electronic mail: baidaulet.urmashev@kaznu.kz*
[e)]*Electronic mail: aidana.amantayeva@kaznu.kz*

Abstract. In this paper, we study numerical methods for solving the Navier-Stokes equations in doubly connected domains. Two methods for solving the problem are considered. The first method is based on constructing a difference problem in variables of the stream function and the vortex of velocity using the uniqueness condition for pressure. The numerical solution of the elliptic equation for stream functions is found as the sum of the solutions of two simple problems of an elliptic type. One problem is with homogeneous boundary conditions, and the other is with a homogeneous equation. An alternative approach to solving the problem is the fictitious domain method with the continuation of the least coefficient. This method does not require satisfying the pressure uniqueness condition, and is simple to implement. An important direction in the development of numerical simulation methods is the study of approximate methods for solving problems of mathematical physics in complex multidimensional areas. To solve many applied problems in irregular areas, the fictitious domain method is widely used, which is characterized by a high degree of automation of programming. The main idea of the fictitious domain method is that the problem is solved not in the original complex domain, but in some other, simpler domain. This allows to create software immediately for a fairly wide class of problems with arbitrary computational domains. The possibilities of applying the fictitious domain method to the problems of hydrodynamics in the variables "stream function, vortex of velocity" are considered in many works. In this paper, we study a numerical method for solving the Navier-Stokes equations in doubly connected domains. A computational finite difference algorithm for solving an auxiliary problem of the fictitious domain method has been developed. The results of numerical modeling of the two-dimensional Navier-Stokes equations by the fictitious domain method with continuation by the lowest coefficient are presented. For this problem, a parallel algorithm was developed using the CUDA architecture, which was tested on various grid dimensions.

INTRODUCTION

The growth in productivity of computer technology and the development of parallel computing contributed to the solution of important practical problems of the industry. One example of such tasks is the assessment of effectiveness and forecasting of oil field development indicators. Due to the complexity of mathematical models describing these processes, calculations for one field can last from several hours to several days. Therefore, the issue of developing effective parallel algorithms that can significantly speed up the calculation becomes relevant.

Along with the classical model of flows in porous media based on the Darcy law [1, 2], a number of other models is widely used to study fluid flows in oil reservoirs, such as the models of N. E. Zhukovsky [3], Forchheimer [4], Navier-Stokes [3, 4]. The use of these models is associated with a violation of the Darcy law under certain conditions, the need for a detailed study of the flow processes near wells, etc.

In this paper, we set the goal of constructing an algorithm for the numerical implementation of an incompressible fluid motion model using the CUDA software and hardware parallel computing architecture. We consider the initial-boundary-value problem for the Navier-Stokes equations in the variables "stream function, velocity vortex" in a two-dimensional doubly connected domain.

The paper considers methods for numerically solving the Navier - Stokes equation in a multiply connected domain. One of the difficulties in numerically solving the Navier - Stokes equation in the variables of the stream function and the velocity vortex in the case of a multiply connected domain is caused by the uncertainty of the values of the stream

International Conference on Analysis and Applied Mathematics (ICAAM 2020)
AIP Conf. Proc. 2325, 020063-1–020063-6; https://doi.org/10.1063/5.0041039
Published by AIP Publishing. 978-0-7354-4069-2/$30.00

function at the internal boundaries. The numerical solution of the Navier-Stokes equations in multiply connected domain was considered in [5, 6], which proposed an explicit method for numerical solution of the Navier-Stokes equations in a doubly connected domain. This problem using the uniqueness condition for pressure was solved in the work of Syrochenko V.P. [7]. In [8], it was concluded that the explicit scheme leads to an unstable calculation. In the present paper, we construct a stable explicit difference scheme for numerically solving the Navier-Stokes equations in a multiconnected domain using the pressure uniqueness condition and the fictitious domain method for solving this problem. To solve this problem, an alternative approximate method is considered based on the fictitious domain method with continuation by lower coefficients. The obtained equations were discretized in the work by the finite difference method; however, in subsequent works, the results of the study will be used in parallel implementation of finite element methods. In conclusion, the results of computational experiments for various grid configurations and analysis of computational acceleration are presented.

Works [9, 10] are devoted to the study of the fictitious domain method for problems with discontinuous coefficients. In [11, 12], an elliptic-type equation with strongly varying coefficients is considered. Interest in the study of such equations is caused by the fact that equations of this type are obtained using the fictitious domain method. A special method is proposed for the numerical solution of an elliptic equation with strongly varying coefficients. A theorem is proved for estimating the rate of convergence of the developed iterative process. A computational algorithm is developed and numerical calculations are carried out to illustrate the effectiveness of the proposed method. In [13], modifications of well-known iterative methods for solving arising grid problems using the fictitious domain method were constructed. The capabilities of the fictitious domain method are illustrated by examples of solving problems of an ideal and viscous incompressible fluid, flows under a hydraulic structure.

Parallel implementations of the fictitious domain method are also known. For example, in [14] a parallel fictitious domain method was constructed for the three-dimensional Helmholtz equation, in [15] for modeling flows loaded with particles and turbulent flow in a channel, in [16] for problems of biomechanics.

Currently, high-performance computing is widely used in research. Every day, computing techniques and hydrodynamic models are developing, which allow the assessment and analysis of various technological processes. In this regard, increases the efficiency of solving scientific problems. Supercomputer technology is widely used in many industries. Computations performed on graphic devices significantly speed up the calculation of «large» tasks, due to its unique architecture [17, 18].

A lot of work has been devoted to the study of the applicability of the CUDA parallel computing architecture, which allows increasing computational performance due to the use of graphic processors. Its many applications to the problems of computational fluid dynamics are known, including the problems of the oil industry [17, 19], the problems of motion of a viscous incompressible fluid [18], the problems of underground hydrogen storage [20] and others [18, 21].

FORMULATION OF THE PROBLEM

To simulate convective flows, we consider the Navier–Stokes equations in the Boussinesq approximation [7]:

$$\frac{\partial u}{\partial t}+u\frac{\partial u}{\partial x}+v\frac{\partial u}{\partial y}+\frac{\partial p}{\partial x}=\frac{1}{\mathrm{Re}}\Delta u,\quad \frac{\partial v}{\partial t}+u\frac{\partial v}{\partial x}+v\frac{\partial v}{\partial y}+\frac{\partial p}{\partial y}=\frac{1}{\mathrm{Re}}\Delta v-\mathrm{Gr}\theta, \tag{1}$$

$$\frac{\partial u}{\partial x}+\frac{\partial v}{\partial y}=0, \tag{2}$$

$$\frac{\partial \theta}{\partial t}+u\frac{\partial \theta}{\partial x}+v\frac{\partial \theta}{\partial y}=\frac{1}{\mathrm{RePr}}\Delta\theta,\ \ (x,y)\in D,\ t\in(0,T] \tag{3}$$

with initial and boundary conditions

$$u=u_0(x,y),\ \ v=v_0(x,y),\ \ \theta=\theta_0(x,y),\ \ (x,y)\in\overline{D},\ t=0, \tag{4}$$

$$u=a_x(x,y,t),\ \ v=a_y(x,y,t),\ \ \theta=\xi(x,y,t),\ \ (x,y)\in\partial D,\ t=[0,T], \tag{5}$$

where u, v are the velocity components, p is the pressure, θ is the temperature, Re is the Reynolds number, Gr is the Grashof number, Pr is the Prandtl number, $\partial D = \gamma_1 \cup \gamma_2$ is the boundary of the domain.

It is convenient to solve problem (1)-(5) by eliminating pressure from the equations of motion and introducing new variables — the stream function and vorticity. An essential role is played by the integral conditions for the uniqueness of pressure. In the work of Ladyzhenskaya O. A. for the unique solvability of the difference scheme for the Navier-Stokes equation, the uniqueness condition for the pressure of the following form is added to the system of equations [22]: $\iint_D p(x,y)\,dx\,dy = 0$. The necessity of setting a condition in this form is due to the fact that the difference analogue of equation (2) is not linearly independent. In the work of Syrochenko V. P. [7] another variant of the pressure uniqueness condition is proposed which is written as

$$\oint_{\gamma_3} \frac{\partial \Pi}{\partial x} dx + \frac{\partial \Pi}{\partial y} dy = 0 \tag{6}$$

where $\Pi = p + \left(u^2 + v^2\right)/2$ is the full pressure.

Introduce the current function ψ and the velocity vortex ω, which are related to the velocity components u, v by the following relations: $u = \dfrac{\partial \psi}{\partial y},\ v = -\dfrac{\partial \psi}{\partial x},\ \omega = \dfrac{\partial u}{\partial y} - \dfrac{\partial v}{\partial x}$.

Problem (1)-(5) in variables ψ, ω is written as follows [7]:

$$\frac{\partial \omega}{\partial t} + \frac{\partial \psi}{\partial y}\frac{\partial \omega}{\partial x} - \frac{\partial \psi}{\partial x}\frac{\partial \omega}{\partial y} = \frac{1}{\mathrm{Re}}\Delta\omega + \mathrm{Gr}\frac{\partial \theta}{\partial x}, \quad \Delta\psi = \omega, \tag{7}$$

$$\frac{\partial \theta}{\partial t} + \frac{\partial \psi}{\partial y}\frac{\partial \theta}{\partial x} - \frac{\partial \psi}{\partial x}\frac{\partial \theta}{\partial y} = \frac{1}{\mathrm{RePr}}\Delta\theta, \ (x,y) \in D,\ t \in (0,T], \tag{8}$$

$$\omega = \alpha(x,y), \ \theta = \phi(x,y), \ (x,y) \in \overline{D}, \ t = 0, \tag{9}$$

$$\psi = \xi_1(x,y,t), \ \frac{\partial \psi}{\partial \vec{n}} = \eta_1(x,y,t), \ (x,y) \in \gamma_1, \ t \in (0,T], \tag{10}$$

$$\psi = \xi_2(x,y,t) + \lambda(t), \ \frac{\partial \psi}{\partial \vec{n}} = \eta_2(x,y,t), \ (x,y) \in \gamma_2, \ t \in (0,T], \tag{11}$$

$$\theta = \beta_l(x,y,t), \ (x,y) \in \gamma_1, \ l = 1,2, \ t \in (0,T], \tag{12}$$

α, ϕ, ξ_i, η_i, β_i, $i = 1,2$ are given functions. Write the condition (6) as follows:

$$\oint \left[\left(\frac{\partial^2 \psi}{\partial t \partial y} + \omega\frac{\partial \psi}{\partial x} + \frac{1}{\mathrm{Re}}\frac{\partial \omega}{\partial y}\right)dx + \left(-\frac{\partial^2 \psi}{\partial t \partial x} + \omega\frac{\partial \psi}{\partial y} - \frac{1}{\mathrm{Re}}\frac{\partial \omega}{\partial x} - \mathrm{Gr}\theta\right)dy\right] = 0. \tag{13}$$

The solution of the difference analogue of problem (7)-(13) is sought in the form

$$\omega^{n+1}(x,y) = \omega_0^{n+1}(x,y) + \lambda^{(n+1)}\omega_1^{n+1}(x,y), \ \ \psi^{n+1}(x,y) = \psi_0^{n+1}(x,y) + \lambda^{(n+1)}\psi_1^{n+1}(x,y), \tag{14}$$

where n is the number of iterations. The first auxiliary problem is as follows:

$$\frac{\omega_0^{n+1} - \omega^n}{\tau} + \frac{\partial \psi^n}{\partial y}\frac{\partial \omega_0^{n+1}}{\partial x} - \frac{\partial \psi^n}{\partial x}\frac{\partial \omega_0^{n+1}}{\partial y} = \frac{1}{\mathrm{Re}}\Delta\omega_0^{n+1} + \mathrm{Gr}\frac{\partial \theta^{n+1}}{\partial x}, \tag{15}$$

$$\Delta\psi_0^{n+1} = -\omega_0^{n+1}, \ (x,y) \in D,$$

$$\psi_0^{n+1}\Big|_{\gamma_1} = 0, \ \ \frac{\partial \psi_0}{\partial n}\Big|_{\gamma_1} = 0, \ \psi_0^{n+1}\Big|_{\gamma_2} = 0, \ \ \frac{\partial \psi_0}{\partial n}\Big|_{\gamma_2} = 0, \tag{16}$$

the second auxiliary problem is as follows:

$$\frac{\omega_1^{n+1}-\omega^n}{\tau}+\frac{\partial \psi^n}{\partial y}\frac{\partial \omega_1^{n+1}}{\partial x}-\frac{\partial \psi^n}{\partial x}\frac{\partial \omega_1^{n+1}}{\partial y}=\frac{1}{\mathrm{Re}}\Delta\omega_1^{n+1}, \tag{17}$$

$$\Delta\psi_1^{n+1}=-\omega_1^{n+1},\ (x,y)\in D,$$

$$\left.\psi_1^{n+1}\right|_{\gamma_1}=0,\ \left.\frac{\partial \psi_1^{n+1}}{\partial n}\right|_{\gamma_1}=0,\ \left.\psi_1^{n+1}\right|_{\gamma_2}=1,\ \left.\frac{\partial \psi_1^{n+1}}{\partial n}\right|_{\gamma_2}=0. \tag{18}$$

We construct a uniform mesh in domain D:

$$D_h=\left\{(x_i,y_j),\ x_i=(i-1)h_1,\ y_j=(j-1)h_2,\ i=0,1,...,n_1,\ j=0,1,...,n_2,\ h_1=\frac{l_1}{n_1-1},\ h_2=\frac{l_2}{n_2-1}\right\}.$$

We suppose that the inner subdomain D_0 is a rectangle:

$$D_{0h}=\left\{(x,y),\ x_{k1}\leq x\leq x_{k2},\ y_{m1}\leq y\leq y_{m2},\ x_i=(i-1)h_1,\ y_j=(j-1)h_2,\ i=0,1,...,n_1,\ j=0,1,...,n_2\right\},$$

nodes of which build in domain D. We consider domain $D_1=\{(x,y),\ x_{k3}\leq x_{k4},\ y_{m3}\leq y\leq y_{m4}\}$ covering domain D_0.

RESULTS AND DISCUSSION

The above method has numerically solved test problem (1)-(5) for the Navier-Stokes equations of a viscous incompressible fluid in variables: stream function, velocity vortex in the Boussinesq approximation.

The temperature distributions and current functions are presented as numerical results. The results were obtained for various cavity sizes, temperature conditions at the boundary, and values that determine the flow of dimensionless parameters — the Grashof Gr and Prantl Pr numbers. The first method is based on constructing a difference problem in variables of the stream function and the vortex of velocity using the uniqueness condition for pressure. This condition allows us to determine the coefficient used in formula (14). The solutions for the function of the current and the velocity vortex are found as the sum of two simple problems. The developed algorithm converges uniformly for a certain amount of iteration, and with the help of the developed numerical algorithm, more accurate results are obtained. The numerical results of this method are presented in Figure 1.

The second approach is based on solving the fictitious domain method with continuation of the lower coefficient. The solution lies with the accuracy ε. This method is simple to implement and does not require the condition of pressure to be unambiguous. Figure 2 show the results of the task posed by the fictitious domain method with a continuation on the lower coefficients.

A parallel algorithm for this task was implemented using the CUDA architecture. When implementing the parallel algorithm on CUDA, two optimization methods were used:

1. Streams of computational data are copied to the internal cells of the subdomain from global memory to shared memory, then boundary data is copied from global memory. In this case, the size of the subdomain does not change [21].

2. We cannot avoid duplicating data from the global memory at the boundary of a subdomain. In the above cases, columns and rows are copied at the boundaries of the subarea. Therefore, you need to change the scheme of two-dimensional decomposition to one-dimensional. Thus, we exclude repeated copying of columns. It is known that in C++ the matrix elements in memory are stored line by line. In this case, each block gets a one-dimensional array, which consists of rows of matrices of the original block.

In the calculations, a uniform grid of 128 x 128, 256 x 256, 512 x 512, 1024 x 1024 and 2048 x 2048 sizes were used. All data were presented as real numbers with single precision (float). A computational experiment was carried out on a personal computer with a quad-core Intel Core i7-3770 3.40 GHz processor and an Nvidia GeForce GTX 550 Ti graphics card. The test result is shown in Figure 3 (a). In the calculation, the optimal block size was 16x16 (the number of threads in one block is 256). Figure 3 (b) shows the performance gain compared to a sequential algorithm depending on the size of the grid.

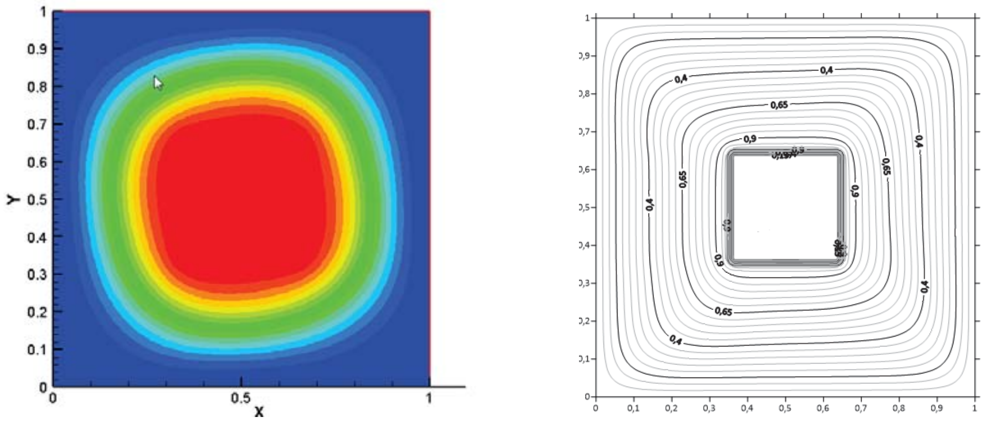

(a) (b)

FIGURE 1. Isolines (a) and isotherms (b). Cavity size is 1.0×1.0, on internal borders $\theta = 1$, $\mathrm{Pr} = 5.39$, $\mathrm{Gr} = 100$

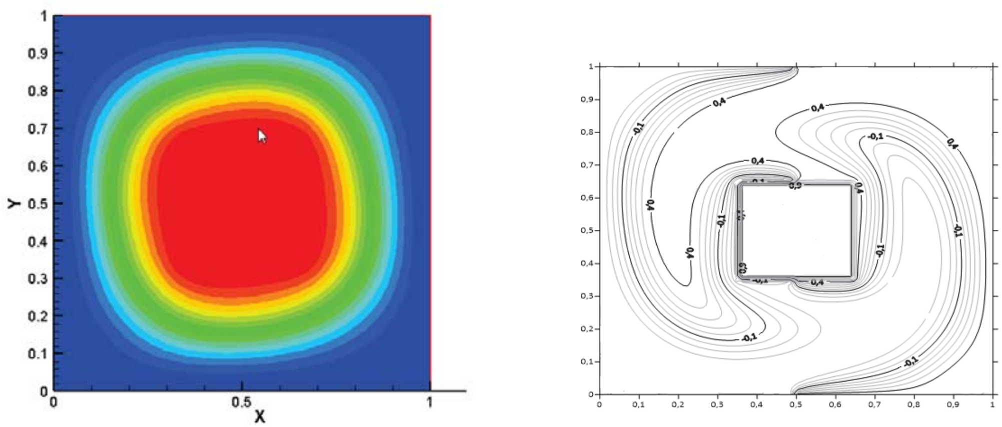

(a) (b)

FIGURE 2. Isolines (a) and isotherms (b). Cavity size is 1.0×1.0, on internal borders (a) $\theta = 0.5$, (b) $\theta = -0.5$, $\mathrm{Pr} = 5.39$, $\mathrm{Gr} = 100$

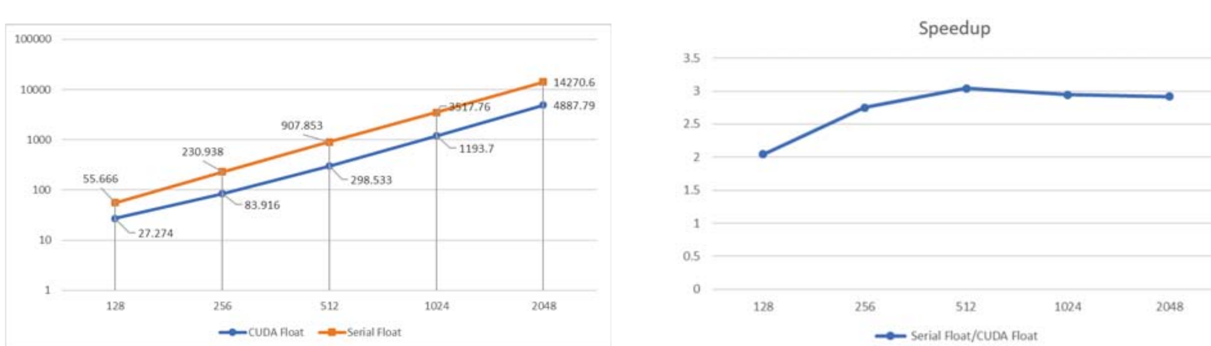

(a) (b)

FIGURE 3. (a) Time of execution of the parallel algorithm on different computational mesh, (b) Acceleration of parallel algorithm on CUDA

CONCLUSION

Thus, in the paper, questions of the numerical implementation of the Navier-Stokes equations in a two-dimensional doubly connected domain using the CUDA parallel computing architecture are investigated. The results of computational experiments show that the use of parallel algorithms using CUDA for this kind of tasks gives good acceleration.

Further research will be aimed at creating parallel algorithms and speeding up computations related to solving nonlinear multiphase filtering problems by finite element methods using the CUDA hardware-software parallel computing architecture.

ACKNOWLEDGMENTS

This work was supported by grant funding for scientific and technical programs and projects of the Ministry of Education and Science of the Republic of Kazakhstan (Grant No. AP08053189).

REFERENCES

1. B. Zhumagulov, N. Temirbekov, and D. Baigereyev, AIP Conference Proceedings **1880**, 060001 (2017).
2. W. Wójcik, N. Temirbekov, and D. Baigereyev, Przeglad Elektrotechniczny **92 (7)**, 24–31 (2016).
3. B. Zhumagulov and V. Monakhov, *Fluid Dynamics of Oil Production* (Elsevier, 2014) pp. 177–178.
4. F. Cimolin and M. Discacciati, Applied Numerical Mathematics **72**, 205–224 (2013).
5. J. From, *Unsteady Flow of an Incompressible Viscous Fluid. Computational Methods in Hydrodynamics* (Publishing House of Moscow State University, 1967) pp. 343–381.
6. D. R. Sood and J. H. E. Elrod, AIAA Journal **12 (5)**, 636–641 (1974).
7. V. P. Syrochenko, Proceedings of the International Conference RDAMM-2001 **6**, 554–562 (2001).
8. J. Adlam, Computers and Fluids **14 (2)**, 141–157 (1986).
9. P. Sun and C. Wang, Applied Numerical Mathematics **152**, 199–220 (2020).
10. P. Sun, Journal of Computational and Applied Mathematics **356**, 81–97 (2019).
11. A. N. Temirbekov and W. Wojcik, International Journal of Electronics and Telecommunications **60 (3)**, 219–223 (2014).
12. A. N. Temirbekov, AIP Conference Proceedings **1759**, 020053 (2016).
13. P. N. Vabishchevich, *The Fictitious Domain Method in Problems of Mathematical Physics* (URSS, 2017) p. 160.
14. E. Heikkola, T. Rossi, and J. Toivanen, SIAM Journal on Scientific Computing **24 (5)**, 1567–1588 (2000).
15. Z. Yu, Z. Lin, X. Shao, and L.-P. Wang, Engineering Applications of Computational Fluid Mechanics **10 (1)**, 160–170 (2016).
16. M. Ruess, V. Varduhn, E. Rank, and Z. Yosibash, 2012 11th International Symposium on Parallel and Distributed Computing , 279–285 (2012).
17. D. Z. Akhmed-Zaki, B. S. Daribayev, T. S. Imankulov, and O. N. Turar, Eurasian Journal of Mathematical and Computer Applications **5 (2)**, 4–13 (2017).
18. D. V. Degi, A. V. Starchenko, and A. A. Trunov, Scientific Internet service: supercomputer centers and tasks: Proceedings International Supercomputer Conference , 346–348 (2010).
19. T. Bekibaev, B. Asilbekov, U. Zhapbasbayev, I. Beisembetov, and B. Kenzhaliev, Bulletin of KazNU. Series mat., fiz., inf. **1 (72)**, 65–78 (2012).
20. A. Koldas and A. Toleukhanov, Bulletin of the NAS of the Republic of Kazakhstan. A Series of Physical and Mathematical Sciences **5**, 181–189 (2013).
21. D. Demidov, A. Egorov, and A. Nuriev, Uchenye Zapiski Kazan University. A Series of Physical and Mathematical Sciences **152**, 142–154 (2010).
22. O. Ladyzhenskaya, *Mathematical Problems of the Dynamics of a Viscous Incompressible Fluid* (Science, 1970).
23. J. C. Thibault and I. Senocak, 47th AIAA Aerospace Sciences Meeting including the New Horizons Forum and Aerospace Exposition (2012).

To Mathematical Modeling of Nonlinear Problem Biological Population in Nondivergent Form with Variable Density

Mirsaid M. Aripov,[1, a)] Shakhlo A. Sadullayeva,[2, b)] and Maftuha Z. Sayfullayeva[1, c)]

[1)] *National University of Uzbekistan named after Mirzo Ulugbek, Uzbekistan*
[2)] *Tashkent University of Information Technologies named after Muhammad al-Khwarizmi, Uzbekistan*

[a)] *Corresponding author: mirsaidaripov@mail.ru*
[b)] *Electronic mail: orif_sh@list.ru*
[c)] *Electronic mail: maftuha87@mail.ru*

Abstract. Mathematical modeling of the nonlinear problem biological population nondivergent form with absorption, variable density are considered. Qualitative properties of considered problem which include the critical and double critical cases are discussed. Results of the numerical experiments are analyzed.

INTRODUCTION

Consider the following Cauchy problem for degenerate parabolic equation in nondivergent form with absorption and variable density

$$Lu \equiv -\frac{\partial u}{\partial t} = u^n \nabla(|x|^l u^{m-1} |\nabla u^k|^{p-2} \nabla u) + \gamma(t)u - b(t)u^q, \tag{1}$$

$$u(0,x) = u_0(x) \geq 0,\ x \in R^N.$$

Here $u(x,t)$ is the population, n, l, k, p are given numerical parameters characterizing media, $0 < \gamma(t), b(t) \in C(0,\infty), q \geq 1$.
Equation (1) in the case $n+k(p-2)+m-1 > 0$ corresponds to slowly diffusion and in the case $n+k(p-2)+m-1 < 0$ it corresponds to fast diffusion equation.

Problem (1), in particular value of numerical parameters, is used for modeling different physical, chemical, biological, spread of an epidemic filtration in gas, liquid, and other processes [1-9]. Many works are devoted to investigate qualitative properties of solutions of Cauchy problem (1) and boundary value problem for particular value of numerical parameters [1-15]. For instance, A. A. Samarskii, V. A. Galaktionov and S. P. Kurdyumov [2] and V. A. Galaktionov [3] studied the properties of self-similar solutions (1), (2) in details when $q > 1$, $n = 0$, $p = 2$, $b(t) = 1$, $\gamma(t) = 0$. In particular, they established a new asymptotic solution for large t in the critical value of the numerical parameter $q = 1 + 2/N$.

Mathematical theory of the porous medium equation ($n = 0$, $l = 0$, $p = 2$, $b(t) = 0$) was considered by J. Vazguez [4]. Chunhua Jin and Jingxue Yin [5] studied properties of self-similar solutions for a class of nondivergent form equations. M. Bertsh, R. D. Passo and M. Ughi [6] established nonuniqueness of solutions of the equation (1) when $q > 1$, $l = 0$, $b(t) = 0$, $\gamma(t) = 1$. C. Z. Yao, Z. Wenshu [7] considered shrinking self-similar solutions of a nonlinear diffusion equation with nondivergent form in the case $b(t) = 0$, $l = 0$, $\gamma(t) = 1$. Blow up property, Fujita type global solvability for double linear parabolic equation with variable coefficient and nonlinear source in the case $n = 0$, $b(t) = 0$, $\gamma(t) = 1$ were studied by P. Cianci, A. V. Martynenko, and A. F. Tedeev [9]. J. N. Zhao [10] considered for p-Laplacian equation case.

In works [13-20] for case $n = 0$, $b(t) = 0$ with different variable density and with source or absorption, authors studied different qualitative properties of solution of the problem (1) based on self-similar approach. In particular estimates of solutions, and free boundary, Fujita type global solvability Cauchy problem, phenomena finite speed of propagation, condition of a space localization, the asymptotic of self-similar solutions, large time asymptotic in critical case [17] of the heat conduction problem with double nonlinearity with absorption at a critical parameter [19, 20], the critical curves of a doubly nonlinear parabolic equation in nondivergent form with a source and a nonlinear boundary flux were considered.

International Conference on Analysis and Applied Mathematics (ICAAM 2020)
AIP Conf. Proc. 2325, 020064-1–020064-6; https://doi.org/10.1063/5.0040820
Published by AIP Publishing. 978-0-7354-4069-2/$30.00

In [11], for equation (1) in case $l = n = 0$, $m = k$, $0 < q < 1$, $b(t) = 0$, by constructing an exact solution and by analyzing it, L. K. Martinson established the following properties of solutions: an inertial effect of a finite velocity of propagation of thermal disturbances, spatial heat localization and finite time localization solution effect.

Considered problem for particular value of numerical parameters under some suitable assumptions, the existence, uniqueness and regularity of a weak solution to the Cauchy problem (1) and their variants have been extensively investigated by many authors [1-11]. Moreover, Z. Xiang, C. Mu and X. Hu [12] investigated the properties of spatial localization, existence and non-existence of global solutions for problem (1) - (2) in case $l = n = 0$, $k = 1$, $b(t) = 0$, $q \geq 1$, $\gamma(t) = 1$.

V. Galaktionov and J. R. King [15] established behavior of blow-up interfaces, an asymptotic analysis of the behavior of blow-up solutions for an inhomogeneous filtration equation with variable density.

P. Zheng, C. Mu, D. Liu, X. Yao, and S. Zhou [21] studied the properties of solution of self-similar equation double nonlinear parabolic equation with source in case $l = n = 0$, $b(t) = 0$ $q \geq 1$.

In this work, we establish the condition of Fujita type global solvability considered problem, estimates of solution for p>l and and free boundary. The critical case $n+k(p-2)+m+n-1 = 0$ and double critical case $n+k(p-2)+m+n-1 = 0$, $p = l$ are considered. The following properties of solutions: an effect of a finite velocity population flash disturbances, spatial localization flash population established. An exact solution for wide class of coefficients $\gamma(t)$, $b(t)$ are obtained. The results of the numerical experience are given.

GENERALIZED RADIAL SYMMETRICAL PRESENTATION OF THE EQUATION (1)

By putting,

$$u(t,x) = \bar{u}(t)w(\tau(t), \varphi(|x|))$$

in (1), where

$$\bar{u}(t) = \exp(\int_0^t b(y)dy),$$

$$\tau(t) = \int_0^t [\bar{u}(y)]^{k(p-2)+n+m-1}dy,$$

$$\varphi(|x|) = \frac{p}{p-l}|x|^{(p-l)/p}, \; if \; p > l,$$

$$\varphi(|x|) = \ln|x|, \; if \; p = l,$$

equation (1) can be reduced to the "radial-symmetric" form

$$\frac{\partial w}{\partial \tau} = w^n \varphi^{1-s}\frac{\partial}{\partial \varphi}\left(\varphi^{s-1}w^{m-1}\left|\frac{\partial w^k}{\partial \varphi}\right|^{p-2}\frac{\partial w}{\partial \varphi}\right) - b_0(\tau)w^\beta = 0, \; if \; p > l, \tag{2}$$

$$\frac{\partial w}{\partial \tau_1} = w^n(\frac{\partial}{\partial \varphi}\left(w^{m-1}\left|\frac{\partial w^k}{\partial \varphi}\right|^{p-2}\frac{\partial w^l}{\partial \varphi}\right) + w^{m-1}\left|\frac{\partial w^k}{\partial \varphi}\right|^{p-2}\frac{\partial w}{\partial \varphi}) - b_0(\tau)w^\beta = 0, \tag{3}$$

if $p = l$, where $b_0(\tau) = \gamma(t)\,[\bar{u}(y)]^{-(k(p-2)+n+m-1)}$, $s = pN/(p-l)$.

Notice that, number s plays role of dimension in equation (2). Presentation of the equation in the form (2), (3) allows us easily construct the Zeldovich-Barenblatt-Pattle type solution [1] to the principal member of the equation (1)

$$\frac{\partial u}{\partial t} = u^n \nabla(|x|^l u^{m-1}\left|\nabla u^k\right|^{p-2}\nabla u). \tag{4}$$

Introduce the functions

$$u_+(\tau,x) = \bar{u}(t)\tilde{u}(\tau)\bar{f}(\eta),$$

$$\eta = \varphi/[\tau_1(\tau)]^{1/p},\ \tilde{u}(\tau) = [T + (\beta-1)\int_0^\tau b_0(y)]^{-1/(\beta-1)},$$

$$\eta = \varphi(|x|)/[\tau(t)]^{1/p},\ \varphi(|x|) = \frac{p}{p-l}\,|x|^{(p-l)/p},\ p > l,$$

$$\tau_1(\tau) = \int_0^t [\tilde{u}(y)]^{k(p-2)+n+m-1}dy,$$

$$b_1 = (k(p-2)+m+n-1)p^{p/(p-1)},\ p > l,$$

$$\eta = \varphi(|x|)/[\tau(t)]^{1/p},\ \varphi(|x|) = \ln|x|,\ if\ p = l,$$

$$\overline{f}(\eta) = \begin{cases} (a - b_1|\eta|^{p/(p-1)})_+{}^{(p-1)/(k(p-2)+m+n-1)},\ if\ k(p-2)+m+n-1 \neq 0 \\ \exp(-\frac{(p-1)\eta^{p/(p-1)}}{k^{(p-2)/(p-1)}p^{1/(p-1)}},\ if\ k(p-2)+m+n-1 = 0 \end{cases}. \tag{5}$$

FUJITA TYPE GLOBAL SOLVABILITY

Theorem 1 *Assume that* $k(p-2)+m+n-1 > 0, \quad p > l,$

$$b_0(\tau)[\tilde{u}(\tau)]^{q-(k(p-2)+m+n)}\tau_1(\tau) < s/p,\ T \geq 0,\ \tau > 0,$$

$$u_0(x) \leq u_+(0,x),\ x \in R^N.$$

Then, there is a global solution to the Cauchy problem (1)-(2) for which the estimate

$$u(t,x) \leq u_+(t,x)\ \in\ Q$$

is valid and for free boundary the estimate
$|x| \leq (\frac{a}{b})^{(p-1)/p} p_1\,[\tau(t)]^{1/(p-l)}$*, holds where* $u_+(t,x)$ *is defined above.*

Critical case: The case $k(p-2)+m+n-1 = 0, \quad p > l$ we will call a *critical case*. In this case behavior of solution of the problem (1) changes. Namely, following statement is true.

Theorem 2 *Assume that* $k(p-2)+m+n-1 = 0, \quad p > l,$

$$b_0(\tau))[\tilde{u}(\tau)]^{q-1}(T+t) < N/p-l),\ T \geq 0,\ t > 0,$$

$$u_0(x) \leq u_+(0,x),\ x \in R^N.$$

Then, there is a global solution to the Cauchy problem (1) for which in Q the estimate

$$u(t,x) \leq u_+(t,x) = \bar{u}(t)\tilde{u}(\tau)\bar{f}(\xi),\ \xi = \varphi(|x|)/(T+\tau(t))^{1/p}$$

holds. Here, $\bar{u}(t),\ \tilde{u}(t),\ \bar{f}(\xi),\ \tau(t)$ *are above defined functions.*

Malthusians model case: $\beta = 1$. When in (1) $\beta = 1$, $k = 1$, $p = 2$ the problem (1) is known as Malthusian population model [1,23]. In this case depending on value numerical parameters we establish property a finite speed of population depth and a space localization.

Theorem 3 *Let us*

$$\beta = 1,\ p > l,\ n + m + k(p-2) > 1,$$

$$\tau_2(\infty) < +\infty,\ \alpha \le s/[p + (k(p-2) + m - 1)s].$$

Then, the solution problem (1) has property a space localization if

$$u_0(x) \le z_1(0,x),\ x \in R^N.$$

For free boundary the estimate

$$|x| \le (a/b_1)^{(p-1)/p}\,[\tau_2(t)]^{1/(p+k(p-2)+m+n-1)s},\ x \in R^N,\ t > 0$$

holds. It is phenomena finite speed of perturbation [1].

Theorem 4 *Assume that*

$$k(p-2) + m + n - 1 = 0,\ p > l,\ u_0(x)\ \le z_+(0,x), x \in R^N \backslash \{0\},$$

$$\beta \ge (k(p-2) + m + n) + (1-q)(p-l)/N, q < 1.$$

Then, there is a global solution to the Cauchy problem (1) - (2) for which in $Q\backslash\{0\}$ the estimate

$$u(t,x)\ \le z_+(t,x) = \bar{u}(t)\tilde{u}(\tau)\exp(-\frac{(p-1)\eta^{p/(p-1)}}{k^{(p-2)/(p-1)}p^{1/(p-1)}}$$

holds, where

$$\eta = \varphi(|x|)/(T+t)^{1/p}, \tilde{u}(\tau) = (T + (\beta-1)\tau)^{-1/(\beta-1)}, \eta = \varphi[T+\tau]^{-1/p}.$$

Double critical case: The case $k(p-2) + m + n - 1 = 0, \quad p = l$ we will call a *double critical* case.

Theorem 5 *Assume $k(p-2) + m + n - 1 = 0, \quad p = l, \quad u_0(x) \le z_+(0,x), \quad x \in R^N\backslash\{0\}, \quad \beta \ge 1 + p$. Then, there is a global solution to the Cauchy problem (1)-(2) for which in $Q\backslash\{0\}$ the estimate*

$$u(t,x) \le z_2(t,x) = \bar{u}(t)\tilde{u}(\tau)(T+t)^{-1/p}\exp(-\frac{(p-1)\eta^{p/(p-1)}}{k^{(p-2)/(p-1)}p^{1/(p-1)}}, \mathit{in}\ Q\backslash\{0\}$$

holds, where

$$\eta = \ln(|x|)/(T+t)^{1/p}, \tilde{u}(\tau) = (T + (\beta-1)\int_0^\tau b_0(y)dy)^{-1/(\beta-1)}, T \ge 0.$$

Proof. Proof all Theorems based on comparison principle [1]. As comparison functions, we used the functions constructed above $u_+(t,x), \quad z_+(t,x), z_1(t,x), z_2(t,x)$. Further, we also checked it is satisfying the conditions $L(u_+) \le 0,\ L(z_+)\ \le 0, L(z_1) \le 0, L(z_2) \le 0$ for applying comparison principle.

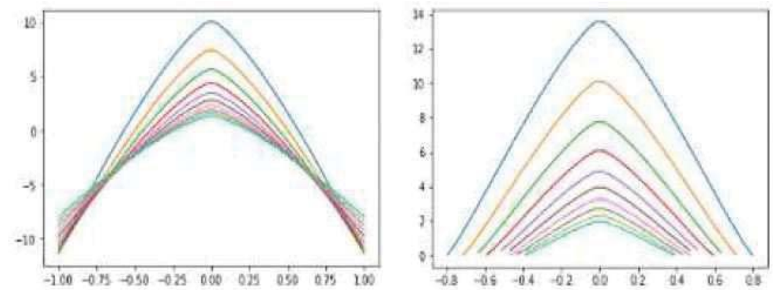

FIGURE 1. Parameters values: (left) n=1.1, p=4, k=1.3, m=1.3 (right) n=1.1, p=4, k=1.1, m=1.1

THE EXACT SOLUTION AND NONLINEAR PHENOMENA

It is proved that equation (1) has the following exact solution.

$$u(t,x) = \bar{u}(t)a(\tau)(f(\tau) - \varphi^{\gamma})_+^{\gamma_1},\ \gamma = p/(p-1),$$

$$\gamma_1 = (p-1)/(k(p-2)+m+n-1),$$

where functions $a(\tau),\ f(\tau)$ satisfy to the system of algebraic equation

$$\begin{aligned} &-\gamma\gamma_1 a(\tau)\tfrac{df}{d\tau} + b_1(\tau)a^q = (\gamma k\gamma_1)^{p-1}\gamma\gamma_1 a^{n+m+k(p-2)} f(\tau), \\ &\tfrac{da}{d\tau} + (\gamma k\gamma_1)^{p-1}[(\gamma\gamma_1 + s)]a^{k(p-2)+n+m} = 0,\ s = pN/(p-l). \end{aligned} \tag{6}$$

By the analysis of solutions, the following nonlinear effects observed: the inertial finite speed of propagation, the effect of a spatial localization of population flash, the effect of finite time of existence of population flash. Notice that this solution in the case $n = 0$, $k = 1$, $l = 0$, $b(t) = 0$ was constructed in the work [16].

RESULTS OF NUMERICAL EXPERIMENTS

Main problem for numerical calculation is to find appropriate initial approximation so that suggested numerical method quickly converges to the solution with necessary accuracy. Based on qualitative properties of solutions established above the numerical calculations are analyzed. For the numerical calculations used modification method [5] suggested for numerical calculation of weak wave type solution to porous media equation. Computational experiments showed the sweep method is stable and provides a unique solution. Results of a numerical experiments showed, usage estimates of solutions and free boundary are good appropriate for construction of iteration process quickly converging to solution of the considered problem keeping nonlinear effects. Due to appropriate initial approximation depending value the numerical parameters reached quickly convergence to solution initial problem. Number iteration in each case not more than three. Obtained results is true for porous media equation, p-Laplacian equation with variable density. Some results of numerical experiments are given below. Numerical calculations were performed by using Python3.

CONCLUSION

In the work, the critical and double critical cases established due to as representation of the double nonlinear parabolic equation with variable density with absorption in "radial symmetrical" form. This presentation of an initial equation gave possibility to easy construct Zeldovoch- Barenbatt-Pattle type [1] solutions for critical cases as comparison functions. Using an algorithm of splitting Fujita type global solvability, considered problem covering all early results of other authors is established. We established the behavior of solution of the Cauchy problem for considered critical cases. The following phenomenon is finite speed of population flash and a space localization of population depth. Results of a numerical experiments showed that usage estimates of solutions and free boundary are good appropriate for construction of iteration process quickly converging to solution of the considered problem keeping nonlinear effects.

ACKNOWLEDGES

This work was supported by grants of Fundamental Investigation OT-F-4-30 (2017-2020) Republic of Uzbekistan.

REFERENCES

1. M. Ughi, Ann. Mat. Pura Appl. **143**, 385-400 (1986).
2. A. A. Samarskii, V. A. Galaktionov, S. P. Kurdyomov, and A. P. Mikhailov, *Blow-up in Quasilinear Parabolic Equations* (Walter de Gruyter, Berlin, 1995).
3. V. A. Galaktionov, S. P. Kurdyumov, and A. A. Samarskiy, Mathematics of the USSR-Sbornik **54(2)**, 421-455 (1986).
4. J. L. Vazquez, *The Porous Medium Equation: Mathematical Theory (Oxford Math. Monogr., Oxford University Press, Oxford, 2007).*
5. *C. Jin and J. Yin, Nonlinear Differential Equations and Applications **20**, 873-893 (2013).*
6. *M. Bertsh, R. Dal Passo, M. Ughi, Anali di Matematica pura e dapplicate **CLXI**, 57-81 (1992).*
7. *Y. Zhengan and Z. Wenshu, J. Math. Anal. Appl. **325**, 183-204 (2007).*
8. *S. Wang, M. X. Wang, and C. H. Xie, Z. Angew. Math. Phys. **51**, 149-159 (2000).*
9. *P. Cianci, A. V. Martynenko, and A. F. Tedeev, Nonlinear Analysis: Theory, Methods & Applications A **73(7)**, 2310-2323 (2010).*
10. *Z. Wenshu and Y. Zhengen, Acta Mathematica Scienta **30(B(5))**, 1679-1686 (2010).*
11. *L. K. Martinson, J. Computational and Mathematical Physics **24(3)**, 462-467 (1984).*
12. *Z. Xiang, C. Mu, and X. Hu, Applications **68(7)**, 1940-1953 (2008).*
13. *J. N. Zhao, Journal of Differential Equations **121(2)**, 329-383 (1995).*
14. *S. Zhou, X. Bai, and S. Zheng, J. Math. Anal. Appl. **373**, 252-263 (2011).*
15. *V. Galaktionov and J. R. King, Journal of Applied Mathematics **57**, 53-77 (1996).*
16. *M. M. Aripov and M. Z. Sayfullaeva, Math. Modeling Mathematical Modeling **3(2)**, 46-51 (2019).*
17. *M. Aripov, A. Mukimov, and B. Mirzayev, Mathematics and Statistics **7(5)**, 205-217 (2019).*
18. *M. M. Aripov and D. K. Muhamediyeva, IOP Conf. Series: Journal of Physics: Conference Series **1441**, 012131 (2020).*
19. *M. Aripov, The Fujita and Secondary Type Critical Exponents in Nonlinear Parabolic Equations and Systems, Differential Equations and Dynamical Systems, 2018, 9-24*
20. *M. Aripov and J. R. Raimbekov, Journal of Siberian Federal University. Mathematics & Physics **12(1)**, 1-13 (2019).*
21. *P. Zheng, C. Mu, D. Liu, X. Yao, and S. Zhou, Abstr. Appl. Anal. **2012**, Article ID 109546 (2012).*

Mathematical Modelling of Covid-19 with the Effect of Vaccine

Nezihal Gokbulut,[1, 2, a)] Bilgen Kaymakamzade,[1, 2, b)] Tamer Sanlidag,[3, c)] and Evren Hincal[1, 2, d)]

[1)] *Department of Mathematics, Near East University, Nicosia, Mersin 10, Turkey*
[2)] *Mathematics Research Center, Near East University, Nicosia, Mersin 10, Turkey*
[3)] *DESAM Institute, Near East University, Nicosia, Mersin 10, Turkey*

[a)] *Corresponding author: nezihal.gokbulut@neu.edu.tr*
[b)] *Electronic mail: bilgen.kaymakamzade@neu.edu.tr*
[c)] *Electronic mail: trsanlidag@yahoo.com*
[d)] *Electronic mail: evren.hincal@neu.edu.tr*

Abstract. Covid-19 is the most recently discovered infectious disease affecting the countries all around the world. SARS-CoV-2, which is a member of coronavirus family, is the virus that makes the infection. Until the 28th of September 2020, almost 34 million people infected by the virus and more than 1 million people died all around the world. One of the most discussed ideas about the disease to die out is vaccination. In our study, we tried to analyze this idea and show the effect of vaccine for Covid-19. Our work starts with constructing an SVI mathematical model. Afterwards, we made the analyze of our model. Then, by taking into consideration of incoming passengers and precautions that should be taken, we used the vaccination idea with changing the percentage of vaccinated people in a population. In last section, we used numerical simulations to support our idea. In our work, we conclude that vaccination is substantially effective if we consider the other things that affect the disease which is incoming passengers and precautions like wearing mask, maintaining social distance, etc.

INTRODUCTION

Nowadays, the whole world is struggling with the epidemic called Covid-19. Disease can caught by an infection of the virus SARS-CoV-2, which is a member of coronavirus family. It is a respiratory disease that seriously affects lungs also [1]. When an infected person coughs, speaks or sneezes, people that are susceptible can get infected. From the point of symptoms and mode of transmission, Covid-19 shows similarities with other diseases caused by influenza viruses [2]. Ever since it became a pandemic, governments trying to make right decisions to prevent the spread. However, with the removal of restrictions on transportation between countries, the disease started to spread rapidly. In order to prevent the increase in spread of epidemic because of removal of these restrictions, people should comply with hygiene rules, wear masks, maintain social distance, and not to be in crowded environments unless necessary. As of September 28, 2020, there has been nearly 34 million Covid-19 infection with more than 1 million deaths in the world [3].

From the beginning of the epidemic, scientists are trying to find a solution to reduce the transmission and death rates. There are many ideas for the disease to die out in time, including herd immunity and vaccine [4]. For viruses, it has been stated that vaccine has a huge contribution in global health [5]. In order to prevent from influenza infection, which has many similarities with Covid-19, vaccine is the most effective option [6]. Influenza type A, also known as H1N1, became severe in April 2009 and in October 2009, vaccination for the disease started after the declaration of the disease as "pandemic" by WHO, in June 2009. According to the estimations, 700,000-1,500,000 clinical cases, hospitalization of 4,000-10,000 people and 200-500 deaths prevented, by means of vaccine, between 2009-2010 [7, 8].

The paper is organized as follows: first it is given model. Then, we gave the analysis of the model. Lastly, we gave numerical simulations to support the idea that vaccine is the most effective way for Covid-19 if people obey the rules stated above and the travel between countries restricted.

MODEL FORMULATION

In the model, there are four compartments as susceptible individuals S, infected individuals I, vaccinated individuals V, and recovered individuals R in a population. Here susceptible compartment includes the people that do not obey the rules we mentioned, the incoming passengers and the ones that are not vaccinated. The parameters used in the model are given in Table 1. The system is given as follows:

International Conference on Analysis and Applied Mathematics (ICAAM 2020)
AIP Conf. Proc. 2325, 020065-1–020065-5; https://doi.org/10.1063/5.0040301
Published by AIP Publishing. 978-0-7354-4069-2/$30.00

$$
\begin{cases}
\frac{dS}{dt} &= \Lambda - \beta S(t)I(t) - rS(t) - \mu S(t), \\
\frac{dV}{dt} &= rS(t) - kV(t)I(t) - (1-k)V(t) - \mu V(t), \\
\frac{dI}{dt} &= e^{-\mu\tau}(\beta S(t- \ \tau) + kV(t-\tau))I(t-\tau) - (d+\gamma+\mu)I(t), \\
\frac{dR}{dt} &= (1-k)V(t) + (d+\gamma+\mu)I(t).
\end{cases}
\tag{1}
$$

TABLE 1. Parameters of the model

Parameters	Descriptions
Γ	Recruitment of individuals
β	Transmission coefficient of susceptible individuals to the infected compartment
r	Rate of vaccination
k	Probability of vaccinated individuals to be infected
μ	Natural death rate
d	Death rate from the disease
τ	Incubation period
γ	Recovery rate

By using the system (1) and next generation matrix method, basic reproduction number R_0 calculated as

$$
R_0 = \frac{e^{-\mu\tau}}{(\gamma+\mu+d)(r+\mu)}\left[\beta + \frac{kr}{\mu+1-k}\right]. \tag{2}
$$

For details, [9] can be checked.

GLOBAL STABILITY ANALYSIS

Global stability analysis of the equilibrium points are explained in [9], in detail. For the stability, authors dealt with the following two theorems.

Theorem 1 *The disease free equilibrium is globally asymptotically stable if* $R_0 < 1$.

Theorem 2 *The endemic equilibrium is globally asymptotically stable.*

NUMERICAL SIMULATIONS

In this section, we discussed the relation between the spread of the disease and percentage of vaccinated people and susceptible compartment in a population. All of the ratios calculated by using the data taken from 50 countries which has the highest number of cases.

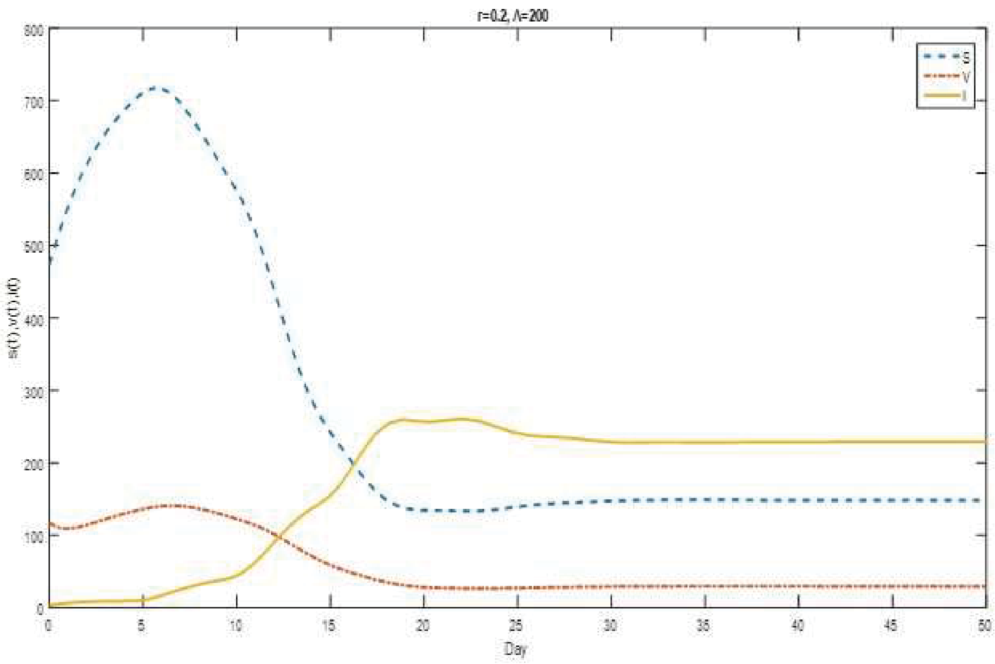

FIGURE 1. Parameter values: $\beta = 0.0035$, $k = 0.000001$ $\mu = 0.005$, $d = 0.0375$, $\tau = 4.6$ days, and $R_0 = 3.36$

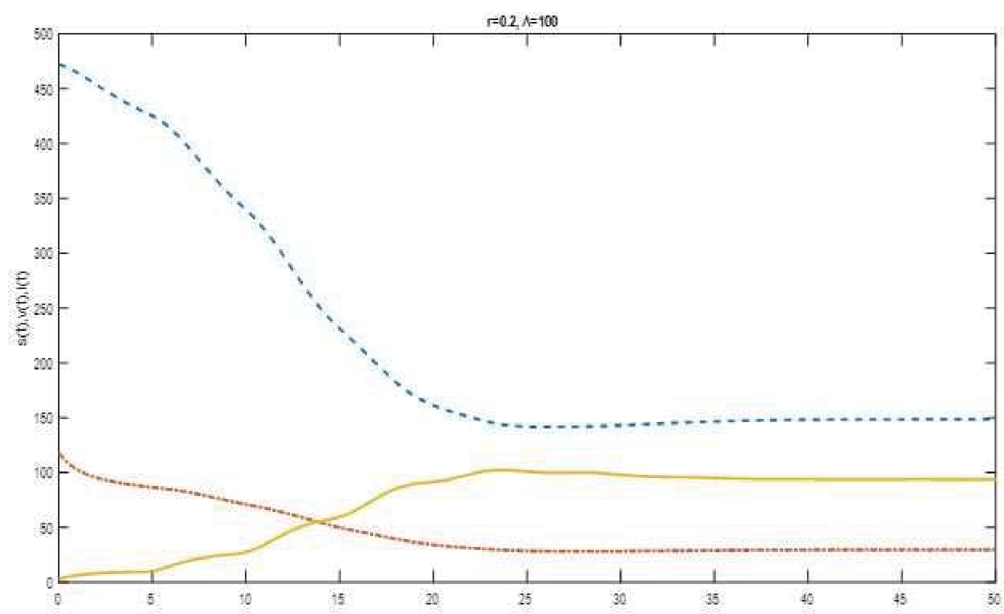

FIGURE 2. Parameter values: $\beta = 0.0035$, $k = 0.000001$ $\mu = 0.005$, $d = 0.0375$, $\tau = 4.6$ days, and $R_0 = 2.37$

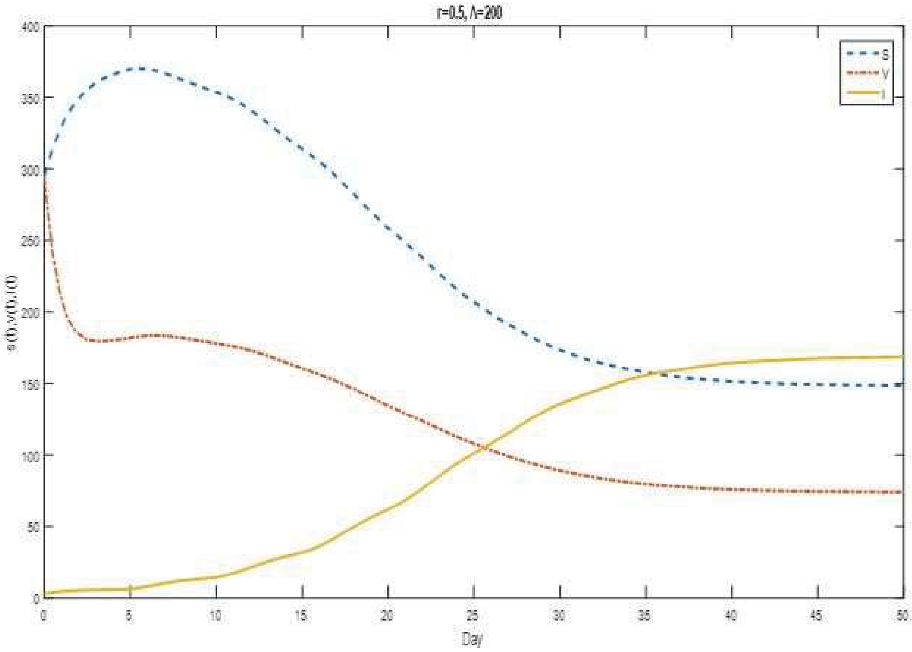

FIGURE 3. Parameter values: $\beta = 0.0035$, $k = 0.000001$ $\mu = 0.005$, $d = 0.0375$, $\tau = 4.6$ days, and $R_0 = 1.98$

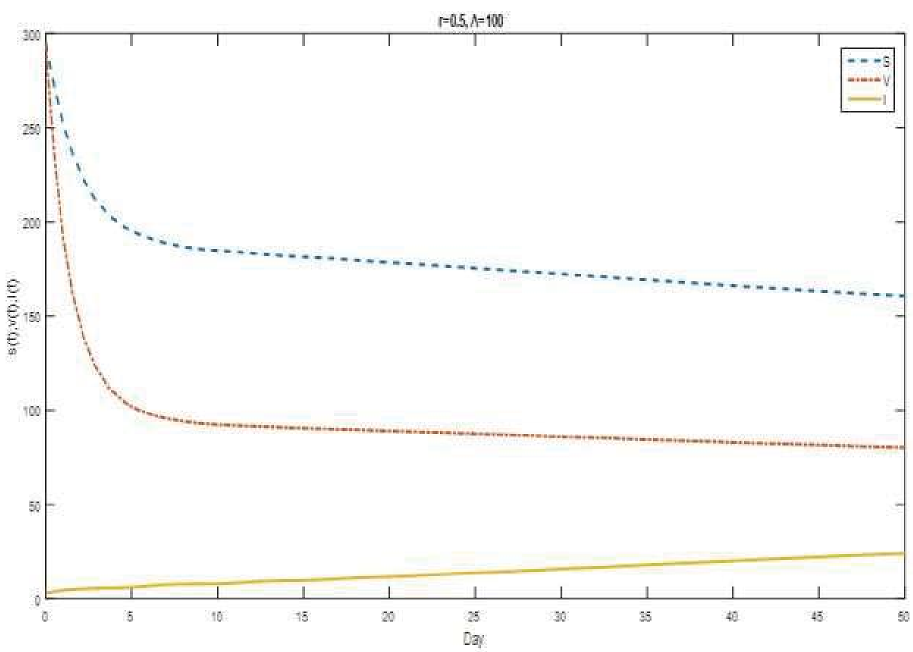

FIGURE 4. Parameter values: $\beta = 0.0035$, $k = 0.000001$ $\mu = 0.005$, $d = 0.0375$, $\tau = 4.6$ days, and $R_0 = 0.96$

RESULTS AND DISCUSSIONS

In this paper, the effect of vaccine verified. In order to see the effect of the vaccine it is assumed that 20% and 50% of the population are vaccinated. As a result of this, we can see from Figure 1 and Figure 3, in order to get a serious reaction, major percentage of the population should be vaccinated. On the other hand, there is a lot to think about such as the vaccine reaching every country, the cost of the vaccine, and the hesitation of people about whether or not to be vaccinated. So, we can not say that vaccine is enough for the disease to die out in time. Figure 2 shows that susceptible compartment is an important effect for the infectiousness of Covid-19. The decrease in susceptible compartment causes decrease in infected people with the implementation of vaccine. The predominant effect can achieved if enough people vaccinated in a population with the decrease in susceptible compartment as can be seen easily in Figure 4.

ACKNOWLEDGEMENTS

The publication has been prepared with the support of Mathematical Research Center.

REFERENCES

1. What does Covid-19 do to your Lungs?, https://www.webmd.com/lung/what-does-covid-do-to-your-lungs#1 (accessed 19 September, 2020).
2. C. Jiang, X. Yao, Y. Zhao, et. al., Elsevier Public Health Emergency Collection **22(6)**, 236-244 (2020).
3. Covid-19 coronavirus pandemic, https://www.worldometers.info/coronavirus/ (accessed 19 September, 2020).
4. What it would take for herd immunity to stop the Coronavirus pandemic, https://www.wsj.com/articles/what-it-would-take-for-herd-immunity-to-stop-the-coronavirus-pandemic-11600594201 (accessed 28 September, 2020).
5. B. Greenwood, Philos Trans R Soc Lond B Biol Sci. **369(1645)**, (2014).
6. C. Mameli, I. Cocchi, et. al., Front Pediatr. **7**, (2019).
7. Influenza A virus subtype H1N1, https://en.wikipedia.org/wiki/Influenza_A_virus_subtype_H1N1 (accessed 28 September, 2020).
8. R. H. Borse, S. S. Shrestha, A. E. Fiore, et. al., Emerging Infectious Diseases **19(3)**, 439-448 (2013).
9. B. Kaymakamzade and E. Hincal, AIP Conference Proceedings **1997**, 020025 (2018).

Numerical Study of Nonlocal BVP for a Third Order Partial Differential Equation

Allaberen Ashyralyev[1, 2, 3, a)] and Kheireddine Belakroum[4, b)]

[1)] *Department of Mathematics, Near East University, Nicosia, TRNC, Mersin 10, Turkey*
[2)] *Peoples' Friendship University of Russia (RUDN University), Ul Miklukho Maklaya 6, Moscow, 117198, Russian Federation*
[3)] *Institute of Mathematics and Mathematical Modeling, 050010, Almaty, Kazakhstan*
[4)] *Department of Mathematics, University of Mentouri Brothers- Constantine, Algeria*

[a)] *Electronic mail: allaberen.ashyralyev@neu.edu.tr*
[b)] *Corresponding author: kheireddinebelakroum@gmail.com*

Abstract. In the present study, first and second order of accuracy difference schemes for the numerical solution of the boundary value problem with nonlocal conditions for a one-dimensional third order partial differential equation are presented. Results of numerical experiments are provided.

INTRODUCTION

The subject of third order partial differential equations with time and space variables and nonlocal boundary conditions has been growing fast in the last years. In the last decades, the development of numerical techniques for the solution of nonlocal boundary value problems has been an important research topic in many branches of science and engineering. Numerical solution of third order partial differential equations with a nonlocal conditions to be a major research area with widespread applications in modern physics and technology. Note that these type of boundary value problems have been studied widely in the literature (for instance, see [1-14]).

The authors M. Deneche and A. Memou in paper [9] investigated nonlocal boundary value problem

$$\begin{cases} \frac{\partial^3 u(t)}{\partial t^3} + \frac{\partial}{\partial x}\left(a(x,t)\,\frac{\partial u}{\partial x}\right) = f(x,t),\ 0<t<T, 0<x<1, \\ u(x,0)=0,\ \frac{\partial u}{\partial t}(x,0)=0, \frac{\partial^2 u}{\partial t^2}(x,T)=0,\ x\in(0,1), \\ u(0,t)=0,\ t\in[0,T], \int_0^1 u(x,t)dx=0,\ t\in[0,T] \end{cases}$$

for third-order partial differential equations with integral conditions. This paper was proved the existence and uniqueness of a strong solution for a linear equation. The authors were also used energy inequalities and the density of the range of the generated operator.

In the paper [6] the nonlocal boundary value problem for the third order partial differential equation

$$\begin{cases} \frac{d^3 u(t)}{dt^3} + \mu\frac{d^2 u(t)}{dt^2} + A\frac{du(t)}{dt} = f(t), \quad 0<t<1, \mu>0, \\ u(0) = \gamma u(\lambda) + \varphi, \quad u'(0) = \alpha u'(\lambda) + \psi, |\gamma|<1, \\ u''(0) = \beta u''(\lambda) + \xi, \left|1+\alpha\beta e^{-\mu\lambda}\right| > \left(|\alpha+\beta| + \frac{\frac{\mu}{2}(|\alpha-\beta|}{\sqrt{\delta-\frac{\mu^2}{4}}}\right)e^{-\frac{\mu\lambda}{2}}, 0<\lambda\le 1 \end{cases}$$

in a Hilbert space H with a self-adjoint positive definite operator A was investigated. The main theorem on the stability estimates for the solution of problem is proved.

NUMERICAL EXPERIMENTS

When the analytical methods do not work properly, the numerical methods for obtaining approximate solutions of partial differential equations play an important role in applied mathematics. We can say that there are many considerable works in the literature (for instance, see [2, 3, 4, 5]). In this section for the approximate solution of a nonlocal

International Conference on Analysis and Applied Mathematics (ICAAM 2020)
AIP Conf. Proc. 2325, 020066-1–020066-8; https://doi.org/10.1063/5.0040592
Published by AIP Publishing. 978-0-7354-4069-2/$30.00

boundary value problem, we will use the first and second order of accuracy difference schemes. Numerically we show that the second order of accuracy for the approximate solution of the problem are more accurate than the first order of accuracy difference scheme. We apply a procedure of modified Gauss elimination method to solve the problem. Results of numerical experiences are given.

The First Order of Accuracy Difference Scheme

We consider the nonlocal boundary value problem

$$\begin{cases} \dfrac{\partial^3 u(t,x)}{\partial t^3}+4\dfrac{\partial^2 u(t,x)}{\partial t^2}-\dfrac{\partial^3 u(t,x)}{\partial t\partial x^2}=f(t,x), \\ f(t,x)=2e^{-t}\sin x, 0<t<1,\ 0<x<\pi, \\ u(0,x)=\frac{1}{4}u(1,x)+\left(1-\dfrac{1}{4e}\right)\sin x,\ 0\le x\le\pi, \\ u_t(0,x)=\frac{1}{4}u_t(1,x)-\left(1-\dfrac{1}{4e}\right)\sin x,\ 0\le x\le\pi, \\ u_{tt}(0,x)=\frac{1}{4}u_{tt}(1,x)+\left(1-\dfrac{1}{4e}\right)\sin x,\ 0\le x\le\pi, \\ u(t,0)=u(t,\pi)=0,\ 0\le t\le 1 \end{cases} \tag{1}$$

for a third order partial differential equation. The exact solution of problem (1) is

$$u(t,x)=e^{-t}\sin x.$$

For the approximate solutions of boundary value problem (1), applying formulas

$$\frac{u(t_{k+2})-3u(t_{k+1})+3u(t_k)-u(t_{k-1})}{\tau^3}-u'''(t_k)=O(\tau),$$

$$\frac{u(1)-u(1-\tau)}{\tau}-u'(1)=O(\tau),$$

$$\frac{u(x_{n+1})-2u(x_n)+u(x_{n-1})}{h^2}-u''(x_n)=O(h^2), \tag{2}$$

and

$$\begin{cases} \dfrac{u'(t_{k+1})-2u'(t_k)+u'(t_{k-1})}{\tau^2}-u'''(t_{k+1})=O(\tau), \\ \dfrac{u(\tau)-u(0)}{\tau}-u'(0)=o(\tau), \dfrac{u(1)-u(1-\tau)}{\tau}-u'(1)=O(\tau), \\ \dfrac{u(2\tau)-2u(\tau)+u(0)}{\tau^2}-u''(0)=O(\tau), \\ \dfrac{u(1)-2u(1-\tau)+u(1-2\tau)}{\tau^2}-u''(1)=O(\tau). \end{cases}$$

We get the first order of accuracy in t difference scheme

$$\begin{cases} \dfrac{u_n^{k+2}-3u_n^{k+1}+3u_n^k-u_n^{k-1}}{\tau^3}+4\dfrac{u_n^{k+2}-2u_n^{k+1}+u_n^k}{\tau^2} \\ -\dfrac{u_{n+1}^{k+2}-u_{n+1}^{k+1}-2\left(u_n^{k+2}-u_n^{k+1}\right)+u_{n-1}^{k+2}-u_{n-1}^{k+1}}{\tau h^2}=f(t_k,x_n), \\ f(t_k,x_n)=2e^{-t_k}\sin x_n,\ t_k=k\tau,\ 1\le k\le N-2\ , \\ 1\le n\le M-1, \\ N\tau=1,\ x_n=nh,\ 1\le n\le M-1,\ Mh=\pi, \\ u_n^0=\frac{1}{4}\ u_n^N+\left(1-\dfrac{1}{4e}\right)\sin x_n,\ 0\le n\le M, \\ \dfrac{u_n^1-u_n^0}{\tau}=\frac{1}{4}\dfrac{u_n^N-u_n^{N-1}}{\tau}-\left(1-\dfrac{1}{4e}\right)\sin x_n, 0\le n\le M, \\ \dfrac{u_n^2-2u_n^1+u_n^0}{\tau^2}=\frac{1}{4}\dfrac{u_n^N-2u_n^{N-1}+u_n^{N-2}}{\tau^2}+\left(1-\dfrac{1}{4e}\right)\sin x_n, \\ 0\le n\le M, \\ u_0^k=u_M^k=0, 0\le k\le N. \end{cases} \tag{3}$$

It is the system of algebraic equations and it can be written in the matrix form

$$\begin{cases} A\ u_{n+1}+Bu_n+Cu_{n-1}=D\varphi_n, \quad 1\le n\le M-1, \\ u_0=\vec{0},\ \ u_M=\vec{0}. \end{cases} \tag{4}$$

Here,

$$A=C=\begin{bmatrix} 0 & 0 & 0 & 0 & \cdots & 0 & 0 & 0 \\ 0 & 0 & a & -a & \cdots & 0 & 0 & 0 \\ 0 & 0 & 0 & a & \cdots & 0 & 0 & 0 \\ \vdots & \vdots & \vdots & \vdots & \ddots & \vdots & \vdots & \vdots \\ 0 & 0 & 0 & 0 & \cdots & 0 & a & -a \\ 0 & 0 & 0 & 0 & \cdots & 0 & 0 & 0 \\ 0 & 0 & 0 & 0 & \cdots & 0 & 0 & 0 \end{bmatrix}_{(N+1)\times(N+1)},$$

$$B=\begin{bmatrix} X & \cdots & Z \\ \vdots & \ddots & \vdots \\ W & \cdots & Y \end{bmatrix}_{(N+1)\times(N+1)},$$

where

$$X=\begin{bmatrix} 1 & 0 & 0 & 0 & 0 \\ b & -3b+4d & 3b-c-8d & b-c+4d & 0 \\ 0 & b & -3b+4d & 3b-c-8d & b-c+4d \\ 0 & 0 & b & -3b+4d & 3b-c-8d \\ 0 & 0 & 0 & b & -3b+4d \end{bmatrix},$$

$$Z = \begin{bmatrix} 0 & 0 & 0 & 0 & -\frac{1}{4} \\ 0 & 0 & 0 & 0 & 0 \\ 0 & 0 & 0 & 0 & 0 \\ 0 & 0 & 0 & 0 & 0 \\ 0 & 0 & 0 & 0 & 0 \end{bmatrix},$$

$$W = \begin{bmatrix} 0 & 0 & 0 & 0 & 0 \\ 0 & 0 & 0 & 0 & 0 \\ 0 & 0 & 0 & 0 & 0 \\ -\dfrac{1}{\tau} & \dfrac{1}{\tau} & 0 & 0 & 0 \\ \dfrac{1}{\tau^2} & -\dfrac{2}{\tau^2} & \dfrac{1}{\tau^2} & 0 & 0 \end{bmatrix},$$

$$Y = \begin{bmatrix} 0 & 3b-c-8d & b-c+4d & 0 & 0 \\ 0 & -3b+4d & 3b-c-8d & b-c+4d & 0 \\ 0 & b & -3b+4d & 3b-c-8d & b-c+4d \\ 0 & 0 & 0 & \dfrac{1}{4\tau} & -\dfrac{1}{4\tau} \\ 0 & 0 & -\dfrac{1}{4\tau^2} & \dfrac{1}{2\tau^2} & -\dfrac{1}{4\tau^2} \end{bmatrix},$$

$$a = \frac{1}{\tau h^2},\ b = -\frac{1}{\tau^3},\ \ c = \frac{2}{\tau h^2}, d = \frac{1}{\tau^2},$$

$$\varphi_n = \begin{bmatrix} \varphi_n^0 \\ \vdots \\ \varphi_n^N \end{bmatrix}_{(N+1)\times 1}, \left\{ \begin{array}{l} \varphi_n^k = \ f(t_k, x_n) = 2e^{-t_k} \sin x_n, \\ t_k = k\tau, 1 \le k \le N-2,\ 1 \le n \le M-1, \\ \\ \varphi_n^0 = \left(1 - \dfrac{1}{4e}\right) \sin x_n, 0 \le n \le M, \\ \varphi_n^{N-1} = -\left(1 - \dfrac{1}{4e}\right) \sin x_n, 0 \le n \le M, \\ \varphi_n^N = \left(1 - \dfrac{1}{4e}\right) \sin x_n, 0 \le n \le M \end{array} \right\}$$

and $D = I_{N+1}$ is the identity matrix,

$$u_s = \begin{bmatrix} u_s^0 \\ \vdots \\ u_s^N \end{bmatrix}_{(N+1)\times 1},\ \ s = n, n \pm 1.$$

Therefore, for the solution of the matrix equation (4), we will use the modified Gauss elimination method. We seek a solution of the matrix equation by the following form:

$$u_n = \alpha_{n+1} u_{n+1} + \beta_{n+1},\quad n = M-1, ..., 1, \tag{5}$$

where $u_M = \vec{0}$, $\alpha_j \quad (j = 1, ..., M-1)$ are $(N+1)\times(N+1)$ square matrices, $\beta_j \quad (j = 1, ..., M-1)$ are $(N+1)\times 1$ column matrices, α_1, β_1 are zero matrices and

$$\begin{aligned} &\alpha_{n+1} = -\left(B + C\alpha_n\right)^{-1} A_n, \\ &\beta_{n+1} = \left(B + C\alpha_n\right)^{-1} \left(D\varphi_n - C\beta_n\right), n = 1, ..., M-1. \end{aligned} \tag{6}$$

TABLE 1. Errors analysis

N,M	$N=M=20$	$N=M=40$	$N=M=80$
Difference scheme (3)	$1.1806e-02$	$5.8856e-03$	$2.9381e-03$

The errors are computed by

$$E_M^N = \max_{1\le k\le N-1, 1\le n\le M-1} \left| u(t_k,x_n) - u_n^k \right| \tag{7}$$

of the numerical solutions, where $u(t_k,x_n)$ represents the exact solution and u_n^k represents the numerical solution at (t_k,x_n) and the results are given in Table I. As it is seen in Table I, we get some numerical results. If N and M are doubled, the value of errors decrease by a factor of approximately $1/2$ for first order difference scheme.

The Second Order of Accuracy Difference Schemes

Now, we will consider the high order of accuracy difference schemes for the approximate solution of the problem (1), for the approximate solution of boundary value problem (1), applying formulas (2),

$$\frac{u(t_{k+2}) - 3u(t_{k+1}) + 3u(t_k) - u(t_{k-1})}{\tau^3} - \frac{3}{4}u'''(t_k) - \frac{1}{4}u'''(t_{k+2}) = O(\tau^3),$$

$$\frac{3u(1) - 4u(1-\tau) + u(1-2\tau)}{2\tau} = u'(1) + O(\tau^2), \tag{8}$$

and

$$\begin{cases} \dfrac{u(t_{k+1}) - 2u(t_k) + u(t_{k-1})}{\tau^2} - \dfrac{1}{2}\left[u''(t_{k+1}) + u''(t_{k-1})\right] = O(\tau^2), \\[2ex] \dfrac{u(t_{k+1}) - 2u(t_k) + u(t_{k-1})}{\tau^2} - \dfrac{1}{2}u''(t_k) - \dfrac{1}{4}\left[u''(t_{k+1}) + u''(t_{k-1})\right] = O(\tau^2), \\[2ex] \dfrac{-u(2\tau) + 4u(\tau) - 3u(0)}{2\tau} - u'(0) = O(\tau^2), \\[2ex] \dfrac{3u(1) - 4u(1-\tau) + u(1-2\tau)}{2\tau} - u'(1) = O(\tau^2), \\[2ex] \dfrac{-3u(3\tau) + 4u(2\tau) - 5u(\tau) + 2u(0)}{\tau^2} - u''(0) = O(\tau^2), \\[2ex] \dfrac{-3u(1) + 4u(1-\tau) - 5u(1-2\tau) + 2u(1-3\tau)}{\tau^2} - u''(1) = O(\tau^2). \end{cases}$$

We get the second order of accuracy in t difference scheme

$$
\begin{cases}
\dfrac{u_n^3-3u_n^2+3u_n^1-u_n^0}{\tau^3} \\
-\dfrac{u_{n+1}^3-2u_n^3+u_{n-1}^3+u_{n+1}^2-2u_n^2+u_{n-1}^2}{4\tau h^2} \\
+\dfrac{\left(u_{n+1}^1-2u_n^1+u_{n-1}^1\right)+\left(u_{n+1}^0-2u_n^0+u_{n-1}^0\right)}{4\tau h^2}+4\dfrac{u_n^3-u_n^2-u_n^1+u_n^0}{2\tau^2} \\
=\dfrac{f(t_1,x_n)+f(t_2,x_n)}{2}=(e^{-t_1}+e^{-t_2})\sin x_n, \\
1\le n\le M-1, \\
\dfrac{u_n^{k+2}-2u_n^{k+1}+2u_n^{k-1}-u_n^{k-2}}{2\tau^3} \\
-\dfrac{u_{n+1}^{k+2}-2u_n^{k+2}+u_{n-1}^{k+2}-\left(u_{n+1}^{k-2}-2u_n^{k-2}+u_{n-1}^{k-2}\right)}{8\tau h^2} \\
-\dfrac{u_{n+1}^{k+1}-2u_n^{k+1}+u_{n-1}^{k+1}-\left(u_{n+1}^{k-1}-2u_n^{k-1}+u_{n-1}^{k-1}\right)}{4\tau h^2}+4\dfrac{u_n^{k+2}-2u_n^k-u_n^{k-2}}{2\tau^2} \\
=f(t_k,x_n),\ f(t_k,x_n)=2e^{-t_k}\sin x_n, \\
t_k=k\tau,\ 2\le k\le N-2\ ,\ 1\le n\le M-1, \\
N\tau=1,\ x_n=nh,\ 1\le n\le M-1,\ Mh=\pi, \\
u_n^0=\frac{1}{4}\ u_n^N+\left(1-\dfrac{1}{4e}\right)\sin x_n,\ 0\le n\le M, \\
\dfrac{-u_n^2+4u_n^1-3u_n^0}{2\tau}=\frac{1}{4}\dfrac{3u_n^N-4u_n^{N-1}+u_n^{N-2}}{2\tau}-\left(1-\dfrac{1}{4e}\right)\sin x_n, \\
0\le n\le M, \\
\dfrac{-u_n^3+4u_n^2-5u_n^1+2u_n^0}{\tau^2}=\frac{1}{4}\dfrac{2u_n^N-5u_n^{N-1}+4u_n^{N-2}-u_n^{N-3}}{\tau^2} \\
+\left(1-\dfrac{1}{4e}\right)\sin x_n, 0\le n\le M, \\
u_0^k=u_M^k=0, 0\le k\le N.
\end{cases}
\tag{9}
$$

This system can be written in the matrix form (4), too. Here,

$$
A=C=\begin{bmatrix}
0 & 0 & 0 & 0 & 0 & \cdots & 0 & 0 & 0 & 0 & 0 \\
a & a & -a & -a & 0 & \cdots & 0 & 0 & 0 & 0 & 0 \\
\frac{1}{2}a & a & 0 & -a & -\frac{1}{2}a & \cdots & 0 & 0 & 0 & 0 & 0 \\
\vdots & \vdots & \vdots & \vdots & \vdots & \ddots & \vdots & \vdots & \vdots & \vdots & \vdots \\
0 & 0 & 0 & 0 & 0 & \cdots & 0 & -a & -\frac{1}{2}a & 0 & 0 \\
0 & 0 & 0 & 0 & 0 & \cdots & a & 0 & -a & -\frac{1}{2}a & 0 \\
0 & 0 & 0 & 0 & 0 & \cdots & \frac{1}{2}a & a & 0 & -a & -\frac{1}{2}a \\
0 & 0 & 0 & 0 & 0 & \cdots & 0 & 0 & 0 & 0 & 0 \\
0 & 0 & 0 & 0 & 0 & \cdots & 0 & 0 & 0 & 0 & 0
\end{bmatrix}_{(N+1)\times(N+1)},
$$

$$
B=\begin{bmatrix} X & \cdots & Z \\ \vdots & \ddots & \vdots \\ W & \cdots & Y \end{bmatrix}_{(N+1)\times(N+1)},
$$

where

$$
X=\begin{bmatrix} 1 & 0 & 0 & 0 & 0 \\ -2b-2a+4c & 6b-2a-4c & -6b+2a-4c & 2b+2a+4c & 0 \\ -b-a+4c & 2b-2a & -8c & -2b+2a & b+a+4c \\ 0 & -b-a+4c & 2b-2a & -8c & -2b+2a \\ 0 & 0 & -b-a+4c & 2b-2a & -8c \end{bmatrix},
$$

$$
Z=\begin{bmatrix} 0 & 0 & 0 & 0 & -\frac{1}{4} \\ 0 & 0 & 0 & 0 & 0 \\ 0 & 0 & 0 & 0 & 0 \\ 0 & 0 & 0 & 0 & 0 \\ 0 & 0 & 0 & 0 & 0 \end{bmatrix},
$$

$$
W=\begin{bmatrix} 0 & 0 & 0 & 0 & 0 \\ 0 & 0 & 0 & 0 & 0 \\ 0 & 0 & 0 & 0 & 0 \\ \frac{-3}{2\tau} & \frac{2}{\tau} & \frac{1}{2\tau} & 0 & 0 \\ \frac{2}{\tau^2} & -\frac{5}{8\tau^2} & \frac{4}{\tau^2} & \frac{-1}{\tau^2} & 0 \end{bmatrix},
$$

$$
Y=\begin{bmatrix} -8c & -2b+2a & b+a+4c & 0 & 0 \\ 2b-2a & -8c & -2b+2a & b+a+4c & 0 \\ -b-a+4c & 2b-2a & -8c & -2b+2a & b+a+4c \\ 0 & 0 & -\dfrac{1}{8\tau} & \frac{1}{2\tau} & -\dfrac{3}{8\tau} \\ 0 & \dfrac{1}{4\tau^2} & -\dfrac{1}{\tau^2} & \dfrac{5}{4\tau^2} & -\dfrac{1}{2\tau^2} \end{bmatrix},
$$

$$
a=\frac{1}{4\tau h^2},\ b=\frac{1}{2\tau^3}, c=\frac{1}{2\tau^2}
$$

$$
\varphi_n=\begin{bmatrix} \varphi_n^0 \\ \vdots \\ \varphi_n^N \end{bmatrix}_{(N+1)\times 1},
\left\{\begin{array}{l}
\varphi_n^k = f(t_k,x_n) = 2e^{-t_k}\sin x_n, \\
t_k = k\tau, 1 \le k \le N-2,\ 1 \le n \le M-1, \\
\varphi_n^1 = \dfrac{f(t_1,x_n)+f(t_2,x_n)}{2} = (e^{-t_1}+e^{-t_2})\sin x_n, \\
1 \le n \le M-1, \\
\varphi_n^0 = \left(1-\dfrac{1}{4e}\right)\sin x_n, 0 \le n \le M, \\
\varphi_n^{N-1} = -\left(1-\dfrac{1}{4e}\right)\sin x_n, 0 \le n \le M, \\
\varphi_n^N = \left(1-\dfrac{1}{4e}\right)\sin x_n, 0 \le n \le M
\end{array}\right\}
$$

TABLE 2. Errors analysis

N, M	$N = M = 20$	$N = M = 40$	$N = M = 80$
Difference scheme (9)	$8.8717e-04$	$2.4416e-04$	$6.3723e-05$

for difference scheme (9). Therefore, for the solution of the matrix equation (4), we will use the same formulas (5),

(6) and the errors are computed by formula (7). Numerical results are given in following table
As it is seen in Table II, we get numerical results for difference scheme (9). Note that if N and M are doubled, the value of errors decrease by a factor of approximately $1/4$ for second order of accuracy in t difference schemes (9).

REFERENCES

1. Yu. P. Apakov and S. Rutkauskas, Nonlinear Anal.:Modelling Control **16**, 255–269 (2011).
2. A. Ashyralyev and N. Aggez, Numerical Functional Analysis and Optimization **25**, 439–462 (2004).
3. A. Ashyralyev and N. Aggez, and F. Hezenci, AIP Conference Proceedings **1470**, 130–132 (2012).
4. A. Ashyralyev and D. Arjmand, Applied Mathematics and Computation **188**, 1483–190 (2007).
5. A. Ashyralyev, D. Arjmand, and M. Koksal, Journal of the Franklin Institute **346(7)**, 651–662 (2009).
6. A. Ashyralyev and K. Belakroum, AIP Conference Proceedings **2183(1)**, (2019).
7. A. Ashyralyev, Kh. Belakroum, and A. Guezane-Lakoud, Electronic Journal of Differential Equations, **2017(53)**, 1–11 (2017).
8. A. Ashyralyev and P. E. Sobolevskii, *New Difference Schemes for Partial Differential Equations* (Birkhäuser Verlag, Basel, Boston, Berlin, 2004).
9. M. Denche and A. Memou, Journal of Applied Mathematics **11**, 533–567 (2003).
10. Z. Direk and M. Ashyraliyev, Advances in Difference Equations **2014(1)**, 1-8 (2014).
11. H.O. Fattorini, *Second Order Linear Differential Equations in Banach Spaces* (Elsevier Science Publishers B.V., Amsterdam, 1985).
12. L. J. Guo, J. P.Sun and Y. H. Zhao, Electronic Journal of Differential Equations **2007**, (2007).
13. P. K. Palamides and A. P. Palamides, Electronic Journal of Qualitative Theory of Differential Equations **2008(14)**, 1-15 (2008).
14. Y. Wang and Sh. Zheng, Boundary Value Problems **2009(1)**, 484879 (2009).

An Algorithm for Control Correction in Nonlinear Point-to-Point Control Problem

Mikhail Dmitriev[1, 2, a)] and Dmitry Makarov[1, 2, b)]

[1)] *Federal Research Center "Computer Science and Control" of Russian Academy of Sciences, 119333, Moscow, Russia*
[2)] *Moscow Institute of Physics and Technology, 141701, Moscow, Russia*

[a)] *Electronic mail: mdmitriev@mail.ru*
[b)] *Corresponding author: makarov@isa.ru*

Abstract. Firstly, a perturbation based correction of an admissible open-loop control in an unperturbed problem is constructed in the form of linear feedback. The constructed control transfers the perturbed system to a neighborhood of a given point. Secondly, then the resulting feedback is refined to reach the end point. The proposed algorithm is illustrated by numerical experiments.

INTRODUCTION

In recent years, in connection with the rapid development of the direction associated with the problems of real-time control of autonomous objects motions, it became necessary to develop new algorithms for solving point-to-point control problems. In some works, researchers rely on the selection of initial constructions for the final trajectory (for example, see the trajectory planning method in [1, 2]). Then the resulting initial trajectory and the corresponding control are selected taking into account the problem constraints and, as a result, an acceptable trajectory and the corresponding admissible control solving the point-to-point problem are obtained.

Such an inverse approach has a significant advantage over traditional algorithms of the optimal control theory, because using specific problem properties, such as geometric and spatial features of motion caused by constraints, one can quickly calculate a qualitative image of an admissible trajectory, which allows one to quickly construct an admissible control.

However, this approach is not applicable in many practical problems due to the dimensionality of objects and non-linearity in their mathematical models. Here we demonstrate some intermediate variant between direct and inverse approaches to finding an admissible point-to-point control. It consists in a searching and the application of the algorithm of a system simplifications combination and using the qualitative properties of models and their optimization. Such an approach can lead to more efficient and rational solutions and corresponding numerical algorithms.

To search for an admissible point-to-point control that transfers a dynamic system to a given state in a finite time, for example, one can use model simplifications associated with introducing various small parameters into the model, which will allow asymptotic expansions to be used to refine qualitative approximations to solutions and to construct extrapolation procedures (see, for example, works related to the penalty functions method [3, 4, 5]).

In this paper, we consider the solution of a perturbed nonlinear point-to-point problem based on control correction using a small parameter characterizing perturbations of the right-hand sides of the system. The control correction in the form of optimal synthesis determines an approximate algorithm for constructing an admissible control based on the solution of a limiting, simplified point-to-point control problem.

THE PROBLEM STATEMENTS

Let us consider the next point-to-point control problem

$$\begin{gathered}\dot{x} = F_0(t,x,u) + \varepsilon F_1(t,x,u), \quad x_0(0) = x^0, \quad x_0(T) = x^T, \\ 0 < \varepsilon \le \varepsilon_0, \quad x \in X \subset R^n, \quad u \in U \subseteq R^r,\end{gathered} \tag{1}$$

where x is a state vector, u is a control vector, ε_0 is a sufficiently small positive number, X and U are corresponding closed or open sets of admissible values of state and control vectors.

The small positive parameter ε is considered to be known. Suppose that for $\varepsilon = 0$ we know the admissible continuously differentiable program control $u_0(t)$ that transfers the unperturbed system from the initial position to the final

International Conference on Analysis and Applied Mathematics (ICAAM 2020)
AIP Conf. Proc. 2325, 020067-1–020067-5; https://doi.org/10.1063/5.0040367
Published by AIP Publishing. 978-0-7354-4069-2/$30.00

given state in time T

$$\begin{gathered}\dot{x}_0 = F_0(t, x_0, u_0), \quad x_0(0) = x^0, \quad x_0(T) = x^T, \\ u_0(t) \in U, \quad x_0(t) \in X,\end{gathered} \tag{2}$$

and it is assumed that the trajectory and control satisfy the constraints and are continuously differentiable vector functions for all $0 \leq t \leq T$.

As the experience of finding open-loop controls for optimal control problems with a small parameter shows, both with various constraints and without them (see, for example, [6]), the use of common optimization and control methods is effective in the vicinity of asymptotic behavior. Because asymptotic behavior, taking into account at least part of the structure of the solution, can be often in local neighborhoods of extremum points. Therefore, the idea arises of representing an admissible solution to the perturbed problem in the form of formal first-order asymptotic approximations, where all members or part of them are sought in the feedback form.

So, we are looking for admissible trajectory and control in the form

$$x_1(t,\varepsilon) = x_0(t) + \varepsilon x_1(t), \quad u_1(x,t,\varepsilon) = u_0(t) + \varepsilon u_1(x + \varepsilon x_1, t, \varepsilon), \tag{3}$$

assuming here that $u_0(t)$ the is an open-loop control and $u_1(x + \varepsilon x_1, t, \varepsilon)$ is a closed-loop one, which transfers the system (1) to a specified neighborhood of the given final state $x(T) = x^T$.

In view of (2), for x_1, and u_1 we obtain the following problems

$$\dot{x}_0 = F_0(t, x_0(t), u_0(t)), \quad x_0(0) = x^0, \quad x_0(T) = x^T, \tag{4}$$

$$\dot{x}_1 = F_{0,x}(t, x_0(t), u_0(t))x_1(t) + F_{0,u}(t, x_0(t), \quad u_0(t))u_1(t) + F_1(t, x_0(t), u_0(t)), \quad x_1(0) = 0, \quad x_1(T) = 0, \tag{5}$$

where $F_{0,x} = \frac{\partial F_0}{\partial x}, F_{0,u} = \frac{\partial F_0}{\partial u}$.

Due to the smallness of ε, it can be established that, under quite general conditions on the right-hand sides of (1), the u_0 transfers the system to a sufficiently small neighborhood of the given end point. However, the open-loop control obtained in this way are not able to respond to arising errors. Therefore, in this neighborhood, as is often done in applications, it is desirable to make a correction via some feedback control u_1.

In this case, on the one hand, the correction feedback control should take into account the structure of the system and be a solution in a simplified system. On the other hand, this correction should be the only solution to some control problem and contribute to the tendency of x_1 to 0 on the right end. It is known from computational experiments that these conditions are fulfilled by the choice of an auxiliary problem in the form of a linear-quadratic control problem in which control is unique, representable in the form of feedback, which often has stabilizing properties.

For example, under the conditions of controllability and observability in a stationary linear system, the transition process in a closed-loop system disappears quite quickly, i.e. trajectories tend to 0 over a sufficiently large period of time. Taking into account the above, for the unambiguous choice of $u_1(t)$ we will construct it by solving the following optimal control problem

$$J(u_1) = \frac{1}{2}\int_{t_0}^{T} \left(x_1{}'(\tau)Q(\tau)x_1{}'(\tau) + u_1{}'(\tau)R(\tau)u_1(\tau)\right)d\tau \to \min_{u_1,\, u_0+\varepsilon u_1 \in U},$$

on the trajectories of system (5) under phase constraints $x_0(t) + \varepsilon x_1(t) \in X$. Here Q and R are the positive definite matrices, turning during the control design. This problem solution without phase constraints has the form [7]

$$u_1(x_1,t) = -R^{-1}(t)B^T(t)(P(t)x_1 + q(t)) = -R^{-1}(t)B^T(t)P(t)x_1 - R^{-1}(t)B^T(t)q(t) = k(x_1(t),t) + p(t),$$

where $k(x_1(t),t) = -R^{-1}(t)B^T(t)P(t)x_1$, $p(t) = -R^{-1}(t)B^T(t)q(t)$, P and q are defined from the following equations

$$\begin{aligned}\dot{P} &= -A^T P - PA + PBR^{-1}B^T P - Q, \quad && P(T) = 0, \\ \dot{q} &= (PBR^{-1}B^T P - A^T)q + Pl, && q(T) = 0,\end{aligned}$$

and $A(t) = F_{0,x}(t, x_0(t), u_0(t))$, $B(t) = F_{0,u}(t, x_0(t), u_0(t))$, $l(t) = F_1(t, x_0(t), u_0(t))$.

To take constraints into account and to improve the accuracy of control, we introduce in u_1 an additional term ω as follows

$$u_1(x_1(t),t) = k(x_1(t),t) + p(t) + \omega(t, c_{i,j}). \tag{6}$$

The components of a vector function ω are represented in the form of the expansions by next system of functions

$$\begin{gathered}\omega_i(\tau(t),c_{i,j}) = \frac{1}{2}c_{i,0} + \sum_{l=1}^{k_\omega} c_{i,2l-1}\cos(j\tau) + c_{i,2l}\sin(j\tau), \\ \tau = \frac{\pi(2t-T)}{T}, \quad t \in [0,T], \quad \tau \in [-\pi,\pi], \quad i = 1,..,r, \quad j = 0,1,...,2k_\omega.\end{gathered} \tag{7}$$

In (7) a parameter $k_\omega \geq 0$ determines the number of terms in series and the vectors of unknown coefficients $c_{i,j}$ are determined by solving the residual minimization problem for each i-th coordinate of the vector-function $\omega(t)$

$$e'e \to \min_{c_{i,j}},$$

where

$$e = x(T) - x\left(t, u_0(t) + \varepsilon\left(k(x_1(t),t) + p(t) + \omega(t,c_{i,j})\right)\right)\big|_{t=T}, \quad i = 1,..,r,\ j = 0,...,2k_\omega,$$

and $u_0(t)$, $k(x_1(t),t), p(t)$ are already known.

Let's note also that the offered correction algorithm for point-to-point control is close to the method, illustrated in [8] on specific control tasks for spacecraft.

NUMERICAL EXPERIMENTS

Let us consider the problem

$$\begin{aligned}\dot{x}_1 &= x_2, \\ \dot{x}_2 &= u_1 - \varepsilon(x_2x_1), \\ \dot{x}_3 &= u_2 + \varepsilon(x_2x_3),\end{aligned} \quad x(0) = \begin{bmatrix} 0.5 \\ 0 \\ 2 \end{bmatrix}, \quad x(1) = \begin{bmatrix} 1 \\ 1 \\ 1 \end{bmatrix}, \quad |u_1| \leq 2, |u_2| < 2. \tag{8}$$

In the zero approximation of this problem it is easy to construct the next admissible trajectory and control

$$\begin{gathered} x_{0,1} = 0.5t^2 + 0.5, \quad x_{0,2} = t, \quad x_{0,3} = -t + 2, \\ u_{0,1} = 1, \quad u_{0,2} = -1, \end{gathered}$$

where $x_{0,i}$ and $u_{0,j}$ are coordinates of vectors x_0 and u_0 accordingly, $i = 1,2,3,\ j = 1,2$.

We have the following matrices for (8)

$$F_0 = \begin{bmatrix} x_2 \\ u_1 \\ u_2 \end{bmatrix}, F_1 = \begin{bmatrix} 0 \\ -x_2x_1 \\ x_2x_3 \end{bmatrix}, F_{0,x}(t,x_0(t),u_0(t)) = \begin{bmatrix} 0 & 1 & 0 \\ 0 & 0 & 0 \\ 0 & 0 & 0 \end{bmatrix}, F_{0,u}(t,x_0(t),u_0(t)) = \begin{bmatrix} 0 & 0 \\ 1 & 0 \\ 0 & 1 \end{bmatrix},$$
$$F_1(t,x_0(t),u_0(t)) = \begin{bmatrix} 0 \\ -0.5t(t^2+1) \\ t(2-t) \end{bmatrix}.$$

The unit weight matrices Q and R of corresponding dimensions were used for the control u_1 construction and the parameter $k_\omega = 1$ was used for ω design. The Fig. 1 shows the coordinates of closed-loop systems along the controls u_0, $u_1 = u_0 + \varepsilon(k(x_1(t),t) + p(t))$ and $u_\omega = u_0 + \varepsilon(k(x_1(t),t) + p(t) + \omega(t))$ for $\varepsilon = 1$, and the Fig. 2 presents these controls themselves.

The Table I shows the terminal error values $J(u) = (x(T,u) - x^T)'(x(T,u) - x^T)$ along different control for various ε. As one may see, for all considered cases, $u_1(x,t,\varepsilon)$ is more effective then control $u_0(t)$ and u_ω is better then $u_1(x,t,\varepsilon)$. Let us note that the superiority of $u_1(x,t,\varepsilon)$ of over $u_0(t)$ is retained even in the case of $\varepsilon = 1$, where the introduction of the parameter is, in fact, formal, and the system is no more weakly nonlinear.

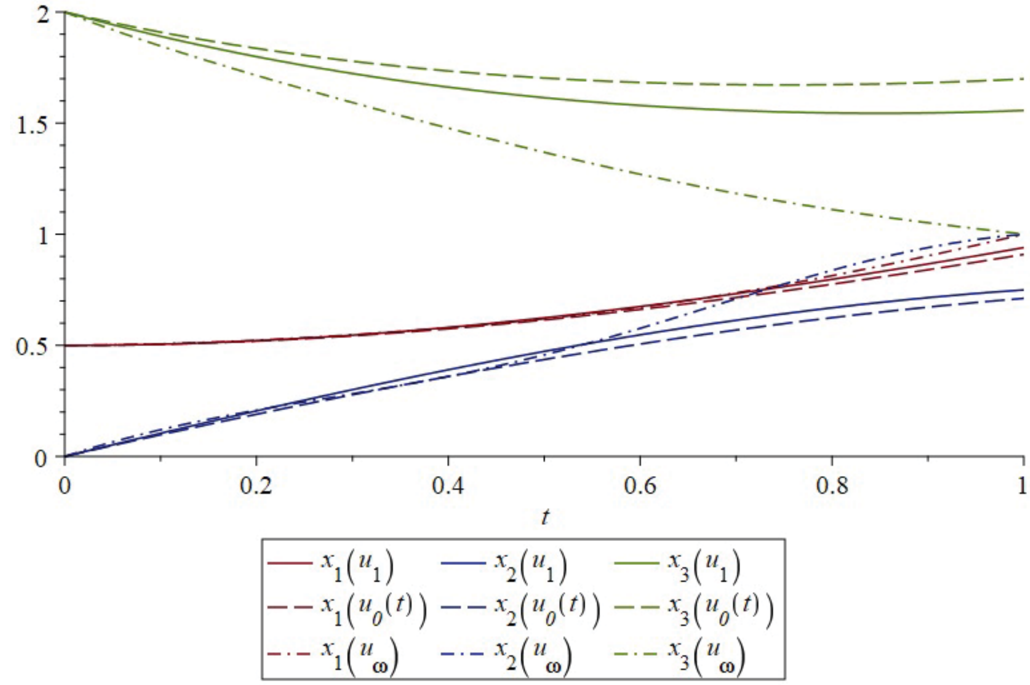

FIGURE 1. Trajectories of closed-loop systems along various controls for $\varepsilon = 1$

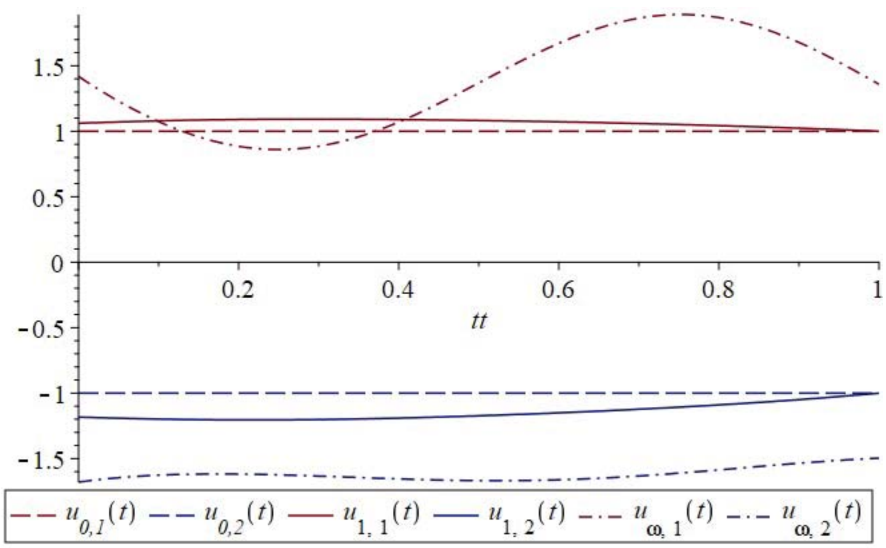

FIGURE 2. Controls time evaluations for $\varepsilon = 1$

TABLE 1. Values of J for various ε

ε	$J(u_0)$	$J(u_1)$	$J(u_\omega)$
1	0.5801	0.3688	$5.7335 * 10^{-8}$
0.5	0.1471	0.0931	$7.1214 * 10^{-8}$
0.1	$0.5949 * 10^{-2}$	$0.3703 * 10^{-2}$	$1.8095 * 10^{-6}$
0.01	$0.5966 * 10^{-4}$	$0.3701 * 10^{-4}$	$1.2832 * 10^{-7}$

CONCLUSION

The paper proposes an algorithm for constructing a correction of an admissible control in a nonlinear point-to-point control problem. The correction consists of two terms. The first one is constructed using an auxiliary linear-quadratic control problem and has a feedback form. The second one is intended to clarify the solution and fulfill the constraints on the coordinates of the system and control. It is open-loop control and is based on the solution of the nonlinear programming problem. Note that this problem is solved in the neighborhood of the control with the first correcting term, which is already found. That reduces the solution search time. The experiments showed the effectiveness of the proposed approach.

ACKNOWLEDGMENTS

This work was supported by RFBR (projects No 18-37-20032, 18-01-00551a).

REFERENCES

1. K. S. Yakovlev, D. A. Makarov, and E. S. Baskin, Scientific and Technical Information Processing **42(5)**, 347–358 (2015).
2. S. Emel'yanov, D. Makarov, A. Panov, and K. Yakovlev, Cognitive Systems Research **39**, 58–72 (2016).
3. V. Y. Glizer and M. G. Dmitriev, Dokl. Akad. Nauk SSSR **231(1)**, 21–23 (1976), in Russian.
4. V. Y. Glizer and M. G. Dmitriev, Differential equations **17(9)**, 994–998 (1981), in Russian.
5. M. G. Dmitriev and D. A. Makarov, AIP Conference Proceedings **1997** (2018), DOI: 10.1063/1.5048995.
6. A. Y. Gornov, M. G. Dmitriev, and A. I. Tyatyushkin, "Experience in solving optimal control problems with a boundary layer," (VINITI DEP, Moscow, 1985) p. 19, in Russian.
7. K. A. Pupkov and N. D. Egupov, "Methods of classical and modern theory of automatic control: A textbook in 5 volumes," (Publishing house MSTU. Bauman, Moscow, 2004) p. 744, 2nd ed., in Russian.
8. V. V. Malyshev, A. V. Starkov, and A. V. Fedorov, Herald of computer and information technologies **9(99)**, 7–12 (2012), in Russian.

On the Boundedness of Solution of the First Order Ordinary Differential Equation with Involution

Allaberen Ashyralyev[1, 2, 3, a)] and Twana Abbas[1, b)]

[1)]Department of Mathematics, Near East University, Nicosia, Mersin 10, Turkey
[2)]Peoples' Friendship University of Russia (RUDN University), 6 Miklukho-Maklaya St, Moscow 117198, Russian Federation
[3)]Institute of Mathematics and Mathematical Modeling, 050010, Almaty,Kazakhstan

[a)]Electronic mail: allaberen.ashyralyev@neu.edu.tr
[b)]Corresponding author: twana.margaret@gmail.com

Abstract. In the present paper, the initial value problem for the first order ordinary differential equation with involution is studied. We obtain equivalent initial value problem for the second order ordinary differential equations to the initial value problem for first order linear differential equations with involution. Theorem on stability estimates for the solution of the initial value problem for the first order ordinary linear differential equation with involution is proved. Theorem on existence and uniqueness of bounded solution of initial value problem for first order ordinary nonlinear differential equation with involution is proved.

INTRODUCTION

Differential equations with involution appear in mathematical models of ecology, biology, and population dynamics (see, e.g, [1-7] and the reference given therein).

Our goal in this paper is to investigate the boundedness of the solution of the initial value problem for the first order ordinary differential equation with involution

$$iy'(t) = f(t;y(t);y(u(t)), t \in I = (-\infty,\infty), y(t_0) = y_0. \tag{1}$$

Here and in future $u(t)$ is involution function, that is $u(u(t)) = t$, and t_0 is a fixed point of u. Problem (1) does not seem to yield directly to any techniques that for ordinary differential equations without involution term can be used them in (1). Therefore, we consider the first order linear differential equations with involution. We obtain equivalent initial value problem for the second order ordinary differential equations to the initial value problem for first order linear differential equations with involution. Theorem on stability estimates for the solution of the initial value problem for the first order ordinary linear differential equation with involution is established. Finally, Theorem on existence and uniqueness of bounded solution of initial value problem for the first order nonlinear ordinary differential equation with involution is proved.

LINEAR ORDINARY DIFFERENTIAL EQUATIONS WITH INVOLUTION

Let $C^\infty[I]$ be set of all differentiable functions for all degrees.

Theorem 1 *Let $u(t)$ be a continuous function that it is own inverse on an open interval $I, u \in C^\infty[I]$, and $t_0 \in I$ be a fixed point of u. Let y_0 be any real number and each of $a(t)$, $b(t)$ be a function of class C^∞ on I, such that $b(t)$ does not vanish on the interval I, then the problem*

$$iy'(t) = a(t)y(t) + b(t)y(u(t)) + f(t), t \in I, y(t_0) = \varphi \tag{2}$$

is equivalent to the following problem for the second order ordinary differential equation

$$\begin{cases} iy''(t) = p(t)y(t) + q(t)y'(t) + F(t), t \in I, \\ y(t_0) = \varphi, y'(t_0) = -\imath\left(a(t_0)\varphi + b(t_0)\varphi + f(t_0)\right), \end{cases} \tag{3}$$

where

$$p(t) = \left[a'(t) - \frac{b'(t)}{b(t)}a(t) + ia(t)a(u(t))u'(t) - ib(t)b(u(t))u'(t)\right],$$

International Conference on Analysis and Applied Mathematics (ICAAM 2020)
AIP Conf. Proc. 2325, 020068-1–020068-8; https://doi.org/10.1063/5.0040392
Published by AIP Publishing. 978-0-7354-4069-2/$30.00

$$q(t) = a(t) + a(u(t))u'(t) + \frac{ib'(t)}{b(t)},$$

and

$$F(t) = ia(u(t))u'(t)f(t) - \frac{b'(t)}{b(t)}f(t) - ib(t)u'(t)f(u(t)) + f'(t).$$

The proof of Theorem 1 is based on approaches of proof of Theorem 1 of paper [1] on the first order linear differential equation with involution. Now we consider the initial value problem

$$iy'(t) = by(\pi - t) + ay(t) + f(t), t \in I, y\left(\frac{\pi}{2}\right) = \varphi \tag{4}$$

for the first order ordinary differential equation with involution. We are interested in studying the stability of problem (4) on I. In general cases of a and b the solution of (4) is not bounded on I. It is important in applications. Applying Theorem 1, we get the equivalent initial value problem

$$\begin{cases} y''(t) - (b^2 - a^2)y(t) = F(t), \\ F(t) = -af(t) + bf(\pi - t) - if'(t), t \in I, \\ y\left(\frac{\pi}{2}\right) = \varphi, y'\left(\frac{\pi}{2}\right) = -i(a+b)\varphi + f\left(\frac{\pi}{2}\right) \end{cases} \tag{5}$$

for the second order ordinary differential equation. We will obtain the solution of the problem (5). There are three cases: $a^2 - b^2 > 0, a^2 - b^2 = 0, a^2 - b^2 < 0$. In the first case $a^2 - b^2 = m^2 > 0$. Substituting m^2 for $a^2 - b^2$ into equation (5), we get

$$y''(t) + m^2 y(t) = F(t), t \in I.$$

Applying Laplace and inverse Laplace transforms, we get

$$y(t) = \cos(mt)\, y(0) + \frac{1}{m}\sin(mt)\, y'(0) + \frac{1}{m}\int_0^t \sin(m(t-y))\, F(y)dy.$$

Now, we obtain $y(0)$ and $y'(0)$. Taking the derivative, we get

$$y'(t) = -m\sin(mt)\, y(0) + \cos(mt)\, y'(0) + \int_0^t \cos(m(t-y))\, F(y)dy.$$

Putting $F(y) = -af(y) + bf(\pi - y) - if'(y)$, we get

$$y(t) = \cos(mt)\, y(0) + \frac{1}{m}\sin(mt)\, y'(0)$$

$$+\frac{1}{m}\int_0^t \sin(m(t-y))\left[-af(y) + bf(\pi - y) - if'(y)\right]dy, \tag{6}$$

$$y'(t) = -m\sin(mt)\, y(0) + \cos(mt)\, y'(0)$$

$$+\int_0^t \cos(m(t-y))\left[-af(y) + bf(\pi - y) - if'(y)\right]dy. \tag{7}$$

Substituting $\frac{\pi}{2}$ for t into equations (6) and (7) gives us

$$y\left(\frac{\pi}{2}\right) = \cos m\frac{\pi}{2}\ y(0) + \frac{1}{m}\sin m\frac{\pi}{2}\ y'(0)$$

$$+\frac{1}{m}\int\limits_0^{\frac{\pi}{2}} \sin m\left(\frac{\pi}{2}-y\right)\left[-af(y)+bf(\pi-y)-if'(y)\right]dy,$$

$$y'\left(\frac{\pi}{2}\right) = -m\sin m\frac{\pi}{2}\ y(0) + \cos m\frac{\pi}{2}\ y'(0)$$

$$+\int\limits_0^{\frac{\pi}{2}} \cos m\left(\frac{\pi}{2}-y\right)\left[-af(y)+bf(\pi-y)-if'(y)\right]dy.$$

Applying initial conditions $y\left(\frac{\pi}{2}\right)=\varphi, y'(\frac{\pi}{2}) = -i\left\{(a+b)\varphi+f\left(\frac{\pi}{2}\right)\right\}$, we obtain

$$\begin{cases} \cos\left(\frac{m\pi}{2}\right)\ y(0)+\frac{1}{m}\sin\left(\frac{m\pi}{2}\right)\ y'(0) = \varphi-\alpha_1, \\ -m\sin\left(\frac{m\pi}{2}\right)\ y(0)+\cos\left(\frac{m\pi}{2}\right)\ y'(0) = -i\left\{(a+b)\varphi+f(\frac{\pi}{2})\right\}-\alpha_2. \end{cases}$$

Here

$$\alpha_1 = \frac{1}{m}\int\limits_0^{\frac{\pi}{2}} \sin\left(m\left(\frac{\pi}{2}-y\right)\right)\left[-af(y)+bf(\pi-y)-if'(y)\right]dy,$$

$$\alpha_2 = \int\limits_0^{\frac{\pi}{2}} \cos\left(m\left(\frac{\pi}{2}-y\right)\right)\left[-af(y)+bf(\pi-y)-if'(y)\right]dy.$$

Since

$$\Delta = \begin{vmatrix} \cos\left(\frac{m\pi}{2}\right) & \frac{1}{m}\sin\left(\frac{m\pi}{2}\right) \\ -m\sin\left(\frac{m\pi}{2}\right) & \cos\left(\frac{m\pi}{2}\right) \end{vmatrix} = \cos^2 m\frac{\pi}{2}+\sin^2 m\frac{\pi}{2} = 1 \neq 0,$$

we have that

$$y(0) = \frac{\Delta_0}{\Delta} = \begin{vmatrix} \varphi-\alpha_1 & \frac{1}{m}\sin\left(\frac{m\pi}{2}\right) \\ -i\{(a+b)\varphi+f(\frac{\pi}{2})\}-\alpha_2 & \cos\left(\frac{m\pi}{2}\right) \end{vmatrix}$$

$$y(0) = \cos\left(\frac{m\pi}{2}\right)[\varphi-\alpha_1]+\frac{1}{m}\sin\left(\frac{m\pi}{2}\right)\left[-i\left\{(a+b)\varphi+f(\frac{\pi}{2})\right\}-\alpha_2\right],$$

$$y'(0) = \frac{\Delta_1}{\Delta} = \begin{vmatrix} \cos\left(\frac{m\pi}{2}\right) & \varphi-\alpha_1 \\ -m\sin\left(\frac{m\pi}{2}\right) & -i\left\{(a+b)\varphi+f\left(\frac{\pi}{2}\right)\right\}-\alpha_2 \end{vmatrix}$$

$$y'(0) = -\cos\left(\frac{m\pi}{2}\right)\left[i\left\{\varphi+f\left(\frac{\pi}{2}\right)\right\}+\alpha_2\right]+m\sin\left(\frac{m\pi}{2}\right)[\varphi-\alpha_1].$$

Putting $y(0)$ and $y'(0)$ into equation (6), we get

$$y(t)=\cos m\left(t-\frac{\pi}{2}\right)\varphi+\frac{1}{m}\sin m\left(\frac{\pi}{2}-t\right)\left[i\{(a+b)\varphi+f\left(\frac{\pi}{2}\right)\right]$$

$$-\frac{1}{m}\int_{t}^{\frac{\pi}{2}}\sin m(t-y)\left[-af(y)+bf(\pi-y)-if'(y)\right]dy. \tag{8}$$

Since $\cos m(t)$and $\sin m(t)$ are bounded functions on I, we can obtain stability estimates in this case for the solution of the problem (4). In the second case $a^2-b^2=0$. Then,

$$y''(t)=F(t). \tag{9}$$

Integrating this equation, we get

$$y'(t)-y'\left(\frac{\pi}{2}\right)=\int_{\frac{\pi}{2}}^{t}F(s)ds$$

and integrating last equation, we get

$$y(t)-y\left(\frac{\pi}{2}\right)-y'\left(\frac{\pi}{2}\right)\left(t-\frac{\pi}{2}\right)=\int_{\frac{\pi}{2}}^{t}(t-s)F(s)ds.$$

Applying initial conditions $y\left(\frac{\pi}{2}\right)=\varphi, y'\left(\frac{\pi}{2}\right)=-i\left\{(a+b)\varphi+f\left(\frac{\pi}{2}\right)\right\}$, we get

$$=\varphi+\left(\frac{\pi}{2}-t\right)i\left\{(a+b)+f\left(\frac{\pi}{2}\right)\right\}-\int_{t}^{\frac{\pi}{2}}(t-y)F(y)dy.$$

Since t *is* not bounded function on I, in general, we can not obtain stability estimates of the solution for problem (4) for this case.
In the third case $a^2-b^2=m^2<0$. Substituting $-m^2$ for a^2-b^2 into equation (5), we get

$$y''(t)-m^2y(t)=F(t), t\in I.$$

Applying Laplace and inverse Laplace transforms, we get

$$y(t)=\cosh(mt)y(0)+\frac{1}{m}\sinh(mt)y'(0)+\frac{1}{m}\int_{0}^{t}\sinh(m(t-y))F(y)dy.$$

Now, we obtain $y(0)$ and $y'(0)$. Taking the derivative, we get

$$y'(t)=-m\sinh(mt)y(0)+\cosh(mt)\ y'(0)+\int_{0}^{t}\cosh(m(t-y))F(y)dy.$$

Putting $F(y)=-af(y)+bf(\pi-y)-if'(y)$, we get

$$y(t)=\cosh(mt)y(0)+\frac{1}{m}\sinh(mt)y'(0)$$

$$+\frac{1}{m}\int_{0}^{t}\sinh(m(t-y))\left[-af(y)+bf(\pi-y)-if'(y)\right]dy, \tag{10}$$

$$y'(t) = m\sinh(mt)\ y(0) + \cosh(mt)\ y'(0)$$

$$+\int_0^t \cosh(m(t-y))\left[-af(y)+bf(\pi-y)-if'(y)\right]dy. \tag{11}$$

Substituting $\frac{\pi}{2}$ for t into equations (10) and (11), we get

$$y(\frac{\pi}{2}) = \cosh m\frac{\pi}{2}\ y(0) + \frac{1}{m}\sinh m\frac{\pi}{2}\ y'(0)$$

$$+\frac{1}{m}\int_0^{\frac{\pi}{2}} \sinh m(\frac{\pi}{2}-y)\left[-af(y)+bf(\pi-y)-if'(y)\right]dy,$$

$$y'\left(\frac{\pi}{2}\right) = m\sinh m\frac{\pi}{2}\ y(0) + \cosh m\frac{\pi}{2}\ y'(0)$$

$$+\int_0^{\frac{\pi}{2}} \cosh m\left(\frac{\pi}{2}-y\right)\left[-af(y)+bf(\pi-y)-if'(y)\right]dy.$$

Applying initial conditions $y\left(\frac{\pi}{2}\right)=\varphi, y'(\frac{\pi}{2}) = -i\left\{(a+b)\varphi+f\left(\frac{\pi}{2}\right)\right\}$, we obtain

$$\begin{cases} \cosh\left(\frac{m\pi}{2}\right)\ y(0) + \frac{1}{m}\sinh\left(\frac{m\pi}{2}\right)\ y'(0) = \varphi - \alpha_1, \\ m\sinh\left(\frac{m\pi}{2}\right)\ y(0) + \cosh\left(\frac{m\pi}{2}\right)\ y'(0) = -i\left\{(a+b)\varphi + f(\frac{\pi}{2})\right\} - \alpha_2. \end{cases}$$

Here

$$\alpha_1 = \frac{1}{m}\int_0^{\frac{\pi}{2}} \sinh\left(m\left(\frac{\pi}{2}-y\right)\right)\left[-af(y)+bf(\pi-y)-if'(y)\right]dy,$$

$$\alpha_2 = \int_0^{\frac{\pi}{2}} \cosh\left(m\left(\frac{\pi}{2}-y\right)\right)\left[-af(y)+bf(\pi-y)-if'(y)\right]dy.$$

Since

$$\Delta = \begin{vmatrix} \cosh\left(\frac{m\pi}{2}\right) & \frac{1}{m}\sinh\left(\frac{m\pi}{2}\right) \\ m\sinh\left(\frac{m\pi}{2}\right) & \cosh\left(\frac{m\pi}{2}\right) \end{vmatrix} = \cosh^2 m\frac{\pi}{2} - \sinh^2 m\frac{\pi}{2} = 1 \neq 0,$$

we have that

$$y(0) = \frac{\Delta_0}{\Delta} = \begin{vmatrix} \varphi-\alpha_1 & \frac{1}{m}\sinh\left(\frac{m\pi}{2}\right) \\ -i\{(a+b)\varphi+f\left(\frac{\pi}{2}\right)\}-\alpha_2 & \cosh\left(\frac{m\pi}{2}\right) \end{vmatrix}$$

$$y(0) = \cosh\left(\frac{m\pi}{2}\right)[\varphi-\alpha_1] + \frac{1}{m}\sinh\left(\frac{m\pi}{2}\right)\left[-i\left\{(a+b)\varphi+f\left(\frac{\pi}{2}\right)\right\}-\alpha_2\right],$$

$$y'(0) = \frac{\Delta_1}{\Delta} = \begin{vmatrix} \cosh\left(\frac{m\pi}{2}\right) & \varphi-\alpha_1 \\ m\sinh\left(\frac{m\pi}{2}\right) & -ia+b+f(\frac{\pi}{2})-\alpha_2 \end{vmatrix}$$

$$y'(0) = -\cosh\left(\frac{m\pi}{2}\right)\left[i(a+b)\,\varphi + f\left(\frac{\pi}{2}\right) + \alpha_2\right] - m\sinh\left(\frac{m\pi}{2}\right)[\varphi - \alpha_1].$$

Putting $y(0)$ and $y'(0)$ into equation (10), we get

$$y(t) = \cosh m\left(t - \frac{\pi}{2}\right)\varphi - \frac{1}{m}\sinh m\left(\frac{\pi}{2} - t\right)\left[i\{(a+b)\,\varphi + f\left(\frac{\pi}{2}\right)\right]$$

$$-\frac{1}{m}\int_t^{\frac{\pi}{2}} \sinh m(t-y)\left[-af(y) + bf(\pi - y) - if'(y)\right]dy.$$

Since $cosh(mt)$ and $\sinh(mt)$ are not bounded functions on I, in general, we can not obtain stability estimates of the solution for problem (4) for this case.

Theorem 2 *Assume that* $0 \neq |b| < |a|$. *Then the problem (4) is stable and the following stability estimate holds*

$$\sup_{t\in I}|y(t)| \leq \left(1 + \frac{|a| + |b|}{\sqrt{a^2 - b^2}}\right)\left[|\varphi| + \int_{-\infty}^{\infty}|f(y)|\,dy\right]. \tag{12}$$

Proof. Applying formula (8), we get

$$y(t) = \cos\sqrt{a^2-b^2}\left(t - \frac{\pi}{2}\right)\varphi + \frac{i}{\sqrt{a^2-b^2}}\sin\sqrt{a^2-b^2}\left(\frac{\pi}{2} - t\right)(a+b)\,\varphi \tag{13}$$

$$-\frac{1}{\sqrt{a^2-b^2}}\int_t^{\frac{\pi}{2}} \sin\sqrt{a^2-b^2}(t-y)\left[-af(y) + bf(\pi - y)\right]dy$$

$$+i\int_t^{\frac{\pi}{2}} \cos\sqrt{a^2-b^2}(t-y)f(y)dy.$$

The proof of estimate (12) is based on the formula (13) and the triangle inequality.

NONLINEAR ORDINARY DIFFERENTIAL EQUATIONS WITH INVOLUTION

We consider the initial value problem

$$iy^{'}(t) = by(-t) + ay(t) + f(t, y(t)), t \in I, y(0) = \varphi \tag{14}$$

for the first order nonlinear ordinary differential equation with involution. We are interested in studying the existence and uniqueness of bounded solution of problem (14) on I. In general cases of a and b the solution of (14) is not bounded on I. Let $C(I)$ be the complete space of all continuous functions defined on the interval I with the metric d defined by[9]

$$d(x,y) = \sup_{t\in I}|x(t) - y(t)|.$$

Theorem 3 *Assume that* $|b| < |a|, a \in (-\infty, 0)$ *and* f *is continuous and bounded function on the region*

$$P = \{(t,x) : -\infty < t < \infty,\ |x - \varphi| < M\}.$$

Suppose that f satisfies a Lipschitz condition on P with respect to its second argument, that is, there is a constant l such that for $(t,x)\,,(t,y)\in P$

$$|f(t,x)-f(t,y)|\leq l\,|x-y|\,. \tag{15}$$

Then, initial value problem (14) has a unique solution $y\in C(I)$. This function y is the limit of the iterative sequence $\{y_n\}_{n=0}^{\infty}$ defined by the recursive Picard iteration formula

$$y_n(t)=\cos\sqrt{a^2-b^2}\left(t-\frac{\pi}{2}\right)\varphi+\frac{i}{\sqrt{a^2-b^2}}\sin\sqrt{a^2-b^2}\left(\frac{\pi}{2}-t\right)(a+b)\,\varphi$$

$$-\frac{1}{\sqrt{a^2-b^2}}\int\limits_{t}^{\frac{\pi}{2}}\sin\sqrt{a^2-b^2}(t-s)\left[-af(s,y_{n-1}(s))+bf\left(\pi-s,y_{n-1}(s)\right)\right]ds$$

$$+i\int\limits_{t}^{\frac{\pi}{2}}\cos\sqrt{a^2-b^2}(t-s)f(s,y_{n-1})ds, n=1,2,...,$$

where $y_0\,(t)$ is an arbitrary continuous function.

Proof. Applying formula (13), we can write problem (14) in the equivalent integral form $y(t)=Ty(t)$. Here

$$Ty(t)=\cos\sqrt{a^2-b^2}\left(t-\frac{\pi}{2}\right)\varphi+\frac{i}{\sqrt{a^2-b^2}}\sin\sqrt{a^2-b^2}\left(\frac{\pi}{2}-t\right)(a+b)\,\varphi$$

$$-\frac{1}{\sqrt{a^2-b^2}}\int\limits_{t}^{\frac{\pi}{2}}\sin\sqrt{a^2-b^2}(t-s)\left[-af\left(s,y(s)\right)+bf\left(\pi-s,y(s)\right)\right]ds$$

$$+i\int\limits_{t}^{\frac{\pi}{2}}\cos\sqrt{a^2-b^2}(t-s)f(s,y)ds.$$

Note that integral form is a Volterra type integral-differential equation of the second kind. Therefore, applying the fixed-point theorem, we can complete the proof of Theorem 3.

CONCLUSION

In the present paper, the initial value problem for the first order differential equation with involution is investigated. Theorem on stability estimates for the solution of the initial value problem for the first order ordinary linear differential equation with involution is proved. Theorem on existence and uniqueness of bounded solution of initial value problem for the first order ordinary nonlinear differential equation with involution is established. Moreover, applying the result of the monograph [8], the single-step stable difference schemes for the numerical solution of the initial value linear and nonlinear problems (4) and (14) for the first order linear and nonlinear differential equations with involution can be presented and studied.

REFERENCES

1. C. E. Falbo, Journal of Interdisciplinary Mathematics **6(3)**, 279–289 (2003).

2. R. M. Nisbet, “Delay-differential equations for structured populations,” in *Structured-Population Models in Marine, Terrestrial, and Freshwater Systems*, edited by S. Tuljapurkar and H. Caswell (Springer US, Boston, MA, 1997) pp. 89–118.
3. A. Ashyralyev and A. M. Sarsenbi, Numerical Functional Analysis and Optimization **38(10)**, 1295–1304 (2017).
4. M. Ashyraliyev, M. Ashyralyyeva, and A. Ashyralyev, Bullition of the Karaganda Univesity-Mathematics **99(3)**, 125–134 (2020).
5. D. Przeworska-Rolewicz, *Equations with Transformed Argument. Algebraic Approach* (Amsterdam, Warszawa, 1997).
6. J. Wiener, *Generalized Solutions of Functional Differential Equations* (Singapore New Jersey, London Hong Kong, 1993).
7. F. T. A.Cabada, *Differential Equations with Involutions* (Atlantis Press, 2015).
8. A. Ashyralyev and P. E. Sobolevskii, *New Difference Schemes for Partial Differential Equations* (Birkhäuser Verlag, Basel, Boston, Berlin, 2004).
9. A. Ashyralyev, *Computational Mathematics* (The South of Kazakhstan State University Named after M.Auezovuku Printing House, Chimkent, 2013).

Relationship Between Financial Stress and Business Confidence in PIGS Countries: Evidence Based on an ARDL Approach

Vusal Mursalzada[1, a)] and Behiye Cavusoglu[2, b)]

[1)] *AZ 1045, Baku, Azerbaycan*
[2)] *Department of Economics, Near East University, 99138, Nicosia, TRNC, Mersin 10, Turkey*

[a)] *Corresponding author: vusal.murselzade@gmail.com*
[b)] *Electronic mail: behiye.cavusoglu@neu.edu.tr*

Abstract. This study investigates the cointegration and causality relationships between business confidence and financial stress for the PIGS countries (Portugal, Italy, Greece, and Spain) based on monthly data covering between January 2008 and December 2019. Panel ARDL methodology and Pooled Mean Group estimation techniques are used to test the short-run and long-run relationships between the variables. The findings indicate that financial stress is significantly and negatively affected by business confidence in the examined countries in both the long run and short run. Furthermore, the current month's financial stress level is negatively affected by the last month's business confidence and financial stress levels. Finally, a univariate causality relationship running from business confidence towards financial stress is revealed.

INTRODUCTION

Initial efforts using certain indicators to understand the general situation of the financial sector commenced in the 1980s. Early indicators included the Monetary Condition Index proposed by the Bank of Canada, the Bloomberg Financial Condition Index, Goldman Sachs FCI, etc. Towards the end of the 1990s, a financial stress began to be used by academicians and central banks as a concept to represent the total stress of the entire financial system. The popularity of this concept particularly increased after the 2008 financial crisis [1].

Financial stress does not emerge in isolation. The recent financial crisis proved that strong links exist between the financial sector and the real sector and these sectors respond to shocks that occur in the other. Various studies have investigated the possible impacts of financial stress on different economic activities such as unemployment, prices, monetary policy measures, GDP and so on ([2, 3, 4]).

This study investigates the relationship between financial stress and business confidence in the PIGS countries (Portugal, Italy, Greece, and Spain) based on monthly data covering the period January 2008-December 2019. Business confidence surveys are regularly conducted to develop a clear picture of world business and to identify potential challenges. Business confidence indices are designed for different regions and countries to measure overall confidence in businesses [5].

LITERATURE REVIEW

Financial Stress

Multiple studies have investigated financial stress in different contexts. Some studies have been devoted to construct financial stress indices for different countries and regions. The study of Illing and Liu [6] was one of the early studies that devised an FSI for a developed country-Canada. Cardarelli et al. [7] designed an FSI to calculate the financial stress in 17 developed countries, including Spain and Italy. The Central Bank of Turkey [8] published a Financial Stability Report, in which an FSI was designed for the financial sector of Turkey to assess the crisis-time financial performance of the country. Louzis and Vouldis [9] devised an FSI for Greece using the GARCH methodology. Oet et al. [10] presented the Cleveland FSI calculated on a daily basis. This study took four financial markets and eleven variables into account while constructing the FSI. Ekinci [1] calculated the financial stress index for Turkey based on banking and public sectors, stock markets and foreign exchange markets and broke down the Turkish economy into different stress periods. Aboura and van Roye [11] devised an FSI for the French economy using the Markov-Switching Bayesian VAR model and indicated low and high stress periods.

Another strand of the literature has investigated the financial stress index (FSI) in relation to different economic activities. The real effects of financial stress have been comprehensively investigated in the literature. David and

International Conference on Analysis and Applied Mathematics (ICAAM 2020)
AIP Conf. Proc. 2325, 020069-1–020069-6; https://doi.org/10.1063/5.0040385
Published by AIP Publishing. 978-0-7354-4069-2/$30.00

Hakkio [2] assessed the influence of financial stress on economic activity in the USA and identified two regimes. In a normal regime, the financial stress level is low and the level of economic activity is high. A reverse condition occurs when the US economy operates in a distressed regime. In the distressed regime, the impact of financial stress on economic activity becomes larger than the normal regime. Li and St-Amant [12] found that financial stress lessens the output growth in Canada. Mallick and Sousa [4] investigated the real effects of financial stress in the Eurozone markets. They determined that financial stress is strongly and negatively affected by tight monetary policies. On the other hand, their findings showed that unexpected variations in the FSI and output fluctuations are closely related in the Eurozone. Van Roye [13] devised an FSI for Germany and examine how financial stress affects economic activity in that country. The findings showed that inflation rates and GDP are severely dampened when financial stress is high. Short-term nominal interest rates also substantially drop as a result of high financial stress. Hubrick and Tetlow [14] investigated the impacts of financial stress on the real economy. They found that monetary policy reactions differ in stress and non-stress periods. Nazlioglu et al. [3] investigated the financial stress-oil prices relationship, looking for volatility spillovers. They used WTI crude oil prices and the Cleveland Financial Stress Index as variables and examined the relationship between them in pre-crisis, crisis, and post-crisis periods. The study results showed that substantial spillovers exist between energy and financial markets. Malega and Horvath [15] found that financial stress affects prices, unemployment, interest rates, and output levels in the Czech Republic and has significantly negative effects for the economy. Aboura and van Roye [11] found that during high financial stress periods, economic activity significantly reduces in France.

Business Confidence

Sood [16] stated that business confidence or expectations surveys are regularly conducted in different countries. Such surveys investigate business conditions and the expectations of firms and can therefore be effective tools for determining the short-term characteristics of economies. Many studies have devised business confidence indices on different economic areas. Oral et al. [5] constructed the Real Sector BCI for Turkey. Santero and Westerlund [17] found that business and consumer confidence indices can help to explain the overall economic situation and make forecasts. They also found that business confidence indicators are more effective for economic analysis than consumer confidence indicators, as a looser relationship exists between output fluctuations and consumer confidence indicators. Cevik et al. [18] investigated how business confidence affects stock returns using the ISM manufacturing index as a business confidence indicator and found that regime-switching probabilities in the US stock markets are affected by the business confidence factor. Sum and Chorlian [19] examined the dynamic effects of business confidence and consumer confidence on stock market risk premiums. They identified that when business confidence and consumer confidence experience shocks, stock market risk premiums immediately show a positive response. Furthermore, the results indicated that business and consumer confidence levels together explain around 7.4% of the variations in risk premiums of stock markets. Ayuningtyas and Koesrindartoto [20] also examined the relationship among the same variables for Indonesia from 2000 to 2013. They found that quarterly stock indices are significantly and positively affected by business confidence in Indonesia. Tibulca [21] investigated how business confidence in the manufacturing sector is affected by fiscal policy decisions. The author used change in taxation to quantify fiscal policy and found that only 15% of the business confidence level can be explained by taxation. Furthermore, the findings indicated that the impact of change in taxation on business confidence is much higher in Japan than in OECD Eurozone member states. The paper of De Jongh and Mncayi [22] investigated the relationship between business confidence, investments, and economic growth in South Africa from 1995Q1 to 2017Q4. Using the autoregressive distributed lag (ARDL) model, they found a significant positive relationship among the variables. The Granger causality results further proposed that "the BCI acts as a key leading indicator for investment and growth in the economy". Khan and Upadhayaya [23] examined whether business investment growth is influenced by the business confidence level in the US and revealed that business confidence can predict investment growth in that country. In addition, they found that the forecasting power of business confidence is much stronger than traditional determinants.

Many studies have investigated the FSI and BCI separately. To the best of the authors' knowledge, this is the first study to examine the financial stress – business confidence nexus. We have employed panel ARDL and Pooled Mean Group estimators together with panel causality analysis to prove the relationship between the two variables.

DATA AND METHODOLOGY

The Pooled Mean Group Estimation method is largely used in studies with large sample sizes and a high number of observations [24]. This model is an effective method in dynamic non-stationary panels. The method calculates the cointegration relationship among variables and it is possible to obtain short-run and long-run results from this model. A basic requirement for the model to yield valid results is that the variables must be I(0) or I(1). Pesaran et al. [25] excluded the existence of I(2) variables for ARDL estimation. This can be tested using unit root tests for both variables at levels and at the first differences. The general formula of the PMG estimator can be modelled as below:

$$Y_{it} = \sum_{j=1}^{p} \lambda_{ij} y_{i,t-j} + \sum_{j=0}^{q} \delta_{ij} X_{i,t-j} + \mu_t + \varepsilon_{it},$$

where the number of cross sections $i = 1, 2, ..., n$ and time $t = 1, 2, 3, ..., \lambda$. $X_{i,t}$ is a vector of $K \times 1$ regressors, λ_{ij} is a scalar, and μ_t is a group specific effect.

TABLE 1. Panel Unit Root Test Summary

Business Confidence Index Level Method	Statistic	Probability
Levin, Lin Chu	-0.46452	0.3211
Im, Pesaran and Shin W-stat	-185.866	0.0315
ADF - Fisher Chi-square	153.800	0.0522
PP - Fisher Chi-square	105.484	0.2286
1st difference		
Levin, Lin Chu	-177.995	0.0375
Im, Pesaran and Shin W-stat	-627.841	0.0000
ADF - Fisher Chi-square	591.381	0.0000
PP - Fisher Chi-square	340.695	0.0000

TABLE 2. Panel Unit Root Test Summary

Financial Stress Index Level Method	Statistic	Probability
Levin, Lin Chu	-148.364	0.0690
Im, Pesaran and Shin W-stat	-302.326	0.0013
ADF - Fisher Chi-square	247.767	0.0017
PP - Fisher Chi-square	301.222	0.0002
1st difference		
Levin, Lin Chu	-872.604	0.0000
Im, Pesaran and Shin W-stat	-156.301	0.0000
ADF - Fisher Chi-square	201.725	0.0000
PP - Fisher Chi-square	376.139	0.0000

Various methodologies have been employed in the literature to test the relationship between two variables, depending on the characteristics of the data. After running several tests, panel ARDL model developed by Pesaran and Smith [26] and Pesaran et al. [24] was found to be effective for the analysis. Pesaran and Smith [26] and Pesaran et al. [24] also proposed the Pooled Mean Group Estimator within the panel ARDL method, which is an efficient estimator as parameters are estimated for each country and then for the group in this model. The PMG estimator allows the short run parameters to act heterogeneously across countries, but in the long run, it considers parameters to be homogenous [27]. Pesaran et al. [24] linked the existence of homogeneity in the long run to several factors such as common technology usage or common institutional improvements. The ARDL model allows the estimation of short-run parameters via the Error Correction Model. Error correction terms in this model are derived from ARDL long-run relationships.
To estimate the relationship between FSI and BCI with an ARDL model, we first introduce the unit root test to examine the stationarity of our variables. Panel unit root test results to determine the stationarity of the business confidence index (BCI) are indicated in Table 1. The E-views software presents a summary of different unit root tests in one table. The null hypotheses of all four tests is that the variable is subject to unit root. Three of the four tests approve that there is unit root at level. The alternative hypothesis is accepted in all four tests conducted at the 1st difference.

TABLE 3. Kao Residual Cointegration Test

	t-Statistic	Prob.
ADF	-2.983.303	0.0014
Residual variance	0.003126	
HAC variance	0.001430	

TABLE 4. Pedroni Residual Cointegration Test. Null Hypothesis: No cointegration

	Statistic	Prob.	Statistic	Prob.
Panel v-Statistic	4.589.211	0.0000	2.129.615	0.0166
Panel rho-Statistic	-1.113.020	0.0000	-1.474.675	0.0000
Panel PP-Statistic	-5.966.604	0.0000	-7.466.503	0.0000
Panel ADF-Statistic	-5.460.399	0.0000	-5.580.743	0.0000
Group rho-Statistic	-1.098.371	0.0000		
Group PP-Statistic	-7.071.321	0.0000		
Group ADF-Statistic	-5.829.654	0.0000		

Thus, the variable BCI is an I(1) variable. The unit root test results for the financial stress index (FSI) variable are presented in Table 2.

The test results largely show that there is no unit root either at the level or at the first difference. Thus, FSI is an I(0) variable. Proving that none of the variables are integrated at the second difference meets the main condition of the panel ARDL method.

Cointegration and causality tests can also be useful tools to further explain the behavior of variables. Searching for cointegration is a helpful step, although not strongly required, to provide evidence that the long-run results are common across countries, which is a necessary step to conduct PMG estimation. Two cointegration tests were used to check whether the two variables are cointegrated or not, which are the Kao Residual Cointegration Test and Pedroni Residual Cointegration Test. The results of these tests are presented in Table 3 and Table 4. The null hypothesis

TABLE 5. Long Run Cointegration Results

Variable	Coefficient	Std. Error	t-Statistics	Probability
BCI	-0.041460	0.004810	-8.620.170	0.0000

of the test supports that there is no cointegration between variables. As the probability value is less than 5%, the null hypothesis must be rejected and the existence of long-run cointegration must be accepted. The Pedroni Residual Cointegration test results further strengthen the evidence of long-run cointegration. The Pedroni [**?**] test consists of different within-dimension and between-dimension statistics (see Table 4). As all probability values for the panel and group indicators are less than 5%, the alternative hypothesis of the existence of panel cointegration between variables can be accepted. However, the Pedroni test can only indicate the presence of cointegration among the variables, but is unable to estimate the long-run relationship. Thus, we use the panel ARDL method suggested by Pesaran et al. [26]. The ARDL approach firstly examines a long-run cointegration relationship among the variables and then estimates the coefficients of the variables. The Pooled Mean Group Estimator developed by Pesaran et al. [24] provides the estimation results in Table 5.

Accepting the FSI as the dependent variable, the long-run results indicate that there is a negative significant relationship between the variables. It indicates that BCI negatively affects FSI in the long run, which is a reasonable finding. According to the cointegration results, a one unit increase in the business confidence index is accompanied by an approximate 0.04 unit decrease in the financial stress index in the long run.

The study investigates the short run cointegration between FSI and BCI. The results show that only up to the 1st lag of both variables can affect the dependent variable in the short run. Specifically, the 1st lag of FSI is significant and negatively affects the current FSI. Also, BCI is a significant explanatory variable to explain FSI. According to the short-run test results, BCI has negative affect on FSI. However, the 1st lag of BCI is significant and it positively affects FSI in the short run. The Error Correction Term is significant and negative, which is a desirable outcome for our study (see Table 6). The short-run cointegration results indicate that a 1 unit increase in the business confidence index results in an approximate 0.09 unit decrease in the financial stress index. The findings also show that a 1 unit increase in the last month's FSI results in a 0.12 unit decrease in the current FSI. Furthermore, a 1 unit increase in the

TABLE 6. Short Run Cointegration Results

Variable	Coefficient	Std. Error	t-Statistic	Probability
COINTEQ01	-0.205827	0.068309	-3.013.188	0.0027
D(FSI(-1))	-0.123799	0.046383	-2.669.078	0.0078
D(FSI(-2))	-0.085211	0.045586	-1.869.248	0.0621
D(FSI(-3))	-0.030927	0.033828	-0.914259	0.3610
D(BCI)	-0.093915	0.015551	-6.038.979	0.0000
D(BCI(-1))	0.073090	0.022768	3.210.253	0.0014
D(BCI(-2))	-0.052855	0.055840	-0.946537	0.3443
D(BCI(-3))	0.029587	0.034422	0.859519	0.3904
C	0.879385	0.289790	3.034.556	0.0025

TABLE 7. Granger Causality Test

Null Hypothesis:	Obs	F-Statistic	Prob.
FSI does not Granger Cause BCI	568	201.503	0.1343
BCI does not Granger Cause FSI		671.407	0.0013

last month's BCI results in a 0.07 unit decrease in the current month's FSI.

To check the causal relationship between variables, the Granger Causality test is conducted [27]. The test results prove that there is a unidirectional relationship running from BCI to FSI (see Table 5).

CONCLUSION

The popularity of financial stress levels in economies as general measurements of financial stability has increased, particularly after the 2008 financial crisis. Previous studies have extensively investigated the potential outcomes of high financial stress levels on different sectors of the economy. This study examined the short-run and long-run relationship between financial stress and business confidence. To the best of the authors' knowledge, the relationship between these variables has not been examined well, if at all. The findings of the study revealed that business confidence negatively affects financial stress in the long term and in the short term in the PIGS countries. Hence, when confidence and expectations in business environment strengthen, financial stress decreases in these countries. The study also found that business confidence causes financial stress in the PIGS countries, but the reverse causality running from financial stress towards business confidence was not found.

ACKNOWLEDGEMENTS

The publication has been prepared with the support of the Near East University, Nicosia, Turkey.

REFERENCES

1. A. Ekinci, Dogus Universitesi Dergisi **14(2)**, 213-229 (2013).
2. T. Davig and C. Hakkio, Economic Review **95(2)**, 35-62 (2010).
3. S. Nazlioglu, U. Soytas, and R. Gupta, Energy Policy **82**, 278-288 (2015).
4. S. K. Mallick and R. M. Sousa, International Review of Financial Analysis **30**, 1-17 (2013).
5. E. Oral, E. Dilara, and T. Hamsici, Central Bank Review **5(1)**, 23-54 (2005).
6. M. Illing and Y. Liu, Journal of Financial Stability **2(3)**, 243-265 (2006).
7. R. Cardarelli, S. Elekdag, and S. Lall, *Financial Stress, Downturns, and Recoveries* (No. 2009-2100) International Monetary Fund, 2009.
8. Central Bank of Turkey, (2009). *Financial stability Report*, 8, May. Retrieved from https://www.tcmb.gov.tr/wps/wcm/connect/EN/TCMB+EN/Main+Menu/Publications/Reports/Financial+Stability+Report/. Last access: 11 July 2020.
9. D. P. Louzis and A. T. Vouldis, *A Financial Systemic Stress Index for Greece, Bank of Greece*, Financial Stability Department Working Paper, January 2011.

10. M. V. Oet, R. Eiben, T. Bianco, D. Gramlich, and S. J. Ong, The Financial Stress Index, 2011.
11. S. Aboura and B. Van Roye, *Financial stress and economic dynamics: an application to France.* Retrieved from https://hal.archives-ouvertes.fr/hal-01526393. Last access: 11 July 2020.
12. F. Li and P. St-Amant, *Financial stress, monetary policy, and economic activity* (No. 2010-12). Bank of Canada.
13. B. Van Roye, *Financial stress and economic activity in Germany and the Euro Area* (No. 1743). Kiel Working Paper, 2011.
14. K. Hubrich and R. J. Tetlow, Journal of Monetary Economics **70**, 100-115 (2015).
15. J. Malega and R. Horváth, Prague Economic Papers **26(3)**, 257-268 (2017).
16. A. Sood, *Business Confidence: The NCAER Survey.* In Proceedings of the Joint ADB/OECD/ESC AP Workshop on Harmonizing and Strengthening Business Tendency Surveys in Developing Countries in the Asia Pacific Region held on (pp. 21-24), 2000.
17. T. Santero and N. Westerlund, *Confidence Indicators and Their Relationship to Changes in Economic Activity* (OECD Publishing, 1996).
18. E. Cevik, T. Korkmaz, and E. Atukeren, Applied Financial Economics **12(4)**, 299–312 (2012).
19. V. Sum and J. Chorlian, International Journal of Economics and Finance **5(9)**, 45-49 (2013).
20. R. Ayuningtyas and D. P. Koesrindartoto, *The Relationship between Business Confidence, Consumer Confidence, and Indexes Return: Empirical Evidence in Indonesia Stock Exchange.* In International Conference on Trends in Economics, Humanities and Management, 21-25, 2014.
21. I. L. Tibulca, Journal of Eastern Europe Research in Business & Economics **2015**, 1 (2015).
22. J. De Jongh and P. Mncayi, International Journal of Economics and Finance Studies **10(1)**, 115-133 (2018).
23. H. Khan and S. Upadhayaya, *Does business confidence matter for investment?*, Empirical Economics, 1-33 (2019).
24. M. H. Pesaran and Y. Shin, R. P. Smith, Journal of the American Statistical Association **94(446)**, 621-634 (1999).
25. M. H. Pesaran, Y. Shin and R. P. Smith, *Pooled Estimation of Long-Run Relationships in Dynamic Heterogeneous Panels* (No. 9721, Faculty of Economics, University of Cambridge, 1997).
26. M. H. Pesaran and R. Smith, Journal of Econometrics **68(1)**, 79-113 (1995).
27. M. E. Bildirici, Gcb Bioenergy **6(6)**, 717-726 (2014).

A Comparative Analysis of Fluoride, Magnesium, and Calcium Phosphate Materials on Prevention of White Spot Lesions Around Orthodontic Brackets with Using pH Cycling Model

Selda Lale[a)]

Department of Orthodontics, Near East University Faculty of Dentistry, Nicosia, Mersin 10, Turkey

[a)]*Corresponding author: selda.lale@neu.edu.tr*

Abstract. One common negative side effect of orthodontic treatment with fixed appliances is the development of white spot lesions (WSLs) around brackets. This study aimed to compare the efficacy of various oral hygiene practices in preventing enamel demineralization around orthodontic brackets under similar in-vitro conditions. The study included 90 extracted bovine incisors, which were randomized into 6 groups. The changes in the demineralization degree were evaluated by measuring the Ca^{+2} concentration (mg/dL) in the demineralization solution at days 5, 10, 15, 19. The procedures were carried out at the Medical Biochemistry Laboratory at Near East University Hospital. Calcium content of each beaker was measured with the Abbott Architect c8000 biochemistry autoanalyzer system using the Arsenazo III method.

INTRODUCTION

One of the most common negative side effects of fixed orthodontic treatment is the development of incipient caries lesions [1].

Studies have shown that while it takes at least 6 months for caries to develop in a patient not submitted to orthodontic treatment, it takes around 1 month [2, 3] to develop in an orthodontic patient because of the difficulty these patients have with performing oral hygiene [4]. This information shows the rapid progression of this disease and the need for continual follow-up of these patients [2]. Investigations have put the incidence of white spot lesion(WSL) during orthodontic treatment with fixed appliances at 73% to 95% [5, 6].

Although there are many methods for the effective control of this initial stage of caries disease, prevention and early and accurate detection of WSLs is a great challenge to orthodontists [7].

However, when the WSLs are found during clinical practice, the lesions are found to have opacity, at least. At present, a few studies have focused on the degree of remineralization of the already-formed WSLs and the prognosis of remineralization therapy. Despite this, there are several questions as follows:

1. Can we prevent the WSLs before they occur?
2. Does prophylactic treatment during orthodontic treatment reduce the occurrence of the WSLs?
3. How should we choose the most effective and correct method when we have such a wide range of products and new materials?

Therefore, the aim of the present study was to investigate the preventive effect of the medical minerals gel and compare it with that of two types of varnishes (fluoride varnish and CPP-ACP varnish), which have been proved to be effective as protective agents, by using methods of observing the changes in visual score and amount of demineralization. If this study finds that medical minerals gel is effective in prevention, then this gel may possibly be added to the list of advised products that can be used to reduce demineralization and the occurrence of WSLs during orthodontic treatment.

APPLICATIONS AND CYCLING MODEL

Tooth Preparation

Ninety incisor teeth were collected from the mandibles of 3-year-old fifteen bovines (negative BSE test) and selected. The selection criteria included intact buccal enamel surfaces without the WSLs, visible cracks, or enamel irregularities.

The teeth were debrided and stored in 0.1% thymol solution at $4°C$. For standardization of the exposed enamel surface, 4 x 6 mm^2 window was created that was placed $5mm$ gingivally to the incisal edge and in the mesiodistal center of the clinical crown. All teeth were painted with a thin coat of acid-resistant nail polish on all surfaces

International Conference on Analysis and Applied Mathematics (ICAAM 2020)
AIP Conf. Proc. 2325, 020070-1–020070-5; https://doi.org/10.1063/5.0040352
Published by AIP Publishing. 978-0-7354-4069-2/$30.00

excluding the window area. Metal lower incisor brackets (3M Unitek, MN, USA) were bonded with a light-cured resin composite cement (Transbond XT, 3M Unitek, MN, USA) at the center of the exposed area [8] which can be seen in Figure 1.

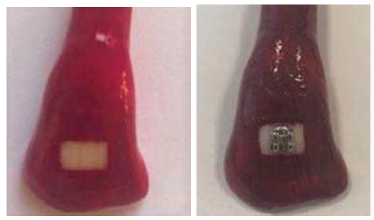

FIGURE 1. Images of teeth before and after bonding the brackets. Left picture represents before bonding the bracket: Nail varnish painted around the exposed enamel surface. Right picture represents after bonding the bracket: Exposed enamel around the bracket represents the area of interest

Visual Assessment

The exposed enamel surfaces of each tooth were examined visually by two examiners in accordance with the scoring criteria established by Ekstrand et al. [9] (listed in Table 1). Only lesions scoring 1 were included in the study. The same visual assessment was conducted at day 19 to evaluate the colour and opacity changes of enamel around brackets.

TABLE 1. Visual examination criteria used in the selection and assessment of teeth [9].

Score	Visual Assessment Criterion
1	No, or slight, change in enamel translucency after air-drying for 5 seconds.
2	Opacity or discoloration hardly visible on the wet surface but visible after air-drying.
3	Visible opacity or discoloration without air-drying.
4	Localised enamel breakdown with opacity or greyish discoloration from the underlying dentin.
5	Cavitation in opaque or discolored enamel exposing the dentin.

pH Cycling Model

After the materials were applied as described later, the groups were cycled in a 25*ml* demineralization solution at 37°*C* for 8 hours per day; each tooth was placed in a separate beaker [10]. Following 8 hours of exposure to the demineralization cycle, the teeth were placed in remineralization solution in separate beakers [8] for approximately 15 hours until the next demineralization cycle [10]. Details can be seen in Table 2.

TABLE 2. Explanation of pH Cycling Model

Cycling Model	Exposure Time to Solutions	Components of Solutions
Demineralization	8 h/ day	Lactic acid and adjusted to pH 4.5 with sodium NaOH
Remineralization	15h/ day	20 mmol/l $NaHCO_3$, 3 mmol/l NaH_2PO_4, and 1 mmol/l $CaCl_2$ at neutral pH

Assigning to Groups of Treatments and Cycling Procedure

Under the same severity, six groups were established based on the prevention method as shown in Table 3.

TABLE 3. Treatment Groups. Here FT denotes fluoride toothpaste, NFT denotes non-fluoride toothpaste, FV+FT denotes fluoride varnish plus fluoride toothpaste, CPP-ACP+FT denotes CPP-ACP varnish plus fluoride toothpaste and MMG+NFT denotes medical minerals gel plus non-fluoride toothpaste

Group 1	Group 2	Group 3	Group 4	Group 5	Group 6
No intervention(control)	FT	NFT	FV+FT	CPP-ACP+FT	MMG+NFT

Each group contained 15 teeth. The duration of the experiment was 19 days. The materials (as listed in Table 4) were applied to the exposed enamel surface around each bracket. All the groups were cycled daily as described before. Varnishes were applied once, at the beginning of the experiment. Medical minerals gel was applied daily according to the manufacturer's instructions and 30 min before starting the next demineralization cycle. Both toothpastes were applied daily, during the remineralization cycle, after immersing in AS for 30 min.

TABLE 4. Composition of commercially available products used in this study.

Material	Composition
Fluoride toothpaste (Colgate Total, Colgate-Palmolive Company, NY, USA)	Sodium fluoride (0.312% (1,450 ppm)), water, glycerin, hydrated silica, sorbitol, PVM/MA copolymer, sodium lauryl sulfate, aroma, carrageenan, sodium hydroxide, propylene glycol, cellulose gum, triclosan, sodium saccharin, limonene, CI 77891 (white pigment).
Non- fluoride toothpaste (R.O.C.S. Pro Brackets & Ortho, 'DRC-Group' Company, Russia)	Sorbitol, silica, glycerin, aqua, xylitol, cocamidopropyl betaine, aroma, xanthan gum, calcium glycerophosphate, bromelain, magnesium chloride, sodium saccharin, sodium benzoate, O-cymen-5-ol, titanium dioxide.
Fluoride varnish (Bifluorid 12, Voco, Cuxhaven,Germany)	Sodium fluoride and calcium fluoride (6%), ethylacetate, pyroxylin, fumed silica, clove oil, ısoamylpropionate.
Casein phosphopeptide-Amorphous Calcium Phosphate(CPP-ACP) varnish (MI varnish, GC, Tokyo, Japan)	Sodium fluoride and CPP-ACP (5%), polyvinyl acetate, hydrogenated rosin, ethanol, silicon dioxide.
Medical minerals gel (R.O.C.S. Medical Minerals; 'DRC-Group' company, Russia)	Aqua, glycerin, xylitol, hydroxyethylcellulose, calcium glycerophosphate, polysorbate-20, aroma, methylparaben, magnesium chloride, hydroxypropyl guar.

Numerical Determination of Calcium Loss (Demineralization)

To assess the amount of demineralization, colorimetric technique were used [11, 12]. The procedures were carried out at the Medical Biochemistry Laboratory at Near East University Hospital. After 8 hours of exposure to the demineralization cycle, the teeth were removed from each beaker. Calcium content of each beaker was measured with the Abbott Architect c8000 biochemistry autoanalyzer system using the Arsenazo III method [13].

The Ca^{+2} content of demineralization solution samples was analyzed for each group at days 5, 10, 15, and 19 to observe change of demineralization according to the days. The lack of Ca^{+2} in demineralization solution is estimated as a measure of the demineralization inhibitory effect of the materials [14].

Statistical Evaluations

Descriptive statistics were calculated. Median differences among the pre- and post treatment visual assessment data for each of the groups were compared using the Bonferroni adjusted Wilcoxon Sign Rank test $(p < 0.001)$ [15, 16].

ANOVA test with the Post-hoc Bonferroni test revealed the significant differences between groups for average demineralization. The results were considered significant at $p = 0.05$. Power analysis was conducted on the Wilcoxon test data to ensure that the sample size and the magnitude of the observed effect were sufficient. The statistical analysis was performed using SPSS software (version 24.0.1, SPSS, Chicago, Ill).

EVALUATION OF NUMERICAL DATA WITH STATISTICAL ANALYSIS

Visual Assessment

A summary of the results of the corresponding statistical analysis via the Bonferroni Adjusted Wilcoxon Sign Rank test is listed in Table 5.

TABLE 5. Median pre- and posttreatment visual examination scores in each group (used products), interquartile ranges and significance levels.

Treatment regime	Control	FT	NFT	FV+FT	CPP-ACP+FT	MMG+NFT
Pretreatment median (interquartile range)	1 (1-2)	1 (1-2)	1 (1-2)	1 (1-2)	1 (1-2)	1 (1-2)
Posttreatment median (interquartile range)	3 (2-3)	2 (2-3)	2 (2-3)	2 (2-3)	1 (1-2)	2 (1-2)
Sample size (n)	15	15	15	15	15	15
Significance level (p)	< 0.001	< 0.001	< 0.001	< 0.001	0.157	< 0.001

These results indicate that the majority of teeth in the CPP-ACP+FT group exhibited no shift in appearance, whereas in the other groups (Control, FT, NFT, FV+FT, MMG+NFT), the visual appearance of the enamel translucency was significantly changed $(p < 0.001)$.

Ca Loss Measurement (Demineralization)

The degrees of demineralization that were evaluated by measuring the Ca^{+2} concentration in the demineralization solution at days 5, 10, 15, 19 for each group and the corresponding A Post-hoc Bonferroni test results of the Ca^{+2} loss measurements confirm the findings of the visual appraisal and indicate that the extent of prevention afforded by the six different treatment regimes investigated in this study for all time points of measurement is in the following order: control $\sim NFT \sim FT \sim FV + FT \sim MMG + NFT < CPP - ACP + FT$ (Table 6).

At all the four time points of measurement (days 5, 10, 15, and 19), the significantly lowest Ca^{+2} concentration in the demineralization solution was observed for the CPP-ACP+FT group.

No advantage was observed for the use of the FV as a supplement to the daily application of the FT during experiment period, but when the MMG was used as a supplement to daily application of the NFT, additional protection was observed at all the time points of measurement.

At day 5, MMG+NFT's preventive efficacy was significantly higher than FV+FT's, but at days 10, 15, and 19, their efficacy was similar. However, at all the time points, MMG+NFT's efficacy was significantly higher than that of control, whereas FV+FT's efficacy was decreased at days 10, 15, and 19 and was close to the efficacy of control.

TABLE 6. The average amount of Ca loss for groups at days 5., 10., 15.,19. (mg/ dL)

Groups	MMG+NFT	FT	FV+FT	CPP-ACP+FT	NFT	Control
At Day 5: Average (mg/dL), Std. Deviation	0.4, 0.07	0.7, 0.11	0.6, 0.15	0.1, 0.09	0.9, 0.21	0.9, 0.19
At Day 10: Average (mg/dL), Std. Deviation	0.6, 0.16	0.9, 0.28	0.8, 0.21	0.2, 0.13	0.9, 0.21	1.2, 0.21
At Day 15: Average (mg/dL), Std. Deviation	0.6, 0.17	0.8, 0.17	0.8, 0.21	0.2, 0.11	0.9, 0.21	1, 0.12
At Day 19: Average (mg/dL), Std. Deviation	0.5, 0.14	1, 0.24	0.8, 0.15	0.3, 0.15	0.9, 0.13	0.9, 0.19

CONCLUSIONS

The findings of this 19-day in-vitro study have indicated that:

1. One-time application of the CPP-ACP varnish as an adjunct to the fluoridated dentifrice is significantly the most protective treatment against demineralization.
2. Daily application of medical minerals gel plus non-F toothpaste exhibited more protection than fluoride varnish plus F toothpaste.
3. There was no clinical advantage of one-time application of 5% sodium fluoride varnish as a supplement to daily

application of fluoride toothpaste.
4. Both toothpastes (fluoride and non-fluoride) had a weak preventive effect.

REFERENCES

1. K. C. Julien, P. H. Buschang, and P. M. Campbell, The Angle Orthodontist **83(4)**, 641–647 (2013).
2. A. Lucchese and E. Gherlone, Eur J Orthodont **35(5)**, 664–668 (2012).
3. E. Tufekci, J. S. Dixon, J. C. Gunsolley, and S. J. Lindauer, The Angle Orthodontist **81(2)**, 206–210 (2011).
4. L. E. A. do Nascimento, M. M. Pithon, R. L. dos Santos, et al., American Journal of Orthodontics and Dentofacial Orthopedics **143(4)**, S72–S77 (2013).
5. S. Lovrov, K. Hertrich, and U. Hirschfelder, Journal of Orofacial Orthopedics/Fortschritte der Kieferorthopädie **68(5)**, 353–363 (2007).
6. A. E. Richter, A. O. Arruda, M. C. Peters, and W. Sohn, American Journal of Orthodontics and Dentofacial Orthopedics **139(5)**, 657–664 (2011).
7. P. E. Benson, A. A. Shah, D. T. Millett, et al., Journal of Orthodontics **32(2)**, 102–114 (2005).
8. C. F. Demito, G. Vivaldi-Rodrigues, A. L. Ramos, and S. J. Bowman, Orthodontics & Craniofacial Research **7(4)**, 205–210 (2004).
9. K. Ekstrand, D. Ricketts, and E. Kidd, Caries Research **31(3)**, 224–231 (1997).
10. S. M. Behnan, A. O. Arruda, C. Gonzalez-Cabezas, et al., American Journal of Orthodontics and Dentofacial Orthopedics **138(6)**, 712.e1–7 (2010).
11. R. V. Kajalkar and A. D. Gaikwad, Int J Eng Res Dev **7(8)**, 8–11 (2013).
12. A. Munshi, N. Reddy, and V. Shetty, Journal-Indian Society of Pedodontics and Preventive Dentistry **19(3)**, 92–102 (2001).
13. C. Bourguignon, A. M. Dupuy, T. Coste, et al., Clinical Biochemistry **47(7-8)**, 636–639 (2014).
14. S. C. T. P. de Souza, K. C. de Araujo, J. R. Barbosa, et al., Acta Odontologica Scandinavica **76(3)**, 188–194 (2018).
15. H. Motulsk, Intuitive Biostatistics: A Nonmathematical Guide to Statistical Thinking (4th ed., Oxford University Press, 2013).
16. M. J. Campbell, D. Machin, and S. J. Walters, Medical Statistics: A Textbook for the Health Sciences (4th ed., Wiley, 2007).